MARINE POLLUTION BULLETIN

Volume 65 Issues 10–12 2012

Ahe Atoll and Pearl Oyster Aquaculture in the Tuamotu Archipelago

Serge Andréfouët and Loic Charpy

The Boulevard Langford Lane Kidlington Oxford OX5 1GB

Amsterdam • Boston • London • New York • Oxford • Paris • Philadelphia • San Diego • St. Louis

Marine Pollution Bulletin 65 (2012) 407–414

Contents lists available at SciVerse ScienceDirect

Marine Pollution Bulletin

journal homepage: www.elsevier.com/locate/marpolbul

Editorial

Recent research for pearl oyster aquaculture management in French Polynesia

1. Introduction

The papers on Ahe Atoll (Fig. 1) compiled in this volume release fresh scientific information relevant for a fairly specific human activity, currently developed mostly in the South Pacific and especially in atolls: black pearl aquaculture. Pearl farming is a commercial activity more than a century-old. It includes the farming of white and gold pearls in Asia and Australia, in both fresh and marine waters. Conversely, black pearl farming is more recent, and mostly associated with Pacific Islands where the production is the highest, and especially from French Polynesia which has dominated the market for the past 20 years (Southgate and Lucas, 2008).

As a human activity conducted in natural lagoon environments, the general topic is of interest for *Marine Pollution Bulletin*. This journal has published papers on a wide array of topics describing the marine environment, its use by human activities, and the related impacts. The suite of manuscripts presented on this special issue on "*Ahe Atoll and Pearl Oyster Aquaculture in the Tuamotu Archipelago*" investigated Ahe Atoll's oceanic wave regime, lagoon hydrodynamics, oyster larval dispersal, reproduction of oysters, lagoon hydrology, phytoplankton and zooplankton communities, oyster's diet, planktonic food webs, and impacts of the farming activity on the lagoon sediments and picoplankton communities. Several of the papers published in this volume tackle subjects that are generally published in journals specialized in aquaculture and biology, but with the huge emergence of aquaculture in recent decades has come greater recognition that the practice is commonly accompanied by deleterious changes. The papers here include ecophysiological papers focused on the pearl oyster *Pinctada margaritifera* and the description of plankton communities. However, all the papers are connected (see below a synthesis of the results) and collectively provide a multidisciplinary and integrated view of a lagoon ecosystem which is seldom available. We are pleased that these papers are published side by side in this issue, for the benefits of scientists and managers interested by human activities in lagoon environments.

2. The aquaculture of pearl oyster in French Polynesia

Black pearl production in French Polynesia tropical lagoons turned in 40 years from the status of a South Seas adventure to the status of an industry, as the second source of income for the country at the end of 1990s, after tourism. In the best years (Fig. 2), black pearl represented 60 MUS$ of income for a country of 250.000 inhabitants. Beyond the magnificent jewel, beyond the beauty of the myriad of colors, lusters and shapes, beyond the prized value, beyond the unique human culture and know-how found around pearl farms, black pearls are fascinating for scientists because they represent the ultimate product of both an exploited lagoon ecosystem and an exploited bivalve, the black lip oyster *Pinctada margaritifera* (Linnaeus, 1758) var. *cumingii* (Jameson, 1901).

Pearl production has always been challenging for the suite of numerous factors and processes that need to be understood and mastered before a black pearl materialize in the hand of a farmer. Throughout the 19th and first half of the 20th century, *P. margaritifera* oysters were harvested by free-divers only for the nacre, and button, industry. Sometimes, natural black pearls were found. In French Polynesia, in 1961, the first attempt to graft oysters with the goal of producing cultivated round pearls was successfully achieved in Hikueru atoll by Jean-Marie Domard and Churoku Muroi. The first farm was established in Manihi atoll in 1968. The two following decades saw the slow rise of a new commercial activity with production in Tuamotu and Gambier archipelagos (e.g., Marutea Sud), with black pearls acquiring the status of high quality gems in international jewellery markets. By the end of the eighties, both archipelagos experienced a black pearl rush, with thousands of Polynesian and foreigners workers returning to remote atolls. Hundreds of new concessions were granted per year on a variety of lagoons. Production rose quickly. Experiments of all kind followed to achieve the most efficient collecting and farming possible, often in logistically challenging remote conditions. Spat collecting was critical. Indeed, the pearl industry required before all the provision of oysters. They were initially harvested from wild stocks, and spat collecting developed rapidly in suitable lagoons to steadily provide to farmers the oysters needed for grafting. Enhanced farming practices yielded an average successful rate of 300–400 sellable pearls for 1000 grafted oysters. On the other hand, transfers of oysters between atolls were frequent, making local populations and lagoons vulnerable to extinction, diseases, and spread of invasive epibionts species. Dedicated governmental services were created to manage and monitor the environmental and socio-economic consequences of what was virtually an entire new field of economic activity coming out of the blue of the Tuamotu and Gambier lagoons. Quickly, despite the growing empirical knowledge developing among farmers, better knowledge of lagoon ecosystem functioning and suitability for pearl farming were needed. This included better knowledge on the physiology of *P. margaritifera*. Scientific research programs were launched, and both lagoon ecosystems and organisms came under the scrutiny of applied and fundamental studies.

http://dx.doi.org/10.1016/j.marpolbul.2012.06.021

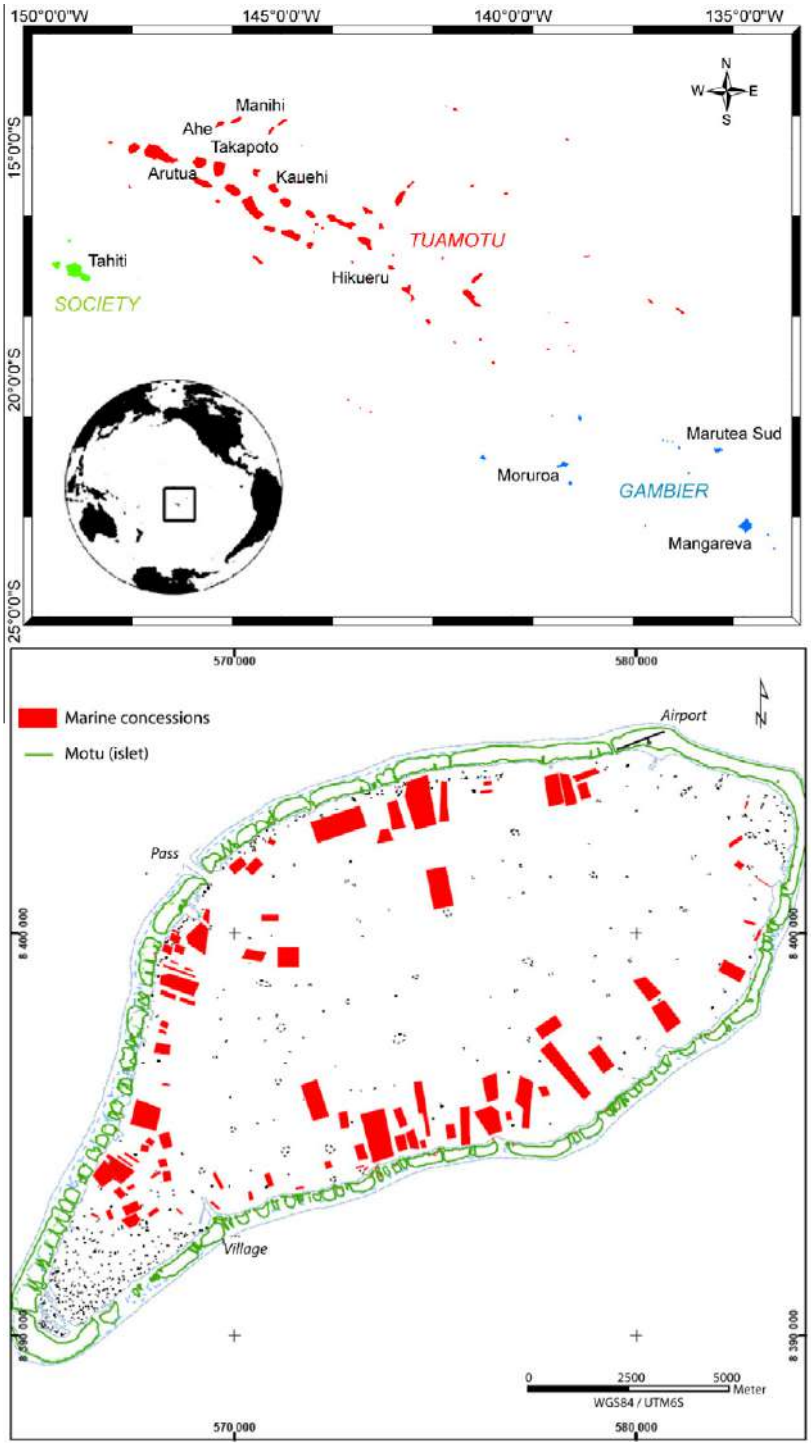

Fig. 1. Top: location map of French Polynesia and Ahe atoll, as well as other sites mentioned in the text. Bottom: map of marine concessions in Ahe atoll, as in 2012. To be compared with the same map in Andréfouët et al. (2006).

In 2011, time came to take a pause and look at the evolution of the situation 20 years after the industry boom. It was also time to assess the status of knowledge and what would be the new priorities. Indeed, like a natural ecosystem, the French Polynesia black pearl industry has reached its climax, collapsed, and is now in a recovery stage. The official numbers from the *Institut de la Statistique de Polynésie Française* (ISPF) show the changes in total exported production, monetary value per gram and total number of concessions since these variables are monitored (Figs. 2 and 3).

Prices collapsed in the year 2000s, due primarily to overproduction of lowest quality pearls and poor management and control of the commercial distribution towards international Asian, American and European markets. Prices plummeted from around 100US$ per gram in 1985 down to less than 5US$ in 2010. Consequently, the number of concessions decreased steadily throughout the Tuamotu and Gambier. In 2010, respectively 425, 102 and 28 concessions were granted for respectively Tuamotu, Gambier (mostly in Mangareva, a high island with a wide lagoon) and Society Archipelagos, thus a total of 555 concessions. In 2011, the last available overall

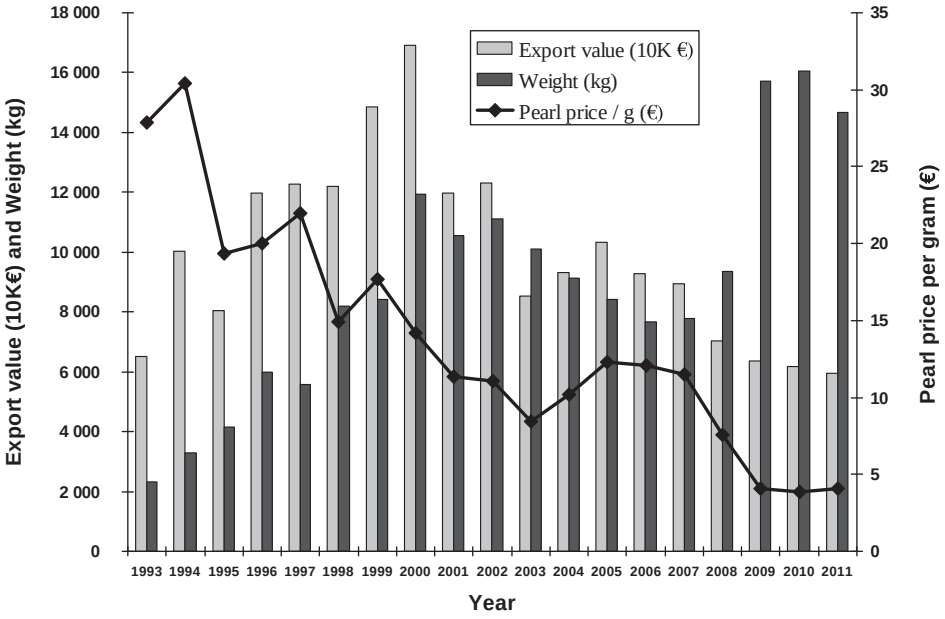

Fig. 2. Evolution from 1993 to 2011 of key indicators: total export value, total weight, and price per gram. Data source: Institut Polynésien de la Statistique.

number is 541. In 1999, 2745 concessions were active. Small family businesses took a heavy toll with the collapse of the prices. They represented in 2011 80% of the farms for 20% of the export market. The total concession area is now limited to 10000 hectares all lagoons included. In 2011, this represented 26 atolls and 4 islands. Among them, 15 atolls are collecting atolls.

The industry is now trying to rebuild the equilibrium between offer and demand, with the hope that curves of prices per pearl and per gram will rise. Pearl quality is closely monitored for exportation. Eleven millions pearls have been controlled in 2010, which represented 18.3 tons. Low quality pearls are destroyed and farmers receive a fixed rate of 0.5 US$ per destroyed gram as a compensation. In 2010, 400 kg of these poor quality pearls have been disregarded. In addition, commercial promotion and selling networks are also restructured.

The aquaculture of black pearl in French Polynesia has thus modified the livelihoods of thousands of islanders in the past 30 years. It has also reshaped the atollscape, with numerous farms, buildings, pontoons and boats appearing and disappearing along shores and coral pinnacles. Tens of thousands of buoys and millions of hanging lines dot the lagoons, spread in the official 10000 hectares of concessions all over French Polynesia. Millions of oysters have been artificially hanging in the water column instead of living on deep atoll floors. Naturally separated oyster populations have been mixed, and species of sponges, anemones (in particular *Aiptasia pallida)* and other epibionts have been introduced in lagoons. Massive local and widespread mortalities have occurred that remain poorly explained due to insufficient *in situ* monitoring of environmental conditions, given the remoteness of atolls and associated monitoring costs. The exact ecological impact of the pearl industry remains unknown to date and will likely be a future direction of investigation. In the past, however, research programs investigated how the lagoon ecosystem carrying capacities could sustain the industry, what could be the best aquaculture practices, and what were the sanitary risks for the cultivated stocks. We review hereafter these past axes of research.

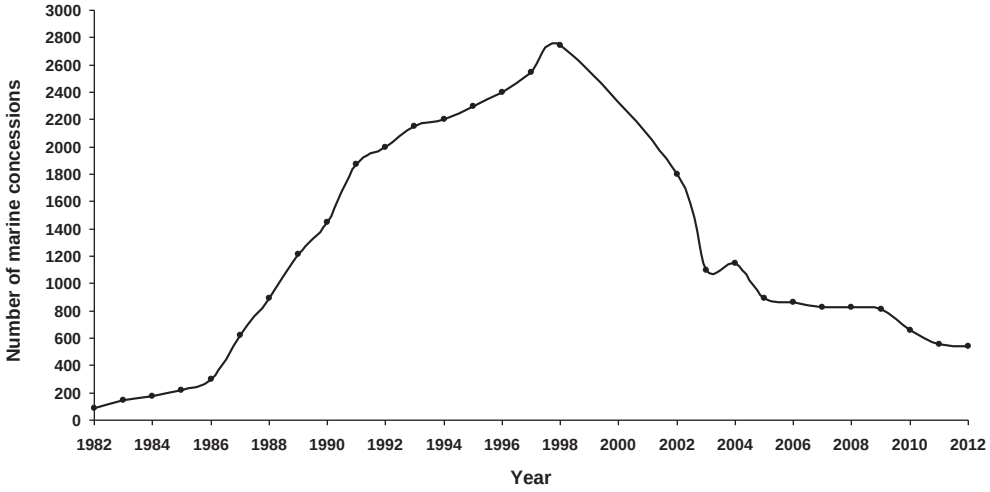

Fig. 3. Thirty years of evolution in number of pearl farming and collecting marine concessions in French Polynesia.

3. Past research on pearl oyster and atoll lagoons

From the early 1980s till to date, research activities have accompanied the black pearl industry. The *Etablissement pour la Valorisation des Activités Aquacoles et Marines* (EVAAM) was created in 1983 to assist farmers and to develop the market. This is in addition to all the empirical individual research activities taking place in farms to enhance spat collecting, grafting, and farming. Initially, research was not seen as a priority by professionals. Confidentiality of knowledge ruled between farmers. However, massive mortalities in 1985–1986 in Takapoto Atoll showed that virtually nothing was known on the interactions between *P. margaritifera* and its environment, its capacity to resist to environmental stressors, and possible pathogens. These assessments were beyond the capacities of farmers alone and new research programs were needed.

Atoll have been studied for decades in French Polynesia and elsewhere, but not always with a focus imposed by one bivalve species and black pearl production. The ATOLL, CYEL, and TYPATOLL projects in particular have looked at general aspects of the ecology and functioning of various atoll lagoons, some specifically selected for their lack of human activities (Dufour and Harmelin-Vivien, 1997). Besides description of planktonic and benthic communities, scientists looked very early at primary production, nutrient limitations and organic matter recycling in both the water column and sediments (Sournia and Ricard, 1975; Charpy and Charpy-Roubaud, 1990; Delesalle and Sournia, 1992; Dufour et al., 2001). The atolls used for nuclear tests (Moruroa and Fangatau) were also intensively studied (Guille et al., 1993; Tartinville et al., 1997). Finfish fisheries were investigated in Tikehau Atoll (Intes et al., 1995). Stocks of giant clams have been studied since at least Salvat (1967) and are still of objects of investigations in the Eastern Tuamotu (Andréfouët et al., 2005; Gilbert et al., 2006). Ciguatera poisoning has also been a major concern for human population health in French Polynesia (Bagnis et al., 1985). Finally, the geology and geomorphology of atolls have been studied and mapped under the light of late Holocene sea level variations, lithospheric processes, and exposure to dominant swell (McNutt and Menard, 1978; Pirazzoli et al., 1988; Andréfouët et al., 2001a).

The *Programme General de Recherche sur la Nacre* (PGRN, standing for Nacre General Research Program), was launched in 1990 and reoriented the research performed on atolls towards black pearl aquaculture issues. The focus set by scientists was primarily on understanding the trophic capacity of the lagoons, and the ecophysiologic and metabolic capacities of oysters (feeding regime, growth, reproduction, respiration) as well as its resistance to temperature and high population density stress. The pilot atoll was Takapoto, where a field station allowed running long term *in situ* experiments. In selected lagoons, a network of stations was set with volunteering farmers to monitor environmental conditions (Pouvreau and Prasil, 2001). In addition, research on aquaculture practices focused on the processing of oysters and lines to clean epibionts and trophic competitors. The PGRN aimed to disseminate results to farmers by various means: on site training, newsletters in both French and Tahitian, meetings etc. The program also led to numerous doctoral studies conducted in the new French Polynesia university, and yielded an abundant scientific literature (e.g., Charpy, 1996; Niquil et al., 1998; Zanini and Salvat, 2000; Buestel and Pouvreau, 2000; Torréton et al., 2002). These papers clarified the dominant planktonic communities, trophic flux and limiting nutrients found in atoll lagoons, and their variations according to atoll morphology and hydrodynamic regime (Charpy et al., 1997; Andréfouët et al., 2001b; Dufour et al., 2001).

This first coordinated research, which terminated in October 1999, provided practical advice to farmers to optimize densities, collecting methods, and epibiont clean-ups. It also enhanced knowledge on the biology and ecophysiology of *P. margaritifera* (Pouvreau et al., 2000a,b). It clarified the links between Takapoto environment and oyster physiology and sources of food. A major conclusion was that lagoons (at least Takapoto Atoll) were not food-limiting given their current loads of cultivated animals (Niquil et al., 2001). In atoll lagoons, organic particles < 5 μm (heterotrophic bacteria, autotrophic bacteria and phytoplankton < 5 μm) generally represented more than 70% of the living carbon biomass whereas particles between 5 μm and 200 μm (protozoan, phytoplankton > 5 μm, appendiculates and metazoan larvae) represent less than 30%. PGRN demonstrated that the low retention efficiency of the dominant < 5 μm planktonic communities by *P. margaritifera* was largely offset by the efficient grazing of the larger size-fraction plankton and protozoan (Loret et al., 2000a,b), and by exceptionally high pumping rates (Pouvreau et al., 1999, 2000c; Yukihira et al., 1998). However, not all aspects of the planktonic food chain were understood, including the role of various zooplankton compartments and the influence of possible competitors.

The PGRN recommendations for a second phase of research were to investigate the risks related to pathogen spreads, the processus controlling the quality of the pearl (in particular those controlling the color and mineralization and the influence of the type of nucleus used), and also the influence of environmental parameters on spat collection. Indeed the success of this activity remained highly variable in space and time (Andréfouët et al. 2006). After the PGRN, researches were not anymore necessarily coordinated within a single program. Instead, the *Service de la Perliculture* (Pearl Aquaculture Service) managed since 2002 individual actions with the various research organisms involved in the activities.

Numerous programs were launched in the past five years, using a variety of source of funding. In 2008 and 2009, the PERDUR project aimed for a better resource sustainability and farmers profits (Hui et al., 2011; Thomas et al., 2011a; Yaroshewski, 2011). The ADEQUA research consortium was launched in 2008 to coordinate during 4 years the activities related to the understanding of the quality of the pearl (e.g., Joubert et al., 2010; Linard et al., 2011; Montagnani et al., 2011). Meantime, the project REGENPERL specifically looked at physiologic (Le Moullac et al., 2011) and genetic aspects (Lemer and Planes, 2012) and a network dedicated to the monitoring of sanitary conditions was developed. Larval dispersal in Ahe atoll was studied, and the larval ecology of *P. margaritifera* was characterized leading to the development of a bioenergetic growth model (Thomas et al., 2011b). Finally, late 2007, a European Community funded project was launched under the auspices of the *Service de la Perliculture* to investigate in Ahe Atoll and Takaroa Atoll the trophic regime of oysters and the hydrodynamic forcing on spat collection. The compilation of papers published in this special issue and summarized below present the main finding of this project for Ahe Atoll.

4. New results from Ahe atoll

Ahe Atoll was selected by a European Fund for Development project for its major position in the hierarchy of pearl and spat producers. Ahe atoll is located in the North-western part of the Tuamotu Archipelago, 500 km North-East of Tahiti. Its lagoon covers 145 km^2 with a mean depth close to 40 m and a maximum depth of around 70 m. One active pass is located in the western part of the lagoon and several reef-flat spillways (hoa, less than 50 cm depth) are distributed along the reef rim, mainly in the south and west part sectors (Dumas et al., 2012). The overall aperture is low, and Ahe can be defined as a semi-closed atoll.

In May 2012, 77 farms were registered. They covered 1188 hectares of lagoonal space (Fig. 1). In December 2007, these numbers were respectively 83 farms and 1320 hectares, illustrating the continuous decrease of the activity. The number of authorized collecting stations was 1050 in May 2012, each about 200 m long. The total number of cultivated oysters could represent up to 15 millions oysters.

The bulk of the Ahe project was accomplished between 2008 and 2010, with field work occurring from mid-2008 to end of 2009. Three different activities took place. First, using numerical tools never applied before in the Tuamotu atolls, the objective was to characterize the circulation of the lagoon to understand better the source of variability in spat collecting. Second, the objectives were to characterize the planktonic communities of Ahe lagoon at different seasons also using new investigation approaches never used before in Tuamotu atoll lagoons. As much as possible, the influence of pearl farming on planktonic communities was assessed. Third, biology and ecophysiology of oysters at adult and larval stages was investigated. Reproduction, grazing and larval dispersal were monitored *in situ* in several periods under different environmental conditions. This third project component benefited from additional source of funding.

The hydrodynamic component of the project had two main subcomponents following Andréfouët et al. (2006) recommendations: an oceanic and a lagoon sub-component. The oceanic and atmospheric forcing of the atoll was classically studied using meteorological data and model. However, the wave regime of the atoll was characterized at high spatial resolution (5 km) using both wave numerical model and satellite altimetry data (Andréfouët et al., 2012). The study shows that Ahe atoll experienced an atypical wave regime, with lower wave height year round than other Tuamotu atolls. This is due to the level of protection of the atoll provided by south Tuamotu atolls. The consequences are that Ahe's lagoon renewal rate is controlled by tide, and not waves. To precisely study the circulation and renewal rates of Ahe's lagoon, Dumas et al. (2012) implemented a high resolution (100 m) 3D numerical model using the Mars3D software and assumptions, using finite difference techniques in a sigma coordinate framework. The model was calibrated and validated using one year of intensive field data acquisition. It provided simulated quantitative data on the three main residual barotropic structures inside the lagoon, under different wind conditions. This demonstrated that the pass played a major role in the hydroscape of the lagoon. It defined areas of high flushing rates, areas of dilution and areas of retention. Circulation is driven by wind. Wind (generally from the east and south-east directions) creates a general overturning circulation parallel to the wind direction and contributes to bring nutrients to the downwind upwelling areas.

The 3D model was fully used by Thomas et al. (2012a) to complete with connectivity matrices and dispersal scenarios the mapping of the distribution and the dynamics of bivalve larvae as observed *in situ* (Thomas et al., 2012b). Models were run under climatological and realistic wind condition scenarios. The connectivity modelling provided maps of the most suitable areas for spat collection under different weather conditions. The hydrodynamic 3D model was refined for this objective by using a vertical swimming sub-model validated *in situ* (Thomas et al., 2012b).

Larval dispersal is itself the consequences of the factors that control the reproduction of oysters. Fournier et al. (2012a) investigated in Ahe Atoll the influence of natural plankton concentration on maturation and spawning of *P. margaritifera*, during a 4 months survey. Plankton concentration (chlorophyll a) and microscope counts were compared with oysters reproduction activity, measured with gonadic index, gonado-visceral dry weights and histology. Fournier et al. (2012a) concluded that gametogenesis rate was mainly related to plankton concentration and that spawning occurred when maximal gonad storage was reached. The main spawning synchronizing factor was plankton concentration. Understanding at least the chlorophyll spatio-temporal variations are thus a priority for predicting the timing of spawning. In their sampling stations, Fournier et al. (2012a) reported that plankton concentration fluctuations were mainly related to the wind regime, and to the overturning circulation and upwelling effects described by Dumas et al. (2012).

The hydrology of the lagoon was characterized during the larval experiments (Thomas et al., 2010), during the hydrodynamic surveys (Dumas et al., 2012) and during the plankton surveys (Charpy et al., 2012). Because different depth limits and stations were considered, and because of the fairly high wind regime experienced during each field period, conclusions were not always in agreement between studies in terms of stratification. Neither Charpy et al. (2012) and Thomas et al. (2010) reported stratification for any of their campaigns. However, according to Dumas et al. (2012), slight thermal and salinity stratifications can occur. The general overturning circulation evidenced by Dumas et al. is likely to be responsible for the mixing of the lagoon water body. In light to medium wind conditions, the overturning circulation weakens, allowing the development of a slight vertical stratification. In more intense wind, the circulation is strong enough to prevent stratification, by upwelling to windward of the bottom cold water and downwelling to leeward of the surface warm water.

Charpy et al. (2012) reported on the general hydrologic characteristics of the lagoon, and compared them to previously studied atolls. The vertical and spatial distribution observed on phytoplankton biomass (extracted chlorophyll) in Ahe was fairly homogeneous, with a significant increase in the southwest of the lagoon under windy conditions. Phytoplankton biomass was also in the same range as other atoll lagoons, as well as nutrient concentrations. Nitrogen is probably the first limiting factor for phytoplankton production (DIN: P ratio <3) but N-enrichment by benthic N_2-fixing cyanobacteria needs to be precisely investigated. The benthic interface was assumed to deliver only up to 28% of the nitrogen phytoplankton demanded. Lefebvre et al. (2012) refine the assessment of spatio-temporal variability through estimations of photosynthetic parameters (using pulse amplitude modulation fluorometry) and primary production (^{13}C incorporation) measurements of the size structured phytoplankton biomass (<2 μm and >2 μm), in addition to traditional incubation of carbon isotopes. Primary production was dominated by the picophytoplankton, but its biomass specific primary productivity was lower than in other atoll lagoons. They showed significant spatial (sites) and temporal (seasonal and day to day) effects on the measured processes for the two size fractions of phytoplankton. The variables size fraction of the phytoplankton, water temperature, season, the interaction term station * fraction and site, explained significantly the variance of the data set using redundancy analysis. However, no significant trends over depth were observed in the range of 0–20 m. A consistent clear spatial pattern was found with the south and north sites different from the two central stations for most of the measured variables. This pattern was explained by the different barotropic cells highlighted by Dumas et al. (2012) in their hydrodynamic study. Lefebvre et al. (2012) hypothesized the existence of a fast regeneration mechanism of nitrogen through pulses, a process that fuels the larger phytoplankton's production better than the picophytoplankton one. Sediment interface and cultured oysters were good candidates to explain, at least partly, the fast regeneration processes of nitrogen organic material. A precise spatial evaluation of the cultured pearl oyster stock remain necessary for future studies, as well as measurements of nutrient ambient conditions, preferentially with flux methods using carbon

and nitrogen tracers rather than measurement of nutrient stocks that are rapidly assimilated and transformed by autotrophs (Furnas et al., 2005).

Charpy et al. (2012) suggests that relatively low particulate organic carbon content compared to other lagoons localized at the same latitude could reflect the impact of pearl oyster aquaculture. However, this impact does not appear on phytoplankton biomass. Indeed, as shown by Fournier et al. (2012b), oysters do not feed directly on phytoplankton, but rather graze heterotrophic plankton. Fournier et al. (2012b) refined the knowledge on *P. margaritifera* diet by demonstrating with the flow through chamber method that the main factor influencing clearance rates of pearl oysters was the biovolume of planktonic particles. Thus, the diet of *P. margaritifera* was mainly driven by fluctuation of the relative biomass of the nano- micro- planktonic communities. Both heterotrophic nano- and micro-plankton represented an important part of the diet of *P. margaritifera* depending on their relative biomass in the water column. The picoplankton communities displayed the lowest clearance rates but represented however a detectable contribution to the diet. Whether or not this selective grazing may induce a change in plankton assemblage in cultivated lagoons compared to uncultivated ones remain unknown.

Pearl farming could impact lagoons in different ways. First, the population of oysters hanging on lines may induce changes in the planktonic communities but this remains unproven to date. Second, lines hanging above the lagoon floors can modify the flux of material at the sediment interface. Gaertner-Mazouni et al. (2012) quantified benthic nutrient fluxes and sedimentation rates for two stations located under pearl oyster frames, and two control stations away from the pearl culture facility. They concluded that aquaculture increased sedimentation rates but probably by modification of local currents and not by the release of additional organic material. No organic enrichment in sediments was demonstrated. Conversely, they showed that maximum values of benthic nitrogen fluxes were recorded in stations directly under the influence of pearl oyster culture. These benthic nitrogen fluxes could contribute up to 28% of the nitrogen demand in the water column. Third, human populations around farms could directly impact the lagoon. Bouvy et al. (2012a) concluded from faecal indicator bacteria that there was no evidence that human sewage had any impact on picoplankton throughout the atoll. They concluded that Ahe atoll belongs to the type of unproductive aquatic system, without high external inputs of inorganic nutrients issuing from human activities, as defined by Duarte and Agusti (1998).

Three papers in this issue refine knowledge of planktonic communities of atoll lagoons. First, Bouvy et al. (2012b) investigate with one survey per atoll the virioplankton and bacterioplankton in Ahe and Takaroa atolls, in comparison with the surrounding oligotrophic ocean. The role of virioplankton in lagoons was unknown while viruses are the numerically dominant biological entities in the ocean and viral infection is a major structuring process in the dynamics of marine microbial communities. For instance, viral lysis of autotrophic and heterotrophic microorganisms influences the rate of nutrient cycling through microbial food webs. Most virioplankton in the environment infect bacterioplankton and, in general, the distributions of viral populations often mirror the bacterial distributions. However, Bouvy et al. (2012b) suggest that the distribution patterns of virioplankton are apparently not coupled in Ahe and Takaroa. Fractions of infected bacterial cells were all extremely low, among the lowest recorded in both marine and freshwater systems. Differences between atolls occurred, with a mean virus-to-bacteria ratio significantly lower in Ahe than in Takaroa. This is consistent with the hypothesis that this ratio is likely to increase in environments that favor fast bacterial growth given the estimated longer residence times in Takaroa compared to Ahe.

Michotey et al. (2012) investigated the prokaryotes communities of Ahe lagoon using molecular techniques. Heterotrophic prokaryotes are important for the mineralization of organic matter and they are the only one able to use directly dissolved organic matter (DOM). The produced prokaryotic biomass is grazed by nanoplankton (nanoflagellates and ciliates), that is successively consumed by micro-zooplankton and organisms of higher trophic level that in turn produce DOM. This microbial loop allows the transfer of energy to the higher levels of the trophic web by recycling of organic matter. All sequences retrieved by Michotey et al. (2012) were affiliated within bacterial (*Cyanobacteria,* and heterotrophic *Proteobacteria* and *Flavobacteria*) or archaeal superkingdoms. Communities and operational taxonomic units were analysed according to dry/rainy seasons and free-living/particle-attached state. Variations of these communities were also assessed in relation to an oceanic-lagoon gradient, and inside the lagoons at different locations and depth. Bacterial density was higher in the lagoon compared to ocean and a seasonal trend was observed. No spatial pattern of bacterial abundance and diversity within the lagoon was detected, nor the influence of the planktonic/attached states was noticed. Archaeal abundance showed seasonal tendency and particle-prevalence, but no differences between lagoon and oceanic location was observed. The spatio-temporal pervasiveness found by Michotey et al. (2012) for the heterotrophic groups (*Marinovum, Flavobacteria* and *Erytrobacter*) confirms that in Ahe atoll, the microbial loop can be predominant (Pagano et al., 2012) and the community is heterotrophic.

Finally, Pagano et al. (2012) completed within Ahe lagoon the assessment of planktonic communities and food webs by investigating during three periods the space–time variations of metazooplankton communities and their abundance according to environmental (salinity, temperature, wind), and trophic factors (phytoplankton, bacteria, heterotrophic nanoflagellates, and ciliates) distribution. Zooplankton plays a major role in the functioning, productivity and food webs of aquatic ecosystems. Zooplanktonic organisms have an herbivorous-detritivorous diet and can exert a strong grazing pressure on phytoplanktonic biomass. Zooplankton, including larvae of *P. margaritifera*, are themselves a food source for organisms of the upper trophic levels such as planktivorous fish and carnivorous invertebrates. In Ahe, the meroplankton, mainly bivalve and gastropod larvae, was dominant. Holoplankton was dominated by copepods. Results highlighted the wind influence on the horizontal distribution of the zooplankton communities that are consistent with the hydrodynamic structures described by Dumas et al. (2012). The metazooplankton was bottom-up controlled by trophic resources. Then, the low nanophytoplankton biomass in contrast to the high abundance of picophytoplankton, nanoflagellates and nano-particle grazers confirmed the importance of the microbial loop in the planktonic food web of Ahe lagoon. The dominance of bivalve larvae suggested potential major community change arising from aquaculture activities, but the influence of the wild populations could not be discarded.

5. Conclusion and perspectives

Following Takapoto Atoll in the nineties during the PGRN program, Ahe Atoll has been since 2007 the main research site for black pearl aquaculture in French Polynesia. As briefly presented above and in detail in this issue, new methods applied to both old and new questions provided a wealth of fresh results on atoll lagoon environments, oyster ecophysiology, planktonic communities and trophic relationships. In particular, the detailed study of the lagoon circulation provided the spatial and hydrodynamic context of the biological observations. This yielded a first integrated view of the lagoon biophysical functioning, which now needs to

be refined and modelled more extensively. Indeed, the next steps consist in coupling the hydrodynamic larval dispersal model with a larval bioenergetic growth model (Thomas et al., 2011b). The result would be a model of larval dispersal taking into account currents but also environmental and food conditions. Development of a bioenergetic growth model is also planned for adults. A series of experiments in Ahe Atoll planned in 2012–2013 will collect new data to meet these goals, also using new methodological approaches.

Another objective for French Polynesias is to expand the research to other lagoons where natural spat collection occurs. A priority is Mangareva Island in the Gambier Archipelago. Mangareva consists of a large deep lagoon surrounding several small high islands where black pearl farming is still active and productive. On-going projects will investigate larval dispersal and *Pinctada margaritifera* ecophysiology in very different environmental and hydrodynamic conditions than those found in Ahe or Takapoto. It is also planned to monitor occurrences of spawning events using the condition index (ratio of wet weight of the visceral mass to shell weight) (Le Moullac et al., 2012). Together, spawning monitoring and larval dispersal modelling will enhance the accuracy of the spat collecting forecast system that French Polynesia aimed at.

All these future activities on Ahe and Mangareva are currently planned in the POLYPERL (2012–2014) and BIODIPERL (2012–2013) recently funded projects. Finally, we point out that the professionals involved in pearl farming in the various atolls and islands are generally supportive of research activities. Their support is essential, and a great motivation, to conduct the researches presented here elsewhere. Therefore, on the long run, additional atolls should be studied, such as Arutua and Kaeuhi. The modelling, environmental and ecophysiological work pioneered in Ahe should provide for these atolls an objective foundation to establish spatial zoning plans in their lagoons. For the benefits of farmers, space and concessions would be allocated according to the most optimal areas for collecting larvae, and for growing juvenile oysters and grafted adults.

Acknowledgements

The 9th European Development Fund (grant POF/001/002N°1 to S.A. and L.C.) through the French Polynesia Service de la Perliculture, supported all the studies presented in this special issue on Ahe atoll and pearl oyster aquaculture. We warmly acknowledge the 26 reviewers who helped for this special issue, for their time and suggestions for improvement. We are grateful to Charles Sheppard, Editor-in-Chief, for welcoming this special issue in *Marine Pollution Bulletin*. We also appreciated the help from Becky Rives-Roberts and Sara Bebbington at Elsevier during the realization of this volume. Pascal Correia provided the Fig. 3, using the latest 2012 data on concessions available at Direction of Marine Resources of French Polynesia.

References

Andréfouët, S., Claereboudt, M., Matsakis, P., Pagès, J., Dufour, P., 2001a. A. Typology of atolls rims in Tuamotu archipelago (French Polynesia) at landscape scale using SPOT-HRV images. Int. J. Remote Sens. 22, 987–1004.

Andréfouët, S., Pagès, J., Tartinville, B., 2001b. Water renewal time for classification of atoll lagoons in the Tuamotu Archipelago (French Polynesia). Coral Reefs 20, 399–408.

Andréfouët, S., Gilbert, A., Yan, L., Remoissenet, G., Payri, C., Chancerelle, Y., 2005. The remarkable population size of the endangered clam *Tridacna maxima* assessed in Fangatau atoll (Eastern Tuamotu, French Polynesia) using *in situ* and remote sensing data. ICES J. Mar. Sci. 62, 1037–1048.

Andréfouët, S., Ouillon, S., Brinkman, R., Falter, J., Douillet, P., Wolk, F., Smith, R., Garen, P., Martinez, E., Laurent, V., Lo, C., Remoissenet, G., Scourzic, N., Gilbert, A., Deleersnijder, E., Steinberg, C., Choukroun, S., Buestel, D., 2006. Review of solutions for 3D hydrodynamic modeling applied to aquaculture in South Pacific atoll lagoons. Mar. Pollut. Bull. 52, 1138–1155.

Andréfouët, S., Ardhuin, F., Queffeulou, P., Gendre, R.L., 2012. Island shadow effects and the wave climate of the Western Tuamotu Archipelago (French Polynesia) inferred from altimetry and numerical model data. Mar. Pollut. Bull. 65, 415–424.

Bagnis, R., Bennett, J., Barsinas, M., Chebret, M., Jacquet, G., Lechat, I., Mitermite, Y., Perolat, P.H., Rongeras, S., 1985. Epidemiology of ciguatera in French Polynesia from 1960 to 1984. In: Gabrie, C., Salvat, B. (Eds.), Proceedings of the Fifth International Coral Reef Congress, vol. 4, pp. 475–482.

Bouvy, M., Combe, M., Bettarel, Y., Dupuy, C., Rochelle-Newall, E., Charpy, L., 2012a. Uncoupled viral and bacterial distributions in coral reef waters of Tuamotu Archipelago (French Polynesia). Mar. Pollut. Bull. 65, 506–515.

Bouvy, M., Dupuy, C., Pagano, M., Barani, A., Charpy, L., 2012b. Do human activities affect the picoplankton structure of the Ahe atoll lagoon (Tuamotu Archipelago, French Polynesia)? Mar. Pollut. Bull. 65, 516–524.

Buestel, D., Pouvreau, S., 2000. Particulate matter in Takapoto lagoon waters: potential food for cultivated pearl oysters. Oceanolog. Acta 23, 193–210.

Charpy, L., 1996. Phytoplankton biomass and production in two Tuamotu atoll lagoons (French Polynesia). Mar. Ecol. Prog. Ser. 145, 133–142.

Charpy, L., Charpy-Roubaud, C.J., 1990. Trophic structure and productivity of the lagoonal communities of Tikehau atoll (Tuamotu Archipelago, French Polynesia). Hydrobiologia 207, 43–52.

Charpy, L., Dufour, P., Garcia, N., 1997. Particulate organic matter in sixteen Tuamotu atoll lagoons (French Polynesia). Mar. Ecol. Prog. Ser. 151, 55–65.

Charpy, L., Rodier, M., Fournier, J., Langlade, M.-J., Gaertner-Mazouni, N., 2012. Physical and chemical control of the phytoplankton of Ahe lagoon, French Polynesia. Mar. Pollut. Bull. 65, 471–477.

Delesalle, B., Sournia, A., 1992. Residence time of water and phytoplankton biomass in coral reef lagoons. Cont. Shelf Res. 12, 939–949.

Duarte, C.M., Agusti, S., 1998. The CO2 balance of unproductive aquatic ecosystems. Science 281, 234–236.

Dufour, P., Harmelin-Vivien, M., 1997. A research program for a typology of atoll lagoons: strategy and first results. In: Lessios, H.A., Macintyre, I.G. (Eds.), 8th Int.. Coral Reef Symp., Panama, pp. 843–848.

Dufour, P., Andréfouët, S., Charpy, L., Garcia, N., 2001. Atolls morphometry control nutrient regime in their lagoons. Limnology Oceanography 46, 456–461.

Dumas, F., Le Gendre, R., Thomas, Y., Andréfouët, S., 2012. Tidal flushing and wind driven circulation of Ahe atoll lagoon (Tuamotu Archipelago, French Polynesia) from in situ observations and numerical modelling. Mar. Pollut. Bull. 65, 425–440.

Fournier, J., Levesque, E., Pouvreau, S., Le Pennec, M., Le Moullac, G., 2012a. Influence of plankton concentration on gametogenesis and spawning of the black lip pearl oyster *Pinctada margaritifera* in Ahe atoll lagoon (Tuamotu archipelago, French polynesia). Mar. Pollut. Bull. 65, 463–470.

Fournier, J., Dupuy, C., Bouvy, M., Couraudon-Réale, M., Charpy, L., Pouvreau, S., Le Moullac, G., Le Pennec, M., Cochard, J.-C., 2012b. Pearl oysters *Pinctada margaritifera* grazing on natural plankton in Ahe atoll lagoon (Tuamotu archipelago, French Polynesia). Mar. Pollut. Bull. 65, 490–499.

Furnas, M., Mitchell, A., Skuza, M., Brodie, J., 2005. In the other 90%: phytoplankton responses to enhanced nutrient availability in the Great Barrier Reef Lagoon. Mar. Pollut. Bull. 51, 253–265.

Gaertner-Mazouni, N., Lacoste, E., Bodoy, A., Peacock, L., Rodier, M., Langlade, M.-J., Orempuller, J., Charpy, L., 2012. Nutrient fluxes between water column and sediments: potential influence of the pearl oyster culture. Mar. Pollut. Bull. 65, 500–505.

Gilbert, A., Andréfouët, S., Yan, L., Remoissenet, G., 2006. The giant clam *Tridacna maxima* communities of three French Polynesia islands: comparison of their population sizes and structures at early stages of their exploitation. ICES J. Mar. Sci. 63, 1573–1589.

Guille, G., Goutière, G., Sornein, J., 1993. Les atolls de Mururoa et de Fangataufa (Polynésie française) I. Géologie, Pétrologie, Hydrogéologie. Editions Louis Jean, 168pp.

Hui, B., Vonau, V., Moriceau, J., Tetumu, R., Vanaa, V., Demoy-Schneider, M., Suquet, M., Le Moullac, G., 2011. Hatchery-scale trials using cryopreserved spermatozoa of black-lip pearl oyster (*Pinctada margaritifera*). Aquat. Living Res. 24, 219–223.

Intes, A., Caillart, B., Charpy-Roubaud, C.-J., Charpy, L., Harmelin-Vivien, M., Galzin, R., Morize, E., 1995. Tikehau: an atoll of the Tuamotu Archipelago. Atoll Res. Bull. vol. 415.

Joubert, C., Piquemal, D., Marie, B., Manchon, L., Pierrat, F., Zanella-Cleon, I., Cochennec-Laureau, N., Gueguen, Y., Montagnani, C., 2010. Transcriptome and proteome analysis of *Pinctada margaritifera* calcifying mantle and shell: focus on biomineralization. BMC Genomics 11, 613.

Lefebvre, S., Claquin, P., Orvain, F., Véron, B., Charpy, L., 2012. Spatial and temporal dynamics of size-structured photosynthetic parameters (PAM) and primary production (13C) of pico- and nano-phytoplankton in an atoll lagoon. Mar. Pollut. Bull. 65, 478–489.

Lemer, S., Planes, S., 2012. Translocation of wild populations: conservation implications for the genetic diversity of the black-lipped pearl oyster *Pinctada margaritifera*. Mol. Ecol.. http://dx.doi.org/10.1111/j.1365-294X.2012.05588.x.

Le Moullac, G., Soyez, C., Sham-Koua, M., Levy, P., Moriceau, J., Vonau, V., Maihota, M., Cochard, J.C., 2011. Feeding the pearl oyster *Pinctada margaritifera* during reproductive conditioning. Aquac. Res.. http://dx.doi.org/10.1111/j.1365-2109.2011.03045.x.

Le Moullac, G., Tiapari, J., Tessier, H., Martinez, E., Cochard, J.C., 2012. Growth and gonad development of the tropical blacklip pearl oyster, *Pinctada margaritifera* (L.), in the Gambier archipelago (French Polynesia). Aquac. Int. 20, 305–315.

Linard, C., Gueguen, Y., Moriceau, J., Soyez, C., Hui, B., Raoux, A., Cuif, J.P., Cochard, J.C., Le Pennec, M., Le Moullac, G., 2011. Calcein staining of calcified structures in pearl oyster *Pinctada margaritifera* and the effect of food resource level on shell growth. Aquaculture 313, 149–155.

Loret, P., Le Gall, S., Dupuy, C., Blanchot, J., Pastoureaud, A., Delesalle, B., Caisey, X., Jonquieres, G., 2000a. Heterotrophic protists as a trophic link between picocyanobacteria and the pearl oyster *Pinctada margaritifera* in the Takapoto lagoon (Tuamotu Archipelago, French Polynesia). Aquat. Microb. Ecol. 22, 215–226.

Loret, P., Pastoureaud, A., Bacher, C., Delesalle, B., 2000b. Phytoplankton composition and selective feeding of the pearl oyster *Pinctada margaritifera* in the Takapoto lagoon (Tuamotu Archipelago, French Polynesia): in situ study using optical microscopy and HPLC pigment analysis. Mar. Ecol. Prog. Ser. 199, 55–67.

McNutt, M., Menard, H.W., 1978. Lithospheric flexure and uplifted atolls. J. Geophys. Res. 83, 1206–1212.

Michotey, V., Guasco, S., Boeuf, D., Morezzi, N., Durieux, E., Charpy, L., Bonin, P., 2012. Spatio-temporal diversity of free-living and particle-attached prokaryotes in the tropical lagoon of Ahe atoll (Tuamotu Archipelago) and its surrounding oceanic waters. Mar. Pollut. Bull. 65, 525–537.

Montagnani, C., Marie, B., Marin, F., Belliard, C., Riquet, F., Tayale, A., Zanella-Cléon, I., Fleury, E., Gueguen, Y., Piquemal, D., Cochennec-Laureau, N., 2011. Pmarg-pearlin is a matrix protein involved in nacre framework formation in the pearl oyster *Pinctada margaritifera*. Chembiochem 12 (13), 2033–2043.

Niquil, N., Jackson, G.A., Legendre, L., Delesalle, B., 1998. Inverse model analysis of the planktonic food web of Takapoto atoll (French Polynesia). Mar. Ecol. Prog. Ser. 165, 17–29.

Niquil, N., Pouvreau, S., Sakka, A., Legendre, L., Addessi, L., Le Borgne, R., Charpy, L., Delesalle, B., 2001. Trophic web and carrying capacity in a pearl oyster farming lagoon (Takapoto, French Polynesia). Aquat. Living Res. 14, 165–174.

Pagano, M., Sagarra, P.-B., Champalbert, G., Bouvy, M., Dupuy, C., Thomas, Y., Charpy, L., 2012. Metazooplankton communities in the Ahe atoll lagoon (Tuamotu Archipelago, French Polynesia): Spatiotemporal variations and trophic relationships. Mar. Pollut. Bull. 65, 538–548.

Pirazzoli, P.A., Montaggioni, L.F., Salvat, B., Faure, G., 1988. Late holocene sea-level indicators from twelve atolls in the central and eastern Tuamotu (Pacific Ocean). Coral Reefs 7, 57–68.

Pouvreau, S., Jonquieres, G., Buestel, D., 1999. Filtration by the pearl oyster, *Pinctada margaritifera*, under conditions of low seston load and small particle size in a tropical lagoon habitat. Aquaculture 176, 295–314.

Pouvreau, S., Bacher, C., Heral, M., 2000a. Gametogenic cycle and reproductive effort of the tropical blacklip pearl oyster, *Pinctada margaritifera* (Bivalvia: Pteriidae), cultivated in Takapoto atoll (French Polynesia). Aquaculture 186, 117–144.

Pouvreau, S., Bacher, C., Héral, M., 2000b. Ecophysiological model of growth and reproduction of the black pearl oyster, *Pinctada margaritifera*: potential applications for pearl farming in French Polynesia. Aquaculture 186, 117–144.

Pouvreau, S., Bodoy, A., Buestel, D., 2000c. In situ suspension feeding behaviour of the pearl oyster, *Pinctada margaritifera*: combined effects of body size and weather-related seston composition. Aquaculture 181, 91–113.

Pouvreau, S., Prasil, V., 2001. Growth of the black-lip pearl oyster, *Pinctada margaritifera*, at nine culture sites of French Polynesia: synthesis of several sampling designs conducted between 1994 and 1999. Aquat. Living Res. 14, 155–163.

Salvat, B., 1967. Importance de la faune malacologique dans les atolls polynésiens. Cahier du Pacifique 11, 7–49.

Sournia, A., Ricard, M., 1975. Phytoplankton and primary productivity in Takapoto atoll, Tuamotu Islands. Micronesica 11, 159–166.

Southgate, P., Lucas, J., 2008. The Pearl Oyster. Elsevier, Oxford, 575pp.

Tartinville, B., Deleersnijder, E., Rancher, J., 1997. The water residence time in the Mururoa atoll lagoon: sensitivity analysis of a three-dimensional model. Coral Reefs 16, 193–203.

Thomas, Y., Garen, P., Courties, C., Charpy, L., 2010. Spatial and temporal variability of the pico- and nanophytoplankton and bacterioplankton in a deep Polynesian atoll lagoon. Aquat. Microb. Ecol. 59, 89–101.

Thomas, Y., Belliard, C., Garen, P., Gueguen, Y., Montagnani, C., 2011a. Development of in situ hybridisation using 16S rRNA gene to monitor black-lip pearl oyster, *Pinctada margaritifera*. larvae in plankton samples. Aquat. Living Res. 24, 27–34.

Thomas, Y., Garen, P., Pouvreau, S., 2011b. Application of a bioenergetic growth model to larvae of the pearl oyster *Pinctada margaritifera* L.. J. Sea Res. 66 (4), 331–339.

Thomas, Y., Garen, P., Bennett, A., Le Pennec, M., Clavier, J., 2012a. Multi-scale distribution and dynamics of bivalve larvae in a deep atoll lagoon (Ahe, French Polynesia). Mar. Pollut. Bull. 65, 453–462.

Thomas, Y., Le Gendre, R., Garen, P., Dumas, F., Andréfouët, S., 2012b. Bivalve larvae transport and connectivity within the Ahe atoll lagoon (Tuamotu Archipelago), with application to pearl oyster aquaculture management. Mar. Pollut. Bull. 65, 441–452.

Torréton, J.P., Pagès, J., Talbot, V., 2002. Relationships between bacterioplankton and phytoplankton biomass, production and turnover rates in Tuamotu lagoons. Aquat. Microb. Ecol. 28, 267–277.

Yukihira, H., Klumpp, D.W., Lucas, J.S., 1998. Effects of body size on suspension feeding and energy budgets of the pearl oysters *Pinctada margaritifera* and *P. maxima*. Mar. Ecol. Prog. Ser. 170, 119–130.

Yaroshewski, V., 2011. Genetic effect of pearl culture practices on the black-lipped pearl oyster (Pinctada margaritifera) in French Polynesia. PhD Dissertation, Dalhousie University, Halifax Nova Scotia.

Zanini, J.M., Salvat, B., 2000. Assessment of deep water stocks of pearl oysters at Takapoto atoll (Tuamotu Archipelago, French Polynesia). Coral Reefs 19, 83–87.

Serge Andréfouët *
Institut de Recherche Pour le Développement, UR 227 CoRéUs, BP A5, 98848 Nouméa, New Caledonia
* *Tel.: +687 26 08 00; fax: +687 26 43 26.*
E-mail address: serge.andrefouet@ird.fr (S. Andréfouët).

Loic Charpy
Institut de Recherche Pour le Développement, MIO, UR235, BP 529, 98713 Papeete, French Polynesia

Alain Lo-Yat
Direction des Ressources Marines, B.P 20, 98713 Papeete, Tahiti, French Polynesia

Cédrik Lo [1]
Direction des Ressources Marines, B.P 20, 98713 Papeete, Tahiti, French Polynesia

[1] Present address: Institut Français de Recherche Pour l'Exploitation de la Mer, Centre Océanologique du Pacifique, BP 7004, 98719 Taravao, Tahiti, French Polynesia.

Marine Pollution Bulletin 65 (2012) 415–424

Contents lists available at SciVerse ScienceDirect

Marine Pollution Bulletin

journal homepage: www.elsevier.com/locate/marpolbul

Island shadow effects and the wave climate of the Western Tuamotu Archipelago (French Polynesia) inferred from altimetry and numerical model data

Serge Andréfouët [a,*], Fabrice Ardhuin [b], Pierre Queffeulou [b], Romain Le Gendre [a,1]

[a] IRD, UR 227 CoRéUs, BP A5, 98848 Nouméa cedex, New Caledonia
[b] Ifremer, Laboratoire d'Océanographie Spatiale, B.P. 70, 29280 Plouzané, France

ARTICLE INFO

Keywords:
Wave field
Island shadow effect
Altimeter
Wave model
Aquaculture
Society Archipelago

ABSTRACT

To implement a numerical model of atoll lagoon circulation, we characterized first the significant wave height (*Hs*) regime of the Western Tuamotu Archipelago and the local attenuation due to the protection offered by large atolls in the south Tuamotu. Altimetry satellite data and a WAVEWATCH III two-way nested wave model at 5 km resolution from 2000 to 2010 were used. Correlation between altimetry and model was high (0.88) over the period. According to the wave model, the archipelago inner seas experienced attenuated *Hs* year-long with a yearly average *Hs* around 1.3 m vs a minimum of 1.6 m elsewhere. The island shadow effect is especially significant in the austral winter. In contrast with southern atolls, Western Tuamotu experienced only few days per year of *Hs* larger than 2.5 m generated by very high *Hs* southern swell, transient western local storms, strong easterly winds, and during the passage of distant hurricanes.

1. Introduction

In coral reef environments, hydrodynamics is one of the major physical forcing factor controlling, among other key processes, trophic productivity, biodiversity accumulation, dominance of certain types of community structures and their vulnerability and resilience to disturbances (Madin and Connolly, 2006; Walker et al., 2008). Hydrodynamics can have two contrasted roles regarding recovery and resilience. For instance, on the one hand, it may contribute to recovery through current-driven larval dispersal. On the other hand, it may bring destruction of habitats by large waves and reef erosion (see Hopley, 2011, for updated encyclopedia entries and reviews on the subject). Reefs and lagoons are exposed differently to hydrodynamic forcing because of the natural variability at regional to local scales of tides, winds, waves and currents. Although the general action of hydrodynamics, and in particular waves, are well known, the proper quantitative characterization of the hydrodynamic regime of a specific site has been seldom achieved. This is true within a reef system, to understand the small scale variabilities present within an atoll, a bay or along a reef system (e.g. Kench 1998; Hoeke et al. 2011), but this is also true at archipelago-scale between islands and reefs.

Local variability in dominant communities, functioning and vulnerabilities at an archipelago scale are related to the modification, within the archipelago, of the meso-scale hydrodynamical patterns. For instance, the topology of islands and the induced sheltering between islands may substantially modify the local wind and wave and energy regime, and therefore modify the type of dominant communities (Goldberg and Kendrick, 2004). To date, three approaches have been conducted to characterize differences in wave exposure within an archipelago or around a large island. A qualitative approach where coastline stretches are ranked according to a relative level of protection (“sheltered”, “exposed”, etc.) (Goldberg and Kendrick, 2004), a quantitative approach where fetch-based model and GIS compute a time-integrated exposure (Ekebom et al., 2003) and a quantitative approach based on actual wave measurements, coupled with physical or biophysical models (Storlazzi et al., 2005; Hoeke et al., 2011).

In atolls, one of the main types of coral reef complexes in the world, three hydrodynamic domains can be defined: the oceanic forereef, the rim and the lagoon. The lagoon is a bounded body of water that is closed or open to exchanges with the ocean depending on the structure of the rim (Andréfouët et al., 2001). In atolls of the Tuamotu Archipelago (French Polynesia), lagoons are the prime locations for the development of pearl oyster aquaculture, tourism and reef fisheries (Andréfouët et al., 2006). The former is a dominant economic activity for the country (Andréfouët et al., 2012). The Western Tuamotu region is a geographic area of high economic importance. Three major atolls for the pearl oyster industry are present, namely Ahe, Takaroa and Manihi (Fig. 1). Historically, a

* Corresponding author. Tel.: +687 26 08 00; fax: +687 26 43 26.
E-mail address: serge.andrefouet@ird.fr (S. Andréfouët).
[1] Present address: Ifremer, LERN, Avenue du Général de Gaulle, 14520 Port-en-Bessin, France.

0025-326X/$ - see front matter © 2012 Elsevier Ltd. All rights reserved.
http://dx.doi.org/10.1016/j.marpolbul.2012.05.042

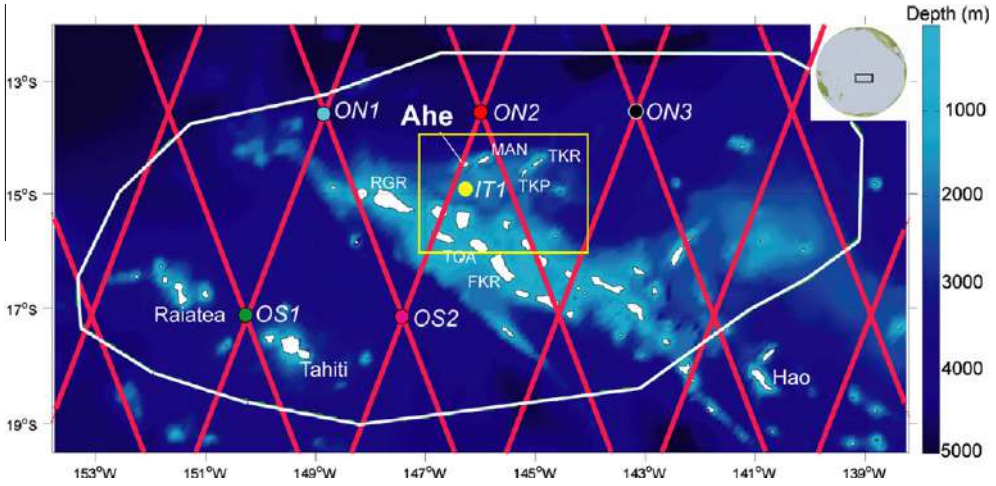

Fig. 1. Location map. In the centre of the Pacific Ocean, the Western Tuamotu (yellow box) and the focal atoll, Ahe, are shown, as well as the boundary of the WAVEWATCH III model (white line) at 0.05° resolution, the TOPEX-Jason acquisition tracks (red line), and the location of the six time-series of modeled *Hs*, five of them being in the ocean away from the atolls at the intersection of altimetry tracks (ON1, ON2, ON3, OS1, OS2) and one being a inner Tuamotu point (IT1), next to a track. Atolls and islands are in white. Atolls mentioned in the text: FKR: Fakarava, RGR: Rangiroa, TOA: Toau, MAN: Manihi, TKP: Takapoto, TKR: Takarao (For interpretation of the references to colour in this figure legend, the reader is referred to the web version of this article.).

fourth atoll of this area, Takapoto, was a major site in the eighties-nineties, but its black pearl industry collapsed and the focus shifted to the other atolls. Ahe was the target of a large interdisciplinary study between 2008 and 2010 (see collection of papers for this issue). Here, we focus the interpretation of our results on this atoll, although most of the conclusions remain valid for the other nearby atolls as well.

A wealth of empirical knowledge exists for each atoll and lagoon after more than 20 years of exploitation, but better knowledge on lagoon trophic and hydrodynamic functioning is a high priority for stakeholders in order to sustain a production of high quality pearls and understand how to optimize the collection of oyster larvae in the field (Thomas et al., 2012). Specifically, understanding the variability in spat collection is necessary. The success of this activity depends, in part, on how currents disperse larvae within the lagoon. Larvae dispersal can be studied by numerical solutions, and we followed this path to characterize the lagoonal circulation with the development of a 3D numerical model validated by field measurements (Dumas et al., 2012; Thomas et al., 2012).

Andréfouët et al. (2006) recommended first a proper characterisation of the atmospheric and oceanic forcing of the lagoon boundaries. In addition to tide, the wind and wave regimes were needed in priority. Indeed, it has been showed that wind directly influences the lagoon circulation, while ocean waves break along the rim and indirectly influence the lagoon by initiating water transport across the rim towards the lagoon (Atkinson et al., 1981; Tartinville et al., 1997; Kraines et al., 1999). Depending on the location, number and depth of spillways and passes along its rim, an atoll lagoon is efficiently renewed by a combination of tide and wave-driven flows through the rim (Kench, 1998; Tartinville et al., 2000; Andréfouët et al., 2001; Callaghan et al., 2006; Dumas et al., 2012).

During the first weeks of *in situ* work in Ahe in 2008, it appeared that the responses of flows through rim spillways to high swell events forecasted by Météo France meteorological services were unusually low, compared to our previous experiences in the Tuamotu (Andréfouët et al., 2001). In Andréfouët et al. (2001), we interpreted such peculiar low response to high swells by a specific rim geomorphology found in specific atolls (e.g. uplifted rims). This hypothesis cannot be ruled out, but these specific atolls were also protected by other atolls which effectively block the wave energy (e.g. Pawka et al., 1984). We hypothesized that the regional island shadowing effects due to the presence of other atolls could be responsible for the specific low responses of Ahe atoll to swell. The problem of the representation of atolls and islands in numerical models subgrids highlighted this shadow effect due to the atolls relative position, but the induced variation in swell amplitude within the archipelago remained undescribed (Chawla and Tolman, 2008; Delpey et al., 2010). Reasons for this poor knowledge are the absence of permanent *in situ* wave measurements, with only semi-quantitative wave information provided by atmospheric infrasound and seismic noise (Barruol et al., 2006). Therefore, an objective of the present study was also to quantify for the first time the significant wave height (*Hs*) attenuation around Ahe atoll due to the regional spatial distribution of atolls and islands. For this objective, we turned to quantitative satellite-based and modeling approaches.

In this study, we first provide a comparison of model *vs* altimetry data for the region of interest, at different spatial and temporal resolutions. As explained below, because altimetry data are relatively poor in spatial coverage and revisiting time, the model-altimetry data comparison is useful afterwards to justify the characterization of the wave regime using the model data only. Finally, using 11 years of modeled *Hs*, we identified the high wave events around Ahe atoll. The identification of these events using altimetry data alone would not have been possible given the short time these events may last, and, in some cases, their small spatial domain of influence.

2. Material and methods

2.1. Study site

The Western Tuamotu Archipelago is defined here by a box bounded by 14°–16° South- 144°–147° West, centered between the group of the main pearl oyster aquaculture atolls (Ahe, Manihi, Takapoto, Takaroa) and the barrier of the large south atolls (such as Rangiroa, Toau, Fakarava) (Fig. 1).

Local *Hs* measured in one location result from the propagation of wave fields across a larger region. The regional domain considered here is defined by a polygon including the Central Tuamotu, the entire Society Archipelago in the southwest corner, and about

2° of open Pacific Ocean north and south of the Tuamotu (Fig. 1). This configuration allows studying swell generated by distant storms when they reach the Western Tuamotu, as well as local wind-generated waves.

2.2. Characterisation of significant wave height and altimetry-model comparison

Here we investigate the spatial patterns of the wave field using a combination of satellite altimetry observation and numerical models. Satellite altimeter data has been shown to give very robust and accurate estimates of *Hs* (Queffeulou, 2004; Zieger et al., 2009; Queffeulou and Croizé-Fillon, 2010; Abdalla et al., 2011). The model is completely independent of the satellite data which is not assimilated. The model provides a daily full spatial and temporal coverage. This is an interesting complement to the satellite spatial and temporal coverage which is limited to narrow tracks (e.g. Fig. 1), revisited every few days at best (10 days for the TOPEX-Jason missions). The model also provides estimates of all sea state variables, and not just the *Hs* which is estimated by the altimeter. Thus, we also looked at the attenuation of waves for different dominant wave directions. For this we used the mean wave direction with a careful analysis of swell partition information. Indeed a mean direction in the presence of several wave systems can be completely meaningless.

The wave model is an implementation of a two-way nested WAVEWATCH III® modeling framework (Tolman, 2008, 2009, hereafter WW3). The two domains of interest are a 0.5° global grid in which a 0.05° resolution is nested. The extent of the inner domain is the white polygon shown in Fig. 1. It should be noted that the subgrid island blocking scheme of Tolman (2003, 2007) is used in both grids. These two domains are part of a set of grids used for forecasting and hindcasting (Magne et al., 2010). The wave model is forced by European Center for Medium-Range Weather Forecasts (ECMWF) operational analyses for the years 2006–2011 and by the Climate Forecast System Reanalysis (CFSR) (Saha et al., 2010) for the years 1988–2005. The sea ice mask is taken from CFSR or ECMWF, and for the years 2002–2009 it is complemented by a mask for small icebergs (Ardhuin et al., 2011a). Due to relative biases between these two wind fields, the model was re-tuned for CFSR winds by lowering the wind-wave growth term BETAMAX from 1.52 to 1.33. This provided a similar small bias in the two simulations and, in the model driven by CFSR winds, practically removed the important negative bias (−10% or so) for very large waves (*Hs* > 9 m) that was present in the model driven by ECMWF winds.

The two model domains use the wave generation and dissipation parameterizations proposed by Ardhuin et al. (2010). These parameterizations were specifically designed to match the swell dissipation that was measured over long distances with synthetic aperture radar data (Ardhuin et al. (2009a), Ardhuin et al. (2009b), Collard et al., 2009; Delpey et al., 2010). Finally, the model also includes coastal reflections for both resolved and subgrid shorelines, with a constant reflection coefficient of 5% and 10%, respectively, following a procedure described by Ardhuin et al. (2011b). WW3 output is given every 3 h. The hindcasted period runs from 2000 to 2010, for a total of 11 years. The full hindcast database is available at http://www.tinyurl.com/iowagaftp.

To complement previous global scale validations (Ardhuin et al., 2010), we re-examined altimeter observations in order to validate the WW3 model outputs in the western Tuamotu region. The altimeter significant wave height data are from the Ifremer altimeter *Hs* database (Queffeulou and Croizé-Fillon, 2010), which is updated regularly and calibrated using methods developed in Queffeulou (2004). Altimeter-derived *Hs* are provided along acquisition tracks with repeating visiting time that are different between missions and satellites (ERS-2, ENVISAT, TOPEX, Poseidon, Jason-1, Geosat Follow-On, Jason-2). A first comparison between WW3 and altimetry can be made for all concurrent data across the domain, during the entire period considered.

Then, to study *Hs* time-series around Ahe atoll for specific locations, and to maximize the number of collocations between altimetry and model during the 2000–2010 period, we used TOPEX and Jason acquisition tracks to identify five locations where altimetry and model could be optimally compared across time in our focal region (Fig. 1). These five locations correspond to the five open ocean track intersections which were the closest to Ahe atoll. The five points (ON1, ON2, ON3, OS1, OS2) were located at −13.5S, −148.75W; −13.5S, −146W; −13.5S, −143.25W; −17.25S, −150.25W; −17.25S, −147.50W, respectively. The revisiting time-period of TOPEX and Jason sensors provide one measurement every 10 days, yielding two measurements on a track intersection every 10 days. The 2002–2010 Jason-1 data set was expended with Geosat Follow-On (GFO) 2000–2008 data and with ENVISAT 2002–2010 data acquired near these points.

For all altimetry *vs* WW3 comparison, for any given day, the modeled *Hs* the closest in time with the altimetry *Hs* were used to compute monthly bias and standard deviations, thus the time difference was always lower than 1 h and 30 min.

2.3. Climatology of the Western Tuamotu wave regime

Since we aim to provide a first-order description of the swell regime in the Western Tuamotu based primarily on *Hs*, we did not use all the different wave variables provided by WW3. WW3 provides both wind wave and swell data and their different spectral decomposition, offering the possibility to discriminate different processes. Also full directional-frequency wave spectra have been stored at a few locations. In practice this information was not systematically used here since the total *Hs* and directions could often be readily interpreted in terms of trade-winds, events, and long-distance swell influence because of their preferential directions.

Monthly mean of WW3 *Hs* were computed to achieve a picture of the average situation, but to avoid a temporal smoothing effect of the spatial patterns, the 11 years of WW3 outputs for the regional domain were examined day by day to identify recurrent patterns of wave amplitude and directions, as well as events. Similar inspection of long term oceanographic spatial data were made by Soto et al. (2009) to detect short term dispersal of river plumes and transient river-coral reef connectivity using ocean color data from the SeaWiFS sensor. These wave events were short time periods of high *Hs* from any direction. Conversely, time periods of very low *Hs* were also interesting, since absence of waves have led to poor renewal of water in some atolls without passes, quick disequilibrium of the hydrological conditions, and dystrophic events (Adjeroud et al., 2001).

Altimetry data covers a longer time period than the WW3 period analyzed here. A monthly and 3-month mean, along-track, climatology of 1992–2010 *Hs* from the TOPEX and Jason missions was compiled. This *Hs* climate was obtained with TOPEX, Jason 1 and Jason 2 data covering respectively the period from 25/09/1992 to 11/08/2002; from 11/08/2002 to 26/01/2009; and from 26/01/2009 to 31/12/2010.

2.4. Quantification of the island shadow effect

Modelled *Hs* at the five locations ON1, ON2, ON3, OS1, OS2 were compared to modeled *Hs* at a sixth location (named IT1) in the south of Ahe atoll, in the centre of the Western Tuamotu box (Fig. 1). This inner Tuamotu location was used to measure *Hs* attenuation compared to open ocean *Hs* around the Western Tuamotu and in the region. In addition, the altimetry 1992–2010

climatology provided a mean to check with observations the long term influence of island on the Western Tuamotu wave regime.

3. Results and discussion

3.1. General patterns from altimetry and model-altimetry comparisons

The altimetry climatology (Fig. 2) shows that the Western Tuamotu, and especially the vicinity and the south of Ahe atoll, are areas of lower *Hs* compared to other regional values, all year-long. In December–February, northern swell modulates slightly this trend with *Hs* reaching 1.8 m next to Ahe, but from March to November, *Hs* remained below 1.6 m. Immediately south of the larger Tuamotu atolls, *Hs* was for the same period well above 1.8 m, thus a systematic decrease of at least 0.2 m between ocean and inner Tuamotu seas. Regionally, the north of the Tuamotu by 12°S and 142–146°W displayed between March and November a lower *Hs* compared to west of 150°W, where *Hs* was systematically above 2 m. The climatology thus suggests a significant island effect with lower *Hs* down-wave and down-wind from the atolls, especially with southern swell.

During the studied period, considering the entire data set (714,091 points, considering each available day and each altimetry sensor), the comparison of WW3 *vs* altimetry yielded a regression of $Hs_{WW3} = 0.834 \cdot Hs_{alt} + 0.152$, with a 0.88 correlation coefficient (Fig. 3). To test if the discrepancy could be explained by the time difference between the two *Hs* estimates, we kept only the data concurrent by <30 min. The overall correlation remained the same ($Hs_{WW3} = 0.838 \cdot Hs_{alt} + 0.144$, $n = 175{,}410$), but the correlation for large *Hs* (>4 m) was enhanced (not shown).

When looking at collocated time-series, *Hs* measured by the various altimetry missions and *Hs* from WW3 were in good agreement (Fig. 4), with a 5–15% underestimation by WW3. For the entire period, monthly standard deviations between the two data sets ranged between 0.2 and 0.3 m, except for few months. A significant increase in monthly bias occurred with ENVISAT in

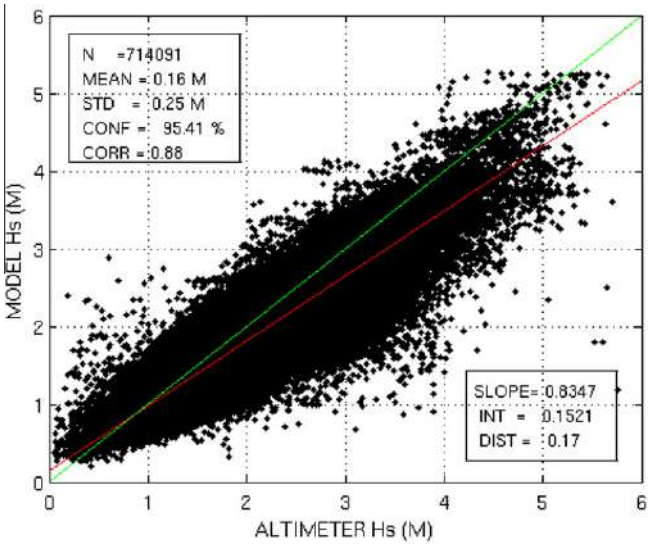

Fig. 3. Scatter-plot of collocated significant wave height (*Hs*) from altimetry and from the WAVEWATCH III model. Data were ±1 h 30 apart, corresponding to a spatial difference of 5–7 km at most. Data number (N), mean value (MEAN) and standard deviation (STD) of differences altimeter minus model *Hs*. Confidence level (CONF) and correlation (COR). Slope and intercept (INT) of the inertial regression line, average distance to the line (DIST). Red: inertial regression line. Green: $y = x$ line (For interpretation of the references to colour in this figure legend, the reader is referred to the web version of this article.).

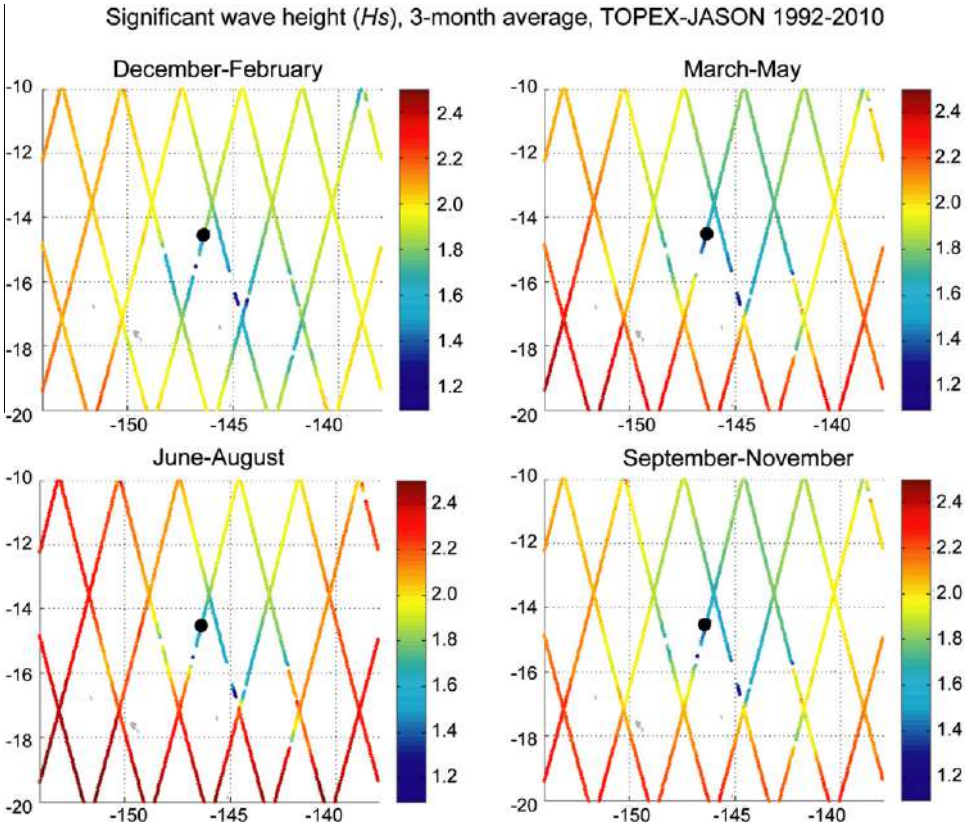

Fig. 2. Altimetry-derived 3-monthly mean *Hs* (in meters) plots for the period 1992–2010. The lowest *Hs* are observed in the south of Ahe atoll (black dot), in the north of the barrier made by the large atolls.

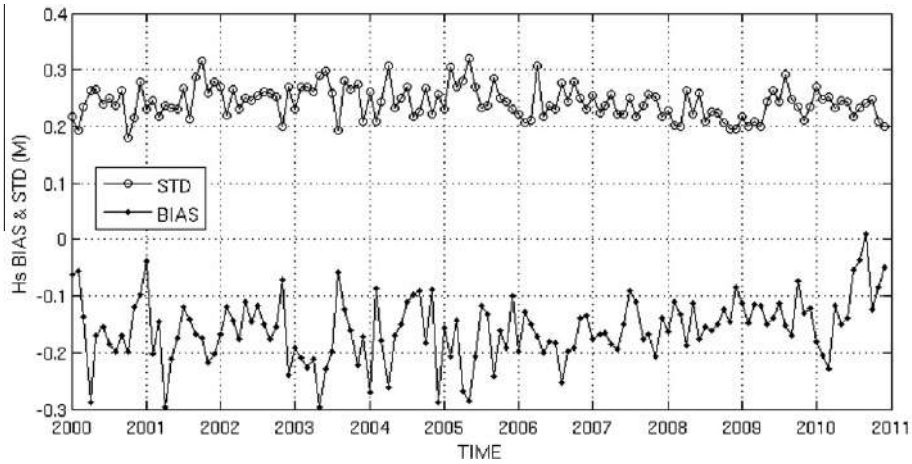

Fig. 4. Over the entire WAVEWATCH III high resolution spatial domain (Fig. 1), time-series of monthly bias and standard-deviation measured between the WAVEWATCH III significant wave height *Hs* and altimetric *Hs* estimated between 2000 and 2010 by Jason 1 (2002–2010), GFO (2000–2008) and ENVISAT (2002–2009).

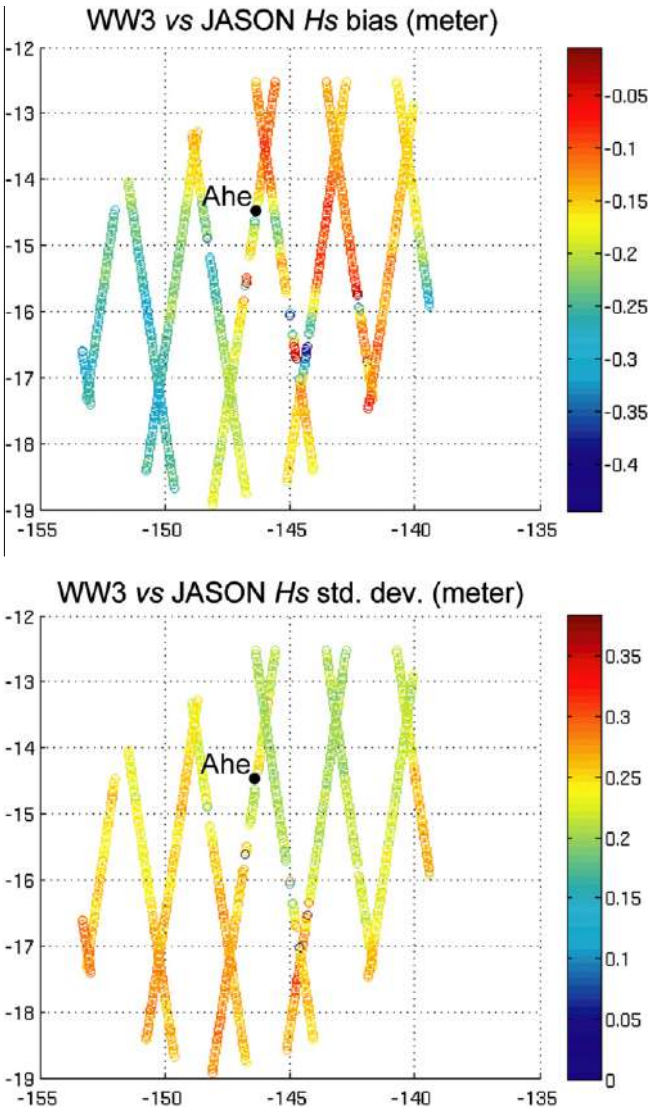

Fig. 5. Over the entire period of observations, spatial variations in the domain of interest (Fig. 1), along Jason altimetry tracks, of standard deviation and bias between WAVEWATCH III and altimetry-derived significant wave height (*Hs*, in meters) (For interpretation of the references to colour in this figure legend, the reader is referred to the web version of this article.).

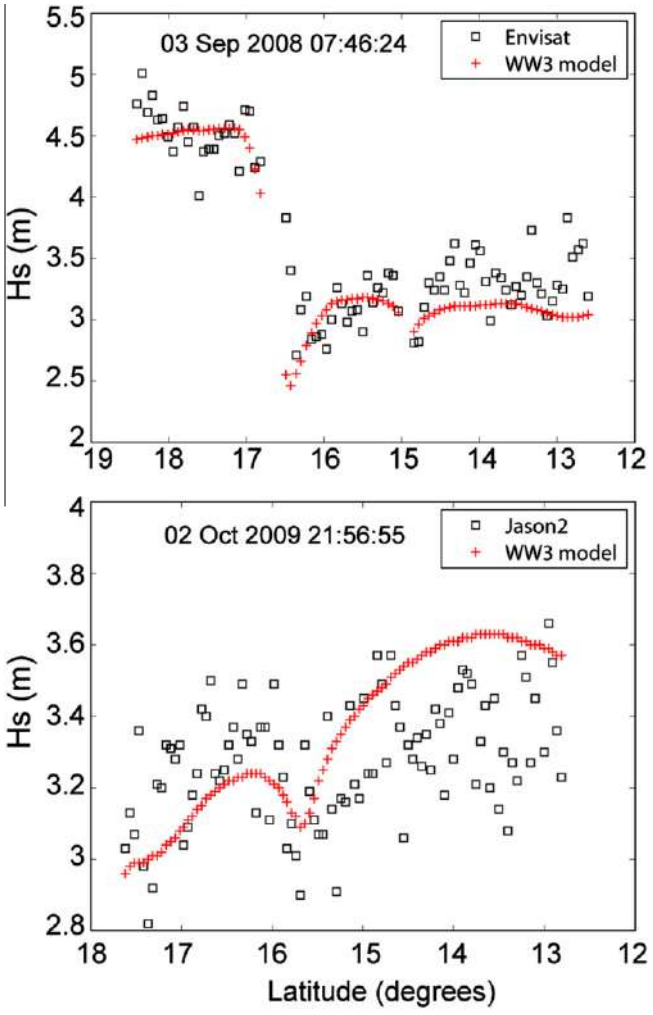

Fig. 6. For two selected days of high *Hs* in the regional domain (see also Fig. 10), along-track altimetry *vs* WAVEWATCH III comparison of significant wave eight (*Hs*). Date and starting time of acquisition are shown. Time period of altimeter acquisition is about 3 min for each plot.

2010, and this year was discarded (data not shown). The reason was a change in ENVISAT processing starting in February 2010 (Queffeulou, 2011).

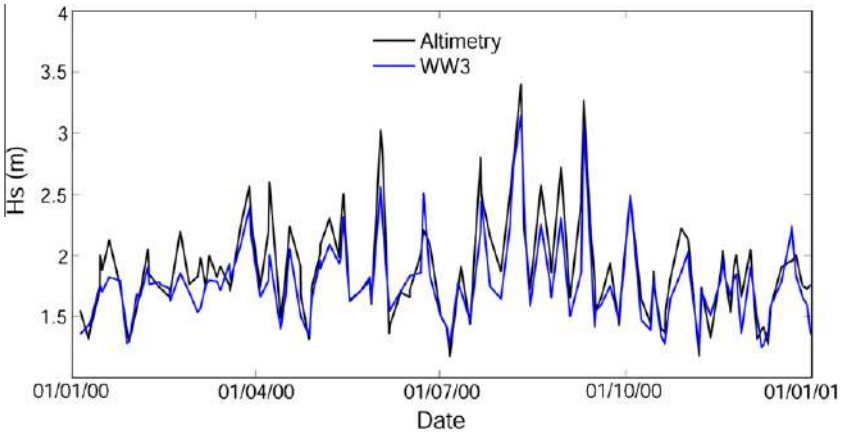

Fig. 7. Time-series of significant wave height (*Hs*) from WAVEWATCH III (WW3) and from altimetry for the year 2000, for one of the 6 focal points (ON1 here) shown Fig. 1. For each altimetry measurement, the most concurrent WW3 output is conserved.

The bias between altimetry and model varied spatially. When looking at the differences between WAVEWATCH III and the January 2002–January 2009 Jason data, overall, the pattern is a northeast to southwest increasing gradient (Fig. 5). Within this gradient, a patch of local higher discrepancy is evident in the south of Ahe (in green Fig. 5a), although the discrepancy is only about 5 cm higher than nearby values and is not as high as in the ocean domain of the southwest corner of the domain. These observed local discrepencies could reflect some difficulty in modeling accurately the shelter effect of small islands. The bias suggests a general underestimation of *Hs* by the model, compared to altimetry.

Looking at modeled *vs* altimetry data along an altimeter track for a particular day clarifies the dispersal of observations over a short time interval. As an example, for two specific days of high *Hs* in the domain, Fig. 6 shows the dispersal of the model *vs* altimetry data along one acquisition track, during a period of altimeter data acquisition lasting <3 min. The overall trends are in agreement, but with both underestimation and overestimation of *Hs*, around ±0.2–0.5 m for any specific moment in time.

Specifically for the 5 selected locations (ON1, ON2, ON3, OS1, OS2), the agreement between WW3 and altimetry was similar to that of the entire domain, with some interannual variations. An example of time-series for the year 2000 for ON1 is shown in Fig. 7. For the data in Fig. 7, the linear regression relationship was $Hs_{WW3} = 0.764 \cdot Hs_{alt} + 0.340$, $n = 132$.

In conclusion, for all the different time and spatial scales for which we compared WW3 and altimetry (Figs. 3–7), we found a good agreement, and more importantly a clarification of the range of uncertainties we needed to account for before concluding on *Hs* variations in the domain of interest. With this information in hand, WW3 high resolution results could be used with confidence to characterize the wave climate and assess the island shadow effects on *Hs*.

3.2. Island effects, wave regime and events

Besides the altimetry climatology observations that suggest an island effect in the Western Tuamotu (Fig. 2), time series of high resolution 0.05° WW3 *Hs* data at the 6 locations of interest confirmed that location IT1, in the south of Ahe and protected by other atolls, has a consistent significantly lower *Hs* year round, for all years, than all the other locations (Fig. 8). The yearly average at IT1 is systematically 0.3–0.35 m lower than at ON2, and 0.5–0.6 m lower than at OS2 (Fig. 8). Among the 5 other locations, considering the yearly average (Fig. 8), there is clear ranking that reveals the cumulated level of protection of each location. ON1, despite its northern location, is directly protected only in the case of south eastern wave. For south and south-western swells, ON1 is far less protected by Society Islands than ON2 and ON3 by the Tuamotu.

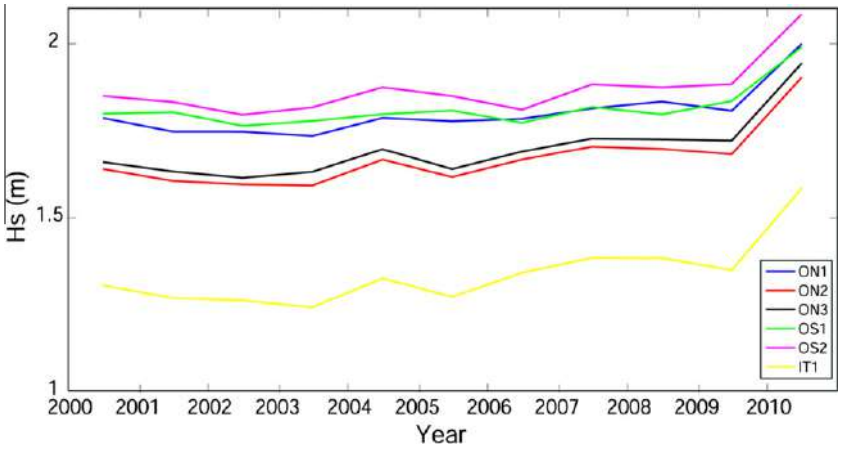

Fig. 8. Yearly average of WAVEWATCH III significant wave height (*Hs*) for the 6 locations (Fig. 1). IT1, the most protected location, is well separated from the 5 other oceanic ones. A group made of OS1, OS2 and ON1 have higher average *Hs* than the group made of ON2 and ON3. The ranking is consistent with the level of protection offered by the Tuamotu and Society Island since ON1 is not in the lee of the Tuamotu for southwest and south swells.

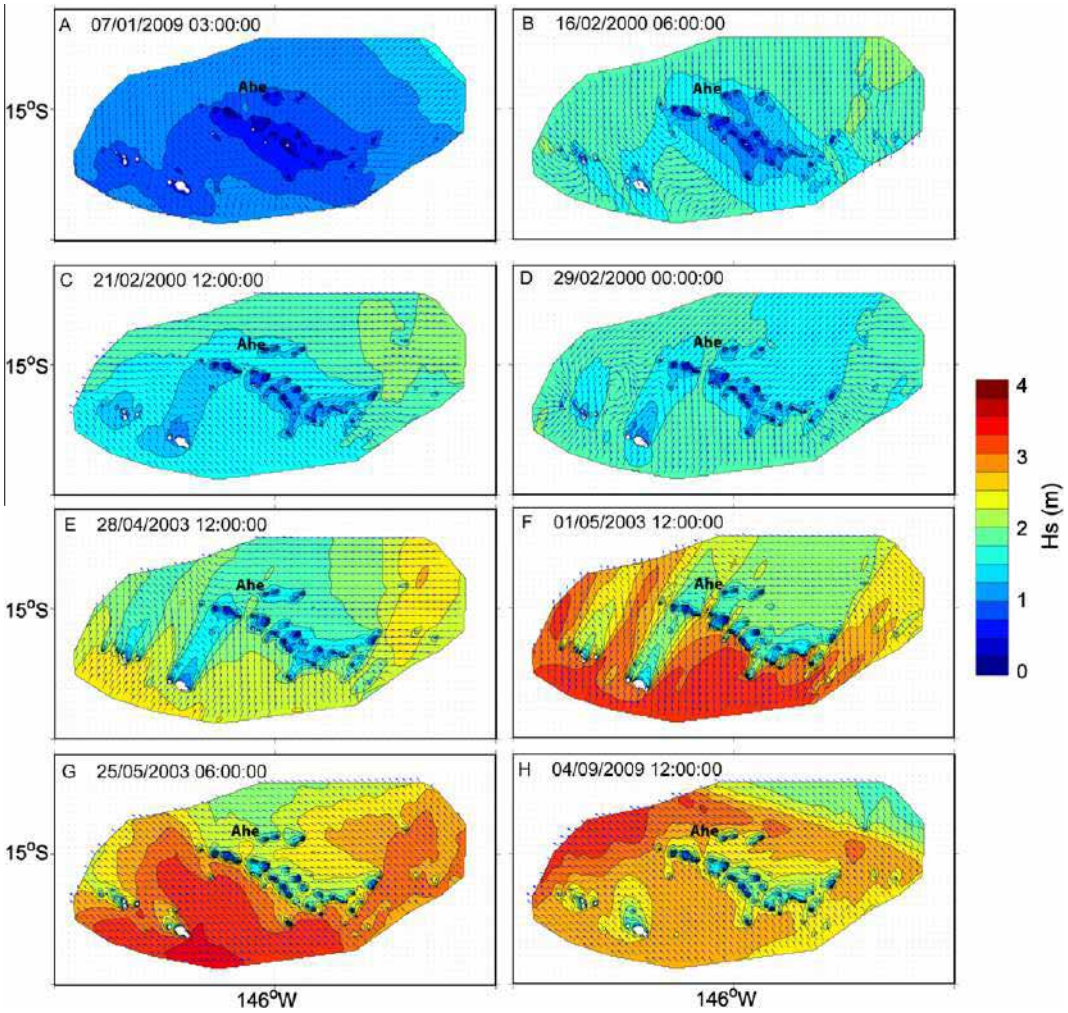

Fig. 9. Typical configurations of WAVEWATCH III significant wave height *Hs* in the region and in the Western Tuamotu. Selected days and hours are shown to highlight the intricate spatial patterns occurring in the archipelago, without smoothing when averaging over a long period.

Ahe atoll and the Western Tuamotu are not always protected from waves. Examination of the high resolution *Hs* and directions allowed identifying the typical configurations occurring year long, for the processed decade, for which Ahe is impacted by waves or protected by nearby atolls (Fig. 9).

In the Austral summer (November–March), the wave regime is dominated by an overall low *Hs*. In the north, south and west of the Tuamotu, wave directions may vary respectively north to east, southeast to southwest, and southeast to northeast (going clockwise). Fig. 9a–d illustrates a range of these configurations, which result from the relative contributions of moderate swell from distant north latitudes and local wind wave. The Tuamotu Archipelago acts as a barrier to northern swell (Fig. 9a), and Ahe is not protected in that case. Wave direction was the most erratic north of the Society archipelago (location OS1, data no show).

Starting in the austral winter, in April and till October, the combination of stronger tradewinds (northeast–southeast, clockwise) and stronger southern swells results in a more complex wave conditions (Fig. 9e–h). It also stabilizes the mean wave direction north and west of the Society Archipelago. Northern swell (as in Fig. 9b) disappears. Periods of low *Hs* and calm occur between periods of moderate to high swells (Fig. 9e–h). This is the period where the spatial patterns generated by island shadow effects are the most variables. In particular, the Fig. 9e–h presents several configurations of island shadowing effects with wave trains coming from the southwest, south and southeast directions. Wave from the southeast are effectively blocked by the barrier of southern atolls (Fig. 9g), given the incidence angle between the direction of atolls and the direction of the waves. Otherwise, south and southwest wave trains can propagate within the archipelago on narrow corridors (Fig. 9f). Under these conditions, the wavescape is the patchiest, with substantial variations of *Hs* over short distances. Note also the quasi-steady dominant wave direction (east), north of the Tuamotu, under the tradewind influence. In the panels Fig. 9e–f, this east direction is perpendicular to the dominant direction south of Tuamotu. Note also the significant shadowing effect induced by Tahiti and Moorea islands in southwest conditions (Fig. 9e and f). The last panel Fig. 9h shows a configuration occurring in austral winter after a period of high wind from the southeast, which builds high *Hs* in the western part of the domain due to a long regional fetch.

It should be pointed out that *Hs* remained consistently below 2.5 m in these typical situations, even when waves reach the atoll (south–southwest directions). We investigated with WW3 how the regional domain and the western Tuamotu experienced high waves during short term (1–8 days) events. Events bringing high amplitude waves in the region (arbitrarily set at $Hs > 3.75$ m) could be categorized in 4 groups.

- Type 1 event: the southern swells generated by distant storms in high south latitudes can bring high northward *Hs*. These events occurred every year, between April and November

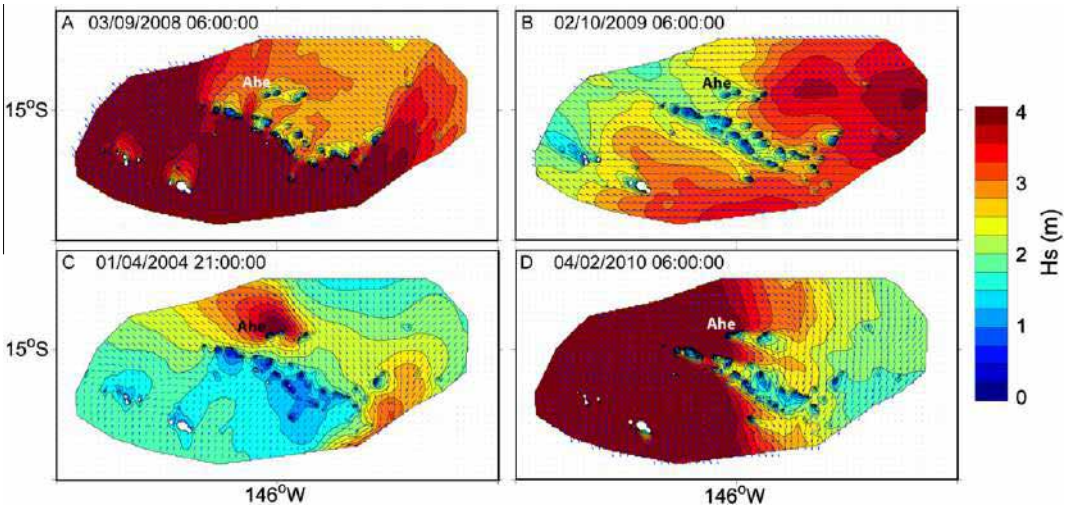

Fig. 10. Examples of remarkable events bringing significant wave height *Hs* above 3.75 m in the region, from the high resolution WAVEWATCH III model. Dates and hour are GMT time. Panels A–D represent respectively the event types 1–4 described in the text.

without clear repetitivity. They bring a region-wide increased *Hs*, up to 4.8 m in the south of the WW3 zoom area (Fig. 1) during 2–4 days. The most dramatic episode in the processed period occurred early September 2008 (Fig. 10a). Ahe appeared well protected during these events from the southern swell, but a cumulated effect of the residual southern swell and local wind waves brought *Hs* to 3.22 m (the yearly maximum, see Table 1), compared to 4.8 m next to Tahiti Island (at OS2). A tongue of northward wave crosses the Tuamotu, but Ahe itself is mostly impacted by wave generated by local eastern winds during these periods (Fig. 10a). Note also the significant shadowing effect induced by Tahiti-Moorea islands. Personal observations in Ahe in September 2008 confirm that no dramatic swells hit the atoll at this moment. Spillways reacted only moderately and the lagoon level did not reach an unusual value, continuing to oscillate according to tide variations (Dumas et al., 2012).

- Type 2 event: high waves with *Hs* > 3.75 m can be generated in the East of the regional domain by high easterlies wind, especially in June–September. Ahe is protected in this configuration by the two eastward atolls Takapoto and Takaroa. This type of event happened twice in 2009, corresponding to the strongest episodes recorded in the decade (Fig. 10b, Table 1).
- Type 3 event: Ahe atoll can be subjected to very localized waves generated by western transient storms (Fig. 10c). These are localized storms that cross in one or 2 days the regional domain. *Hs* reached up to 4 m on the northwestern side of Ahe during these events. These events did not occur every year, but Tuamotu experienced in 2004 and 2005 several of them (Table 1).
- Type 4 event: distant hurricanes generate high waves in the domain. The only example in our 11-year our time series was from hurricane Oli in early February 2010 (Fig. 10d). The hurricane passed in the southwest of the domain and seriously impacted the Australes Island in the south of French Polynesia. *Hs* reached 3.85 m around Ahe during this event, which is the highest *Hs* provided by the WW3 model in 11 years (Table 1).

The Figs. 9 and 10 are extracted from animations that show WW3 outputs across the 11 years of data. These animations are available on request to the authors.

No high *Hs* waves in our 11-year time series came from the North, from distant storms. Overall, Ahe atoll was subjected to *Hs* > 2.5 m only a few days per year (Fig. 7 and Table 1). In 2001, this threshold was reached for one day only (Table 1). Nevertheless, Ahe remains exposed to high waves generated by hurricanes and by western localized storms, although the later passed extremely quickly. It would be possible to further characterize more

Table 1
Summary of high WAVEWATCH III *Hs* for each year at location IT1 in the south of Ahe atoll (see Fig. 1). For instance, in 2010 during 26 days *Hs* was above 2.5 m. These 26 days consist in 5 periods of consecutive days throughout the year, one of them corresponding to an event of type 4, with the passage of hurricane Oli (lasting 8 days) that brought *Hs* up to 3.85 m that year. A day is included if *Hs* > 2.5 m for at least 3 h. An event is characterized by *Hs* > 3.75 m in the region (there are 4 different types of events, see text). An event occurring in the region may, or not, be related to the occurrence of the maximum *Hs* in IT 1. In 2007, 2006, 2002 and 2001, no concurrent events occurred in the region at the time of the maximum *Hs* but they were related to eastern waves, generated by local winds, so a process similar to the events of type 2.

Year	*Hs* max (m)	Date of *Hs* max	Related corresponding event	Total number of days with *Hs* > 2.5 m	Number of clusters of consecutive days with *Hs* > 2.5 m
2000	3.08	10-September	Type 1	4	2
2001	2.53	06-August		1	1
2002	2.59	01-October		2	1
2003	2.90	08-July	Type 2	7	3
2004	2.86	02-April	Type 3	3	2
2005	3.10	24-February	Type 3	4	2
2006	2.72	12-June		8	4
2007	2.78	30-August		8	2
2008	3.22	03-September	Type 1	8	3
2009	3.27	20-February	Type 2	17	6
2010	3.85	04-February	Type 4	26	5

finely these wave trains according to their periods, and quantify the level of vulnerability of Ahe for each different type of events. This will be part of a subsequent study.

3.3. WAVEWATCH III high resolution model and the characterization of coral reef exposure

To the best of our knowledge, this study is the first to use a 5 km high spatial resolution wave model to investigate the wave climate within a coral reef archipelago. The high temporal and spatial resolution allowed identifying trends and events, at a daily time-scale, and the spatial variability associated with the local topology of reef and islands. In comparison, to achieve at least one measurement per day, using only altimetry data would lead to enlarge substantially (up to 500 km) the spatial domain of integration around the focal study area (Tartinville and Rancher, 2000; Andréfouët et al., 2001).

Here, we only reported *Hs* results, and we used the decomposition between wind waves and swells provided by WAVEWATCH III to infer the source of the wave (local or distant) (not shown). This study is a first step of the analysis of the wave climate of a coral reef region before using more detailed outputs on all the available frequencies.

It could be possible to use other wave data sets spanning longer periods, such as the ERA-40 and ERA-Interim models. ERA Interim is the latest ECMWF global atmospheric reanalysis of meteorological observations from 1989 to the present, which displays major improvements over ERA-40 (1958–2001) (Dee and Uppala, 2009). However, their coarser resolution compared to the WAVEWATCH III model used here, and our direct use of altimetry data for a period long enough limit the interest of these models for our purposes. These data sets could be interesting to detect modifications of the wave regime due to climate change, but this is out of the scope of the present study.

The analysis performed here should be repeated elsewhere in other archipelagoes, possibly at higher spatial resolution thanks to availability of unstructured grids in most wave models (e.g. Benoit et al., 1996; Ardhuin et al., 2009a,b). Indeed, exposure to waves and wind is often a hydrodynamic parameter explaining the different type of communities existing on a section of reefs and the processes involved (see Edmunds et al., 2010 for a French Polynesia example, in Moorea Island). This exposure is seldom, if ever, quantified directly from observations or numerical wave models. Instead, other indirect GIS approaches based on wind climatology and fetch model have been used (e.g., Ekebom et al., 2003; Harborne et al., 2006; Burrows et al., 2008). The reason is that these methods, with little technical expertise, allowed answering the question of the influence of a time-integrated exposure on biological communities. But the development of online data servers providing high quality, high resolution wave model data similar to what we used here offers new perspectives for coastal ecologists (Hoeke et al., 2011).

3.4. Implications for Ahe atoll hydrodynamic functioning and modeling

In a companion study aimed at modeling the hydrodynamics of Ahe atoll lagoon (Dumas et al., 2012), *in situ* measurements of flows through the atoll rim in shallow spillways highlighted weak currents year round. Velocities and flows were responding to waves and tides fluctuations, but remained low compared to measurements made on other atolls (Andréfouët et al., 2001). This is a direct consequence of *Hs* attenuation around Ahe atoll, especially for southern swells. As a consequence, and considering the small number of functional spillways, flows generated by wave radiation stress were not a significant driver of the Ahe lagoon circulation, in contrast with other atolls like Majuro in Marshall Islands (Kraines et al., 1999). Thus, Dumas et al. (2012) parameterized the Ahe lagoon model with a standard, low, average flow at its boundaries, which allowed reproducing well a variety of physical and biological *in situ* measurements (Dumas et al., 2012; Thomas et al., 2012). This situation is likely specific, and besides the Takaroa, Manihi and Takapoto atolls located near Ahe, other less protected Tuamotu atolls would certainly need to use a realistic *Hs vs* velocity parameterization, especially for atolls with wide open reef flats such as Arutua, another important pearl oyster aquaculture site in the southern exposed part of the Tuamotu, which is directly facing the southern swells. Generalization from one atoll to another is certainly possible, but after quantification of the relative exposure of the different rim sections to swell energy.

4. Conclusion

This study (1) described the use of modeling tools to characterize the wave climate at high resolution in an archipelago environment, complementing previous use of scarce altimetry data and GIS fetch-model approaches; (2) it described the wave climate of one archipelago and highlights the temporal and spatial variations occurring at short distance due to the shadowing effects of islands relative to each others. Specifically, it shows that Ahe atoll, the focal atoll of a large interdisciplinary study, is subjected to an attenuated wave regime due to its northward sheltered position and is forced by an atypical wave regime compared to most other Tuamotu Archipelago atolls; (3) it justified the relaxed boundary rim-parametrization that has been implemented to model the atoll lagoon circulation (Dumas et al., 2012).

The combined use of high resolution wave model and altimetry data offers new perspectives to characterize the hydrodynamic forcing of numerous ecological, biological and geochemical processes in reef and lagoon environments. We predict that this study will pave the way for similar characterization elsewhere. In addition, this study has focused on the significant wave height regime only. Other aspects should be investigated in the future, including the energy of the wave trains according to their spectral decomposition.

Acknowledgements

This study was funded by the 9th European Development Fund (Grant POF/001/002N1 to S.A. and Loic Charpy, IRD) through the French Polynesia Service de la Perliculture. F.A. is supported by ERC Grant #240009 "IOWAGA" and US National Ocean Partnership Program, under Grant N00014-10-10383.

References

Abdalla, S., Janssen, P.A.E.M., Bidlot, J.R., 2011. Altimeter near real time wind and wave products: random error estimation. Marine Geodesy 34, 393–406.

Adjeroud, M., Andréfouët, S., Payri, C., 2001. Mass mortality of macrobenthic communities in the lagoon of Hikueru atoll (French Polynesia). Coral Reefs 19, 287–291.

Andréfouët, S., Pagès, J., Tartinville, B., 2001. Water renewal time for classification of atoll lagoons in the Tuamotu Archipelago (French Polynesia). Coral Reefs 20, 399–408.

Andréfouët, S., Ouillon, S., Brinkman, R., Falter, J., Douillet, P., Wolk, F., Smith, R., Garen, P., Martinez, E., Laurent, V., Lo, C., Remoissenet, G., Scourzic, B., Gilbert, A., Deleersnijder, E., Steinberg, C., Choukroun, S., Buestel, D., 2006. Review of solutions for 3D hydrodynamic modeling applied to aquaculture in South Pacific atoll lagoons. Marine Pollution Bulletin 52, 1138–1155.

Andréfouët, S., Charpy, L., Lo-Yat, A., Lo, C., 2012. Recent research for pearl oyster aquaculture management in French Polynesia. Marine Pollution Bulletin. 65, 407–414.

Ardhuin, F., Chapron, B., Collard, F., 2009a. Observation of swell dissipation across oceans. Geophysical Research Letters 36, L06607.

Ardhuin, F., Marié, L., Rascle, N., Forget, P., Roland, A., 2009b. Observation and estimation of Lagrangian, Stokes and Eulerian currents induced by wind and waves at the sea surface. Journal of Physical Oceanography 39, 2820–2838.

Ardhuin, F., Rogers, E., Babanin, A., Filipot, J.-F., Magne, R., Roland, A., van der Westhuysen, A., Queffeulou, P., Lefevre, J.-M., Aouf, L., Collard, F., 2010. Semi-empirical dissipation source functions for wind-wave models. Part I. Definition, calibration and validation. Journal of Physical Oceanography 40, 1917–1941.

Ardhuin, F., Tournadre, J., Queffeulou, P., Girard-Ardhuin, F., Collard, F., 2011a. Observation and parameterization of small icebergs: drifting breakwaters in the southern ocean. Ocean Modelling 39, 405–410.

Ardhuin, F., Stutzmann, E., Schimmel, M., Mangeney, D.A., 2011b. Ocean wave sources of seismic noise. Journal of Geophysical Research 116 (C9), C09004. http://dx.doi.org/10.1029/2011JC006952.

Atkinson, M., Smith, S.V., Stroup, E.D., 1981. Circulation in Enewetak atoll lagoon. Limnology Oceanography 26, 1074–1083.

Barruol, G., Reymond, D., Fontaine, F.R., Hyvernaud, O., Maurer, V., Maamaatuaiahutapu, K., 2006. Characterizing swells in the southern Pacific from seismic and infrasonic noise analyses. Geophysical Journal International 164, 516–542.

Benoit, M., Marcos, F., Becq, F. 1996. Development of a third generation shallow-water wave model with unstructured spatial meshing. In Proceedings of the 25th International Conference on Coastal Engineering, Orlando, ASCE, 465–478.

Burrows, M.T., Harvey, R., Robb, L., 2008. Wave exposure indices from digital coastlines and the prediction of rocky shore community structure. Marine Ecology-Progress Series 353, 1–12.

Callaghan, D.P., Nielsen, P., Gourlay, M.R., Ballock, T.E., 2006. Atoll lagoon flushing forced by waves. Coastal Engineering 53, 691–704.

Chawla, A., Tolman, H.L., 2008. Obstruction grids for spectral wave models. Ocean Modelling 22, 12–25.

Collard, F., Ardhuin, F., Chapron, B., 2009. Monitoring and analysis of ocean swell fields from space. New methods for routine observations. Journal of Geophysical Research-Oceans 114, C07023.

Dee, D.P., Uppala, S., 2009. Variational bias correction of satellite radiance data in ERA-interim reanalysis. Quarterly Journal of the Royal Meteorological Society 135, 1830–1841.

Delpey, M.T., Ardhuin, F., Collard, F., Chapron, B., 2010. Space-time structure of long ocean swell fields. Journal of Geophysical Research-Oceans 115, C12037.

Dumas, F., Le Gendre, R., Thomas, Y., Andréfouët, S., 2012. Tidal flushing and wind driven circulation of Ahe atoll lagoon (Tuamotu Archipelago, French Polynesia) from in situ observations and numerical modelling. Marine Pollution Bulletin 65, 425–440.

Edmunds, P.J., Leichter, J.J., Adjeroud, M., 2010. Landscape-scale variation in coral recruitment in Moorea, French Polynesia. Marine Ecology-Progress Series 414, 75–89.

Ekebom, J., Laihonen, P., Suominen, T., 2003. A GIS-based step-wise procedure for assessing physical exposure in fragmented archipelagos. Estuarine Coastal and Shelf Science 57, 887–898.

Goldberg, N.A., Kendrick, G.A., 2004. Effects of island groups, depth, and exposure to ocean waves on subtidal macroalgal assemblages in the Recherche archipelago, Western Australia. Journal of Phycology 40, 631–641.

Harborne, A., Mumby, P., Zychaluk, K., Hedley, J., Blackwell, P., 2006. Modeling the beta diversity of coral reefs. Ecology 87, 2871–2881.

Hoeke, R., Storlazzi, C., Ridd, P., 2011. Hydrodynamics of a bathymetrically complex fringing coral reef embayment: wave climate, in situ observations, and wave prediction. Journal of Geophysical Research-Oceans 116, C04018.

Hopley, D., 2011. Encyclopedia of Modern Coral Reefs. Structure, Form and Process. Springer, Berlin, pp. 1206.

Kraines, S., Susuki, A., Yanagi, T., Isobe, M., Guo, X., Komiyama, H., 1999. Rapid water exchange between the lagoon and the open ocean at Majuro Atoll due to wind, waves, and tide. Journal Geophysical Research 104, 15635–15654.

Kench, P.S., 1998. Physical processes in an Indian Ocean atoll. Coral Reefs 17, 155–168.

Madin, J.S., Connolly, S.R., 2006. Ecological consequences of major hydrodynamic disturbances on coral reefs. Nature 444, 477–480.

Magne, R., Ardhuin, F., Roland, A., 2010. Prévisions et rejeux des états de mer du globe à la plage (waves forecast and hindcast from global ocean to the beach). European Journal of Environmental and Civil Engineering 14, 149–162.

Pawka, S.S., Inman, D.L., Guza, R.T., 1984. Island sheltering of surface gravity-waves – model and experiment. Continental Shelf Research 3, 35–53.

Queffeulou, P., 2004. Long term validation of wave height measurements from altimeters. Marine Geodesy 27, 495–510.

Queffeulou, P., Croizé-Fillon, D., 2010. Global altimeter SWH data set, version 7, <ftp://ftp.ifremer.fr/ifremer/cersat/products/swath/altimeters/waves/>.

Queffeulou, P., 2011. Updated altimeter SWH validation for ENVISAT, Jason-1 and Jason-2. Technical Report, IFREMER, LOS, BP 70, 20280 Plouzané, France.

Saha, S. et al., 2010. The NCEP climate forecast system reanalysis. Bulletin of the American Meteorological Society 91, 1015–1057.

Soto, I., Andréfouët, S., Hu, C., Muller-Karger, F.E., Wall, C.C., Sheng, J., Hatcher, B.G., 2009. Physical connectivity in the Mesoamerican Barrier Reef System inferred from 9 years of ocean color observations. Coral Reefs 28, 415–425.

Storlazzi, C.D., Brown, E.K., Field, M.E., Rodgers, K., Jokiel, P.L., 2005. A model for wave control on coral breakage and species distribution in the Hawaiian Islands. Coral Reefs 24, 43–55.

Tartinville, B., Deleersnijder, E., Rancher, J., 1997. The water residence time in the Mururoa atoll lagoon: sensitivity analysis of a three-dimensional model. Coral Reefs 16, 193–203.

Tartinville, B., Rancher, J., 2000. Wave-induced flow over Mururoa atoll reef. Journal of Coastal Research 16, 776–781.

Thomas, Y., Le Gendre, R., Garen, P., Dumas, F., Andréfouët, S., 2012. Bivalve larvae transport and connectivity within the Ahe atoll lagoon (Tuamotu Archipelago), with application to pearl oyster aquaculture management. Marine Pollution Bulletin. 65, 441–452.

Tolman, H.L., 2003. Treatment of unresolved islands and ice in wind wave models. Ocean Modelling 5, 219–231.

Tolman, H.L., 2007. Automated grid generation for WAVEWATCH III. Technical Report 254, Environ. Canada, Toronto, Ont., Canada.

Tolman, H.L., 2008. A mosaic approach to wind wave modeling. Ocean Modelling 25, 35–47.

Tolman, H.L., 2009. User manual and system documentation of WAVEWATCH III™ version 3.14, Technical Report 276, NOAA/NWS/NCEP/MMAB.

Walker, S.J., Degnan, B.M., Hooper, J.N.A., Skilleter, G.A., 2008. Will increased storm disturbance affect the biodiversity of intertidal, nonscleractinian sessile fauna on coral reefs? Global Change Biology 14, 2755–2770.

Zieger, S., Vinoth, J., Young, I.R., 2009. Joint calibration of multiplatform altimeter measurements of wind speed and wave height over the past 20 years. Journal of Atmospheric and Oceanic Technology 26, 2549–2564.

Marine Pollution Bulletin 65 (2012) 425–440

Contents lists available at SciVerse ScienceDirect

Marine Pollution Bulletin

journal homepage: www.elsevier.com/locate/marpolbul

Tidal flushing and wind driven circulation of Ahe atoll lagoon (Tuamotu Archipelago, French Polynesia) from *in situ* observations and numerical modelling

F. Dumas [a,*], R. Le Gendre [d,1], Y. Thomas [c], S. Andréfouët [b]

[a] *Ifremer, DYNECO/PHYSED, BP 70, 29280 Plouzané, France*
[b] *IRD, UR 227 CoRéUs, BP A5, 98848 Nouméa Cedex, New Caledonia*
[c] *Ifremer, DPFOM LPI, Presqu'île du Vivier, 29840 Argenton, France*
[d] *Ifremer, LERN, avenue Général de Gaulle, 14520 Port-en-Bessin*

ARTICLE INFO

Keywords:
Lagoon circulation
French Polynesia
Residence time
Connectivity
MARS3D
Aquaculture

ABSTRACT

Hydrodynamic functioning and water circulation of the semi-closed deep lagoon of Ahe atoll (Tuamotu Archipelago, French Polynesia) were investigated using 1 year of field data and a 3D hydrodynamical model. Tidal amplitude averaged less than 30 cm, but tide generated very strong currents (2 m s^{-1}) in the pass, creating a jet-like circulation that partitioned the lagoon into three residual circulation cells. The pass entirely flushed excess water brought by waves-induced radiation stress. Circulation patterns were computed for climatological meteorological conditions and summarized with stream function and flushing time. Lagoon hydrodynamics and general overturning circulation was driven by wind. Renewal time was 250 days, whereas the e-flushing time yielded a lagoon-wide 80-days average. Tide-driven flush through the pass and wind-driven overturning circulation designate Ahe as a wind-driven, tidally and weakly wave-flushed deep lagoon. The 3D model allows studying pearl oyster larvae dispersal in both realistic and climatological conditions for aquaculture applications.

1. Introduction

Pearl oyster aquaculture is a major source of income for French Polynesia and Cook Islands, and is gaining increasing momentum in different Pacific Island countries. The beautiful black pearls, produced mostly in atoll lagoons, have been the main source of incomes for French Polynesia in the past years, especially between 1995–2003 (Andréfouët et al., 2012a). Tuamotu Archipelago atoll lagoons are essential sources of both spats and adult *Pinctada margaritifera* oysters due to their natural and imported large stocks and their adequate environment for oysters reproduction and growth. An adequate environment is primarily characterized by its bio-physical regime dependant on temperature, water renewal time, and planktonic food availability, both in quality and quantity. The bio-physical regime of the lagoon is largely dependent on the hydrodynamic regime of the lagoon, which is itself dependent on the atoll geomorphology and the atmospheric and oceanic forcing on the atoll boundaries (Andréfouët et al., 2006).

Atolls have different morphologies. Their general saucer-shape lagoon morphology is bounded by a rim which can be completely closed by a continuous emerged rim, or very open to the ocean with continuous submerged reef flats. Open atolls have wide reef flats along most of the perimeter of the atoll, draining waters from the ocean towards the lagoon when waves break along the rim crest. Accordingly, Callaghan et al. (2006) have described wave-driven lagoon-scale processes of flushing in Manihiki and Rakahanga Atolls (Cook Islands). A semi-closed atoll will have few of these reef flats, called also *hoa*, compared to an open atoll. Sometimes, these openings make no more than few tens of meters for an entire atoll. These closed and semi-closed atolls are typical of Tuamotu Archipelago, where they are more frequent than elsewhere.

In addition to the amount of reef flats, atolls may have one or several deep passages allowing water transfer that are driven by local tide cycles. Pugh (1979) provided a simple model of tidal energy dissipation within the deep passage of Aldabra Atoll (Seychelles) and showed that tidal energy dissipation was critically linked to tidal range, lagoon areas and depth of the channel. This induced an attenuated and slightly delayed tide cycle in the lagoon compared to the ocean. In the past, Tuamotu atolls have been ranked according to the number of passes (Salvat, 2009), but this descriptive view is fonctionnaly limited. More functional typologies have been proposed, that relate geomorphology, water renewal mechanisms, and hydrobiological regime (Delesalle and Sournia, 1992; Dufour et al., 2001; Andréfouët et al., 2001).

Atoll water renewal characteristics have been defined and measured in different manners. Andréfouët et al. (2001) based their estimation of a renewal time with a lagoon-scale index dependant on geomorphology and wave-driven flows across the rim openings

* Corresponding author. Tel.: +33 298224676; fax: +33 298224864.
E-mail address: fdumas@ifremer.fr (F. Dumas).
[1] Ifremer, Dyneco, BP 70, 29280 Plouzané, France.

0025-326X/$ - see front matter © 2012 Elsevier Ltd. All rights reserved.
http://dx.doi.org/10.1016/j.marpolbul.2012.05.041

(reef flats and passes). In contrast, Tartinville et al. (1997) characterized for Mururoa atoll an intra-lagoon, spatially-explicit, residence time thanks to field observations and numerical modelling. They also provided a sensitivity analysis of this residence time to various physical forcing variables like wind, waves, tide and stratification. As pointed out by Andréfouët et al. (2006), to be useful for pearl oyster aquaculture management, a lagoon-scale hydrobiological approach is not satisfactory, and a fine-scale intra-lagoon characterization is necessary. To achieve a proper intra-lagoon spatially-explicit hydrobiological characterization, three-dimensional (3D) hydrodynamic numerical models are the tools of choice. They require proper calibration and validation and come with their own limitations, but they allow hypothesis-testing and measuring sensitivity to different forcing factors.

In order to contribute to the management of the pearl oyster aquaculture in Ahe atoll, we used *in situ* measurements and numerical models to characterize the exchanges between the lagoon and the ocean and the main regimes of lagoonal water circulation. In this paper we present the pilot study site, Ahe atoll, with its semi-closed lagoon. Then, we present the suite of *in situ* measurements used to calibrate and validate the model. The various hydrodynamic patterns observed in the hoa, the pass and within the lagoon water body are detailed, as well as the exchanges across the atoll rim and the dynamic response of the sea level. Sensitivity to waves, wind and tidal conditions are discussed. Model outputs are compared to *in situ* measurements throughout. Afterwards, the model is used to characterize the lagoon circulation and map the lagoon e-flushing time. Ahe lagoon hydrodynamic functioning is then discussed, especially in the light of other lagoons described in the literature.

2. Materials and methods

2.1. Study site

Ahe atoll is located in the north-western part of the Tuamotu Archipelago (14°29′S–146°18′W), about 500 km north-east from Tahiti (Fig. 1a). The lagoon is a 142 km^2 deep water body (Fig. 1b) with an average depth of 41 m, and contains numerous pinnacles rising to the surface. The volume of the inner water body is 5.9×10^9 m^3. A detailed lagoon-wide acoustic bathymetric survey revealed that the deeper areas are made of honeycomb-like

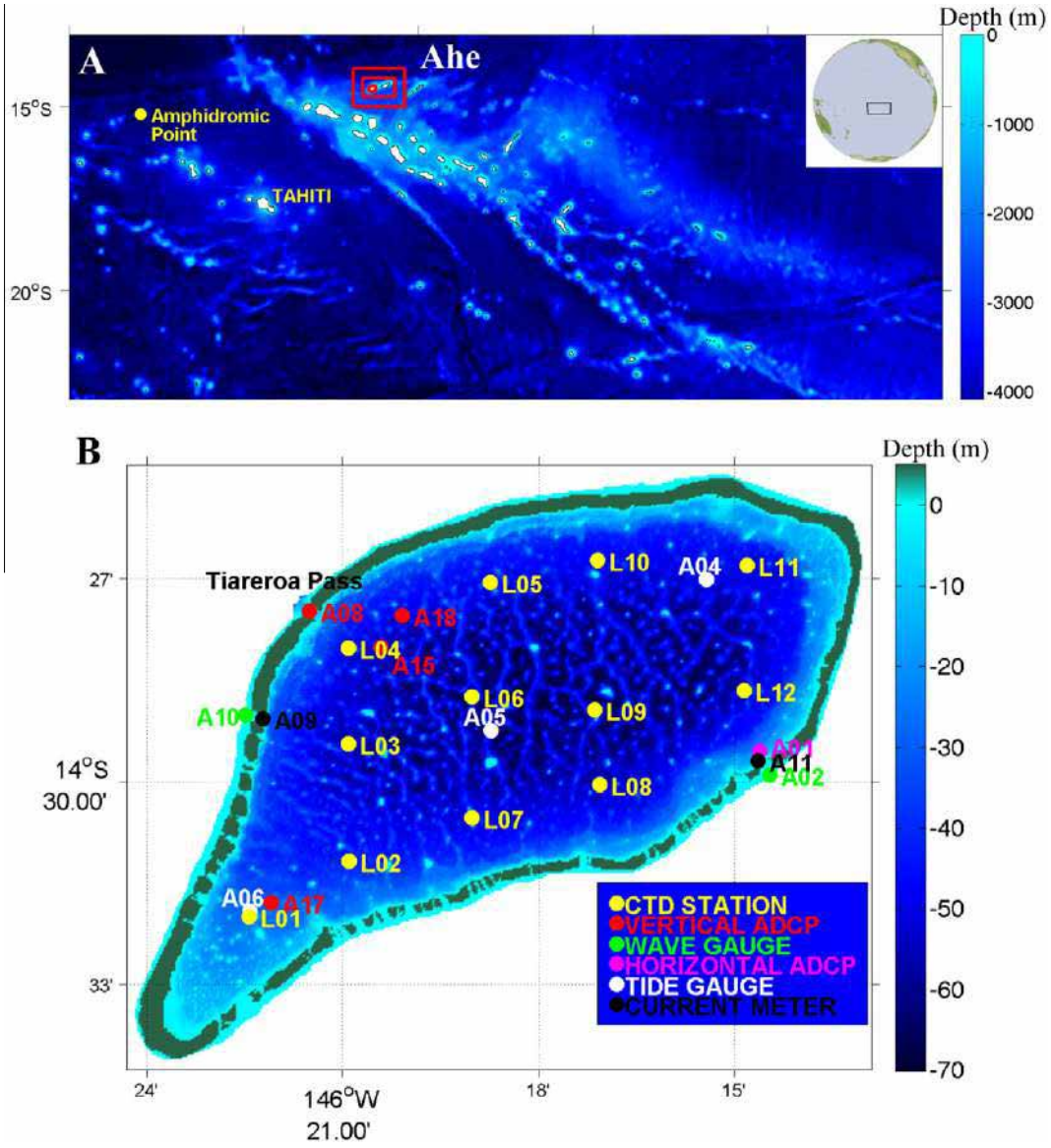

Fig. 1. (A) Map of French Polynesia islands. The extent of this frame is the same as the coarse computational domain. Nested ranks are also shown. (B) Bathymetry of Ahe atoll and locations of the sampling stations, per instrument type (see Table 2).

Table 1
Instrument deployment schedule (date are DD/MM/YY).

	Leg 1	Leg 2	Leg 3	Leg 4	Leg 5
Begins	02/12/08	09/02/09	24/04/09	28/06/09	28/09/09
Ends	08/02/09	24/04/09	28/06/09	28/09/09	07/11/09

cellular structures probably of karstic origin, in which individual basins reach up to 70 m deep.

The lagoon is an almost closed water body connected to the open ocean through a 11-meter deep, 200-meter wide pass. The *Tiareroa* pass is located on the north-west side of the atoll rim (Fig. 1b). Several very shallow hoa (about 30 cm deep, between 10 and 300-meter wide, with a total cumulated width of 4 km), represent about 5% of the rim perimeter (77 km). Hoa are present on the southern side and on the north-western side of the rim. The northern part of the rim located east from the pass, and most of the eastern part of the rim, are completely closed to water exchanges (Fig. 1b).

The wave regime around Ahe atoll is described by Andréfouët et al. (2012b). Ahe atoll benefits from a sheltered position due to the relative position of nearby atolls. It is very efficiently sheltered from the southern oceanic waves by a series of large southward atolls, and it is also sheltered, although less efficiently, on its east side by Takaroa and Takapoto atoll. North swells generated by northwest Pacific depressions occur from November to March and they hit directly Ahe's northern rim, but wave height in the north of the atoll is typically low with an average wave height around 1.7 m, including the contribution of wind waves. As a result, Ahe is mostly exposed year round to wind waves generated locally by dominant easterly tradewinds, which are stronger from April to October. Andréfouët et al. (2012b) showed that Ahe is exposed to wave height above 2.5 m only a few days per year.

Ocean tidal amplitudes near Ahe atoll are small (around 40 cm) due to its proximity to a M2 amphidromic point (Fig. 1a).

2.2. In situ hydrodynamic measurements

Continuous physical measurements were made during nearly 1 year between December 2008 and early November 2009. *In situ* data acquisition took place during 5 legs of continuous recording, with data downloading and instrument maintenance occurring

Table 2
Description of moored instrument deployments used for this study. See Fig. 1 for locations of stations. SP = sampling period.

Station	Location	Instrument	Depth (m)	Legs deployed	Sampling
A02	14°29.909′S 146°14.466′W	Tide and wave recorder TWR-2050	6.8	1,2,3,4,5	SP waves: 20 min SP tide: 10 min
A04	14°27.086′S 146°15.435′W	Pressure recorder DR-1050	50.5	1,2	SP: 10 s
A05	14°29.326′S 146°18.727′W	Pressure recorder TGR-1050	53.7	1,2,3	SP: 10 s
A06	14°31.989′S 146°22.429′W	Pressure recorder DR-1050	25	1,2,3	SP: 10 s
A08	14°27.488′S 146°21.511′W	ADCP Sentinel (1200 kHz)	17	1	SP: 10 min Bin size: 0.5 m
A09	14°29.077′S 146°22.224′W	Current-meter Aanderaa RCM7	0.8	1,2,3,4,5	SP: 10 min
A10	14°29.024′S 146°22.488′W	Pressure recorder TGR-1050	6.1	1,2,3,4,5	SP: 1 s for leg 1, 2 s for others
A11	14°29.698′S 146°14.639′W	Current-meter Aanderaa RCM7	0.8	3,4,5	SP: 10 min
A15	14°28.021′S 146°20.422′W	ADCP Sentinel (1200 kHz)	22	3	SP: 10 min Bin size: 2 m
A17	14°31.791′S 146°22.092′W	ADCP Sentinel (1200 kHz)	20	4	SP: 20 min Bin size: 2 m
A18	14°27.549′S 146°20.097′W	ADCP Sentinel (1200 kHz)	20	5	SP: 10 min Bin size: 2 m

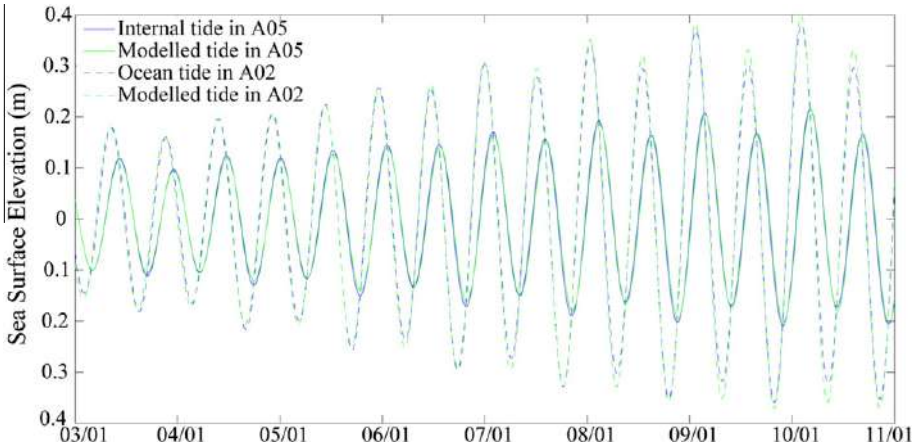

Fig. 2. Half spring-neap tidal cycle (January 2009) of sea surface elevation in A05 (lagoon) and A02 (ocean). Model *versus in situ* data are displayed, but they are in very close agreement and overlap almost perfectly.

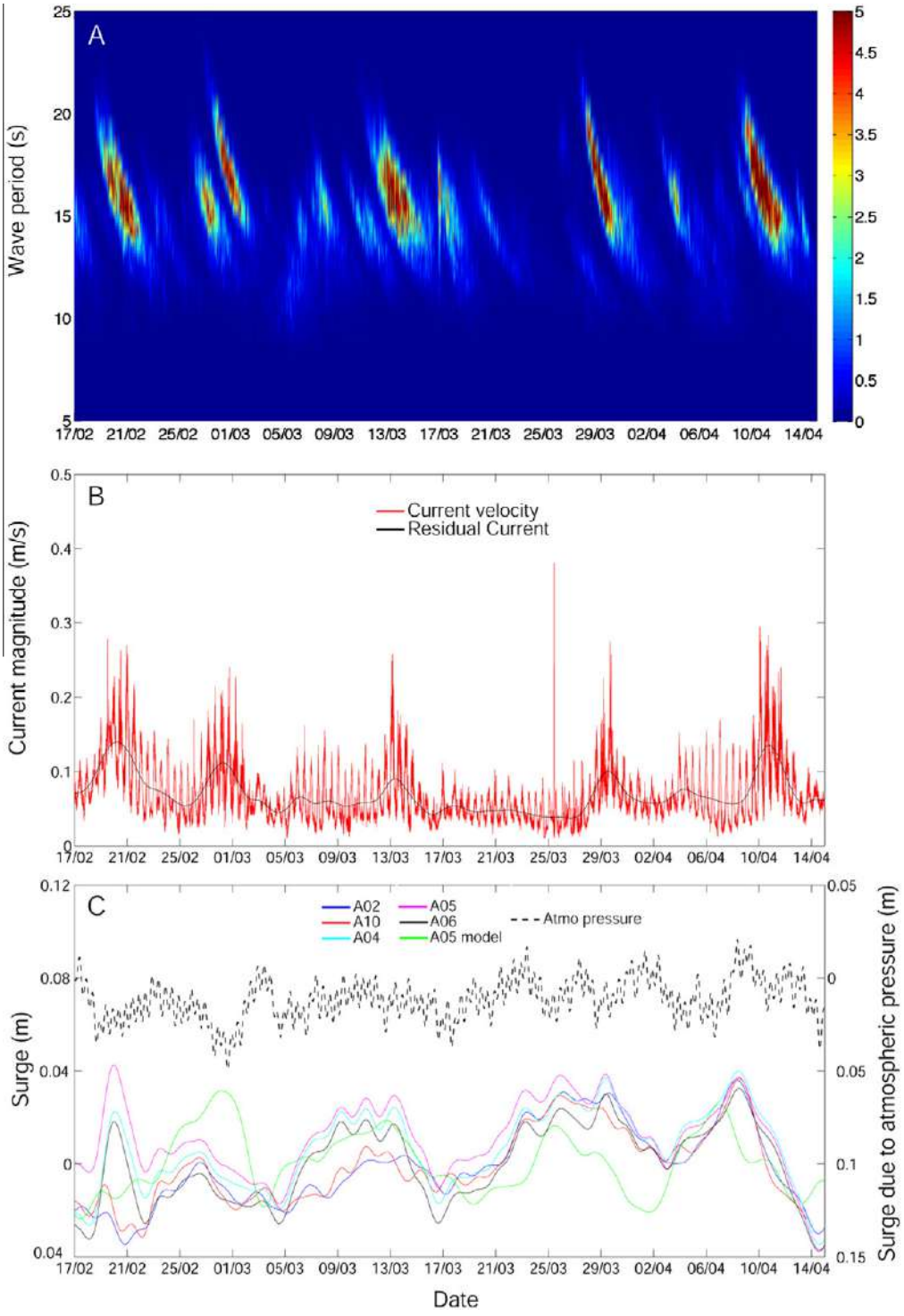

Fig. 3. (A) Forereef wave energy spectra (color bar in $m^2\ Hz^{-1}$) in A10 (in front of the northern hoa, Fig. 1) from mid-February–mid-April 2009. (B) Concurrent instantaneous and tidally filtered currents in A09 (northern hoa). (C) Concurrent de-tided sea surface elevations inside and outside of the lagoon and inverse barometer surge.

every 2 months, at the exception of the last leg which lasted 3 months (Table 1).

The global strategy for data acquisition was to measure in a coordinated fashion the incident waves on the forereef, water levels and tide inside and outside the lagoon, currents through the rim (hoa and pass), and currents in different locations inside the atoll for a better understanding of the circulation. The sampling was designed to assess the co-influences between the processes taking place at the lagoon boundary and inside the lagoon. Table 2 explains the instruments deployment. For each leg, the mooring locations were the same except for the upward-looking 1200 kHz acoustic Doppler current profiler (ADCP, RD Instruments Workhorse Sentinel) which was used in different locations from one leg to another.

Two functional (i.e. always active with flowing waters) hoa were selected and instrumented. One was located on the northwest (Station A09) and one on the southeast side (Station A11). For measuring current velocities, rotor current meters (Aanderaa

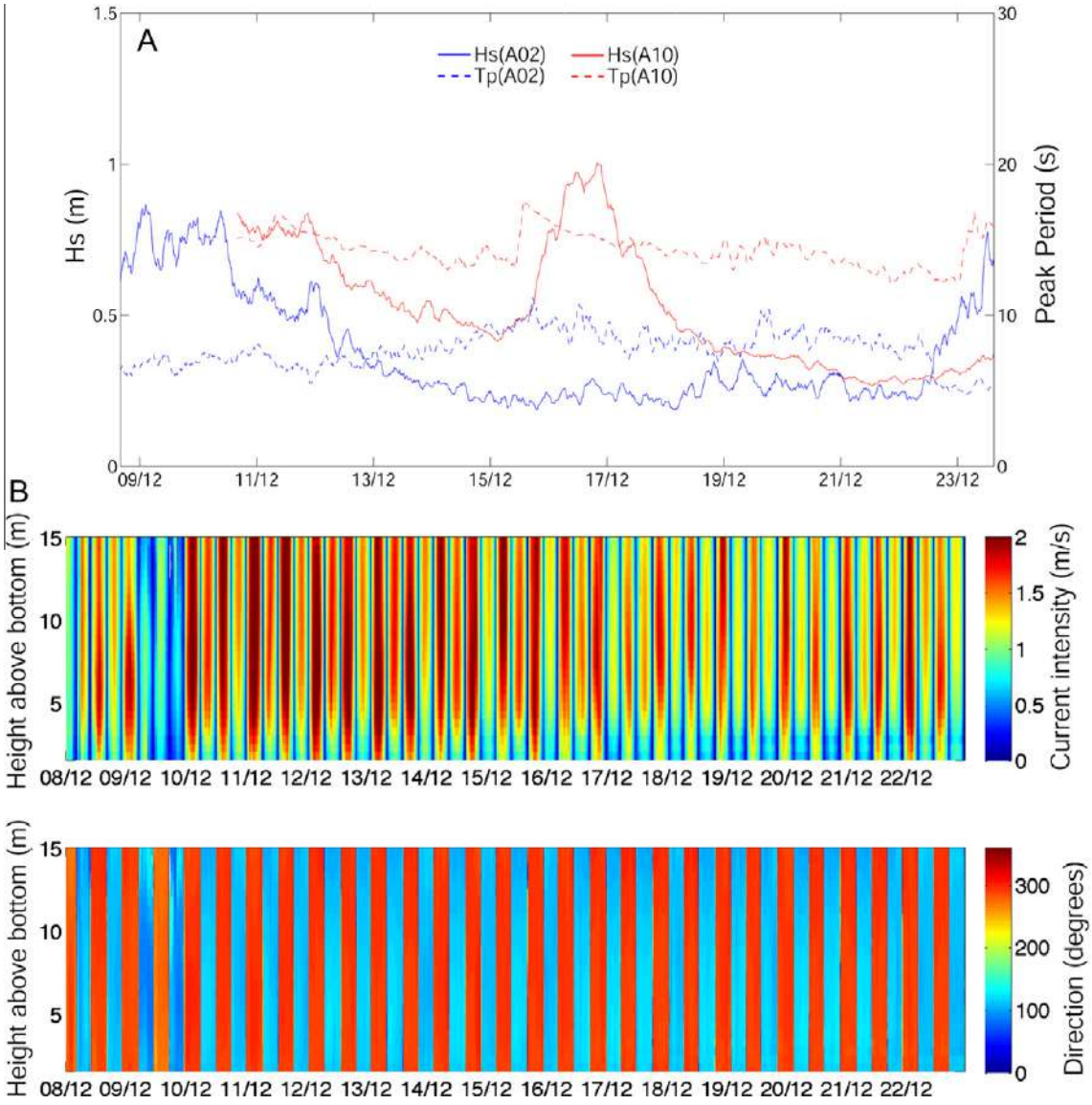

Fig. 4. (A) Significant wave height and peak period in A02 (southern hoa) and A10 (northern hoa) in December 2008. (B) Concurrent vertical profile of instantaneous current intensity and direction from the ADCP in the pass (A08). The current flows outbound around 340° (red), and inward around 120° (blue). (For interpretation of the references to colour in this figure legend, the reader is referred to the web version of this article.)

RCM7) were used, casted in concrete with their blades disassembled. This system measured velocities every 12 s, then stores an average value over a 10 min time step.

The north incident waves as well as sea levels were measured using a pressure recorder (TGR-1050, RBR), moored on the external oceanic forereef slope (Station A10). This sensor sampled pressure every 1 or 2 s. On the south side of the atoll, a tide and wave recorder (TWR-2050, RBR) was also deployed (Station A02). Its sampling period for tide was 10 min. Measurements were the average of 1 min-long acquisition at 2 Hz. Wave data were stored every 20 min using burst lengths of 512 samples at 2 Hz.

For the lagoon tide characterization, three pressure recorders were moored aligned in Ahe longitudinal axis (Stations A04, A05, A06). They recorded pressure data every 10 s.

During the first leg, the vertical Sentinel ADCP was moored in the pass (Station A08) to evaluate the magnitude of the main exchanges between ocean and lagoon. Other lagoon sites were also investigated using additional vertical current profiler in this first leg, and with the Sentinel subsequently. This includes the sector near the pass (with Stations A15 and A18). A location in the south-west of the lagoon (Station A17) was also monitored to study recirculation phenomenon. For all legs, the vertical profiler averaged currents over 250 pings per ensemble. Ensemble interval was generally set to 10 min except for the fourth leg which lasted 1 month longer than the others.

During each field campaign aimed at downloading data and servicing the instruments, hydrologic surveys were carried out to provide profiles of temperature, salinity, oxygen and pH along the water column at Stations L01 to L12 using a multi-parameter profiler CTD Seabird SBE 19 plus.

2.3. Post-processing

The pressure data from the recorder in A10 were transformed to depth data, and converted to surface wave-height data using inverse Fourier transforms. The processing of de-tided signals (levels in Fig. 2, currents in Fig. 3 and flow in Fig. 4) has been performed using Demerliac filter (Demerliac, 1974). This filter is specifically

designed to remove tidal harmonic constituents from any signal using a 72 hour window. For level analysis, in order to have all the signals centered on the same vertical referential, mean value of depth over the entire duration of the time series was subtracted from instantaneous values. Tide harmonic analysis was made with the T_tide toolbox (Pawlowicz et al., 2002).

2.4. Numerical modelling

The MARS3D numerical model used here has been described in detail by Lazure and Dumas (2008). In short, it is a standard model based on classical assumptions (Boussinesq approximation, hydrostatic balance assumed) that leads to a set of equations that is solved using finite difference techniques in a sigma coordinate framework. The resolution is based on mode splitting as in Blumberg and Mellor (1987). The turbulent eddy diffusivity and viscosity are assessed using the Gaspar (1990)'s turbulence closure.

To model Ahe lagoon, four different levels of nesting were required (Fig. 1a). The first three levels are bi-dimensional horizontal approximation. They describe the open boundary conditions of the atoll, including astronomical and meteorological tides. The wider model is forced by a sea level signal harmonically composed from FES2004 (Lyard et al., 2006), accounting for an inverse barometric correction estimated from the NCEP Global Data Assimilation System (GDAS) pressure field. The barotropic mode (sea surface height and mean vertical velocity) along the open marine boundaries is thus provided by the immediately wider model of the embedment.

The bathymetry at the nodes of the grids were obtained from various sources: ETOPO1 bathymetry grid was used for the large scale. For the deep atoll slopes, we digitized nautical charts from the French Oceanographic and Hydrographic Service (SHOM). Inside the lagoon, bathymetry (Fig. 1a) has been mapped using a single beam acoustic sensor on east–west oriented tracks spaced 50 m apart. The pass and some large pinnacles were surveyed following a finer mesh of about 10 m resolution.

The detailed inner hydrodynamic model has a spatial resolution of 100 m. It encompasses entirely the lagoon, the rim and most of the external slope. On the vertical axis, 23 sigma layers are distributed to represent both the bottom and the surface boundary layers.

The atmospheric forcings were computed thanks to bulk formulae following Luyten and de Mulder (1992). These formulae require wind velocity at 10 m, pressure at the sea level, relative humidity and air temperature at 2 m, and finally fractional cloud cover. These meteorological conditions were obtained from a Meteo France weather station located at the Takaroa station (14°28.460′S–146°2.285′W). Hourly data of wind intensity and direction, pressure at sea level, temperature and cloud cover were gathered, and given the Ahe-Takaroa distance (150 km) and lack of any orographic effects in atolls, Takaroa data were considered valid for Ahe. At the scale of the process examined here, we considered that meteorological conditions could be taken homogeneous over the modelled area. An alternative choice would be to use GDAS analysis, but the 50 km spatial resolution does not provide a significant enhancement compared to the Takaroa meteo station data. Moreover, GDAS temporal (6 h) were far worse than local data.

2.5. The e-flushing time

There are various ways of investigating the retention capability of a semi enclosed water body like Ahe. A useful bulk variable is the renewal time. It has been defined as the ratio of the total volume of the water mass to the incoming flow that flushes it. This gives an integrated measurement at lagoon-scale. However, the retention capability varies in space. It is inherently constrained by the morphology of the basin (independent of time) but it also depends on dynamic time-dependent forcing factors such as tide, wind and flow forced by waves. To refine the notions of retention that have been introduced by Thomas et al. (2012a,b) for larval dispersal and spat collecting, we introduce hereafter the e-flushing time.

E-flushing time aims to map the most favourable retention areas, and their variability with respect to forcing. It helps understanding the numerical experiences shown by Thomas et al. (2012,b). The e-flushing time is defined as follows: at a given location, it is the time needed to decrease a concentration of tracers (e.g., larvae) by a factor $e = 2.718$. Thus the concentration is about 60% lower than the initial concentrations. The e-flushing time is estimated with the model, using passive tracer homogeneously distributed in the lagoon water body at the initial time. Initial concentrations are fixed, equal to 1 unity.m^{-3}. Every water flux entering the lagoon (either by the main pass or the hoa) has a null concentration. The transport equation is then integrated along with dynamical evolution of the flow to update the concentrations and the current e-flushing time.

3. Results

3.1. Tide

The tidal spectra was mostly made of components that are in the tide-generating potential. Accordingly, it is of oceanic type because non linear effects giving birth to interaction with waves are very weak. The harmonic constituents at Station A02 are provided in Table 3. The M2 amplitude was 23 cm and the sum of the main semi-diurnal components reached 34 cm whereas the main diurnal components reached 4 cm, thus slightly less than a tenth of the semi-diurnal. This defined a mostly semi-diurnal with diurnal irregularities tidal regime. The mean tidal range was around 50 cm, decreasing to 31 cm during neap tide and increasing up to 73 cm in spring tide. As modelled by Pugh (1979), tidal energy was severely dissipated by the Tiareroa pass, thus the lagoon inner tide amplitude was limited to 20 cm during neap tide and 32 cm during spring tide. Associated to this damping, a significant delay between the inner and outer tide was observed corresponding to a M2 phase of 54°, or in other words almost a two hours lag. The three tidal gauges (A04, A05, A06, Fig. 1b) within the lagoon showed that at least the M2 component is homogeneous throughout the lagoon, although phase shifts of 0.2° (i.e. 25 s) between A04 and A06 could be calculated. No differences greater than a millimeter in amplitude were detected between the three lagoon sites.

Fig. 2 compares the pure astronomical tide reconstructed from the five main components extracted from gauges A02 (ocean) and A05 (central lagoon) and the model at the same locations. Except the five main components M2, S2, N2, O1 and K1, others have an amplitude of about 1 mm or less, and thus they were neglected afterwards. Models and observations are in good agree-

Table 3
Comparison of measured and modeled tidal harmonic constituents between open ocean in Station A02 and lagoonal tide in Station A05.

Harmonic constituent	A02 H (m)	A02 model H (m)	A02 G (°)	A02 model G (°)	A05 H (m)	A05 model H (m)	A05 G (°)	A05 model G (°)
M2	0.236	0.249	98.29	93.72	0.139	0.139	154.04	156.14
S2	0.065	0.075	57.46	63.23	0.032	0.034	123.63	134.87
N2	0.049	0.049	77.04	76.33	0.024	0.023	140.00	143.63
K1	0.029	0.022	93.46	87.36	0.020	0.017	137.48	135.97
O1	0.012	0.012	32.00	10.51	0.009	0.009	69.60	59.53

ment. Outside the lagoon (A02), Table 3 shows that the amplitudes differ from less than 1.5 cm at most, whereas the phase lag (except curiously for O1, the weakest wave) is of the order of 5°, representing a 10-min lag for semi-diurnal components. This slight discrepancy between model and observations is explained by the use of FES2004 and the bathymetry ETOPO1. Within the lagoon, observations and model fitted perfectly (Fig. 2), with time delay less than 15 min and amplitude difference which are lower than 2 cm. The good agreement suggests that our bottom parameterization was sufficient (bottom drag coefficient, which is based on a log law approximation, and roughness set to 3.5 mm; lateral friction was accounted for in the bottom friction parameterisation and the sigma vertical framework) and that the influence of the pass due to its geometry was also correctly represented at the 100 m spatial resolution used here.

3.2. Waves, current in hoa, and lagoon surge

This section analyses the variation of sea surface elevation in the lagoon, after filtering out the astronomical tide. An example of sequence is shown for February–April 2009, for the different stations (Fig. 3c). In relation to oceanic surface and lagoon surface elevation, the distribution of wave energy measured on the north side of the rim according to the wave period (Fig. 3a) shows the effect of incoming waves generated in higher northern latitudes. The dispersion effect is visible on the spectra Fig. 3a as the longer wave arrives first, in agreement with the dispersion relation of linear Airy waves in infinite depth, which implies that longer waves propagate faster. In Fig. 3, the period of the swell reaching Ahe varied from 19 to 13 s, and its significant wave height reached up to 1.40 m (observed on the 5th of January – not shown). Current velocities measured at Station A09 in the northern hoa during the same period are shown Fig. 3b. The current intensity appeared very well correlated with the sea state observed at Station A10 in the ocean. The black curve Fig. 3b is the intensity of the current filtered by Demerliac filter to remove tide effects. The maxima fit very well with wave trains observed outside the atoll at point A10. The instantaneous de-tided current may be of the order of 28 cm s^{-1} when waves are present, and it peaked at 30 cm s^{-1} the 10th of April 2009 in Fig. 3. Strongest velocities were measured at 38 cm s^{-1} the 16th September 2009 (not shown). Tidal influence was evident too in the hoa unfiltered signal (red curve, Fig. 3b). The current in the hoa peaked at high tide and was minimum at low tide. Even without significant waves from the north, the hoa remained active with a light residual current at few cm s^{-1} (Fig. 3b). As the cumulated length of the few hoa on the northern

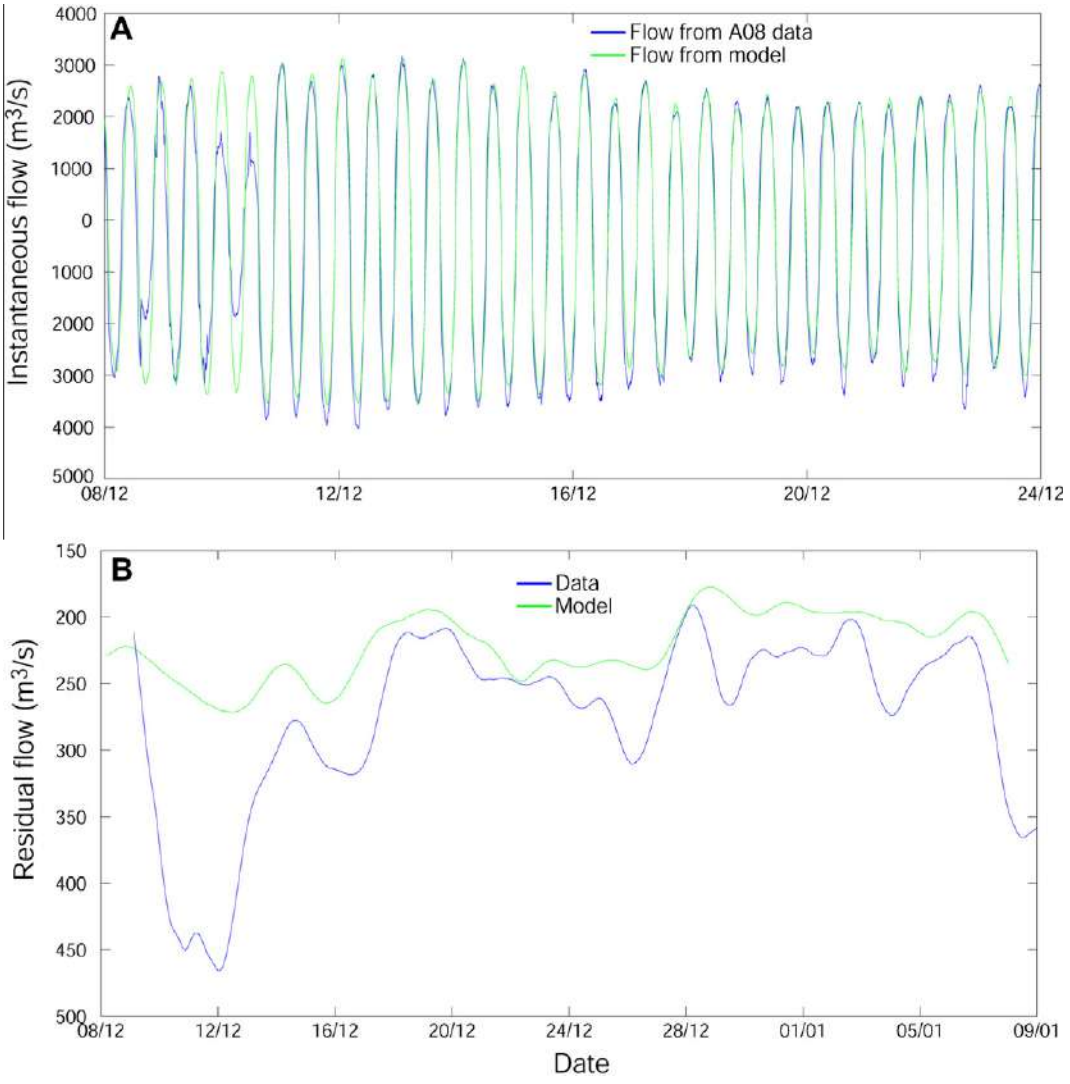

Fig. 5. (A) Instantaneous flow through the pass section deduced from the observations and simulated by the model, in December 2008. (B) Residual flow through the pass section (A08) from the observations and the model, during 1 month.

side of the rim is nearly 500 m, assuming all hoa work in the same manner, the cumulated water flux entering the atoll by the northern side is about 50 $m^3 s^{-1}$.

Time series of current from the southern hoa (Station A11) show the same behaviour as the north hoa, with a modulation with respect to the tidal signal and a good correlation with the significant wave height measured outside the rim in front of the hoa (Station A2). A commonly observed sea state (Hs = 1.5 m and Tm = 8 s) generates tidally filtered currents of 15 cm s^{-1} within the southern hoa. The strongest currents over the period of the survey occurred on the 4th of October 2009. The tidally filtered currents peaked to 50 cm s^{-1}, during a time where significant wave height and peak period estimated by WAVEWATCH III model (Andréfouët et al., 2012b) were 2.5 m and 8 s respectively.

Given the low variability and low velocity of hoa current observed during the entire survey both in the north and south sectors, the hoa parameterisation has been simplified in the model. Velocity across all hoa has been tuned permanently to a mean value of 10 cm s^{-1}, which was the average value observed over the entire observation period (1 year). Under the assumption that all southern hoa work in the same manner at the same time, this average value induces a mean inflow during a half tidal cycle of 103 $m^3 s^{-1}$. This is ten to twenty times smaller (i.e. 1340 to 2010 $m^3 s^{-1}$) than the flux exchanged through the main pass during the same time by the tide alone as previously evidenced. If we consider that the volume extracted through the pass during half a tidal cycle is not the same as the one re-entering during the next half-tidal cycle, it appears that over the year, on average, the contribution of the hoa to the flush was weak, and an order of magnitude lower to tidal flushing. During short energetic events when wave height was above 2.5 m, the velocity in the hoa can reach about 50 cm s^{-1} (e.g., 4th of October 2009). In that case, hoa contribution was only two to four times weaker than the tidal flushing, and it could be considered significant compared to pass flushing.

During the entire survey (December 2008–November 2009), the maximum lagoon surge amplitude observed was only 6 cm, observed for example the 8th February 2009 (Fig. 3c). All gauges (A04, A05, A06) generally reacted in the same manner, but some difference occurred the 20th February with a 2.5 cm difference between A06 and A05, and again on the 13th and the 25th of March. This weak difference and the consistent reaction of the three gauges show that water level variations are rather homogeneous lagoon-wide. Fig. 3c shows that the mean sea level computed by the model is in agreement with the observations (i.e. −4 cm to 4 cm). A clear signal, with a period of a fortnight, is visible in the observation and is well reproduced by the model. The largest discrepancy occurred on the 21st of February 2009 when the signal observed in northern hoa (15 cm s^{-1}) was stronger than the signal forced into the model. The resulting surge was thus underestimated by the model at this date. In addition, on the 1st of March 2009, the model reacted more rapidly to a shift in the atmospheric pressure than what was observed.

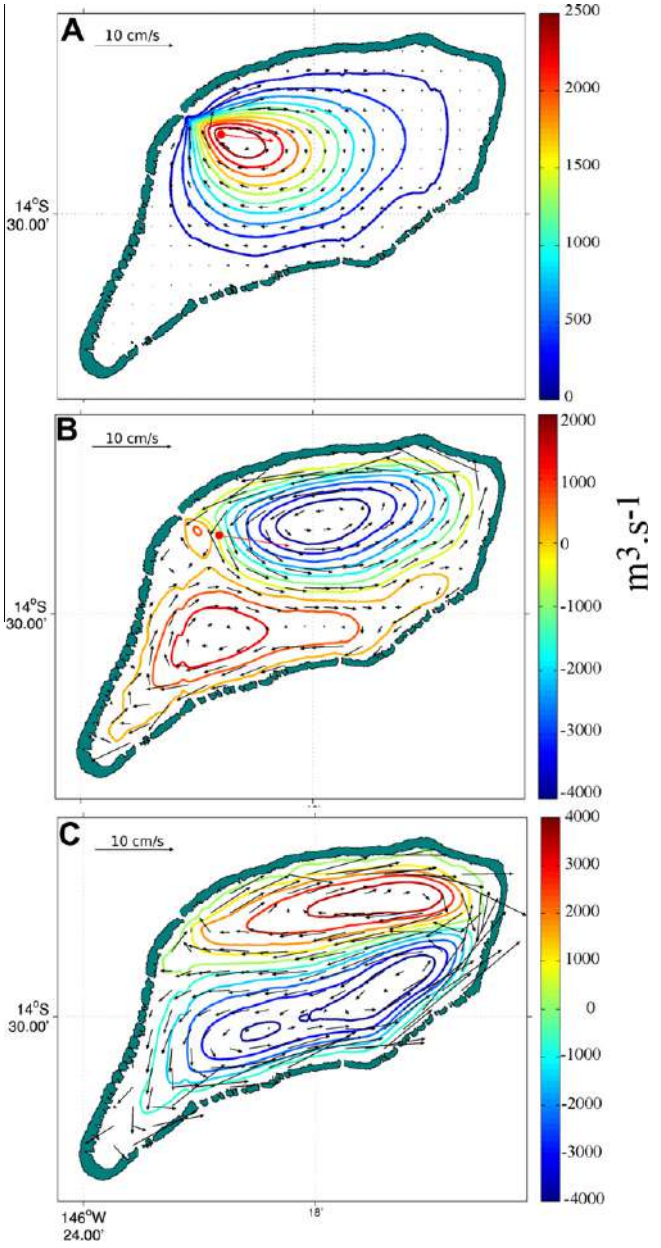

Fig. 6. (A) Barotropic stream function (contours in $m^3 s^{-1}$. Note that scales are different per panel) and barotropic current fields of the tidally filtered, modelled, current field (BSF). The flow is driven by tide alone. Estimates from ADCP measurements are shown by the red arrow (B) BSF with the flow driven by tide and stationary average tradewinds (107° – 8 m s^{-1}). (C) BSF with the flow driven by tide and stationary western winds (270° – 8 m s^{-1}). (For interpretation of the references to colour in this figure legend, the reader is referred to the web version of this article.)

3.3. Exchanges through the pass

The instantaneous current profiles measured in the middle of the pass (Station A08, first leg, see Table 1) showed that the current was essentially bidirectional (340° during ebb tide and 120° during flood tide) and tightly coupled to tide variations (Fig. 4). The current is thus clearly semi-diurnal. Over the period (a fortnight), tidal reverse was always clearly visible even the 10th of December 2008 when the flood was severely dampened. The tidal reverse always happened in less than ten minutes (Fig. 4b). The intensity of the current ranged from 1.2 m s^{-1} (neap tide) to 2.5 m s^{-1} (spring tide), except during the 10th December event.

The vertical profiles showed the classical decrease expected next to the bottom due to the friction. The thickness of this bottom boundary layer was about 4 m. Above this boundary layer, the profile was usually rather homogeneous up to the surface, even if maximum regularly occurred (9th, 18th, 21st) 6 m above the bottom. Also, the current was systematically stronger during ebb tide than flood tide. The direction was almost homogeneous along the vertical axis: only a slight veering was noticeable during flood from 140° at the bottom to 120° at the surface.

The flow through the pass has been estimated using the ADCP current profiles and a bathymetric transect passing through the ADCP mooring. The model used to build an integrated flow through

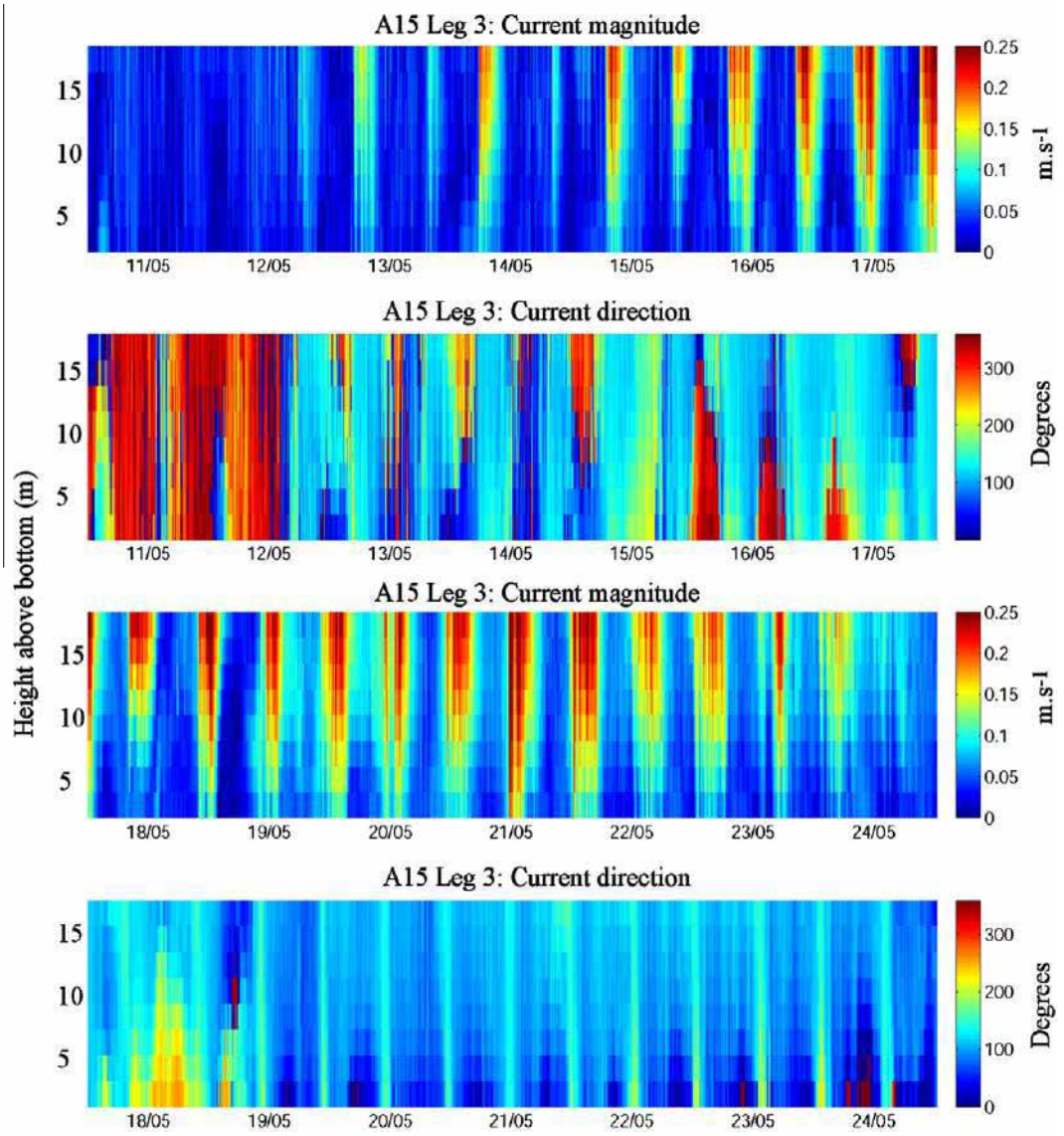

Fig. 7. Vertical profiles of currents observed at location A15.

the whole section of the pass relied on the assumption that the main equilibrium of the forces that drive the flow at any point of the section is between external pressure gradient and friction, thus giving :

$$\frac{\partial \zeta}{\partial n} = \frac{\overline{u}^2}{\mathrm{St}^2 H^{4/3}}$$

if the bottom friction is parameterised thanks to Strikler (St) coefficient, $\overline{u}$ is the vertically averaged current, ζ is the sea surface elevation, H is the total water depth. This equation at Station A08 provided the sea surface slope. Assuming the surface slope is constant along the transect and knowing H, we deduce $\overline{u}$ along the section, and finally integrate the flow through the pass (Fig. 5a). Instantaneous flows (Fig. 5a) were clearly semi-diurnal, varying from 2000 $m^3\ s^{-1}$ (neap tide) to 3000 $m^3\ s^{-1}$ (spring tide). The total amount of water passing through the pass during half a period was thus 0.03–0.045 km^3 (or 5–8‰ of the total lagoon volume). Spread over the lagoon, this volume would correspond to a tidal range of 20–35 cm, which is in agreement with our tide observations.

Fig. 5b (bottom panel) shows the residual (i.e. tidally filtered with the Demerliac filter) flow through the pass for the entire period of ADCP measurement. This residual flow was always oriented outward from the lagoon (thus the negative y-axis in Fig. 5b). The mean residual flow over the period was 270 $m^3\ s^{-1}$. It peaked at 470 $m^3\ s^{-1}$ on the 12th of December 2008. Secondary peaks occurred the 17th, 26th of December and again the 4th and 8th of January. Fig. 4a clearly shows that these peaks corresponded either to large waves measured in front of the northern hoa at Station A10 (17th of December) or in front of the southern hoa at Station A02 (26th of December, not shown), or in front of both hoa (12th of December). The highest residual peak corresponds to both hoa being active. Since all the hoa sections summed to 4000 m (split between 500 m in the northern part and 3500 m in the southern part), and considering a mean hoa depth of 50 cm and that the 470 $m^3\ s^{-1}$ of the main peak were uniformly spread among all hoa (supposed active during this event), we obtain an average velocity of 23.5 cm s^{-1} in each hoa. This velocity is consistent with our measured velocities. Moreover, a mean pass outflow of 270 $m^3\ s^{-1}$ led to a 13.5 cm s^{-1} residual velocity in the hoa, close to the value shown Fig. 3b.

Since the model was parameterized with a stable value of hoa current velocity, the model could not reproduce finely in the pass the main peaks, which were thus themselves explained by waves

Table 4
Residual current measured by ADCP under various meteorological conditions at various locations within the lagoon.

Wind conditions/ station	A15	A17	A18
No wind Mean current over the vertical	**Period:** 22/05/2009–26/05/2009 **Mean wind (over the period) at Takaroa station**: 2 m s^{-1}/110° u = 0.0672 m s^{-1} v = −0.0088 m s^{-1} Norm = 0.0678 m s^{-1} Direction = 97.5°	**Period:** 04/08/2009–08/08/2009 **Mean wind (over the period) at Takaroa station**: 2.5 m s^{-1} /170° u = 0.0033 v = −0.0004 Vitesse = 0.0034 Direction = 98.4°	**No available observation**
Trade wind Mean current over the vertical	**Period:** 27/05/2009–06/06/2009 **Mean wind (over the period) at Takaroa station** : 8.5 m s^{-1},114° u = 0.0891 m s^{-1} v = −0.0136 m s^{-1} Vitesse = 0.0901 m s^{-1} Direction = 98.8°	**Period:** 12/09/2009–20/09/2009 **Mean wind (over the period) at Takaroa station**: 7.9 m s^{-1},112° u = 0.0012 m s^{-1} v = −0.0028 m s^{-1} Vitesse = 0.003 m s^{-1} Direction = 149°	**Period:** 03/10/2009–08/10/2009 **Mean wind (over the period) at Takaroa station**: 8.65 m s^{-1},114° u = 0.0343 m s^{-1} v = 0.0188 m s^{-1} Vitesse = 0.0391 m s^{-1} Direction = 55°
Trade wind Current at 2 m below the surface	**Period:** 27/05/2009–06/06/2009 **Mean wind (over the period) at Takaroa station**: 8.5 m s^{-1},114° u = 0.0981 m s^{-1} v = −0.0333 m s^{-1} Vitesse = 0.1036 m s^{-1} Direction = 110°	**Period:** 12/09/2009–20/09/2009 **Mean wind (over the period) at Takaroa station** : 7.9 m s^{-1},112° u = −0.0133 v = −0.0032 Vitesse = 0.0137 Direction = 256°	**Period:** 03/10/2009–08/10/2009 **Mean wind (over the period) at Takaroa station**: 8.65 m s^{-1},114° u = 0.0343 m s^{-1} v = 0.0188 m s^{-1} Vitesse = 0.0391 m s^{-1} Direction = 55°
Trade wind Current at 3 m above the bottom	**Period:** 27/05/2009–06/06/2009 **Mean wind (over the period) at Takaroa station** : 8.5 m s^{-1},114° u = 0.0687 m s^{-1} v = 0.0078 m s^{-1} Vitesse = 0.0691 m s^{-1} Direction = 183°	**Period:** 12/09/2009–20/09/2009 **Mean wind (over the period) at Takaroa station** : 7.9 m s^{-1},112° u = 0.003 m s^{-1} v = 0.00033 m s^{-1} Vitesse = 0.003 m s^{-1} Direction = 84°	**Period:** 03/10/2009–08/10/2009 **Mean wind (over the period) at Takaroa station** : 8.65 m s^{-1},114° u = 0.0343 m s^{-1} v = 0.0188 m s^{-1} Vitesse = 0.0391 m s^{-1} Direction = 55°

forcing hoa currents (see above). Nevertheless, the simulated pass residual flux was oriented outside the lagoon at all times, with an order of magnitude in agreement with observations. Thus, the model reproduced correctly the process of a lagoon filled by hoa and emptied by the pass.

We concluded that the model was able to reproduce correctly the climatological circulation at the lagoon boundary, through the hoa and the pass, with simulations in agreement with measurements, and discrepancies well explained by the parameterization used (with fixed velocities in hoa). The model was then used to investigate the main patterns of the circulation inside the lagoon.

3.4. Residual circulation patterns

Observations suggest that the main driving mechanism of the lagoon circulation that must be accounted for were tide and wind forcing, and not waves, due to the small hoa residual velocities measured year long. For the numerical simulations, tidal conditions were taken realistic whereas the wind forcing was set stationary. The winds observed at the Takaroa meteorological station and considered representative of the synoptic wind were very stable and typical of trade winds. Its interannual mean speed and direction was 8 m s^{-1} and 107°, respectively.

The horizontal residual eulerian currents were properly characterized by the transport or the vertically averaged currents $(\bar{u}, \bar{v})$. It is rather straightforward to see that the transport associated with these currents computed under stationary conditions are divergence-free so that a stream function (ψ) could be derived as : $(h\bar{u}, h\bar{v}) = (-\frac{\partial\psi}{\partial y}, \frac{\partial\psi}{\partial x})$. The isolines of this stream function computed from stationary divergence-free current field coincide with the trajectories of particles that are freely advected in this field. The distance between isolines can be interpreted in terms of flow: the more two isolines are spaced the weaker is the flow passing in between. Thus the isolines reveal neatly the circulation structures, in particular the retention structures which are evidenced as closed circulation cells.

Fig. 6 shows the barotropic current function computed under various stationary meteorological conditions. Fig. 6a shows the transport associated to the tidal circulation only. The pass jet influence was remarkable whereas the transport was very weak elsewhere. The large residual circulation patterns showed that the tidal jet entering through the pass spread preferentially to the east and north-east and went out by pumping water from the south east, giving rise to large cyclonic (or clockwise) circulation patterns. ADCP profiles under weak wind conditions (less than 2 m s^{-1} over 3 days) at point A15 (Fig. 7) showed residual barotropic current in rather good agreement in direction. However; the intensity of the observed current was twice the modeled one. When a climatological wind was activated (Fig. 6b and c), the stream function displayed two main barotropic circulation structures: under climatological trades (6b) a large anticlockwise circulation patterns, located in the north occupied two third of the water body with residual currents of the order of 5 cm s^{-1}. Then, a weaker clockwise circulation patterns appeared in the south. Its shape was strongly constrained by the atoll rim. Two ADCP observations (Table 4) confirmed that in the vicinity of the pass (A15), the residual barotropic current was oriented to the east. Again, measurements showed velocities that double the model prediction. ADCP also confirmed that the residual current in the south (A18) was very weak (<1 cm s^{-1}). Finally, under climatological tradewind conditions, the tidal jet residual influence next to the pass was not visible anymore. It was probably reinforcing the northern circulation cell by spreading to the southeast during flood and pumping from the east-northeast during ebb.

Under western wind conditions (6c) two main spatial patterns emerged. The northern pattern has shifted and flattened along the northern rim and the circulation has been reversed (clockwise). The southern pattern expanded and spread to the east occupying the southern part of the lagoon. Its circulation has also been reversed. In both patterns, the residual currents reached 6 cm s^{-1}. The residual influence of the tidal jet was also modulated by the wind. It seems that it spread along the northern rim and pumped

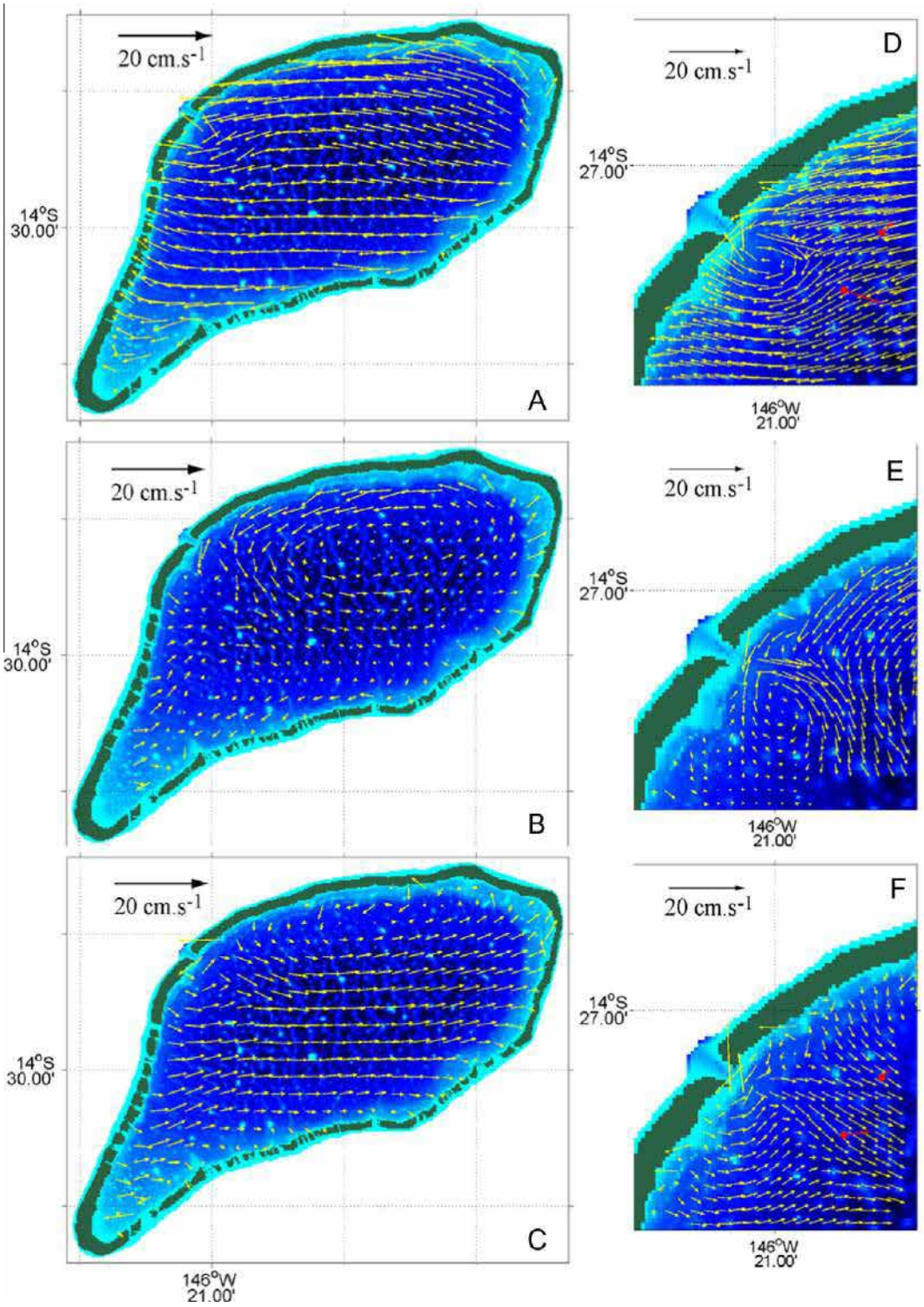

Fig. 8. Modelled residual at 2 m, 15 m below the surface and 2 m above the bottom (A–C). Panels D–F illustrate a zoom on the pass. Arrows show the estimates from ADCP measurements at location A15 and A18.

from the southeast. Everything happened as if the wind forced the shallow parts of the lagoon, inducing currents in the direction of the wind. The deeper part was constrained by continuity, and gave birth to backward currents.

The residual effects of the tidal jet appeared tightly linked to the wind conditions. Indeed, Fig. 7 shows vertical ADCP current profiles recorded at location A15 (22 m deep), in the vicinity of the pass. During this period the wind was first shifting from the north to the southwest. We first noticed the currents variability with respect to time. Currents were below 5 cm s^{-1} from the 10th to 12th of May, with no more tidal cycle visible, except on the direction. Then, the wind returned to a more frequent direction (from the southeast, then to the east). The intensity of the current increased (25 cm s^{-1}) till the end of the period, showing again clear tidal cycles. Attenuation along the vertical due to bottom friction was also noticeable. The direction showed the tidal reverse and most of the

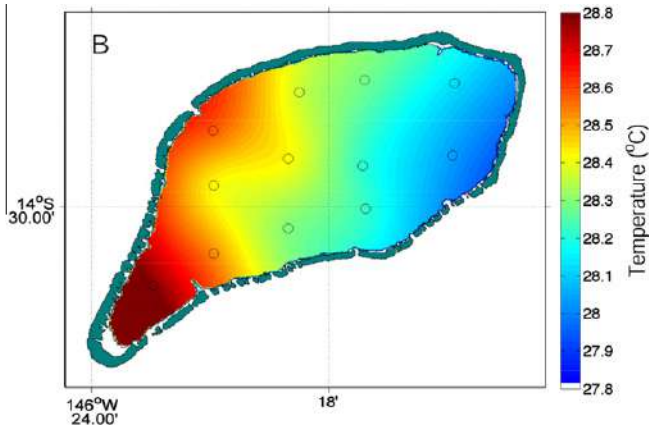

Fig. 9. Sea surface temperature (°C) from CTD casts network achieved the 9th of November 2009. Circles indicate the positions of the 12 measurements, interpolated afterwards.

time the increase of the current modulus from the surface to the bottom, evidencing the bottom Ekman pumping oriented to the right. The surface veering expected to the left at the surface is not seen, likely because an Ekman spiral cannot develop under these conditions. The current reached its maximum on the 21st of May when the wind was blowing again from the east with moderate intensity (6 m s^{-1}).

Last but not least, it clearly appears on Fig. 6a and b that the residual barotropic flow was oriented in the same direction than the wind in the shallow waters whereas it is oriented against the wind in the deeper waters. This can be noticed in both trades and west wind conditions. The Fig. 10 shows that the water column was better mixed in the shallow part of the lagoon. The wind generated current was rather homogeneous along the vertical, giving a vertical averaged current oriented in the direction of the wind on both side of the lagoon. As long as water cannot be accumulated leeward, a return current occurred in the mid part of the basin below the wind generated current.

3.5. The two-layers overturning circulation

Under climatological conditions, the simulated vertical structure circulation yielded a two-layers, overturning, circulation (Fig. 8a and c). The surface currents homogeneously flow downwind at a speed of 10 cm s^{-1}, representing the expected order of magnitude of several percent of wind speed (i.e. 8 m s^{-1}). This downwind layer lies on top of a return layer characterized by currents an order of magnitude slower, typically of few cm s^{-1}. In the middle part (Fig. 8b) of the lagoon, below the Ekman layer (15 m) the barotropic structure seen on Fig. 6a is again noticeable. It also shows that a Ekman spiral could not develop due to the basin shape constraints.

The top layer was about ten meter thick (Fig. 10), which is consistent with the structure showed by Tartinville et al. (1997, Fig. 5) for Mururoa atoll. According to the model, it is thinner in the deeper part of the lagoon. It is thicker in the shallower part, where the bottom mixed layer probably merge with the surface one, mixing the water column.

In the vicinity of the pass (Fig. 8d–f) the flow was the most complex. At the surface, the tidal jet counteracts the effect of the wind (Fig. 8d). The ADCP measurements below the surface at location A15 and A18 2 m were in rather poor agreement with the model. Below 15 m deep, both intensity and direction were in better agreement (Fig. 8f). Model and data show deep residual currents oriented against the wind direction.

The overturning circulation was confirmed by hydrological observations. Fig. 9 shows sea surface temperature (SST) horizontal distribution for the 9th of November 2009, according to CTD casts performed on the L01 to L12 hydrological network stations (Fig. 1b). Wind conditions were close to climatology conditions. For that day, data revealed a clear lagoon-wide thermal stratification which lasted over a week. The SST structure confirmed the circulation structure, with cold waters being upwelled windward along the east side of the rim, and warmer waters being pushed downwind in the southwestern corner of the lagoon.

3.6. The e-flushing time

The eulerian residual currents structure analysis from the previous section does not yield in a straightforward way a view of residence time, since the turbulent fluxes are not accounted for. This point was also discussed by Tartinville et al. (1997). We confirm their conclusions achieved on Mururoa atoll that the large lagoon horizontal gyres seen on the transport stream function tend to trap water parcels, and increase the residence time. This assumption was confirmed here by the computation of the e-flushing time. Fig. 11a shows this e-flushing time computed under typical climatological trade winds. The patterns fit very well with the structure

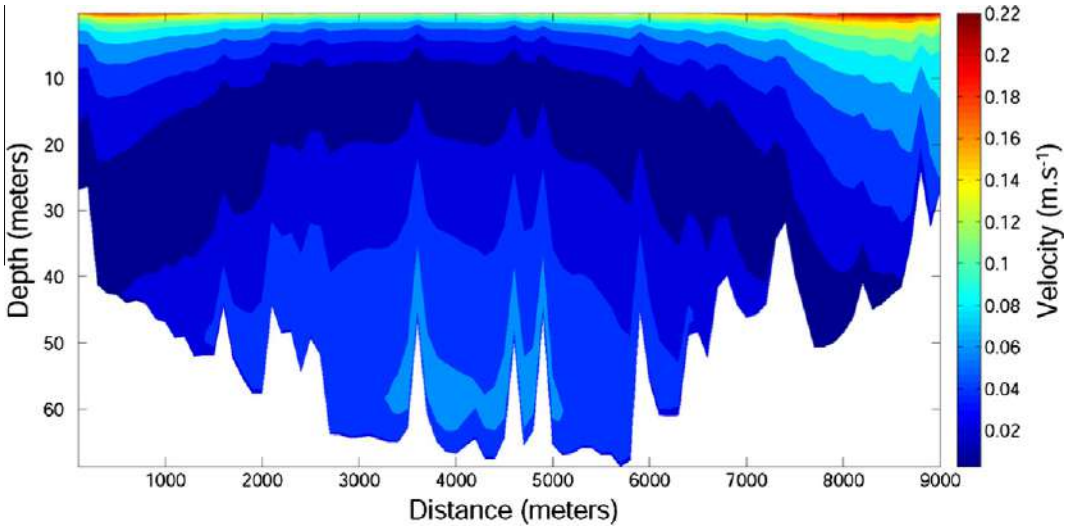

Fig. 10. Middle lagoon (146°18′W) north–south vertical section of the residual currents modelled under stationary trade winds (in m s^{-1}).

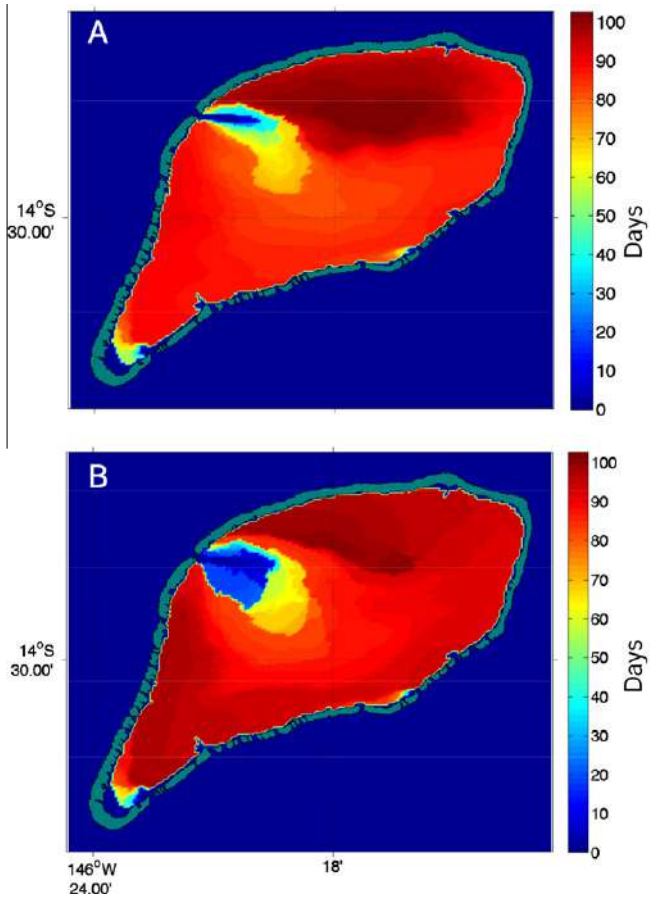

Fig. 11. (a) Resulting e-flushing time under stationary trade winds (107° – 8 m s^{-1}). (b) e-flushing time under realistic winds measured from January to April 2009.

of the stream function (Fig. 6b). The northern gyre shown previously coincided here with a trapped water mass with a e-flushing time greater than 100 days. The pass played a significant role in separating the lagoon into three water-bodies. In the vicinity of the pass, the e-flushing time was lower, about 50–60 days. To the north and to the south, e-flushing times were larger, around 80 days to the south, more than 100 days to the north, and reached 140 days in the core of the northern circulation cell. Furthermore, this structure was rather homogeneous along the vertical (not shown), fitting well with the stream function structure. This is in agreement with the fact that the shorter time scale of the flow is associated with vertical diffusion. The average e-flushing time over the entire domain was about 80 days.

Fig. 11b shows the same quantity computed under a realistic sequence of winds taken from the beginning of January 2009–April 2009. The orders of magnitude were about the same and the structures were similar to the climatological conditions patterns. Nevertheless some differences can be pointed out:

- The influence of the pass was larger towards the south.
- The extension of the north cell was reduced but its e-flushing time remained similar (above 100 days).
- The south cell was clearly reinforced. Its water body seemed to be more isolated, and its e-flushing increased to up to 90 days.

The e-flushing time could be averaged over the entire lagoon during the realistic wind conditions. We obtained a result close to the climatological situation, with an average of 80 days.

4. Discussion

4.1. Residence time, renewal time and e-flushing time

Residence time is a key variable to characterize a water body. Different computation schemes have been proposed (see Jouon et al., 2006 for review), and we have defined here the e-flushing time. Previous studies (Atkinson et al., 1981, Delesalle and Sournia 1992, Tartinville et al., 1997; Kraines et al., 1999; Andréfouët et al., 2001) offered lagoon-scale measurements, typically by establishing a budget between water inputs and outputs at the lagoon boundary, or if spatial numerical methods were involved, they computed the average time needed for a tracked particle to leave the lagoon. The power of a well validated, trustable, numerical 3D model is of course to provide a spatially-explicit view (a map) of the variations of residence time in the focal lagoon, itself leading to an integrated lagoon-scale water renewal time when needed (Andréfouët et al., 2001). For Ahe lagoon, if we consider the average output residual flux through the main pass estimated by the ADCP measurements and if we assume that all the water entering through the hoa is eventually flushed out by the pass, then the water body is renewed at the rate of this flow. This was estimated at around 260 m^3 s^{-1}, which for a 5.9 km^3 lagoon volume, yields a renewal time of 252 days. This renewal time is not what is observed in the computed e-flushing time (Fig. 11). Indeed, the model accounts for the spatial structure of the circulation and specifically for the action of the tidal flow through the pass. As demonstrated in the previous sections, the pass partitions the lagoon into three circulation cells. Inbound flows entering the lagoon through the southern rim does not flow homogenously and directly to the pass. This flow is trapped in the various cells of circulation where the e-flushing time is above 80 days almost everywhere except in the vicinity of the pass.

In terms of larval dispersal and spat collecting, the e-flushing time is relevant assuming there is a synchronous and homogeneous spawning at the initial time, over the entire domain. Illustrations of the spatial variations in terms of retention, accumulation and exports are provided by Thomas et al. (2012a,b) who complete the picture given here.

4.2. Tide-driven lagoon flushing and circulation

The lagoon water flushing through the pass influences primarily the lagoonal volume next to the pass (Fig. 11). The net flushing is significant, under the assumption that the water mass re-entering the lagoon is not the same than the water that just left. This process could rapidly renew the water body even if the residual flow of this purely tidal-driven process is quantitatively null. Under the above assumption, the Ahe model suggests that tidal flushing decreases the renewal time: the mean e-flushing – which could be considered of the same order of magnitude as the renewal – time is around 80 days whereas the renewal time is of 252 days. This is in contrast with Callaghan et al. (2006) who concluded that wave flushing was more efficient than pure tidal flushing. Of course atolls studied by Callaghan et al. (2006) did not have a pass, had larger reef flat width to perimeter ratios, and likely had a different, more energetic, wave climate. We conclude here for Ahe that tide is the major flushing driver as long as it is combined to wind forcing. In fact, the internal circulation induced by tide alone (Fig. 6a) is very weak and yields lagoon scale renewal time and average e-flushing time far longer than those obtained when the wind is blowing. Tartinville et al. (1997) made similar observations for Mururoa atoll, although Kraines et al. (1999) insisted that in Majuro Atoll, the main flushing driver was the radiation-stress-driven flow (i.e. wave flushing) from the reef flats through the hoa.

4.3. Overturning circulation and stratification

CTD casts have been performed in Ahe atoll lagoon in 2008–2009 during surveys aimed at characterizing relationships between pearl oyster larvae densities and hydrological conditions (Thomas et al., 2012a,b). The same L02-L12 stations were used here to compute a mean average stratification presented on Fig. 12. Fig. 12 confirms a frequent detectable stratification occurring in Ahe lagoon, with surface and bottom SST differences in 2008 and 2009, depending on wind speed (averaged here over the 3 days preceding the observations). The wind component the most correlated with the stratifications is the one projected on the 35° axis of the lagoon, in other words parallel the largest atoll dimension. However, most of the time the thermal stratification is very weak: in 80% of the observed situations, they are below 0.3 °C. It is also noticeable that negative thermal stratifications (i.e. bottom temperature higher than surface temperature) frequently occurs and seems to be compensated by negative haline stratification.

With winds blowing above 3 m s^{-1} in the 35° direction, the stratifications are very weak (less than 0.2 °C), whereas in light to medium wind conditions, the lagoon waters may get stratified. Observed stratification frequently reach above 0.4 °C, and up to 1.2 °C (in November 2009). Typically, under such thermal flux and wind conditions, the water column is stratified. This is seen oceanward just outside the lagoon on CTD casts performed at the same time. Casts showed a sharp thermocline located at 45 m. Thermal stratification appeared much more limited in the lagoon. The de-stratification cannot be explained easily by direct mixing due to wind, neither because of bottom friction generated turbulence, since bottom currents remained very weak. The general overturning circulation is likely to be responsible for the mixing of the lagoon water body. In light to medium wind conditions, the overturning circulation weakens, allowing the development of a vertical stratification. In more intense wind, the circulation is strong enough to prevent stratification, by upwelling windward the bottom cold water and downwelling leeward the surface warm water. This explanation is confirmed by the weak stratifications observed under light wind conditions. This probably shows that wind direction rather than wind intensity make the overturning circulation more or less efficient tin mixing the water column. The most intense stratification over the 3 years (2007–2009) was observed during period of wind coming from 130° (November 8–10th 2009), a direction which significantly departs from the climatological tradewinds (i.e. 107°). Nevertheless, the stratification in Ahe appear limited in intensity and in time. This could explain why stratification was neither reported by Atkinson et al. (1981) in Enewetak nor Kraines et al. (1999) in Majuro, although it may occur in Ahe.

4.4. Comparing atoll lagoons hydrodynamics: towards a functional typology of Pacific Ocean atolls?

Following Atkinson et al. (1981), Ahe atoll lagoon can be classified as a "deep" lagoon not only because of its average depth but in the sense that circulation is dominated by wind and not by tide, and because the primary wind-driven circulation pattern is a downwind surface flow and a returning upwind deep flow. However, Ahe lagoon departs from the circulation scheme described by Atkinson et al. (1981) for Enewetak lagoon in the Marshall Islands, and by von Arx (1948) for Bikini lagoon, also in the Marshall Islands. In Enewetak, radiation stress due to breaking waves on the windward eastern side are an important forcing factors of water exchanges and circulation, but not in Ahe. The geomorphology of the atolls are also very different with three passes in Enewetak, each with their own behaviour, *versus* one in Ahe. These passes oriented the deep water flows in Enewetak, but not in Ahe. Moreover, in terms of water exchanges, whereas Atkinson et al. (1981) reported a net positive (albeit weak) outflow across the Enewetak leeward rim margin, in Ahe, the entire windward wave-driven flow was flushed through the pass. Indeed, if we consider at Ahe that the average speed within the hoa are of the order of 10 cm s^{-1} as observed, this yields a total windward flux (assuming that all the southern hoa work in the same way) of the order of 260 m^3 s^{-1}. On the leeward side, the maximum speed observed was around 20 cm s^{-1} giving a total output flux of 30 m^3 s^{-1}. In the same time, the mean output flux in the main pass was around 260 m^3 s^{-1}. The conclusion is that the lagoon water body received water windward but flushed entirely this excess water through the main pass.

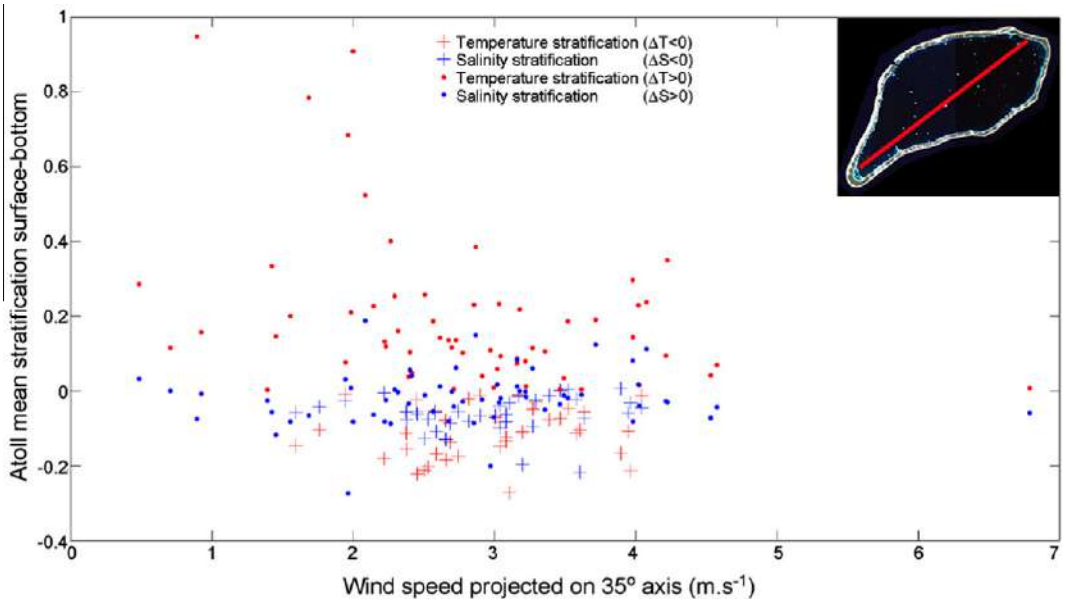

Fig. 12. Mean thermal and haline stratifications (surface minus bottom) computed over the eleven stations of the CTD observation network. Red dots are positive thermal stratifications, blue dots are haline stratification. Same for the crosses that show negative thermal stratification. The *x*-axis is the average wind over the past 3 days projected on the 35° axis (largest dimension) of the lagoon. (For interpretation of the references to colour in this figure legend, the reader is referred to the web version of this article.)

The circulation patterns and computed time scales in Ahe appear very close to Mururoa's (Tartinville et al., 1997) despite the different morphology (5 km wide pass, 33 mean depth in Mururoa *versus* a 0.2 km wide pass and 41 m mean depth in Ahe). Hoa played a minor role in both atolls. Typical velocity observed in the hoa were weak (around 10 cm s^{-1} and in case of Ahe peaking at 35 cm s^{-1}) (Tartinville and Rancher, 2000) and their depth and cumulated length were small compared to the perimeter of the rim. Thus, most aspects of the circulation were driven by wind and tide, justifying their classifications as "Deep" lagoons (Atkinson et al., 1981). However, the rim geomorphology plays a significant role and influence the circulation in the lagoons: in Ahe, the pass divided the circulation inside the lagoon into three main cells whereas the 5 km-long pass in Mururoa confined only a single cell along the southern rim. Barotropic transport was weaker in Ahe, with the stream function peaking at 300 $m^3 s^{-1}$ in Ahe *versus* 1500 $m^3 s^{-1}$ in Mururoa under the same wind forcing (i.e. about 8 m s^{-1}). Renewal times obtained with comparable methods were of comparable magnitude with 80 and 100 days in Ahe and Mururoa, respectively.

Despite the differences primarily explained by a semi-closed geomorphology, Ahe atoll shares several general circulation features with previously describe Pacific open atolls, such as Bikini (von Arx, 1948), Enewatak (Atkinson et al., 1981), Mururoa (Tartinville et al., 1997) and Majuro (Kraines et al., 1999). The vertical structure circulation that we obtain by simulation in Ahe lagoon has already been described for Bikini, Enewatak and Mururoa. In contrast, for atolls without passes, excess waters due to wave radiation stress cannot be flushed through these passes. Instead, flushing occurs by gravity when the lagoon surface reaches an elevation allowing water to flow oceanward across the rim located on the protected side of the atoll, from the opposite direction of the incident waves. The hydrodynamic functioning of such a closed atoll (in the sense that there is no pass) has been formalized by Callaghan et al. (2006) for two Cook Islands atolls (Manihiki and Rakahanga). They described a flushing mechanism driven by wave pumping on the exposed side of the rim and modulated by the ocean tide. A key feature is that lagoon water levels remain above the ocean level regardless of the tidal phase.

5. Conclusion

If we consider the small completely closed atolls (no pass, neither any functional reef flats, such as Taiaro and Clipperton, in Leclerc et al. (1999) and Charpy et al. (2010)), the small atolls with no passes but with reef flats (Manihiki and Rakahanga studied by Callaghan et al. (2006)), the small open but deep and compartmentalized atoll (Palmyra, Gardner et al., 2011), the large open atolls with passes and reef flats (Enewetak, Bikini, Majuro, Mururoa studied by authors cited above), the case study represented by Ahe atoll (medium size, deep atoll, semi-closed with passes and few reef flats) offers a different geomorphological setting, and not surprisingly a somewhat different scheme and set of conclusions compared to all the previous studies.

Among the studied Pacific atolls, only Majuro, Mururoa, Ahe and Takaroa (unpublished results, but similar study as Ahe presented here) lagoons have been studied with 3D numerical models to our knowledge (Andréfouët et al., 2006). Other atolls have been characterized from *in situ* physical and hydrobiological measurements only but they equally contribute to establish the continuum of variations in atoll hydrodynamics functioning. Since there are no large, closed atolls in the Pacific Ocean (nor elsewhere), the geomorphological range of studied atolls is now getting significant and quite complete. Establishing a hydrodynamical typology of lagoons based only on geomorphology would be a first logical step, but each atoll needs to be related to its physical boundary conditions to be rigorous and before generalizing. A previous atoll classification based on water renewal time was established for Tuamotu Archipelago according to geomorphology and wave forcing (Andréfouët et al., 2001). Wave forcing is a critical parameter that can vary widely between atolls at short distance. For instance, Ahe and Takaroa atolls wave climate is quite different than atolls only 100 km away due to the sheltering barrier-effects of large atolls in the south (Andréfouët et al., 2012b). Lagoon-scale variables were used for this previous Tuamotu atoll classification, but an atoll typology based on the relative importance of the wind-driven, tide-driven, wave-driven, and density-driven processes on the internal lagoon circulation is now shaping up.

In terms of aquaculture, the results obtained here highlight the weak flushing of Ahe lagoon that itself leads to renewal time and e-flushing time that appear very long (at least some tenths of days) compared to the larval life of the pearl oyster *P. margaritifera* (15–30 days, Thomas et al., 2012a,b). Thus, the retention capability of Ahe appears very interesting in regards to larval dispersal and the potential for spat collecting, contributing to explain analytically why Ahe is one of the most important producers of pearl oyster juveniles in French Polynesia.

Finally, the 3D model of Ahe lagoon will provide the needed diagnostic tool to characterize the physical mechanisms that control the spatio-temporal variations of biological variables in the water column, such as planktonic communities.

Acknowledgements

This study was funded by the 9th European Development Fund (Grant POF/001/002N°1 to Serge Andréfouët and Loic Charpy, IRD) through the French Polynesia Service de la Perliculture. The authors are grateful to the colleagues who participated to the numerous surveys and to the project in general, specifically Alain Loyat (Project manager), Joël Orempuller, Nicolas Maihota, Jean-Yves Panché, David Varillon, Francis Gallois, Mainui Tanetoa, and Nahiti Vernaudon, from IRD-Tahiti, IRD US191 in Nouméa and Service de la Perliculture. Useful insights were provided by Sylvain Ouillon and Pascal Douillet in the early stages of the project. Météo France and the French Hydrographic Service provided data for this study. GéoPolynésie (Christian Friot) was contracted for the bathymetry survey of Ahe atoll.

References

Andréfouët, S., Pagès, J., Tartinville, B., 2001. Water renewal time for classification of atoll lagoons in the Tuamotu Archipelago (French Polynesia). Coral Reefs 20, 399–408.

Andréfouët, S., Ouillon, S., Brinkman, R., Falter, J., Douillet, P., Wolk, F., Smith, R., Garen, P., Martinez, E., Laurent, V., Lo, C., Remoissenet, G., Scourzic, B., Gilbert, A., Deleersnijder, E., Steinberg, C., Choukroun, S., Buestel, D., 2006. Review of solutions for 3D hydrodynamic modeling applied to aquaculture in South Pacific atoll lagoons. Marine Pollution Bulletin 52, 1138–1155.

Andréfouët, S., Charpy, L., Lo-Yat, A., Lo, C., 2012a. Recent research for pearl oyster aquaculture management in French Polynesia. Marine Pollution Bulletin 65, 407–414.

Andréfouët, S., Ardhuin, F., Quefeullou, P., Le Gendre, R., 2012b. Island shadow effects and the wave climate of the Western Tuamotu Archipelago (French Polynesia) inferred from altimetry and numerical model data. 65, 415–424.

Atkinson, M., Smith, S.V., Stroup, E.D., 1981. Circulation in Enewetak atoll lagoon. Limnology and Oceanography 26, 1074–1083.

Blumberg, A. F. and G. L. Mellor (1987). A description of a three-dimensional coastal ocean circulation model, Three-Dimensional Coastal ocean Models, edited by N. Heaps, 208 pp., American Geophysical Union, 1987.

Callaghan, D., Nielsen, P., Cartwright, N., Gourlay, M., Baldock, T., 2006. Atoll lagoon flushing forced by waves. Coastal Engineering 53, 691–704.

Charpy, L., Rodier, M., Couté, A., Perrette-Gallet, C., Bley-Loëz, C., 2010. Clipperton, a possible future for atoll lagoons. Coral Reefs 29, 771–783.

Delesalle, B., Sournia, A., 1992. Residence time of water and phytoplankton biomass in a coral reef lagoons. Continental Shelf Research 12, 939–949.

Demerliac, A., 1974. Calcul du niveau moyen journalier de la mer. Rapport du service hydrographique de la marine 741, 49–57.

Dufour, P., Andréfouët, S., Charpy, L., Garcia, N., 2001. Atoll morphometry controls lagoon nutrient regime. Limnology and Oceanography 46, 456–461.
Gardner, J.P.A., Garton, D.W., Collen, J.D., 2011. Near-surface mixing and pronounced deep-water stratification in a compartmentalised, human-disturbed atoll lagoon system. Coral Reefs 30, 271–282.
Gaspar, P., Grégoris, Y., Lefevre, J., 1990. A simple eddy kinetic energy model for simulations of the oceanic vertical mixing: tests at Station Papa and long-term upper ocean study site. Journal of Geophysical Research 95 (C9), 179–193.
Jouon, A., Douillet, P., Ouillon, S., Fraunié, P., 2006. Calculations of hydrodynamic time parameters in a semi-opened coastal zone using a 3D hydrodynamic model. Continental Shelf Research 26, 1395–1415.
Kraines, S., Suzuki, A., Yanagi, T., Isobe, M., Guo, X., Komiyama, H., 1999. Rapid water exchange between the lagoon and the open ocean at Majuro Atoll due to wind, waves, and tide. Journal of Geophysical Research 104 (C7), 15635–15653.
Lazure, P., Dumas, F., 2008. An external-internal mode coupling for a 3D hydrodynamical model for applications at regional scale (MARS). Advances in Water Resources 31, 233–250.
Leclerc, A.M., Baptiste, P., Texier, D., Broc, D., 1999. Density induced water circulation in atoll coral reefs: a numerical study. Limnology and Oceanography 44, 1268–1281.
Luyten, P.J., De Mulder, T., 1992. A module representative surface fluxes of momentum and heat. Technical report No. 9 MAST-0050-C (Mumm), 30pp.
Lyard, F., Lefevre, F., Letellier, T., Francis, O., 2006. Modelling the global ocean tides: modern insights from FES2004. Ocean Dynamics 56, 394–415.
Pawlowicz, R., Beardsley, B., Lentz, S., 2002. Classical tidal harmonic analysis including error estimates in MATLAB using T_TIDE. Computers and Geosciences 28, 929–937.
Pugh, D.T., 1979. Sea levels at Aldabara atoll, Mombasa and Mahé, western equatorial Indian Ocean, related to tides, meteorology and ocean circulation. Deep Sea Research 26, 237–258.
Salvat, B., 2009. Dominant benthic mollusks in closed atolls, French Polynesia. Galaxea 11, 197–206.
Tartinville, B., Rancher, J., 2000. Wave-induced flow over Mururoa atoll reef. Journal of Coastal Research 16, 776–781.
Tartinville, B., Deleersnijder, E., Rancher, J., 1997. The water residence time in the Mururoa atoll lagoon: sensitivity analysis of a three-dimensional model. Coral Reefs 16, 193–203.
Thomas, Y., Le Gendre, R., Garen, P., Dumas, F., Andréfouët, S., 2012a. Bivalve larvae transport and connectivity within the Ahe atoll lagoon (Tuamotu Archipelago), with application to pearl oyster aquaculture management. Marine Pollution Bulletin 65, 441–452.
Thomas, Y., Garen, P., Bennett, A., Le Pennec, M., Clavier, J., 2012b. Multi-scale disctribution and dynamics of bivalve larvae in a deep atoll lagoon (Ahe, French Polynesia). Marine Pollution Bulletin. 65, 453–462.
Von Arx, W.S., 1948. The circulation systems of Bikini and Rongelap lagoons. Transactions, American Geophysical Union 29, 861–870.

Marine Pollution Bulletin 65 (2012) 441–452

Contents lists available at SciVerse ScienceDirect

Marine Pollution Bulletin

journal homepage: www.elsevier.com/locate/marpolbul

Bivalve larvae transport and connectivity within the Ahe atoll lagoon (Tuamotu Archipelago), with application to pearl oyster aquaculture management

Y. Thomas [a,b,*], R. Le Gendre [c,1], P. Garen [b], F. Dumas [d], S. Andréfouët [c]

[a] Ifremer, DPFOM LPI, Presqu'île du Vivier, 29840 Argenton, France
[b] Ifremer, COP, BP 7004, 98719 Taravao, Tahiti, French Polynesia
[c] IRD, UR 227 CoRéUs, BP A5, 98848 Nouméa Cedex, New Caledonia
[d] Ifremer, DYNECO/PHYSED, BP 70, 29280 Plouzané, France

ARTICLE INFO

Keywords:
Transport model
Connectivity
Bivalve larvae
Pearl oyster
Atoll lagoon
French Polynesia

ABSTRACT

Patterns of bivalve larvae dispersal in the deep Ahe atoll lagoon was studied by using a numerical 3D transport model (MARS3D) coupled with a vertical swimming sub-model, forced mainly by tide and wind-induced currents. The simulations were validated against observations of larval dispersal monitored several days throughout the lagoon. Connectivity matrices describing larval exchanges inside the lagoon were inferred. Larvae displayed a significant dispersal capacity at the lagoon scale, especially with dominant eastern winds. With southeastern winds, larvae mostly remained in their origin sector. The total export rate of the larvae, toward the ocean through the pass and shallow lagoon borders, was independent of the wind conditions, with 1% of the total concentration exported per day. However, the tide-driven currents efficiently flushed larvae in sectors close to the pass. Connectivity matrices suggest that the south and west sectors were more suitable for spat collecting and that central sectors would be efficient sanctuaries if genitors were accumulated.

1. Introduction

More than 70% of the benthic invertebrates present a planktonic life stage during their larval development (Thorson, 1950). The settlement of these species, defined as the integration of juveniles in a population (Connell, 1985), is one of the main processes governing temporal variations and spatial structure of the adult populations (Ellien et al., 2004). Numerous studies are investigating the physical and biological factors that influence settlement and the consequences on adult population structure, larval dispersal, export rates, and spatial connectivity (Eckman, 1996; Grantham et al., 2003; Shanks et al., 2003; Cowen et al., 2007). In tropical ecosystems, significant research efforts have investigated the connectivity of populations through modelled larval dispersal between source input sectors and sink settlement locations, so as to protect, preserve and manage biodiversity (Roberts, 1997; Swearer et al., 1999; Botsford et al., 2009; Munday et al., 2009; Kool et al., 2010). Most of these efforts focussed on large-scale oceanic dispersal with coarse resolution model. Few studies have investigated realistically small coastal domains at high spatial resolution, and even fewer the dispersal patterns within semi-closed water bodies like atoll lagoons (see review of atoll lagoon modelling in Andréfouët et al. (2006)). Atoll lagoons are generally saucer-shaped basins, with an average depth closer to 20–30 m, reaching ~70 m in its maximum. Atolls fine-scale topography may be complex, with frequent coral patches that reach vertically to the surface (pinnacles). Landscape is made of small islands and reef-flat spillways (*hoa*, less than 50 cm depth) distributed along the atoll rim in various possible configurations (Andréfouët et al., 2001a). Deeper passes through the rim, generally narrow (few tens of meters) with a few meters depth in its shallowest part, may be present in Tuamotu atolls. Flows though these passes is primarily modulated by tides. The moderate depth and semi-closed status of Western Tuamotu atolls suggest that lagoon circulation forcing can be dominated by either winds or waves (Andréfouët et al., 2006).

Like for all bentho-pelagic species in their own environment, diversity and structure of molluscan populations in atoll lagoons is highly dependent on local factors such as habitat type (substrate type, light intensity, depth, etc.) and water circulation and current (Pante et al., 2006). The abundance and distribution of adult populations would thus be dependent on the success of larval life and fixing process (Adjeroud et al., 2000). Larval dispersal processes have been studied at various spatial scales with population genetics (Siegel et al., 2003), *in situ* tracking of larval cohorts (McQuaid and Phillips, 2000) and by numerical modelling (Verdier-Bonnet et al., 1997; Edwards et al., 2006; Viard et al., 2006; North et al.,

* Corresponding author at: Ifremer, DPFOM LPI, Presqu'île du Vivier, 29840 Argenton, France. Tel.: +33 2 98 89 29 43; fax: +33 2 98 89 29 59.
E-mail address: yoann.thomas1@gmail.com (Y. Thomas).
[1] Present address: Ifremer, LERN, Avenue du Général de Gaulle, 14520 Port-en-Bessin, France.

0025-326X/$ - see front matter © 2012 Elsevier Ltd. All rights reserved.
doi:10.1016/j.marpolbul.2011.12.027

2008; Jolly et al., 2009). Some of these modelling exercises have quantified the effect of hydrological conditions on selected specie dispersal taking into account realistic estimates of mortality and larval behaviour (Levin, 2006). Specifically, even considering the low swimming capacity of invertebrate larvae in comparison to water speed and flow, it appeared that swimming behaviour, especially vertically, might significantly influence transport and dispersal (Shanks and Brink, 2005; Guizien et al., 2006; North et al., 2008).

In Ahe atoll, French Polynesia, recent studies put in evidence the lagoon-scale spatio-temporal heterogeneity of the bivalve larvae concentrations and the consequences for collection of the targeted black-lip pearl oyster for the local aquaculture industry (Thomas et al., 2012). In French Polynesian atoll lagoons, the black-lip pearl oyster (*Pinctada margaritifera cumingii*, Linné 1758) farming plays a major socio-economic role since the 1990s (Andréfouët and Charpy, 2012). The entire farming activity relies on the collection of black-lip pearl oyster juveniles on artificial collectors. However, collecting success has remained unpredictable with large spatio-temporal variations (Brié, 1999) and pearl farms activities remained vulnerable to steady availability of oysters. Andréfouët et al. (2006) recommended a spatially explicit numerical modelling approach to study and forecast spat collecting potential on Polynesian atoll lagoons. Dumas et al. (2012) made this recommendation a reality using the hydrodynamical model MARS3D (Lazure and Dumas, 2008) implemented for the deep atoll lagoon of Ahe atoll in French Polynesia. Here, we extend the hydrodynamical and circulation modelling work of Dumas et al. (2012) to the simulation and validation of bivalve larvae transport in Ahe atoll.

Specifically, the objectives of the present study are (1) to calibrate, integrate and validate a model of vertical swimming for the bivalve larvae, (2) to validate the transport model integrating the swimming sub-model with data acquired *in situ* and (3) to evaluate the intra-lagoonal connectivity patterns and quantify exchanges between potential sink and source sectors. The consequences of larval dispersal on pearl oyster settlement variability and aquaculture management are discussed.

2. Materials and methods

2.1. Study site

Ahe atoll is located in the North-western part of the French Polynesian Tuamotu Archipelago, 500 km North-East of Tahiti island (Fig. 1). Ahe lagoon covers 145 km^2 with a mean depth close to 40 m. One active pass is located in the western part of the lagoon and several reef-flat spillways (*hoa*, less than 50 cm depth) are distributed along the reef rim, mainly in the south and west part sectors (Dumas et al., 2012). The overall aperture is low, and Ahe can be defined as a semi-closed atoll.

Ahe is submitted to dominant easterly tradewinds, which are stronger from April to October. According to a meteorological station located in a nearby atoll (Dumas et al., 2012), the mean annual wind is around 6 m s^{-1}, from 107°, with a winter season, from April to October, showing southeastern wind trend (135°, 7 m s^{-1}) and a warm season with eastern winds (90°, 6 m s^{-1}). Ocean tidal amplitudes near Ahe atoll are small (around 40 cm) due to its proximity to an amphidromic point (Dumas et al., 2012).

2.2. Biological model description

Species *P. margaritifera var. cumingii*, known under the name: black-lip pearl oyster, is a molluscan from the *Pteriidae* family. *P. margaritifera* is found in the Indo-Pacific coral reef ecosystems, from the Red Sea to the Central America. This species is particularly abundant in the Polynesian Archipelago. The black-lip pearl oyster fixes itself mostly in lagoons, between 0 and 50 m depth, thanks to its byssus. Preferred substrates are coral on pinnacles and dead substrate, as well as debris from coral and mollusc shell on lagoon sandy bottom. The bulk of the natural stock was found below 30 m depth in the few atolls where the natural stock was assessed (e.g., Takapoto atoll, Zanini and Salvat, 2000). Maturity can be reached during the first year, followed by an important gonad development during the second year (Tranter, 1958; Thielley, 1993; Pouvreau et al., 2000). Gametogenesis is quick (1 month), and is observed throughout any given year with a significant asynchronism. Nonetheless, austral summer is the more favourable period (Pouvreau et al., 2000). At each spawning event, released gamets corresponds to 10% of the total flesh weight (Pouvreau et al., 2000). Females propagate up to 40–50 millions of eggs (50 μm) at each spawn. Males propagate 10–100 time more spermatozoa (5 μm). The first larval stage (D-larva, 80 μm), is reached after 24 h. A ciliate organ (the velum) allows swimming and feeding activities. The lifespan of the larval stage, observed in hatcheries averages 21 days for *P. margaritifera* (Doroudi and Southgate, 2003). However, depending on environmental conditions (e.g., temperature, food concentration), lifespan may vary from 15 to more than 30 days (Thomas et al., 2011). At the end of their development, larvae reach

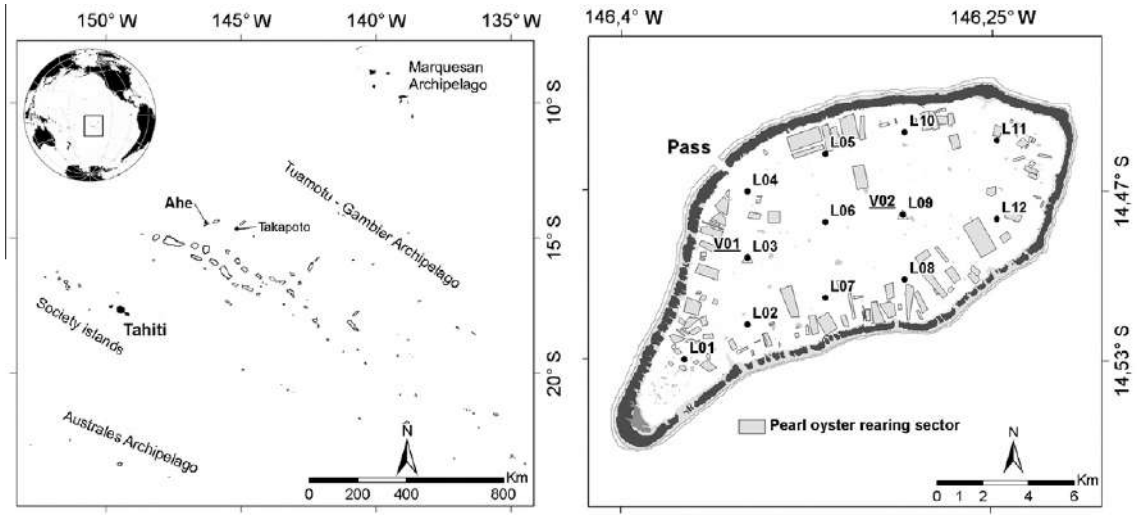

Fig. 1. Location and general morphology of Ahe atoll, with positions of the sampling stations to study vertical cycles (V01 and V02), and lagoon wide concentrations (L01–L12).

230 μm length on average. After metamorphosis, young spats (250 μm) fixe themselves to the substratum with a byssus. The growth is fast, and juveniles reach 10–12 cm length after 2 years. Adult life duration may be more than 12 years, with a theoretical maximum length of 18 cm depending on atolls (Sims, 1994; Pouvreau and Prasil, 2001).

During our surveys, in 2007 and 2008, almost 10% of the Ahe lagoon area was dedicated to black-lip pearl oyster rearing (adult oysters, Fig. 1). The total stock of cultivated pearl oysters was estimated at 15 million individuals (Perliculture Service, pers. comm.). The extent of the wild population remains unknown. The exact position of each collection line is also unknown, but the extent and boundaries of each concession, and the number of lines per concession are registered. With nearly 1245 recorded spat collection stations (with a theoretical 600 collectors per station), distributed mainly in the western part of the lagoon, Ahe is one of the most important juvenile producers in French Polynesia.

2.3. The bio-physical larval transport model

Larval transport and dispersal were simulated with the 3-D hydrodynamic model MARS3D, which resolves the ocean dynamics equations (Lazure and Dumas, 2008). This model implements a set of partial differential equations resolved with finite differences. It simulates the ocean dynamics under the combined effect of tide, wind and thermal exchanges between the ocean and the atmosphere. The specifics of implementation for Ahe are explained by Dumas et al. (2012). In short, the model is constrained by a horizontal cell size of 100 m by 100 m, as a compromise between a correct representation of the physical structures governing the circulation (pass, bathymetric variations, *hoa*) and the calculation cost. The vertical spatial resolution of the model respects the range of water depths in Ahe lagoon with 23 sigma-vertical layers. These sigma-vertical layers are tightened close to the bottom and to the surface in order to better represent velocity gradients in the interface layers. With maximum water flows observed *in situ* close to 2–3 m s^{-1}, a time step of 10 s was used, allowing model stability.

To model Ahe lagoon, four different levels of nesting were required. The first three levels are bi-dimensional horizontal approximation to describe the open boundary conditions of the atoll, including astronomical and meteorological tides. These are: Rank 0 for all the Polynesia (3 km grid); Rank 1 for the vicinity of Ahe and the nearby Manihi atolls (1 km grid): Rank 2 for a close-up on Ahe and Manihi atolls (300 m grid). The wider model is forced by a sea level signal harmonically composed from FES2004 (Lyard et al., 2006), accounting for an inverse barometric correction estimated from the NCEP Global Data Assimilation System (GDAS) pressure field. The barotropic mode (sea surface height and mean vertical velocity) along the open marine boundaries is thus provided by the immediately wider model of the embedment. Finally, the detailed inner hydrodynamic model has a spatial resolution of 100 m. It encompasses entirely the lagoon, the rim and the external slope. For the simulations presented here, water entrance through each *hoa* was forced during 6 h around the high tide with water flowing at 0.5 m s^{-1}, in agreement with to the mean velocity measured *in situ*. A complete description of the model and its validation can be found in Dumas et al. (2012).

The hydrodynamic model was coupled with an advection/dispersal module, itself integrating a model allowing reproducing the dial vertical swimming of the bivalve larvae. To summarise, the larval transport simulated Eulerian transport since the state variables were calculated at a fixed point. Larval distribution was thus described as a network of larval concentrations, transported as a function of time by the water flow network (as calculated by the dynamics equations) and by the vertical swimming displacement (as established by *in situ* observations). The larvae exported to impracticable sectors for farming activity, into the ocean, the pass or shallow waters (less than 5 m-deep), may be remobilized into the global larval pool *via* inbound exchanges through the pass and the *hoa*, or from the shallow waters to the deeper one.

Larval vertical displacement may result from three types of forcing: swimming, convection and turbulent mixing. *In situ* observations showed that bivalve larvae follow a dial migration toward the surface during the night and toward the bottom during the day (Thomas et al., 2012). The sub-model of vertical migration coupled to the transport model empirically simulated the vertical migration of the larvae depending on the swimming behaviour observed *in situ*. Here, no horizontal movement was introduced into the swimming model in agreement with the fact that oysters' larvae swim helicoidally with a limited horizontal displacement (North et al., 2008; Troost et al., 2008).

The swimming model simulates vertical displacement velocity of larvae as a function of the hour of the day, according to a sinusoid centred on 0, forcing a positive velocity during the night (going up) and a negative velocity (going down) during the day:

$$v = \alpha \sin(\omega t + \varphi) \quad (1)$$

with v the vertical velocity (m h^{-1}), α the half-amplitude of the sinusoid (m h^{-1}), ω the pulsation ($\omega = 2\pi/T$) (rad h^{-1}) with T the period, t the time (h) and φ the phase at the origin of the sinusoid (radian).

2.4. Larval transport model validation

2.4.1. Swimming model validation

Data used to calibrate/validate the vertical swimming model came from two deep stations, V01 and V02 (50 m deep), located in the west and the central-east part of the lagoon, respectively (Fig. 1). Water samplings were realised by pumping from a boat over the whole range of five layers (0–10, 10–20, 20–30, 30–40 and 40–50 m). A mesh retained larvae with a length between 40 and 250 μm. Water was sampled from each layer with a continuous flow and a pipe diving speed of 1 m every 30 s, providing an average pumping rate of 43 ± 4 l m^{-1}. Each station was sampled every 4 h, from 8 h AM, during a 24-h cycle. The two stations were successively visited at a 24-h interval. These day/night cycles were studied in April 2007, July 2007 and February 2008.

The swimming model was firstly calibrated into a 1-D model, simulating the concentration variations into five 10-m layers according to the hour and vertical velocity. The calibration step was made on three of the 24-h cycles, showing the smaller wind velocity in order to avoid the turbulences effect and to only consider the active displacement of the larvae. Next, the calibrated model was implemented into the 3-D model and validated for the entire 24-h cycles, with realistic conditions of wind and tide. No significant difference in global concentration being measured between the samples of each cycle, we considered a unique amount of larvae, without supply or diluting effect.

2.4.2. Lagoon scale validation

Validation data came from a larval sampling survey conducted throughout Ahe lagoon on 12 stations, L01–L12, during a 18 day-period in May 2007 (Fig. 1). Water sampling was realised every 2 days in the morning by pumping from a boat from the surface to 5 m above the bottom with a continuous flow rate and a pipe diving speed of 1 m every 10 s, providing an average pumping rate of 14 ± 5 l m^{-1}. A mesh retained larvae with a length between 40 and 250 μm. The 12 stations were sampled during the same day, with a delay of about 4 h between the first and the last station. That enabled to avoid the sampling of the same water mass. During this survey, a major spawning event occurred the 8 May and was

Table 1
Larval concentration observed the 8 May 2007, after the spawning event.

Station	Larval concentration ($\times 10^3$ m^{-3})
L01	79.5
L02	9.8
L03	7.2
L04	3.6
L05	0
L06	10.1
L07	4.7
L08	4.2
L09	0
L10	8.0
L11	0
L12	4.7

identified on almost all the stations (Table 1). Larvae were morphologically very close to the pearl oyster and were assimilated to this specie. The cohort was isolated during the days following the spawning event, until the 26 May, by the modal decomposition method of Bhattacharya (software: FISAT-II, FAO-ICLAM, Italie, http://www.fao.org/fi/oldsite/STATIST/FISOFT/FISAT/index.htm).

For validation purposes, the initial larval concentration data recorded *in situ* on the twelve stations (Table 1) were interpolated and extrapolated to every cell of the transport model. On every cell of the model, the initial concentrations were considered homogenous along the water column. A spin-up period of 10 days before the spawning event was applied in order to stabilize the model. At every date of the sampling period, larval concentrations simulated on the 12 stations (1 cell for each station) were extracted and compared to *in situ* observations.

2.5. Connectivity measurement

The theoretical simulations described in the following section aimed to measure the connectivity level existing between different sectors of the Ahe lagoon by using the swimming bivalve larvae as tracers. For bentho-pelagic species, connectivity is dependent on the dispersal phase, from the spawning event to the end of the fixing process (including the choice of a substrate and the metamorphosis) (Cowen et al., 2007). Connectivity was measured here for a period corresponding to the larval lifespan before fixing which is 15–30 days. Therefore, the effect of the larval lifespan variability on connectivity was evaluated by running 30-days long simulations.

Twelve sectors were defined around the sampling stations (Fig. 2) and a specific tracer was associated for each sector to track larvae from one sector to another. For each sector, the initial local larval concentrations were of 100 m^{-3}, homogeneous in x, y, z directions. Indeed, the first larval stages (i.e. first 24 h), are less mobile and then are submitted to homogenisation. So, we considered here the veliger D-stage for initial condition, with homogeneous concentrations.

For these simulations, we defined three wind conditions: mean annual wind (107° globally E, 6 m s^{-1}), cold season mean wind (135° globally SE, 7 m s^{-1}) and warm season mean wind (90° E, 6 m s^{-1}). The mean annual wind was calculated from 2 years of daily recordings extracted from Takaroa meteorological station, an atoll 150 km west of Ahe. The cold and warm season trends were extracted from the same data set. Data were compared to the meteorological climatologies in this region to avoid using unusual conditions.

For the results, larval plume was observed every 5 days between $t = 0$ and 30 days. Larval dispersal was thus represented after 0, 5, 15 and 30 days for source Sectors 1, 3, 6, 10 and 12. These sectors were deemed representative of the different trends observed by modelling. Connectivity was evaluated after 15, 20, 25 and 30 days, corresponding to the larval lifespan.

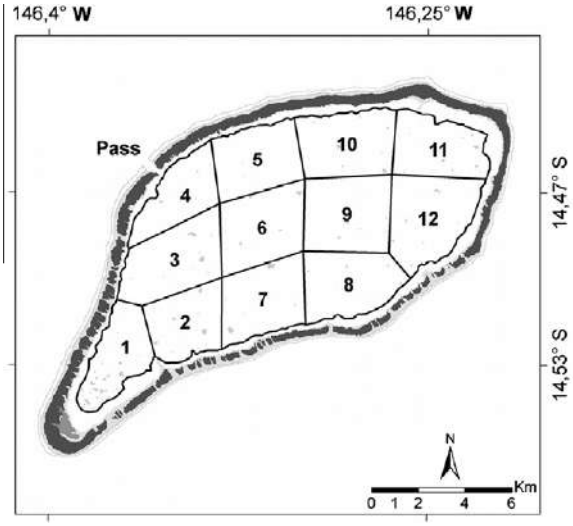

Fig. 2. The 12 Sectors defined for the connectivity analysis.

2.6. Data analyses

The goodness-of-fit of the swimming and transport models outputs (Y) *vs in situ* observations (X) was evaluated by linear regression and tested against the model $Y = X$ at an alpha error threshold of 5%. The R^2 coefficient of determination evaluates the level of variance explained by the model.

A transition probability matrix formalised the connectivity synthetically. This matrix reflect the probability for a larvae emitted from a sector i at time t to be transported into the sector j after $t + k$, k being the larval lifespan (Paris et al., 2007). This probability was calculated as the ratio between the larval concentration coming from the sector i and measured into the sector j after $t + k$ and the initial larval concentration into the sector i (North et al., 2008). In the results section, only the connectivity matrix for a lifespan of 20 days, corresponding to the mean larval lifespan, is presented. Auto-supply rate, corresponding to the probability for a larva to settle into its own source sector, was computed the same way. Self-recruitment was thus evaluated after 15, 20, 25 and 30 days.

The export rate for a given sector i corresponds to the proportion of the larvae that escaped from the system *via* the pass and *via* the rim shallow waters, below 5 m depth, which correspond to unsuitable sectors for farming activity. Nonetheless, larvae exported in these sectors may be remobilized into the global pool. The total export rate, e, was calculated with:

$$e = (1 - r) \quad (2)$$

with r the retention rate. r is defined as the ratio between the number of larvae coming from the i sector found in all other sectors than i at time t, and the initial number of larvae in the sector i. Export rate was extracted after 1, 2, 5, 10, 15, 20, 25 and 30 days of dispersal.

Multiple ANOVA with Tukey test were applied on arcsinus transformed data to test the effect of the various factors (*i.e.* time, sector) on connectivity and export rates.

3. Results

3.1. Model calibration and validation

The swimming model parameterization gave a maximal vertical velocity corresponding to a half-amplitude (α) of 1.5 m h^{-1} or

0.42 mm s^{-1} (Table 2). The model period, (T = 24 h) yielded a pulsation, ω, of 0.26 rad h^{-1} and a phase at the origin, φ, of 1.45 rad. Consequently, maximal rising velocity occurred in the middle of the night, at 00:00, and the maximal descent velocity in the middle of the day, at 12:00.

At the exception of the V02 station in April 2007 (simulation B, Fig. 3), vertical migration was correctly reproduced by the swimming model, with a descent to the depths during the day and a rise towards the surface at night. The discrepancy for V02/April 2007 came from a poor match between the predicted day–night variations and the unusual observed stable concentrations.

For the large lagoon-scale validation, Fig. 4 shows the variations of simulated and measured concentrations averaged for the 12 stations during the 18 days period. The general trend was an exponential decrease of concentrations. The agreement was satisfactory ($y = x$; $R^2 = 0.55$; $p < 0.0001$), but we note an overestimation at the end of the simulations periods. Standard deviation of the mean, which was large at the beginning of the dispersal, for both observations and simulations, decreased with time, suggesting a homogenisation of concentrations lagoon-wide.

Details for each station are provided on Fig. 5. Overall, for the entire period, concentrations were under-estimated by the model ($y = 0.85x$, $R^2 = 0.50$, $p < 0.0001$). The agreements were more satisfactory for the southern and central stations than in the north and east. For instance, for L01, the predictions were near perfect ($y = x$, $R^2 = 0.9$, $p < 0.0001$) with quick decrease and stabilization to low concentration levels. For L03 ($y = x$, $R^2 = 0.8$, $p < 0.0001$) the agreement was good, including for the peak of concentrations measured the 14th May 2007. Conversely, for L02, simulated concentrations were underestimated at the beginning of the period, before converging to observed value. For L04, simulated concentrations were overestimated at the beginning of the period, before converging. For L10, fairly stable simulations do not reproduce well the variability observed *in situ*. For L12, we report both under and overestimation in succession.

3.2. Intra-lagoon connectivity

3.2.1. Mean annual wind scenario

Year-round, the mean wind direction was 107°. Fig. 6 presents larval dispersal after 0, 5, 15 and 30 days for source Sectors 1, 3, 6, 10 and 12. In general, after day 15, homogenisation at the lagoon scale occurred despite contrasting situations before that day. From the western Sector 1, larvae propagated quickly to the north along the west side of the lagoon. Then they dispersed to the east first, and throughout the lagoon afterwards. From Sector 3, larvae propagated eastwards first then throughout the lagoon. From the central Sector 6, larvae dispersed towards the southeast, then the west, then after day 15 throughout the lagoon homogeneously. Conversely, larvae from Sector 10 remained in Sector 10 for about 15 days before dispersing. Finally, eastern Sector 12 larvae quickly dispersed westwards, both along the north and south shores, before diffusing in the entire lagoon.

The connectivity matrices (Fig. 7) summarised the level of exchanges between each of the 12 Sectors after 20 days of simulation. Anova and Tukey test were performed in order to characterise the spatio-temporal patterns. The four time-steps (15, 20, 25 and 30 days) appeared significantly different in average, with a decrease in exporting probability between source and arrival sectors (data not shown). Seven source groups with homogeneous exporting probability were found:

- Sector 9, in the east-centre of the lagoon, with a mean export probability of 8.5 ± 0.9%, was a homogeneous source for all sectors.
- Sectors 6 and 12, in the centre and east of the lagoon, with a mean export probability of 7.7 ± 1.0%, were source for all sectors with higher probability of export to the western sectors (2, 3, 4, 5).
- Sectors 3, 7 and 8, in the west and south, with a mean export probability of 6.7 ± 1.0%, were source for all sectors with higher probability of export to the western sectors (2, 3, 4).

Table 2
Parameters of the vertical swimming model for the larvae.

Parameter	Symbol	Unit	Value
Half-amplitude	α	m h^{-1}	1.5
Period	T	h	24
Pulsation	ω	rad h^{-1}	0.26
Phase	φ	rad	1.45

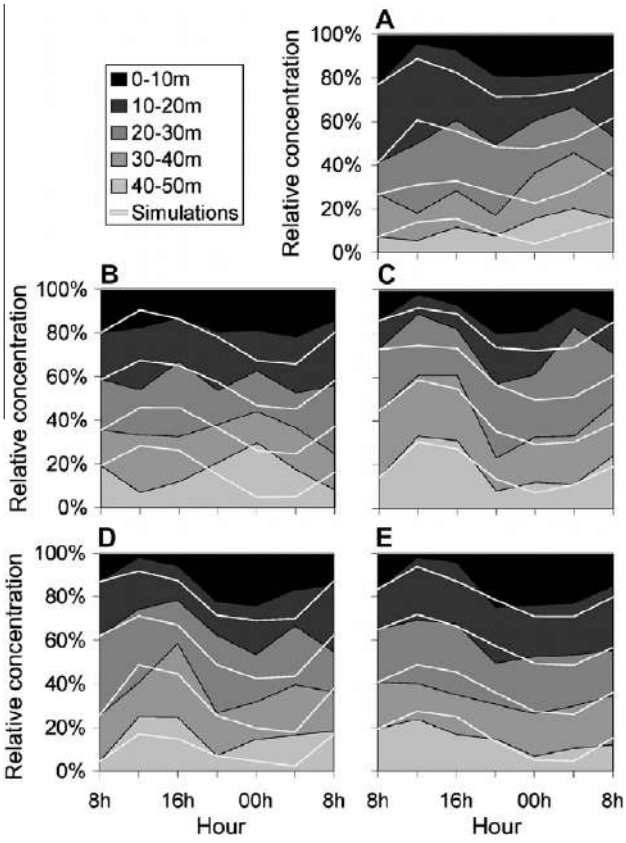

Fig. 3. Comparison between relative larval abundance measured for each vertical 10 m section during five 24-h cycles and simulated by the swimming model. (A) Station V01, April 2007; (B) Station V02, April 2007; (C) Station V01, August 2007; (D) Station V01, February 2008; (E) Station V02, February 2008.

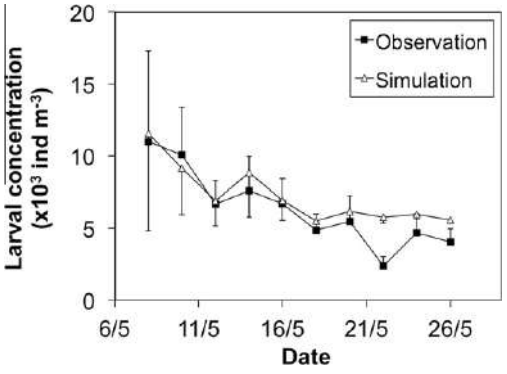

Fig. 4. Average ± standard error larval concentrations evolution for 12 stations (L01–L12), observed and simulated from 8 to 26 May 2007.

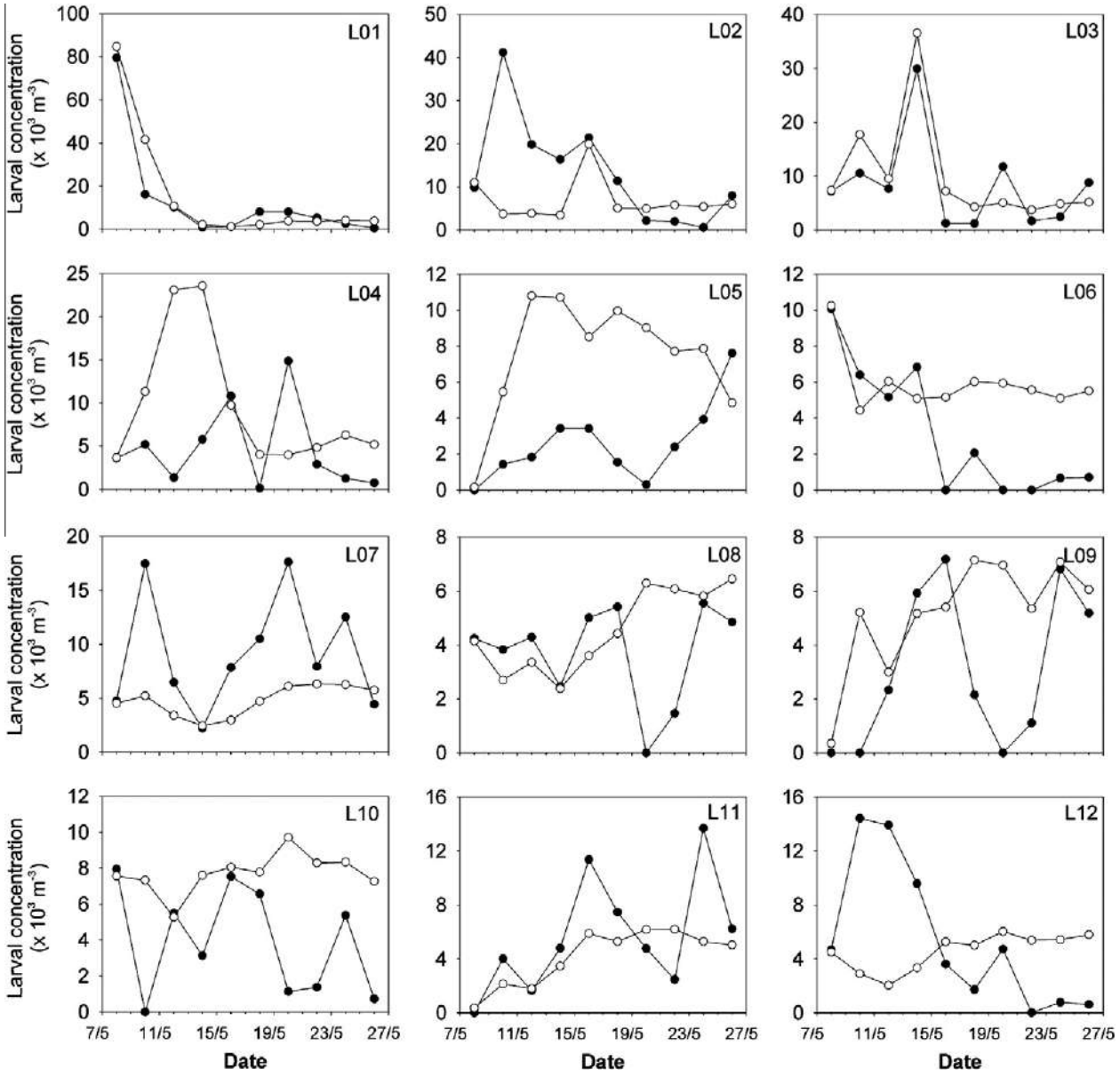

Fig. 5. Individual larval concentrations evolution per station (L01–L12), observed (black circle) and simulated (open circle) between the period: 8 to 26 May 2007.

- Sector 10, in the northeast, with a mean export probability of 5.9 ± 1.2%, was source for all sectors, but with higher probabilities of export to the north sectors (4, 5, 10, 11).
- Sector 5, in the north, with a probability of 5.0 ± 0.7%, was source for all sectors.
- Sectors 2 and 11, in the southwest and northeast, with a mean export probability of 4.7 ± 1.0%, were small contributors, mainly for western and northeastern sector for respectively Sectors 2 and 11.
- Sectors 1 and 4, in the west and northwest, with a mean export probability of 3.3 ± 0.5%, export homogeneously throughout the lagoon.

3.2.2. Winter wind scenario

In austral winter (June–September) winds were stronger and more south-easterly than year round. Mean wind direction was 135°. Larval dispersal in these conditions appeared significantly different than when considering an annual mean wind condition (see above) (Fig. 8).

Indeed, for western and eastern sectors, larvae remained in their source sectors during the 30 days of simulation. For Sector 1 in the west, simulations reported a slight transport of larvae northwards along the western shore. Larvae from Sectors 3 and 6 displayed similar trends, concentrating in the centre of the lagoon, between the south and north shores. Larvae from these two sectors almost never reached the western sectors. Larvae from Sectors 10 and 12 also remained stable, with slight westwards transfer along the north shore.

The averaged export probabilities appeared significantly different between day 15, 25 and 30, with a decrease in export probability between source and arrival sectors (data not shown). But no significant differences were measured between day 15 and 20 and day 20 and 25. Five source groups with homogeneous exporting probability were extracted from the statistical analysis of the connectivity results (Fig. 7):

- Sectors 9 and 12, in the centre and east, with a mean export probability of 8.5 ± 3.4%, mainly exported to eastern sectors (9, 10, 11, 12) and partly by centre-north sectors (2, 4, 5, 6).

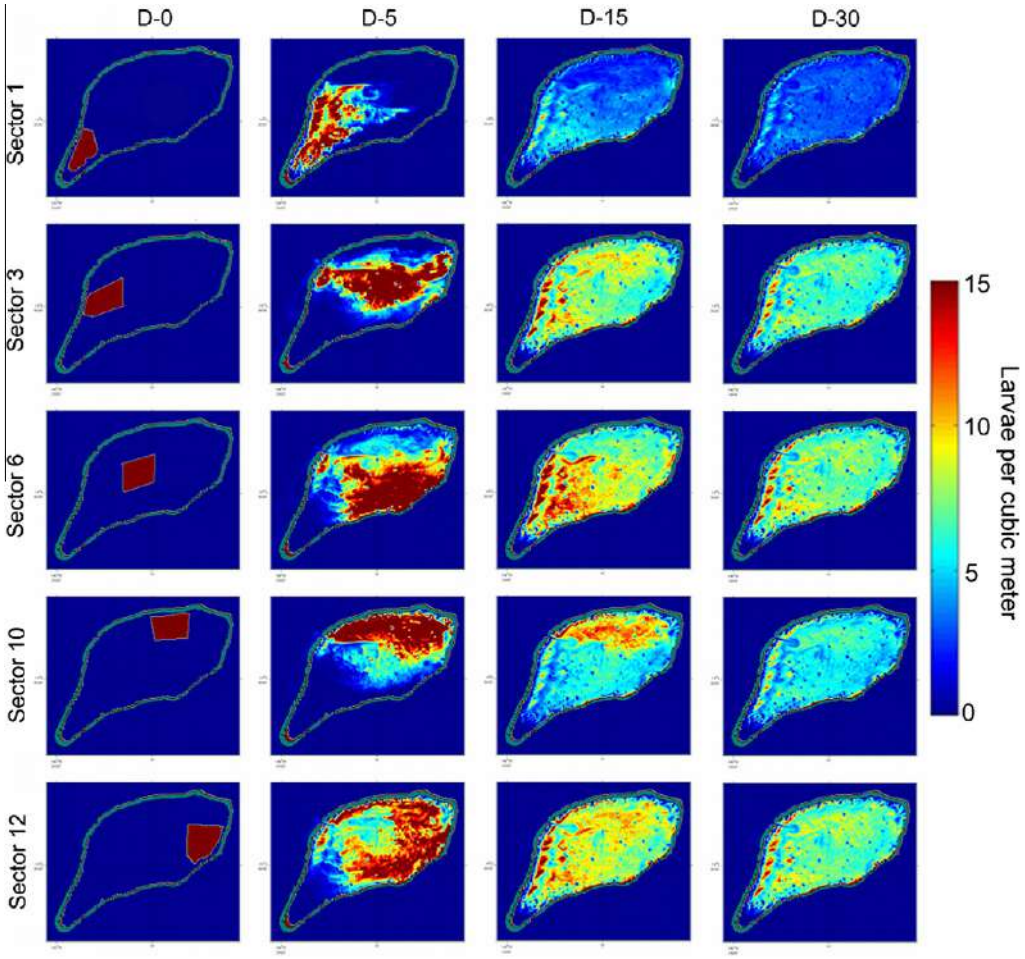

Fig. 6. Maps of larval concentration in Ahe lagoon, simulated by mean annual wind conditions (107°, 6 m s^{-1}), dispersed from the sectors: 1, 3, 6, 10 and 12, after 0, 5, 15 and 30 days of simulation.

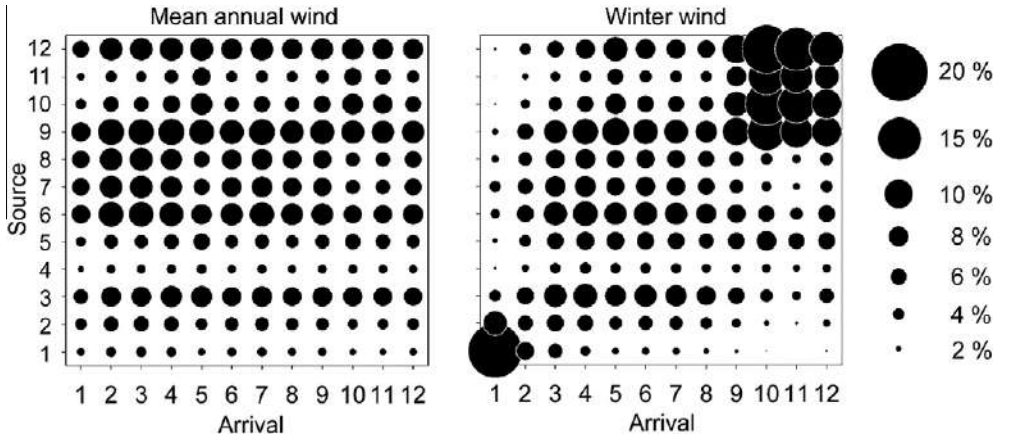

Fig. 7. Connectivity matrices between the 12 Sectors, giving the export probability between source and arrival sectors after 20 days of simulations with mean annual wind (left) and winter wind (right).

– Sectors 3, 6 and 10, in the centre-west and north, with a mean export probability of 6.8 ± 2.4%, mainly exported to western sectors (3, 4, 5, 6, 7, 8) but with a high retention in the eastern part of the lagoon (Sectors 9, 10, 11, 12) for the Sector 10.

– Sectors 5, 7, 8 and 11, in the north, south and east, with a mean export probability of 5.6 ± 2.0%. Sector 5 exports homogeneously in the lagoon, except to the Sector 1. Sectors 7 and 8 mainly export to the western sectors (2, 3, 4, 5, 6, 7, 8). Finally, Sector 11 is a source for the eastern sectors (9, 10, 11, 12).

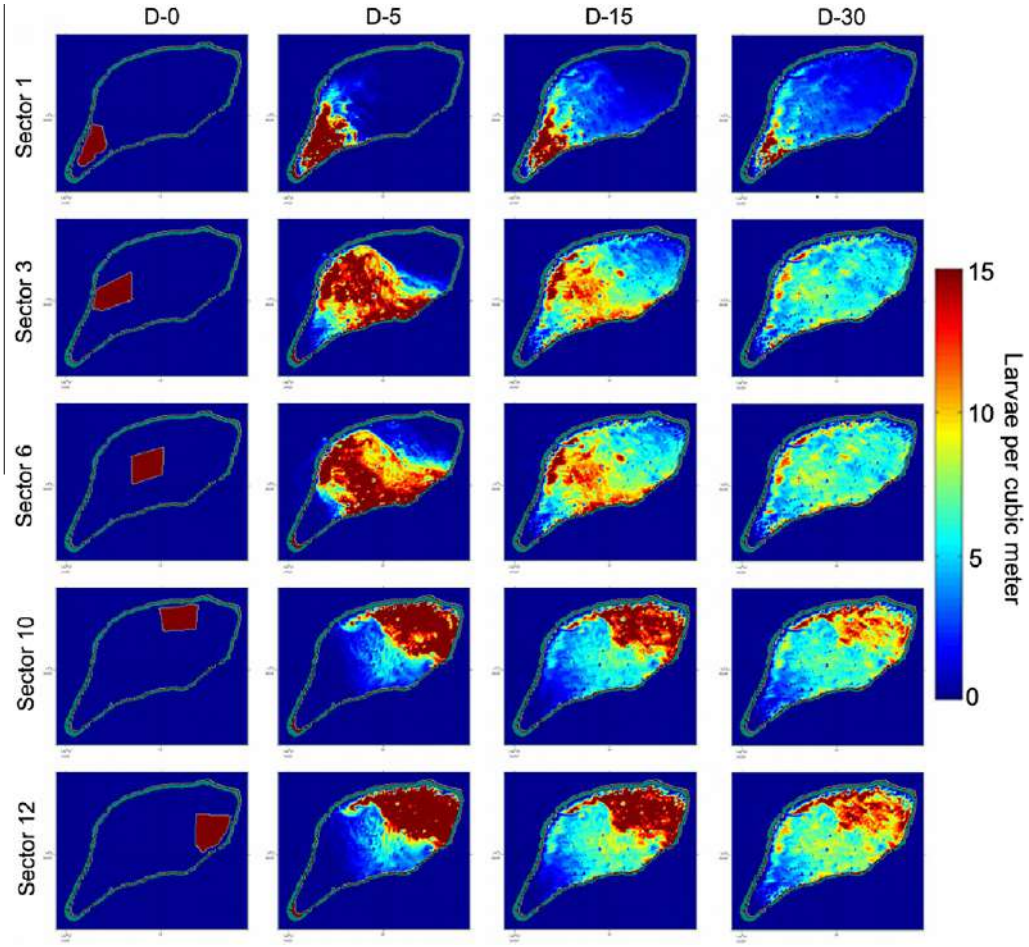

Fig. 8. Maps of larval concentration in Ahe lagoon, simulated by winter wind conditions (135°, 7 m s^{-1}), dispersed from the sectors: 1, 3, 6, 10 and 12, after 0, 5, 15 and 30 days of simulation.

- Sector 2, in the southwest, with a mean export probability of 4.5 ± 1.9%, highly retained larvae in the western part of the lagoon.
- Sectors 1 and 4, in the west and northwest, with a mean export probability of 3.6 ± 2.7%. Sector 1 showed a high retention in the western sectors (1, 2, 3) and no export in the east. Sector 4 showed very small probability values, concentrated in the centre of the lagoon.

3.2.3. Summer wind scenario

In austral summer (October–May) the mean trade wind direction was 90°. Thus, close to the annual mean conditions, and indeed simulations showed for the summer similar patterns that what we previously described for the annual mean. Therefore, we hereafter discuss the mean annual and summer patterns *vs* the mean winter patterns.

3.2.4. Self-recruitment patterns

The connectivity matrix diagonal quantifies self-recruitment for each sector. It appeared significantly higher in winter wind conditions ($p < 0.0001$), with an average, between days 15 and 30, of 9% compared to 6.4% in mean annual condition. Winter self-recruitment was especially high in Sectors 1, 9, 10, 11 and 12 in the western and eastern sectors (Fig. 9). Conversely, the Sector 4 displayed the lowest self-recruitment rate with a 3.7% average. Self-recruitment decreased significantly between days 15 and 30 of the simulations for the mean annual condition ($p < 0.0001$), decreasing from 7.6% to 5.5% and not significantly from 11.1% to 7.3% for winter wind conditions.

3.3. Export

The mean export rate from the lagoon was not significantly different between each wind-dependent scenario ($p > 0.05$). It reached an average 28% after 30 days (Fig. 10, right). This export rate was variable across the lagoon (Fig. 10, left). Sector 4, displayed the highest export rate, with an average 45% between days 15 and 30 for the two wind conditions. For the mean annual wind scenario, Sector 4 showed significantly higher rates than a group of 6 Sectors: 1, 2, 7, 8, 9 and 12. The other sectors showed no significant difference. For the winter scenario, the Sector 4 was significantly higher than Sectors 1, 9, 10, 11, 12. These last 5 Sectors showed also significantly lower exporting rates than Sectors 2, 3, 6, 7 and 8. The largest differences between the two scenarios appeared in the eastern part of the lagoon. Indeed, the only significant differences between the two wind conditions were measured on Sectors 10 and 11, which showed higher export rates with mean annual wind. After 5 days of simulation (Fig. 10, right), the mean export rate obeyed to a linear trend, with a slope of 0.9% per day, thus suggesting that nearly 1% of the larvae were exported every day.

4. Discussion

4.1. Larval transport model validation

To the best of our knowledge, the present study presents for the first time in an atoll environment a validated model of bivalve larvae vertical migration, coupled with a hydrodynamic model.

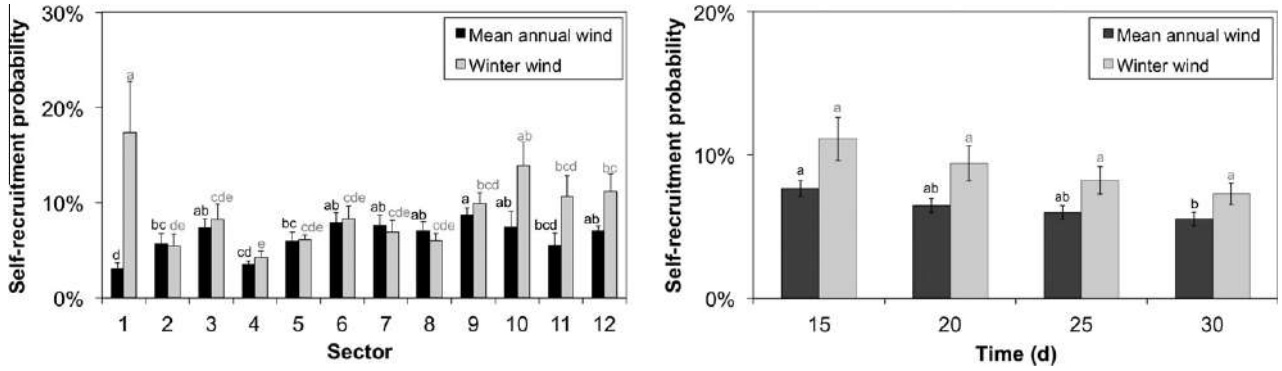

Fig. 9. Left: average ± standard error self-recruitment probability between 15 and 30 days for the 12 different sectors, and according to the different wind conditions (mean annual, winter). Right: evolution of the self-recruitment probability averaged (±standard error) across the entire lagoon according to time (15, 20, 25 and 30 days) and according to the different wind conditions. Letters give significant differences between stations/time (Tukey test).

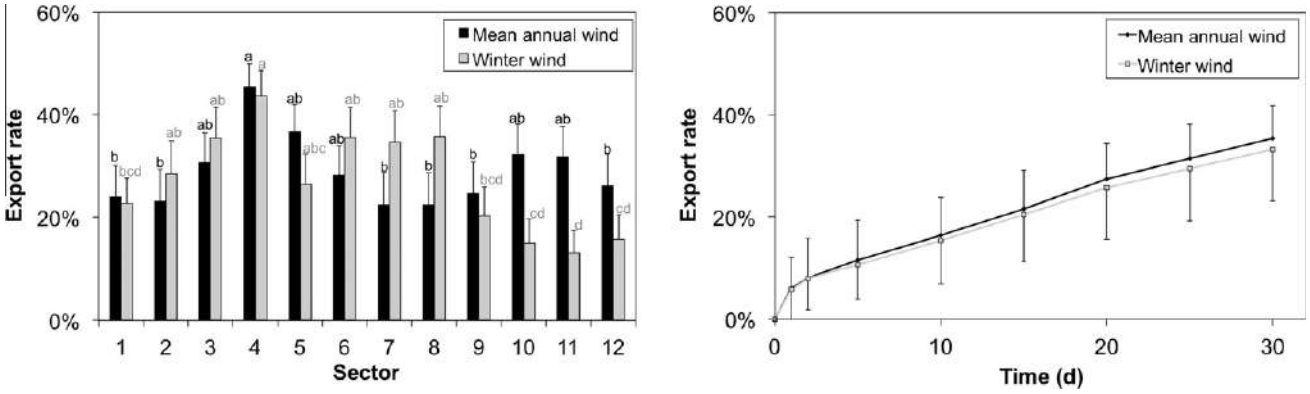

Fig. 10. Left: average ± standard error export rate between 15 and 30 days for the 12 different sectors and according to the different wind conditions (mean annual, winter). Right: evolution of the export rate averaged (±standard error) across the lagoon, according to time (15, 20, 25 and 30 days) and different wind conditions. Letters give significant differences between stations/time (Tukey test).

The vertical 1-D swimming model was validated locally with extensive *in situ* observations but it remains a first-order empirical model based on day–night cycles. It did not account for larval development stage. Larvae swimming abilities evolve during their development, in speed and direction (Troost et al., 2008) and Eq. (1) was not modulated accordingly. Furthermore, no changes were applied according to environmental factors such as salinity, temperature, food availability and hydrodynamic turbulences which are all factors influencing larval behaviour (Eckman et al., 1994; Dekshenieks et al., 1996). Here, the vertical swimming speed, with a maximal speed of 0.42 mm s^{-1}, was in agreement with previous works on bivalves species (Troost et al., 2008). The vertical swimming model simulations were also in good agreement with our observations, although some discrepancies were showed at station V02 in April 2007. Indeed, we measured high larval concentrations in deep layers at night, while a migration toward the surface was expected. In fact, wind speed during this survey was high at the beginning, over 8 m s^{-1}, from SE (130°), and decreased progressively to reach 4 m s^{-1} from ENE (70°) at the end of the 24-h cycle. These wind conditions were the highest and the most variable that we encountered. Considering that larvae submitted to strong turbulent mixing may react by following a sinking strategy, this could likely explain the discrepancies between observation and simulations.

Once the hydrodynamic and the larval behaviour models were coupled, the study of larval dispersal by hydrodynamic transport and vertical periodic sinusoidal migration became possible. Results appeared realistic, being validated against data from a field campaign that opportunistically bracketed a spawning event. Simulated and observed concentrations were in agreement across time, and the simulation of larvae dispersal was deemed satisfactory. The model seemed to reproduce correctly the progressive decrease of larval concentrations due to dilution and exports through the pass and along the water exchanges areas of the shoreline. An important standard deviation was observed at the beginning of the simulation for both observed and simulated concentrations. This variation was likely the consequence of spatial heterogeneity during the spawning event. The decrease of spatial variation, consistent with the lagoon scale homogenisation of concentrations (i.e., decrease in standard deviation) was well reproduced by the model. However, the model did not use a mortality rate. Larvae were expected to die due to predation and food deprivation (Eckman, 1996), but the good agreement between simulations and observations seemed to suggest that natural mortality could be very low in Ahe atoll, or that most mortality occur in the first 2 days of larval life. Indeed, mortality rates is highest in early life stages in the first couple of days (Pechenik, 1999) and in the last stages, due to higher predation and likely longer periods of starvation (Hofmann et al., 2004). Here; these early stages were not taken into account since capture and census in the field yielded larvae already 1–2 days old. Conversely, the expected actual higher mortality during the last stages could explain the general overestimation of simulated larval concentrations at the end of the simulated periods.

The agreement between simulations and observations was also satisfactory for most individual stations but several factors can explain the existing discrepancies. For station 12, discrepancies can

be explained if the sampling missed the arrival of the cohort. Indeed, the source of larvae can be very local (Scheltema, 1986), and larvae may have been detected only after 1 or 2 days after the initial dispersal, which is likely what we captured in the field. Other sources of discrepancies are due to the spatial scale mismatch between *in situ* station (a point data) and simulated data. The later integrates values from the extent of a model grid cell, thus from a 10,000 m^2 area. Furthermore, larvae can form patches and groups that may aggregate at various space scales (Garland and Zimmer, 2002). For stations 4 and 5 located next to the pass, given the speed of the current and the extent of the influence of the pass in the lagoon (Dumas et al., 2012), small time lags between observations and models at these stations can also explain differences. All model values were extracted at 10 AM, but field data were measured between 8:00 and 12:00 AM. Finally, a likely source of discrepancy lied in the extraction of one cohort data from a pool of observations. The theoretical decomposition of modes in order to identify and monitor cohort's abundance is not necessarily free of errors.

The largest discrepancy observed between observations and simulation was observed close to the 20th of May, when observed larval concentrations decreased strongly in L05, 06, 08, 09 and 10, without increase elsewhere. This event was concomitant with a rainy period (7 mm day^{-1}), showing a decrease in temperature (−2 °C) and a decrease in insolation. The agreement between observation and simulation being satisfactory after this event, this could explain a large part of the discrepancy observed. Indeed, larvae might have migrated very close to the bottom (*i.e.* out of the sampling domain) during this rainy period.

4.2. Larval dispersal schematic diagram

Larval dispersal simulations provide a tool to diagnose the influence of environmental conditions (mostly wind) on the transport of larvae between sources and sinks sectors (including self-recruitment) and export rates. Simulations presented here revealed a strong dispersal potential within Ahe atoll lagoon, from one sector to the other, especially when the wind is blowing from the east (mean annual and summer period). Conversely, southeast wind, in winter, tends to increase self-retention, especially in the east and west sectors. If we simplify our 12-sector view into a 6-sector view based on the typology of behaviour highlighted in the result section, we obtain (Fig. 11):

- Sector Southwest (a, previously Sector 1): export larvae to the north and retain them in respectively easterlies and south-easterlies conditions.
- Sector West (b, previously Sectors 3, 4): facing the pass, it shows strong larval export and transport to the atoll centre in all type of wind conditions.
- Sector South (c, previously Sectors 2, 7, 8): with limited potential for transport, principally towards sector (b).
- Sector Centre (d, previously Sectors 6, 9): export larvae eastward and southward respectively in easterlies and south-easterlies conditions.
- Sector North (e, previously Sectors 5, 10, 11): export larvae westward in easterlies conditions, and display an almost exclusive retention during south-easterlies conditions.
- Sector East (f, previously Sectors 12): export rapidly larvae northwards and westwards, and exclusively northwards in respectively easterlies and south-easterlies conditions.

In short, wind coming from the east promotes larval transport between sectors and especially between east and west sectors. Concentrations are more easily homogenised lagoon-wide in these conditions. When the southeast winds blow, the situation is different. The limiting returning upwind deep flow (Dumas et al., 2012) promotes retention in the eastern and western sectors and limit export potential. This functioning is intimately related to the wind-dependent hydrodynamic behaviour of the atoll. In their study of the tidal flushing and wind driven circulation of Ahe atoll lagoon, Dumas et al. (2012), showed that the pass divided the lagoon in three main circulation cells located in the north, centre and south of the lagoon. When the wind blows from southeast, the three main cells are reinforced. The west and east sectors are more separated from the pass sector and their flushing time increase. This explains the strong retention (i.e. self-recruitment) measured in the western and eastern sectors. Furthermore, 95% of the Ahe atoll rim is completely closed to water exchanges. Only the pass and *hoa* are open to water exchanges. The flow in the pass is tide-driven. The flow in *hoa* are both tide and wave-driven, with an inflow only during a half tide cycle around high tide. Cumulated inflow through all the *hoa* is 10–20 times smaller than the volume exchanged through the main pass during the same time (Dumas et al., 2012). Since the only existing outflow that exists is through the pass, the atoll rim is thus a true boundary for larval dispersal.

4.3. Consequences for spat collection

Spatio-temporal variations in bivalve fixation (and thus on pearl oyster collecting) are theoretically dependant on the adults spatial distribution, spawning periods and occurrences, larval survival and thus environmental forcing and food availability, dispersal potential, potential chemical attraction and finally availability of suitable substrate for fixations when the larval development is completed (Rodriguez et al., 1993; Adjeroud et al., 2000; Pante et al., 2006). This study has clarified the dispersal potential of larvae coming from different sectors. In Ahe atoll lagoon, the stock of wild pearl oysters is unknown, but aquaculture farms alone raised in 2007 a substantial total of 15 millions adults spread across the lagoon, except in the eastern sectors where farms are far less numerous, and in the deep central sectors that are unpractical for daily operations. The preferred sectors by professionals for spat collections are currently the western sectors.

In term of aquaculture management, this study provides clues to understand the variations in pearl oyster spat collecting success. Indeed, larvae displayed significant dispersal capacity at the lagoon scale, promoted at least by the wind-driven and tide-driven circulation. Our simulations suggest that in all conditions, the western sectors are best sectors to collect larvae. If the wind blows from the east, the western part of the lagoon is a sink, and if the wind comes from the southeast, most larvae are retained. Thus, there are fewer chances of shortages and loss year long, especially after the spawning periods. This potential is likely enhanced given the high concentrations of farms and concessions in this sector. The southern and central part of the lagoon appeared to be good sources of larvae for other sectors, with favourable self-recruitment rates as well. Since the central part of the lagoon is less used for farming activities, this sector could be an efficient sanctuary if genitors were accumulated there, as well-placed an additional source of larvae.

This study showed the capability of a 3D transport model to properly simulate the larval dispersal at the lagoon-scale. This provides a decision-support tool well tuned for the aquaculture application as described by Andréfouët et al. (2006). Indeed, circulation model outputs are technically effective for collecting spats and cost-effective for the industry when they identify suitable collecting areas without years of trials and errors by farmers. Dispersal model are only one part of the equation. Better knowledge of factors controlling recruitment variability will also enable to better understand the wild populations structure and to rationalise a collecting strategy for aquaculture. In particular, gametogenesis,

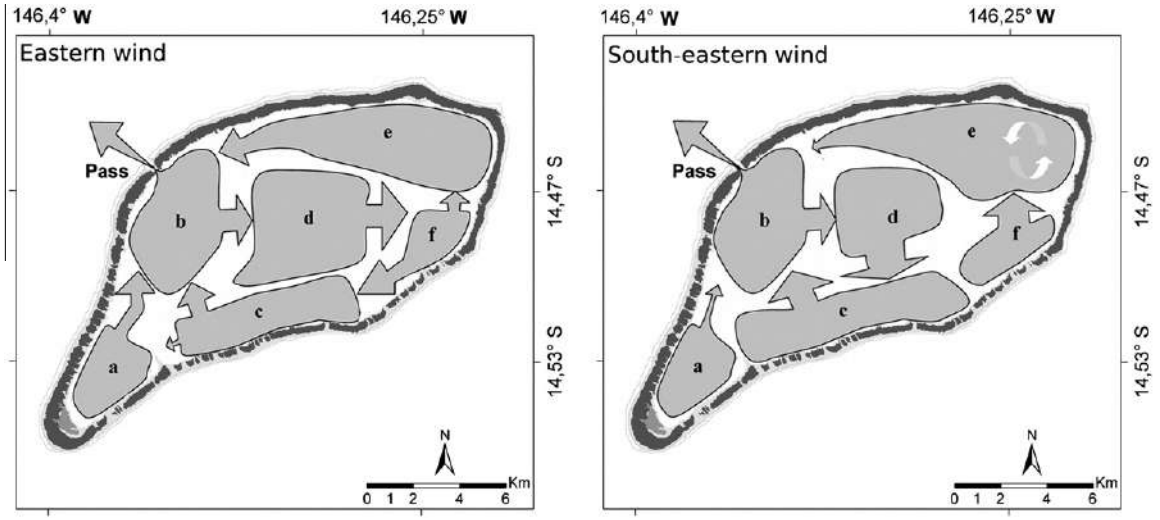

Fig. 11. Schematic view of larval exchanges according to the different eastern and south-eastern wind conditions and according to the different sectors (simplified here in 6 Sectors). Arrows widths are representative of exchange rates.

spawning and larval growth potential also determine spat collection variability (Fournier et al., 2012; Thomas et al., 2012). Coupling biology and physic-based approaches is now needed to perpetuate the pearl oyster aquaculture.

In addition to the general lagoon-scale wind-driven dispersal potential highlighted here, this study also revealed smaller-scale structures due to the influence of the pass, especially for the central northern sector. Given the small influence of the *hoa* in Ahe atoll, no other small-scale structural effects have been evidenced in Ahe. It is likely that lagoon coral pinnacles also have local-scale effects on larval survival, dispersal, retention and fixation but this scale was not considered here. Further work on geomorphologically different atolls could lead to highlight different regimes of water renewal, circulation and dispersal patterns (Andréfouët et al., 2001a,b). This warrants further investigation. It is however reasonable to state that for atolls with geomorphology and environmental forcing comparable to Ahe, the functioning will likely be very similar.

Acknowledgements

This study was co-funded by the French institute for the exploitation of the sea (Ifremer) and the government of French Polynesia (Research Delegation) and the 9th European Development Fund (EDF). The authors are grateful to the Ifremer and EDF teams who participated in the experiments conducted on Ahe atoll. We finally thank two anonymous reviewers for their valuable suggestions and comments in the revision of the original manuscript.

References

Adjeroud, M., Andréfouët, S., Payri, C., Orempuller, J., 2000. Physical factors of differentiation in macrobenthic communities between atoll lagoons in the Central Tuamotu Archipelago (French Polynesia). Marine Ecology-Progress Series 196, 25–38.

Andréfouët, S., Charpy, L., Lo-yat, A., Lo, C., 2012. Recent reseach for pearl oyster aquaculture management in French Polynesia. Marine Pollution Bulletin. 65, 407–414.

Andréfouët, S., Claereboudt, M., Matsakis, P., Pagès, J., Dufour, P., 2001a. Typology of atoll rims in Tuamotu Archipelago (French Polynesia) at landscape scale using SPOT HRV images. International Journal of Remote Sensing 22, 987–1004.

Andréfouët, S., Ouillon, S., Brinkman, R., Falter, J., Douillet, P., Wolk, F., Smith, R., Garen, P., Martinez, E., Laurent, V., Lo, C., Remoissenet, G., Scourzic, B., Gilbert, A., Deleersnijder, E., Steinberg, C., Choukroun, S., Buestel, D., 2006. Review of solutions for 3D hydrodynamic modeling applied to aquaculture in South Pacific atoll lagoons. Marine Pollution Bulletin 52, 1138–1155.

Andréfouët, S., Pages, J., Tartinville, B., 2001b. Water renewal time for classification of atoll lagoons in the Tuamotu Archipelago (French Polynesia). Coral Reefs 20, 399–408.

Botsford, L.W., White, J.W., Coffroth, M.A., Paris, C.B., Planes, S., Shearer, T.L., Thorrold, S.R., Jones, G.P., 2009. Connectivity and resilience of coral reef metapopulations in marine protected areas: matching empirical efforts to predictive needs. Coral Reefs 28, 327–337.

Brié, C., 1999. Etude experimentale du collectage de naissain de *Pinctada margaritifera* (Linné, 1758) à Takapoto, atoll des Tuamotu; en Polynesie Française. Mémoire EPHE, p. 87.

Connell, J.H., 1985. The consequence of variation in initial settlement *vs* postsettlement mortality in rocky intertidal communities. Journal of Experimental Marine Biology and Ecology 93, 11–45.

Cowen, R.K., Gawarkiewic, G., Pineda, J., Thorrold, S.R., Werner, F.E., 2007. Population connectivity in marine systems an overview. Oceanography 20, 14–21.

Dekshenieks, M.M., Hofmann, E.E., Klinck, J.M., Powell, E.N., 1996. Modeling the vertical distribution of oyster larvae in response to environmental conditions. Marine Ecology-Progress Series 136, 97–110.

Doroudi, M.S., Southgate, P.C., 2003. Embryonic and larval development of *Pinctada margaritifera* (Linnaeus, 1758). Molluscan Research 23, 101–107.

Dumas, F., Le Gendre, R., Andréfouët, S., 2012. Tidal flushing and wind driven circulation of Ahe lagoon (Tuamotu Archipelago, French Polynesia) from *in situ* observations and numerical modelling. Marine Pollution Bulletin. 65, 425–440.

Eckman, J.E., 1996. Closing the larval loop: linking larval ecology to the population dynamics of marine benthic invertebrates. Journal of Experimental Marine Biology and Ecology 200, 207–237.

Eckman, J.E., Werner, F.E., Gross, T.F., 1994. Modeling some effects of behavior on larval settlement in a turbulent boundary-layer. Deep-Sea Research Part II – Topical Studies in Oceanography 41, 185–208.

Edwards, K.P., Hare, J.A., Werner, F.E., Blanton, B.O., 2006. Lagrangian circulation on the southeast US continental shelf: implications for larval dispersal and retention. Continental Shelf Research 26, 1375–1394.

Ellien, C., Thiebaut, E., Dumas, F., Salomon, J.C., Nival, P., 2004. A modelling study of the respective role of hydrodynamic processes and larval mortality on larval dispersal and recruitment of benthic invertebrates: example of *Pectinaria koreni* (Annelida: Polychaeta) in the Bay of Seine (English channel). Journal of Plankton Research 26, 117–132.

Fournier, J., Levesque, E., Pouvreau, S., Le Pennec, M., Le Moullac, G., 2012. Influence of plankton concentration on gametogenesis and spawning of the black lip pearl oyster *Pinctada margaritifera* in Ahe atoll lagoon (Tuamotu archipelago, French polynesia). Marine Pollution Bulletin 65, 463–470.

Garland, E.D., Zimmer, C.A., 2002. Hourly variations in planktonic larval concentrations on the inner shelf: emerging patterns and processes. Journal of Marine Research 60, 311–325.

Grantham, B.A., Eckert, G.L., Shanks, A.L., 2003. Dispersal potential of marine invertebrates in diverse habitats. Ecological Applications 13, S108–S116.

Guizien, K., Brochier, T., Duchene, J.C., Koh, B.S., Marsaleix, P., 2006. Dispersal of *Owenia fusiformis* larvae by wind-driven currents: turbulence, swimming behaviour and mortality in a three-dimensional stochastic model. Marine Ecology-Progress Series 311, 47–66.

Hofmann, E.E., Powell, E.N., Bochenek, E.A., Klinck, J.A., 2004. A modelling study of the influence of environment and food supply on survival of *Crassostrea gigas* larvae. Ices Journal of Marine Science 61, 596–616.

Jolly, M.T., Guyard, P., Ellien, C., Gentil, F., Viard, F., Thiebaut, E., Jollivet, D., 2009. Population genetics and hydrodynamic modeling of larval dispersal dissociate

contemporary patterns of connectivity from historical expansion into European shelf seas in the polychaete *Pectinaria koreni*. Limnology and Oceanography 54, 2089–2106.

Kool, J.T., Paris, C.B., Andréfouët, S., Cowen, R.K., 2010. Complex migration and the development of genetic structure in subdivided populations: an example from Caribbean coral reef ecosystems. Ecography 33, 597–606.

Lazure, P., Dumas, F., 2008. An external-internal mode coupling for a 3D hydrodynamical model for applications at regional scale (MARS). Advances in Water Resources 31, 233–250.

Levin, L.A., 2006. Recent progress in understanding larval dispersal: new directions and digressions. Integrative and Comparative Biology 46, 282–297.

Lyard, F., Lefevre, F., Letellier, T., Francis, O., 2006. Modelling the global ocean tides: modern insights from FES2004. Ocean Dynamics 56, 394–415.

McQuaid, C.D., Phillips, T.E., 2000. Limited wind-driven dispersal of intertidal mussel larvae: *in situ* evidence from the plankton and the spread of the invasive species Mytilus galloprovincialis in South Africa. Marine Ecology-Progress Series 201, 211–220.

Munday, P.L., Leis, J.M., Lough, J.M., Paris, C.B., Kingsford, M.J., Berumen, M.L., Lambrechts, J., 2009. Climate change and coral reef connectivity. Coral Reefs 28, 379–395.

North, E.W., Schlag, Z., Hood, R.R., Li, M., Zhong, L., Gross, T., Kennedy, V.S., 2008. Vertical swimming behavior influences the dispersal of simulated oyster larvae in a coupled particle-tracking and hydrodynamic model of Chesapeake Bay. Marine Ecology-Progress Series 359, 99–115.

Pante, E., Adjeroud, M., Dustan, P., Penin, L., Schrimm, M., 2006. Spatial patterns of benthic invertebrate assemblages within atoll lagoons: importance of habitat heterogeneity and considerations for marine protected area design in French Polynesia. Aquatic Living Resources 19, 207–217.

Paris, C.B., Cherubin, L.M., Cowen, R.K., 2007. Surfing, spinning, or diving from reef to reef: effects on population connectivity. Marine Ecology-Progress Series 347, 285–300.

Pechenik, J.A., 1999. On the advantages and disadvantages of larval stages in benthic marine invertebrate life cycles. Marine Ecology-Progress Series 177, 269–297.

Pouvreau, S., Gangnery, A., Tiapari, J., Lagarde, F., Garnier, M., Bodoy, A., 2000. Gametogenic cycle and reproductive effort of the tropical blacklip pearl oyster, *Pinctada margaritifera* (Bivalvia: Pteriidae), cultivated in Takapoto atoll (French Polynesia). Aquatic Living Resources 13, 37–48.

Pouvreau, S., Prasil, V., 2001. Growth of the black-lip pearl oyster, *Pinctada margaritifera*, at nine culture sites of French Polynesia: synthesis of several sampling designs conducted between 1994 and 1999. Aquatic Living Resources 14, 155–163.

Roberts, C.M., 1997. Connectivity and management of Caribbean coral reefs. Science 278, 1454–1457.

Rodriguez, S.R., Ojeda, F.P., Inestrosa, N.C., 1993. Settlement of benthic marine invertebrates. Marine Ecology-Progress Series 97, 193–207.

Scheltema, R.S., 1986. On dispersal and planktonic larvae of benthic invertebrates – an eclectic overview and summary of problems. Bulletin of Marine Science 39, 290–322.

Shanks, A.L., Brink, L., 2005. Upwelling, downwelling, and cross-shelf transport of bivalve larvae: test of a hypothesis. Marine Ecology-Progress Series 302, 1–12.

Shanks, A.L., Grantham, B.A., Carr, M.H., 2003. Propagule dispersal distance and the size and spacing of marine reserves. Ecological Applications 13, S159–S169.

Siegel, D.A., Kinlan, B.P., Gaylord, B., Gaines, S.D., 2003. Lagrangian descriptions of marine larval dispersion. Marine Ecology-Progress Series 260, 83–96.

Sims, N.A., 1994. Growth of wild and cultured black-lip pearl oysters, *Pinctada margaritifera* (L) (Pteriidae; Bivalvia), in the Cook islands. Aquaculture 122, 181–191.

Swearer, S.E., Caselle, J.E., Lea, D.W., Warner, R.R., 1999. Larval retention and recruitment in an island population of a coral-reef fish. Nature 402, 799–802.

Thielley, M., 1993. Etude cytologique de la gamétogenèse, de la sex-ratio et du cycle de reproduction chez l'huître perlière *Pinctada margaritifera* (L) var. *cumingii* (Jameson), (mollusques, bivalves). Comparaison avec le cycle de *Pinctada maculata* (Gould). Th Univ Tahiti, Polynésie Française, p. 233.

Thomas, Y., Garen, P., Bennett, A., Le Pennec, M., Clavier, J., 2012. Multi-scale distribution and dynamics of bivalve larvae in a deep atoll lagoon (Ahe, French Polynesia). Marine Pollution Bulletin. 65, 453–462.

Thomas, Y., Pouvreau, S., Garen, P., 2011. Application of a bioenergetic growth model to larvae of the pearl oyster *Pinctada margaritifera* L. Journal of Sea Research 66, 331–339.

Thorson, G., 1950. Reproductive and larval ecology of marine bottom invertebrates. Biological Reviews 25, 1–45.

Tranter, D.J., 1958. Reproduction in Australian pearl oysters (*Lamellibranchia*) IV. *Pinctada margaritifera* (*Linnaeus*). Australian Journal of Marine and Freshwater Research 9, 509–525.

Troost, K., Veldhuizen, R., Stamhuis, E.J., Wolff, W.J., 2008. Can bivalve veligers escape feeding currents of adult bivalves? Journal of Experimental Marine Biology and Ecology 358, 185–196.

Verdier-Bonnet, C., Carlotti, F., Rey, C., Bhaud, M., 1997. A model of larval dispersion coupling wind-driven currents and vertical larval behaviour: application to the recruitment of the annelid Owenia fusiformis in Banyuls Bay, France. Marine Ecology-Progress Series 160, 217–231.

Viard, F., Ellien, C., Dupont, L., 2006. Dispersal ability and invasion success of *Crepidula fornicata* in a single gulf: insights from genetic markers and larval-dispersal model. Helgoland Marine Research 60, 144–152.

Zanini, J.M., Salvat, B., 2000. Assessment of deep water stocks of pearl oysters at Takapoto atoll (Tuamotu Archipelago, French Polynesia). Coral Reefs 19, 83–87.

Marine Pollution Bulletin 65 (2012) 453–462

Contents lists available at SciVerse ScienceDirect

Marine Pollution Bulletin

journal homepage: www.elsevier.com/locate/marpolbul

Multi-scale distribution and dynamics of bivalve larvae in a deep atoll lagoon (Ahe, French Polynesia)

Y. Thomas [a,b,*], P. Garen [b], A. Bennett [b], M. Le Pennec [c], J. Clavier [d]

[a] Ifremer, DPFOM LPI, Presqu'île du Vivier, 29840 Argenton, France
[b] Ifremer, COP, BP 7004, 98719 Taravao, Tahiti, French Polynesia
[c] Université de Polynésie Française, BP 6570, 98702 Faa'a, Tahiti, French Polynesia
[d] CNRS, UMR 6539 (LEMAR), IUEM, Technopôle Brest-Iroise, Place N. Copernic, 29280 Plouzané, France

ARTICLE INFO

Keywords:
Bivalve larvae
Distribution patterns
Vertical migration
Pinctada margaritifera settlement
Deep atoll lagoon
French Polynesia

ABSTRACT

Bivalve larvae and hydrographic parameters were sampled over a range of spatio-temporal scales in a deep atoll lagoon. Bivalve larvae abundances were very high throughout the year: 18,550 m^{-3} in average. Larvae were (i) concentrated at mid-depth with nocturnal ascent and diurnal descent, (ii) heterogeneously dispersed at the lagoon scale, (iii) subject to day-to-day variation in abundance and (iv) transferred between different parts of the lagoon providing evidence of intra-lagoonal connectivity. The primacy of physical factors was seen on large spatial scale with the diluting effect of water renewal and transfers by hydrodynamics. On smaller spatial scale, the primacy of biological processes was recognised, with larval swimming activity leading to dial vertical migration correlated with food concentration. Variations in larval abundance were driven by bivalve reproductive activity correlated with meteorological conditions (*i.e.* windy periods). Finally, relationship between bivalve larvae patterns and pearl oyster (*Pinctada margaritifera*) settlement structuring is discussed.

1. Introduction

The majority of marine invertebrates have a planktonic larval stage at the beginning of their lives. This planktonic step appears to be a key determinant for adult distribution and abundance since the distribution and abundance of sessile populations are determined by a combination of pre- and post-settlement factors (Olson and Olson, 1989; Cowen et al., 2000; Levin, 2006). Besides endogenous factors, like feeding capacity and metabolic processes (Pace et al., 2006), bivalve larval growth and survival depend on external pressures from predation (Troost et al., 2009) and a wide variety of environmental factors, *i.e.* temperature, salinity, food quality and availability (Eckman, 1996; Doroudi et al., 1999; Powell et al., 2002; Hofmann et al., 2004). Moreover, as for all zooplankton communities, bivalve larvae distributions exhibit spatial patterns (Pinel-Alloul, 1995; Avois-Jacquet, 2002). These patterns are generated and maintained by physical factors, like hydrodynamics, and biological processes such as larval swimming activity (Haury et al., 1978; Garland et al., 2002; Masson et al., 2004; Badylak and Phlips, 2008). Since zooplankton distributions and environmental processes are 'scale-dependent', a range of spatial and temporal scales should be considered for studying zooplankton variability and understanding its driving mechanisms (Borcard et al., 2004).

The determinants of marine population dispersal remains one of the fundamental challenges for marine ecology and oceanography (Cowen et al., 2006). In tropical ecosystems, numerous studies address fish or coral larval dispersal, mainly to understand the connectivity between source and recipient sectors so as to protect, preserve and manage biodiversity (Roberts, 1997; Swearer et al., 1999; Botsford et al., 2009; Munday et al., 2009). In atoll lagoons, the diversity and structure of mollusc populations are highly related to local factors like substrate types or hydrodynamic conditions (Pante et al., 2006). Nonetheless, most of the mechanisms explaining abundance and distribution variability of adult populations remain obscure and could be attributed to larval development success and settlement processes (Adjeroud et al., 2000).

In French Polynesian atoll lagoons, reared stocks of the black-lip pearl oyster (*Pinctada margaritifera*, Linné, 1756) are added to wild populations, increasing the abundances of bivalves. Pearl oyster farming plays a major socio-economic role in French Polynesia with 81 million euros in exports and about 5000 jobs in 2008 (ISPF, 2008). This activity is entirely sustained by the wild collection of juveniles on artificial collectors, although the levels of spat collected are unpredictable. Efficient management of *P. margaritifera* production requires the ability to understand distribution of larvae, and identify suitable zones for spat collection. Among the 15 French Polynesia collecting atolls, Ahe atoll is one of the main

* Corresponding author at: Ifremer, DPFOM LPI, Presqu'île du Vivier, 29840 Argenton, France. Tel.: +33 2 98 89 29 43; fax: +33 02 98 89 29 59.
E-mail address: yoann.thomas1@gmail.com (Y. Thomas).

0025-326X/$ - see front matter © 2012 Elsevier Ltd. All rights reserved.
doi:10.1016/j.marpolbul.2011.12.028

producers of *P. margaritifera* juveniles and was chosen as a reference site to study bivalve larvae ecology.

The goals of this study were to quantify the spatio-temporal heterogeneity of bivalve larvae abundances, and develop plausible scenarios involving physical or biological mechanisms to explain observed patterns of variation. The link between larval patterns and *P. margaritifera* settlement variability is discussed.

2. Materials and methods

2.1. Sampling site

Ahe atoll is located in the Northwestern part of the French Polynesian Tuamotu Archipelago, 500 km northeast of Tahiti islands (Fig. 1). Ahe lagoon has a 145 km^2 area with a mean depth close to 40 m. Ahe is defined as a semi-enclosed atoll with a mean residence time of 34 days (Pagès and Andréfouët, 2001; Dumas et al., 2012). One active pass is located in the western part of the lagoon and several reef-flat spillways (less than 50 cm depth) are distributed along the reef rim, mainly in the south and west part of the lagoon (Andréfouët and Yamano, 2012). Almost 10% of the Ahe lagoon area is dedicated to black-lip pearl oyster rearing. The total stock of cultivated pearl oysters, located in breeding line and excluding spat on collectors, is judged to be 15 million individuals (Perliculture Service, pers. comm.), although the extent of the wild population remains unknown. With nearly 1240 spat collection stations and with 600 collectors per station, Ahe is one of the most important producers of pearl oyster juveniles in French Polynesia.

2.2. Sampling design

A multi-scale spatial and temporal approach was developed to assess larval abundance and size distribution and hydrographic parameters at local (*i.e.* horizontal and vertical) and lagoon scales, according to nycthemeral, day-to-day and seasonal dynamics.

2.2.1. Day-to-day lagoon-scale sampling

Sampling was made at 12 stations (L01–L12) distributed throughout the lagoon (Fig. 1). Stations were visited successively every 2 days in the morning, from L12–L01. Water was sampled at each station from the surface to 5 m above the bottom. To assess the seasonal dynamics, four surveys were carried out, in April–May 2007, July–August 2007, November 2007 and February–March 2008. For technical reasons, day-to-day samplings were of different durations: 29, 15, 20 and 29 days during these periods, respectively.

2.2.2. Local transect

Two north south transects (Fig. 1) of 10 stations separated by 100 m were sampled in the west and the central-east part of the lagoon, respectively. Water was sampled on each station from the surface to 5 m above the bottom. The two transects were successively sampled at 24-h interval. Three transect samplings surveys were carried out, in April 2007, May 2007 and July 2007, giving a total of 6 profiles; 3 for each transect.

2.2.3. 24-h cycle vertical sampling

Two deep stations, V01 and V02 (50 m deep), located in the west and the central-east part of the lagoon, respectively (Fig. 1), were sampled over the whole range of five layers (0–10, 10–20, 20–30, 30–40 and 40–50 m). Each station was sampled with a frequency of 4 h from 08:00 h over a 24-h cycle. The two stations were successively visited at a 24-h interval. These day/night cycles were studied in April 2007, July 2007 and February 2008, giving a total of six cycles; 3 for each station.

2.3. Zooplankton sampling method

Plankton was sampled from a boat by pumping at an average flow rate of 5 $m^3\ h^{-1}$. A pipe of 32 mm diameter was connected to the pump and immersed to the sampling depth. The mean sample volumes were of 560, 740 and 430 l for each of the lagoonal, transect and vertical samples, respectively. Pumped water was prefiltered on a 250 μm mesh and plankton was retained on a 40 μm mesh. Samples were immediately preserved in 72% ethanol.

In the laboratory, each sample was transferred into a 16 cm diameter glass dish and spread evenly. Three transversal bands covering the dish width and disposed at the first quarter, middle and third quarter of the dish diameter were scanned at 6400 ppp with an Epson V750*Pro* scanner. The sum of the three scanned surfaces corresponded to 6% of the total dish surface and therefore to 6% of the total sample. On each scan, bivalve larvae were visually enumerated and automatically measured using NIvision® image analysing software. The major axis of the adjusted ellipse was used to describe larval size. In 2007, the specific identification of bivalve larvae was difficult and did not allow *P. margaritifera* and *Pinctada*

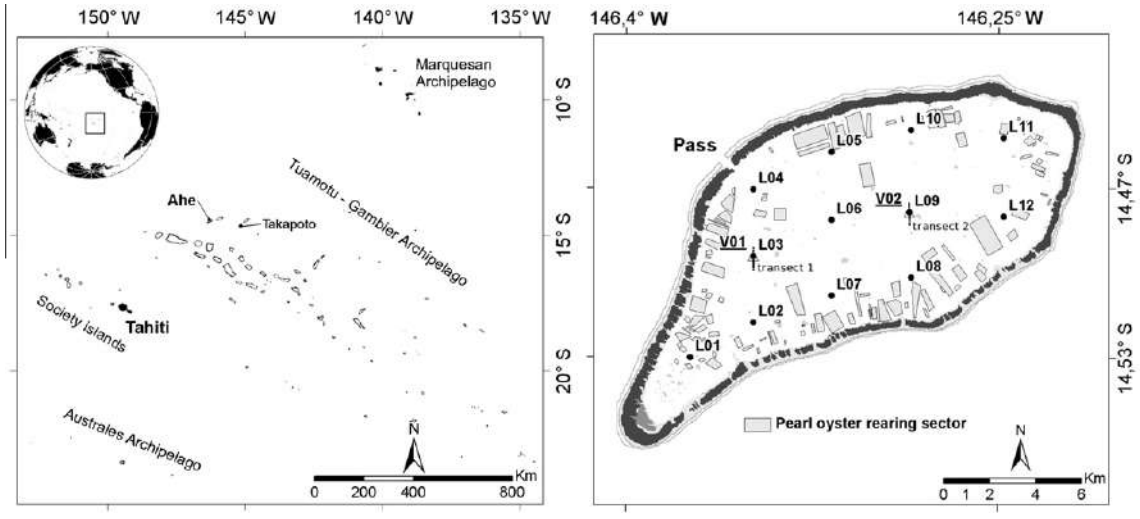

Fig. 1. Left: localisation of the Ahe lagoon. Right: morphology of the Ahe lagoon and positions of the sampling stations in the lagoon; 'L': lagoon scale, 'V': vertical scale (24-h cycles), 'Transect': local scale.

maculata (Gould, 1850) to be distinguished (Paugam et al., 2006), thus no species distinction could be made at the larval stage for this study.

2.4. Experimental spat collection

We studied black-lip pearl oyster settlement concurrently with planktonic bivalve larvae distribution, in order to assess any direct links between them. Three experimental collectors, of the type used in the industry (*i.e.* loops of black flat polypropylene, knitted onto a 30 cm monofilament polyethylene line), were immersed at 6 depths (5, 10, 15, 25, 35 and 45 m) at 2 stations (V01 and V02) for 6 weeks in April–May 2007, July–August 2007, November–December 2007 and February–March 2008. In the laboratory, spat were retrieved from the collectors and fixed in a 72% ethanol solution. Three groups: *P. margaritifera*, *P. maculata* and 'other bivalves' spat were identified and enumerated.

2.5. Environmental parameters

Vertical profiles of salinity (practical salinity unit), temperature (°C) and *in vivo* chlorophyll *a* ($\mu g\ l^{-1}$), were carried out *in situ* with a multi-parameter probe (SBE S19*Plus*, Sea-Bird Electronics Inc.) at each sampling station. Hourly wind direction and velocity were obtained from Takaroa atoll meteorological station (Météo France data) located about 120 km east of Ahe (145°3′4″W, 14°28′57″S). Wind direction and velocity were recorded in the field with a mobile anemometer during the 24-h cycles. A detailed description of spatial and temporal variation of environmental parameters can be found in Thomas et al. (2010).

2.6. Data analysis

Median size was used to characterise the population of larvae species. Knowing the median size provides a first description of community composition by inferring the developmental stage and species structure. The coefficient of variation ($CV = \sigma/\mu$) was calculated for larval abundance and size so as to quantify the degree of variability on various scales. To represent lagoon scales patterns, data were standardised by the standard score: $z = (V - \mu)/\sigma$ where V is the median size value or larval concentration. After $\log(x + 1)$ transformation of abundances for data normalisation and variance homogenisation, one-way ANOVA was applied to test the effects of space and time at the different scales. A post hoc Scheffé's pair-wise multiple comparison test was performed when significant differences were detected.

A Hierarchical Cluster Analysis (HCA), using similarity coefficient (*i.e.* Pearson correlation coefficient), was performed on all the daily abundances and median sizes ($n = 1200$), to identify homogeneous groups of stations at the lagoon scale in order to ease result interpretations.

Spearman correlations were used to test the relationships between bivalve larvae abundances and environmental parameters. Since all the data of the 4 sampling campaigns were introduced to calculate the correlation coefficient, the distribution of the data did not reach the normality. This has motivated the choose of the Spearman's rank correlation coefficient, which makes the coefficient less sensitive to non-normality in distributions. Finally, the mean depth distribution of the larvae (*ZCM*), described by Fortier and Leggett (Fortier and Leggett, 1982), was calculated for the 24-h cycles:

$$ZCM = \sum c_i d_i$$

where c_i is the concentration frequency at the ith depth interval and d_i is equal to the mid-depth of the ith interval.

3. Results and discussion

3.1. Vertical structure and dynamics

Bivalve larvae abundances were heterogeneously distributed through the water column ($p < 0.001$) (Table 1, Fig. 2a). Larvae were concentrated between 15 and 35 m depth. The mean *CV* calculated on the whole vertical profile was 38%. In addition, the population median size was unevenly distributed, with the largest larvae between 15 and 35 m depth (Fig. 2b).

Larvae exhibited vertical migration according to the day/night cycles (Figs. 3 and 4). No significant effect of the hour of the day was measured on the total concentration (Table 1), demonstrating the homogeneity of total abundances during the surveys. Larval abundances increased in the deeper layer during the day until 16:00 h and then increased in the upper layers until midnight. This cycle was mainly observed in the upper 10 m layer where larval concentration was systematically higher at night than during the day (Fig. 3). A slight variation of the mean depth distribution, *ZCM*, was measured with 26.5 m during the day and 23 at night (Fig. 4). This pattern implies nocturnal ascent and daytime descent but was disrupted by windy conditions, mainly during the two first surveys on the V02 station where day/night migration was not clear due to winds of 5.8 and 7.6 $m\ s^{-1}$, respectively, comparing to the 3.8, 3.8, 3.7 and 4.1 $m\ s^{-1}$ measured during the 4 others surveys. No specific pattern could be identified in the median size (data not shown) according to 24-h dynamics.

The vertical heterogeneity of bivalve larvae abundance observed in Ahe atoll is in agreement with a previous study in the Takapoto lagoon, with maximum larval concentration at mid-depth (pers. comm. Garen). Similar patterns were described for bivalve larvae by Garland et al. (2002) in an inner-shelf of North Carolina (USA) and by Raby et al. (1994) in the Baie des Chaleurs, Quebec, Canada. Various stimuli were suggested that might explain the vertical swimming behaviour of bivalve larvae, like salinity or temperature discontinuity, light intensity, food availability or avoidance of predators (Raby et al., 1994; Knights et al., 2006). In Ahe lagoon, the vertical distribution was positively correlated with temperature and food concentration (*i.e.* Chl *a in vivo*) (Table 2). These results must be considered cautiously because correlations are not causal relationships. Nonetheless, temperature (or saline) discontinuities may have a significant influence on the vertical swimming ability (*i.e.* speed) of bivalve larvae (see *e.g.* Dekshenieks et al., 1996). But this influence was always described with high variation levels in T or S and mostly for species from temperate area. That is why; specific experimental protocols need to be developed to better know the effect of various T and S gradients on tropical species larvae. However, autotrophic communities and bivalve larvae seem to follow similar dial dynamics, apparently driven by light intensity, as suggested by the day/night pattern observed. This swimming behaviour is however hampered by windy conditions, probably due to water column homogenisation. No specific pattern was observed in median sizes of larval cohorts during the 24-h cycles studied. Species-specific larval behaviour at this stage could instead be invoked to describe the vertical distribution (Baker, 2003).

3.2. Large-scale distribution and dynamics

Bivalve larvae were present in the plankton of Ahe lagoon at each of the sampling periods. The average abundance ranged from $15.8 \pm 0.6 \times 10^3\ m^{-3}$ in November 2007 to $21.3 \pm 1.1 \times 10^3\ m^{-3}$ in April–May 2007 (Table 3). This constant presence is in agreement with the continuous reproductive patterns described for tropical bivalves (Pouvreau et al., 2000). Average concentrations were

Table 1
Results of the one-way ANOVA tests. In the comments column, numbers give the depth level (m) or the survey number (1: April–May, 2: July–August, 3: November and 4: February–March), and the letters give the homogenous groups.

Parameter	Factor	DF	*F*	*p*	Comment
Larval concentration	Station	1	18.03	<0.0001	V01 > V02
	Depth	4	5.55	0.0003	5a 15bc 25c 35abc 45ab
	Hour	5	0.42	0.836	=
Larval median size	Station	1	150.52	<0.0001	V01 < V02
	Depth	4	4.76	0.001	5ab 15a 25a 35ab 45b
	Hour	5	0.60	0.732	=
P. margaritifera spat density	Station	1	8.53	0.006	V01 < V02
	Survey	3	5.18	0.004	1a 2b 3b 4ab
	Depth	5	9.57	<0.0001	5a 10ab 15abc 25bc 35c 45c
P. maculata spat density	Station	1	1.97	0.169	V01 = V02
	Survey	3	6.40	0.001	1a 2b 3ab 4a
	Depth	5	7.91	<0.0001	5ab 10a 15a 25ab 35c 45bc
Other bivalves spat density	Station	1	10.317	0.003	V01 < V02
	Survey	3	11.15	<0.0001	1a 2c 3ab 4bc
	Depth	5	8.63	<0.0001	5a 10a 15a 25a 35a 45b

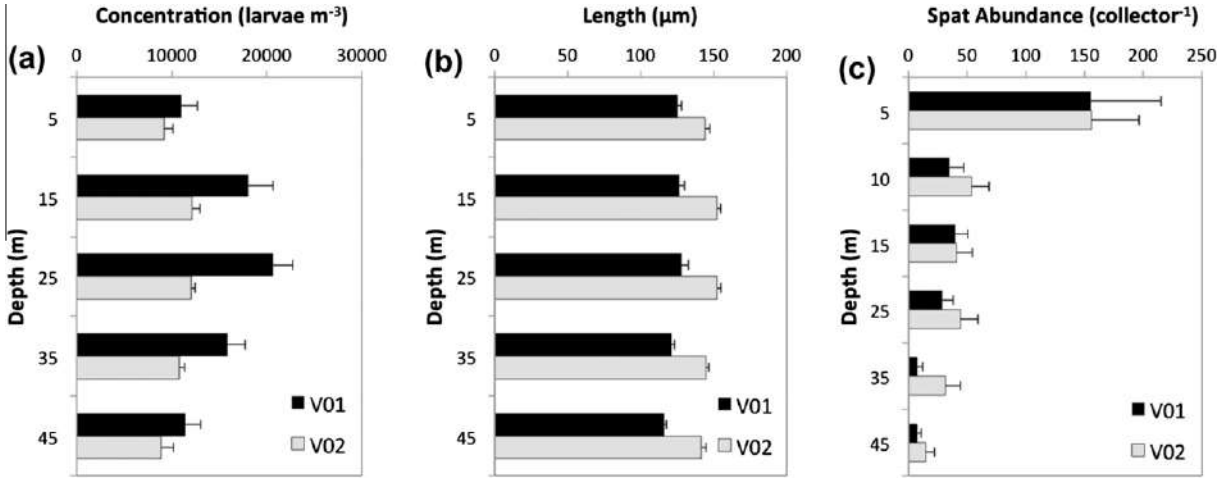

Fig. 2. (a) Vertical patterns of bivalve larvae abundance, (b) bivalve larvae median size and (c) *P. margaritifera* spat settlement density at the two stations V01 and V02. Data correspond to averages ± standard error, calculated on the three sampling periods: April–May 2007, July–August 2007 and February–March 2008.

higher than in other atolls. In addition, bivalve larvae contribute to a large part of the zooplankton abundance in the Ahe lagoon with a contribution of 53.3 ± 13.2% to the abundance (Pagano et al., 2012). In their study of Tikehau lagoon (French Polynesia), Blanchot et al. (1989) reported a mean bivalve larvae concentration of 0.9×10^3 m^{-3}, ranging from 0.2×10^3 to 1.9×10^3 m^{-3}, and corresponding to 6% of the plankton abundance. An average concentration of 2.1×10^3 m^{-3}, ranging from 0.3×10^3 to 35.4×10^3 m^{-3} was measured in the Takapoto lagoon (French Polynesia) (Garen, unpublished data).

The larval concentration in Ahe lagoon appeared also very high compared with other ecosystems. A coastal lagoon of southern Portugal had an average bivalve larvae concentration around 4.7×10^3 m^{-3} (Chicharo and Chicharo, 2000), and the inner-shelf off North Carolina yielded 9.8×10^3 m^{-3} (Garland et al., 2002).

The abundant population of adults in Ahe lagoon certainly explain the permanent larval abundance, which is also modulated, by larval mortality due to predation, export, and starvation. In Ahe, only the reared *P. margaritifera* stock numbers are well known (ca. 15×10^6 individuals), not including oysters on collectors that are breeders from the age of approximately 6 months to 1 year. Although no data are available on the wild bivalve populations in Ahe lagoon, 6 bivalve species are likely present given their abundance in other Polynesian atoll lagoons: *Arca ventricosa* (Lamarck, 1819), *P. maculata*, *Crassostrea cucullata* (Born, 1778), *Spondylus varians* (Sowerby, 1829), *Chama iostoma* (Conrad, 1837) and *Tridacna maxima* (Röding, 1798). An evaluation of the wild population broodstocks should be made in Ahe lagoon to evaluate the relative contribution of these species to the entire bivalve community. Our spat settlement measurement suggest that *P. maculata* would be dominant since it accounts for almost 80% of the total density (see below). Nonetheless, species selectivity of collectors is unknown and it would be hazardous to draw any direct conclusion about wild stock from this result.

During our surveys, the variability of larval abundance appeared lower on the local scale than on the large scale. Larval abundance was constant or exhibited gradient shape along the two transects (Fig. 5). This observation meant that interpretation mistakes due to small-scale patchy patterns were minimised.

Bivalve larvae abundances were heterogeneously distributed at the lagoon scale (Fig. 6), with a general pattern showing (i) a low concentration area in front of the pass, (ii) a high concentration area along the east reef rim and (iii) a more variable concentration area in the southwest sector. The extent of the southern high concentration sector was the most variable feature, with a minimal area during the August survey, which was the windiest period, and a shift of the 'poorest' area towards the west coast of the lagoon. A significant east–west gradient was revealed for the median

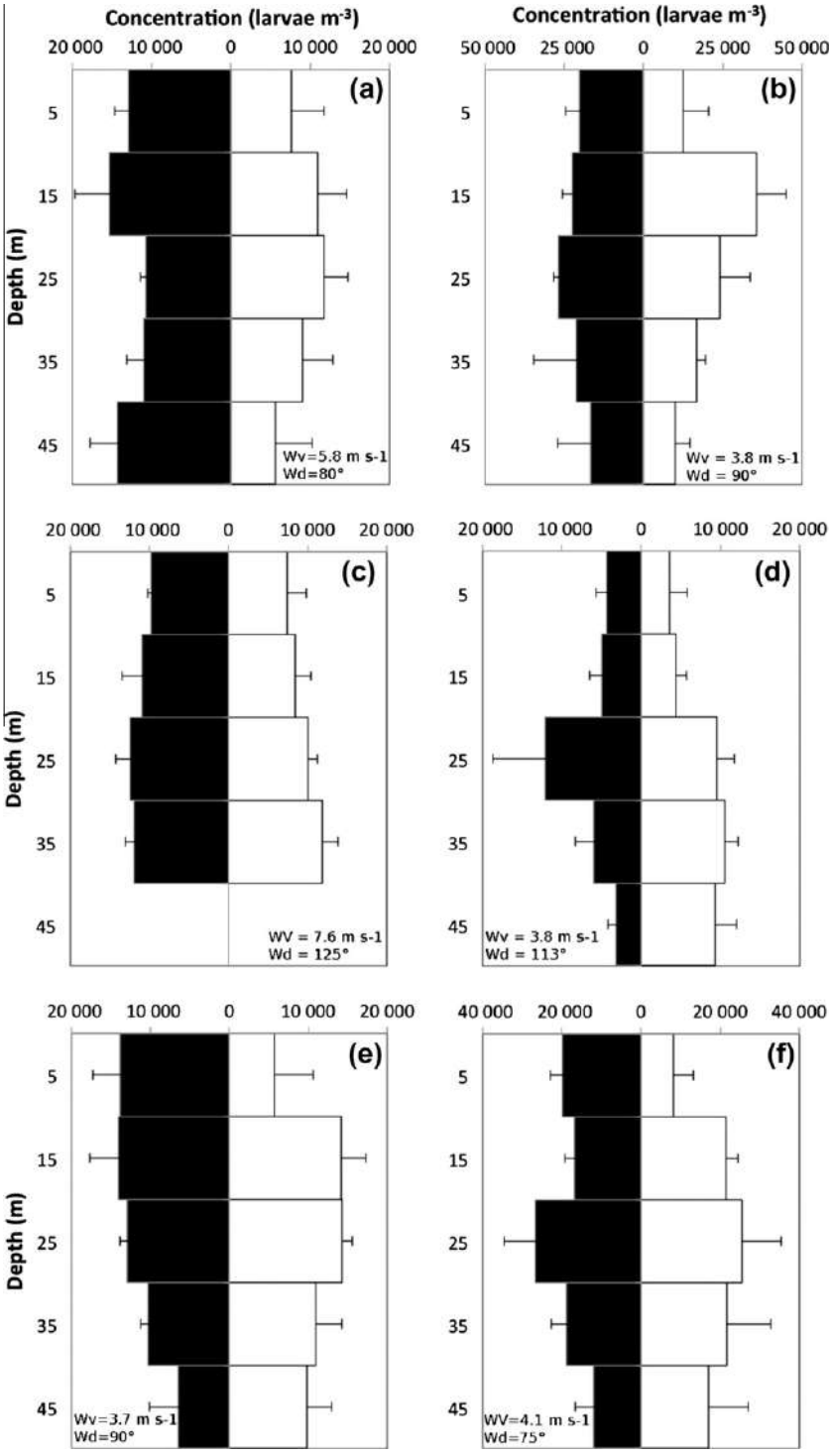

Fig. 3. Vertical distribution of bivalve larvae concentration (±standard error) during the day (open) and at night (black): (a) V02-April 07, (b) V01-April 07, (c) V02-July 07, (d) V01-July 07, (e) V02-February 08 and (f) V01-February 08. Day means correspond to four measurements: 08:00, 12:00, 16:00 and 08:00 the second day and night means to three measurements: 20:00, 00:00 and 04:00. Wind velocity (Wv) and direction (Wd) are indicated on the plots.

size of bivalve larvae cohorts, showing higher values in the eastern sector at every survey (Fig. 6). A similar large-scale pattern was described by Carleton and Doherty (1998) in the Taiaro atoll lagoon, with different zooplankton assemblages in windward and leeward parts of the lagoon, which they interpreted as a result of both hydrodynamic circulation and species-specific behaviour.

Ahe should be regarded as a deep lagoon, with a 40 m average depth and maximum depth over 70 m. In such deep lagoons, circulation patterns are mostly wind-driven, with surface circulation going downwind and a 'compensatory' upwind current of deep water (Atkinson et al., 1981). Since the majority of larvae were actually distributed in deep layers, the vertical distribution of bivalve larvae could explain some of the observed large-scale patterns, the larvae being subjected to the 'compensatory' upwind current leading to high larval concentration along the eastern reef rim. This observation is confirmed by the study of Pagano et al. (2012) in the Ahe lagoon, describing heterogeneity in zooplankton assemblage, with species showing a migratory behaviour

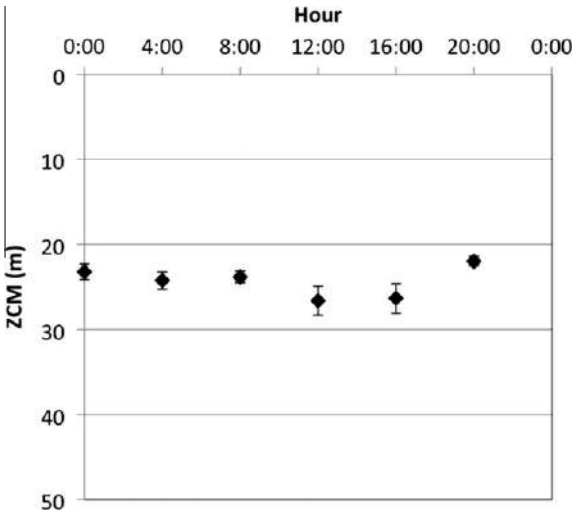

Fig. 4. Dial variation of the mean depth distribution of the larvae, *ZCM*. Data correspond to the averages ± standard error calculated on the overall 24-h cycles data set.

concentrated in the western part of the atoll and a high concentration of bivalve larvae in the eastern part by windy conditions. The large-scale pattern could also be related to the broodstock distribution, as the majority of the cultivated broodstock is located close to the reef rim around the lagoon. The central part of the lagoon has deep waters, with few reefs suitable as adult habitat (Adjeroud et al., 2000; Pante et al., 2006). Nonetheless, the high transport potential for larvae observed in our study (see below) and confirmed by the modelling study of Thomas et al. (2012) on the larval transport and connectivity in the Ahe lagoon, seem to minimise the effect of the broodstock location, mainly by eastern winds.

In atoll lagoons, tide residual transport and direct influence on planktonic communities exhibit a general low pattern and are mostly confined to the vicinity of the pass (Tartinville et al., 1997). In our study, the diluting effect of the pass was obvious and corroborated by the positive correlation between larval abundances and distance from the pass (Table 2). Stations L04, L05 and L06, located in front of the pass, and extended toward the east, were mainly submitted to this diluting effect.

The Hierarchical Cluster Analysis (HCA) allowed four groups of stations with similar abundance and median size patterns and dynamics to be identified (Fig. 7): a western confined sector A, corresponding to the L01 station; a sector B, separated in two groups: one in front of the pass covering the L02, L03 and L04 station and a second in southeast, covering the stations L08, L09 and L12; an extended north sector, C, covering the stations L05, L06, L10 and L11; and a small south sector, D, corresponding to the station L07. HCA did not provide any explanation or interpretation, so the results need to be considered carefully. Indeed, as our HCA analysis did not include weighting by location proximity, the spatial and temporal continuity of two-day step data used for the HCA may induce positive spatial autocorrelations (Schabenberger and Gotway, 2005). This analyse is mainly used to simplify the short-time scale patterns presentation and interpretation.

Short time-scale variations were recorded in wind velocity, mostly during the three first surveys (Fig. 8a). In addition, high day-to-day variations in phytoplankton biomass were observed, concurrent to stratification/mixing events, showing higher

Table 2
Spearman correlation among the studied environmental parameters (LARV = larval abundance, SAL = salinity, TEMP = temperature, Chl *a* = *in vivo* Chlorophyll-a, Dist pass = distance from pass, Dist east-reef = distance from eastern reef and WV = wind velocity) according to the three spatial scales studied.

Scale		LARV	SAL	TEMP	Chl *a*	Dist pass
Lagoon	SAL	0.04				
	TEMP	0.06	−0.06			
	CHLA	0.07	0.30***	0.37***		
	Dist pass	0.42***	0.03	−0.09*	0.08*	
	Dist east-reef	−0.37***	0.02	0.01	−0.16***	−0.85***
	WV	0.04	0.17***	0.13**	0.12**	–
Transect	SAL	−0.39**				
	TEMP	0.02	−0.59***			
	CHLA	0.30*	−0.16	0.14		
	Dist pass	0.07	0.05	−0.26*	0.34**	
	Dist east-reef	−0.19	−0.06	0.24	−0.29*	−0.75***
Vertical	SAL	−0.33***	–			
	TEMP	0.43***	−0.33***	–		
	CHLA	0.14*	0.01	−0.14	–	

* $p < 0.05$.
** $p < 0.01$.
*** $p < 0.001$.

Table 3
Water temperature, bivalve larvae concentration: mean ± standard error (*n*); and spat density of *P. margaritifera*, *P. maculata* and other bivalve species on collectors: mean of 6 depths ± standard error (*n*, relative proportion) during four survey periods (letters indicate significant differences between surveys: $p < 0.05$).

			April–May	July–August	November	February–March
Water temperature (°C)			29.3 ± 0.001^{a} ($>10^4$)	27.2 ± 0.001^{b} ($>10^4$)	28.2 ± 0.001^{c} ($>10^4$)	28.6 ± 0.001^{d} ($>10^4$)
Bivalve larvae ($\times 10^3$ m^{-3})			21.3 ± 1.1^{a} (194)	17.4 ± 0.8^{ab} (96)	15.8 ± 0.6^{b} (132)	19.7 ± 0.9^{ab} (180)
Spat (collector^{-1})	V01	*P. margaritifera*	35 ± 7^{a} (12, 0.52)	11 ± 6^{b} (6, 1.5)	15 ± 8^{ab} (6, 0.39)	88 ± 35^{a} (14, 2.12)
		P. maculata	5853 ± 2188^{a} (*8*, 86.50)	570 ± 166^{b} (6, 78.01)	3238 ± 1568^{ab} (*6*, 80.76)	3742 ± 1149^{ab} (*6*, 90.27)
		Other bivalves	879 ± 198^{a} (*8*, 12.98)	150 ± 52^{b} (*6*, 20.49)	756 ± 259^{ab} (*6*, 18.85)	315 ± 117^{ab} (*6*, 7.61)
	V02	*P. margaritifera*	61 ± 13^{a} (*12*, 1.64)	81 ± 49^{a} (*6*, 4.65)	42 ± 18^{a} (*6*, 0.99)	49 ± 18^{a} (*12*, 0.75)
		P. maculata	2408 ± 1007^{b} (*8*, 65.04)	1369 ± 585^{b} (*6*, 78.99)	3017 ± 1177^{b} (*6*, 71.61)	5941 ± 1755^{a} (*8*, 91.29)
		Other bivalves	1233 ± 288^{a} (8, 33.32)	284 ± 67^{c} (6, 16.37)	1154 ± 335^{ab} (6, 27.40)	518 ± 118^{b} (8, 7.96)

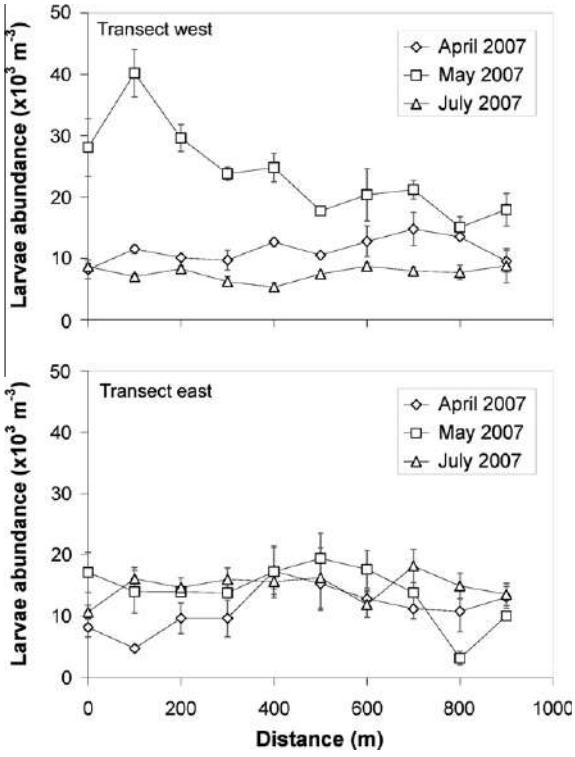

Fig. 5. Bivalve larvae abundance variation (mean ± standard error) along the west (up) and east (down) transects, during three sampling surveys.

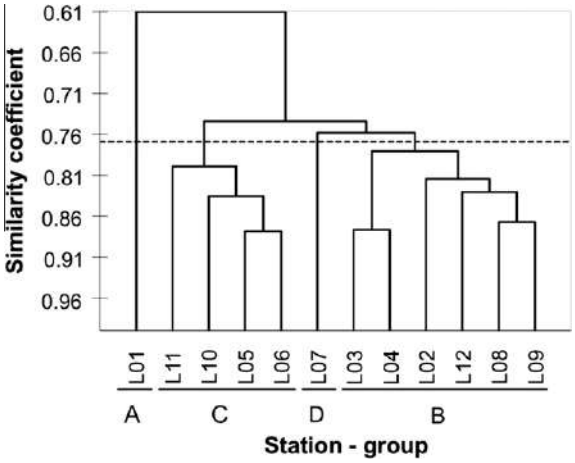

Fig. 7. Dendrogram extracted from the Hierarchical Cluster Analysis.

concentration in the deeper layers (Fig. 8b). The bivalve larvae abundances and median size variations are presented on Fig. 8c and d with a two-day step frequency, according to the four groups identified by the Hierarchical Cluster Analysis: A, B, C and D. The mean coefficients of variation calculated for sectors A, B, C and D were 101%, 30%, 32% and 54%, respectively. These high levels of variation were mainly supported by the first and last surveys. Four successive increases in abundance were then observed with increasing intensity during the fourth survey in sector A (Fig. 8c). A specific event occurred during the first survey, on 8 May, with a synchronous increase in the four sectors. The abundance rise recorded in sector A also appeared delayed in the adjacent D area, as seen during the first survey, after the 8 May, and during the last survey, after the second and third 'larval blooms', on 19 and 25 February.

The 'larval blooms' observed during the first and last surveys were correlated with high wind occurrence, leading to the homogenisation of the water column that was recorded through the Chl *a* *in vivo* measurement (Fig. 8b). As revealed by the day-to-day recording, abundance variations appeared to be mostly sustained by punctual increases, which were dominant in sector A. These events were related to a decrease in median size and could then be linked to spawning events. The southwest zone can, therefore, be considered as a 'source area' for larvae, sustained by multiple 'spawning events' identified by the simultaneous increase in abundance and decrease in median size. Indeed, this sector gathers an important pearl oyster stock and several reefs suitable as adult habitat. Nevertheless, bivalve larvae abundance decreased rapidly after these 'spawning events' in L01 and reached lower values than in other areas, providing evidence of export. This west–east transfer through the southern part of the lagoon is supported by the delay of abundance rises described between sectors A and D (Fig. 8c). Furthermore, westward extension of the B and C groups shows evidence of east–west transfers.

A system like the counter-rotating bodies of water described by Atkinson et al. (1981) in the Enewetak atoll lagoon could explain these east–west transfers without north–south communication.

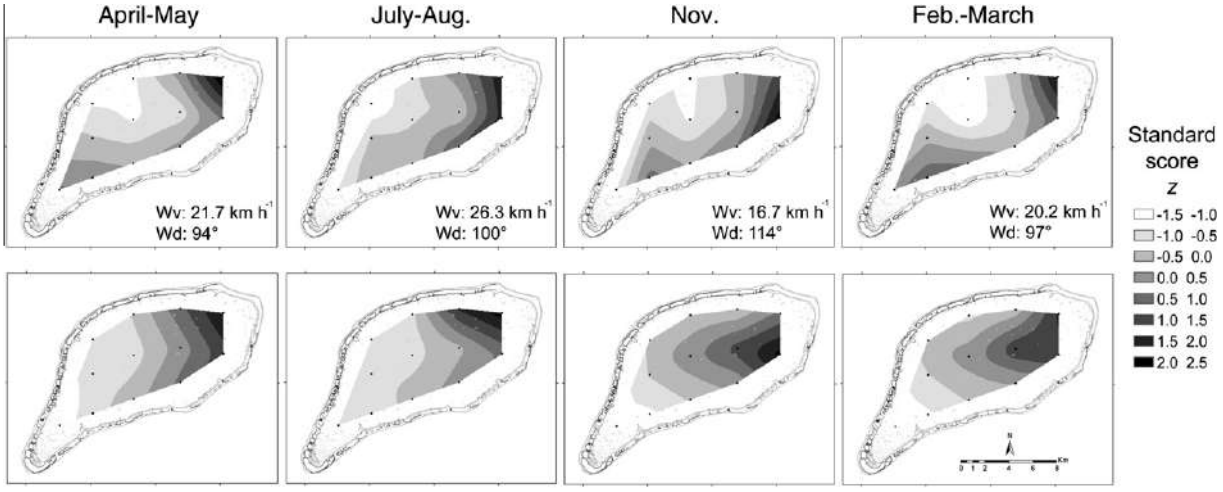

Fig. 6. Spatial variation of bivalve larvae abundance (up) and bivalve larvae median size (down), in the four surveys: (a) April–May 2007, (b) July–August 2007, (c) November 2007 and (c) February–March 2008. All data were standardised (standard score *z*). Mean wind velocity (Wv) and wind direction (Wd) are indicated on the maps.

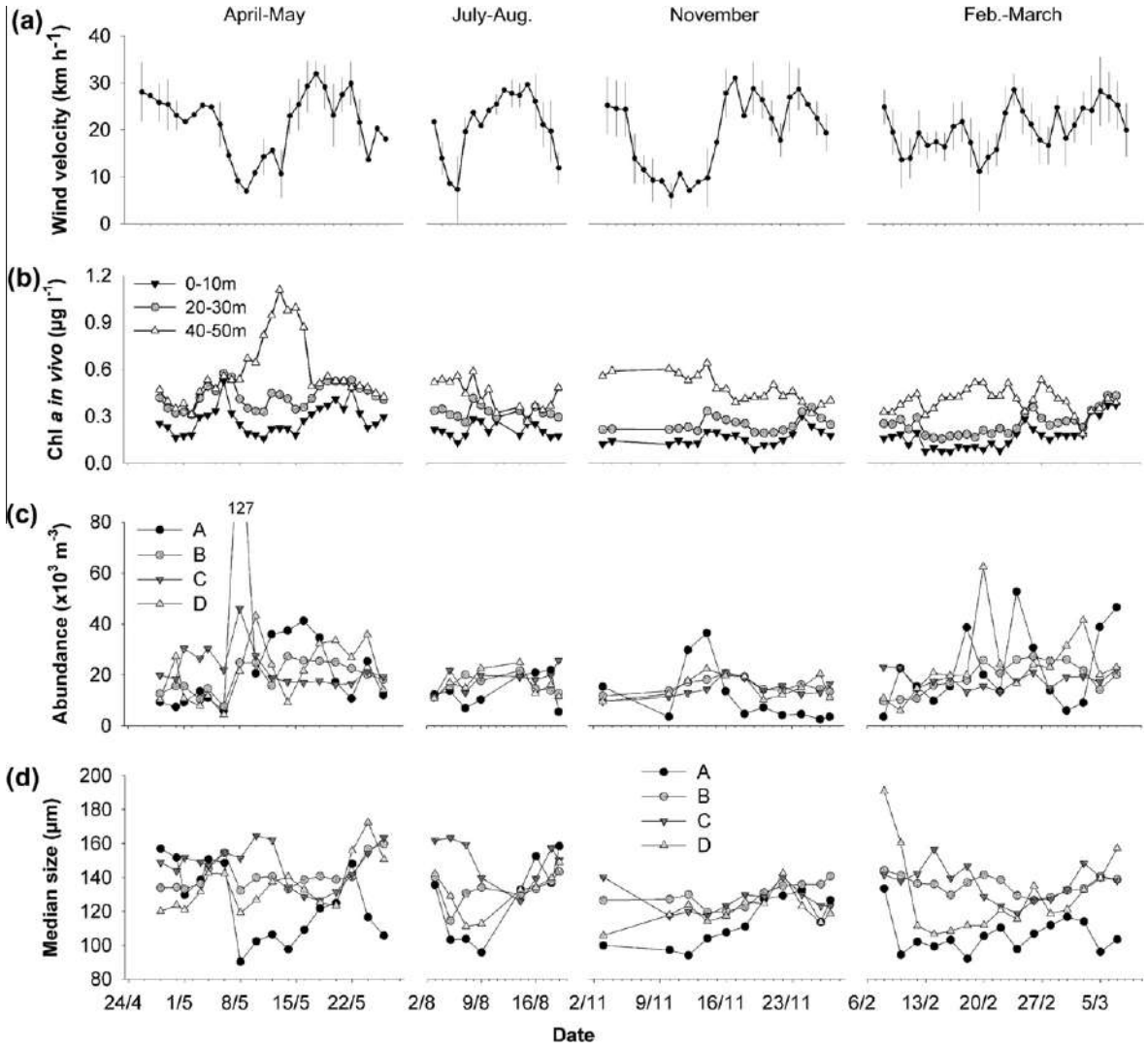

Fig. 8. Day-to-day variation in wind velocity, Chl *a in vivo* concentration by 10 m depth layers, abundance of bivalve larvae and median size of bivalve larvae for the four groups of stations: A, B, C and D, during the four surveys: April–May 2007, August 2007, November 2007 and February–March 2008.

Indeed, this kind of functioning has been recently described in Ahe lagoon by Dumas et al. (2012), with the stream function displaying three main barotropic circulation structures: a flat clockwise cell along the southern rim, an anticlockwise circulation cell in the middle of the atoll, and a clockwise circulation loop along the northern rim. In addition, a high connectivity level between sectors of the Ahe lagoon has been recently confirmed by Thomas et al. (2012), through a 3D modelling study of the larval transport. Indeed, they showed that the west–east transfer of larvae was supported by eastern winds, observed during the summer period, and related to the activation of a compensatory current in the deep layers. For winds coming from the southeast, mainly observed during the winter, a lower compensatory current, induced by a low fetch, implies higher retention of the larvae in their origin area.

3.3. Bivalve larvae patterns related to environmental factors

Correlations between environmental parameters and bivalve larvae abundances at the three spatial scales studied are presented in Table 2. Spatio-temporal variability of environmental parameters such as the temperature, salinity and phytoplanktonic communities in the Ahe lagoon were described by Thomas et al. (2010). Distances from the pass and from the eastern reef were added to the analysis in order to extract the effects of water renewal and geomorphology.

At the lagoon scale, larval abundances revealed a significant positive correlation with distance from the pass and negative correlation with distance from the eastern reef. At the local scale (*i.e.* transects), larval abundance showed significant positive correlation with Chl *a in vivo* and negative correlation with salinity. Finally, at the vertical scale, larval abundance exhibited a significant positive correlation with temperature and *in vivo* Chl *a*, and a negative correlation with salinity.

Maximal larval concentrations were recorded during the warmest periods. As already mentioned, this pattern must largely be related to oyster broodstock reproductive activity that, despite continuous reproduction, reaches a maximum during warm periods (Pouvreau et al., 2000). Reproductive pattern itself appeared closely linked to hydro-biological and/or meteorological events on a short time-scale, according to the synchronous 'spawning events' correlated with high wind occurrences recorded during the first and last surveys (Fig. 7). Bivalve molluscs are known to have stress-induced reproductive triggers (Fujikura et al., 2007). Windy conditions could, therefore, provide a physical stress factor that triggers reproduction by current modification, water mixing or the consequent modification of hydro-biological parameters (*e.g.*

food concentration and/or availability). Indeed, Fournier et al. (2012) showed recently that *P. margaritifera* developed a clear opportunistic strategy of reproduction in which gametogenesis rate and spawning are directly related to plankton concentration, itself correlated to the wind speed.

The spatial patterns described in our study showed significant heterogeneity, in agreement with the 'multiple driving force hypothesis' described by Pinel-Alloul (1995), and defined as the combination of biotic and abiotic factors controlling environmental heterogeneity. We demonstrated the primacy of abiotic factors controlling bivalve larvae heterogeneity at a large spatial scale and a greater importance of biological processes at smaller scales. At the lagoon scale, bivalve larvae abundances were then positively correlated with the distance from the pass, indicating a significant diluting effect. In addition, abundances were negatively correlated with the distance from the eastern reef, which could partly be related to hydrodynamic effects on retention or through the effect of the compensatory current in deep layers (Thomas et al., 2012). At last, the large scale heterogeneity in larval concentration may be related to the trophic resource heterogeneity described by Thomas et al. (2010) and the opportunistic strategy of reproduction of *P. margaritifera* described by Fournier et al. (2012), with higher plankton concentration close to the east and west reefs, corresponding to the sectors most concentrated in larvae. On the smallest scales, larval abundances were significantly correlated with temperature, salinity and food concentration, and exhibited vertical swimming behaviour leading to vertical structuring of abundances.

3.4. Bivalve species settlement patterns

P. margaritifera spat appeared largely under-represented on collectors, with a relative proportion of 1.6% compared with 80.3% and 18.1% for the *P. maculata* and 'other bivalves', respectively (Table 3). *P. margaritifera* spat settlement on artificial collectors showed a low but significant difference ($p = 0.044$) between the two stations, with higher densities at V02 (Table 3). The maximum *P. margaritifera* spat recruitment was recorded at 5 m depth with a strong decrease below this layer (Fig. 2). No significant seasonal difference was recorded at the V02 station, and maxima were recorded in April–May and February–March at V01.

P. maculata spat showed maximum density in the first 25 m (data not shown). No significant difference was recorded between stations ($p > 0.05$), both showed lower abundances in August and higher during warm periods in April and February.

'Other bivalves' showed significantly lower density at 45 m (data not shown) with higher abundances at V02. The same seasonal trend was recorded at both stations, showing maxima during the first and third surveys.

Several studies indicate spatial and temporal variability of benthic invertebrate larvae settlement over a wide range of scales (Porri et al., 2008). Beside the substrate selection, most studies explain this temporal and spatial variation by two related factors: hydrodynamics and larval supply (Friedman and Bell, 1999). In our case, significant spatio-temporal variations were found for the *P. margaritifera* spat settlement. The two collecting stations exhibited different patterns: the eastern sector showing no seasonal variation, but higher settlement performances, and the western stations showing a more seasonal pattern, with higher performances during warm periods. These observations could be related to the distribution of bivalve larvae cohorts on a large scale, with high concentrations in the east and a more variable southwest area. The larval phase of *P. margaritifera* has a duration of 3–4 weeks in the laboratory (Southgate and Beer, 1997). Larvae could, therefore, be exported from the southwest sector to an area with higher residence time until they reach the competent stage necessary for settlement (Le Pennec et al., 2003). Higher larval median sizes found in the eastern part of the lagoon and east-to-west connectivity in the western part of the lagoon measured during eastern wind periods corroborate this observation. As observed during the July–August survey, the windiest conditions coincided with lowest settlement westward and increasing settlement eastward, indicating that windy conditions provide favourable circumstances for west to east transport.

Vertical heterogeneity was found with maximum *P. margaritifera* settlement at 5 m depth, which is in agreement with previous studies and industry recommendations (Friedman and Bell, 1999). However these observations differ from those made in Takapoto lagoon, where more than half of the wild stock was found in the 30–40 m depth layer (Zanini and Salvat, 2000). Specific behaviour related to artificial substrates (*i.e.* collectors) might explain the characteristics of oysters in Ahe atoll, as chemical cues (*e.g.* biofilm coverage) and substrate type (*i.e.* deep colour, roughness) are key parameters determining attractiveness for settlement (Doroudi and Southgate, 2002; Su et al., 2007), and may be depth-dependent. In addition, *P. margaritifera* spat appeared to be particularly under-represented, mainly in comparison with *P. maculata* spat. Inter-specific competition could, therefore, contribute to a part of the spatio-temporal variation in settlement on collectors.

4. Conclusion

Despite the low variability of hydro-biological parameters commonly assumed in atoll lagoons, we recorded significant heterogeneity of bivalve larvae abundances in the range of the spatio-temporal scales we examined. According to the 'measured heterogeneity' concept, defined as the product of the observer's perspective (Pinel-Alloul, 1995), bivalve larvae appeared (i) concentrated at mid-depth with nocturnal ascent and daytime descent, (ii) heterogeneously dispersed at the lagoon scale, (iii) exhibited day-to-day abundance variations and (iv) transferred between sectors of the lagoon. These transfers provide evidence for intra-lagoonal connectivity and, therefore, for potential source and sink sectors. According to the 'functional heterogeneity' concept (Pinel-Alloul, 1995), which arises from the ecological interactions between ecological entities and their environment, we identified (i) the primacy of physical factors at a large spatial scale, with the diluting effect of renewal and large-scale hydrodynamic transfers, and (ii) the primacy of biological processes at smaller scales, showing larval swimming activity leading to vertical migrations positively correlated with food concentration. Small time-scale abundance variations also appeared to be driven by reproductive activity, itself correlated with meteorological conditions (*i.e.* windy periods). Finally, we demonstrated the positive relationship between bivalve larvae abundance and *P. margaritifera* settlement abundance. However, only species identification at larval stages should provide more information between small-scale larval patterns and spat settlement. To this end, whole mount *in situ* hybridisation technique recently developed to allow the discrimination of closely-related pearl oyster larvae species found in the French Polynesian atolls (Thomas et al., 2011), might be a relevant tool.

Acknowledgements

This study was funded by the Institut Français de Recherche pour l'Exploitation de la Mer (Ifremer) and the French Polynesian government (research delegation) with technical support of the Service de la Perliculture. Authors wish to express their gratitude to the Ifremer and Service de la Perliculture staff for their efficient help during sample collection. We also thank the Pa'umotu: the Maifano family for their effective assistance on Ahe atoll. We thank H. McCombie for her helpful comments and English revision.

References

Adjeroud, M., Andréfouët, S., Payri, C., Orempuller, J., 2000. Physical factors of differentiation in macrobenthic communities between atoll lagoons in the Central Tuamotu Archipelago (French Polynesia). Marine Ecology-Progress Series 196, 25–38.

Andréfouët, S., Yamano, H., 2012. High resolution mapping of semi-enclosed atoll rims for the characterisation of hydrodynamic processes: the case of Ahe and Takaroa (Tuamotu Archipelago). Submitted for publication.

Atkinson, M., Smith, S.V., Stroup, E.D., 1981. Circulation in Enewetak atoll lagoon. Limnology and Oceanography 26, 1074–1083.

Avois-Jacquet, C., 2002. Variabilité spatiale multiéchelle du zooplancton dans un lagon récifal côtier. phD dissertation, Université Paris 6, France Université de Montréal, Canada.

Badylak, S., Phlips, E.J., 2008. Spatial and temporal distributions of zooplankton in Tampa Bay, Florida, including observations during a HAB event. Journal of Plankton Research 30, 449–465.

Baker, P., 2003. Two species of oyster larvae show different depth distributions in a shallow, well-mixed estuary. Journal of Shellfish Research 22, 733–736.

Blanchot, J., Charpy, L., Le Borgne, R., 1989. Size composition of particulate organic matter in the lagoon of Tikehau atoll Tuamotu Archipelago pacific ocean. Marine Biology 102, 329–340.

Borcard, D., Legendre, P., Avois-Jacquet, C., Tuomisto, H., 2004. Dissecting the spatial structure of ecological data at multiple scales. Ecology 85, 1826–1832.

Botsford, L.W., White, J.W., Coffroth, M.A., Paris, C.B., Planes, S., Shearer, T.L., Thorrold, S.R., Jones, G.P., 2009. Connectivity and resilience of coral reef metapopulations in marine protected areas: matching empirical efforts to predictive needs. Coral Reefs 28, 327–337.

Carleton, J.H., Doherty, P.J., 1998. Tropical zooplankton in the highly-enclosed lagoon of Taiaro atoll (Tuamotu Archipelago, French Polynesia). Coral-Reefs 17, 29–35.

Chicharo, L.M.Z., Chicharo, M.A., 2000. Short-term fluctuations in bivalve larvae compared with some environmental factors in a coastal lagoon (South Portugal). Scientia Marina 64, 413–420.

Cowen, R.K., Lwiza, K.M.M., Sponaugle, S., Paris, C.B., Olson, D.B., 2000. Connectivity of marine populations: open or closed? Science 287, 857–859.

Cowen, R.K., Paris, C.B., Srinivasan, A., 2006. Scaling of connectivity in marine populations. Science 311, 522–527.

Dekshenieks, M.M., Hofmann, E.E., KlinckJ, M., Powell, E.N., 1996. Modeling the vertical distribution of oyster larvae in response to environmental conditions. Marine Eccology Progress Series 136, 97–110.

Doroudi, M.S., Southgate, P.C., 2002. The effect of chemical cues on settlement behaviour of blacklip, pearl oyster (*Pinctada margaritifera*) larvae. Aquaculture 209, 117–124.

Doroudi, M.S., Southgate, P.C., Mayer, R.J., 1999. The combined effects of temperature and salinity on embryos and larvae of the black-lip pearl oyster, *Pinctada margaritifera* (L.). Aquaculture Research 30, 271–277.

Dumas, F., Le Gendre, R., Thomas, Y., Andréfouët, S., 2012. Tidal flushing and wind driven circulation of Ahe lagoon (Tuamotu Archipelago, French Polynesia) from *in situ* observations and numerical modelling. Marine Pollution Bulletin. 65, 425–440.

Eckman, J.E., 1996. Closing the larval loop: linking larval ecology to the population dynamics of marine benthic invertebrates. Journal of Experimental Marine Biology and Ecology 200, 207–237.

Fortier, L., Leggett, W.C., 1982. Fickian transport and the dispersal of fish larvae in estuaries. Canadian Journal of Fisheries and Aquatic Sciences 39, 1150–1163.

Fournier, J., Levesque, E., Pouvreau, S., Le Pennec, M., Le Moullac, G., 2012. Influence of plankton concentration on gametogenesis and spawning of the blacklip pearl oyster *P. margaritifera* in Ahe atoll lagoon (Tuamotu Archipelago, French Polynesia). Marine Pollution Bulletin. 65, 463–470.

Friedman, K.J., Bell, J.D., 1999. Variation in abundance of blacklip pearl oyster (*Pinctada margaritifera* Linne.) spat from inshore and offshore reefs in Solomon islands. Aquaculture 178, 273–291.

Fujikura, K., Amaki, K., Barry, J.P., Fujiwara, Y., Furushima, Y., Iwase, R., Yamamoto, H., Maruyama, T., 2007. Long-term in situ monitoring of spawning behavior and fecundity in *Calyptogena* spp. Marine Ecology-Progress Series 333, 185–193.

Garland, E.D., Zimmer, C.A., Lentz, S.J., 2002. Larval distributions in inner-shelf waters: the roles of wind-driven cross-shelf currents and diel vertical migrations. Limnology and Oceanography 47, 803–817.

Haury, L., McGowan, J., Wiebe, P., 1978. Patterns and processes in the time-space scales of plankton distribution. In: Steele, J.H. (Ed.), Spatial Pattern in Plankton Communities. Plenum Press, New York, pp. 277–327.

Hofmann, E.E., Powell, E.N., Bochenek, E.A., Klinck, J.A., 2004. A modelling study of the influence of environment and food supply on survival of *Crassostrea gigas* larvae. Ices Journal of Marine Science 61, 596–616.

ISPF, 2008. Regards sur l'économie de l'année 2008. Institut de la Statistique de la Polynésie française, Regards No. 19, p. 94.

Knights, A.M., Crowe, T.P., Burnell, G., 2006. Mechanisms of larval transport: vertical distribution of bivalve larvae varies with tidal conditions. Marine Ecology-Progress Series 326, 167–174.

Le Pennec, M., Paugam, A., Le Pennec, G., 2003. The pelagic life of the pectinid pecten maximus – a review. Ices Journal of Marine Science 60, 211–223.

Levin, L.A., 2006. Recent progress in understanding larval dispersal: new directions and digressions. Integrative and Comparative Biology 46, 282–297.

Masson, S., Pinel-Alloul, B., Dutilleul, P., 2004. Spatial heterogeneity of zooplankton biomass and size structure in southern Quebec lakes: variation among lakes and within lake among epi-, meta- and hypolimnion strata. Journal of Plankton Research 26, 1441–1458.

Munday, P.L., Leis, J.M., Lough, J.M., Paris, C.B., Kingsford, M.J., Berumen, M.L., Lambrechts, J., 2009. Climate change and coral reef connectivity. Coral Reefs 28, 379–395.

Olson, R.R., Olson, M.H., 1989. Food limitation of planktonic marine invertebrate larvae – does it control recruitment success? Annual Review of Ecology and Systematics 20, 225–247.

Pace, D.A., Marsh, A.G., Leong, P.K., Green, A.J., Hedgecock, D., Manahan, D.T., 2006. Physiological bases of genetically determined variation in growth of marine invertebrate larvae: a study of growth heterosis in the bivalve *Crassostrea gigas*. Journal of Experimental Marine Biology and Ecology 335, 188–209.

Pagano, M., Sagarra, P.B., Champalbert, G., Bouvy, M., Dupuy, C., Thomas, Y., Charpy, L., 2012. Metazooplankton communities in the Ahe atoll lagoon (Tuamotu Archipelago, French Polynesia): Spatiotemporal variations and trophic relationships. Marine Pollution Bulletin 65, 538–548.

Pagès, J., Andrefouet, S., 2001. A reconnaissance approach for hydrology of atoll lagoons. Coral Reefs 20, 409–414.

Pante, E., Adjeroud, M., Dustan, P., Penin, L., Schrimm, M., 2006. Spatial patterns of benthic invertebrate assemblages within atoll lagoons: importance of habitat heterogeneity and considerations for marine protected area design in French Polynesia. Aquatic Living Resources 19, 207–217.

Paugam, A., D'Ollone, C., Cochard, J.C., Garen, P., Le Pennec, M., 2006. The limits of morphometric features for the identification of black-lip pearl oyster (*Pinctada margaritifera*) larvae. Journal of Shellfish Research 25, 959–967.

Pinel-Alloul, B., 1995. Spatial heterogeneity as a multiscale characteristic of zooplankton community. Hydrobiologia 300, 17–42.

Porri, F., McQuaid, C.D., Lawrie, S.M., Antrobus, S.J., 2008. Fine-scale spatial and temporal variation in settlement of the intertidal mussel perna perna indicates differential hydrodynamic delivery of larvae to the shore. Journal of Experimental Marine Biology and Ecology 367, 213–218.

Pouvreau, S., Gangnery, A., Tiapari, J., Lagarde, F., Garnier, M., Bodoy, A., 2000. Gametogenic cycle and reproductive effort of the tropical blacklip pearl oyster, *Pinctada margaritifera* (Bivalvia: Pteriidae), cultivated in Takapoto atoll (French Polynesia). Aquatic Living Resources 13, 37–48.

Powell, E.N., Bochenek, E.A., Klinck, J.M., Hofmann, E.E., 2002. Influence of food quality and quantity on the growth and development of *Crassostrea gigas* larvae: a modeling approach. Aquaculture 210, 89–117.

Raby, D., Lagadeuc, Y., Dodson, J.J., Mingelbier, M., 1994. Relationship between feeding and vertical distribution of bivalve larvae in stratified and mixed waters. Marine Ecology-Progress Series 103, 275–284.

Roberts, C.M., 1997. Connectivity and management of Caribbean coral reefs. Science 278, 1454–1457.

Schabenberger, O., Gotway, C.A., 2005. Statistical Methods for Spatial Data Analysis. Texts in Statistical Science ed. Chapman and hall, CRC, p. 488.

Southgate, P.C., Beer, A.C., 1997. Hatchery and early nursery culture of the blacklip pearl oyster (*Pinctada margaritifera* L.). Journal of Shellfish Research 16, 561–567.

Su, Z.X., Huang, L.M., Yan, Y., Li, H.X., 2007. The effect of different substrates on pearl oyster *Pinetada martensii* (Dunker) larvae settlement. Aquaculture 271, 377–383.

Swearer, S.E., Caselle, J.E., Lea, D.W., Warner, R.R., 1999. Larval retention and recruitment in an island population of a coral-reef fish. Nature 402, 799–802.

Tartinville, B., Deleersnijder, E., Rancher, J., 1997. The water residence time in the Mururoa atoll lagoon: sensitivity analysis of three-dimensional model. Coral-Reefs 16, 193–203.

Thomas, Y., Belliard, C., Garen, P., Gueguen, Y., Montagnani, C., 2011. Development of *in situ* hybridisation of 16S rRNA to monitor black-lip pearl oyster (*Pinctada margaritifera* L.) larvae. Aquatic Living Resources 24, 27–34.

Thomas, Y., Garen, P., Courties, C., Charpy, L., 2010. Spatial and temporal variability of the pico- and nanophytoplankton and bacterioplankton in a deep Polynesian atoll lagoon. Aquatic Microbial Ecology 59, 89–101.

Thomas, Y., Le Gendre, R., Garen, P., Dumas, F., Andréfouët, S., 2012. Bivalve larvae transport and connectivity within the Ahe atoll lagoon (Tuamotu Archipelago), with application to pearl oyster aquaculture management. Marine Pollution Bulletin. 65, 441–452.

Troost, K., Gelderman, E., Kamermans, P., Smaal, A.C., Wolff, W.J., 2009. Effects of an increasing filter feeder stock on larval abundance in the Oosterschelde estuary (SW Netherlands). Journal of Sea Research 61, 153–164.

Zanini, J.M., Salvat, B., 2000. Assessment of deep water stocks of pearl oysters at Takapoto atoll (Tuamotu Archipelago, French Polynesia). Coral Reefs 19, 83–87.

Marine Pollution Bulletin 65 (2012) 463–470

Contents lists available at SciVerse ScienceDirect

Marine Pollution Bulletin

journal homepage: www.elsevier.com/locate/marpolbul

Influence of plankton concentration on gametogenesis and spawning of the black lip pearl oyster *Pinctada margaritifera* in Ahe atoll lagoon (Tuamotu archipelago, French polynesia)

Jonathan Fournier [a], Emmanuelle Levesque [a], Stephane Pouvreau [b], Marcel Le Pennec [c], Gilles Le Moullac [a,*]

[a] IFREMER, Centre du Pacifique, BP 7004, 98719 Taravao, Tahiti, French Polynesia
[b] IFREMER, UMR 100, Presqu'île du Vivier, 29840 Argenton, France
[c] University de la Polynésie Française, EA42639, BP 6570, 98702 Faa'a, Tahiti, French Polynesia

ARTICLE INFO

Keywords:
Pearl Oyster
Gametogenesis
Spawning
Phytoplankton
French Polynesia

ABSTRACT

Pearl culture industry represents one of the dominant business sector of French Polynesia. However, it still entirely relies on unpredictable spat collection success. Our aim was to assess the influence of natural plankton concentration fluctuations on maturation and spawning of the black lip pearl oyster *Pinctada margaritifera*, during a 4 months survey conducted in Ahe atoll lagoon. Plankton concentration was assessed by chlorophyll *a* extraction and by microscope counts while gonadic index, gonado-visceral dry weights and histology were used to measure pearl oysters reproduction activity. We found that (i) plankton concentration fluctuations were mainly related to wind regime, (ii) gametogenesis rate was mainly related to plankton concentration, (iii) spawning occurred when maximal gonad storage was reached, (iv) plankton concentration was the main spawning synchronizing factor. These results contribute explaining *P. margaritifera* spat collection variability in French Polynesian atoll lagoon.

1. Introduction

Pearl culture industry represents one of the dominant business sector and source of income in French Polynesia. However, it still entirely relies on unpredictable natural reproduction and spat collection success. Indeed, large spatio-temporal variability of recruitment rates of the pearl oyster *Pinctada margaritifera* has been reported Andréfouët et al., 2006; Thomas et al., 2012a and a better knowledge of the factors determining its reproduction is thus of particular interest.

Reproductive cycle of bivalve is generally driven by annual temperature cycles and by food availability (Bayne and Newell, 1983; Gervis and Sims, 1992; Sastry, 1979).

Most studies on bivalve reproduction have been conducted in temperate coastal ecosystems which are characterized by strong seasonal differences. Typically, temperature peaks in summer and concentration of phytoplankton is generally higher during spring, summer and early autumn than in late autumn and winter (Gómez and Gorsky, 2003; Valiela and Cebrián, 1999). In these environments, most bivalve species display an annual reproductive cycle characterized by a resting period during the coldest months of the year with spawning inhibited under a given temperature threshold (Dutertre et al., 2009). During spring and summer, the most favorable period for gametogenesis and spawning, food availability has a major impact on spawning frequency and reproduction effort (Enríquez-Díaz et al., 2008; Mac Donald and Thompson, 1985; Ruiz et al., 1992; Saucedo et al., 2002; Saxby, 2002). In addition to the seasonal determinism of gametes production and spawning, Bayne (1976) distinguished two types of energy management strategies used by bivalves to support gametogenesis. First, a "conservative strategy" where energy storage occurs prior to gametogenesis. Second, an "opportunistic strategy" where gametogenesis and storage can occur simultaneously.

However, both reproductive cycles and storage strategies are not species specific and a great plasticity has been observed between different populations of the same species. These differences were explained either by an adaptative physiological response to local environmental conditions or by genetic differences between populations (Hilbish and Zimmerman,1988; Loosanoff and Nomejko, 1951; Paulet et al., 1988; Thompson, 1984).

In tropical ecosystems, characterized by low seasonal variations and high water temperature, gametogenesis is generally continuous and spawning can occur all year long (Arjarasirikoon et al., 2004; Baqueiro-Cárdenas and Aldana-Aranda, 2000; Fournier, 1992; García-Domínguez et al., 1996; Gervis and Sims, 1992; Lefort and Clavier, 1994; Luna-González et al., 2000).

* Corresponding author.
E-mail address: gilles.le.moullac@ifremer.fr (G. Le Moullac).

0025-326X/$ - see front matter © 2012 Elsevier Ltd. All rights reserved.
http://dx.doi.org/10.1016/j.marpolbul.2012.03.027

In the atoll lagoons of the Tuamotu archipelago (French Polynesia), temperatures are high and stable (between 25 °C and 31 °C) while plankton and particulate organic carbon concentrations are low with little seasonal differences but with high day to day fluctuations (Buestel and Pouvreau, 2000; Charpy et al., 1997; Thomas et al., 2010). In these lagoons, *P. margaritifera* has a continuous and fast gametogenesis leading to frequent asynchronous spawning all year long (Pouvreau et al., 2000a,b). Pouvreau et al. (2000b) and Le Moullac et al. (2012) further demonstrated that *P. margaritifera* had low energy storage abilities and could therefore be defined as an "opportunistic" bivalve, investing all energy surplus into its reproduction. However, the precise influence of natural fluctuations of plankton composition and concentration on gametogenesis and spawning of pearl oysters remain poorly known.

In the present study, we aim to measure the influence of natural plankton concentration fluctuations on maturation and spawning of the black lip pearl oyster *P. margaritifera* during a four months survey conducted in Ahe atoll lagoon. To reach this goal, we used digitized images of visceral-mass sections (including gonads) to calculate a quantitative descriptor of gonadal maturity. We measured chlorophyll *a* concentration as a proxy for phytoplankton concentration and we estimated microplankton concentration by microscope counts of dinoflagellates, diatoms and ciliates.

2. Materials and methods

For convenience sake, on all graphs, time is represented in days. Day 1 represents the 7th of February 2009 and Day 120 represents the 6th of June 2009.

2.1. Study site

This study was conducted in Ahe atoll lagoon, located 500 km northeast of Tahiti island in the north of the Tuamotu archipelago (Fig. 1). Ahe lagoon has an area of 142 km^2 and a mean depth close to 42 m with several maxima close to 70 m. Ahe is defined as a semi-enclosed atoll. There is one active pass in the west part of the lagoon and several reef-flat spillways (<50 cm depth) are distributed along the reef rim, mainly in the south and west parts of the lagoon. The average water renewal time (ratio of lagoon volume to average water input rate) was estimated at 34 days (Pagès et al., 2001). Dumas et al. (2012) recently characterized with numerical models the spatial variation of residence and flushing time in different weather conditions, and the average renewal time was estimated to be around 80 days.

To study the reproduction of *P. margaritifera*, 2000 6-years old pearl oysters were hung at low density (<20 pearl oysters m^{-3}) in December 2008 on a breeding line located in the north east of Ahe lagoon at approximately 3 km off the coast, at 10 m deep (Fig. 1). Experiments started in February 2009.

2.2. Meteorological and hydrological parameters

Hourly wind direction and velocity were obtained from Takaroa atoll meteorological station (Météo France data) located about 120 km east of Ahe (145°3′4″W, 14°28′57″S). Daily mean of wind velocity was calculated from initial wind speed hourly values. Water temperature (°C) and salinity (PSU) were obtained from a Sea Bird (SBE V19 plus) probe immersed at a depth of 10 m at the experimental breeding station (Fig. 1).

2.3. Plankton concentrations

Plankton concentration was measured at the breeding site every 3 days, between the 11th of February (Day 5) and the 2nd of June (Day 116). All sampling and analysis were done in triplicate. Water was sampled at 10 m deep with a 5 l Niskin bottle and gently transferred into 5 l containers which were kept in the dark in an isotherm container and immediately brought back to the laboratory for analysis. Phytoplankton concentration was measured on all samples while microplankton enumeration was carried out on samples collected between the 11th of March (Day 33) and the 19th of May (Day 102) only.

Methods used to measure phytoplankton and microplankton concentration is described in details by Fournier et al. (2012). Briefly, phytoplankton concentration was assessed by measuring chlorophyll *a* (Chl *a*) concentration for two size fractions: <2 μm (Chl *a* <2 μm) and >2 μm (Chl *a* >2 μm). Water samples of 200 ml were filtrated sequentially on 2 μm Millipore filters and on GFF filters. Chl *a* concentration was measured with a Tuner Design TD 700 fluorometer equipped with the set of optical filters recommended by Welschmeyer (1994) for direct measurement of Chl *a*. Total phytoplankton (Chl *a* Tot.) concentration was defined as the sum of Chl *a* <2 μm concentration and of Chl *a* >2 μm concentration.

To assess microplankton concentration, water samples (200 ml) were fixed with alcalin lugol iodine. Enumeration of dinoflagellates, diatoms and dinoflagellates was carried out after sedimentation in Utermohl settling chambers (Hydro bios combined plate chamber), at 400 magnification with a Leica DMI 3000 inverted microscope and following the systematic literature (Kahl, 1931; Lee et al., 1985; Paulmier, 1997; Ricard, 1987; Sournia, 1986).

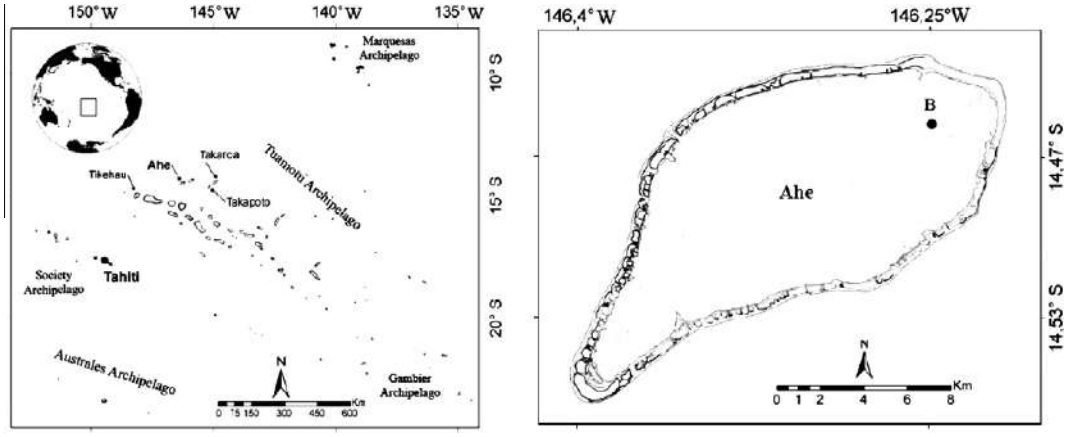

Fig. 1. Location of Ahe atoll and location of the experimental breeding station (B) in Ahe lagoon.

2.4. Dissection and dry flesh weight, gonadic index and maturity stages

Every 10 days, 80 pearl oysters were randomly collected from the breeding line between 18th of February 2009 (Day 12) and 5th of June 2009 (Day 119). After collection, pearl oysters were cleaned from epibionths and immediately brought back to laboratory. Dorso-ventral height and antero-posterior length (Gervis and Sims, 1992) were measured to the nearest mm with a soft stainless ruler. Mantle + gills, muscle and gonado-visceral mass were dissected, drained during 1 h on absorbent paper and weighted to the nearest 0.01 g. Wet weight of drained gonado-visceral mass (GVM), mantle + gills (MAN) and abductor muscle (MUS) were then converted into dry weights using their respective moisture content: 86% for GVM, 87% for MAN and 75% for MUS. These values come from average moisture content of 215 freeze dried pearl oysters sampled in Ahe lagoon, collected, dissected and drained as described above (unpublished personal data).

From each set of 80 oysters, we measured the gonadic index of 40 randomly selected oysters and assessed their histological maturity stages. Specifically, gonado-visceral mass of pearl oysters were fixed during 5 days in a solution of 10% formalin prepared with seawater; transferred into 70% ethanol for preservation; cut in the sagittal plane and digitized with an Epson 2400 scanner. On the digitized images, gonad areas (GA, in pixels) and total gonado-visceral mass areas (GVMA, in pixels) were measured with the help of Image J freeware (http://www.rsbweb.nih.gov/ij/). Gonadic index (GI, in %) was then computed for each individual using the following equation: GI = GA/GVMA.

Once digitized, gonado-visceral mass sampled between the 25th of March (Day 47) and the 9th of May (Day 92) were dehydrated through a graded ethanol series, embedded in paraffin, sectioned at 3–4 μm on a rotary microtome, stained with Giemsa dye and, finally, mounted on microscope slides. Sections were made in the gonad area, between the proximal end of the gut loop and the base of the foot.

Slide preparations were examined under a light microscope at 200x magnification to assess maturity stages, which were based on the description made by Pouvreau et al. (2000a):

(1) Stage 0: indeterminate or inactive, no evidence of gonadal development.
(2) Stage 1: early gametogenesis, follicles small, gonia numerous.
(3) Stage 2: actively developing but mature gametes are not observed.
(4) Stage 3: near ripe follicles with mature gametes.
(5) Stage 4: spawning ripe, follicles distended, confluent and entirely filled.
(6) Rp: partially spawned, partially empty lumen.
(7) Rt: spent, completely empty lumen.

2.5. Data analysis, statistics

Mean of GI, of GVM dry weight, of MAN dry weight and of MUS dry weight were calculated for each sampling date. Since data were not normal, we used the non parametric Kruskal–Wallis test for the comparison of these four variables among sampling dates. A *posteriori* multiple comparisons were carried out using the non parametric Steel–Dwass test (Critchlow and Fligner, 1991; Spurrier, 2006).

As data were not normal, confidence intervals of GI, GVM dry weight, MAN dry weight and MUS dry weight were calculated using a boot strap method (Efron and Tibshirani,1986).

Spearman correlation analyzes were used to examine the relationships between wind velocity and concentration of Chl *a* <2 μm, Chl *a* >2 μm, Chl *a* Tot., dinoflagellates, diatoms and ciliates.

2.6. Relationships between reproduction intensity and plankton concentration

To characterize the relationships between reproductive activity of pearl oysters and plankton concentration, we used a Spearman correlation analysis between the absolute variation of GI and the running mean of phytoplankton concentration.

The absolute variation of GI between two sampling dates was calculated using the following equation: $GIV = |GI_D - GI_{D-10}|$, where GIV = absolute gonadic index variation (%), GI = mean gonadic index of pearl oysters at the sampling date D (GI_D) and at the previous sampling date (10 days before $GI_D = GI_{D-10}$). Then, we calculated the running mean of phytoplankton concentration for six periods of time (5, 10, 15, 20, 25 and 30 days). Finally, we associated each GIV value with the values of running means calculated for the day corresponding to GI_D sampling date and we used a Spearman correlation analysis to test the relationships between GIV and the 6 running means of phytoplankton concentration.

We used the same procedure to test the relationships between phytoplankton concentration and variations of GVM, MAN and MUS dry weights.

In all tests, significance was determined with an alpha level of 0.05.

All analysis were conducted with the R freeware (http://www.r-project.org/).

3. Results

3.1. Hydrobiological parameters

Oxygen concentration and salinity were stable during the period of our study (6.0 ± 0.1 mg l^{-1} and 36.2 ± 0.0 PSU, respectively). Water temperature ranged from 28.6 °C to 29.2 °C and maximum daily variation was 0.3 °C.

Wind speed ranged from 0.7 m s^{-1} to 11 m s^{-1} (Fig. 2a). When blowing from the east to south direction, wind velocity was higher than 6 m s^{-1} whereas it was lower than 6 m s^{-1} when blowing from west to north direction. Temperature, salinity, wind speed and wind direction corresponded to the usual climatic conditions expected during this period of the year (Buestel and Pouvreau, 2000; Thomas et al., 2010).

Chl *a* Tot. ranged from 0.22 μg l^{-1} to 0.60 μg l^{-1}. Mean concentration of Chl *a* <2 μm (0.23 μg l^{-1}) was significantly higher than mean concentration of Chl *a* >2 μm (0.14 μg l^{-1}) (Wilcoxon test, $W = 157$, $p = 0.000$). However, between Day 52 and Day 65, Chl *a* >2 μm concentration was higher than Chl *a* <2 μm concentration (Fig. 2b).

The mean dinoflagellates concentration was 20.0 ± 13.1 × 10^3 cell l^{-1}. The mean diatoms concentration was 7.3 ± 12.2 × 10^3 cell l^{-1} and the mean concentration of ciliates was of 1.4 ± 1 × 10^3 cell l^{-1}. Dinoflagellates constituted the dominant microplankton community (Fig. 2c) except between Days 54 and 71 when diatoms concentration reached up to 6 × 10^5 cell l^{-1}.

All peaks of Chl *a* Tot. concentration occurred at the time of wind velocity peaks (Fig. 2a, Days 15, 34, 57, 64,73, 99, 103 and 116). The lowest Chl *a* Tot. concentrations were measured during low wind periods (Fig. 2a, Days 23, 78 to 92 and 109). Chl *a* Tot. concentration and wind velocity were significantly correlated (Table 1).

The four peaks of microplankton concentration were concurrent to Chl *a* >2 μm concentration peaks (Fig. 2b and c, Days 34, 57, 64 and 99). Similarly, the lowest microplankton concentration corresponded to the lowest Chl *a* >2 μm concentration (Fig. 2b and c, Days 73–92). Chl *a* >2 μm and microplankton concentrations were also significantly correlated (Table 1).

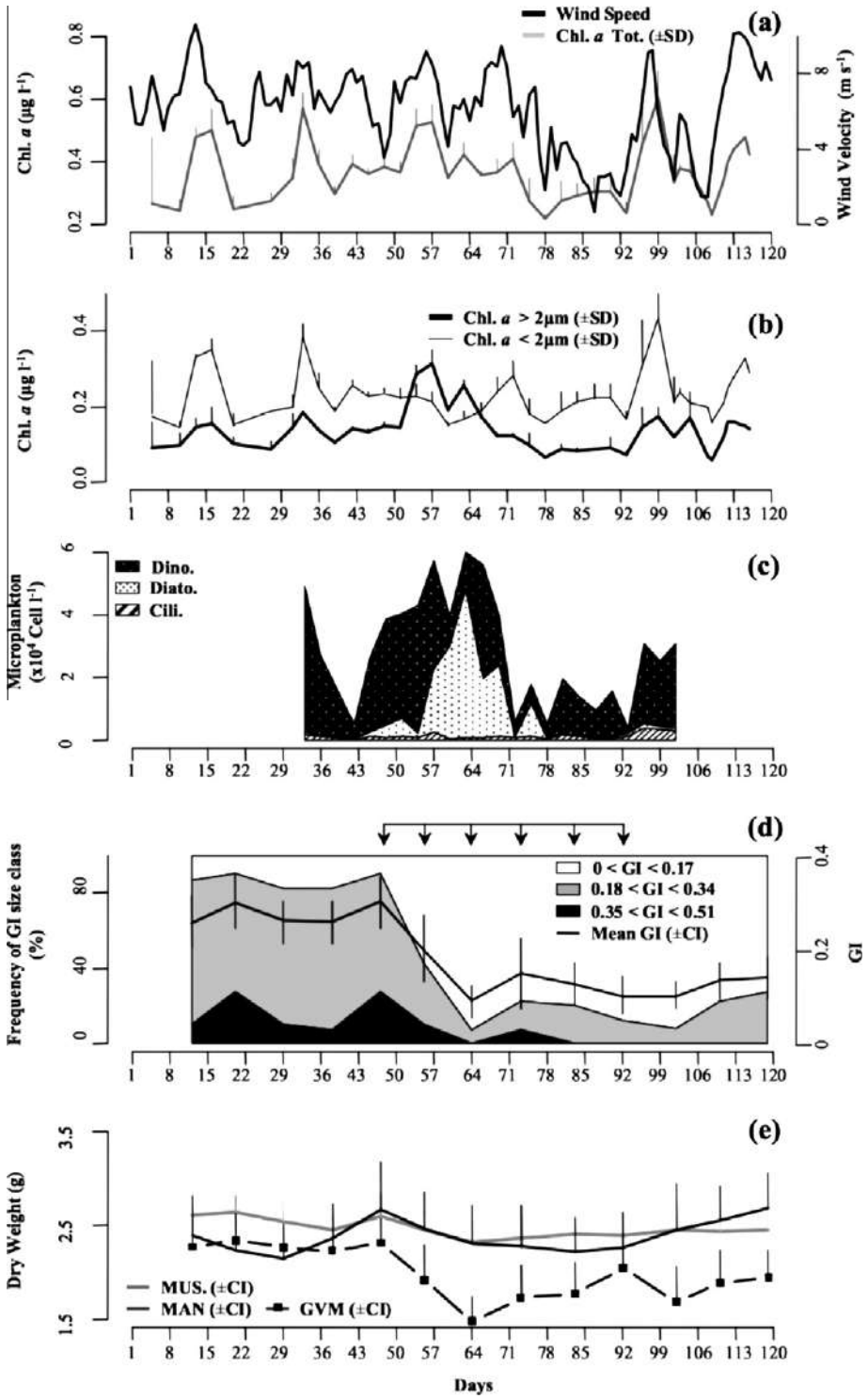

Fig. 2. (a) Wind velocity and total phytoplankton concentration (Chl *a* Tot.), (b) Chl *a* >2 µm and Chl *a* <2 µm concentration; (c) dinoflagellates (Din.), diatoms (Diat.) and ciliates (Cili.) concentrations; (d) mean gonad-index and frequency of 3 size class of gonadic index; (e) dry weight of abductor muscle (MUS), of Mantle + Gills (MAN) and of gonado-visceral mass (GVM). All parameters were measured in Ahe atoll lagoon between the 7th of February 2009 (day 1) and the 6th of June 2009 (day 120). On (d), arrows indicate the dates at which maturity stages of pearl oysters were assessed by histology.

3.2. GI and maturity stages

The fluctuations of the mean gonadic index (GI) and of the GI size class frequencies observed during our study are presented in Fig. 2d. Mean GI displayed significant variations between sampling dates (Table 2).

From Day 12 to Day 47, the mean GI was at its highest and ranged from 0.24 to 0.29, with more than 70% of pearl oysters presenting a GI > 0.17. Between Day 47 and Day 64, a major spawning occurred. The mean GI decreased sharply from 0.29 down to 0.08 while the frequency of low GI (<0.17) increased from 10% to 93%. Between Day 64 and Day 119, mean GI reached its lowest value (ca. 0.14) and low GI (<0.17) frequency was high (70%).

The histological maturity stages also confirmed the main spawning event. Indeed, the frequency of ripe individuals decreased from 85% to 8% between Day 47 and Day 64 (Fig. 3).

Table 1
Relationships between wind velocity (W.V.) and concentration of phytoplankton <2 μm (Chl *a* <2 μm), phytoplankton >2 μm (Chl *a* >2 μm), total phytoplankton (Chl *a* Tot.), dinoflagellates (Dino.), diatoms (Diato.), ciliates (Cili.) and total microplankton (MicPk), *r* = Spearman's rho, *p* = *p*-value. Significant correlations are indicated in bold type characters (α = 0.05).

	W.V.	Chl. *a* tot.	Chl. *a* >2 μm	Chl. *a* <2 μm	Dino.	Diato.
Chl *a* Tot	***r* = 0.56**					
	***p* = 0.000**					
Chl *a* >2 μm	***r* = 0.53**	–				
	***p* = 0.000**					
Chl *a* <2 μm	***r* = 0.43**	–	***r* = 0.45**			
	***p* = 0.005**		***p* = 0.004**			
Dino.	***r* = 0.46**	***r* = 0.54**	***r* = 0.62**	*r* = 0.35		
	***p* = 0.026**	***p* = 0.007**	***p* = 0.002**	*p* = 0.103		
Diato.	***r* = 0.49**	*r* = 0.21	***r* = 0.56**	*r* = −0.26	*r* = 0.21	
	***p* = 0.018**	*p* = 0.326	***p* = 0.005**	*p* = 0.224	*p* = 0.335	
Cili.	*r* = 0.33	*r* = 0.35	*r* = 0.20	*r* = 0.29	*r* = 0.52	***r* = 0.11**
	p = 0.129	*p* = 0.106	*p* = 0.371	*p* = 0.185	*p* = 0.118	***p* = 0.000**
MicPk.	***r* = 0.59**	***r* = 0.56**	***r* = 0.82**	*r* = 0.02	–	–
	***p* = 0.003**	***p* = 0.006**	***p* = 0.000**	*p* = 0.910		

Table 2
Results of Kruskal–Wallis tests used for the comparisons of gonadic index (GI), gonado-visceral mass dry weight (GVM DW), mantle + gills dry weight (Ma. DW), muscle dry weight (Mu. DW) among sampling dates.

Test	*df*	*Khi*^{2}	*p*
GI among sampling date	12	246	0.000
GVM DW among sampling date	12	172.6	0.000
Ma. DW among sampling date	12	52.7	0.000
Mu. DW among sampling date	12	23.3	0.025

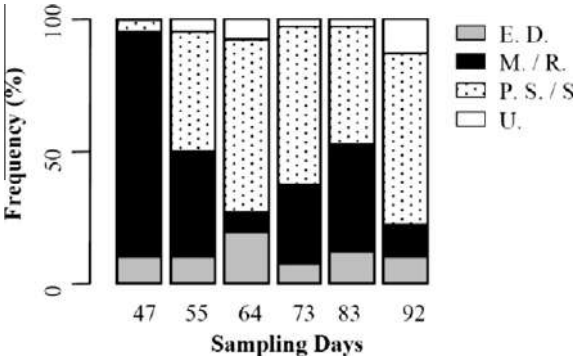

Fig. 3. Frequency of maturity stages observed by histology between the 25th of March (day 47) and the 9th of May (day 92). E.D. = early development (=stage 1 + 2), M./R. = maturing + ripe (=stage 3 + 4), P.S./S. = partially spawn + spent (=stage Rp + Rt), U = lack of gonadal tissue.

During the study period, maturation was faster (between Day 12 and 20, Day 38 and 47, Day 64 and 73) and spawning was more intense (between Day 20 and 29, Day 47 and 55, Day 73 and 83) when the Chl *a* >2 μm concentration was >0.1 μg l^{-1}. Conversely, when Chl *a* >2 μm concentration was <0.1 μg l^{-1}, we only observed slight variations of mean GI (between day 12 and 20, day 38 and 47, day 64 and 73). These graphical observations were confirmed by a significant correlation between GIV and Chl *a* >2 μm concentration running mean (Table 2).

3.3. Dry weights

Variation of mean gonado-visceral mass (GVM) dry weight, mean mantle + gills (MAN) dry weight and mean abductor muscle (MUS) dry weight are presented in Fig. 2e. Mean GVM dry weight, MAN dry weight and MUS dry weight showed significant variations between sampling dates (Table 2).

Between Day 12 and Day 47 GVM dry weight was significantly higher than on Day 64. This confirmed the major spawning event observed during this period.

The MAN dry weight significantly increased when Chl *a* >2 μm concentration was >0.1 μg l^{-1} (from Days 29 to 47 and Days 92 to 119) and significantly decreased during the main spawning event (between Day 47 and Day 74).

Compared to GVM and MAN dry weights, MUS dry weight was rather constant. We only observed a slight increase preceding the major spawning and a slight decrease after.

No significant relationships were reported between GVM dry weight and phytoplankton concentration (Table 3) neither between MUS or MAN dry weight and phytoplankton concentration (data not shown).

4. Discussion

4.1. Hydrobiological parameters

We measured a Chl *a* Tot. mean concentration in the higher range of concentrations reported by Charpy and Blanchot (1998) and Pagès et al. (2001) in other French Polynesian atolls. The maximum concentration of Chl *a* Tot. observed during this study (0.6 μg l^{-1}) was close to values reported by Pagès et al. (2001) in Takaroa atoll lagoon during a phytoplankton bloom. Our mean concentration of ciliates and dinoflagellates were higher than those reported in Takapoto lagoon by Loret et al. (2000) but were in the range of measured in Tikehau lagoon (González et al., 1998).

Previous studies in French Polynesian atolls have shown that plankton concentration variations can be significant at small spatial and/or temporal scale, despite the average low concentrations and the weak seasonal differences (Buestel and Pouvreau, 2000; Charpy et al., 2012; Fournier et al., 2012, González et al., 1998; Pagano et al., 2012; Sournia and Ricard, 1976; Thomas et al., 2010). However, the exact mechanisms responsible for these changes remain unclear. Here, we report that the main fluctuations of Chl *a* >2 μm, Chl *a* <2 μm, diatoms and dinoflagellates concentration were clearly related to the wind regime variations.

The link between wind and plankton concentrations can be explained by a process of nutrient enrichment in the water column. First, in semi enclosed atoll lagoons, high winds (10 m s^{-1}) induce an overturning circulation that brings deep bottom water layer to the windward coast of the atoll (Dumas et al., 2012; Lenhardt, 1991). This process brings nutrients accumulated in deep water layers to the surface layer. Indeed, nutrient release from the sediment added to remineralization of the settling organic particles tend to enrich bottom water layers of atoll lagoons (Charpy and

Table 3
Relationships between GIV (gonadic index variations) and running mean of phytoplankton concentration (phytoplankton <2 μm = Chl *a* <2 μm, phytoplankton > 2 μm = Chl *a* > 2 μm, total phytoplankton = Chl *a* Tot.) calculated for 6 different periods (5–30 days). Relationships between gonado-visceral mass dry weight variation and the same moving averages of phytoplankton concentration; *r* = Spearman's rho, *p* = *p*-value. Significant correlations are indicated in bold type characters ($\alpha = 0.05$).

Period (days)	GIV			Gonado-visceral mass variation		
	<2 μm	>2 μm	Tot.	<2 μm	>2 μm	Tot.
5	$r = -0.45$	$r = 0.20$	$r = -0.20$	$r = -0.15$	$r = 0.43$	$r = 0.15$
	$p = 0.14$	$p = 0.53$	$p = 0.53$	$p = 0.65$	$p = 0.17$	$p = 0.63$
10	$r = -0.36$	$r = 0.49$	$r = 0.15$	$r = -0.01$	$r = 0.4$	$r = 0.4$
	$p = 0.26$	$p = 0.11$	$p = 0.63$	$p = 0.97$	$p = 0.2$	$p = 0.2$
15	$r = -0.32$	$r = \mathbf{0.64}$	$r = 0.44$	$r = -0.11$	$r = 0.42$	$r = 0.49$
	$p = 0.31$	$p = \mathbf{0.03}$	$p = 0.15$	$p = 0.73$	$p = 0.17$	$p = 0.11$
20	$r = -0.22$	$r = \mathbf{0.59}$	$r = 0.43$	$r = 0.10$	$r = 0.18$	$r = 0.38$
	$p = 0.50$	$p = \mathbf{0.04}$	$p = 0.16$	$p = 0.76$	$p = 0.57$	$p = 0.23$
25	$r = -0.34$	$r = 0.39$	$r = 0.29$	$r = -0.04$	$r = 0.13$	$r = 0.18$
	$p = 0.28$	$p = 0.21$	$p = 0.35$	$p = 0.90$	$p = 0.68$	$p = 0.57$
30	$r = -0.27$	$r = 0.34$	$r = 0.31$	$r = 0.06$	$r = 0.10$	$r = 0.22$
	$p = 0.39$	$p = 0.28$	$p = 0.32$	$p = 0.85$	$p = 0.75$	$p = 0.48$

Charpy-Roubaud, 1991; Charpy-Roubaud et al., 1996; Gerber and Marshall, 1982). Since experimental nitrogen and phosphorous enrichment of lagoonal water samples have increased growth and abundance of phytoplankton and heterotrophic flagellates (Ferrier-Pagès and Furla, 2001), this nutrient flow likely enhanced as well the plankton biomass and concentration in the eastern lagoon. Specifically here, south and east winds blowing at speed >6 m s^{-1} probably brought enriched bottom water layer to the surface in the northeastern part of Ahe lagoon which promoted plankton growth and abundance where our breeding line was located. This process is indirectly confirmed by the low concentrations of Chl *a* Tot. observed during west and north winds <6 m s^{-1}, and by results of Fournier et al. (2012) who measured high Chl *a* Tot. concentration (>1 μg l^{-1}) in the northeastern part of the lagoon during steady east and south-east wind in October 2008.

4.2. Reproduction of pearl oysters

Dispersion of individual GI and histological results show that, during the period of our study, *P. margaritifera* exhibited a continuous reproductive activity with an extremely short resting period and a fast initiation of gametogenesis. These results are in agreement with previous studies which reported fast and continuous gametogenesis in tropical bivalves (Arjarasirikoon et al., 2004; Baqueiro-Cárdenas and Aldana-Aranda, 2000; García-Domínguez et al., 1996; Gervis and Sims, 1992).

Moreover, Ahe lagoon displays fairly similar hydrobiological conditions as Takapoto lagoon where Pouvreau et al. (2000b) showed that gametogenesis and spawning were occurring all year long. It is therefore obvious that *P. margaritifera* is characterized by continuous gametogenesis and spawning in Ahe atoll lagoon.

The effect of temperature, food availability and food quality on gametogenesis rate has mainly been studied for temperate species during experimental broodstock conditioning. These conditioning experiments demonstrated that an increase of temperature and food level were matched by an increase of maturation rate until an optimal combination of temperature and food was reached (Chávez-Villalba et al., 2002; Chávez-Villalba et al., 2003; Pronker et al., 2008; Martínez and Pérez, 2003). From a bioenergetic point of view, these results are explained by the global increase of physiological rates when temperature increases and by the increase of energy inflow when food availability increases (Kooijman, 2000). Similar increase of gametogenesis rate with temperature and algae concentrations was observed in *P. margaritifera* conditioning experiments (personnal unpublished data).

Once individuals are mature, a thermal stress is generally used to artificially induce spawning in hatcheries of temperate (Helm and Bourne, 2004) and tropical bivalves (Gervis and Sims, 1992). However, in natural conditions factors inducing spawning remain unclear for temperate bivalves. A combination of several environmental factors have explained spawning, including thermal amplitude, phytoplankton blooms, tidal cycles and lunar phases (Bernard, 2011; Bonardelli et al., 1996; Starr et al., 1990).

Pouvreau et al. (2000b) and Le Moullac et al. (2012) have shown that gametogenesis and spawning of pearl oysters can occur all year long within a temperature range of 23–31 °C. Thus, in Tuamotu atoll lagoons, temperature is not a limiting factor for gametogenesis. The same authors have also concluded that sufficient plankton food is naturally available to sustain constant gametogenesis and spawning all year long. However, our results clearly demonstrate that gametogenesis rate and spawning of pearl oysters are directly related to plankton concentration.

In fact, conditions of food and temperature are met for *P. margaritifera* to produce gametes continuously all year long, but at a rate that varies with plankton concentration. Gametes accumulate in gonads until the maximum storage capacity is reached, which leads to spawning. Thus, when plankton concentration increases, gametogenesis rate increases, the maximum storage size of gonad is reached faster, and the number of individual spawning in the population increases as well.

Plankton concentration is therefore the main spawning synchronizing factor for pearl oysters in atoll lagoons. However, artificial spawning conducted at the Ifremer center of Vairao (Tahiti, French Polynesia) has revealed that female spawning was conditioned to the previous release of the male gametes (Le Moullac, pers com.). The impact of this gender synchronization is unknown *in situ* but is likely to play a role in the spawning synchronization of pearl oysters.

As discussed above, plankton concentration variations can be significant at small spatial and/or temporal scale. Thus, reproduction dynamics of pearl oysters is also likely to be highly variable from one site to another. A peak of plankton concentration at one site could induce a synchronized spawning of all individuals, while at other sites spawning may be reduced to a small percentage of individuals.

Seasonal variations of plankton concentration are commonly assumed to be low in Tuamotu atoll lagoons (e.g. Charpy et al., 1997). However, during the "warm" season (November–April), Buestel and Pouvreau et al. (2000b) and Thomas et al. (2010) measured higher concentration of phytoplankton than during the "fresh" season in Takapoto and Ahe lagoons, respectively. Available data are too scarce to demonstrate the impact of these seasonal variations on reproduction dynamics of pearl oysters. However, Pouvreau et al. (2000b) reported more intense spawning during

the warm season than during the cool season and we also observed a major spawning at the end of the warm season.

To conclude, our results are in agreement with Pouvreau et al. 2000a who showed that *P. margaritifera* was an opportunistic species with very low energy storage abilities and which invest all surplus of energy into its reproduction. More specifically, our results clearly demonstrated that even if spawning can occur all year long, gametogenesis rate and spawning are tightly linked to the variation of food availability which itself is related wind regimes. Thus, spatial and/or temporal variability of the plankton concentration obviously leads to spatial and temporal heterogeneity of spawning intensity in the lagoon.

In association with the results of Thomas et al., 2012a and Thomas et al., 2012b who described the patterns of bivalve larval dispersal and growth in Ahe lagoon, our findings provide a comprehensive description of the processes involved in the inherent variability of spat collection success, observed empirically in Tuamotu atolls after decades of black pearl farming.

In fact, wind regime determines lagoon hydrodynamics regime which drives larval dispersal and impacts both food availability and reproduction dynamics. The monitoring of wind and of >2 μm plankton biomass is therefore a priority to predict spawning and infer subsequent larval dispersal (Thomas et al., 2012b).

Acknowledgements

This study was supported by the European Development Fund, in collaboration with the Service de la Perliculture, the Université de la Polynésie Française and the Institut Français de Recherche pour l'Exploitation de la Mer (Ifremer). We thank Ifremer and Service de la Perliculture staff for their help during field work, A. Lo Yat for his efficient management of the EDF project; the Pa'umotu: R. and W. Richmond, T. Coulombe and M. Maifano for their assistance on Ahe Atoll. We acknowledge the two anonymous reviewers and S. Andréfouët for their comments.

References

Andréfouët, S., Ouillon, S., Brinkman, R., Falter, J., Douillet, P., Wolk, F., Smith, R., Garen, P., Martinez, E., Laurent, V., Lo, C., Remoissenet, G., Scourzic, N., Gilbert, A., Deleersnijder, E., Steinberg, C., Choukroun, S., Buestel, D., 2006. Review of solutions for 3D hydrodynamic modeling applied to aquaculture in South Pacific atoll lagoons. Marine Pollution Bulletin 52, 1138–1155.

Arjarasirikoon, U., Kruatrachue, M., Sretarugsa, P., Chitramvong, Y., Jantataeme, S., Upatham, E., 2004. Gametogenic processes in the pearl oyster, *Pteria penguin* (Roding, 1798) (Bivalvia, Mollusca). Journal of Shellfish Research 23, 403–409.

Baqueiro-Cárdenas, E., Aldana-Aranda, D., 2000. A review of reproductive patterns of bivalve mollusks from Mexico. Bulletin of Marine Science 66 (1), 13–27.

Bayne, B., 1976. Aspects of reproduction in bivalve molluscs. In: Wiley, M. (Ed.), Estuarine Processes. Academic Press, New York, pp. 432–448.

Bayne, B., Newell, R., 1983. Physiological energetics of marine molluscs. In: Saleuddin, A., Wilbur, K. (Eds.), The Mollusca. Academic Press, New York, pp. 491–498.

Bernard, I., 2011. Écologie de la reproduction de l'huître creuse, *Crassostrea gigas*, sur les côtes atlantiques françaises. Vers une explication de la variabilité du captage. PhD Thesis, Université de La Rochelle.

Bonardelli, J.C., Himmelman, J.H., Drinkwater, K., 1996. Relation of spawning of the giant scallop, *Placopecten magellanicus*, to temperature fluctuations during downwelling events. Marine Biology 124, 637–649.

Buestel, D., Pouvreau, S., 2000. Particulate matter in Takapoto lagoon waters: potential food for cultivated pearl oysters. Oceanologica Acta 23, 193–210.

Charpy, L., Blanchot, J., 1998. Photosynthetic picoplankton in French Polynesian atoll lagoons: estimation of taxa contribution to biomass and production by flow cytometry. Marine Ecology Progress Series 162, 57–70.

Charpy, L., Charpy-Roubaud, C., 1991. Particulate organic matter fluxes in a Tuamotu atoll lagoon (French Polynesia). Marine Ecology Progress Series 71, 53–63.

Charpy, L., Dufour, P., Garcia, N., 1997. Particulate organic matter in 16 Tuamotu atoll lagoons (French Polynesia). Marine Ecology Progress Series 151, 55–65.

Charpy, L., Rodier, M., Fournier, J., Langlade, M.J., Gaertner-Mazouni, N., 2012. Physical and chemical control of the phytoplankton of Ahe lagoon, French Polynesia. Marine Pollution Bulletin 65, 471–477.

Charpy-Roubaud, C., Charpy, L., Sarazin, G., 1996. Diffusional nutrient fluxes at the sediment-water interface and organic matter mineralization in an atoll lagoon (Tikehau, Tuamotu Archipelago, French Polynesia). Marine Ecology Progress Series 132, 181–190.

Chávez-Villalba, J., Cochard, J., Le Pennec, M., Barret, J., Enriquez-Diaz, M., Caceres-Martinez, C., 2003. Effects of temperature and feeding regimes on gametogenesis and larval production in the oyster *Crassostrea gigas*. Journal of Shellfish Research 22, 721–731.

Chávez-Villalba, J., Pommier, J., Andriamiseza, J., Pouvreau, S., Barret, J., Cochard, J., Le Pennec, M., 2002. Broodstock conditioning of the oyster *Crassostrea gigas*: origin and temperature effect. Aquaculture 214, 115–130.

Critchlow, D., Fligner, M., 1991. On distribution-free multiple comparisons in the one way analysis of variance. Communication in Statistics Theory and methods 20, 127–139.

Dumas, F., Le Gendre, R., Andréfouët, S., 2012. Tidal flushing and wind driven circulation of Ahe lagoon (Tuamotu Archipelago, French Polynesia) from in situ observations and numerical modelling. Marine Pollution Bulletin 65, 425–440.

Dutertre, M., Beninger, P., Barillé, L., Papin, M., Rosa, P., Barillé, A., Haure, J., 2009. Temperature and seston quantity and quality effects on field reproduction of farmed oysters, *Crassostrea gigas*, in Bourgneuf Bay, France. Aquatic Living Resources 22, 319–329.

Efron, B., Tibshirani, R., 1986. Bootstrap methods for standard errors, confidence intervals, and other measures of statistical accuracy. Statistical Science 1, 54–77.

Enríquez-Díaz, M., Le Pennec, M., Pouvreau, S., Chávez-Villalba, J., 2008. Gametogenesis, reproductive investement, and spawning behavior of the Pacific giant oyster *Crassostrea gigas*: evidence of an environment-dependent strategy. Aquaculture International.

Ferrier-Pagès, C., Furla, P., 2001. Pico- and nanoplankton biomass and production in the two largest atoll lagoons of French Polynesia. Marine Ecology Progress Series 211, 63–76.

Fournier, J., Dupuy, C., Bouvy, M., Courrodon-Real, M., Charpy, L., Pouvreau, S., Le Moullac, G., Le Pennec, M., Cochard, J.C., 2012. Pearl oysters *Pinctada margaritifera* grazing on natural plankton in Ahe atoll lagoon (*Tuamotu archipelago*, French Polynesia). Marine Pollution Bulletin 65, 490–499.

Fournier, M., 1992. The reproductive biology of the tropical rocky oyster *Ostrea iridescens* (Bivalvia: Ostreidae) on the Pacific coast of Costa Rica. Aquaculture 101, 371–378.

García-Domínguez, F., Ceballos-Vásquez, B., Quezada, A., 1996. Spawning cycle of the pearl oyster, *Pinctada mazatlanica* (Hanley, 1856), (Pteriidae) at isla Espiritu Santo, Baja California Sur, Mexico. Journal of Shellfish Research 15, 297–303.

Gerber, R., Marshall, N., 1982. Characterization of the suspended particulate organic matter and feeding by the lagoon zooplankton at Enewetak atoll. Bulletin of marine science 32, 290–300.

Gervis, M., Sims, N., 1992. The Biology and Culture of Pearl Oysters (Bivalvia: Pteriidae). Management ICLARM (Eds.), Manilla.

Gómez, F., Gorsky, G., 2003. Annual microplankton cycles in Villefranche Bay, Ligurian Sea, NW Mediterranean. Journal of Plankton Research 25, 323–339.

González, J., Torréton, J., Dufour, P., Charpy, L., 1998. Temporal and spatial dynamics of the pelagic microbial food web in an atoll lagoon. Aquatic Microbial Ecology 16, 53–64.

Helm, M., Bourne, N., 2004. Hatchery culture of bivalves, a practical manual. In: Lovatelli, A. (Ed.). FAO, Rome.

Hilbish, T., Zimmerman, K., 1988. Genetic and nutritional control of the gametogenic cycle in *Mytilus edulis*. Marine Biology 98, 223–228.

Kahl, A., 1931. Urtiere oder protozoa. In: Dahl, F., Dahl, M., Bischoff, H. (Eds.), Die Tierwelt Deutschlands und der angrenzenden Meeresteile. Gustav Fischer, Jena.

Kooijman, S., 2000. Dynamic Energy and Mass Budgets in Biological Systems. Cambridge University Press, Cambridge.

Lee, J., Hutner, S., Bovee, E. (Eds.), 1985. An illustrated Guide to the Protozoa. Allen Press, Lawrence, KS.

Lefort, Y., Clavier, J., 1994. Reproduction of *Annachlamys flabellata*, *Comptopallium radula* and *Mimachlamys gloriosa* (Mollusca: Pectinidae) in the south-west lagoon of New Caledonia. Aquatic Living Resources 7, 39–46.

Le Moullac, G., Tiapari, J., Teissier, H., Martinez, E., Cochard, J., 2012. Growth and Gonad Development of the Tropical Black-lip Pearl Oyster, *Pinctada margaritifera* (L.), in the Gambier archipelago (French Polynesia). Aquaculture International. 20, 305–315.

Lenhardt, X., 1991. Hydrodynamique des lagons d'atoll et d'île haute en Polynésie Française. ORSTOM, Etudes et Thèse, Paris.

Loosanoff, V., Nomejko, C., 1951. Existence of physiologically-different races of oysters, *Crasostrea virginica*. Biological Bulletin 101, 151–156.

Loret, P., Le Gall, S., Dupuy, C., Blanchot, J., Pastoureaud, A., Delesalle, B., Caisey, X., et al., 2000. Heterotrophic protists as a trophic link between picocyanobacteria and the pearl oyster *Pinctada margaritifera* in the Takapoto lagoon (Tuamotu Archipelago, French Polynesia). Aquatic Microbial Ecology 22, 215–226.

Luna-González, A., Cácerer-Martinez, C., Zúñiga-Pacheco, C., López-López, S., Ceballos-Vázques, B., 2000. Reproductive cycle of Argopecten ventricosus (Sowerby 1842) (Bivalvia: Pectinidae) in the Rada del Puerto de Pichilingue, B.C.S., Mexico and its relation to temperature, salinity, and food. Journal of Shellfish Research 19, 107–112.

Mac Donald, B., Thompson, R., 1985. Influence of temperature and food availability on the ecological energetics of the giant scallop *Placopecten magellanicus*. II. Reproductive output and total production. Marine Ecology Progress Series 25, 295–303.

Martínez, G., Pérez, H., 2003. Effect of different temperature regimes on reproductive conditioning in the scallop *Argopecten purpuratus*. Aquaculture 228, 153–167.

Pagano, M., Sagarra, P., Champalbert, G., Bouvy, M., Dupuy, C., Thomas, Y., Charpy, L., 2012. Metazooplankton communities in Ahe atoll lagoon (Tuamotu Archipelago, French Polynesia): spatiotemporal variations and trophic relationships. Marine Pollution Bulletin 65, 438–548.

Pagès, J., Andréfouët, S., Delesalle, B., Prasil, V., 2001. Hydrology and trophic state in Takapoto Atoll lagoon: comparison with other Tuamotu lagoons. Aquatic living resources 14, 183–193.

Paulet, Y., Lucas, A., Gerard, A., 1988. Reproduction and larval development in two *Pecten maximus (L.)* populations from Brittany. Journal of Experimental Marine Biology and Ecology 119, 145–156.

Paulmier, G., 1997. Tintinnides (Ciliophora, Oligotrichida, Tintinnina) de l'atalntique boréal. de l'océan indien et de quelques mers adjacentes: Mediterranée mer Caraïbe, mer Rouge. Inventaires et distribution. Observations basées sur les loricas. Rapport Ifremer, DRV/RH/97-17, 191p.

Pouvreau, S., Bacher, C., Héral, M., 2000a. Ecophysiological model of growth and reproduction of the black pearl oyster, *Pinctada margaritifera*: potential applications for pearl farming in French Polynesia. Aquaculture 186, 117–144.

Pouvreau, S., Gangnery, A., Tiapari, J., Lagarde, F., Garnier, M., Bodoy, A., 2000b. Gametogenic cycle and reproductive effort of the tropical blacklip pearl oyster, *Pinctada margaritifera* (*Bivalvia: Pteriidae*), cultivated in Takapoto atoll (French Polynesia). Aquatic Living Resources 13, 37–48.

Pronker, A., Nevejan, N., Peene, F., Geijsen, P., Sorgeloos, P., 2008. Hatchery broodstock conditioning of the blue mussel *Mytilus edulis* (Linnaeus 1758). Part I. Impact of different micro-algae mixtures on broodstock performance. Aquaculture International 16, 297–307.

Ricard, M., 1987. Diatomosphycées. In Atlas du phytoplancton marin. In: Sournia A. (Ed.), Editions du Centre National de la Recherche Scientifique, vol. 2. Paris, pp 1–297.

Ruiz, C., Abad, M., Sedano, F., García-Martin, L., Sánchez-López, J., 1992. Influence of seasonal environmental changes on the gamete production and biochemical composition of *Crassostrea gigas* (Thunberg) in suspended culture in El Grove, Galicia, Spain. Journal of Experimental Marine Biology and Ecology 155, 249–262.

Sastry, A., 1979. Pelecypoda (Excluding Ostreidae). In: Giese, A., Pearse, J. (Eds.), Reproduction of Marine Invertebrates. Academic Press, New York, pp. 113–265.

Saucedo, P., Racotta, I., Villarreal, H., Monteforte, M., 2002. Seasonal changes in the histological and biochemical profile of the gonad, digestive gland, and muscle of the calafia mother of pearl oyster, *Pinctada mazatlanica* (Hanley, 1856) associated with gametogenesis. Journal of Shellfish Research 21, 127–135.

Saxby, S., 2002. A review of Food Availability, Sea Water Characteristics and Bivalve Growth Performance at Coastal Culture Sites in Temperate and Warm Temperate Regions of the World. Fisheries Research (Fisheries, p. 42). Department of Fisheries, Perth, Western Australia.

Starr, M., Himmelman, J., Therriault, J., 1990. Direct coupling of Marine Invertebrates Spawning with phytoplankton blooms. Science 247, 1071–1074.

Sournia, A., 1986. Atlas du phytoplancton marin. Introduction, Cyanophycées, Dictyochophycées, Dinophycées et Raphidophycées, vol. 1. Editions du CNRS, Paris, 219p.

Sournia, A., Ricard, M., 1976. Données sur l′ hydrologie et la producativité d'un atoll fermé (Takapoto, Iles Tuamotu). Vie Milieu 26, 243–279.

Spurrier, J., 2006. Additional tables for steel–Dwass–Critchlow–Fligner distribution-free multiple comparisons of three treatments. Communications in Statistics - Simulation and Computation 35, 441–446.

Thomas, Y., Garen, P., Bennett, A., Le Pennec, M., Clavier, J., 2012a. Multiscale distribution and dynamics of bivalve larvae in a deep atoll lagoon (Ahe, French Polynesia). Marine Pollution Bulletin 65, 453–462.

Thomas, Y., Garen, P., Courties, C., Charpy, L., 2010. Spatial and temporal variability of the pico-and nanophytoplankton and bacterioplankton in a deep Polynesian atoll lagoon. Aquatic microbial ecology 59, 89–101.

Thomas, Y., Le Gendre, R., Garen, P., Dumas, F., Andréfouët, S., 2012b. Bivalve larvae transport and connectivity within the Ahe atoll lagoon (Tuamotu Archipelago), with application to pearl oyster aquaculture management. Marine Pollution Bulletin 65, 441–452.

Thompson, R., 1984. The reproductive cycle and physiological ecology of the mussel *Mytilus edulis* in a subarctic, non-estuarine environment. Marine Biology 79, 277–288.

Valiela, I., Cebrián, J., 1999. Seasonal patterns in phytoplankton biomass in coastal ecosystems. Journal of Plankton Research 21, 429–444.

Welschmeyer, N., 1994. Fluorometric analysis of chlorophyll *a* in the presence of chlorophyll *b* and pheopigments. Limnology and Oceanography 39, 1985–1992.

Marine Pollution Bulletin 65 (2012) 471–477

Contents lists available at SciVerse ScienceDirect

Marine Pollution Bulletin

journal homepage: www.elsevier.com/locate/marpolbul

Physical and chemical control of the phytoplankton of Ahe lagoon, French Polynesia

Loïc Charpy [a,*], Martine Rodier [b], Jonathan Fournier [c], Marie-José Langlade [a], Nabila Gaertner-Mazouni [d]

[a] IRD, MIO, UR235, IRD Tahiti, BP 529, 98713 Papeete, French Polynesia
[b] IRD, MIO, UR235, IRD New Caledonia, BP A58, 98848 Nouméa, New Caledonia
[c] IFREMER, COP, BP 7004, 98719 Taravao, Tahiti, French Polynesia
[d] Université de la Polynésie Française, Tahiti, French Polynesia

ARTICLE INFO

Keywords:
Atoll
Nutrients
Phytoplankton
Aquaculture

ABSTRACT

The environmental characteristics of Ahe deep lagoon (Tuamotu Archipelago, French Polynesia) were studied over 3 years with the aim of explaining the spatial and temporal variability of the natural food available for pearl oysters with a special focus on phytoplankton biomass and global photosynthesis/respiration ratio of the lagoon. Chlorophyll averaged 0.34 ± 0.01 μg L^{-1} and our findings did not confirm increased phytoplankton biomass in deep lagoonal waters. Phytoplankton production appears to be limited firstly by nitrogen and respiratory processes overpass photosynthetic processes at least in the northeastern edge of the atoll. Grazing by pearl oysters in culture seems to decrease the POC concentration but not the phytoplankton biomass. Oysters graze mainly on non chlorophyllian particles.

1. Introduction

In atoll lagoons, planktonic processes are partially controlled by physical and chemical factors (Charpy-Roubaud et al., 1990; Charpy, 2001; Charpy and Blanchot, 1998; Charpy et al., 1997; Dufour et al., 2001, 1999). Shallow lagoons have widely been assumed to present environmental homogeneity as they are routinely considered well-mixed (Buestel and Pouvreau, 2000; Charpy, 1996; Gonzalez et al., 1998; Torreton and Dufour, 1996). In the deep Ahe lagoon, Thomas et al. (2010) found that phytoplankton biomass, estimated by *in vivo* fluorescence, was higher in the deep layer than in the upper layer. The authors considered that the main factors potentially driving this vertical phytoplankton structure could be photoinhibition in the upper layers and a bottom effect providing more favorable nutrient conditions in the deeper layers.

This paper presents baseline data on the physical and chemical characteristics and phytoplankton biomass in the deep Ahe lagoon subject to pearl oyster farming influence. The main objectives of this study were thus to describe the vertical and spatial distribution of phytoplankton and improve our understanding of the mechanisms controlling the phytoplankton distribution in an exploited lagoon in comparison to other atolls. The nutrient status was also evaluated and the heterotrophy or autotrophy balance assessed, taking into account the effect of pearl oyster culture.

2. Materials and methods

2.1. Study site

Ahe atoll (14.5°S, 146.3°W) is located in the northwestern part of the French Polynesian Tuamotu Archipelago, at 500 km northeast of Tahiti Island. Ahe lagoon measures 142 km^2, and has a maximum depth of 70 m and a mean depth of 42 m. It is defined as a semi-enclosed atoll. There is one active pass in the western part of the lagoon, and several reef-flat spillways (<50 cm depth) are distributed along the reef rim, mainly in the southern and western part. Ahe lagoon hosts significant pearl oyster aquaculture industry. In 2008, there were 86 farms, but plummeting pearl prices have meant that only 65 farms are still in business as in late 2010 (Lo-Yat pers. comm.). However, it still remains nearly 1350 spat collection stations and almost 11% of the lagoon dedicated to black-lip pearl oyster rearing.

2.2. Sampling

Sampling was conducted over a total of 5 expeditions covering the 2008–2010 period (May 2008, October 2008, February 2009, August 2009 and October 2010). A 4-station SW-to-NE transect (L01, L03, L09 and L11) of the lagoon was explored one to three times on each expedition, with another station L04 explored in August 2008. A further station (OCE) located just outside the lagoon near the main passage was also sampled one to two times over the 5 expeditions (Fig. 1). Sampling operations were always performed between 8 and 10 a.m.

* Corresponding author.
E-mail address: loic.charpy@ird.fr (L. Charpy).

0025-326X/$ - see front matter © 2011 Elsevier Ltd. All rights reserved.
doi:10.1016/j.marpolbul.2011.12.026

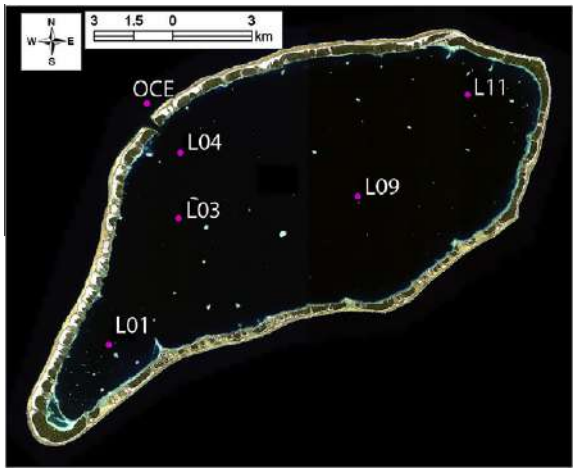

Fig. 1. Sampling stations prospected between 2008 and 2010.

2.3. Hydrological profiles

Vertical profiles of salinity, temperature, pH and dissolved oxygen were measured using an YSI multi-parameter probe (model 600). The pH probe was calibrated using NBS (NIST) buffers.

2.4. Dissolved and particulate material

Discrete water samples were taken at 0.5, 5, 10, 15, 20, 30, 40 m depth using a 5 L Niskin bottle.

2.4.1. Nutrients

Ammonium (NH_4^+) and soluble reactive phosphate (SRP) were analyzed within 1–2 h post-sampling at the field laboratory set up on Ahe atoll. Ammonium concentrations were determined on a Trilogy fluorometer (Turner Designs) using the fluorometric and o-phthaldialdehyde (OPA) method described in Holmes et al. (1999). To limit sample contamination, the OPA reagent was instantly injected into the samples onboard ship. SRP concentrations were measured manually with a Shimadzu UV-mini 1240 spectrophotometer (cell length: 10 cm), using the molybdenum blue reaction (Murphy and Riley, 1962).

Nitrate (NO_3^-), nitrite (NO_2^-) and silicate ($Si(OH)_4$) were analyzed post-expedition on $HgCl_2^-$–preserved samples (Kattner, 1999) at the IRD's Nouméa centre lab (New Caledonia). Determinations were performed by colorimetry using a Technicon Autoanalyzer III system (Aminot and Kérouel, 2004; Strickland and Parsons, 1972).

2.4.2. POC/PON

Particulate organic carbon (POC) was measured on the first 4 expeditions, while particulate organic nitrogen (PON) was measured on the fourth expedition only. A total of 500 mL of sea water was filtered on a pre-combusted (24 h at 450 °C) 25 mm Whatman GF/F filter. All filters were further oven-dried at 60 °C for 24 h and then stored dry until analysis. POC and PON analysis was performed within 1 month of collection on an Integra-CN mass spectrometer (PDZ Europa) calibrated with glycine references at every batch of 10–15 samples. The accuracy of our analytical system was also regularly verified using reference materials from the International Atomic Energy Agency (IAEA, Analytical Quality Control Services).

2.4.3. Chlorophyll a

Chlorophyll a (Chl *a*) was used as a proxy for phytoplankton biomass in the lagoon, and was measured for two size fractions: <2 μm and total. Water samples (0.5 L) were filtered on Whatman GF/F for total Chl *a* biomass and fractionated by serial filtration on 2 μm Millipore filters and GF/F for the >2 μm Chl *a* size class. Chlorophyll was immediately extracted with methanol then analyzed after 1 h using the fluorometric procedure described in (Welschmeyer, 1994) on a TD 700 fluorometer (Turner Designs) calibrated with pure Chl *a* standard (Sigma).

2.5. Plankton oxygen budget

Continuous O_2 measurements were performed in 2009 at station L11 using an SBE 19Plus CTD profiler (Sea-Bird Electronics Inc., USA) fitted with a SBE 43 sensor and a Clark polarographic membrane, settled at 10 m depth over 3.5 successive months (from February 7 to May 21). This method was carried out to give an estimate of plankton respiration and net and gross primary production. The probe was placed 30 m above the bottom to avoid potential bottom influence. The observed changes in dissolved oxygen (Q, g O_2 m^{-2} h^{-1}) can be described by the equation:

$$Q = P_G - R + D_{in} \quad (1)$$

where P_G is rate of gross phytoplankton production, R is plankton community rate of respiration, and D_{in} is oxygen flux due to diffusion. We consider $D_{in} = 0$ as the probe was settled far from the surface (10 m depth).

3. Results

3.1. Meteorological and hydrological conditions

During the year 2008, rainfall varied between 0 and 34 mm h^{-1} with an average of 0.1 mm h^{-1}, air temperature varied between 22 and 31 °C with an average of 27 °C, percent humidity varied between 48 and 96, and wind speed between 0 and 14 m s^{-1} with an average of 7 m s^{-1}. In 2009, rainfall varied between 0 and 22 mm h^{-1} with an average of 0.2 mm h^{-1}, air temperature varied between 23 and 33 °C with an average of 29 °C, percent humidity varied between 54 and 94, and wind speed varied between 0 and 10 m s^{-1} with an average of 3.8 m s^{-1}. Wind was mainly ESE (32%) and E (30%); data from Takaroa meteorological station 100 km from Ahe. No data are available for 2010.

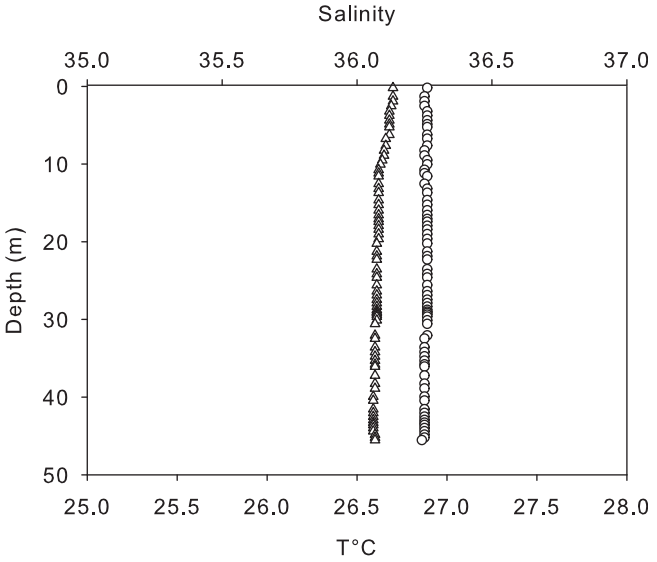

Fig. 2. Depth profiles of temperature (triangles) and salinity (circles) at station L11 in October 2010.

During the 5 expeditions, water temperature and salinity were homogenous between stations and from the surface to the bottom (Fig. 2). Temperature averaged 28.29 ± 0.01 °C (±SE). The lowest temperatures were recorded in October 2008 and 2010 (26.93 ± 0.01 °C and 26.87 ± 0.01 °C, respectively) while the highest temperatures were recorded in February 2009 (29.25 ± 0.01 °C) which corresponds to the austral summer (Fig. 3).

Salinity averaged 36.64 ± 0.005. The highest salinities were recorded in May 2008 (36.97 ± 0.003) while the lowest salinities were recorded in October 2010 (36.24 ± 0.006; Fig. 3). Temperature and salinity was significantly higher in the lagoon than at station OCE ($P < 0.001$, two-way ANOVA): +0.07 °C for temperature and +0.02 in May and 0.25 in October 2008 for salinity.

Vertical profiling of dissolved oxygen and pH was performed only in February 2009; O_2 and pH vertical distribution were homogenous with no clear differences between stations. In the lagoon, all stations and depths pooled, morning O_2 saturation was 98.13 ± 0.01% and pH was 8.08 ± 0.002. At station OCE, O_2 saturation was 98.43 ± 0.02% and pH 8.19 ± 0.002 over the 0–50 upper layer.

3.2. Nutrients and organic matter

The nutrient data reported in Table 1 were collected during the last cruise in October 2010; for logistics reasons, no data are available for the other cruises.

In October 2010, nutrient concentrations were low and distributed evenly through the lagoon. Ammonia concentrations were below 0.05 μM and were even undetectable outside of the pearl-farming areas. Nitrate concentrations ranged between 0.05 and 0.10 μM. Nitrite concentrations remained low (<0.06 μM) generally followed the same spatial pattern as nitrate. Average DIN ($NO_3^- + NO_2^- + NH_4^+$) concentration was 0.11 ± 0.01 μM ($n = 16$). Dissolved inorganic phosphorus (SRP) concentrations were relatively similar through the lagoon, and averaged 0.26 ± 0.01 μM ($n = 16$). $Si(OH)_4$ concentrations were also very similar through the lagoon, and averaged 1.54 ± 0.03 μM ($n = 16$).

Nutrient concentrations in surrounding oceanic waters (0.14 ± 0.03 μM DIN and 0.23 ± 0.01 μM SRP, $n = 5$) were close to lagoonal nutrient concentrations values.

During the 2008–2009 period (Fig. 4), POC varied from 23 μg C L^{-1} (station L04) up to 582 μg C L^{-1} (station L01), with an average of 159 ± 6 μg C L^{-1} ($n = 130$). The POC concentration at station L04, which was located close to the passage, was thus 4-fold lower than in other stations. PON (measured only in August 2009) varied from 5.1 up to 41.1, with an average of 23.5 ± 1.5 μg N L^{-1} ($n = 34$). Average C:N was 6.3 ± 0.1 (mol:mol). POC and PON were not measured at station OCE.

3.3. Phytoplankton biomass and production

Chl *a* concentrations inside the lagoon varied over a 10-fold range (i.e. from 0.08 to 0.85 μg L^{-1}), and averaged 0.34 ± 0.01 μg L^{-1} ($n = 177$). Percentage of picophytoplankton (Chl $a < 2$ μm) ranged from 48.9% to 100% (average: 78.4 ± 0.7%, $n = 160$).There was no significant relationship between Chl *a* and depth ($F = 0.861$, $P = 0.447$). In contrast, two-way ANOVA showed a significant effect of sampling station and period ($F = 31.6$, $P < 0.001$ and $F = 5.7$, $P < 0.001$) on lagoon Chl *a* content. The highest Chl *a* levels were found at station L01 and the highest percent contributions of picoplankton were recorded at station L11 (Fig. 5). Phytoplankton biomass was higher in February and May than in other months, while percent of picoplankton remained similar (Fig. 6).

"Oceanic" waters were less Chl *a*-rich than the lagoonal waters, with Chl *a* concentrations varying between 0.07 and 0.26 μg L^{-1}, but the biomass was still dominated by picoplankton (54.1–86.8% of Chl $a < 2$ μm).

Average plankton respiration measured at station L11 during the night was −4.81 ± 0.39 μg O_2 L^{-1} h^{-1} ($n = 46$) while net O_2 budget during daylight was +4.02 ± 0.46 μg O_2 L^{-1} h^{-1} ($n = 39$). Therefore, over a 24-h period, oxygen budget was negative. Estimated gross primary production during daylight was 8.8 μg O_2 L^{-1} h^{-1}.

4. Discussion

4.1. Environmental conditions and nutrient status

Lagoon temperature and salinity showed a quasi-homogeneous vertical structure (Fig. 2), with no stratification whatever the season. The constant wind during our surveys, mainly from the E and ESE, is probably responsible for the observed homogeneity. Similarly, spatial variability remained relatively low, except at station L11 located SW of the atoll where temperature and salinity were the lowest due to the shallowness of this station. The lower temperature observed in October 2010 (26.87 ± 0.01 °C) is likely due to the strong La Niña which affected the Pacific from June 2010 to April 2011 (Ref. NOAA site). Indeed during La Nina events, negative SST anomalies of 3–5 °C may be observed across the equatorial Central Pacific Ocean.

There were no significant temperature and salinity differences between the lagoon and surrounding waters. This reflects the short residence time of water inside the lagoon (~34 d), estimated by

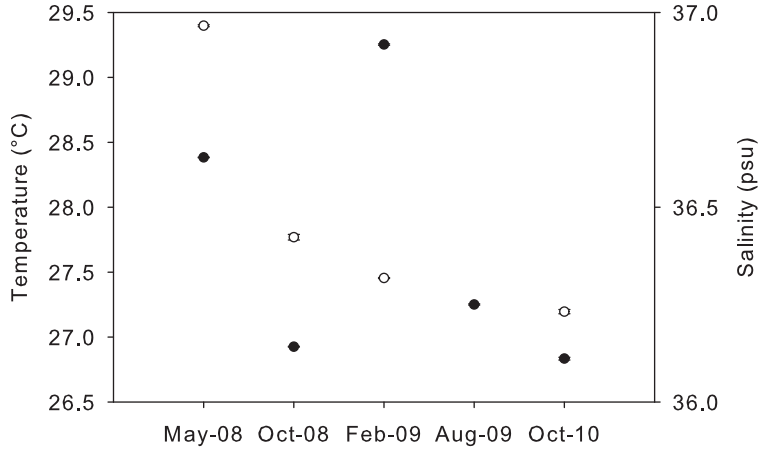

Fig. 3. Temporal variability (averages ± SE) for temperature (black circles) and salinity (open circles) in Ahe lagoon between 2008 and 2010.

Table 1
Nutrients (μM) and nutrient ratios (mol:mol) in October 2010. DIN = $NH_4^+ + NO_3^- + NO_2^-$; SRP = dissolved inorganic phosphorus.

Date	Station	Depth	NH_4^+	NO_2^-	NO_3^-	DIN	SRP	$Si(OH)_4$	DIN/SRP	DIN:Si
10/21/2010	OCE	0.5	0.04	0.022	0.121	0.183	0.26	1.68	0.70	0.11
		10	0.01	0.011	0.089	0.110	0.25	1.31	0.44	0.08
		20	0.01	0.013	0.084	0.107	0.22	1.36	0.49	0.08
		30	0.00	0.013	0.062	0.075	0.22	1.52	0.34	0.05
		50	0.04	0.029	0.160	0.229	0.22	1.57	1.04	0.15
10/22/2010	L01	0.5	0.03	0.026	0.072	0.128	0.26	1.60	0.49	0.08
		10	0.03	0.018	0.098	0.146	0.43	1.68	0.34	0.09
		20	0.03	0.032	0.070	0.132	0.23	1.57	0.57	0.08
		27	0.08	0.025	0.086	0.191	0.28	1.39	0.68	0.14
10/23/2010	L03	0.5	0.05	0.011	0.085	0.146	0.29	1.85	0.50	0.08
		10	0.01	0.007	0.06	0.077	0.28	1.65	0.28	0.05
		20	0.02	0.009	0.055	0.084	0.23	1.67	0.37	0.05
		40	0.02	0.008	0.086	0.114	0.23	1.19	0.50	0.10
10/23/2010	L09	0.5	0.02	0.008	0.058	0.086	0.25	1.62	0.34	0.05
		10	0.01	0.007	0.058	0.075	0.24	1.58	0.31	0.05
		20	0.01	0.003	0.064	0.077	0.24	1.55	0.32	0.05
		40	0.04	0.014	0.068	0.122	0.25	1.61	0.49	0.08
10/23/2010	L11	0.5	0.02	0.018	0.128	0.166	0.25	1.31	0.66	0.13
		10	0.01	0.007	0.053	0.070	0.25	1.60	0.28	0.04
		20	0.01	0.005	0.068	0.083	0.25	1.45	0.33	0.06
		40	0.02	0.008	0.058	0.086	0.25	1.50	0.34	0.06

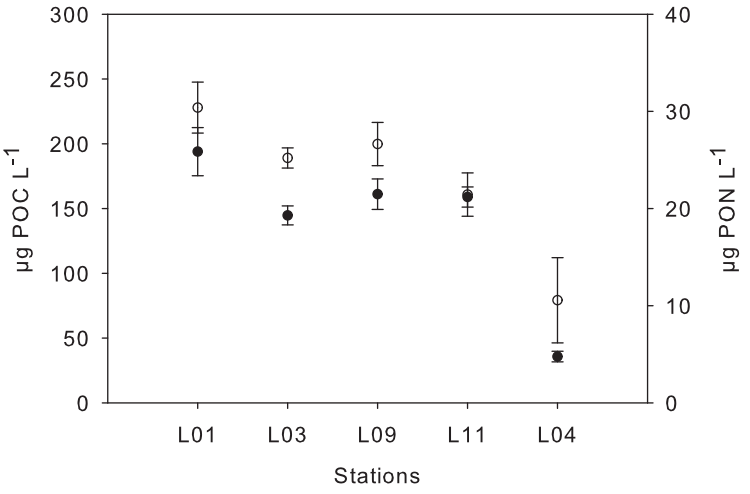

Fig. 4. Spatial variability (averages ± SE) for particulate organic carbon (POC, black circles) and particulate organic nitrogen (PON, open circles) in Ahe lagoon between 2008 and 2009.

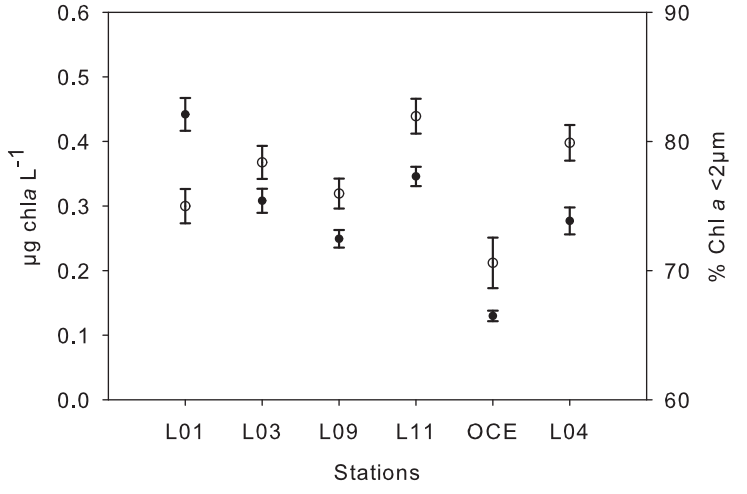

Fig. 5. Spatial distribution (averages ± SE) for chlorophyll *a* (Chl *a*, black circles) and percent of phytoplankton cells of size <2 μm (open circles) in Ahe lagoon and surrounding oceanic water (OCE) for the 2008–2010 period.

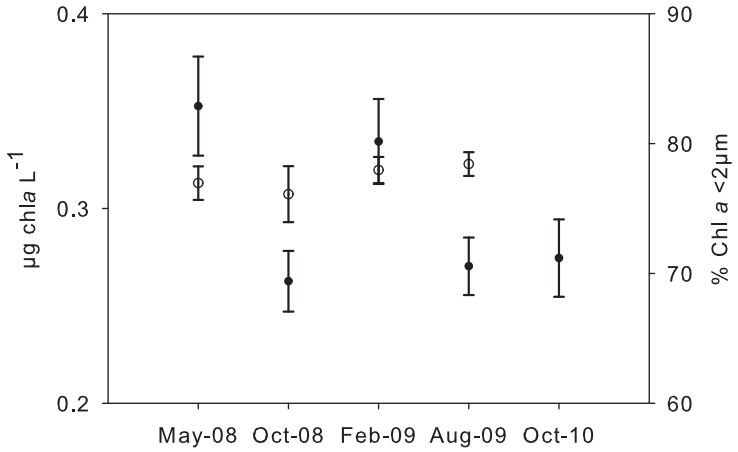

Fig. 6. Temporal variability (averages ± SE) for chlorophyll *a* (Chl *a*, black circles) and percent of phytoplankton cells with a size <2 µm (open circles) in Ahe lagoon for the 2008–2010 period.

Pagès and Andrefouet (2001) and based on the ratio of lagoon volume to average water input rate.

Ahe lagoon was low-N and P-nutrient (DIN = 0.11 ± 0.01 µM; SRP = 0.26 + 0.01 µM), at least in October 2010. Average DIN:SRP ratio (0.42 ± 0.03) was considerably lower than the Redfield ratio of 16:1 (Redfield et al., 1963), indicating that phytoplankton growth is mainly constrained by nitrogen availability. These values correspond, however, to the intermediate period between dry and rainy season, but do not reflect potential seasonal or annual variability (such as rainfall variability). The nutrient conditions in Ahe are comparable to those observed over two seasons in 12 Tuamotu lagoons during the TYPATOLL program (Dufour et al., 2001): low DIN and SRP concentrations and DIN:SRP ratios <3 (Dufour et al., 2001). Moreover, by comparing our data to other tropical coral reef lagoons in the Pacific, Great Barrier Reef lagoon (Furnas et al., 2005) and southwest lagoon of New Caledonia (Torreton et al., 2010), the N-limitation appears to be a common feature in tropical coral reef lagoons.

In such nutrient-limited conditions, phytoplankton growth can only be sustained by nutrient inputs from external sources. In Ahe, nitrogen fluxes at the water–sediment interface were measured *in situ* using benthic transparent hemispheres (Gaertner-Mazouni et al., 2012). Maximum values of benthic nitrogen fluxes (DIN) were recorded in stations directly under the influence of pearl oyster culture 32.06 and 35.6 µmol m^{-2} d^{-1}. These benthic fluxes could contribute to a 3–28% of the nitrogen demands for primary production.

For comparison, in Tikehau lagoon, N flux at the water–sediment interface accounted for less than 6.8% of the N requirements of lagoonal primary production (Charpy-Roubaud et al., 1996). On the other hand, nutrient budget analysis between lagoon and open ocean evidenced that oceanic waters are not an important N source for the lagoon. Surface oceanic water around Tuamotu atolls typically has average nutrient concentrations of 0.02 µM DIN and 0.21 µM SRP (Dufour et al., 1999). However, higher DIN values at the OCE station in October 2010, especially at 50 m (0.23 µM), indicates a possible surface N-enrichment due to turbulent vertical mixing of the waters along the shelf break, as observed in Tikehau atoll (Charpy-Roubaud et al., 1990).

Dinitrogen (N_2) fixation is reported as another source of nitrogen for lagoonal waters. In Tikehau atoll, Charpy-Roubaud et al. (2001) found that total lagoonal benthic N_2 fixation contributed 24.4% of the total nitrogen requirement for the benthic primary production. Like in Tikehau, we found benthic nitrogen-fixing cyanobacteria in various stations of Ahe. Benthic N_2 fixation is probably an important source of nitrogen for Ahe lagoon.

Average silicate concentration in Ahe (1.55 ± 0.05 µM) was relatively low but slightly higher than average silicate concentration in other Tuamotu atolls (1.0 ± 0.1 µM; Dufour et al., 1999). The DIN:$Si(OH)_4$ ratio found in Ahe (0.07 ± 0.01) was higher than the DIN:$Si(OH)_4$ ratio found during the TYPATOLL program (0.04 ± 0.01), but in both cases the values are lower than the Redfield ratio of 1:1, which shows no evidence of potential Si limitation, in such N-limited conditions.

POC and PON contents and C:N ratio are in the mid-range of the values reported by Charpy et al. (1997) for 16 other Tuamotu atoll lagoons. In their paper, the authors found that the POC concentration was inversely correlated to the latitude of each lagoon. They interpret this result as an influence of the waters deriving from the Peruvian and equatorial upwellings. Ahe is located at nearly the same latitude as Tikehau and Rangiroa but its POC content was lower; this difference could be due to the impact of pearl oyster aquaculture. Indeed, in 1996, there were very little aquaculture in these 2 atolls.

4.2. Phytoplankton distribution, control and productivity

According to our extracted Chl *a* data, the phytoplankton biomass appears to be homogeneously distributed from the surface to the bottom and dominated by the <2 µm fraction. Our chlorophyll values (0.34 ± 0.01 µg L^{-1}) and the high percent contribution of picoplankton are in the range of the extracted Chl *a* values (0.01–0.52 µg L^{-1} Chl *a* < 2 µm and 0–0.24 µg L^{-1} Chl *a* > 2 µm) measured at 5 m depth in Ahe lagoon by Thomas et al. (2010) 1 year before us (2007–2008). However, Thomas et al. (2010) using *in vivo* Chl *a* estimates conclude on a vertical gradient of phytoplankton biomass, increasing with depth. We consider that extracted Chl *a* gives a more reliable measure of phytoplankton biomass, and the *in vivo* gradient observed by Thomas et al. (2010) may be due to an increase in fluorescence with depth rather than any real biomass increase. In our case, the homogeneous distribution of Chl *a* indicates no photoinhibition in the upper layer in agreement with Lefebvre et al. (2012) and could be explained (1) by low nutrient inputs from the benthic system at the sediment–water interface as measured by Gaertner-Mazouni et al. (2012): 1.75–855 µmol N m^{-2} d^{-1}, and (2) by strong mixing in the absence of thermohaline stratification.

The spatial heterogeneous distribution of chlorophyll can be attributed to the NE surface current (Dumas et al., 2012) which accumulates phytoplankton biomass in the SW part of the lagoon (Station L01). On the other hand, we do not have any

hypotheses to explain the increase of phytoplankton biomass in February and May.

The Chl *a* concentrations found in Ahe are in the upper range (second position) of values reported for 16 Polynesian atoll lagoons by Charpy et al. (1997) during TYPATOLL expeditions: 0.03 ± 0.01 μg Chl *a* L^{-1} (Tekokota) to 0.43 ± 0.03 (Reka-Reka). This relatively high Chl *a* concentrations in a lagoon with pearl farms compared to non exploited ones, suggests that grazing by pearl oysters *Pinctada margaritifera* does not significantly decrease Chl *a* concentration, unless phytoplankton growth be enhanced by some N input from filter feeders metabolism. There is no available data to conclude on the positive effect of feeder on phytoplankton; conversely, recent work conducted in Ahe by Fournier et al. (2012) on pearl oyster grazing has found that the diet of *P. margaritifera* is composed mainly of heterotrophic (without Chl *a*) nano- and micro-plankton and not of phytoplankton. The negligible influence of the oysters on the planktonic network and the importance of heterotrophic protists in the diet of *P. margaritifera* have also been formally demonstrated in Takapoto atoll by Niquil et al. (2001) and by Loret et al. (2000), respectively.

The high contribution of picoplankton (Chl *a* < 2 μm) to total phytoplankton biomass fit with observations in other Polynesian atolls made by Charpy et al. (1997). Such high contribution is typical of low DIN concentration as evidenced by Jacquet et al. (2006) in the SW New Caledonia lagoon. In Ahe, diatoms represent only between 10% and 34% in abundance of the phytoplankton with a size >2 μm (Lefebvre, pers. com.).

Chl *a* measured at station OCE outside the lagoon (0.13 ± 0.01 μg Chl *a* L^{-1}) was lower than the average measured within the lagoon but higher than the average Chl *a* content of the oceanic waters prospected during the TYPATOLL program (0.05 ± 0.00 μg Chl *a* L^{-1}). As stated earlier, station OCE was prospected with a small speedboat from close to the atoll rim (less than 300 m away) and was possibly under the influence of surface N-enrichment due to turbulent vertical mixing of the waters along the shelf break as evidenced by DIN data.

Phytoplankton production estimated from gross O_2 budget, assuming a photosynthetic coefficient of 1, was equivalent to 6.6 μg C L^{-1} d^{-1}. This estimation is within the range of values obtained in Ahe using ^{13}C uptake (Lefebvre et al., 2012), in Tikehau and Takapoto (Charpy, 1996) and in the SW lagoon of New Caledonia (Torreton et al., 2010) using ^{14}C uptake.

The oxygen budget of the north-eastern edge of the lagoonal water was negative over a 24 h period, suggesting that respiratory processes play a greater role than oxygen production, as further attested by the low pH values. Indeed, the fact that pH values were lower inside the lagoon than in surrounding oceanic water can be attributed to respiration processes that are significant in both water column and by benthic organisms, pearl oysters included. The importance of respiration processes in water column and sediment and the impact of these respiration processes on pH and O_2 concentrations have already been reported for another Polynesian atoll (Tikehau) by Charpy-Roubaud et al. (1996). Such net heterotrophy was also observed in the New Caledonia SW lagoon by Torreton et al. (2010).

5. Conclusions

Physical and chemical characteristics of Ahe lagoon are very similar to other prospected coral reef lagoons of the Tuamotu Archipelago. Phytoplankton biomass (extracted chlorophyll) was in the same range as other atoll lagoons and distributed homogeneously with depth. Spatial variability exists with a significant increase in the SW of the lagoon due to wind effect. Nutrient concentrations are low and typical of other Tuamotu atolls. Nitrogen is probably the first limiting factor for phytoplankton production (DIN: P ratio <3) but N-enrichment by benthic N_2-fixing cyanobacteria was still not evaluated. The relatively low POC content compared to other lagoons localized at the same latitude can reflect the impact of pearl oyster aquaculture. Such impact does not appear onto phytoplankton biomass, pearl oysters mainly grazing onto heterotrophic plankton but could also be explained by a rapid turnover of the primary producers, as it was recorded in other shellfish farming zones. Further studies are thus needed to confirm these assumptions of the influence of oyster culture and the contribution of the benthic system. The water column of the Ahe lagoon seems to be net heterotrophic due to animal respiration including pearl oysters.

Acknowledgements

This work was supported by the European Development Fund, the French Agency of Development (AFD), the National Institute of Water and Atmospheric Research (NIWA) in collaboration with the Service de la Perliculture and the University of French Polynesia. We should like to thank all the colleagues for their valuable help in collecting samples and Raita and Willy for their warm hospitality in Ahe.

References

Aminot, A., Kérouel, R., 2004. Hydrologie Des Ecosystemes Marins. Paramètres et analyses, Ifremer.
Buestel, D., Pouvreau, S., 2000. Particulate matter in Takapoto lagoon waters: potential food for cultivated pearl oysters. Oceanol. Acta 23, 193–210.
Charpy, L., 1996. Phytoplankton biomass and production in two Tuamotu atoll lagoons (French Polynesia). Mar. Ecol. Prog. Ser. 145, 133–142.
Charpy, L., 2001. Phosphorus supply for atoll biological productivity. Coral Reefs 20, 357–360.
Charpy, L., Blanchot, J., 1998. Photosynthetic picoplankton in French Polynesian atoll lagoons: estimation of taxa contribution to biomass and production by flow cytometry. Mar. Ecol. Prog. Ser. 162, 57–70.
Charpy, L., Dufour, P., Garcia, N., 1997. Particulate organic matter in sixteen Tuamotu atoll lagoons (French Polynesia). Mar. Ecol. Prog. Ser. 151, 55–65.
Charpy-Roubaud, C., Charpy, L., Cremoux, J.L., 1990. Nutrient budget of the lagoonal waters in an open Central South Pacific atoll Tikehau Tuamotu, French Polynesia. Mar. Biol. 107, 67–74.
Charpy-Roubaud, C., Charpy, L., Sarazin, G., 1996. Diffusional nutrient fluxes at the sediment-water interface and organic matter mineralization in an atoll lagoon (Tikehau, Tuamotu Archipelago, French Polynesia). Mar. Ecol. Prog. Ser. 132, 181–190.
Charpy-Roubaud, C., Charpy, L., Larkum, A.W.D., 2001. Atmospheric dinitrogen fixation by benthic communities of Tikehau Lagoon (Tuamotu Archipelago, French Polynesia) and its contribution to benthic primary production. Mar. Biol. 139, 991–997.
Dufour, P., Charpy, L., Bonnet, S., Garcia, N., 1999. Phytoplankton nutrient control in the oligotrophic South Pacific subtropical gyre (Tuamotu Archipelago). Mar. Ecol. Prog. Ser. 179, 285–290.
Dufour, P., Andrefouët, S., Charpy, L., Garcia, N., 2001. Atoll morphometry controls lagoon nutrient regime. Limnol. Oceanogr. 46, 456–461.
Dumas, F., Le Gendre, R., Thomas, Y., Andréfouët, S., 2012. Tidal flushing and wind driven circulation of Ahe atoll lagoon (Tuamotu Archipelago, French Polynesia) from *in situ* observations and numerical modeling. Mar. Pollut. Bull. 65, 425–440.
Fournier, J., Dupuy, C., Bouvy, M., Courrodon-Real, M., Charpy, L., Pouvreau, S., Le Moullac, G., Le Pennec, M., Cochard, J.-C., 2012. Pearl oysters *Pinctada margaritifera* grazing on natural plankton in Ahe atoll lagoon (Tuamotu archipelago, French Polynesia). Mar. Pollut. Bull. 65, 490–499.
Furnas, M.J., Mitchell, A., Skuza, M., Brodie, J., 2005. In the other 90%: phytoplankton responses to enhanced nutrient availability in the Great Barrier Reef Lagoon. Mar. Pollut. Bull. 51, 253.
Gaertner-Mazouni, N., Lacoste, E., Bodoy, A., Peacock, L., Rodier, M., Langlade, M.J., Orempuller, J., Charpy, L., 2012. Nutrient fluxes between water column and sediments: potential influence of the pearl oyster culture. Mar. Pollut. Bull. 65, 500–505.
Gonzalez, J.M., Torreton, J.P., Dufour, P., Charpy, L., 1998. Temporal and spatial dynamics of the pelagic microbial food web in an atoll lagoon. Aquat. Microb. Ecol. 16, 53–64.
Holmes, R.M., Aminot, A., Kérouel, R., Hooker, B.A., Petersen, B.J., 1999. A simple and precise method for measuring ammonium in marine and freshwater ecosystems. Can. J. Fish. Aquat. Sci. 56, 1801–1808.
Jacquet, S., Delesalle, B., Torreton, J.P., Blanchot, J., 2006. Response of phytoplankton communities to increased anthropogenic influences (southwestern lagoon, New Caledonia). Mar. Ecol. Prog. Ser. 320, 65–78.

Kattner, G., 1999. Storage of dissolved inorganic nutrients in seawater: poisoning with mercuric chloride. Mar. Chem. 67, 61–66.
Lefebvre, S., Claquin, P., Orvain, F., Véron, B., Charpy, L., 2012. Spatial and temporal dynamics of size-structured photosynthetic parameters (PAM) and primary production (^{13}C) of pico- and nano-phytoplankton in an atoll lagoon. Mar. Pollut. Bull. 65, 478–489.
Loret, P., Le Gall, S., Dupuy, C., Blanchot, J., Pastoureaud, A., Delesalle, B., Caisey, X., Jonquieres, G., 2000. Heterotrophic protists as a trophic link between picocyanobacteria and the pearl yoster *Pinctada margaritifera* in the Takapoto lagoon (Tuiaomotu Archipelago, French Polynesia). Aquat. Microb. Ecol. 22, 215–226.
Murphy, J., Riley, J.P., 1962. A modified single solution method for the determination of phosphate in natural waters. Anal. Chim. Acta 26, 31–36.
Niquil, N., Pouvreau, S., Sakka, A., Legendre, L., Addessi, L., Le Borgne, R., Charpy, L., Delesalle, B., 2001. Trophic web and carrying capacity in a pearl oyster farming lagoon (Takapoto, French Polynesia). Aquat. Living Resour. 14, 165–174.
Pagès, J., Andrefouet, S., 2001. A reconnaissance approach for hydrology of atoll lagoons. Coral Reefs 20, 409–414.
Redfield, A.C., Ketchum, B.H., Richards, F.A., 1963. The influence of organisms on the composition of seawater. In: Hill, M.N. (Ed.), The Sea. Interscience, pp. 26–77.
Strickland, J.D.H., Parsons, T.R., 1972. A Practical Handbook of Seawater Analysis, second ed. Fisheries Research Board of Canada, Ottawa.
Thomas, Y., Garen, P., Courties, C., Charpy, L., 2010. Spatial and temporal variability of the pico- and nanophytoplankton and bacterioplankton in a deep Polynesian atoll lagoon. Aquat. Microb. Ecol. 59, 89–101.
Torreton, J.P., Dufour, P., 1996. Temporal and spatial stability of bacterioplankton biomass and productivity in an atoll lagoon. Aquat. Microb. Ecol. 11, 251–261.
Torreton, J.P., Rochelle-Newall, E., Pringault, O., Jacquet, S., Faure, V., Briand, E., 2010. Variability of primary and bacterial production in a coral reef lagoon (New Caledonia). Mar. Pollut. Bull. 61, 335–348.
Welschmeyer, N.A., 1994. Fluorometric analysis of chlorophyll a in the presence of chlorophyll *b* and pheopigments. Limnol. Oceanogr. 39, 1985–1992.

Marine Pollution Bulletin 65 (2012) 478–489

Contents lists available at SciVerse ScienceDirect

Marine Pollution Bulletin

journal homepage: www.elsevier.com/locate/marpolbul

Spatial and temporal dynamics of size-structured photosynthetic parameters (PAM) and primary production (^{13}C) of pico- and nano-phytoplankton in an atoll lagoon

Sébastien Lefebvre [a,*], Pascal Claquin [b], Francis Orvain [b,c], Benoît Véron [b], Loïc Charpy [d]

[a] Université de Lille 1 sciences et technologies, UMR CNRS 8187, LOG (Laboratoire d'Océanologie et Géosciences), Station Marine de Wimereux, 28 Avenue Foch, 62930 Wimereux, France
[b] Université de Caen Basse-Normandie, FRE3484 CNRS BioMEA, Esplanade de la Paix, BP 5186, 14032 Caen Cedex, France
[c] CNRS, UMR 7208 BOREA, Muséum d'Histoire Naturelle, CRESCO, 38 Rue du Port Blanc, 35800 Dinard, France
[d] Aix-Marseille University, Mediterranean Institute of Oceanography (MIO), IRD, UR 235, BP529, 98713 Papeete, French Polynesia

ARTICLE INFO

Keywords:
Pulse amplitude modulation
Electron transport rate
Carbon incorporation
Coral reefs
Ahe atoll
Nutrient availability

ABSTRACT

Atoll lagoons display a high diversity of trophic states due mainly to their specific geomorphology, and probably to their level and mode of human exploitation. We investigated the functioning of the Ahe atoll lagoon, utilized for pearl oyster farming, through estimations of photosynthetic parameters (pulse amplitude modulation fluorometry) and primary production (^{13}C incorporation) measurements of the size structured phytoplankton biomass (<2 μm and >2 μm). Spatial and temporal scales of variability were surveyed during four seasons, over 16 months, at four sites within the lagoon. While primary production (P) was dominated by the picophytoplankton, its biomass specific primary productivity (P^B) was lower than in other atoll lagoons. The variables size fraction of the phytoplankton, water temperature, season, the interaction term station * fraction and site, explained significantly the variance of the data set using redundancy analysis. No significant trends over depth were observed in the range of 0–20 m. A clear spatial pattern was found which was persistent over the seasons: south and north sites were different from the two central stations for most of the measured variables. This pattern could possibly be explained by the existence of water cells showing different water residence time within the lagoon. Photoacclimation strategies of the two size fractions differed through their light saturation coefficient (higher for picophytoplankton), but not through their maximum photosynthetic capacity (ETR_{max}). Positive linear relationships between photosynthetic parameters indicated that their dynamic was independent of light availability in this ecosystem, but most probably dependent on nutrient availability and/or rapid changes in the community structure. Spatial and temporal patterns of the measured processes are then further discussed in the context of nutrient availability and the possible role of cultured oysters in nutrient recycling.

1. Introduction

Atolls are ring-shaped coral reefs, each enclosing a lagoon, and are characterized by a very small land area compared to the total area. Most of these coral reef ecosystems are situated in the Pacific or Indian ocean under tropical or sub-tropical climates (Kinsey and Hopley, 1991). Atoll lagoons are highly productive ecosystems compared to the oligotrophic surrounding waters and often support significant aquaculture production (e.g. pearl oyster farming) and fisheries (Sournia and Ricard, 1976). The atoll geomorphology and its correlated water residence time greatly influence its trophic status and food web organization (Pagès et al., 2001). As their geomorphology differs from one another, this leads to a wide range of lagoon ecological functioning; each lagoon being a stable state of a given trophic state (Dufour and Harmelin-Vivien, 1997).

Atoll lagoons can be viewed as continuous reactors in the oligotrophic ocean, efficiently processing the low nutrient tropical waters (Furnas et al., 1990; Hatcher, 1997). In atoll lagoons with greater depth than classical coral reef ecosystems, biomass of phytoplankton is usually low (between 0.2 and 0.6 μg Chl a L^{-1}), but provides most of the total primary production with high rates of biomass specific primary production (from 2.6 to 21 mg C mg Chl a^{-1} h^{-1}, Charpy et al., 1997). Autotrophic picoplankton (<2 μm) such as cyanobacteria (*Synechococcus* and *Prochlorococcus* species) and picoeukaryotes accounts for most of the biomass (usually >80%) and most of the primary production (>60%) of the phytoplankton; the remaining part being carried out by cells of larger sizes belonging to nanophytoplankton such as Dinophyta, Haptophyta and diatoms (Delesalle et al., 2001).

* Corresponding author. Tel.: +33 3 21 99 29 25; fax: +33 3 21 99 29 01.
E-mail address: sebastien.lefebvre@univ-lille1.fr (S. Lefebvre).

0025-326X/$ - see front matter © 2012 Elsevier Ltd. All rights reserved.
http://dx.doi.org/10.1016/j.marpolbul.2012.04.011

In order to define an atoll lagoon typology, Delesalle and Sournia (1992), and later Charpy et al. (1997) and Pagès et al. (2001), compared the trophic state of numerous atoll lagoons (30 atolls for the most complete study). At this macroscopic scale, they found that water residence time (i.e. the opposite of water renewal rate) and biomass of phytoplankton were positively correlated between atolls. Torréton et al. (2002) observed the same pattern for primary production on a more restricted number of atolls (12). Besides these, studies of spatio-temporal variability within single atolls are scarce. Torréton et al. (2002) stated that there were no spatial or seasonal variations in primary production within 12 atoll lagoons. On the contrary, Delesalle et al. (2001) recorded spatial heterogeneity in phytoplankton biomass during some seasons in Takapoto atoll. Actually, only one large data set incorporating spatio-temporal variability (on a monthly scale) of phytoplankton biomass and primary production has so far been published (Takapoto and Tikehau atolls; Charpy, 1996). The spatio-temporal patterns were neither presented nor discussed in this study because all sites were pooled horizontally. Water residence time varies daily due to differences in swell, wind or tide conditions (Andréfouët et al., 2001), and varies spatially within atoll lagoons depending on water circulation (Dumas et al., 2012). This may generate significant variations in the trophic state of a single atoll in its temporal and spatial components, as observed in New Caledonia lagoon (Torréton et al., 2007, 2010).

Tuamotu atoll lagoons host highly productive pearl oyster (*Pinctada margaritifera*) farming. Oysters are cultivated on suspended ropes so that these suspension feeders can access the pelagic environment food sources. Pearl oysters are able to process seston from 5 to 7 μm (Pouvreau et al., 2000). Consequently, they are not sustained directly by the main compartment of phytoplankton i.e. picoplankton. Mixotrophic and heterotrophic cells serve as a trophic link between picoplankton and the oysters (Loret et al., 2000). In the size range of cells that can be processed by oysters, carbon concentration of hetero-mixotrophs and autotrophs are in the same order of magnitude (Loret et al., 2000). Estimating primary production of the larger cell (>2 μm nanophytoplankton) is crucial in evaluating the carrying capacity of these lagoon atolls for filter feeders and also for aquaculture. In addition, the introduction of cultured bivalves into an ecosystem can lead to complex spatio-temporal patterns with local depletion of seston (Officer et al., 1982; Prins et al., 1995) and localized increases in nutrient regeneration (Grangeré et al., 2010). Hence, the primary productivity can be increased at the costs of the filtered and regenerated biomass.

The aim of our study was to determine the photosynthetic parameters and the primary production of the size structured phytoplankton biomass (<2 μm and >2 μm) of an atoll lagoon exploited for pearl oyster farming (Ahe atoll). Our study was the first to pay attention to the spatial (lagoon surface and depth) together with temporal (seasonal and day to day) variations. We hypothesized that geomorphology (and subsequent water residence time and water circulation) and aquaculture activities of the Ahe atoll, may lead to differences in primary production compared to previous studied atolls. In addition to traditional incubation of carbon isotopes, we used the pulse amplitude modulation (PAM) fluorometry method, based on variable chlorophyll fluorescence of photosystems II (PSII), which allows fast measurements of the electron transport rate (ETR) and subsequent photosynthetic parameters, to unravel the physiological and photoacclimation status of the phytoplankton.

2. Materials and methods

2.1. Study site

The Ahe atoll (14.5° S, 146.3° W) is located in the northwestern part of the French Polynesia Tuamotu Archipelago 500 km northeast of the main island, Tahiti. The lagoon has a surface area of about 142 km^2, and a mean depth of 41.7 m, with several deeper areas around 70 m. Ahe is defined as a semi-enclosed atoll (Fig. 1). One active pass is located in the western part of the lagoon (209 m width and 10 m deep) and several reef-flat spillways (30 cm deep on average) are distributed along the reef's rim (ca 5% of the total perimeter), mostly in the southern part of the lagoon (Dumas et al., 2012). The average water residence time is estimated at 252 days (Dumas et al., 2012). Ahe lagoon supports an important pearl oyster aquaculture industry. In 2008, there were 86 farms, but after the dramatic fall in the price of pearls, there remained only 65 farms at the end of 2010 (Lo-Yat A., pers. com.).

2.2. Sampling design

Four different surveys were conducted in May (14, 16, 20 and 23) and October (16 and 20) 2008, and February (17, 21 and 24), and August (20, 21 and 24) 2009. Samples were collected from three different depths (0.5 m, 10 m and 20 m), at four different sites (L01, L03, L09 and L11), along a northeastern/southwestern transect (Fig. 1), giving a total of 12 water samples per sampling day. Two to four daily samplings were carried during each season, between 8 am and 10 am and on the same date. On one occasion in August 2009, sites were not sampled on the same date: L01 and L03 on the 20th; L09 and L11 on the 21th. Samples were taken using a Niskin bottle (5 L), and kept in plastic bags in the dark until further processing.

2.3. Irradiance and water temperature

Vertical profiles of water temperature were measured using a YSI 600 probe coupled to an ultra miniature light intensity recorder (MDS-MkV/L, Alec electronics). Irradiance was also measured continuously using the same equipment cis above close to the site L11 at a depth of 5 m.

2.4. Size-structured primary production

The stable isotope ^{13}C was used to measure primary production. Polycarbonate Nalgene flasks (600 mL) were filled from the plastic bags kept in the dark within 2 h of sampling with 0.6 mL of ^{13}C-labeled sodium bicarbonate solution added (6 g of $NaH^{13}CO_3$, 99% ^{13}C, in 250 mL of de-ionized water, Eurisotop). The final concentration of ^{13}C in each bottle was 285.7 μmol $^{13}C\ L^{-1}$ on average. Bottles from the different sites were all incubated at the same site (L11) at their respective sampling depth. Incubation started between 10 am and 11 am and lasted between 4 and 6 h. After incubation, 300 mL of the flasks contents were filtered onto a precombusted 25 mm Whatman GF/F glass filter (total) and 300 mL were fractionated by serial filtration onto a 2 μm Millipore polycarbonate filter and GF/F for the <2 μm size class. At the end of filtration, 100 μL of 0.5 N HCl were added to the filters to remove any carbonates. After 3 h, the filters were rinsed with distilled water to remove the acid and dried for 24 h at 60 °C. Isotopic enrichment ($\delta^{13}C$) and carbon content were measured 1 month later using an elemental analyzer (Eurovector) for particulate C (% C) coupled to an isotope ratio mass spectrometer (IRMS GV Isoprime instrument) for C isotopes. Analytical precision was estimated at 0.05 for $\delta^{13}C$, and 0.005 for % C based on repeated internal standards. Carbon fixation rates (primary production: P) were calculated according to Slawyk et al. (1977) using the natural $\delta^{13}C$ for phytoplankton of 1.089. Biomass specific primary production rates (P^B) were calculated using the chlorophyll *a* concentration data carried out on the same data set by Charpy et al. (2012).

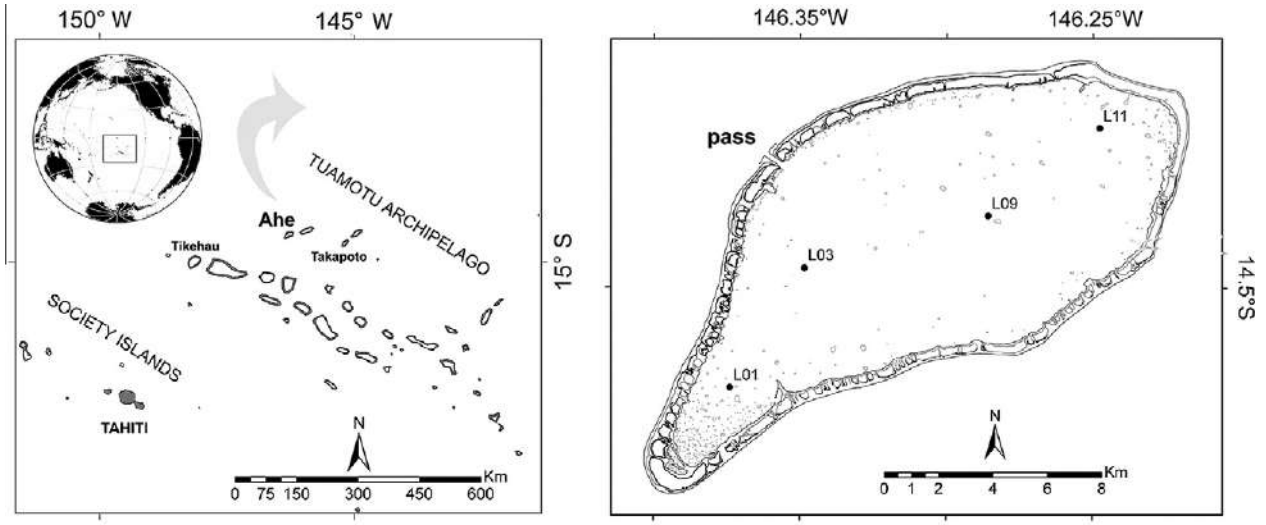

Fig. 1. Map of the Ahe atoll lagoon with an indication of the four sampling sites in the lagoon.

2.5. Size-structured variable chlorophyll fluorescence of photosystems II

1 L of each sample was filtered onto a 2 μm Millipore filter under low vacuum to sample nanophytoplankton, the filtrate being stored for further processing. The 2 μm filter was then placed in a 15 mL darkened tube filled with 10 mL of 0.2 μm filtered seawater and gently homogenized. The filtrate (500 mL) was filtered under a low vacuum onto a 0.2 μm Millipore filter to recover the picoplankton. The 0.2 μm filter was processed as for the 2 μm filter. Samples were kept in the darkened tubes for at least 15 min before pulse amplitude modulation (PAM) fluorometry and were randomly handled. For each sampling date, the whole process for the 24 samples lasted 5 h.

Variable chlorophyll *a* fluorescence was measured using a PAM fluorometer including a PAM-control unit and a cuvette WATER-ED-universal emitter-detector unit (Walz, Effeltrich, Germany). This apparatus is equipped with a modulated measuring red light (LED emission at 650 nm), and with the actinic and saturating red lights (LEDs emission 660 nm).

Irradiances were calibrated against a microspherical quantum sensor (US-SQS/L) within the cuvette. Samples were injected into the cuvette with a darkened plastic pipette from the darkened tube to avoid any exposure to light. The maximum quantum yield (F_v/F_m) of photosystems II (PSII) was measured after reaching a stable fluorescence signal (around one minute) by applying a saturating flash of 1.2 s at around 3800 μmol photons m^{-2} s^{-1}. F_v/F_m is calculated by dividing the variable fluorescence (F_v) by the maximum fluorescence after dark acclimation (F_m). F_v is the difference between F_m and the minimum fluorescence in the dark (F_0).

Steady State Light Curves (SSLCs) were then performed by exposing the samples to eight steps of increasing irradiance. The duration of the irradiance steps was 60 s. The electron transport rate (ETR in μmol e^- mg Chl a^{-1} s^{-1}) was calculated at each level of irradiance, as the product of the effective quantum yield of PSII ($\Delta F/F'_m$), the delivered irradiance (E in μmol photons m^{-2} s^{-1}), the spectrally averaged (400–700 nm) Chl *a* specific absorption coefficient (a^* in m^2 mg Chl a^{-1}) and the proportion of photosystems II on total photosystems (PSII/PStot, no unit):

$$\mathrm{ETR} = \Delta F/F'_m \; E \; a^* \; \mathrm{PSII/PStot}$$

ΔF is determined by applying a saturating flash and is the difference between the maximum fluorescence in actinic light during each light step of the SSLCs (F'_m) and the stable fluorescence before the saturating flash (F_s). a^* and PSII/PStot values were extracted from Johnsen and Sakshaug (2007) by averaging published values on related pigment groups acclimated to high light (Chromophyta for >2 μm and Cyanobacteria for <2 μm). For <2 μm and >2 μm fractions respectively, we used values of 0.038 and 0.015 m^2 mg Chl a^{-1} for a^* and 0.24 and 0.75 for PSII/PStot. Non photochemical quenching (NPQ) development during the SSLCs was calculated as $\mathrm{NPQ} = (F_m - F'_m/F'_m)$.

2.6. Statistics

The light (E) responses to the electron transport rate (ETR/E) curves were constructed using the model of Eilers and Peeters (1988) since 9 curves out of a total of 247 steady state light curves (SSLCs) showed some photoinhibition. This model makes it possible to estimate the maximum ETR (ETR_{max}), which is the asymptote of the curve; the maximum light use efficiency (α), which is the slope at the beginning of the curve; and the light saturation coefficient (E_K), calculated as (ETR_{max}/α). Curve fitting was achieved using the downhill simplex method of the Nelder–Mead model, and standard deviation of parameters was estimated by an asymptotic method. All fittings were tested by analysis of variance ($P < 0.001$), residues being tested for normality and homogeneity of variance, and parameter significance by Student's t-test ($P < 0.05$). All the curve fitting processes and associated statistics were coded in MATLAB R2008b (MathWorks Natick, Massachusetts, USA).

Redundancy analysis (RDA) was used to identify which explanatory variables played a significant role in the determination of explained variables of the two phytoplankton size fractions: primary production (P), ETR_{max}, α, E_K, maximum quantum yield (F_v/F_m), non-photochemical quenching (NPQ), and chlorophyll *a* biomass ($B^{Chl\ a}$); biomass specific primary production (P^B) and E_k were considered as supplementary because they are calculated from other variables. Water temperature and irradiance were chosen as environmental variables. Phytoplankton size fraction (>2 μm and <2 μm), site (L01, L03, L09 and L11), depth (0.5 m, 10 m and 20 m), and season (4 modalities) variables were also considered as explanatory variables. The interaction terms site * season, fraction * season and fraction * site were also tested as explanatory variables. Wind speed, wind direction, rain and daily cumulative irradiance, which were measured under a reduced spatio-temporal

design, were considered as supplementary explanatory variables as well as date. Explained variables were log transformed, centered and standardized. From a linear combination of the explanatory variables, RDA extracted synthetic gradients (i.e. ordination axes) that maximize the separation between the explained variables. The ordination diagrams were interpreted using the biplot rule (ter Braak and Verdonschot, 1995). Explanatory variables were ranked in order of importance and selected by manual forward selection (Monte Carlo unrestricted permutations: 999). Only explanatory variables which presented a *P*-value lower than 0.05 were kept in the model. RDA was performed with Canoco software (Microcomputer Power, Ithaca, New-York, USA).

Generalized linear models (GLM) were used to test for significant differences between the fixed factors season, site and their interaction for the explained variables (P, ETR_{max}, α, E_K, F_v/F_m, NPQ, $B^{Chl\ a}$, P^B and E_K). Based on the RDA results, GLM were conducted on variables of each of the two size fractions of phytoplankton separately, and depth values were pooled and considered as replicates. When analyzes were significant, means were compared using a post-hoc Tuckey test. Analysis of covariance was used to test for significant differences in the regression relationships (ETR_{max} vs. α or ETR_{max} vs. E_K) between the two size fractions of phytoplankton. Paired *t*-tests were used to test for significant differences between the two size fractions when using the whole dataset. For all statistical tests, homogeneity of variance and normality of residuals were checked. These statistical tests were performed using Minitab 15 (Minitab Inc., USA).

3. Results

3.1. Meteorological environment

In May and October 2008, the mean water temperature was 28.4 °C and 26.9 °C, respectively, and in February and August 2009, it was 29.2 °C and 27.3 °C, respectively, (Table 1). The difference between the sites was less than 0.3 °C, and the south site (L01: see in Fig. 1) was generally the warmest. Integrated irradiance over the day at 5 m depth was lower in the 2009 surveys than the 2008 surveys, (except for May 20; Table 1).Wind speed was lower and more variable during the May 2008 survey than for the other surveys (Table 1).

3.2. Photosynthetic parameters and primary production: general trends

Maximum electron transport rate (ETR_{max}) of the two classes of phytoplankton did not differ significantly (paired *t*-test, $P = 0.97$; Fig. 2). For the <2 μm size class, ETR_{max} varied from 0.07 to 4.13 μmol e^- mg Chl a^{-1} s^{-1} with a mean of 1.78 μmol e^- mg Chl a^{-1} s^{-1} ± 1.02 sd (Table 2). For >2 μm size class, ETR_{max} varied from 0.26 to 4.00 μmol e^- mg Chl a^{-1} s^{-1} with a mean of 1.71 μmol e^- mg Chl a^{-1} s^{-1} ± 0.85 sd (Table 2). Maximum light use efficiency (α) was significantly lower for the <2 μm size class (mean of 2.5×10^{-3} μmol e^- mg Chl a^{-1} s^{-1} (μmol photons m^{-2} s^{-1})$^{-1}$) than for the >2 μm size class (mean of 4.2×10^{-3} μmol e^- mg Chl a^{-1} s^{-1} (μmol photons m^{-2} s^{-1})$^{-1}$; paired *t*-test $P < 0.001$; Fig. 2). The light saturation coefficient (E_K) was significantly higher for the <2 μm size class (mean of 693.9 μmol photons m^{-2} s^{-1}) than for the >2 μm size class (mean of 413.4 μmol photons m^{-2} s^{-1}; paired *t*-test $P < 0.001$; Table 2). Averaged light curves for the two size classes are presented in Fig. 2. Photosynthetic parameters (ETR_{max}, α and E_K) showed significant positive linear relationships to each other (Fig. 3; linear regressions $P < 0.001$). There were significant differences between the slopes of ETR_{max} vs. α relationship for the two classes of phytoplankton (ANCOVA, $P < 0.001$) but not for ETR_{max} vs. E_K relationship (ANCOVA, $P = 0.21$).

Maximum quantum yield (F_v/F_m) was significantly higher (paired *t*-test; $P < 0.001$) for the >2 μm (mean of 0.45) than for the <2 μm size class (mean of 0.29). The two size classes did not show significant levels of non photochemical quenching (NPQ), and no significant differences were found between the two size classes for the maximum NPQ (NPQ_{max}; paired *t*-test; $P > 0.05$; Table 2).

Primary production (P) by the <2 μm fraction was significantly higher than by the >2 μm fraction (paired *t*-test; $P < 0.001$; Table 2). P by the <2 μm fraction ranged from 0.7 to 3.63 mg C m^{-3} h^{-1} with an average of 1.83 mg C m^{-3} h^{-1} ± 1.29 sd and represented 64% of the total P. As a note, the <2 μm fraction contained 78.4% of $B^{Chl\ a}$ (Charpy et al., 2012). P by the >2 μm fraction ranged from 0.19 to 3.26 mg C m^{-3} h^{-1} with an average of 1.17 mg C m^{-3} h^{-1} ± 0.97 sd. The biomass specific primary production rates (P^B) of the >2 μm fraction were significantly higher (mean of 13.68 mg C mg Chl a^{-1} h^{-1} ± 7.92 sd) than the <2 μm fraction (mean of 7.47 mg C mg Chl a^{-1} h^{-1} ± 4.24 sd; paired *t*-test, $P < 0.001$; Table 2).

3.3. Spatio-temporal patterns as revealed by redundancy analysis (RDA)

Size fraction of the phytoplankton (F-ratio = 61.2; $P < 0.001$), water temperature (F-ratio = 24.3; $P < 0.001$), season (F-ratio = 17.8; $P < 0.001$), the interaction term station * fraction (F-ratio = 9.9; $P < 0.001$) and site (F-ratio = 3.2; $P = 0.013$) accounted significantly for 96.5% of the explained variance (axis 1 = 64.4% and axis 2 = 32.1%). Irradiance and depth did not contribute significantly to the model (F-ratio = 1.7 and 1.2 respectively; $P > 0.05$) as well as the interaction terms station * season and fraction * season (F-ratio = 0.7 and 2.3 respectively; $P > 0.05$). Consequently, a linear combination of only size fraction, water temperature, season, station * fraction and site was used to constrain ordination of the axes. RDA displayed 34% of the total variance (axis 1 = 21.5% and axis 2 = 11.8%).

The size fraction of the phytoplankton was correlated with the first ordination axis (Fig. 4a). By projection of the explained variables primary production (P) and chlorophyll a biomass ($B^{Chl\ a}$) on the size fraction vector, one can see that the <2 μm fraction was higher in $B^{Chl\ a}$ and in P (and to a lesser extent, lower in maximum quantum yield (F_v/F_m) and maximum light efficiency (α)) on the contrary to the >2 μm fraction (Fig. 4a). Noticeably, the interaction term fraction * site was also negatively correlated to $B^{Chl\ a}$ and P, meaning that biomass and production did not evolve the same way for the two size fraction of phytoplankton depending on the site (Fig. 4a). The other explained variables were not discriminated by the first axis. Water temperature, site and season were closely correlated with the second ordination axis (Fig. 4a). However, the correlation was positive for site and season (and also the supplementary explanatory variables: daily irradiance, wind speed and date) and negative for water temperature (and also the supplementary explanatory variables: wind direction). Rain was not explained by the first and second axis. It was noticeable that the factor date was confounded with the factor season in direction and intensity. Hence, water temperature was spatially and temporally structured. As for the explained variables, the higher the water temperature was, the higher maximum electron transport rate (ETR_{max}) and light saturation coefficient (E_K; and to a lesser extent F_v/F_m and α) were. Biomass specific primary production (P^B) was negatively correlated to ETR_{max} (Fig. 4a). Maximum non photochemical quenching (NPQ_{max}) was not explained by any of these environmental variables.

The biplot rule also applied to samples (Fig. 4b). A clear discrimination occurred between the two size fractions of phytoplankton

Table 1
Meteorological conditions during the four surveys (May and October 2008, February and August 2009). Cumulative daily irradiance at a 5 m depth, mean irradiance at 5 m depth and mean temperature (based on depth profile) during the samplings done between 8 am and 10 am each sampling date. Rain, mean wind speed and wind direction for each sampling date.

Period	Date	Irradiance (mol photons m^{-2} d^{-1})	Mean irradiance (μmol photons m^{-2} s^{-1})	Water temperature (°C)	Rain (mm day^{-1})	Wind speed (m s^{-1})	Wind direction (°)
May 2008	14	47.3	1198.0	28.37	0	4.3	110.4
	16	51.0	1306.7	28.42	0	2.1	35.0
	20	18.7	188.6	28.38	0.00	1.8	256.3
	23	42.3	1054.9	28.46	2.40	1.9	273.3
October 2008	16	59.2	1618.1	26.90	0.40	9.0	114.2
	20	54.8	1569.8	26.97	0.00	7.9	112.5
February 2009	17	35.2	303.6	29.47	3.60	8.0	113.3
	21	25.0	151.3	29.16	15.40	7.5	108.8
	24	45.1	354.3	29.00	2.8	6.5	107.9
August 2009	21	38.3	860.3	27.36	0	5.4	85.4
	22	24.1	557.0	27.24	7.80	6.7	99.6
	24	38.4	861.8	27.18	0.60	7.0	97.5

along the size fraction vector that was correlated to the first axis. The two size fractions were not similarly structured along the second axis (which was also best explained by water temperature, season and site). For the <2 μm size fraction, May 2008 and February 2009 showed no discrimination between each other and were characterized by higher ETR_{max} and E_K (and to a lesser extent higher F_v/F_m and α) together with lower P (Fig. 4b and see also Table 2 for value). May 2008 was further characterized by lower wind speeds and North and/or West winds. October and August 2009 were clearly distinct and opposite to the two other periods. For the >2 μm size fraction, the gradient between season was similar but the discrimination was lower. Within each season, the lagoon was spatially structured (Fig. 4b), but this spatial structure was not governed by the same explanatory variables depending on the size fraction of the phytoplankton. For the <2 μm size fraction, a north–south gradient was evidenced for P and $B^{Chl\ a}$. For the >2 μm size fraction, a north–south gradient was evidenced for ETR_{max} (and the opposite for P^B).

A closer look on spatio-temporal variability was conducted by a univariate method (Generalized linear model; GLM). This analysis confirmed, on each explained variable taken separately, the tendencies observed on the whole matrix, using RDA. For all variables, there were no significant interactions between the factor site and season ($P > 0.05$). There were no significant seasonal or spatial differences for NPQ_{max} ($P > 0.05$). For the other variables and for the two size fractions of phytoplankton, there were significant seasonal differences ($P < 0.05$). For the <2 μm fraction, P^B and P were higher in October 2008 and August 2009 (39% and 27% on average, respectively) than the two other seasons, and it was the reversed situation for $B^{Chl\ a}$ and ETR_{max} (Fig 5). For the >2 μm fraction, trends were different: P and P^B were higher in October 2008 and February 2009 than the two other seasons (21% and 32% on average, respectively), while ETR_{max} and $B^{Chl\ a}$ declined along the four periods (Fig. 5). The spatial effect was significant for all variables of the >2 μm fraction (except NPQ_{max} see above, and P^B see Fig 6): ETR_{max}, $B^{Chl\ a}$ and P were higher in L01 than in the other sites (by 40% on average; Fig. 6). The spatial effect was also significant for P and $B^{Chl\ a}$ of the <2 μm fraction ($P < 0.05$), L01 and L11 showing higher values for these two variables (Fig 6).

4. Discussion

4.1. General comparison of primary production rates with other atolls

Atoll geomorphology is known as a primary factor controlling its ecology. Ahe atoll lagoon is a deep lagoon atoll (average depth 50 m) with wind-driven water circulation mainly characterized by a down-wind surface flow and a returning up wind deep flow (Dumas et al., 2012). Phytoplankton biomass averaged 0.34 μg Chl a L^{-1} (Charpy et al., 2012), which is at the upper range for atoll lagoons monitored by the Typatoll program (Charpy et al., 1997). Water residence time in Ahe lagoon, estimated to be around 252 days (Dumas et al., 2012), fell within the upper range of water residence time measured for other atoll lagoons (Pagès et al., 2001). This high biomass fits well with the positive relationship between biomass and lagoon water renewal time (Andréfouët et al., 2001; Pagès et al., 2001). Phytoplankton biomass and water renewal time of the Ahe lagoon were comparable to Takapoto (0.34–0.41 μg Chl a L^{-1}, 268 days respectively), another pearl oyster exploited atoll (Charpy et al., 1997; Pagès et al., 2001). Also, contribution of the picoplankton to the total chlorophyll a biomass ($B^{Chl\ a}$) was comparable in the two lagoons (around 80%; Charpy 1996; Charpy et al., 2012).

Primary production (P) estimates in atoll lagoons are scarce in the literature. The most recent measurements were made around the 1990s (Charpy, 1996; Torréton et al., 2002). P estimated here (3.0 mg C m^{-3} h^{-1}) fell within the upper range of P measured in other atolls (0.05–3.8 mg C m^{-3} h^{-1}; Torréton et al., 2002), but were lower than those measured in Takapoto atoll lagoon (3.5 mg C m^{-3} h^{-1} between 1991 and 1994; Charpy, 1996). In our study, biomass specific primary production rates (P^B) of the <2 μm fraction (7.5 mg C mg Chl a^{-1} h^{-1}) were lower than Takapoto lagoon (13.6 mg C mg Chl a^{-1} h^{-1} for <3 μm in Charpy, 1996) while P^B of the >2 μm fraction (13.7 mg C mg Chl a^{-1} h^{-1}) was almost equivalent (15.5 mg C mg Chl a^{-1} h^{-1} for >3 μm in Charpy, 1996). These values of P^B remained high for aquatic ecosystems and were comparable to those measured in temperate coastal waters (Jouenne et al., 2007). In comparison to Takapoto lagoon and with comparable total $B^{Chl\ a}$, the lower P estimated here was mostly explained by a lower P^B of the picoplankton fraction. A side result was that although $B^{Chl\ a}$ of the >2 μm size fraction of phytoplankton was only 21.6% of the whole $B^{Chl\ a}$ in Ahe lagoon, it contributed 36% to the total P. This ratio ($P/B^{Chl\ a}$) was higher than those encountered in the shallower Tikehau or Takapoto atolls (typically 20% of nanophytoplankton biomass contributes 20% of the total primary production, Charpy, 1996).

As the depths of Takapoto and Ahe lagoons are different (25 m and 50 m, respectively), deep mixing could have lowered the average irradiance available for cells, leading to a higher Chl a per cell ratio and consequently a lower P^B (Behrenfeld et al., 2002). However, this does not explain why picophytoplankton would have been more impacted by deep mixing than the nanophytoplankton in Ahe atoll lagoon, as shown by our estimations of P^B. Another explanation stands in the nutrient status of the lagoon. The Ahe lagoon waters are low-nutrient and typically potentially nitrogen

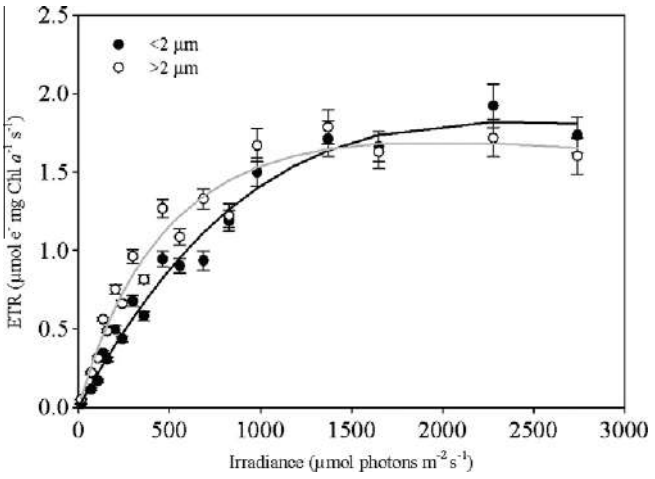

Fig. 2. Electron transport rate (ETR) vs. irradiance curves (mean ± sd) assembling the whole data set for each of the two phytoplankton size fractions (picophytoplankton: <2 µm; nanophytoplankton: >2 µm) and corresponding results of the Eilers and Peeters' model fitting (see material and methods section for further details).

limited (0.11 µmol-N L^{-1}; Charpy et al., 2012) as predicted for large lagoons (Dufour et al., 2001). Deep atolls present a high ratio between water volume and the underlying sediment area, potentially inducing a smaller contribution of the benthic nutrient fluxes to the pelagic system. Actually, fluxes from the benthic interface were considered to fuel only 3–28% of the nitrogen demands for primary production in Ahe atoll lagoon (Charpy et al., 2012). Other sources of nitrogen must maintain P^B of larger cells at a good level. Nutrient pulses do not necessary lead to an increase of nutrient concentration since they are assimilated instantaneously (Furnas et al., 2005). Associated with turbulence, they are recognized to favor production in larger cells relative to smaller ones (Pannard et al., 2007; van Duyl et al., 2002). Firstly, Ahe lagoon was found to be a wind-driven water circulation lagoon (Dumas et al., 2012), which favors turbulence. Secondly, several studies have shown that nutrient fluxes regenerated by macro, can partly control phytoplankton dynamics (Claquin et al., 2010; Fouillaron et al., 2007) and influence the regulation of photosynthetic parameters of the phytoplankton cells (Claquin et al., 2010). The fact that Ahe lagoon waters support high density of oysters, leads us to hypothesize to the existence of a fast regeneration mechanism of nitrogen through pulses, which fuels the larger phytoplankton's production better than the picophytoplankton one (Cox et al., 2006).

4.2. Spatio-temporal variability of measured processes

Statistical analysis, including redundancy analysis and generalized linear models, did not reveal significant interactions between sites and seasons, This means that the spatial structure was persistent over time during the periods of study, a feature, which was not observed in a comparable atoll lagoon (Takapoto; Delesalle et al., 2001). Consequently, spatial and temporal variabilities have been discussed separately.

4.2.1. Spatial variability

Spatial variability of biological variables may be due to underlying environmental constraints (hydrodynamics or biology) and to dynamic processes of these biological variables (growth, predation; Legendre et al., 2002). Water circulation within the lagoon and with the adjacent ocean is the primary factor that can determine the biological and chemical properties of the lagoon waters (Torréton et al., 2007). Under the normal trade wind conditions, Dumas et al., 2012 using a numerical 3D model validated by observations found that the Ahe lagoon waters were divided into three cells. The south and the north cells had higher water residence time than the central one, which was directly impacted by the pass and its aperture to the open ocean. In our study, sampling sites L03 and L09 were located in the central cell, while sites L01 and L11 were located in the south and north cell respectively. Here, the spatial effect differed depending on the size fraction of the phytoplankton. For the picophytoplankton, south and north sites presented higher primary production (P) and chlorophyll a biomass ($B^{Chl\ a}$) and this fitted with the general scheme of the water residence time being positively related to biomass (Pagès et al., 2001) and production (Torréton et al., 2002) stated between atolls. However, this relationship did not hold for the nanophytoplankton in Ahe atoll lagoon, since only the south station had higher $B^{Chl\ a}$ and P. Drivers such as bottom–up or top–down controls of the biomass and primary production were obviously different for the two size fractions of phytoplankton at the spatial scale we considered. This was shown by the significant interaction term site $*$ fraction in the redundancy analysis. Local conditions within atolls could modulate the water residence time vs. biomass relationship, and particularly for the larger phytoplanktons. For instance, the north and south sites presented higher biomass of meta-zooplankton (Pagano et al., 2012).

What we know so far is that the south site is shallower and has a higher density of cultured pearl oyster and a larger human population (Lo-Yat A., pers. com.). High chlorophyll biomass in Takapoto atoll was assumed to coincide with faster nutrient cycling in regions with higher density of pearl oysters (Loret et al., 2000). However, this spatial pattern was not persistent over time in Takapoto (Delesalle et al., 2001). Conversely, the presence of suspension feeders in an ecosystem often leads to a depletion of nanophytoplankton biomass (Grangeré et al., 2010; Prins et al., 1995). In Ahe lagoon, the presence of a water circulation cell with higher residence time, coupled with a shallow depth (up to 25 m), favored high nanophytoplankton biomass and production significantly, in a such way that the higher density of pearl oyster paradoxically did not succeed in depleting the larger phytoplankton's biomass. Although $B^{Chl\ a}$ was higher in this site, the maintenance of a P^B comparable to other sites, also favored high P. Nutrients recycled by cultured oysters and from sediments, could have sustained P^B at a good level, although biomass was high. Additionally, biodeposits from the cultured suspension feeders and sedimentation of trapped particles in mucus produced by the oyster and the surrounding corals (Wild et al., 2004) may provoke a positive budget of organic matter and its subsequent high regeneration in this retention zone. This explanation is further supported by Ahe lagoon observations: nutrient fluxes were higher under oyster culture (Gaertner-Mazouni et al., 2012).

In the present study, significant trends with depths (0–20 m) were not revealed considering the whole data set in the redundancy analysis. Thomas et al. (2010) observed vertical gradients in $B^{Chl\ a}$ (0–40 m depth) of Ahe lagoon waters as measured by *in vivo* fluorescence when winds were under 3 m s^{-1}. In contrast, Charpy et al. (2012) did not observe any vertical gradient in $B^{Chl\ a}$ (neither salinity nor temperature) at the time of this study in the 0–20 m depth. The water circulation in Ahe atoll is wind-driven and was mainly characterized by a down-wind surface flow and a returning up wind deep flow (Dumas et al., 2012) which likely homogenizes the water column under trade wind conditions. The spatio-temporal design in our study was however insufficient to observe such trends when it appeared occasionally and so deeply.

Table 2
Mean (standard error) of maximum electron transport rate (ETR_{max}), maximum light use efficiency (α), light saturation coefficient (E_K), maximum quantum yield of PSII (F_v/F_m), maximum non-photochemical quenching (NPQ_{max}), primary production (P) biomass specific primary production rates (P^B) and phytoplankton biomass ($B^{Chl\ a}$). For a given size fraction, period and site, data were averaged over depth.

Fraction	Period	Sites	ETR_{max}	α	E_k	F_v/F_m	NPQ_{max}	P	P^B	$B^{Chl\ a}$
			μmol e^- mg chl a^{-1} s^{-1}	μmol e^- mg chl a^{-1} s^{-1} (μmol photons m^{-2} $s^{-1})^{-1}$	μmol photons m^{-2}	Relative unit	Relative unit	mg C m^{-3} h^{-1}	mg C mg chl a^{-1} h^{-1}	μg chl a L^{-1}
<2 μm	May 2008	L01	1.61 i(0.16)	0.0028 (0.0002)	588.4 (33.7)	0.35(0.02)	0.11(0.03)	2.35(0.27)	5.89 (0.90)	0.42(0.03
		L03	2.47 i(0.31)	0.0031 (0.0003)	777.7 (67.5)	0.37(0.03)	0.14(0.03)	1.53(0.28)	5.53 (1.25)	0.25(0.04
		L09	2.31(0.37)	0.0027 (0.0003)	828.9 (90.3)	0.32(0.03)	0.10(0.03)	1.21(0.14)	6.83 (1.41)	0.22(0.04
		L11	2.41(0.33)	0.0028 (0.0002)	882.3 (115.4)	0.31(0.02)	0.17(0.03)	1.62(0.23)	6.70 (2.33)	0.34(0.06
	October 2008	L01	1.38(0.39)	0.0016 (0.0003)	764.3 (137.5)	0.20(0.03)	0.09(0.03)	4.05(1.92)	10.18 (2.62)	0.20(0.03
		L03	2.02(0.39)	0.0032 (0.0007)	683.2 (72.5)	0.39(0.03)	0.17(0.04)	1.51(0.27)	9.83 (2.58)	0.18(0.03
		L09	2.26(0.13)	0.0026 (0.0003)	893.0 (75.8)	0.38(0.02)	0.13(0.05)	1.87(0.50)	8.57 (1.79)	0.17(0.02
		L11	1.73(0.29)	0.0022 (0.0008)	944.6 (216.3)	0.35(0.04)	0.12(0.04)	2.36(0.42)	9.61 (1.77)	0.25(0.03
	February 2009	L01	2.20(0.27)	0.0024 (0.0002)	843.2 (73.8)	0.30(0.03)	0.12(0.03)	1.91(0.20)	5.30 (0.76)	0.42(0.04
		L03	2.48(0.22)	0.0029 (0.0002)	877.4 (46.9)	0.31(0.02)	0.10(0.03)	1.30(0.14)	4.88 (0.67)	0.31(0.04
		L09	1.54 l(0.21)	0.0027 (0.0003)	633.1 (94.8)	0.28(0.02)	0.11(0.04)	1.07(0.09)	5.77 (0.53)	0.22(0.02
		L11	1.86 (0.23)	0.0023 (0.0003)	819.7 (37.3)	0.28 (0.02)	0.12 (0.04)	1.68 (0.37)	6.46 (0.91)	0.29(0.04
	August 2009	L01	1.50(0.43)	0.0033 (0.0010)	458.3 (67.2)	0.14(0.03)	0.12(0.04)	2.62(0.21)	9.33 (0.63)	0.29(0.03
		L03	0.54(0.18)	0.0017 (0.0004)	268.1 (42.5)	0.16(0.03)	0.16(0.05)	2.15(0.14)	9.48 (1.27)	0.24(0.03
		L09	0.56(0.14)	0.0019 (0.0003)	292.0 (28.3)	0.18 (0.03)	0.13 (0.05)	1.60 (0.06)	11.27 (1.46)	0.15(0.02
		L11	0.29(0.08)	0.0013 (0.0002)	248.1 (35.1)	0.17(0.04)	0.15(0.05)	1.30(0.14)	8.75 (2.67)	0.20(0.04
>2 μm	May 2008	L01	2.97(0.15)	0.0056 (0.0004)	586.7 (36.2)	0.43(0.06)	0.20(0.05)	1.43(0.31)	9.83 (1.67)	0.14(0.01
		L03	2.41(0.19)	0.0051 (0.0002)	461.4 (17.2)	0.46(0.05)	0.10(0.03)	0.55(0.12)	9.54 (2.29)	0.07(0.01
		L09	2.20(0.24)	0.0047 (0.0003)	481.1 (49.2)	0.41(0.05)	0.09(0.02)	0.55(0.12)	10.52 (2.11)	0.05(0.01
		L11	1.80(0.16)	0.0042 (0.0003)	461.2 (55.1)	0.51(0.03)	0.10(0.02)	1.24(0.37)	14.82 (3.22)	0.07(0.01
	October 2008	L01	1.99(0.17)	0.0037 (0.0003)	537.5 (97.1)	0.49(0.03)	0.12(0.03)	1.23(0.08)	16.69 (0.90)	0.09(0.01
		L03	1.66(0.18)	0.0042 (0.0006)	415.9 (95.1)	0.44(0.03)	0.08(0.03)	1.62(0.38)	15.79 (1.46)	0.07(0.01
		L09	1.12(0.22)	0.0025 (0.0006)	638.4 (156.9)	0.46(0.02)	0.10(0.04)	1.81(0.37)	26.47 (4.90)	0.06(0.00
		L11	1.73(0.29)	0.0022 (0.0008)	944.6 (216.3)	0.35(0.04)	0.12(0.04)	0.63(0.10)	7.01 (1.20)	0.08(0.01
	February 2009	L01	2.70(0.20)	0.0056 (0.0004)	549.4 (41.5)	0.49(0.02)	0.14(0.04)	2.22(0.82)	12.97 (1.89)	0.11(0.02
		L03	1.33(0.08)	0.0054 (0.0009)	321.1 (40.7)	0.46(0.02)	0.15(0.05)	1.42(0.25)	17.84 (3.71)	0.08(0.01
		L09	1.11(0.06)	0.0045 (0.0005)	266.2 (48.1)	0.46(0.02)	0.15(0.05)	1.08(0.17)	14.54 (1.17)	0.07(0.01
		L11	1.14(0.14)	0.0034 (0.0004)	333.9 (49.6)	0.50(0.02)	0.16(0.05)	1.22(0.35)	12.85 (2.07)	0.08(0.01
	August 2009	L01	1.25(0.16)	0.0039 (0.0005)	316.8 (20.0)	0.42(0.02)	0.14(0.04)	1.70(0.15)	20.68 (1.63)	0.08(0.00
		L03	0.72(0.10)	0.0031 (0.0004)	229.6 (11.5)	0.36(0.02)	0.15(0.05)	0.71(0.11)	12.03 (1.78)	0.05(0.00
		L09	0.77(0.08)	0.0031 (0.0003)	239.3 (17.1)	0.37(0.01)	0.19(0.05)	0.71(0.38)	7.32 (1.96)	0.05(0.00
		L11	0.54(0.07)	0.0030 (0.0004)	189.8 (17.2)	0.39(0.05)	0.10(0.05)	0.80(0.22)	16.49 (4.59)	0.05(0.00

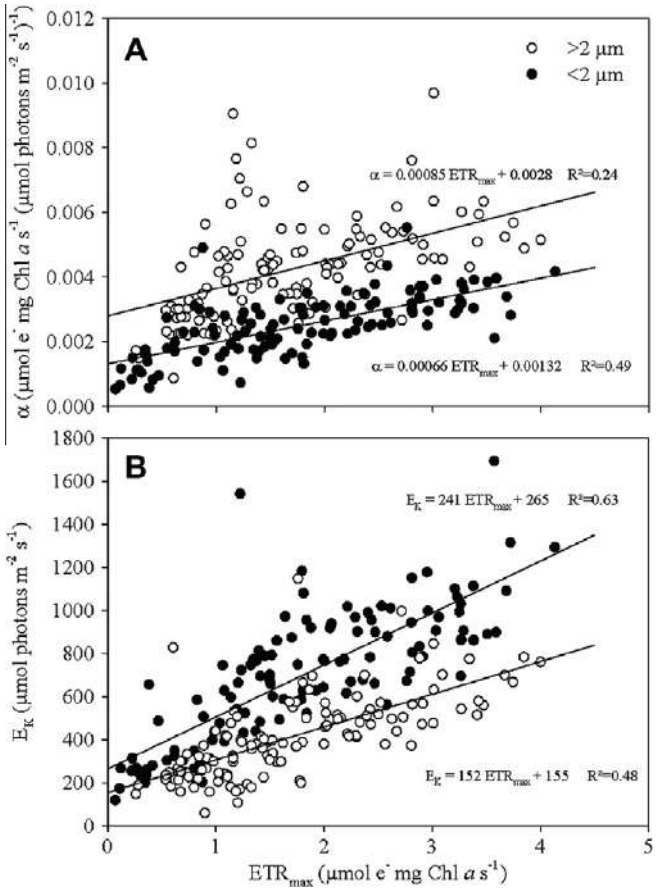

Fig. 3. Linear regressions between photosynthetic parameters using the whole data set for each of the two phytoplankton size fractions (picophytoplankton: <2 µm $n = 118$; nanophytoplankton: >2 µm $n = 123$; $P < 0.001$ for all regressions). (A) Maximum electron transport rate (ETR_{max}) vs. maximum light use efficiency (α). (B) ETR_{max} vs. light saturation coefficient (E_K).

4.2.2. Temporal variability

The season and the date variables were comparable in intensity, as shown by the redundancy analysis. This feature has been observed in other studies in atoll lagoons (Thomas et al., 2010; Torréton et al., 2010). However, the seasonal trends were often not detected because of higher short-term variations (Torréton et al., 2010).

In our study, seasonal changes were mostly linked to water temperature and/or wind changes (and to a lesser extent to cumulative daily irradiance) the latter two being negatively correlated. A clear seasonal change occurred for P^B, P and $B^{Chl\ a}$ for picophytoplankton, the latter two being inversely correlated to P^B. Higher $B^{Chl\ a}$ led to higher P but lower P^B, due to changes in the availability of the nutrients through a bottom-up control (Furnas et al., 2005). Top–down control by variations in the grazers (micro, meso and metazooplankton) biomass with time can be discarded since zooplankton biomass was regulated by the phytoplankton biomass in the Ahe atoll lagoon (Pagano et al., 2012; Thomas et al., 2012). Although, the interaction term fraction * season was not significant in the redundancy analysis when considering the whole data set, it appeared in our study that P^B of nanophytoplankton reacted rather differently to the season effect than the picophytoplankton; it was significantly lower in May 2008 when wind speed was at its lowest, and with a different direction than trade winds. In Ahe atoll lagoon, wind-induced advection of water was the main factor driving water currents, and the formation of three water cells showing different residence time (Dumas et al., 2012). Therefore, changes in wind direction or speed may have indirectly caused short term fluctuations (date variability) in biological processes (such as P^B) which otherwise should remain stable at the seasonal scale (Torréton et al., 2010; Torréton and Dufour, 1996). It is however difficult to disentangle on one hand, the role of water temperature from the role of wind on the other hand, on the biological processes of the phytoplankton.

4.3. Photosynthetic parameters regulations

A significant and linear relationship was observed between the maximum electron transport rate (ETR_{max}) and the maximum light

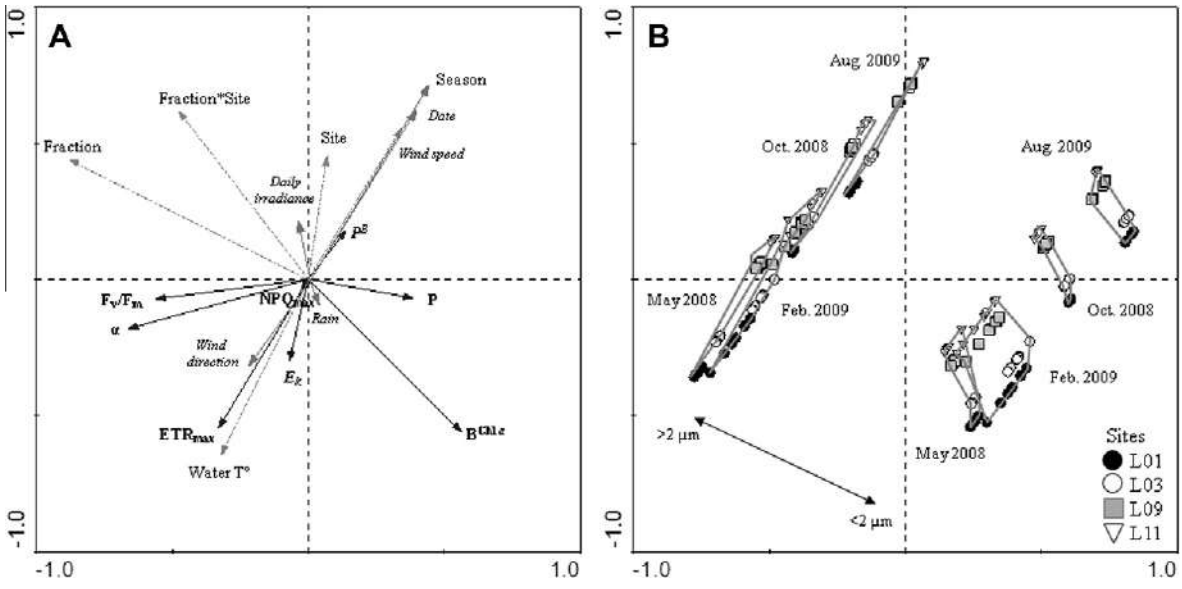

Fig. 4. Factorial maps of redundancy analysis (RDA) showing the contribution of the environmental variables as significant explanatory variables (grey arrows) of photosynthetic parameters, primary production and biomass (black arrows; A) and the position of samplings in each of the four seasons, for the two size fractions of phytoplankton (picophytoplankton: <2 µm; nanophytoplankton: >2 µm) and for the four sites. Explanatory variables: site, fraction, the interaction term fraction * site, season and water temperature (water $T°$). Supplementary explanatory variables in italic: wind direction, wind speed, date, cumulative daily irradiance and rain. Photosynthetic parameters: ETR_{max}, α, E_K, F_v/F_m, NPQ_{max}. Primary production parameters: P and P^B. Biomass: $B^{Chl\ a}$. E_K and P^B are supplementary explained variables. See Table 1 for symbols and abbreviations and see Fig. 1 for location of sites.

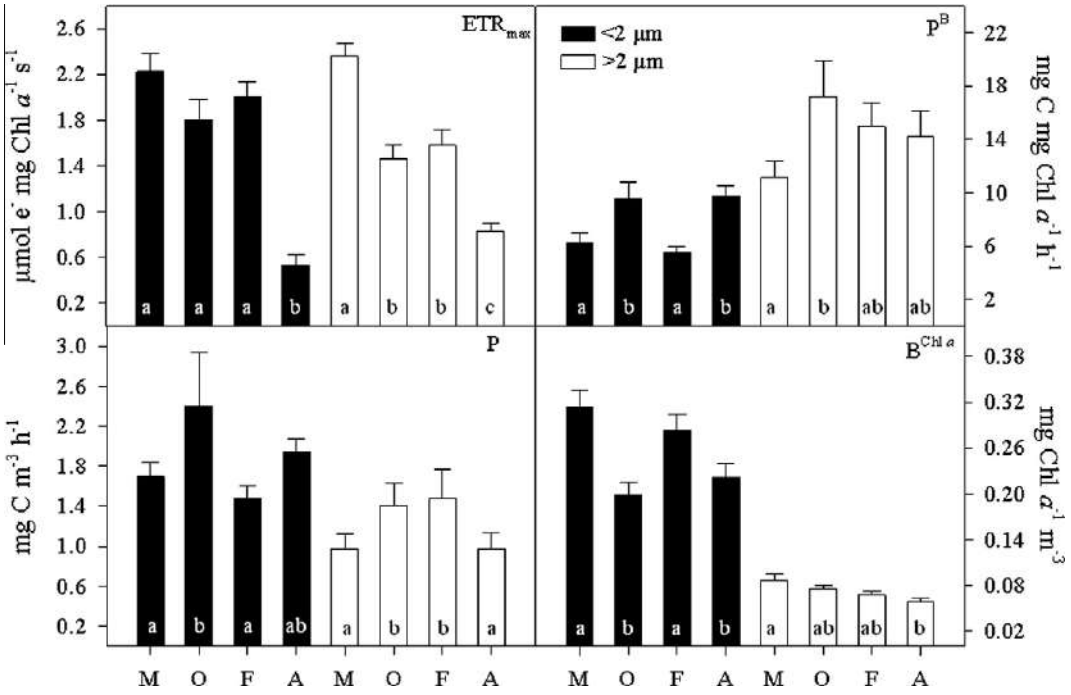

Fig. 5. Mean (standard error) of maximum electron transport rate (ETR_{max}), primary production (P), biomass specific primary production (P^B) and phytoplankton biomass ($B^{Chl\ a}$) for each of the two phytoplankton size fractions (picophytoplankton: <2 µm; nanophytoplankton: >2 µm). For a given season and size fraction, data were averaged over the sites, the dates and the three depths. Means (bars) not sharing a common superscript are significantly different (Tukey post-hoc test at $P < 0.05$).

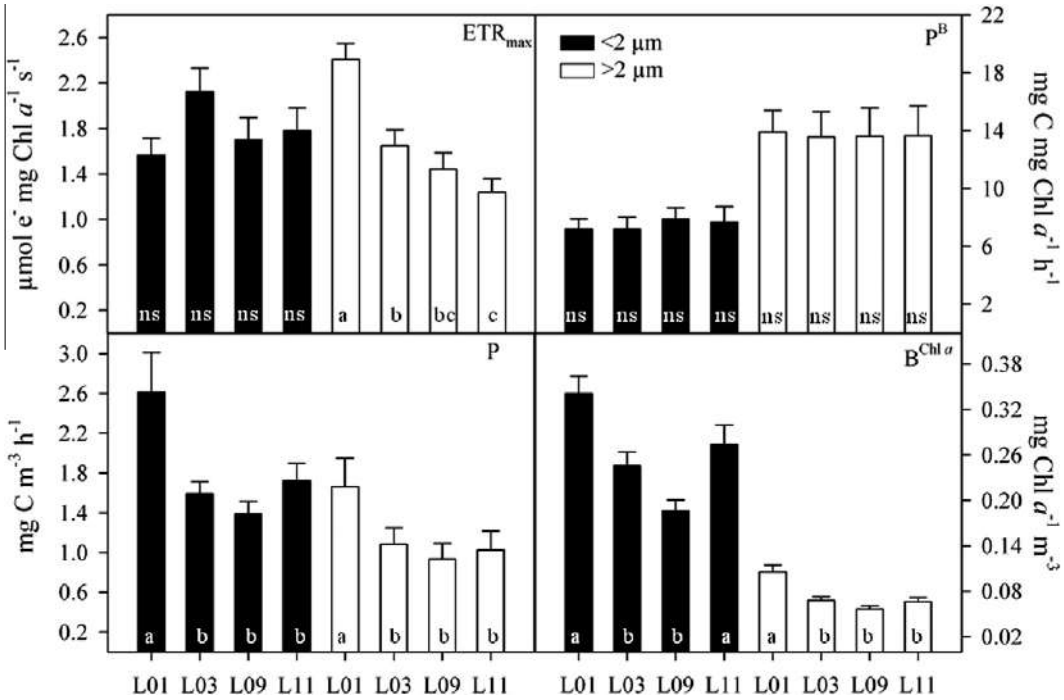

Fig. 6. Mean (standard error) of maximum electron transport rate (ETR_{max}), primary production (P), biomass specific primary production (P^B) and phytoplankton biomass ($B^{Chl\ a}$) for each of the two phytoplankton size fractions (picophytoplankton: <2 µm; nanophytoplankton: >2 µm). For a given site and size fraction, data were averaged over the seasons, the dates and the three depths. Means (bars) not sharing a common superscript are significantly different (Tukey post-hoc test at $P < 0.05$). ns Not significant.

use efficiency (α) for <2 µm and >2 µm fractions (Fig. 3). Behrenfeld et al. (2004) described two types of variability in P/E (Photosynthesis/Irradiance) relationships. Firstly, an uncoupling of maximal photosynthetic capacities and α, which could be linked to photoacclimation mechanisms in response to changing light. Secondly, parallel changes in maximal photosynthetic capacities and α due to pigment variability, nutrient availability or taxonomy (Behrenfeld et al., 2004).

The coupling between ETR_{max} and α suggested that the variation of the photosynthetic parameters was independent of light availability in Ahe atoll. Change in the phytoplankton community on a seasonal scale has been observed in such systems (Bouvy et al., unpublished data and personal unpublished observations) and could have explained partly this co-variability of photosynthetic parameters. Another complementary explanation was that the potential nitrogen limitation occurring in this atoll (Charpy

et al., 2012) could also have impacted on this relationship, as described by Claquin et al. (2010). The maximum quantum yield (F_v/F_m) measured during this study did not confirm such a nutrient limitation (Table 2). The F_v/F_m ratio is frequently used as an indicator of nutrient limitation. This ratio was maximal for nutrient replete cells and declines with nutrient stress. However, Parkhill et al. (2001) have shown that it can remain high and constant under low nutrient concentration when phytoplankton are acclimated to nutrient limitation. In the present study, the F_v/F_m ratio did not reach high values, around (0.6), but did not drop below 0.2 excepted for the <2 μm fraction in August 2009. The F_v/F_m ratio was higher for the >2 μm fraction and varied from 0.4 to 0.54 in May, October and February. This maintenance and stability of the F_v/F_m ratio can be due to nutrient pulses (Claquin et al., 2010), which are recognized to favor larger cells (Pannard et al., 2007; van Duyl et al., 2002) as previously mentioned. The lowest values of the F_v/F_m measured on the <2 μm fraction have to be carefully interpreted because of the state transition mechanisms which occur in photosynthetic organisms and particularly in cyanobacteria. The mechanisms of transition states are a process of changing the balance of energy flows into the photosystems I (PSI) and photosystems II (PSII) reaction centers, by changing the position of light-harvesting complexes, i.e. phycobilisomes in *Synechococcus,* which are able to move between both photosystems (Campbell et al., 1998). After a dark adaptation, numerous light-harvesting complexes can be associated to the PSI, which results in a low F_v/F_m ratio. Cyanobacteria as *Prochlorococcus,* which has no phycobilisomes (Hess et al., 2001) behave as eukaryotic microalgae. The highest initial slope (α) observed on Fig. 2 on >2 μm fraction indicates a higher photosynthetic efficiency of the PSII for this fraction in comparison to the <2 μm fraction, due to a different pigment composition (Johnsen and Sakshaug, 2007). The proportion of PSII on total photosystems (PSII/PStotal) is higher in eukaryotic microalgae (0.55–0.73) than in cyanobacteria (0.24) (Johnsen and Sakshaug, 2007). This different structure of the photosynthetic apparatus could explain the difference that we observed between both fractions by using pulse amplitude modulation (PAM) measurements, which only estimated those parameters on the PSII.

Maximum non-photochemical quenching (NPQ_{max}) values measured during the study were low (0.18; Table 2). Typically, values of NPQ_{max} are higher than 1 (and up to 5) in microalgae cells facing high light levels (Lefebvre et al., 2011). These low NPQ_{max} values indicated a good acclimation to the high light intensities. Low concentration of pigment per cell under high light may probably explain these low NPQ_{max} values (Serodio and Lavaud, 2011). Low light acclimated phytoplankton has more chlorophyll than high light acclimated and therefore absorbs more energy and have higher NPQ_{max}. Further evidence of photoacclimation to high light is the absence of photoinhibition in the ETR vs. light (ETR/E) curves as previously observed in other atoll lagoons (Torréton et al., 2002) and the absence of a depth effect in the measured primary production. Finally, nutrient limitation is known to increase the NPQ_{max} value (Petrou et al., 2008; Rodriguez-Roman and Iglesias-Prieto, 2005). The low NPQ_{max} that we observed may have further indicated the maintenance of photosynthetic parameters by nutrient pulses.

The ratio ETR_{max} on biomass specific primary productivity (ETR_{max}/P^B) allows an estimate of the number of moles of electron necessary to fix onto one mole of carbon i.e. the electrons requirement (θ). The average of electrons requirement was 13.7 ± 5.2 mol electron for the >2 μm fraction and 5.8 ± 2.5 mol electrons for the <2 μm fraction. These values were in the range of those cited in the literature (Gilbert et al., 2000; Morris and Kromkamp, 2003). Estimated θ values for August 2009 were extremely low: 2.5 ± 0.7 mol electron, which is physiologically impossible, because a minimum of 4 mol electron is required when considering only the PSII (Falkowski and Raven, 1997). The θ values that we calculated have consequently to be considered carefully since the estimations of a^* and the number of PSII/PStot were taken from the literature without temporal or spatial variations. However, we observed a significant difference of θ between both fractions. As described many times in the literature, comparisons between ETR and C incorporation or O_2 production is not trivial and many physiological processes, such as the Mehler reaction, light-dependent mitochondrial respiration, PSII heterogeneity, and in lower proportions photorespiration, affect the transport of electrons from the PSII to carbon fixation (Claquin et al., 2004; Flameling and Kromkamp, 1998; Morris and Kromkamp, 2003). Different regulations of the electron stream for PSII to Calvin cycle between both fractions may explain the lowest θ values observed for the <2 μm fraction, these parallel electron pathways being potentially part of a different photoacclimation strategy. A negative correlation was found between ETR_{max} and P^B as revealed by the redundancy analysis (RDA), the ETR_{max} being higher when P^B was lower. This underlines another sink for electrons produced through nitrogen fixation for cyanobacteria, and nitrogen reduction for phytoplankton in general (Babin et al., 1996; Beardall et al., 2009). This electron sink could vary from day to day and on seasonnal scales, depending on nutrient availability, potentially confirming the existence of nutrient pulses in such ecosystem.

5. Conclusion

The properties of the geomorphology of the Ahe atoll (medium size deep atoll semi-closed with passes and few reef flats) were quite different from all previous studies on other atolls, and this has provided different schemes of water mass circulation within the lagoon (Dumas et al., 2012). Not surprisingly, specific wind driven water circulation and local water cells with different water residence time within the lagoon have probably forced the ecological functioning of the lagoon waters in ways that differ from forcing in other atolls.

Our results showed that primary production (P) was slightly lower than in other shallower atolls, which was mainly due to a lower biomass specific primary productivity (P^B) of picophytoplankton, while P^B of nanophytoplankton was maintained at a good level. Photosynthetic parameters measured using pulse amplitude modulation (PAM) indicated that pico- and nano-phytoplankton were acclimated to high light and that the maximum electron transport rate (ETR_{max}) was equivalent between the two fractions. Finally, our results showed significant spatial (sites) and temporal (seasonal and day to day) effects on the measured processes for the two size fractions of phytoplankton. Water temperature and wind significantly explained temporal variability, while we suspected water residence time and possibly spatial heterogeneity of cultured oysters, explained spatial variability.

Together with these results, several indicators (no development of non photochemical quenching, good level of maximal quantum yield, co-variation of photosynthetic parameters and variability of the ETR_{max}/P^B ratio), further indicated that nutrient limitation by nitrogen was not high and probably variable in time (seasons and day to day variations) and space (sites). We now suspect dissolved nitrogen is being delivered under the form of pulses, which together with wind-driven turbulence is known to favor larger phytoplankton. Additionally, benthic interface was assumed to deliver only up to 28% of the nitrogen phytoplankton demanded. Cultured oysters are good candidates to explain, at least partly, the fast regeneration processes of nitrogen organic material. A precise spatial evaluation of the cultured pearl oyster stock is necessary for future studies in this field, as well as measurements of nutrient ambient conditions. However, measurement of nutrient stocks is

not a sensitive method since nutrients are rapidly assimilated and transformed by autotrophs; these measurements must be accompanied by flux methods using carbon and nitrogen tracers (Furnas et al., 2005). Ecosystem modeling as well as experimental works and additional monitoring studies should help to explain the importance of these suspected nutrient pulses.

Acknowledgements

We thank Willie Richmond for technical assistance through the field sampling and Marie-Paule Bataillé (Université de Caen Basse-Normandie) for help in isotope analysis. We thank Yoann Thomas for providing Fig. 1. The authors are grateful to the colleagues who participated in the numerous surveys, and specifically Alain Lo-Yat (Project manager, French Polynesia Service de la Perliculture). Météo France provided data for this study. We thank Peter Magee for English editing (www.englisheditor.webs.com). Finally, we also thank three anonymous reviewers for help in improving the manuscript. This study was funded by the 9th European Development Fund (Grant POF/001/002N1 to Serge Andréfouët and Loic Charpy, IRD) through the French Polynesia Service de la Perliculture.

References

Andréfouët, S., Pagès, J., Tartinville, B., 2001. Water renewal time for classification of atoll lagoons in the Tuamotu Archipelago (French Polynesia). Coral Reefs 20, 399–408.

Babin, M., Morel, A., Claustre, H., Bricaud, A., Kolber, Z., Falkowski, P.G., 1996. Nitrogen- and irradiance-dependent variations of the maximum quantum yield of carbon fixation in eutrophic, mesotrophic and oligotrophic marine systems. Deep-Sea Research. Part I. Oceanographic Research Papers 43, 1241–1272.

Beardall, J., Ihnken, S., Quigg, A., 2009. Gross and net primary production: closing the gap between concepts and measurements. Aquatic Microbial Ecology 56, 113–122.

Behrenfeld, M.J., Maranon, E., Siegel, D.A., Hooker, S.B., 2002. A photoacclimation and nutrient based model of light-saturated photosynthesis for quantifying oceanic primary production. Marine Ecology Progress Series 228, 103–117.

Behrenfeld, M.J., Prasil, O., Babin, M., Bruyant, F., 2004. In search of physiological basis for covariations in light-limited and light-saturated photosynthesis. Journal of Phycology 40, 4–25.

Campbell, D., Hurry, V., Clarke, A.K., Gustafsson, P., Oquist, G., 1998. Chlorophyll fluorescence analysis of cyanobacterial photosynthesis and acclimation. Microbiology And Molecular Biology Reviews 62, 667–683.

Charpy, L., 1996. Phytoplankton biomass and production in two Tuamotu atoll lagoons (French Polynesia). Marine Ecology-Progress Series 145, 133–142.

Charpy, L., Dufour, P., Garcia, N., 1997. Particulate organic matter in 16 Tuamotu atoll lagoons (French Polynesia). Marine Ecology-Progress Series 151, 55–65.

Charpy, L., Rodier, M., Fournier, J., Langlade, M.J., 2012. Physical and chemical control of the phytoplankton of Ahe lagoon (French Polynesia). Marine Pollution Bulletin 65, 471–477.

Claquin, P., Kromkamp, J.C., Martin-Jézéquel, V., 2004. Relationship between photosynthetic metabolism and cell cycle in a synchronized culture of the marine alga *Cylindrotheca fusiformis* (*Bacillariophyceae*). European Journal of Phycology 39, 33–41.

Claquin, P., Longphuirt, S.N., Fouillaron, P., Huonnic, P., Ragueneau, O., Klein, C., Leynaert, A., 2010. Effects of simulated benthic fluxes on phytoplankton dynamic and photosynthetic parameters in a mesocosm experiment (Bay of Brest, France). Estuarine Coastal and Shelf Science 86, 93–101.

Cox, E.F., Ribes, M., Kinzie III, R.A., 2006. Temporal and spatial scaling of planktonic responses to nutrient inputs into a subtropical embayment. Marine Ecology-Progress Series 324, 19–35.

Delesalle, B., Sakka, A., Legendre, L., Pages, J., Charpy, L., Loret, P., 2001. The phytoplankton of Takapoto Atoll (Tuamotu Archipelago, French Polynesia): time and space variability of biomass, primary production and composition over 24 years. Aquatic Living Resources 14, 175–182.

Delesalle, B., Sournia, A., 1992. Residence time of water and phytoplankton biomass in coral-reef lagoons. Continental Shelf Research 12, 939–949.

Dufour, P., Andrefouet, S., Charpy, L., Garcia, N., 2001. Atoll morphometry controls lagoon nutrient regime. Limnology and Oceanography 46, 456–461.

Dufour, P., Harmelin-Vivien, M., 1997. A research program for a typology of atoll lagoons: strategy and first results, In: Lessios, H.A., MacIntyre, I.G. (Eds.), Proceeding of the 8th International Coral Symposium, Panama, pp. 843–848.

Dumas, F., Le Gendre, R., Thomas, Y., Andréfouët, S., 2012. Tidal flushing and wind driven circulation of Ahe atoll lagoon (*Tuamotu Archipelago*, French Polynesia) from in situ observations and numerical modelling. Marine Pollution Bulletin 65, 425–440.

Eilers, P.H.C., Peeters, J.C.H., 1988. A model for the relationship between light intensity and the rate of photosynthesis in phytoplankton. Ecological modelling 42, 199–215.

Falkowski, P.G., Raven, J.A., 1997. Aquatic photosynthesis. Blackwell science, Malden US.

Flameling, I.A., Kromkamp, J.C., 1998. Light dependence of quantum yields for PSII charge separation and oxygen evolution in eucaryotic algae. Limnology and Oceanography 43, 284–297.

Fouillaron, P., Claquin, P., L'Helguen, S., Huonnic, P., Martin-Jezequel, V., Masson, A., Longphuirt, S.N., Pondaven, P., Thouzeau, G., Leynaert, A., 2007. Response of a phytoplankton community to increased nutrient inputs: a mesocosm experiment in the Bay of Brest (France). Journal of Experimental Marine Biology and Ecology 351, 188–198.

Furnas, M., Mitchell, A., Skuza, M., Brodie, J., 2005. In the other 90%: phytoplankton responses to enhanced nutrient availability in the Great Barrier Reef Lagoon. Marine Pollution Bulletin 51, 253–265.

Furnas, M.J., Mitchell, A.W., Gilmartin, M., Revelante, N., 1990. Phytoplankton biomass and primary production in semi-enclosed reef lagoons of the central great-barrier-reef, Australia. Coral Reefs 9, 1–10.

Gaertner-Mazouni, N., Lacoste, E., Bodoy, A., Peakoc, L., Rodier, M., Langlade, M.-J., Orempuller, J., 2012. Nutrients fluxes between water column and sediments: potential influence of the pearl oyster culture. Marine Pollution Bulletin 65, 500–506.

Gilbert, M., Domin, A., Becker, A., Wilhelm, C., 2000. Estimation of primary productivity by chlorophyll *a in vivo* fluorescence in freshwater phytoplankton. Photosynthetica 38, 111–126.

Grangeré, K., Lefebvre, S., Bacher, C., Cugier, P., Ménesguen, A., 2010. Modelling the spatial heterogeneity of ecological processes in an intertidal estuarine bay: dynamic interactions between bivalves and phytoplankton. Marine Ecology-Progress Series 415, 141–158.

Hatcher, B.G., 1997. Coral reef ecosystems: how much greater is the whole than the sum of the parts? Coral Reefs 16, S77–S91.

Hess, W.R., Rocap, G., Ting, C.S., Larimer, F., Stilwagen, S., Lamerdin, J., Chisholm, S.W., 2001. The photosynthetic apparatus of Prochlorococcus: insights through comparative genomics. Photosynthesis Research 70, 53–71.

Johnsen, G., Sakshaug, E., 2007. Bio-optical characteristics of PSII and PSI in 33 species (13 pigment groups) of marine phytoplankton, and the relevance for pulse-amplitude-modulated and fast-repetition-rate fluorometry. Journal of Phycology 43, 1236–1251.

Jouenne, F., Lefebvre, S., Véron, B., Lagadeuc, Y., 2007. Phytoplankton community structure and primary production in a small intertidal estuarine-bay (eastern English Channel, France). Marine Biology 151, 805–825.

Kinsey, D.W., Hopley, D., 1991. The significance of coral reefs as global carbon sinks – response to greenhouse. Global And Planetary Change 89, 363–377.

Lefebvre, S., Mouget, J.-L., Lavaud, J., 2011. Duration of rapid light curves for determining *in situ* the photosynthesis of microphytobenthos biofilm. Aquatic Botany 95, 1–8.

Legendre, P., Dale, M.R.T., Fortin, M.J., Gurevitch, J., Hohn, M., Myers, D., 2002. The consequences of spatial structure for the design and analysis of ecological field surveys. Ecography 25, 601–615.

Loret, P., Le Gall, S., Dupuy, C., Blanchot, J., Pastoureaud, A., Delesalle, B., Caisey, X., Jonquieres, G., 2000. Heterotrophic protists as a trophic link between picocyanobacteria and the pearl oyster *Pinctada margaritifera* in the Takapoto lagoon (Tuamotu Archipelago, French Polynesia). Aquatic Microbial Ecology 22, 215–226.

Morris, E.P., Kromkamp, J.C., 2003. Influence of temperature on the relationship between oxygen- and fluorescence-based estimates of photosynthetic parameters in a marine benthic diatom (*Cylindrotheca closterium*). European Journal of Phycology 38, 133–142.

Officer, C.B., Smayda, T.J., Mann, R., 1982. Benthic filter feeding – a natural eutrophication control. Marine Ecology-Progress Series 9, 203–210.

Pagano, M., Sagarra, P.B., Champalbert, G., Bouvy, M., Dupuy, C., Thomas, Y., Charpy, L., 2012. Metazooplankton communities in the Ahe atoll lagoon (*Tuamotu Archipelago*, French Polynesia). Spatio-temporal variations and trophic relationships. Marine Pollution Bulletin 65, 538–548.

Pagès, J., Andréfouët, S., Delesalle, B., Prasil, V., 2001. Hydrology and trophic state in Takapoto Atoll lagoon: comparison with other Tuamotu lagoons. Aquatic Living Resources 14, 183–193.

Pannard, A., Bormans, M., Lefebvre, S., Claquin, P., Lagadeuc, Y., 2007. Phytoplankton size distribution and community structure: influence of nutrient input and sedimentary loss. Journal of Plankton Research 29, 583–598.

Parkhill, J.P., Maillet, G., Cullen, J.J., 2001. Fluorescence-based maximal quantum yield for PSII as a diagnostic of nutrient stress. Journal of Phycology 37, 517–529.

Petrou, K., Doblin, M.A., Smith, R.A., Ralph, P.J., Shelly, K., Beardall, J., 2008. State transitions and nonphotochemical quenching during a nutrient-induced fluorescence transient in phosphorus-starved *Dunaliella tertiolecta*. Journal of Phycology 44, 1204–1211.

Pouvreau, S., Bodoy, A., Buestel, D., 2000. *In situ* suspension feeding behaviour of the pearl oyster, *Pinctada margaritifera*: combined effects of body size and weather-related seston composition. Aquaculture 181, 91–113.

Prins, T.C., Escaravage, V., Smaal, A.C., Peeters, J.C.H., 1995. Nutrient cycling and phytoplankton dynamics in relation to mussel grazing in a mesocosm experiment. Ophelia 41, 289–315.

Rodriguez-Roman, A., Iglesias-Prieto, R., 2005. Regulation of photochemical activity in cultured symbiotic dinoflagellates under nitrate limitation and deprivation. Marine Biology 146, 1063–1073.

Serodio, J., Lavaud, J., 2011. A model for describing the light response of the nonphotochemical quenching of chlorophyll fluorescence. Photosynthesis Research 108, 61–76.

Slawyk, G., Collos, Y., Auclair, J.C., 1977. Use of C-13 and N-15 isotopes for simultaneous measurement of carbon and nitrogen turnover rates in marine-phytoplankton. Limnology and Oceanography 22, 925–932.

Sournia, A., Ricard, M., 1976. Data on hydrology and productivity of a closed lagoon (Takapoto, Tuamotu Islands). Vie Et Milieu Serie B-Oceanographie 26, 243–279.

ter Braak, C.J.F., Verdonschot, P.F.M., 1995. Canonical corespondence analysis and related multivariate methods in aquatic ecology. Aquatic sciences 57, 255–289.

Thomas, Y., Garen, P., Bennett, A., Le Pennec, M., Clavier, J., 2012. Multi-scale distribution and dynamics of bivalve larvae in a deep atoll lagoon (Ahe, French Polynesia). Marine Pollution Bulletin 65, 453–462.

Thomas, Y., Garen, P., Courties, C., Charpy, L., 2010. Spatial and temporal variability of the pico- and nanophytoplankton and bacterioplankton in a deep Polynesian atoll lagoon. Aquatic Microbial Ecology 59, 89–101.

Torréton, J.-P., Rochelle-Newall, E., Jouon, A., Faure, V., Jacquet, S., Douillet, P., 2007. Correspondence between the distribution of hydrodynamic time parameters and the distribution of biological and chemical variables in a semi-enclosed coral reef lagoon. Estuarine Coastal and Shelf Science 74, 766–776.

Torréton, J.-P., Rochelle-Newall, E., Pringault, O., Jacquet, S., Faure, V., Briand, E., 2010. Variability of primary and bacterial production in a coral reef lagoon (New Caledonia). Marine Pollution Bulletin 61, 335–348.

Torréton, J.P., Dufour, P., 1996. Temporal and spatial stability of bacterioplankton biomass and productivity in an atoll lagoon. Aquatic Microbial Ecology 11, 251–261.

Torréton, J.P., Pagès, J., Talbot, V., 2002. Relationships between bacterioplankton and phytoplankton biomass, production and turnover rate in Tuamotu atoll lagoons. Aquatic Microbial Ecology 28, 267–277.

van Duyl, F.C., Gast, G.J., Steinhoff, W., Kloff, S., Veldhuis, M.J.W., Bak, R.P.M., 2002. Factors influencing the short-term variation in phytoplankton composition and biomass in coral reef waters. Coral Reefs 21, 293–306.

Wild, C., Huettel, M., Klueter, A., Kremb, S.G., Rasheed, M.Y.M., Jorgensen, B.B., 2004. Coral mucus functions as an energy carrier and particle trap in the reef ecosystem. Nature 428, 66–70.

Marine Pollution Bulletin 65 (2012) 490–499

Contents lists available at SciVerse ScienceDirect

Marine Pollution Bulletin

journal homepage: www.elsevier.com/locate/marpolbul

Pearl oysters *Pinctada margaritifera* grazing on natural plankton in Ahe atoll lagoon (Tuamotu archipelago, French Polynesia)

Jonathan Fournier [a], Christine Dupuy [b], Marc Bouvy [c], Marine Couraudon-Réale [a], Loïc Charpy [d], Stephane Pouvreau [e], Gilles Le Moullac [a,*], Marcel Le Pennec [f], Jean-Claude Cochard [g]

[a] IFREMER, Centre du Pacifique, BP 7004, 98719 Taravao, Tahiti, French Polynesia
[b] CNRS and University of La Rochelle, LIENSs, UMR 6250, Batiment ILE, 2 rue Olympe de Gouges, 17000 La Rochelle, France
[c] IRD, UMR 5119, ECOSYM, University of Montpellier 2, Place Eugène Bataillon, 34095 Montpellier Cedex 5, France
[d] IRD, CNRS and University of Méditerranée, UMR UPB, BP 529, 98713 Papeete, French Polynesia
[e] IFREMER, RBE, LPI, UMR 100, Presqu'île du Vivier, 29840 Argenton, France
[f] University de la Polynésie Française, EA42639, BP 6570, 98702 Faa'a, Tahiti, French Polynesia
[g] IFREMER, ODE, ER, Technopole de Brest-Iroise, BP 70, 29280 Plouzané, France

ARTICLE INFO

Keywords:
Pinctada margaritifera
Clearance rates
French Polynesia
Phytoplankton
Protists

ABSTRACT

In atoll lagoons of French Polynesia, growth and reproduction of pearl oysters are mainly driven by plankton concentration. However, the actual diet of black-lip pearl oysters *Pinctada margaritifera* in these lagoons is poorly known. To fill this gap, we used the flow through chamber method to measure clearance rates of *P. margaritifera* in Ahe atoll lagoon (Tuamotu Archipelago, French Polynesia). We found: (i) that pearl oysters cleared plankton at a rate that was positively related to plankton biovolume, (ii) that nanoflagellates were the main source of carbon for the pearl oysters, and (iii) that the quantity and origin of carbon filtrated by pearl oysters was highly dependent on the concentration and composition of plankton. These results provide essential elements for the comprehension of growth and reproduction variability of pearl oysters in atoll lagoons of French Polynesia.

1. Introduction

For the last 40 years, farming of the black-lip pearl oyster *Pinctada margaritifera* has been the main aquaculture activity in French Polynesia atoll lagoons. In 2010, production and annual exportation of black pearls reached up to 12 metric tons, worth approximately 50 million Euros, making this industry the 2nd source of income for French Polynesia after tourism (Service de la Perliculture, pers. com.). However, this industry entirely relies on spat collection successes, which strongly depends on natural reproduction rates and on environmental conditions (Pouvreau et al., 2000a; Thomas et al., 2012).

French Polynesian atoll lagoons have been characterized in the past by stable and homogeneous temperature and salinity (*e.g.* Buestel and Pouvreau, 2000). The planktonic biological processes are controlled by the hydrodynamic regime and specifically by the water residence time (Charpy et al., 1997; Delesalle and Sournia, 1992; Torréton et al., 2002), which is closely linked to atoll geomorphology and water exchanges through the reef rims (Andréfouët et al., 2001; Charpy and Blanchot, 1998; Sournia and Ricard, 1976; Dumas et al., 2012).

The same lagoons were also characterized by concentrations of chlorophyll *a* and particulate organic carbon that rarely exceed 0.6 $\mu g\, l^{-1}$ and 0.4 $mg\, l^{-1}$, respectively (Buestel and Pouvreau, 2000; Charpy et al., 1997); and by the dominance of planktonic particles inferior to 5 μm size which represented more than 70% of the total planktonic biomass (Buestel and Pouvreau, 2000; Charpy and Charpy-Roubaud, 1990; Niquil et al., 1998).

In the 1990s the feeding strategy of *P. margaritifera* was investigated with various methods including laboratory and *in situ* experiments : (1) batch and flow-through chamber methods were used by Pouvreau et al. (1999) and Yukihira et al. (1998b) to measure clearance rates of *P. margaritifera* on various species of cultured algae, (2) batch method was used by Loret et al. (2000a) to study clearance rates of pearl oysters on natural assemblage of ciliates and dinoflagellates, (3) the biodeposit method was used by Pouvreau et al. (2000b) to measure *in situ* clearance rates of pearl oysters in Takapoto lagoon and, finally, and (4) direct sampling of *P. margaritifera* gut content and HPLC analysis was used to determine which phytoplankton taxa were contributing to the pearl oysters' diet (Loret et al., 2000b).

These experiments demonstrated that (i) planktonic particles <2 μm were not efficiently retained, (ii) the diet of *P. margaritifera* included both autotrophic and heterotrophic plankton and (iii) *P. margaritifera* compensated the low concentration of efficiently

* Corresponding author.
E-mail address: gilles.le.moullac@ifremer.fr (G. Le Moullac).

0025-326X/$ - see front matter © 2012 Elsevier Ltd. All rights reserved.
http://dx.doi.org/10.1016/j.marpolbul.2012.03.026

retained planktonic particles (>2 μm) by relatively high pumping rates to meet its energy requirements. However, this knowledge remained too limited to fully characterize, quantitatively, the pearl oysters' diet.

In this context, this study aims to measure the clearance rates of pearl oysters for six types of autotrophic and/or heterotrophic plankton (picoplankton, nanoflagellates, dinoflagellates, ciliates, phytoplankton <2 μm and phytoplankton >2 μm), and to assess their relative contribution to the pearl oysters' diet in Ahe lagoon.

We selected the flow-through chamber method to measure clearance rates for two reasons: (i) it allows keeping the pearl oysters under the influence of natural fluctuations of environmental parameters and (ii) it facilitates repetitive sampling.

Complementary techniques such as flow cytometry, microscope counts and chlorophyll *a* extraction were used to measure the plankton concentration in the flow-through chambers.

2. Material and methods

2.1. Study site

This study was conducted in Ahe atoll lagoon, located 500 km north of Tahiti Island in the north of the Tuamotu Archipelago (Fig. 1). Ahe lagoon measures 142 km^2 with a mean depth close to 42 m. Ahe is defined as a semi-enclosed atoll. One active pass is located in the west part of the lagoon and several reef-flat spillways (less than 50 cm depth) are distributed along the reef rim, mainly in the south and west parts of the lagoon. The average water renewal time (ratio of lagoon volume to average water input rate) was estimated at 80 days (Dumas et al., 2012). With nearly 1350 spat collection stations and almost 11% of the lagoon dedicated to black-lip pearl oyster rearing, Ahe lagoon is a remarkable site for pearl culture and spat collection in French Polynesia.

Our study site and experimental set up were located in the northeast of the lagoon, 30 m off the coast, in a small pile building (Fig. 1). Lagoon depth was approximately 2.5 m. Experimental devices were protected from direct sunlight and rain. Pearl oysters were subjected to natural light regimes and experiments were conducted after an acclimation period of 4 days in the flow-through grazing chambers.

The experiments took place in May 2008 (from 15th to 23rd), October 2008 (from 10th to 23rd) and April/May 2009 (from 28th to 10th). The rate at which pearl-oysters cleared phytoplankton from lagoon water (chlorophyll *a* used as a proxy) was measured during each of these three experimental periods. The rate at which pearl-oysters cleared picoplankton, nanoflagellates, dinoflagellates and ciliates from lagoon water were only measured during October 2008 experiments.

2.2. Environmental parameters

Hourly wind direction and velocity were obtained from Takaroa atoll meteorological station (Météo France data) located about 120 km east of Ahe (145°3′4″W, 14°28′57″S). Lack of any orographic effects around atolls allows using this distant measurement, which was in good agreement with local value and numerical models output at Ahe atoll (Dumas et al., 2012).

Water temperature (°C) and salinity (PSU) were obtained from a Sea Bird probe (SBE V19 plus) immersed at a 10 m depth, next to an experimental breeding station located approximately 3 km away from our study site (Fig. 1).

2.3. Phytoplankton concentration

Water samples (200 ml) were filtered firstly on Millipore filters (2 μm of pore size) and then on GF/F Whatman filters (ca. 0.7 μm pore size). Chlorophyll *a* (Chl *a*) retained on these filters was extracted from phytoplankton cells during 4 h in the dark at 4 °C in 6 ml of methanol 100%. Chl *a* concentration in these extracts was determined using a Turner design TD 700 fluorimeter calibrated with Chl *a* standard (Sigma) and equipped with the set of optical filters recommended by Welschmeyer (1994) for direct measurement of Chl *a*.

We measured concentration of phytoplankton <2 μm (Chl $a < 2$ μm, in μg l^{-1}) and >2 μm (Chl $a > 2$ μm, in μg l^{-1}), respectively from the Chl *a* concentration measured in GF/F filters extracts and from the Chl *a* concentration in Millipore filters extracts. To convert Chl $a > 2$ μm and Chl $a < 2$ μm concentrations into carbon biomass, we used ratios equal to 50 μgC μgChla^{-1} and to 82 μgC μgChla^{-1}, respectively (Charpy and Charpy-Roubaud, 1990; Charpy, 1996).

2.4. Picoplankton concentration

In this study, picoplankton abundance (Pico. in cell l^{-1}) is defined as the sum of bacteria, cyanobacteria (*Synechococcus* sp. and *Prochlorococcus* sp.) and picoeukaryotes abundances.

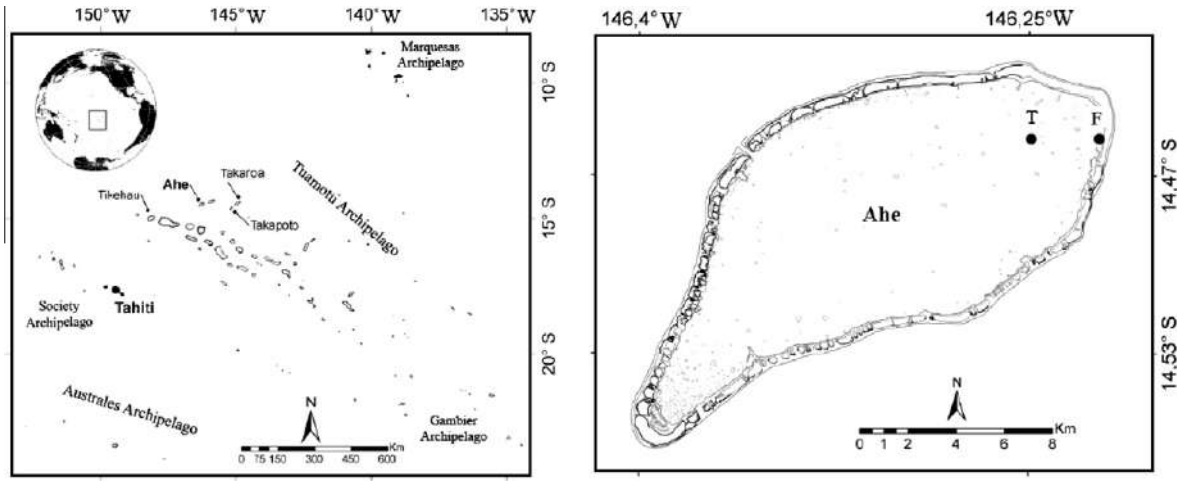

Fig. 1. Location of Ahe atoll. Location of the sites where filtration experiments were carried out (site F) and where we measured water temperature and salinity (site T) in Ahe lagoon (map by courtesy of Yoann Thomas).

Bacteria and picoautotrophic cells were fixed with 0.2 μm filtered formaldehyde (final concentration 2%) and frozen in liquid nitrogen (N_2). Bacterial cells were counted by flow cytometry using the method described by Marie et al. (1997). One milliliter formaldehyde-fixed subsamples were incubated with DAPI at a final concentration of 1/10,000 for 15 min at room temperature in the dark. Each subsample was counted using a MoFlo cytometer (Dako Colorado Inc., Fort Collins, CO, USA). Stained bacterial cells, excited at 488 nm, were enumerated according to their right-angle light scatter (RALS) and green fluorescence (FL1) measured using a 530/30 nm filter. These cell parameters were recorded on a 4 decade logarithmic scale mapped onto 1024 channels. Fluorescent beads (0.94 μm, Polysciences Inc., Warrington, PA, USA) were systematically added to each sample. Standardized RALS and FL1 values (cell RALS and FL1 divided by 0.94 μm beads RALS and FL1, respectively) were used as an estimation of the relative size and nucleic acid content of bacterial cells, respectively (Trousselier et al., 1995). Listmode files were analyzed using SUMMIT software (Dako Colorado Inc., Fort Collins, CO, USA).

Picophytoplankton (*Prochlorococcus* sp. and *Synechococcus* sp. cells) and autotrophic picoeukaryotes counts were performed with the same flow cytometer set up as described above. Cells excited at 488 nm were detected and directly enumerated according to their FALS and RALS properties and their orange fluorescence (585/42 nm) and red fluorescence (>650 nm) due to phycoerythrin and chlorophyll pigments, respectively. Fluorescent beads (0.94 μm) were also systematically added to each sample. Listmode files were analyzed using SUMMIT software (Dako Colorado Inc., Fort Collins, CO, USA).

To calculate an average carbon conversion factor for picoplankton, we used conversion factors of 14 fgC cell^{-1} (Gundersen et al., 2002), 60 fgC cell^{-1}, 178 fgC cell^{-1} (Charpy and Blanchot, 1998) and 836 fgC cell^{-1} (Verity et al.,1992) for bacteria, *Prochlorococcus* sp., *Synechococcus* sp. and for picoeukaryotes, respectively. These values were averages and weighted by the mean abundance of heterotrophic bacteria, *Prochlorococcus* sp., *Synechococcus* sp. and picoeukaryotes measured during this study. This community-scale conversion factor was then use to convert the total picoplankton concentration (cell l^{-1}) into carbon biomass (μgC l^{-1}).

Similarly, to calculate an average biovolume (BV, μm^3) per picoplankton cell we used biovolumes of 0.035 μm^3, 0.11 μm^3, 0.38 μm^3 and 1.2 μm^3 per heterotrophic bacteria (Sakka et al., 2000), *Prochlorococcus* sp. cell, *Synechococcus* sp. cell (Charpy and Blanchot, 1998), and picoeukaryote cell, respectively. These values were weighted by the mean abundance measured for each plankton type.

2.5. Nanoplankton and microplankton concentration

The taxonomic determination of protists was carried out in accordance with systematics literature (Kahl, 1931; Lee et al., 1985; Paulmier, 1997; Ricard, 1987; Sournia, 1986).

For microplankton counts (dinoflagellates and ciliates), water samples (1 l) were fixed with alcalin lugol iodine (2% final concentration). A first period of sedimentation was conducted during 24 h after which the top 900 ml of sample was slowly siphoned off with small-bore tubing. The remaining 100 ml was then stored at 4 °C in the dark before enumeration. A second sedimentation of 24 h was carried out in Utermöhl settling chamber (Hydro-Bios combined plate chamber) and cell enumeration was made at 400 magnification using a Leica DMI 3000B inverted microscope with interference contrast. Cells were counted in every microscope field (at least 60 fields per samples) for five transversal bands covering the settling chamber width and disposed at equal distance of each other.

For nanoplankton counts, water samples (25 ml) were fixed and preserved with paraformaldehyde (1% final concentration). Samples were concentrated to 10 ml with a filtration tower mounted with 0.8 μm pore size black polycarbonate filters (Nuclepore) and stained with DAPI (2.5×10^{-4} g l^{-1} final concentration). Enumeration of stained nanoplanktonic cells was made under UV light excitation on at least 15 randomly selected fields, at the magnification of ×1000.

Nanoplankton and microplankton abundances (in cell l^{-1}) were computed using the following equation:

$$A = (N_C/(N_{MF} \times S_{MF})) \times S_{SC} \times 1000/V_S$$

where A = abundance of nanoplankton or microplankton (cell l^{-1}), N_C = total number of cells (in cell), N_{MF} = number of counted microscopic fields, S_{MF} = area of one microscopic field (mm^2), S_{SC} = area of settling chamber or filter (mm^2), V_S = sample volume (l).

An average biovolume for dinoflagellates (200 cells) and ciliates (about 50 cells) was calculated using the mean length and width of cells, which were determined with a calibrated ocular micrometer.

Using these mean biovolumes and the biovolume to carbon content relationship from Menden-Deuer and Lessard (2000), we calculated the carbon conversion factors for both dinoflagellates and ciliates. These conversion factors were then used to convert dinoflagellates and ciliates concentration (cell l^{-1}) into carbon biomass (μgC l^{-1}).

For nanoplankton cells, we assumed an average biovolume of 509 μm^3 which was calculated from the cell diameters of chlorophytes, prasinophytes and cryptophytes measured by Loret et al. (2000b) in Takapoto lagoon and we assumed an average conversion factor of 4.7×10^{-6} μgC per cell of nanoplankton as in Ferrier-Pagès and Furla (2001).

2.6. Flow through chambers

After a critical analysis of the methodological shortcomings and possible misinterpretations related to the different methods of studying bivalve feeding processes (Bayne, 2004; Filgueira et al., 2006; Pascoe et al., 2009; Petersen, 2004 and Riisgård, 2004 for the most recent reviews) we selected the flow through chamber method for the measurement of *in situ* clearance rates of *P. margaritifera*.

Water was pumped from the lagoon at 1 m deep to a 80 l reservoir tank at a flow rate of approximately 300 l h^{-1}. We used a peristaltic pump to avoid the destruction of fragile planktonic organisms. From this tank, lagoon water was distributed by gravity into flow through grazing chambers. Flow rates were adjusted (between 5 l h^{-1} and 68 l h^{-1}) in each flow through chamber to prevent the pearl oyster from removing more than 30% of chlorophyll *a* (Hawkins et al., 1999). A control flow through chamber without pearl oyster was maintained in the same configuration as our grazing chambers.

To avoid "recirculation issues" and to ensure "sufficient mixing of the exhalant flow with the flow bypassing the bivalve" (Riisgård, 2001), our grazing chambers were divided into three compartments (Fig. 2): the inflow compartment where the water was entering, the grazing compartment where the pearl oyster was filtering and the outflow compartment where the water was siphoned off. Inflow and grazing compartments were separated out by 2 homogenization grids. In the grazing compartment, one pearl oyster was maintained on a PVC support at mid height of the water column and the exhalant flow was directed to the outflow compartment through a PVC reduction of 5 cm of diameter. In the outflow compartment, water was siphoned off 5 cm under the surface.

The siphoned water was sampled with 500 ml graduated test tube simultaneously from the control chamber and from the grazing chambers.

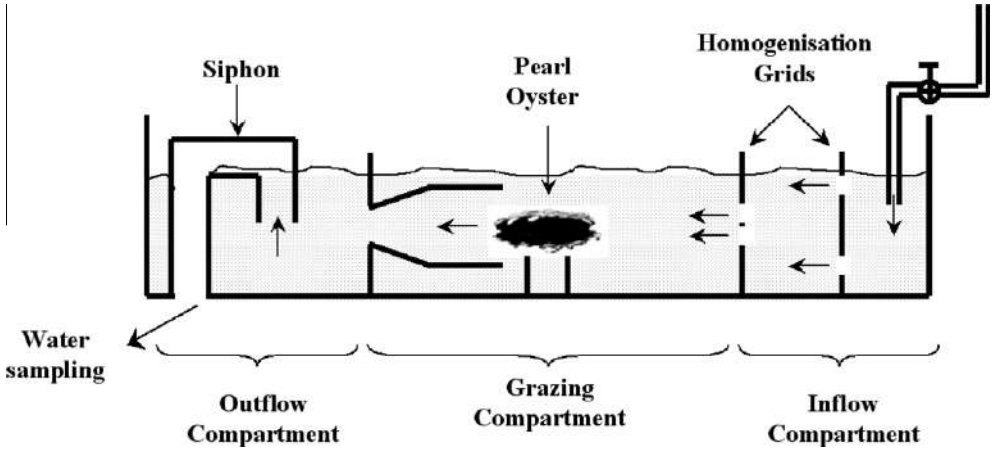

Fig. 2. Flow through grazing chambers were divided into 3 compartments: inflow compartment, grazing compartment and outflow compartment.

Experiments with the smallest pearl oysters (25–30 mm in height) were conducted in 25 l grazing chambers (20 cm in diameter and 50 cm in length) whereas experiments with pearl oysters measuring 41–115 mm in height were conducted in 50 l grazing chambers (20 cm in diameter and 100 cm in length).

All flow trough chambers were emptied and cleaned every single day to remove faeces and pseudofaeces produced by the pearl oysters.

2.7. Pearl oysters

A total of 16 pearl oysters were used during these experiments. In May 2008, experiments were conducted with pearl oysters measuring 42 ± 1 mm in height (mean ± sd) (n = 4) and with 113 ± 4 mm height pearl oysters (n = 2). In October 2008, experiments were conducted with 28 ± 2 mm height pearl oysters (n = 4), and in May 2009, with 75 ± 6 mm height pearl oysters (n = 6). For each size class of pearl oysters, sampling strategy is indicated in Table 1.

The smallest pearl oysters (25–43 mm in height) were bred at the Ifremer center's hatchery of Vairao (Tahiti Island) and were stored in Ahe lagoon at 1 m deep at least 1 week before starting the experiments. Pearl oysters from 74–115 mm came from the "Motu Tahiri" pearl farm in Ahe. All epibionts were cleaned off and pearl oysters were allowed to recover from any potential stress during 3 days before starting the starting the experiments. Sampling was then conducted at least once a day during the experimental periods.

At the end of the experiments, each pearl oyster height was measured and the flesh was freeze dried and weighted. Freeze dried fresh weight (DW in g) was used to normalize clearance rates per g of dry flesh.

2.8. Clearance rates

Clearance rate is defined as the volume of water entirely cleared of plankton by one pearl oyster per unit of time. It was calculated for each plankton type with the following equation, modified from Hildreth and Crisp (1976):

$$CRi = Fr \times (Cc - Cg)/Cg$$

with CRi = clearance rates of pearl-oyster (in l h^{-1}, per individual), Cc and Cg = concentration of plankton at the exit of the control (Cc) and grazing (Cg) flow trough chambers (in µg Chl a l^{-1} or in cell l^{-1}), Fr = flow rate in the grazing flow through chamber (l h^{-1}).

Clearance rates is known to follow an allometric relationship of the type $CR = aDW^b$ with DW = freeze dried fresh weight (in g), a and b = linear regression coefficients of log (CR_i) vs. log (DW) (e.g. Pouvreau et al., 1999). Following this relationship, all CRi values were divided by DW^b and standardized clearance rates (CR) were expressed in l h^{-1} g^{-1}.

2.9. Carbon retention rates

Clearance rates can be defined as the capacity of pearl oysters to filter and retain particles from their environment. However, the amount of carbon retained by *P. margaritifera* also depends on the plankton biomass. To assess the contribution of each plankton type to the diet of *P. margaritifera*, we estimated carbon retention rates by the following equation:

$$RR = CB \times CR,$$

where RR = Retention Rates of carbon in µgC g^{-1} h^{-1}, CB = Carbon Biomass in µgC l^{-1}, CR = Clearance Rates in (l h^{-1}).

2.10. Statistics

All analysis were conducted with the R freeware (http://www.r-project.org/). All data sets were tested for normality (Shapiro-Wilk test) and homogeneity of variance (Bartlett test). In most cases, data had to be log-transformed (natural log of X).

As wind velocity, salinity and water temperature data were not normal, highly heteroscedastic and were also highly asymmetric

Table 1
Mean height ± standard deviation (in mm) and number of oysters (between parentheses) used during our experiments. Sampling strategy (n) for the measurement of clearance rates of pearl oysters (Pico. = picoplankton, Nano. = nanoflagellates, Dino. = dinoflagellates, Cili. = Ciliates, Chl. a < 2 µm and Chl. a > 2 µm = phytoplankton < 2 µm and > 2 µm).

Survey	Oysters height	Chl. a (n)	Pico. (n)	Nano. (n)	Dino. (n)	Cili. (n)
May 2008	42 ± 1 (4)	8	–	–	–	–
	113 ± 4 (2)	9				
October 2008	28 ± 2 (4)	30	22	15	10	10
May 2009	75 ± 6 (6)	50	–	–	–	–

Table 2
Mean ± 95% confidence interval of wind velocity (m s^{-1}), water temperature (°C) and salinity (PSU) measured in May 2008, October 2008 and April/May 2009.

Survey	Wind velocity	Water temp.	Salinity
May 2008	2.83 ± 0.86	28.22 ± 0.03	36.87 ± 0.09
October 2008	8.63 ± 0.41	26.82 ± 0.01	36.16 ± 0.3
May 2009	2.65 ± 0.62	29.10 ± 0.05	36.23 ± 0.01

between surveys, we only used their mean and associated 95% confidence interval (Efron and Tibshirani, 1986) for each survey.

Two-way analysis of variance (ANOVA) were used (i) to compare concentration of Chl *a* among surveys and within size class (>2 μm and <2 μm) and (ii) to compare CR of pearl-oysters among surveys and within size-class of Chl *a* (>2 μm and <2 μm). *A posteriori* multiple comparisons were carried out using Tukey HSD tests.

We used Pearson's correlation to examine relationships between Chl *a* concentration (>2 μm and <2 μm), flow rates in the flow trough grazing chambers and clearance rates of pearl oysters.

For each survey, exact binomial tests were used to compare the percentage of carbon retained by pearl oysters from Chl. *a* < 2 μm and Chl. *a* > 2 μm.

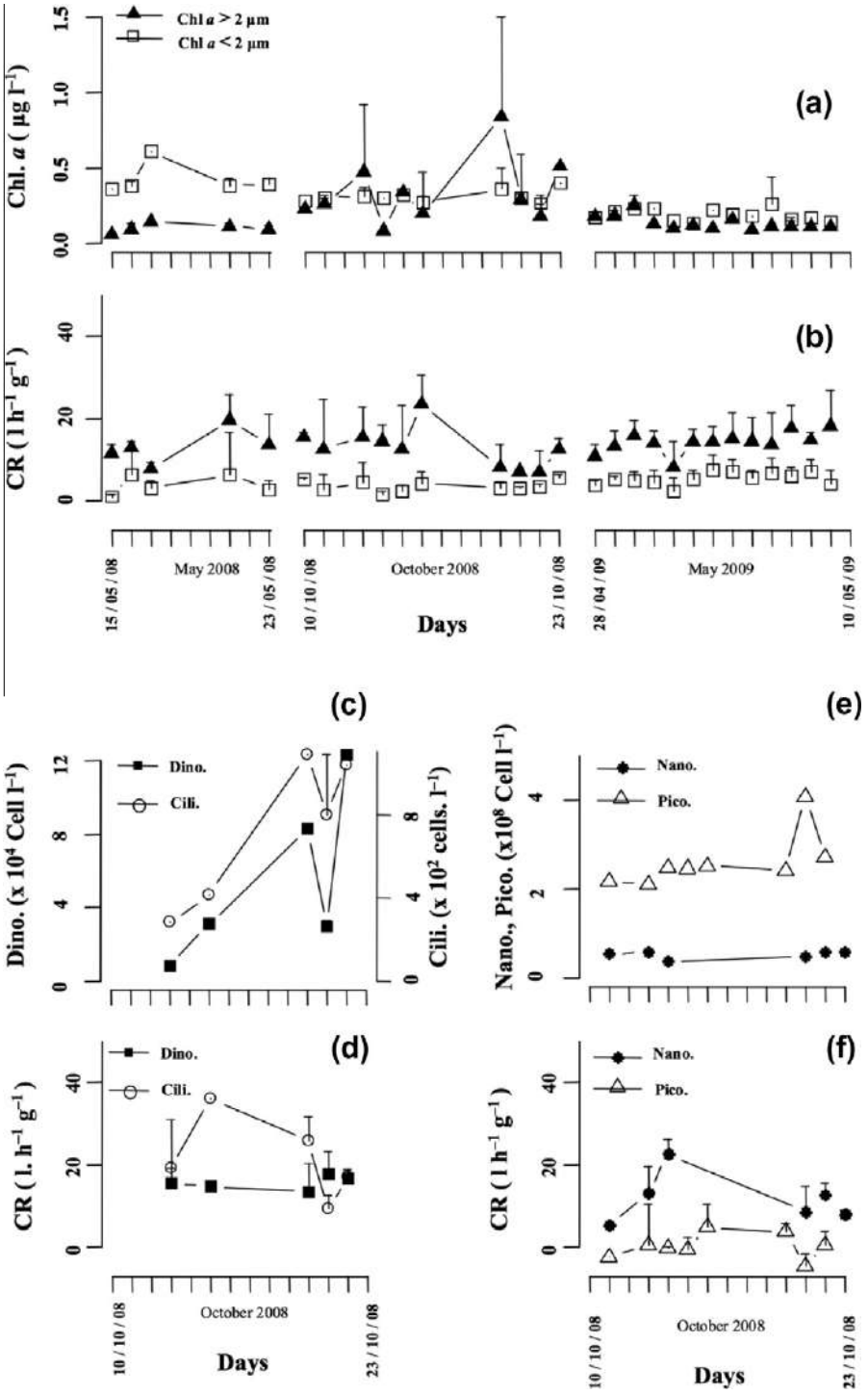

Fig. 3. Abundance of plankton (graphs a, c and e) and clearance of pearl oysters (graphs b, d and f) measured in May 2008, October 2008 and April/May 2009 in Ahe lagoon. (Pico. = picoplankton, Nano. = nanoflagellates, Dino. = dinoflagellates, Cili. = Ciliates, Chl. *a* < 2 μm and Chl. *a* > 2 μm = phytoplankton < 2 μm and > 2 μm).

Table 3
Abundance (in Cell l^{-1} or in µgChl *a* l^{-1}), carbon biomass (CB in µgC l^{-1} and B in %), clearance rates of pearl oysters (in l h^{-1} g^{-1}) and carbon retention rates (carbon retained in µgC h^{-1} g^{-1} and Carb. in %) measured in May 2008, October 2008 and April/May 2009 at our study site (Pico. = picoplankton, Nano. = nanoflagellates, Dino. = dinoflagellates, Cili. = Ciliates, Chl. *a* < 2 µm and Chl. *a* > 2 µm = phytoplankton < 2 µm and > 2 µm).

Survey	Plankton type	Abundance	CB	B (%)		Clearance rates	Carbon retained	Carb (%)	
May 2008	Chl *a* > 2 µm	0.10 ± 0.03	5	13		14.4 ± 6.0	72	32	
	Chl *a* < 2 µm	0.41 ± 0.08	34	87		4.5 ± 6.2	152	68	
October 2008	Chl *a* > 2 µm	0.34 ± 0.32	17	40		13.7 ± 7.8	233	72	
	Chl *a* < 2 µm	0.30 ± 0.06	25	60		3.7 ± 2.5	92	28	
	Pico.	$2.64 \pm 0.71 \times 10^8$	28	10	100%	0.5 ± 5.4	15	0	100%
	Nano.	$5.25 \pm 0.80 \times 10^7$	247	85		11.8 ± 6.6	2918	93	
	Dino.	$5.09 \pm 4.32 \times 10^4$	11	4		15.9 ± 4.1	179	6	
	Cili.	740 ± 354	2	1		18.7 ± 10.0	29	1	
May 2009	Chl *a* > 2 µm	0.14 ± 0.06	7	30		14.6 ± 5.0	102	53	
	Chl *a* < 2 µm	0.20 ± 0.06	16	70		5.6 ± 2.5	92	47	

Table 4
Analysis of variance table for statistical comparisons of concentration Chl. *a* and standardized clearance rates of pearl oysters within size class of Chl. *a* (>2 µm and <2 µm) and between survey.

Analysis	Source	*df*	*F*	*p*
Chl. *a* concentration among survey and size class of Chl *a*	Size class	1	25.3	0.000
	Survey	2	17.9	0.000
	Interaction	2	21.0	0.000
CR of pearl oysters among survey and size class of Chl *a*	Size class	1	154.6	0.000
	Survey	2	2.4	0.089
	Interaction	2	0.3	0.766

Non parametric Kruskal-Wallis tests were used to compare (1) abundance of ciliates, dinoflagellates, nanoplankton and picoplankton measured in October 2008, (2) clearance rates of ciliates, dinoflagellates, nanoplankton and picoplankton measured in October 2008. *A posteriori* multiple comparisons were carried out using the non parametric Steel-Dwass test (Critchlow and Fligner, 1991; Spurrier, 2006).

In all tests, significance was determined with an alpha level of 0.05.

3. Results

3.1. Temperature, salinity, wind direction and speed

Mean water temperature ranged from 26.82 ± 0.01 °C (in October 2008) to 29.1 ± 0.05 °C (in May 2009). Mean salinity ranged from of 36.16 ± 0.03 (in October 2008) to 36.87 ± 0.09 in (May 2008) (Table 2).

East and southeast winds blew continuously in October 2008 with the highest velocity of the three surveys (8.63 ± 0.41 m s^{-1}). In May 2008 and in May 2009, winds were predominantly blowing from the northwest and northeast (more than 75% of the time) with lower velocity (3.0 ± 1.7 m s^{-1} and 2.7 ± 1.4 m s^{-1}, respectively) (Table 2).

3.2. Chlorophyll a: concentration and clearance rates and carbon retention

Variations of Chl *a* < 2 µm and Chl *a* > 2 µm concentrations and of clearance rates are presented in Fig. 3. Both Chl *a* > 2 µm and Chl *a* < 2 µm concentrations showed significant variations between surveys (Tables 3 and 4). Chl *a* > 2 µm was lower than Chl *a* < 2 µm in May 2008 and in May 2009, while concentrations were not significantly different in October 2008, a period when we observed the highest Chl *a* > 2 µm concentration (1.31 µg l^{-1}).

Conversion factors presented in Table 5 were used to convert mean Chl *a* > 2 µm and Chl *a* < 2 µm concentration into carbon biomass. Phytoplankton biomass ranged from 23 µgC l^{-1} (May 2009) to 42 µgC l^{-1} (October 2008).

The biomass temporal trends were similar to concentration trends. In May 2008 and May 2009, biomass of Chl *a* < 2 µm was

Table 5
Average biovolumes (BV in μm^3) and carbon content (C.C. in µgC $Cell^{-1}$ or in µgC µgChla^{-1}) computed from our data and from literature data (Pico. = picoplankton, Nano. = nanoflagellates, Dino. = dinoflagellates, Cili. = Ciliates, Chl. *a* < 2 µm and Chl. *a* > 2 µm = phytoplankton < 2 µm and >2 µm).

Plankton type	B.V.	C.C.
Pico.	0.25	1.1×10^{-7}
Nano.	509	4.7×10^{-6}
Dino.	1606	2.2×10^{-4}
Cili.	18091	2.1×10^{-3}
Chl. *a* > 2 µm	–	50
Chl. *a* < 2 µm	–	82

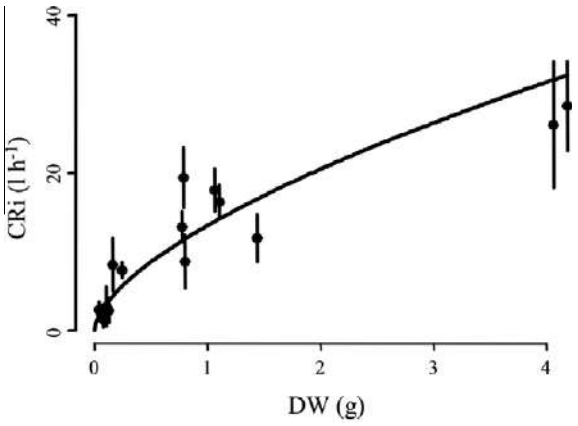

Fig. 4. Allometric relationship between clearance rates (CRi in l h^{-1}) and freeze dried flesh weight (DW in g) of pearl oysters. Each point represents the mean individual clearance rates of pearl-oysters (Chl *a* > 2 µm) with bars corresponding to standard deviation. The curve corresponds to the equation CRi = 13.3 × $DW^{0.62}$.

higher than biomass Chl a > 2 μm while there was no significant difference between biomass Chl a < 2 μm and Chl a > 2 μm in October 2008.

The allometric relationship between Chl a > 2 μm clearance rates and freeze dried dry flesh weight is presented in Fig. 4. Linear regression of log (CRi) on log (DW) was significant (r^2 = 0.87 and p < 0.001, n = 16) and we established that CRi = 13.3 $DW^{0.62}$. This relationship was further used to standardize clearance rates for a 1 g DW pearl oyster (CR = CRi/$DW^{0.62}$).

In all surveys, pearl oysters cleared Chl a > 2 μm at a higher rate than Chl a < 2 μm. Mean CR did not show any significant variations between surveys (Table 4). CR of pearl oysters was not influenced by variations of Chl a < 2 μm and Chl a > 2 μm concentration, neither by flow rates (Table 6).

In May 2008, pearl oysters retained significantly higher quantities of carbon from Chl a < 2 μm than from Chl a > 2 μm. In October 2008, it was the opposite: pearl oysters retained significantly higher quantities of carbon from Chl a > 2 μm than from Chl a < 2 μm. In May 2009, pearl oysters retained similar quantities of carbon from Chl a > 2 μm and from Chl a < 2 μm (Table 3).

3.3. Planktonic microorganisms: concentration, clearance rates and carbon retention

This section presents results of the October 2008 survey, when the contribution of all plankton types to the pearl oysters diet was assessed. Variations of plankton concentrations and clearance rates are presented in Fig. 3. Mean plankton concentration, mean clearance rates and mean carbon retention rates are presented in Table 3.

In October 2008, picoplankton and nanoflagellates were the two most abundant plankton types (Table 3). Picoplankton concentration ranged from 1.92×10^8 cell l^{-1} to 3.09×10^8 cell l^{-1} with a mean of $2.64 \pm 0.71 \times 10^8$ cell l^{-1}. We calculated an average carbon content per cell of picoplankton of 1.1×10^{-7} μgC $Cell^{-1}$ (Table 5). Nanoflagellates concentration ranged from 3.77×10^7 cell l^{-1} to 6.04×10^7 cell l^{-1} with a mean concentration of $5.25 \pm 0.80 \times 10^7$ cell l^{-1}. Dinoflagellates concentration ranged from 0.86×10^4 cell l^{-1} to 12.3×10^4 cell l^{-1} with a mean concentration of $5.09 \pm 4.32 \times 10^4$ cell l^{-1}. From their mean length (14.1 ± 5.0 μm) and width (10.9 ± 3.7 μm), we calculated an average biovolume of 1600 μm^3 and an average carbon content per cell of 2.2×10^{-4} μgC $Cell^{-1}$ (Table 5). Ciliates concentration ranged from 282 cell l^{-1} to 1093 cell l^{-1} with a mean of 740 ± 354 cell l^{-1} (Table 3, Fig. 3). From their mean length (30.3 ± 13.4 μm) and width (23.4 ± 9.4 μm) we calculated an average biovolume of 18,000 μm^3 and an average carbon content per cell of 2.1×10^{-3} μgC $Cell^{-1}$ (Table 5).

The mean concentration of picoplankton, nanoflagellates, dinoflagellates and ciliates were converted into carbon biomass using the conversion coefficients presented in Table 5. The total carbon biomass was 288 μgC l^{-1} and nanoflagellates constituted the bulk of total plankton biomass (85%).

Mean clearance rates of pearl oysters increased with the size of plankton (from 0.5 l h^{-1} g^{-1} for picoplankton to 18.7 l h^{-1} g^{-1} for ciliates) and there was a significant relationship (r^2 = 0.71, p = 0.000, n = 16) between mean clearance rates of pearl oysters and biovolumes of plankton cells : CR = 0.42 ln (BV) + 0.35 (Fig. 5).

Nanoflagellates were the dominant source of carbon retained by pearl oysters in October 2008 (93%). The second source of carbon for pearl oysters were dinoflagellates (6%).

Table 6
Relationship between clearance rates of pearl oyster ($CR_{Chl\ a<2\mu m}$ and $CR_{Chl\ a>2\mu m}$), concentration of phytoplankton <2 μm (Chl a < 2 μm), of phytoplankton >2 μm (Chl a > 2 μm), and flow rates in the grazing chambers. Pearson's product moment correlation (r) and p-values (p) are indicated for each analysis.

	$CR_{Chl\ a<2\mu m}$	$CR_{Chl\ a>2\mu m}$
Chl a > 2 μm	r = −0.08	r = 0.09
	p = 0.434	p = 0.348
Chl a < 2 μm	r = 0.01	r = −0.04
	p = 0.970	p = 0.717
Flow rates	r = 0.20	r = 0.08
	p = 0.050	p = 0.415

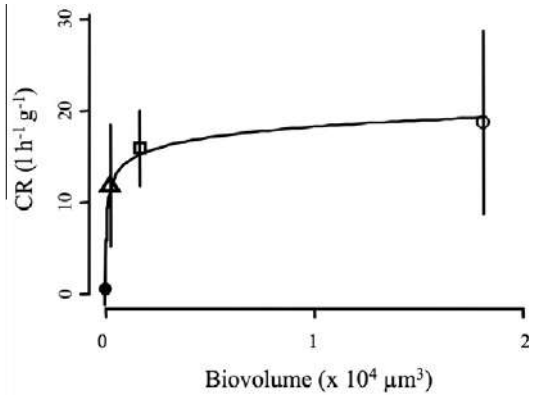

Fig. 5. Relationship between standardized clearance rates of pearl oysters (CR in l h^{-1} g^{-1}) and plankton biovolume (in μm^3). Each point represents the mean CR of pearl-oysters measured in October 2008 in Ahe lagoon (picoplankton = full circle, nanoplankton = empty triangle, dinoflagellates = empty square and ciliates = empty circle). Bars represent standard deviation. Curve represents the equation CR = 0.42 ln (BV) + 0.35.

4. Discussion

4.1. Plankton concentration

Phytoplankton concentration measured during this study was in the upper range of phytoplankton concentration measured in Ahe lagoon and in several other Tuamotu atoll lagoons (Table 7).

In October 2008 phytoplankton concentration reached values >1 μgChl a l^{-1} with a mean concentration above 0.65 μgChl a l^{-1}. In October 2008, we also observed (i) concentration of dinoflagellates being in the upper range of values measured in other lagoons (Takapoto and Tikehau) (Table 7), (ii) concentration of nanoflagellates that were approximately 10 times greater than those measured in Rangiroa, Tikehau and in Ahe lagoon at other sites/

Table 7
Range of plankton concentration (in μgChl a l^{-1} or in Cell l^{-1}) measured during our experiments (This study), at other sites/periods in Ahe atoll lagoon (Ahe) and in other French Polynesian atoll lagoons (Other atolls).

	This study	Ahe	Other atolls
Chlorophyll a	0.25–1.76	0.08–0.85[a]	0.02–1.24[e]
Picoplankton. ($\times 10^8$)	1.9–3.1	1.0–5.1[b]	2.2–23.2[e]
Bacteria. ($\times 10^8$)	0.6–1.9	2.6–7.8[b]	2.2–20.7[e]
Synecococchus. ($\times 10^8$)	0.6–1.4	0.8–1.2[b]	<0.1–2.8[e]
Prochlorococcus. ($\times 10^8$)	0.1–0.8	0.6–1.4[b]	<0.1–1.7[e]
Picoeukaryotes. ($\times 10^6$)	1.4–5.3	2.8–4.6[b]	<0.1–4.9[e]
Nanoflagellates. ($\times 10^6$)	37.0–67.0	5.5–8.5[c]	0.7–2.0[f]
Dinoflagellates. ($\times 10^5$)	0.09–1.2	<0.01–0.03[d]	<0.01–1.90[g]
Ciliates. ($\times 10^3$)	0.3–1.1	<0.01–0.9[d]	<0.01–4.0[g]

[a] Thomas et al. (2010), Fournier et al. (2012), Charpy et al. (2012).
[b] Thomas et al. (2010).
[c] Dupuy (Pers. Com.).
[d] Fournier et al. (2012).
[e] Charpy and Blanchot (1998), Torréton et al. (2002).
[f] González et al. (1998).
[g] González et al. (1998), Loret et al. (2000a).

periods (Table 7), and (iii) concentrations of picoplankton in the lower range of values reported in other atolls (Table 7).

Thus, during the October 2008 experiments, the biomass of >2 μm planktonic particles (nanoplankton + dinoflagellates + ciliates) represented more than 90% of the total planktonic biomass. These observations are unusual in Tuamotu atoll lagoons where the biomass of >2 μm planktonic particles is approximately 36% of the total planktonic biomass, as reviewed by Pouvreau et al. (2000a).

Previous studies in French Polynesian atolls have shown that plankton concentration variations can be significant at small spatial and/or temporal scale, despite the average low concentration of plankton and despite weak seasonal trends (Buestel and Pouvreau, 2000; Charpy et al., 2012; Fournier et al, 2012; González et al., 1998; Pagano et al., 2012; Sournia and Ricard, 1976; Thomas et al., 2010). However, the exact mechanisms responsible for these changes remain unclear. Changes in hydrodynamic regimes are likely causal factors and warrant further investigations. The availability of 3D circulation numerical models will allow in a near future a better understanding of these processes (Dumas et al., 2012).

4.2. Clearance rates

Mean CR of pearl oysters ranged between 11.8 l h^{-1} g^{-1} and 18.7 l h^{-1} g^{-1} for plankton >2 μm (Chl *a* > 2 μm, nanoflagellates, dinoflagellates and ciliates). These values are in the range of CR measured by Yukihira et al. (1998b) (12.3 l h^{-1} g^{-1}) and Pouvreau et al. (1999) (25.9 l h^{-1} g^{-1}) during laboratory experiments with a monospecific solution of *Isochrysis galbana* retained at 98% by *P. margaritifera*.

Clearance rates of *P. margaritifera* are also close to clearance rates of the oyster *Crassostrea gigas* measured under low seston load conditions in Thau lagoon in France (16 l h^{-1} g^{-1} for >5 μm flagellates) (Dupuy et al., 2000).

During our experiments, we did not measure any influence of plankton concentration variations on clearance rates (Table 6). However, bivalves filtration performances are known to decrease when seston load increases (e.g., Pouvreau et al., 2000b for *P. margaritifera*). Species inhabiting high seston load environments display lower clearance rates than species in low seston load environments (Jørgensen, 1996; Yukihira et al., 1998a; Trottet et al., 2008). The low load of atoll lagoons compared to many temperate coastal environments explains the typically high, and stable, CR of *P. margaritifera* (and *C. gigas* when in a low seston load environment).

Clearance of picoplankton by pearl oysters was extremely low compared to clearance of nanoplankton and microplankton. Moreover, there was a clear positive relationship between clearance rates of *P. margaritifera* and biovolume of plankton cells (Fig. 5). This relationship, obtained *in situ*, is in agreement with the relationship between retention efficiency and particle size obtained in laboratory by Pouvreau et al. (1999). Finally, numerous studies have shown that this relationship was explained by the gill structure, and especially by the disposition of cirri on gill filaments (e.g., Pouvreau et al., 1999; Silverman et al., 1996; Wright et al., 1982).

For *P. margaritifera*, *in situ* clearance rates data are scarce in literature. However, comparisons between clearance rates values measured during our experiments and clearance rates values measured by Loret et al. (2000a) in Takapoto lagoon again highlight this obvious relationship between clearance rates and particle size/biovolume.

Indeed, mean CR of small (length: 14.1 μm; width: 10.9 μm) dinoflagellates (16 l h^{-1} g^{-1}) measured during this study was half lower than CR (33 l h^{-1} g^{-1}) of large (length: 83 μm; width: 35 μm) dinoflagellates measured by Loret et al (2000a).

Conversely, mean CR of small (length: 30.3 μm; width: 23.4 μm) ciliates (19 l h^{-1} g^{-1}) measured during this study was in the range of CR of 10 l h^{-1} g^{-1} for *Amphileptus* sp. (length: 55 μm; width: 21 μm) and of 20 l h^{-1} g^{-1} for *Strombidium* sp. (length: 50 μm; width: 30 μm) measured by Loret et al. (2000a) in Takapoto lagoon.

4.3. Carbon retention rates

Obviously, plankton concentration measured in October 2008 was exceptionally high and did not represent the average plankton concentration in Ahe lagoon. Thus, to assess the average amount of carbon retained by pearl oysters in Ahe lagoon, we calculated the average concentration of Chl. *a* < 2 μm, Chl. *a* > 2 μm, picoplankton, nanoflagellates, dinoflagellates and ciliates from literature data (Table 8). Then, we converted these average plankton concentrations into their respective carbon biomass using the conversion factors in Table 5. Finally, we calculated the average carbon retention rates of pearl oysters for each plankton fraction using clearance rates measured in October 2008.

The average biomass of phytoplankton in Ahe was 26 μgC l^{-1} and Chl *a* > 2 μm represented 27% of this biomass. However, pearl oysters retained similar amounts of carbon from Chl *a* < 2 μm and from Chl *a* > 2 μm (ca. 100 μgC h^{-1} g^{-1}) (Table 8).

The average total panktonic carbon biomass was 103 μgC l^{-1} (Table 8). Picoplankton represented 69% of this total carbon biomass and nanoflagellates represented 24%. Finally, dinoflagellates and ciliates represented only 7%. In contrast, carbon retained by pearls oysters originated mainly from nanoflagellates (64%), then from dinoflagellates and ciliates (27%), and finally from picoplankton (8%).

In October 2008, pearl oysters retained almost 8 times more planktonic carbon than average (*ca.* 3000 μgC h^{-1} g^{-1} and 400 μgC h^{-1} g^{-1}, respectively).

In Takapoto lagoon, pearl oysters retained similar quantities of carbon from dinoflagellates (64 μgC h^{-1} g^{-1}) compared to the average in Ahe (70 μgC h^{-1} g^{-1}). Dinoflagellates were larger in

Table 8
Average abundance (in Cell l^{-1} or in μgChl *a* l^{-1}), carbon biomass (CB in μgC l^{-1} and B in %), and carbon retention rates of pearl oysters (carbon retained in μgC h^{-1} g^{-1} and Carb. in %) in Ahe lagoon. (Pico. = picoplankton, Nano. = nanoflagellates, Dino. = dinoflagellates, Cili. = Ciliates, Chl. *a* < 2 μm and Chl. *a* > 2 μm = phytoplankton <2 μm and >2 μm).

Plankton type	Abundance	CB	B (%)		Carbon retained	Carb (%)	
Chl *a* > 2 μm	0.14[a]	7	27		102	49	
Chl *a* < 2 μm	0.23[a]	19	73		105	51	
Pico.	6.5×10^{8}[b]	71	69	100%	38	8	100%
Nano.	5.3×10^{6}[c]	25	24		293	64	
Dino.	2.0×10^{4}[a]	4	4		70	15	
Cil.	1.4×10^{4}[a]	3	3		55	12	

[a] Fournier et al. (2012).
[b] Thomas et al. (2010).
[c] Dupuy (Unp. data.).

Takapoto lagoon but their concentration was lower than in Ahe lagoon (Loret et al., 2000a).

Pearl oysters retained higher quantities of carbon in Takapoto from ciliates (86 μgC h^{-1} g^{-1}) compared to the average in Ahe (55 μgC h^{-1} g^{-1}), where they were smaller and less abundant than in Takapoto (Loret et al., 2000a).

To our knowledge, there is no comparable *in situ* study that has measured the relative contribution of pico- nano- and microplankton to the diet of a tropical bivalve. In temperate environments, Trottet et al. (2008) and Dupuy et al. (2000) investigated the relative contribution of pico- nano- and micro- plankton in the blue mussel diet (*Mytilus edulis*) and in the cupped oyster diet (*C. gigas*), respectively. In Thau lagoon (France), *C. gigas* retained a total of 1634 μgC h^{-1} g^{-1}, and in Grand Entrée lagoon (Canada), total carbon retention of *M. edulis* ranged from 160 μgC h^{-1} g^{-1} to 1467 μgC h^{-1} g^{-1}.

In Thau lagoon, diatoms represented 87% of the total planktonic biomass and 80% of the carbon retained by *C. gigas* while in Grande Entrée lagoon, ciliates represented at least 50% of the total planktonic biomass and at least 70% of the carbon retained by *M. edulis*.

Similarly to these two species, we report for *P. margaritifera* that (i) natural variations in the composition and abundance of plankton lead to important feeding variations and (ii) particles of size >2 μm are the main source of carbon.

4.4. Conclusion and perspectives

The grazing experiments conducted in Ahe lagoon with the flow trough chamber method confirmed the *in situ* high clearance rates of *P. margaritifera* and highlighted the strong relationship between clearance rates and plankton size/biovolume. Our results also clearly demonstrated that, even if atoll lagoons of Tuamotu Archipelago are characterized by a low average biomass of plankton, the variations of this biomass and the variations in the structure of planktonic communities have a major influence on the feeding of pearl oysters. This will help on the long run to understand the inter-lagoon differences of pearl oysters' ecophysiology (growth, reproduction, see Fournier et al., 2012) and therefore the inter-lagoon differences in aquaculture an pearl farming potential.

However, food sources of *P. margaritifera* are highly diversified (Loret et al., 2000a; Nasr, 1984) and it is obvious that several plankton taxa/types were not considered in the present study due to their low concentration such as diatoms, small metazooplankton, coccolithophorids.

Despite their average low abundance, transitory peaks of diatoms, bivalve larvae and other metazoan larvae concentration have been observed in atoll lagoons (Fournier et al., 2012; Pagano et al, 2012; Sournia and Ricard, 1976). These plankton fractions may therefore represent significant food sources for pearl oysters.

For these reasons, further studies on pearl oysters nutrition should focus on the measurement of clearance rates and carbon retention rates of small metazooplankton, coccolithophorids and diatoms.

Acknowledgements

This study was supported by the European Development Fund, in collaboration with the Service de la Perliculture, the University of French Polynesia and the Institut Français de Recherche pour l'Exploitation de la Mer (Ifremer). We thank the Ifremer and Service de la Perliculture staff for their efficient help during field work; the Pa'umotu: R. and W. Richmond, T. Coulombe and M. Maifano, for their effective assistance on Ahe Atoll. We acknowledge the two anonymous reviewers and Serge Andréfouët for their comments.

References

Andréfouët, S., Pagès, J., Tartinville, B., 2001. Water renewal time for classification of atoll lagoons in the Tuamotu Archipelago (French Polynesia). Coral Reefs 20, 399–408.

Bayne, B., 2004. Comparisons of measurements of clearance rates in bivalve molluscs. Marine Ecology Progress Series 276, 305–306.

Buestel, D., Pouvreau, S., 2000. Particulate matter in Takapoto lagoon waters: potential food for cultivated pearl oysters. Oceanologica Acta 23, 193–210.

Charpy, L., 1996. Phytoplankton biomass and production in two Tuamotu atoll lagoons (French Polynesia). Marine Ecology Progress Series 145, 133–142.

Charpy, L., Blanchot, J., 1998. Photosynthetic picoplankton in French Polynesian atoll lagoons:estimation of taxa contribution to biomass and production by flow cytometry. Marine Ecology Progress Series 162, 57–70.

Charpy, L., Charpy-Roubaud, C., 1990. Trophic structure and productivity of the lagoonal communities of Tikehau atoll (Tuamotu Archipelago, French Polynesia). Hydrobiologia 207, 43–52.

Charpy, L., Dufour, P., Garcia, N., 1997. Particulate organic matter in sixteen Tuamotu atoll lagoons (French Polynesia). Marine Ecology Progress Series 151, 55–65.

Charpy, L., Rodier, M., Fournier, J., Langlade, M.J., Gaertner-Mazouni, N., 2012. Physical and chemical control of the phytoplankton of Ahe lagoon, French Polynesia. Marine Pollution Bulletin 65, 471–477.

Critchlow, D., Fligner, M., 1991. On distribution-free multiple comparisons in the one way analysis of variance. Communication in Statistics – Theory and, Methods 20, 127–139.

Delesalle, B., Sournia, A., 1992. Residence time of water and phytoplankton biomass in coral reef lagoons. Continental Shelf Research 12, 939–949.

Dumas, F., Le Gendre, R., Andréfouët, S., 2012. Tidal flushing and wind driven circulation of Ahe lagoon (Tuamotu Archipelago, French Polynesia) from in situ observations and numerical modelling. Marine Pollution Bulletin 65, 425–440.

Dupuy, C., Vaquer, A., Lam-Höai, T., Rougier, C., Mazouni, N., Lautier, J., Collos, Y., Le Le Gall, S., 2000. Feeding rate of the oyster *Crassostrea gigas* in a natural planktonic community of the Mediterranean Thau Lagoon. Marine Ecology Progress Series 205, 171–184.

Efron, B., Tibshirani, R., 1986. Bootstrap methods for standard errors, confidence intervals, and other measures of statistical accuracy. Statistical Science 1, 54–77.

Ferrier-Pagès, C., Furla, P., 2001. Pico- and nanoplankton biomass and production in the two largest atoll lagoons of French Polynesia. Marine Ecology Progress Series 211, 63–76.

Filgueira, R., Labarta, U., Fernandez-Reiriz, M., 2006. Flow-through chamber method for clearance rate measurements in bivalves: design and validation of individual chambers and mesocosm. Limnology and Oceanography: Methods 4, 284–292.

Fournier, J., Levesque, E., Pouvreau, S., Le Pennec, M., Le Moullac, G., 2012. Influence of plankton concentration on gametogenesis and spawning of the black lip pearl oyster *P. margaritifera* in ahe atoll lagoon (Tuamotu Archipelago, French Polynesia). Marine Pollution Bulletin 65, 463–470.

González, J., Torréton, J., Dufour, P., Charpy, L., 1998. Temporal and spatial dynamics of the pelagic microbial food web in an atoll lagoon. Aquatic Microbial Ecology 16, 53–64.

Gundersen, K., Heldal, M., Norland, S., Purdie, D., Knap, A., 2002. Elemental C, N and P cell content of individual bacteria collected at the Bermuda Atlantic Time-series Study (BATS) site. Limnology and Oceanography 47, 1525–1530.

Hawkins, A., James, M., Hickman, R., Hatton, S., Weatherhead, M., 1999. Modelling of suspension-feeding and growth in the green-lipped mussel *Perna canaliculus* exposed to natural and experimental variations of seston availability in the Marlborough Sounds, New Zealand. Marine Ecology Progress Series 191, 217–232.

Hildreth, D., Crisp, D., 1976. A corrected formula for calculation of filtration rate of bivalve molluscs in an experimental flowing system. Journal of the Marine Biological Association of UK 56, 111–120.

Jørgensen, C., 1996. Bivalve filter feeding revisited. Marine Ecology Progress Series 142, 287–302.

Kahl, A., 1931. Urtiere oder protozoa. In: Dahl, F., Dahl, M., Bischoff, H. (Eds.), Die Tierwelt Deutschlands und der angrenzenden Meeresteile. Gustav Fischer, Jena.

Lee, J., Hutner, S., Bovee, E. (Eds.), 1985. An Illustrated Guide to the Protozoa. Allen Press, Lawrence, KS.

Loret, P., Le Gall, S., Dupuy, C., Blanchot, J., Pastoreaud, A., Delesalle, B., Caisey, X., Jonquières, G., 2000a. Heterotrophic protists as a trophic link between picocyanobacteria and the pearl oyster *Pinctada margaritifera* in the Takapoto lagoon (Tuamotu Archipelago, French Polynesia). Aquatic Microbial Ecology 22, 215–226.

Loret, P., Pastoreaud, A., Bacher, C., Delesalle, B., 2000b. Phytoplankton composition and selective feeding of the pearl oyster *Pinctada margaritifera* in the Takapoto lagoon (Tuamotu Archipelago, French Polynesia): in situ study using optical microscopy and HPLC pigment analysis. Marine Ecology Progress Series 199, 55–67.

Marie, D., Partensky, F., Jacquet, S., Vaulot, D., 1997. Enumeration and cell analysis of natural populations of marine picoplankton by flow cytometry using the nucleic acid stain SYBR Green I. Applied and Environmental Microbiology 63, 186–193.

Menden-Deuer, S., Lessard, E., 2000. Carbon to volume relationships for dinoflagellates, diatoms, and other protist plankton. Limnology and Oceanography 45, 569–579.

Nasr, D.H., 1984. Feeding and growth of the pearl oyster *Pinctada margaritifera* (L.) in Dongonab Bay, Red Sea. Hydrobiologia 110, 241–245.

Niquil, N., Jackson, G., Legendre, L., Delesalle, B., 1998. Inverse model analysis of the planktonic food web of Takapoto Atoll (French Polynesia). Marine Ecology Progress Series 165, 17–29.

Pagano, M., Sagarra, P., Champalbert, G., Bouvy, M., Dupuy, C., Thomas, Y., Charpy, L., 2012. Metazooplankton communities in Ahe atoll lagoon (Tuamotu Archipelago, French Polynesia): spatiotemporal variations and trophic relationships. Marine Pollution Bulletin 65, 538–548.

Pascoe, P., Parry, H., Hawkins, A., 2009. Observations on the measurement and interpretation of clearance rate variations in suspension-feeding bivalve shellfish. Aquatic Biology 6, 181–190.

Paulmier, G., 1997. Tintinnides (Ciliophora, Oligotrichida, Tintinnina) de l'atalntique boréal, de l'océan indien et de quelques mers adjacentes: Mediterranée, mer Caraïbe, mer Rouge. Inventaires et distribution. Observations basées sur les loricas Rapport Ifremer, DRV/RH/97-17, 191p.

Petersen, J., 2004. Methods for measurement of bivalve clearance rate-hope for common understanding. Marine Ecology Progress Series 276, 309–310.

Pouvreau, S., Bacher, C., Héral, M., 2000a. Ecophysiological model of growth and reproduction of the black pearl oyster, *Pinctada margaritifera*: potential applications for pearl farming in French Polynesia. Aquaculture 186, 117–144.

Pouvreau, S., Bodoy, A., Buestel, D., 2000b. *In situ* suspension feeding behaviour of the pearl oyster, *Pinctada margaritifera*: combined effects of body size and weather-related seston composition. Aquaculture 181, 91–113.

Pouvreau, S., Jonquières, G., Buestel, D., 1999. Filtration by the pearl oyster, *Pinctada margaritifera*, under conditions of low seston load and small particle size in a tropical lagoon habitat. Aquaculture 176, 295–314.

Ricard, M., 1987. Diatomophycées. In Atlas du phytoplancton marin. Sournia A. (Ed.), Editions du Centre National de la Recherche Scientifique, vol. 2. Paris, pp 1–297.

Riisgård, H., 2001. On measurement of filtration rates in bivalves-the stony road to reliable data: review and interpretation. Marine Ecology Progress Series 211, 275–291.

Riisgård, H., 2004. Intercalibration of methods for measurement of bivalve filtration rates – a turning point. Marine Ecology Progress Series 276, 307–308.

Sakka, A., Legendre, L., Gosselin, M., Delesalle, B., 2000. Structure of the oligotrophic planktonic food web under low grazing of heterotrophic bacteria: Takapoto Atoll, French Polynesia. Marine Ecology Progress Series 197, 1–17.

Silverman, H., Lynn, J., Dietz, T., 1996. Particle capture by the gills of *Dreissena polymorpha*: structure and function of Latero-frontal Cirri. Biological Bulletin 191, 42–54.

Sournia, A., 1986. Atlas du phytoplancton marin. Introduction, Cyanophycées, Dictyochophycées, Dinophycées et Raphidophycées, vol. 1. Editions du CNRS, Paris, 219p.

Sournia, A., Ricard, M., 1976. Données sur l'hydrologie et la producativité d'un atoll fermé (Takapoto, Iles Tuamotu). Vie Milieu 26, 243–279.

Spurrier, J., 2006. Additional tables for Steel–Dwass–Critchlow–Fligner distribution-free multiple comparisons of three treatments. Communications in Statistics – Simulation and Computation 35, 441–446.

Thomas, Y., Garen, P., Bennett, A., Le Pennec, M., Clavier, J., 2012. Multiscale distribution and dynamics of bivalve larvae in a deep atoll lagoon (Ahe, French Polynesia). Marine Pollution Bulletin 65, 453–462.

Thomas, Y., Garen, P., Courties, C., Charpy, L., 2010. Spatial and temporal variability of the pico-and nanophytoplankton and bacterioplankton in a deep Polynesian atoll lagoon. Aquatic Microbial Ecology 59, 89–101.

Torréton, J., Pagès, J., Talbot, V., 2002. Relationships between bacterioplankton and phytoplankton biomass, production and turnover rate in Tuamotu atoll lagoons. Aquatic Microbial Ecology 28, 267–277.

Trottet, A., Roy, S., Tamigneaux, E., Lovejoy, C., Tremblay, R., 2008. Impact of suspended mussels (*Mytilus edulis* L.) on plankton communities in a Magdalen Islands lagoon (Québec, Canada): a mesocosm approach. Journal of Experimental Marine Biology and Ecology 365, 103–115.

Troussellier, M., Courties, C., Zettelmaier, S., 1995. Flow cytometric analysis of coastal lagoon bacterioplankton and picophytoplankton : fixation and storage effects. Aquatic Microbial Ecology 40, 113–119.

Verity, P., Robertson, C., Tronzo, C., Andrews, M., Nelson, J., Sieracki, M., 1992. Relationship between cell volume and the carbon and nitrogen content of marine photosynthetic nanoplankton. Limnology and Oceanography 37, 1434–1446.

Welschmeyer, N., 1994. Fluorometric analysis of chlorophyll a in the presence of chlorophyll b and pheopigments. Limnology and Oceanography 39, 1985–1992.

Wright, R., Coffin, R., Ersing, C., Pearson, D., 1982. Field and laboratory measurements of bivalve filtration of natural marine bacterioplankton. Limnology and oceanography 27, 91–98.

Yukihira, H., Klumpp, D., Lucas, J., 1998a. Comparative effects of microalgal species and food concentration on suspension feeding and energy budgets of the pearl oysters *Pinctada margaritifera* and *P. maxima* (*Bivalvia:Pteriidae*). Marine Ecology Progress Series 171, 71–84.

Yukihira, H., Klumpp, D., Lucas, J., 1998b. Effects of body size on suspension feeding and energy budgets of the pearl oysters *Pinctada margaritifera* and *P. maxima*. Marine Ecology Progress Series 170, 119–130.

Marine Pollution Bulletin 65 (2012) 500–505

Contents lists available at SciVerse ScienceDirect

Marine Pollution Bulletin

journal homepage: www.elsevier.com/locate/marpolbul

Nutrient fluxes between water column and sediments: Potential influence of the pearl oyster culture

Nabila Gaertner-Mazouni [a,*], Elise Lacoste [a], Alain Bodoy [b], Lisa Peacock [c], Martine Rodier [d], Marie-José Langlade [e], Joel Orempuller [e], Loic Charpy [e]

[a] Université de la Polynésie Française, BP 6570, 98702 FAA'A, Tahiti, French Polynesia
[b] IFREMER, COP, BP 7004, 98719 Taravao, Tahiti, French Polynesia
[c] NIWA, P.O. Box 8602, Riccarton, 8440 Christchurch, New Zealand
[d] UMR MIO (IRD, CNRS, Université Méditerranée), IRD New Caledonia, BP A58, 98848 Nouméa, New Caledonia
[e] UMR MIO (IRD, CNRS, Université Méditerranée), IRD Tahiti, BP 529, 98713 Papeete, French Polynesia

ARTICLE INFO

Keywords:
Benthic-pelagic coupling
Pearl oyster
Nutrient fluxes
Sediment interface

ABSTRACT

This study quantifies benthic nutrient fluxes and sedimentation rates in the Ahe Atoll lagoon (French Polynesia), in two stations located under pearl oyster frames, and two control stations away from the pearl culture facility. Dissolved inorganic nitrogen fluxes ranged between 2 and 35 μmol N m^{-2} h^{-1} and Soluble Reactive Phosphorus varied between −3 and 8.2 μmol P m^{-2} h^{-1}. Particulate sedimentation rates beneath the oysters were approximately five times higher than in the control zone and the percentage of small particles (⩽63 μm) were about the twice. In contrast, sediment composition was similar under and outside the direct influence of oyster frames. In this ecosystem, where primary production is dependent on the available nitrogen, our study revealed that, while highly variable, benthic fluxes could sometimes contribute up to 28% of the nitrogen demand for primary production.

1. Introduction

Benthic–pelagic coupling is known to control the planktonic productivity of semi-enclosed systems, such as lagoons. In atoll lagoons, the development of bivalve culture enhances the benthic–pelagic coupling and also controls the system primary production (Grenz et al., 2010; Boucher et al., 1998). Influence of bivalve culture on sediment nitrogen recycling and benthic fluxes have been well described in temperate systems (Mazouni et al., 1996; Mazouni, 2004; Mallet et al., 2006; Alonso-Pérez et al., 2010), but similar studies on exploited tropical ecosystems remain scarce, even though several tropical coral reef lagoons appeared nitrogen limited, such as in Tuamotu, French Polynesia (Dufour and Berland, 1999; Dufour et al., 2001), in Australia (Furnas et al., 2005) and in New Caledonia (Torréton et al., 2010).

As highlighted by Charpy et al. (2012), phytoplankton nitrogen requirements in Ahe lagoon cannot be filled only by the available water column nitrogen concentrations and by ocean water inputs. As a consequence, other nitrogen sources involved in the functioning of these ecosystems need to be quantified to explain these systems' productivity. The present work contributes to this issue, with an assessment of benthic nitrogen fluxes in Ahe Atoll lagoon. By comparing sediment zones directly under and outside the influence of pearl oyster culture, we assessed whether shellfish mariculture activity could enhance (1) nitrogen transfer from the water column towards the sediment interface (e.g. nitrogen sedimentation rates) and (2) nitrogen remineralization and renewal in the water column (e.g. inorganic nitrogen fluxes at the water–sediment interface).

2. Materials and methods

2.1. Study area

Ahe Atoll is located in northwestern Tuamotu Archipelago (French Polynesia), 500 km northeast of Tahiti Island (Fig. 1). Ahe is defined as a semi-enclosed atoll (Thomas et al., 2010). The mean depth is around 40 m and the average water residence time (ratio of lagoon volume to average water input rate) was estimated at 34 days (Pagès and Andréfouët, 2001). Dumas et al. (2012) recently characterized the spatial variation of residence and flushing time in different weather conditions, and the average renewal time was estimated to be around 80 days.

Our measurements were performed at four stations and two depths: 27 and 17 m. Station L01 (beneath pearl oyster spat collectors), P (outside the reared zone, as control), G (close to grafted pearl oyster structures, as control) and GB (beneath grafted pearl oysters structures), during 1 week in October 2010 (Fig. 1).

* Corresponding author.
E-mail address: nabila.gaertner-mazouni@upf.pf (N. Gaertner-Mazouni).

0025-326X/$ - see front matter © 2012 Elsevier Ltd. All rights reserved.
doi:10.1016/j.marpolbul.2012.02.013

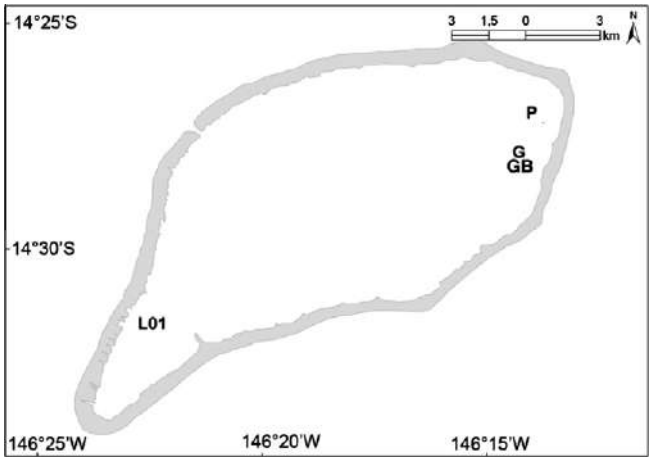

Fig. 1. Location of the sampling stations.

Pearl oyster culture at station L01 consisted of oyster spat collectors. These collectors consisted of ropes of about 1.5 m long, hanging vertically, at a frequency of 3 collectors per meter. The density recorded was 58 ind m^{-2} (total biomass of 129.5 g m^{-2}). Station GB was located under grafted oysters attached to two long lines. The grafted oysters were reared in protected nets, pooled by 20 and 30 individuals. In GB station, density was 14 ind m^{-2} (total biomass of 5560 g m^{-2}).

2.2. Water column characteristics

Water was collected with a 5 l Niskin bottle. Samples were collected from subsurface, and every 10 m at depth. The last sample was taken 2 m above the bottom. The bottle content was used to fill different small bottles for subsequent chemical analyses. The remaining was transferred to plastic tanks for the determination of particulate organic material (POM), seston, and particulate organic nitrogen (PON). These plastic tanks were kept in dark cool boxes, in order to avoid any elevation of temperature and any biological activities of autotrophic materials.

Ammonium concentration was determined fluorometrically with a Turner TD-700, using the ortho-phtaldialdehyde method as described in Holmes et al. (1999). Soluble reactive phosphate (SRP) concentrations were measured manually with a Shimadzu UV-mini 1240 spectrophotometer (cell length: 10 cm), using the molybdenum blue reaction (Murphy and Riley, 1962). These parameters were thus analysed within 2 h after sampling. A second set of samples was fixed using $HgCl_2$ (Kattner, 1999) prior to nitrate and nitrite (NO_{3+2}), Silicates ($Si(OH)_4$) and SRP analyses. All samples were stored in a dry cool place until analysed by colorimetry using a Technicon Autoanalyzer III system (Strickland and Parsons, 1972; Aminot and Kérouel, 2004).

Filtrations were performed immediately upon trip. Whatman GF/F glass filters were previously combusted at 450 °C. They were rinsed with distilled water before filtration of the sample. Water was filtered at 0.7 bars vacuum. Samples were rinsed with a solution of ammonium formiate at 68 g l^{-1}, isotonic with the sea water, in order to remove the salt from the filter before drying. All filters were dried at 50 °C, and weighed. Filters were combusted at 450 °C, and weighed to obtain the total organic material (POM).

2.3. Sediment characteristics

The organic matter in sediments was measured in the three upper centimetres of the sediment, on 3 randomly samples taken by divers, with 4.2 cm corers (surface of 13.8 cm^2). Following the "losses on ignition method", aliquots were dried at 70 °C for 4 h and weighed. Then to assess the sediment carbon we calcinated them at 250 °C for 16 h, and re-weighed after cooling (see Kristensen and Andersen, 1987). A final calcination at 450 °C was performed to obtain the total organic content. Only one sample was analysed at each station. Samples of 100 g of sediment were taken for granulometry analysis. Sediment was dried at 70 °C for 24 h, and fractions were sorted through a standardised column of sieves, according to AFNOR standards NF X 11-506, and weighed after shaking for 15 min.

2.4. Benthic fluxes

Sediment fluxes were measured *in situ* using the benthic flux chambers method (Mazouni et al., 1996; Boucher et al., 1998). Four transparent benthic chambers (clear metacrylate hemispheres) each with a volume of 15 l and a surface of 0.114 m^2 were randomly positioned by SCUBA divers at the different stations, ensuring minimal sediment disturbance. They were hermetically closed and sampling was made using 60 ml syringes every 60 min. The total incubation time was 120 min, in order to calculate fluxes during the initial linear section of the theoretical curve of nutrient production. The fluxes were calculated after the incubation time as the difference between initial and final concentration of nutrient.

2.5. Nitrogen transfer from water column to sediments

A sediment trap was used to quantify the fluxes of POM, PON and PIM to the sediments. Methodological constraints limited the use of sediment particle traps at the different stations. The traps needed to be positioned during 1 day before to be started and then measurements were performed during 2 days. So 7 days were needed for two stations measurements (under pearl oysters and control). The limitation of the field experiment (9 days), did not allow measurements in more than two stations.The model was a Technicap PPS 4/3, with a height of 1 m and an inner aperture of 0.05 m^2 (diameter 0.25 m). The aspect ratio of the trap was then of 4.9. The trap was located by divers at 3 m above the sediment as proposed in previous works (Storlazzi et al., 2011). Filtrations of the material collected in the sediment trap, were performed as described for water column (see Section 2.2), and some filters were used for CHN analyses (PON).

3. Results and discussion

Ammonia, nitrate and nitrites concentrations in the water column were significantly lower than those recorded by Grenz et al. (2010) in New Caledonia, with 0–2 μM N measured at 20 m depth (Table 1). Conversely, SRP concentrations were in the same range of these authors findings, with 0.01–0.3 μM P, as well as for silicates 1.3–5.5 μM $Si(OH)_4$.

Sedimentation rates were significantly different between stations, with a total sedimentation rate five times higher for station L01 (below oyster spats collectors) than in station P (Fig. 2). Similarly, sedimentation rates of POM and PON were respectively three times and seven times higher under oyster facility than at control (Table 1). This result supports the hypothesis that shellfish activity enhances the transfer of particulate material from the water column to the sediment (Vacelet et al., 1996; Mallet et al., 2006). However, although oysters may have contributed to increased sedimentation rates at station L01, organic content of the sediment collected in the traps of the same station (31%) was not higher, and even lower, than POM content at control (46%) (Fig. 3). This may indicate that the sedimentation enhancement is due to the reduction of flow by the rearing structures rather than by oyster

Table 1
Water column characteristics, measured near the bottom and sedimentation rates. Depth (m), water temperature (°C), nutrient concentrations in the water column expressed in μM; PON: particulate organic nitrogen (μmol m^{-2} h^{-1}); TPM: total particulate material (mg dry weight m^{-2} h^{-1}); POM: particulate organic material (mg dry weight m^{-2} h^{-1}).

	Water-column								Sediment		
	Depth	Temperature	NH_4	PO_4	$Si(OH)_4$	NO_2	NO_3	PON	TPM	PON	POM
L01	27	26.8	0.1	0.3	1.4	0.03	0.09	1.5	589.5	32.6	184.8
P	27	26.8	0.01	0.3	1.3	0.02	0.06	1.8	118.8	4.5	55.1
G	17	27	0.05	0.3	1.8	0.03	0.1	1.9	–	–	–
GB	17	27	0.05	0.2	1.4	0.05	0.06	–	–	–	–

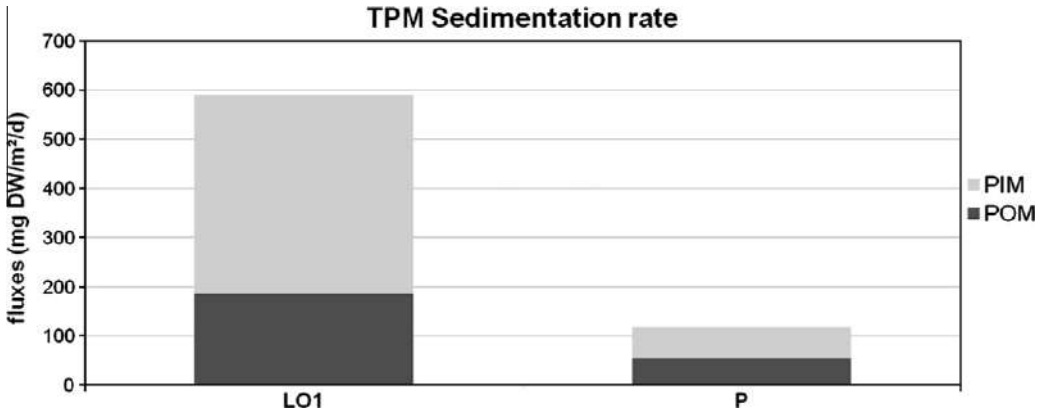

Fig. 2. Comparison of sedimentation rate between the two stations, L01 under oyster culture, and P out of oysters influence (control). Total particulate matter (TPM) is divided into organic (POM) and inorganic (PIM) material. Fluxes are expressed as mg of dry weight per day.

excretion (Nugues et al., 1996). The lower percentage of POM in the traps at the cultured site could be due to a preferential utilization of this organic material by oysters in the water column.

The sediment granulometry corroborates the results on sedimentation rates (Fig. 4). The sediment grain structure was also different between stations. The percentage of small grain size fraction (⩽63 μm) observed below the oysters culture (28% and 15%) for stations L01 and GB was more important than in the outer (control) stations (17% and 5%) at 27 and 17 m depth, respectively. Otherwise, the high percentage of the largest particles recorded in station L01 and GB were mainly due to shell fragments.

While our sedimentation rates are of the same order of magnitude than described under oyster culture (Clavier et al., 1995; Crawford et al., 2003), they correspond to the lowest values reported by these authors. Despite the higher organic sedimentation level we found under oyster culture, the sediment organic content was similar at the two deepest stations (3%). The same pattern (i.e. similar organic matter enrichment) was observed in the shallowest stations whether or not under the direct influence of grafted oysters.

Assessing sediment enrichment is an important issue in evaluating the impact of shellfish farming on lagoon ecosystems. An excessive content of organic matter in the sediment (9–10%) could lead to a degradation of the benthic communities (Chivilev and Ivanov, 1997). Here, the low values of organic matter in Ahe lagoon indicate that the pearl culture influence has not reached a detrimental level for the benthic communities.

Previous studies also found this same discrepancy between organic matter transfer from the water column and the organic content in the sediments (Mallet et al., 2006; Mitchell, 2006). We suggest, based on these results that organic matter transferred from

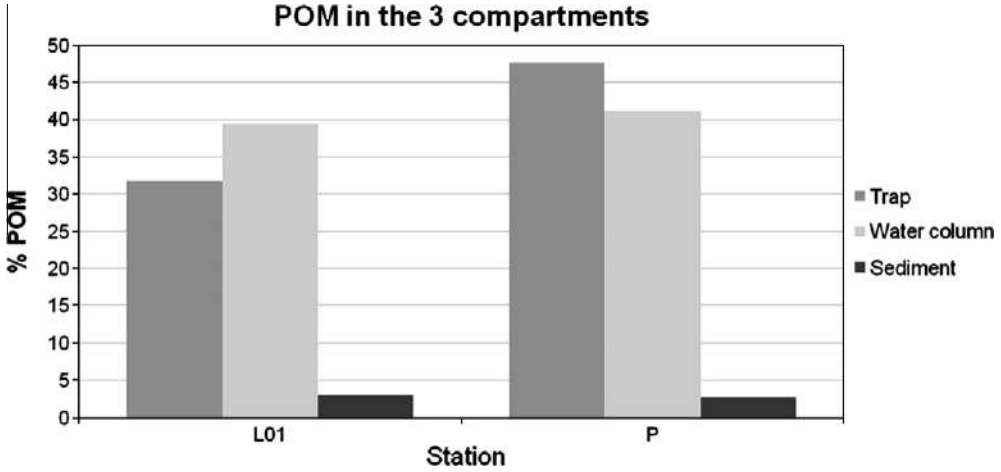

Fig. 3. Percentage of POM contained in the different compartments at the two stations, under pearl oyster spat collectors influence (L01) and outside the pearl oyster spat collectors influence (P-control).

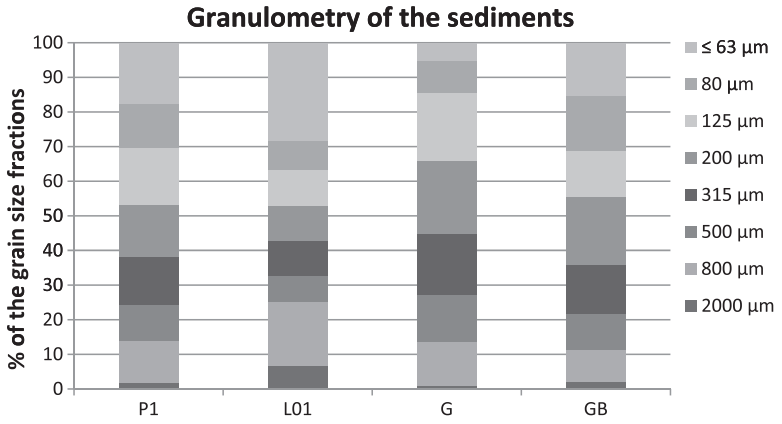

Fig. 4. Sediment granulometry expressed as the percentage of the different particles size fractions.

the water column, is not stored in the sediment, but is either transported and deposited elsewhere or rather used by the local benthic communities. Several studies pointed out that organic material could be consumed rapidly through remineralisation and bioturbation processes at the sediment–water interface, and serve as a source of nutrients to the water column. However, our benthic fluxes data show that maximum values of benthic nitrogen fluxes (DIN) were recorded in stations directly under the influence of pearl oyster culture, with 32 and 36 µmol N m^{-2} h^{-1} for station GB and L01, respectively (Fig. 5). These values are in agreement with Stimson and Larned (2000) and Lourey et al. (2001) in Australia. Grenz et al. (2010) also obtained values from −5 to 70 µmol N m^{-2} h^{-1} of NH_4 from core incubations in New Caledonia lagoon. They are also in agreement with Boucher and Clavier (1990) for NH_4 benthic fluxes found in grey-sand sediment (27.5 ± 4 µmol N m^{-2} h^{-1}) in New Caledonia lagoon. Nevertheless, we found no pattern of nutrient and organic matter benthic fluxes that could be related to pearl oyster culture or to sedimentation rates (Kruskal–Wallis, $p < 0.01$).

SRP fluxes varied between −3 and 8 µmol P m^{-2} h^{-1} (Fig. 6). Maximum values were recorded in the shallowest zone directly under the oyster's facility (station GB). At this station, the sediment interface act as a net source of SRP for the plankton communities. SRP fluxes were in the same range as those measured by Stimson and Larned (2000) and Grenz et al. (2010). Conversely, our results did not correspond with those calculated in Tikehau lagoon by Charpy-Roubaud et al. (1996) who reported 0.03–0.43 µmol P m^{-2} h^{-1} on the basis of diffusive fluxes only (Fick' first law of diffusion). At the deepest stations, whether or not under oyster frames, the variability of SRP fluxes is extreme, indicating SRP uptake or release. These variations cannot be related to the oxic conditions prevailing in the sediments, as they were equivalent for all the stations, with an oxic limit around 3–6 cm (Bodoy, unpublished data). All these aspects highlight that benthic nutrient fluxes in Ahe lagoon seem to be mostly controlled by other biological processes (e.g. bioturbation, microphytobenthic activity, remineralization).

$Si(OH)_4$ fluxes recorded at the water–sediment interface were in the same range as Grenz et al. (2010) in New Caledonia's lagoon at 20 m depth (Fig. 7). They were higher than those calculated by Charpy-Roubaud et al. (1996) in Tikehau lagoon with 0.1–3.3 µmol SiO_2 m^{-2} h^{-1}. When irradiance increased (i.e. in our shallower stations G and GB), $Si(OH)_4$ uptake indicated that they were intercepted by the diatom biofilm as shown in Clavier et al. (1995) and Srithongouthai et al. (2003). Conversely, in the deeper stations, sediments act as a source of silicates to the water column and may thus contribute to the pelagic primary production. Therefore, biofilms at the water sediment interface are likely to modify the solute exchange rates between the sediment and the water column (Srithongouthai et al., 2003). The Chla content of the sediment at station G was about 2.6 times higher than at station P, and 1.3 higher at station L01 (Charpy, unpublished data).

4. Conclusion

This preliminary study of the functioning of the benthic interface in an exploited lagoon in French Polynesia, highlighted its potential contribution to the phytoplankton communities nitrogen demand. While highly variable, benthic nitrogen fluxes could contribute up to 28% of the nitrogen demand in the water column. Furthermore, an indirect influence of the oyster frames was found on nitrogen transfer from the water column. From our results, it appeared that the contribution of the sediments was controlled by the sedimentation rate, the organic matter renewal and the depth.

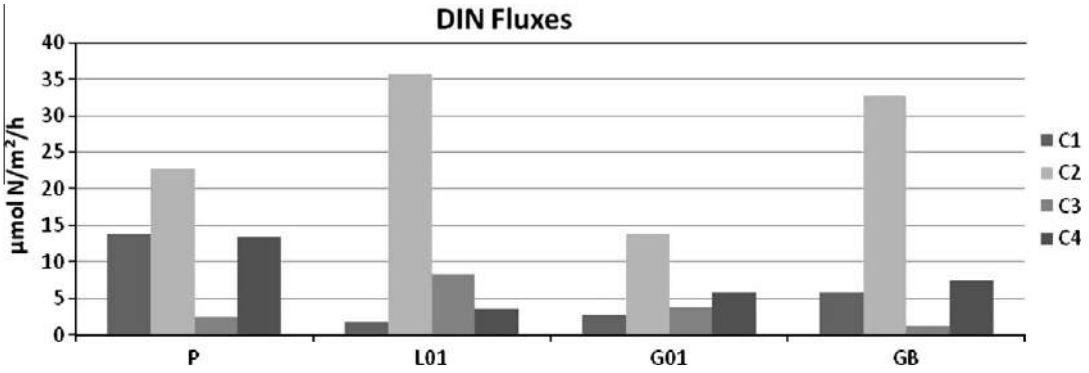

Fig. 5. DIN fluxes at the water–sediment interface measured in the four benthic chambers at the different stations (µmol N m^{-2} h^{-1}).

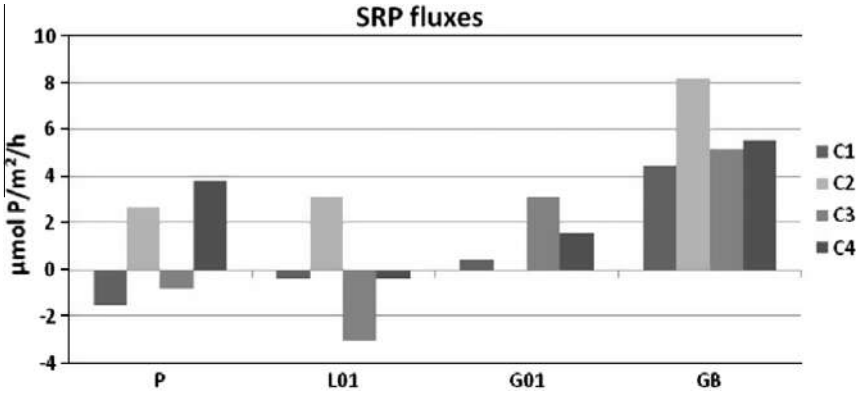

Fig. 6. SRP fluxes at the water–sediment interface measured in the four benthic chambers at the different stations (µmol P m^{-2} h^{-1}).

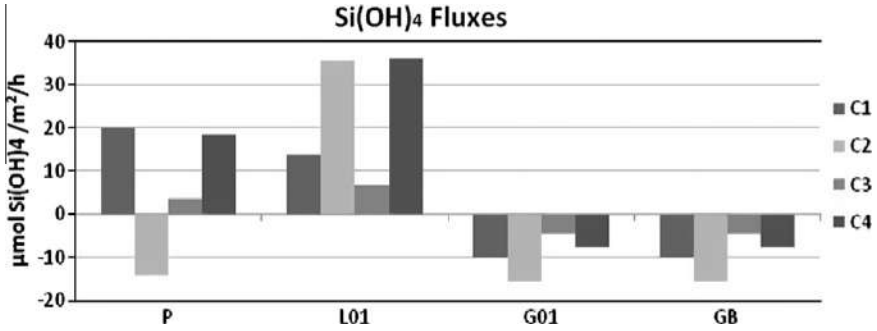

Fig. 7. $Si(OH)_4$ fluxes at the water–sediment interface measured in the four benthic chambers at the different stations (µmol $Si(OH)_4$ m^{-2} h^{-1}).

The benthic system might sustain either nitrogen recycling for the benthic biofilm in shallowest stations (17 m), where the irradiance is sufficient to ensure a high phytobenthic production, or diatom production in the overlying water column, by providing silicates for these planktonic communities. Further investigations are needed to confirm this hypothesis at a larger scale.

Acknowledgements

This work was supported by the European Development Fund, the French Agency of Development (AFD), the National Institute of Water and Atmospheric Research (NIWA) in collaboration with the Service de la Perliculture and the University of French Polynesia. We would like to thank the two anonymous reviewers for their help in improving the manuscript.

References

Aminot, A., Kérouel, R., 2004. Hydrologie des écosystèmes marins. Paramètres et analyses Ifremer.

Alonso-Pérez, F., Ysebaert, T., Castro, C.G., 2010. Effects of suspended mussel culture on benthic–pelagic coupling in a coastal upwelling system (Ria de Vigo, NW Iberian Peninsula). Journal of Experimental Marine Biology and Ecology 382 (2), 96–107.

Boucher, G., Clavier, J., 1990. Contribution of benthic biomass to overall metabolism in New Caledonia lagoon sediments. Marine Ecology Progress Series 64, 271–280.

Boucher, G., Clavier, J., Hily, C., Gattuso, J.P., 1998. Contribution of soft-bottoms to the community metabolism (primary production and calcification) of a barrier reef flat (Moorea, French Polynesia). Journal of Experimental Marine Biology and Ecology 225, 269–283.

Charpy, L., Rodier, M., Fournier, J., Langlade, M.J., Gaertner-Mazouni, N., 2012. Physical and chemical control of the phytoplankton of Ahe lagoon, French Polynesia. Marine Pollution Bulletin 65, 471–477.

Charpy-Roubaud, C., Charpy, L., Sarazin, G., 1996. Diffusional nutrient fluxes at the sediment–water interface and organic matter mineralization in an atoll lagoon (Tikehau, Tuamotu Archipelago, French Polynesia). Marine Ecology Progress Series 132, 181–190.

Chivilev, S., Ivanov, M., 1997. Response of the Arctic benthic community to excessive amounts of nontoxic organic matter. Marine Pollution Bulletin 35 (7–12), 280–286.

Clavier, J., Chardy, P., Chevillon, C., 1995. Sedimentation of particulate matter in the south-west lagoon of New Caledonia: spatial and temporal patterns. Estuarine Coastal and Shelf Science 40 (3), 281–294.

Crawford, C.M., Macleod, C.K.A., Mitchell, I.M., 2003. Effects of shellfish farming on the benthic environment. Aquaculture 224 (1–4), 117–140.

Dumas, F., Le Gendre, R., Thomas, Y., Andréfouët, S., 2012. Tidal flushing and wind driven circulation of Ahe atoll lagoon (Tuamotu Archipelago, French Polynesia) from*in situ*observations and numerical modelling. Marine Pollution Bulletin 65, 425–440.

Dufour, P., Berland, B., 1999. Nutrient control of phytoplanktonic biomass in atoll lagoons and Pacific ocean waters: studies with factorial enrichment bioassays. Journal of Experimental Marine Biology and Ecology 234 (2), 147–166.

Dufour, P., Andréfouët, S., Charpy, L., Garcia, N., 2001. Atoll morphometry controls lagoon nutrient regime. Limnology and Oceanography 46, 456–461.

Furnas, M.J., Mitchell, A., Skuza, M., Brodie, J., 2005. In the other 90%: phytoplankton responses to enhanced nutrient availability in the Great Barrier Reef Lagoon. Marine Pollution Bulletin 51, 253.

Grenz, C., Denis, L., Pringault, O., Fichez, R., 2010. Spatial and seasonal variability of sediment oxygen consumption and nutrient fluxes at the sediment water interface in a sub-tropical lagoon (New Caledonia). Marine Pollution Bulletin 61 (7–12), 399–412.

Holmes, R.M., Aminot, A., Kérouel, R., Hooker, B.A., Peterson, B.J., 1999. A simple and precise method for measuring ammonium in marine and freshwater ecosystems. Canadian Journal of Fisheries and Aquatic Sciences 56 (10), 1801–1808.

Kattner, G., 1999. Storage of dissolved inorganic nutrients in seawater: poisoning with mercuric chloride. Marine Chemistry 67 (1–2), 61–66.

Kristensen, E., Andersen, F.O., 1987. Determination of organic carbon in marine sediments: a comparison of two CHN-analyser methods. Journal of Experimental Biology and Ecology 109, 15–23.

Lourey, M. et al., 2001. Variability of nutrient regeneration rates and nutrient concentrations in surface sediments of the northern Great Barrier Reef shelf. Continental Shelf Research 21 (2), 145–155.

Mallet, A.L., Carver, C.E., Landry, T., 2006. Impact of suspended and off-bottom Eastern oyster culture on the benthic environment in eastern Canada. Aquaculture 255 (1–4), 362–373.

Mazouni, N., 2004. Influence of suspended oyster cultures on the regeneration of nitrogen in a coastal lagoon (Thau, France). Marine Ecology Progress Series 276, 103–113.

Mazouni, N., Gaertner, J.C., Deslous-Paoli, J.M., Landrein, S., Geringer d'Oedenberg, M., 1996. Nutrient and oxygen exchanges at the water–sediment interface in a

shellfish farming lagoon (Thau, France). Journal of Experimental Marine Biology and Ecology 205, 91–113.
Mitchell, I.M., 2006. *In situ* biodeposition rates of Pacific Oysters (Crassostrea gigas) on a marine farm in Southern Tasmania (Australia). Aquaculture 257 (1–4), 194–203.
Murphy, J., Riley, J.P., 1962. A modified single solution method for the determination of phosphate in natural waters. Analytica Chimica Acta 27, 31–36.
Nugues, M., Kaiser, M., Spencer, B., 1996. Benthic community changes associated with intertidal oyster cultivation. Aquaculture 27 (12), 913–924.
Pagès, J., Andréfouët, S., 2001. A reconnaissance approach for hydrology of atoll lagoons. Coral Reefs 20, 409–414.
Srithongouthai, S., Sonoyama, Y.I., Tada, K., Montani, S., 2003. The influence of environmental variability on silicate exchange rates between sediment and water in a shallow-water coastal ecosystem, the Seto Inland Sea, Japan. Marine Pollution Bulletin 47, 10–17.
Storlazzi, C.D., Field, M.E., Bothner, M.H., 2011. The use (and misuse) of sediment traps in coral reef environments: theory, observations and suggested protocols. Coral Reefs 30, 23–38.
Stimson, J., Larned, S., 2000. Nitrogen efflux from the sediments of a subtropical bay and the potential contribution to macroalgal nutrient requirements. Journal of Experimental Marine Biology and Ecology 252 (2), 159–180.
Strickland, J.D.H., Parsons, T.R., 1972. A Practical Handbook of Seawater Analysis, second ed. Fisheries Research Board of Canada, Ottawa.
Thomas, Y., Garen, P., Courties, C., Charpy, L., 2010. Spatial and temporal variability of the pico- and nanophytoplankton and bacterioplankton in a deep Polynesian atoll lagoon. Aquatic Microbial Ecology 59, 89–101.
Torréton, J.P. et al., 2010. Variability of primary and bacterial production in a coral reef lagoon (New Caledonia). Marine Pollution Bulletin 61 (7–12), 335–348.
Vacelet, E., Arnoux, A., Thomassin, B., 1996. Particulate material as an indicator of pearl-oyster excess in the Takapoto lagoon (Tuamotu, French Polynesia). Aquaculture 144 (1–3), 133–148.

Marine Pollution Bulletin 65 (2012) 506–515

Contents lists available at SciVerse ScienceDirect

Marine Pollution Bulletin

journal homepage: www.elsevier.com/locate/marpolbul

Uncoupled viral and bacterial distributions in coral reef waters of Tuamotu Archipelago (French Polynesia)

Marc Bouvy [a,*], Marine Combe [a], Yvan Bettarel [a], Christine Dupuy [b], Emma Rochelle-Newall [c], Loic Charpy [d]

[a] UMR 5119, ECOSYM – Ecologie des systèmes marins côtiers (UM2, CNRS, IRD, Ifremer, UM1), Université Montpellier 2, Place Eugène Bataillon, Case 093, 34095 Montpellier Cedex 5, France
[b] Littoral, Environnement et SociétéS (LIENSs), Université de La Rochelle, UMR 6250 CNRS-ULR, 2 rue Olympe de Gouges, 17000 La Rochelle Cedex, France
[c] UMR 7618, BIOEMCO (UPMC-CNRS-INRA-ENS-IRD-AgroParisTech-Université Paris-Est), Ecole Normale Supérieure, 46 rue d'Ulm, 75005 Paris, France
[d] UMR LOPB (IRD, CNRS, Université Méditerranée), IRD Centre de Tahiti, BP 529, 98713 Papeete, French Polynesia

ARTICLE INFO

Keywords:
Virus
Bacteria
Distributions
Strategy lifes
Coral reef waters

ABSTRACT

This study examined the distribution of virioplankton and bacterioplankton in two coral reef systems (Ahe and Takaroa atolls) in the Tuamotu Archipelago, in comparison with the surrounding oligotrophic ocean. Mean concentrations of 4.8×10^5 and 6.2×10^5 cells ml^{-1} for bacteria and 8.1×10^6 and 4.3×10^6 VLP (virus-like particle) ml^{-1} were recorded in Ahe and Takaroa lagoons, respectively. Chlorophyll-*a* concentrations and dissolved organic matter were higher in Ahe whereas ^3H thymidine incorporation rates were higher in Takaroa. First data on lytic and lysogenic strategies of phages in coral reef environments were discussed in this paper. The fraction of visibly infected cells by viruses was negligible regardless of the lagoon station (mean = 0.15%). However, the fraction of lysogenic cells ranged between 2.5% and 88.9%. Our results suggest that the distribution patterns of virioplankton are apparently not coupled to the spatial dynamics of the bacterioplankton communities.

1. Introduction

There is no doubt of the ecological importance of bacterioplankton in coral reef systems but the role of virioplankton in these ecosystems has, to our knowledge, yet to be studied. Viruses are the numerically dominant biological entities in the ocean and viral infection is a major structuring process in the dynamics of marine microbial communities (Fuhrman, 1999; Suttle, 2005). Viral lysis of autotrophic and heterotrophic microorganisms influences the rate of nutrient cycling through microbial food webs (Proctor and Fuhrman, 1990; Fuhrman, 1999). Recent studies of marine systems have shown that virus mediated mortality of bacterioplankton is greater in nutrient rich habitats where contact rates with potential hosts are high (Weinbauer, 2004).

Most virioplankton in the environment infect bacterioplankton (bacteriophages or, simply, phages) and, in general, the distributions of viral populations often mirror the bacterial distributions (Hewson et al., 2001; Middelboe et al., 2003). Variability amongst coral reef bacterial communities has been investigated at a variety of spatial and temporal scales (Moriarty, 1979; Moriarty et al., 1985; Paul et al., 1986; Hoppe et al., 1988; Gast et al., 1998) and significant variations in abundance, activity and composition have been observed over small spatial and temporal scales (Paul et al., 1986; Gast et al., 1998; van Duyl and Gast, 2001; Frias-Lopez et al., 2002; Rohwer et al., 2002). The role of virioplankton in coral reef systems remain relatively unexplored (Seymour et al., 2005; Mari et al., 2007; Dinsdale et al., 2008), as well as the presence and the roles of viruses associated with healthy and diseased corals which warrant further investigation (Weil et al., 2006; Patten et al., 2008). Nothing is known on the mode of viral infections and the life strategy of virioplankton in coral reef systems.

In addition to their role in the mortality of phyto-and bacterioplankton, viral lysis products (e.g., dissolved organic matter (DOM)) from cells through the viral shunt can be taken up by prokaryotes, thereby stimulating the growth of heterotrophic bacterioplankton (Wilhelm and Suttle, 1999; Thingstad, 2000). Tropical coral lagoon systems are also an interesting environment for the study of carbon cycling, as they are often characterized by low nutrient (DOM) and chlorophyll concentrations (Rochelle-Newall et al., 2008). The recycling of DOM by heterotrophic bacterioplankton is one of the major organic matter transformation pathways and could explain bacterial and viral distributions (Del Giorgio and Davies, 2003). Virioplankton are, therefore, believed to have a significant effect on aquatic environments.

French Polynesia is made up of several groups of islands in the South Pacific gyre with 84 atolls surrounded by oligotrophic

* Corresponding author. Tel.: +33 467144128.
E-mail address: marc.bouvy@ird.fr (M. Bouvy).

0025-326X/$ - see front matter © 2012 Elsevier Ltd. All rights reserved.
doi:10.1016/j.marpolbul.2012.01.001

waters. The lagoons are of great importance to the economy of French Polynesia, where farming of pearl oyster, *Pinctada margaritifera*, is the major source of export earnings (Andréfouët et al., 2012). Though originally benthic, *P. margaritifera* is now reared on suspended ropes and the resulting interactions with pelagic communities raise questions about the ability of planktonic food webs to sustain this increased animal production. In atoll lagoons, the primary production is mainly achieved by picophytoplankton (Charpy, 1996; Charpy and Blanchot, 1996), whereas the biomass is dominated by low-producing bacteria (Torréton and Dufour, 1996). As both picoplankters are in a size range unavailable to oysters (Pouvreau et al., 1999), phagotrophic protists may act as an intermediate between the dominant picoproduction and bivalves (Loret et al., 2000).

To determine the potential role of virioplankton in bacterioplankton dynamics in coral reef systems, the spatial distribution of virus-like particles (VLP) and bacterial communities was determined in the pelagic zone, as well as the dissolved organic carbon and the chlorophyll-*a* concentrations within two atoll lagoons in the Tuamotu Archipelago. The fraction of lysogenic bacterial cells (FLC) and the fraction of infected bacterial cells (FIC) were also determined to infer the prevalence of these two modes of infection. A broad study was made of the VLP and bacterial communities in the benthic zone where there is very little data on virioplankton dynamics at tropical latitudes, especially in coral reef systems.

2. Methods

2.1. Study sites and sampling

This study was conducted in two atolls (Ahe and Takaroa) located 500 km northeast of Tahiti in the north of the Tuamotu Archipelago between August 20 and 30, 2009 (Fig. 1; see details in Thomas et al., 2010). Ahe lagoon is 142 km^2 in area with a maximum depth close to 70 m and can be defined as a semi-enclosed atoll. There is one deep passage to the ocean in the northwest and there are several reef-flats (inferior to 50 cm depth) along the reef rim. Four stations were sampled (A1, A3, A9, A11) situated from the south-west (the deepest A1 with more extensive oyster farming) to the north-east (A11 being the shallowest station with less extensive oyster farms). Water samples were collected at three depths for A1 (1, 10 and 20 m) and at five depths for the others (1, 10, 20, 30 and 40 m). Takaroa lagoon is 85 km^2 in area with a mean depth of 26 m (max depth = 47.5 m). Four stations were sampled (T1, T2, T3, T4) situated from the east (less deep) to the west, with samples taken at three depths (1, 10 and 20 m). The average water residence time is estimated at 76 d in Takaroa, twice that reported for Ahe (34 d) by Andréfouët et al. (2001) and Pagès et al. (2001). Dumas et al. (2012) recently characterized the spatial variation of residence and flushing time in different weather conditions.

The sampling stations were selected to test the spatial distributions of bacterioplankton and virioplankton in the lagoon. For comparison, samples were also taken at three depths (1, 10, and 20 m) outside the two lagoons (about 3.5 km away) in the euphotic oceanic zone.

At each sampling station, a CTD profiler (YSI 600 XM) was deployed to measure temperature and depth. Water samples for nutrient and viral and bacterial parameters were collected in the morning using a 5-l Niskin bottle at each depth, placed directly in acid-washed polyethylene bottles and kept in the dark at *in situ* temperatures until processed in the laboratory within 2 h. Dissolved organic carbon (DOC) analyses were performed on 30 ml subsamples collected in pre-combusted (450 °C overnight) glass vials, preserved with 35 µl 85% phosphoric acid. Samples were stored in the dark until analysis using a Shimadzu TOC VCPH analyzer (Rochelle-Newall et al., 2008). Chlorophyll concentrations were determined fluorometrically after filtration of samples onto Whatman GF/F fiberglass filters and directly extracted using methanol (Yentsch and Menzel, 1963). For bacterial and viral parameters, samples were fixed with prefiltered (0.02 µm) buffered formaldehyde (2% final concentration), stored in liquid nitrogen (−162 °C) and analyzed on return to Montpellier University.

Sediment cores were taken by diving near station A11 (Ahe atoll; 5 m depth) using a PVC tube with 30 mm internal diameter ($n = 4$). Cores were processed immediately after collection, with subsamples taken using 5 ml sterile syringes ($n = 3$). The top centimeter of the core layer was carefully extracted for bacterial and viral analyses.

2.2. Enumeration of virioplankton and bacterioplankton

For water samples, the abundance of bacterioplankton was determined by epifluorescence microscopy using fluorochrome 4′,6′-diamidino-2-phenylindole (DAPI) (Porter and Feig, 1980). The number of virus-like particles (VLPs) contained in triplicates of 50–200 µl samples were determined after particles had been retained on 0.02 µm pore-size membranes (Anodisc) and stained with SYBR Gold (Patel et al., 2007). On each slide, 300–600 bacterioplankton and VLPs were counted in 15–20 fields with final numbers giving a precision of <10% at 95% confidence limit.

Morphologies of virioplankton were also determined using transmission electron microscopy (TEM) (Bettarel et al., 2010). Virioplankton contained in 5 ml aliquots of formalin-fixed samples were harvested by ultracentrifugation onto grids (400 mesh Cu electron microscope grids with carbon coated Formvar film) using a Centrikon TST 41.14 swing-out rotor at 120,000*g* for 2 h. Grids were then stained for 30 s with uranyl acetate (2%, w/w) and VLP were counted and measured using a JEOL 1200EX TEM at 80 kV and a magnification of 40,000. The viral populations were divided into three virus capsid sizes: <60 nm; 60–90 nm; >90 nm. Three morphotypes were distinguished for classifying tailed virioplankton (Caudovirales) according to their shape. Tailed virioplankton with isomeric heads and long non contractile tails were classified as *Siphoviridae*. Tailed virioplankton with isomeric heads and contractile tails were classified as *Myoviridae*. Tailed virioplankton with short tails were classified as *Podoviridae* (Bettarel et al., 2011).

For the sediment samples, viruses and bacteria were extracted and analysed according to the procedure of Danovaro et al. (2001) and analyzed according to the procedures described above. Aliquots of the fixed sediment samples (1 ml) were diluted with tetrasodium pyrophosphate (Ppi-NaCl; 4 ml; 10 mM final concentration) and incubated for 20 min at 4 °C. Samples were then sonicated three times (100 W for 1 min), diluted 200–1000 times with 0.02 µm filtered formaldehyde (2% final concentration). This procedure has been shown to extract most VLPs and bacteria from the sediment (Danovaro et al., 2001).

2.3. Bacterial production (BP)

For both sediment and overlying water, heterotrophic bacterial production was determined by [methyl-^{3}H]-thymidine incorporation (Kirscher and Velimirov, 1999). For water samples, duplicates and one control (zero time) were incubated with (methyl-^{3}H)-thymidine (47 Ci $mmol^{-1}$, Amersham) in the dark at *in situ* temperature. Incubation time was 60 min, with a final thymidine concentration of 20 nM (saturation condition). It was assumed that isotope dilution was negligible at this concentration (Robarts and Zohary, 1993). Radioactivity was counted by liquid scintillation.

For the sediments, two replicates and one control were incubated with labeled thymidine used at saturation point, at a final

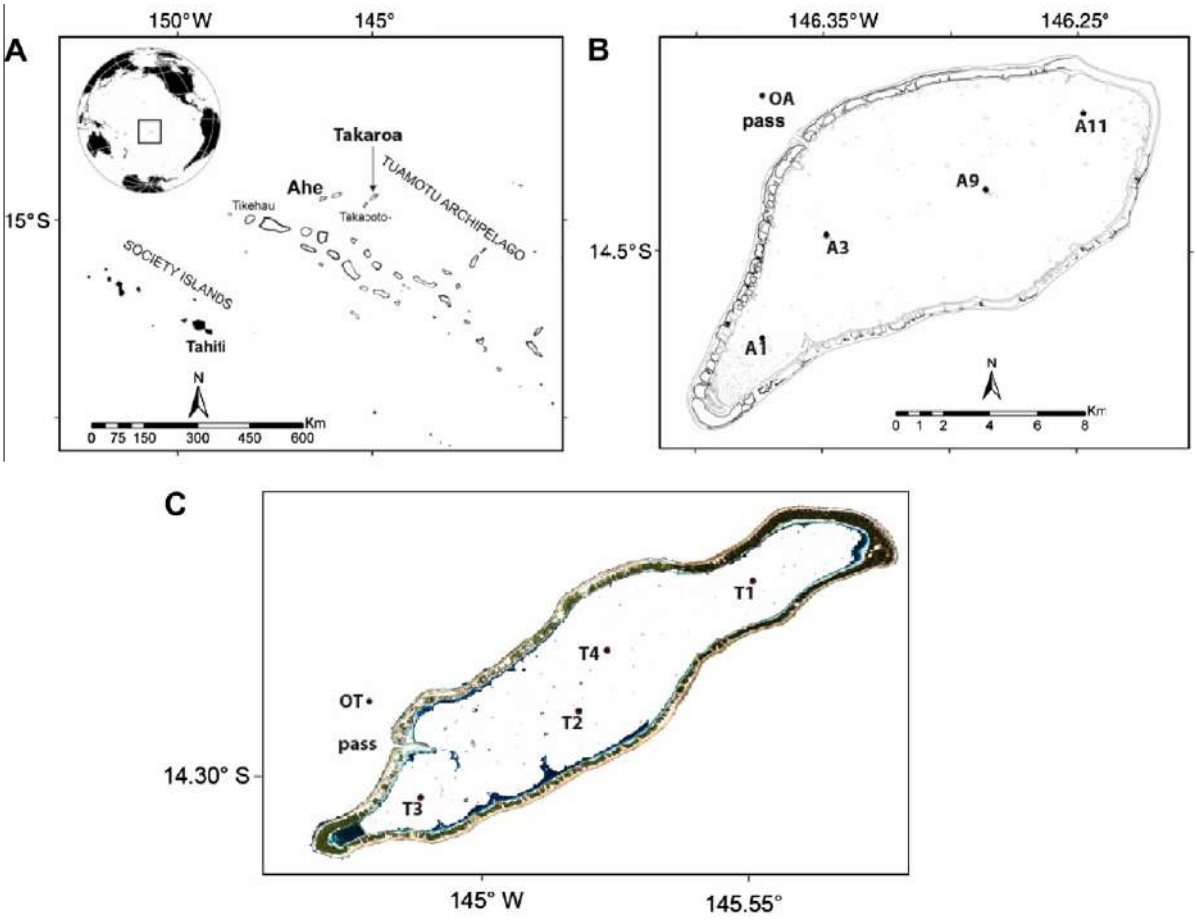

Fig. 1. Location of the stations studied in the two atolls in the Tuamotu Archipelago in French Polynesia (A). Positions of the sampling stations in Ahe (B) and Takaroa (C) lagoon. OA and OT are defined as oceanic stations, respectively in Ahe and Takaroa atoll system.

concentration of 1000 nM (Haglund et al., 2003). 0.5 g sub-samples of wet sediment were incubated in 10-ml centrifugation tubes at *in situ* temperature. Incubation was stopped with formaldehyde after 60 min. Samples were then centrifuged (8500*g*) for 20 min, the supernatant was discarded and the pellet was washed three times with 5 ml of 80% ethanol. Finally, pellets were washed twice with 5 ml of ice-cold TCA (5%), filtered onto a 0.2 μm pore size membrane filter, transferred to vials with 3 ml of 2 N NaOH and heated for 2 h in a water bath at 100 °C. After cooling, 1 ml of the supernatant was transferred to a scintillation vial and a scintillation cocktail was added. For comparison with the literature, bacterial production was estimated using a conversion factor of 2×10^{18} cells produced per mole of thymidine incorporated (Haglund et al., 2003).

2.4. Viral infection of bacterioplankton

Two different viral infection strategies were investigated: the frequency of bacteria killed by lytic phages (lytic infection) and the frequency of lysogenic cells (lysogenic infection). To determine the percentage of lytic bacterial cells (fraction of infected cells; FIC), bacterioplankton contained in duplicate 8 ml aliquots of formalin-fixed samples were harvested by ultracentrifugation at 70,000*g* for 20 min onto 400 mesh Cu grids, stained for 30 s with uranyl acetate (2% w/w) and examined at ×40,000 by TEM at 80 kV to distinguish between virus-infected and uninfected bacterial cells (Weinbauer and Höfle, 1998). At least 500 bacterial cells were inspected per grid. To estimate virally-induced bacterial mortality (VIBM), the fraction of infected cells (FIC) was calculated from the fraction of visibly infected cells (FVIC) (expressed as a percentage) using the formula: $FIC = 7.11 \times FVIC$ (Weinbauer et al., 2002). Only samples from the water columns were analyzed for viral infection. The fraction of lysogenic bacteria (FLC) was estimated following the method described by Mei and Danovaro (2004), based on the prophage induction in the bacterioplankton from the pelagic zone. For each sample, three subsamples (10 ml) were taken and mitomycin C (1 μg ml^{-1} final concentration, Sigma Chemical Co, No. M-0503) was added to 2 of these, the untreated subsample serving as a control. Both samples were formalin-fixed after being incubated for 12 h (Mei and Danovaro, 2004; Weinbauer et al., 2003). Prophage induction was calculated as the difference in viral abundance between mitomycin C treated (Vm) and control incubations (Vc). The fraction of lysogenic bacterioplankton cells (FLC) was calculated as: $FLC\ (\%) = 100\ [(Vm - Vc)/(BS \times BAC_{t0})]$, with BS = burst size (number of virus per bacteria) and BAC_{to} = bacterial abundance at the start of the experiment, i.e. before the addition of mitomycin C (Weinbauer et al., 2003).

2.5. Statistical analysis

The measured concentrations and distributions of bacterioplankton and virioplankton were compared between the two lagoons and within the water columns. Data were not systematically normally distributed and thus, the non parametric Mann–Whitney test was used to test differences in biological parameters and physico chemical parameters between the two

atolls. All values are reported as means ± standard deviation (SD) unless otherwise stated. All statistical analyses were performed using Sigma Stat version 3.5.

3. Results

3.1. Physical and chemical conditions

The water temperature was comparable in the two atoll lagoons, with a mean of 27.2 °C. In the oceanic zone, values were not significantly different from those recorded in the atolls (26.8 ± 0.58 °C; Table 1). Chlorophyll-*a* concentrations were significantly different between the two atolls ($p = 0.001$), with higher values found for Ahe (0.32 ± 0.10 μg l^{-1}). In oceanic zones, chlorophyll concentrations were significantly lower than those in the lagoons (0.13 ± 0.04 μg l^{-1}; $p = 0.003$) (Table 1). Mean values of DOC concentrations were low and not statistically different ($p > 0.05$) between the stations and the lagoons (107.6 ± 53.9 μM for Ahe and 87.4 ± 8.6 μM for Takaroa). No significant difference was observed between the concentrations in the lagoons and the oceanic zones (82.9 ± 3.9 μM). Mean concentrations of these physico-chemical parameters did not vary significantly according to depth whatever the stations.

3.2. Planktonic bacterial and viral abundance

Total bacterial abundances differed significantly between Ahe (6.2×10^5 cells ml^{-1}) and Takaroa atolls (4.8×10^5 cells ml^{-1}) ($p = 0.028$) (Table 2). Concentrations of bacterioplankton were significantly higher in the lagoons (5.6×10^5 cells ml^{-1}) than in the ocean (2.9×10^5 cells ml^{-1}) ($p = 0.001$). Virus like particle (VLP) concentrations were significantly different between Ahe (4.3×10^6 VLP ml^{-1}) and Takaroa atolls (8.1×10^6 cells ml^{-1}) ($p < 0.001$). However, there was no correlation between the viral and the bacterial concentrations ($r = -0.05$; $p < 0.774$; $n = 30$). There was a significant difference in virioplankton abundance between the lagoon and ocean sites ($p = 0.174$) with a lower mean in oceanic sites (4.2×10^6 VLP ml^{-1}). The mean virus-to-bacteria ratio (VBR) was 7.6 for Ahe, significantly lower than the ratio (17.6) observed for Takaroa ($p < 0.001$) (Table 2). No significant difference in VLP abundance was noted according to the depth and the stations studied inside a lagoon (Figs. 2 and 3). Virioplankton smaller than 60 nm were clearly dominant at all stations studied inside the lagoon and in the oceanic zones (Table 3). They accounted for nearly 95% of the total community for all stations, with the exception of station A11 (87.3%) located in the northern part of the Ahe atoll. There were relatively few virioplankton larger than 90 nm at all stations (Table 3). Almost 75% of the total viral community belonged to the *Siphoviridae*. No significant difference between the viral morphotypes was observed between lagoon stations and oceanic zone. The rest of the community comprised virioplankton from the *Myoviridae* and *Podoviridae* families.

3.3. Benthic bacterial and viral abundances

Mean of benthic bacterial concentrations were $68 \pm 62 \times 10^5$ cells ml^{-1} ($n = 4$), nearly 10 times more abundant than planktonic bacterial cells observed in the same station (A11). Mean abundances of benthic viruses were 40 times ($197 \pm 3 \times 10^5$ VLP ml^{-1}; $n = 4$) more abundant than virioplankton. The mean virus-to-bacteria ratio (VBR) was higher in the benthic zone (51.0 ± 36.4) than in the water column (11.6 ± 0.4) in the same station. The mean rate of ^{3}H thymidine incorporation was 1000-fold higher in the sediments ($10 \pm 3.9 \times 10^3$ pmol l^{-1} h^{-1}) than in the overlying waters (10.5 pmol l^{-1} h^{-1}).

3.4. Planktonic bacterioplankton activity

The ^{3}H thymidine incorporation rates in bacterial cells were significantly lower ($p < 0.001$) in the Ahe lagoon (mean = 5.9 ± 3.1

Table 1
Values of temperature (Temp; °C), concentrations of chlorophyll-*a* (Chlor-a; μg l^{-1}) and dissolved organic carbon (DOC; μM) at each depth sampled in the two atolls. OA and OT: oceanic stations.

AHE				TAKAROA			
Depth (m)	Temp (°C)	Chlor-*a* (μg l^{-1})	DOC (μM)	Depth (m)	Temp (°C)	Chlor-*a* (μg l^{-1})	DOC (μM)
Atoll stations							
A1				T1			
1	27,47	0,44	95,3	1	27,12	0225	99,9
10	27,45	0,50	168,5	10	27,28	0165	99,9
20	27,43	0,28	97,8	20	27,28	0243	95,6
A3				T2			
1	27,3	0,34	90,0	1	27,18	0145	76,6
10	27,29	0,34	96,2	10	27,25	0158	93,2
20	27,28	0,39	88,4	20	27,25	0159	85,9
A9				T3			
1	27,17	0,27	84,8	1	27,24	0215	79,5
10	27,13	0,16	83,6	10	27,25	0213	75,0
20	27,12	0,15	259,5	20	27,19	0239	84,3
A11				T4			
1	27,16	0,27	73,3	1	NA	0135	79,9
10	27,12	0,31	73,5	10	NA	0159	89,2
20	27,11	0,36	80,7	20	NA	0143	89,0
Mean	**27.25**	**0.32**	**107.6**	**Mean**	**27.23**	**0.18**	**87.4**
Std	**0.14**	**0.10**	**53.9**	**Std**	**0.05**	**0.04**	**8.6**
Ocean station							
OA				OT			
1	26,1	0,14	80,0	1	NA	0089	82,9
10	27,12	0,13	88,7	10	NA	0104	85,5
20	27,1	0,19	83,0	20	NA	0156	77,3
Mean	**26.77**	**0.15**	**83.9**	**Mean**	**NA**	**0.12**	**81.9**
Std	**0.58**	**0.03**	**4.4**	**Std**	**NA**	**0.04**	**4.2**

Table 2
Mean and standard deviations (n = 3 or 4 according to the depth) of viral and bacterial parameters for the pelagic zone of the different lagoon stations and oceanic zones in Ahe and Takaroa.

SITE	Bacteria conc. (10^5 cells ml^{-1})	Virus conc. (10^6 VLP ml^{-1})	VBR	^{3}H thymidine incorporation (pmol l^{-1} h^{-1})	Burst size	FIC (%)	FLC (%)
AHE							
A1	5.6 (2.8)	4.9 (1.4)	9.9 (3.7)	10.5 (5.0)	76	0.27	88.9 (17.1)
A3	6.1 (1.5)	0.6 (1.1)	7.4 (4.2)	4.6 (1.4)	19	0.23	7.9 (1.2)
A9	5.8 (1.9)	4.7 (1.0)	8.7 (3.3)	5.4 (2.2)	30	0.34	Nd
A11	7.1 (0.7)	3.8 (1.1)	5.3 (1.3)	4.9 (0.8)	20	0.47	Nd
Mean (lagoon)	**6.2**	**4.3**	**7.6**	**5.9**	**42.1**	**0.32**	**Nd**
Std (lagoon)	**1.7**	**1.1**	**3.4**	**3.1**	**31.6**	**0.11**	**Nd**
OA (ocean)	3.8 (1.1)	2.1 (0.4)	5.8 (2.9)	4.6 (4.5)	0	0	2.5 (0.8)
TAKAROA							
T1	5.4 (1.9)	7.1 (0.7)	14.0 (4.7)	13.4 (4.5)	26	0.31	7.4 (1.0)
T2	4.6 (0.9)	7.7 (3.2)	16.0 (3.9)	8.1 (1.1)	30	0.35	Nd
T3	3.6 (1.2)	7.5 (3.1)	21.5 (8.2)	8.8 (0.7)	0	0	Nd
T4	5.6 (2.2)	7.8 (6.3)	12.6 (9.5)	15.3 (15.4)	25	0.28	Nd
Mean (lagoon)	**4.8**	**8.1**	**17.6**	**9.3**	**20.2**	**0.23**	**Nd**
Std (lagoon)	**1.6**	**2.5**	**5.2**	**3.2**	**13.6**	**0.16**	**Nd**
OT (ocean)	1.9 (1.1)	6.4 (1.1)	39.1 (18.4)	6.7 (3.2)	0	0	8.0 (2.2)

VBR: virus to bacteria ratio; FIC: frequency of infected cells; FLC: frequency of lysogenic cells.
OA and OT: oceanic stations.
Nd: not determined.

pmol l^{-1} h^{-1}) than in the Takaroa lagoon (mean = 9.3 ± 3.2 pmol l^{-1} h^{-1}). The mean values for the oceanic zones, were lower (4.6 and 6.7 pmol l^{-1} h^{-1}), but not significantly different from those observed in lagoons (p = 0.289).

3.5. Life strategies of virioplankton

In the water column, the fraction of infected cells (FIC) ranged from 0% to 0.5% (mean = 0.15%). No significant difference of FIC was observed regardless of the station (p = 0.85) and the atoll (p = 0.75). At the oceanic stations, no bacterial cells were infected at any site or depth sampled. The burst size (the number of VLP counted in a bacterial cell) varied significantly with the highest values observed in Ahe lagoon (mean = 42.1) compared to Takaroa lagoon (17.6). The mean burst size was 28.2 ± 21.5 (Table 2).

The fraction of lysogenic cells (FLC) differed significantly between the stations inside an atoll, with the fraction of lysogenic cells in the total bacterial community ranging from 2.5% (station A11) to 88.9% (station A1) (Table 2). Unlike the results for lytic infection, all the bacterial communities from the ocean stations had a significant fraction of lysogenic cells (2.5–8%).

After compiling all the data, no significant correlation was observed between bacterial and viral abundance or between ^{3}H-thymidine incorporation rates and bacterial abundance. Bacterial abundances and chlorophyll concentrations were not significantly correlated, regardless of site, nor were the bacterial abundances and the DOC concentrations. The only significant correlation observed was between the ^{3}H thymidine incorporation rates and DOC concentrations in the Takaroa atoll (r = 0.594; p < 0.04).

4. Discussion

Many studies have dealt with the viral compartment in tropical ecosystems (Seymour et al., 2005; Dinsdale et al., 2008; Weinbauer et al., 2010) by exploring the relationship between bacterial and viral distributions. This study provides new data on these two biological components in two coral reef systems, and especially on a variety of viral parameters. To the best of our knowledge, this study provided the first data on lytic and lysogenic strategies of phages in coral reef environments. Other secondary results reported viral and bacterial parameters in the benthic compartment (at one site), knowing that this domain is seldom studied in these systems (e.g., Paul et al., 1993; Patten et al., 2008).

Bacterial numbers in the water column overlying coral reefs (e.g., in the northern Great Barrier Reef) are around 2–6 × 10^5 cells ml^{-1} (Moriarty, 1979). Levels of bacterial production and activity are generally higher above coral reefs than in the surrounding waters (Moriarty et al., 1985; Hoppe et al., 1988) owing to the high concentrations of dissolved and particulate organic matter that are released into the overlying reef waters by corals (Ferrier-Pages et al., 1998; van Duyl and Gast, 2001) and benthic algae (Ducklow, 1990). The relationship between production (^{3}H incorporation rates) and DOC concentrations was only observed in this study in the Takaroa atoll (r = 0.594; p = 0.04; n = 30). In the Ahe lagoon, the high concentrations observed in A9 at a depth of 20 m are potentially due to sedimentary release of potentially low bioavailabilily DOC. Similarly, at station A1, located closer to the atoll rim, the inputs of coral mucus derived DOC should not be ignored (Wild et al., 2004). Rochelle-Newall et al. (2008), working in a barrier reef system proposed that the shifts in the degree of coupling between dissolved primary production and hence, DOC concentrations and bacterial activity in the water column were due to inputs from coral reef mucus or from other inputs of terrestrial origin. In our work, it is probable that the terrestrial inputs were minimal, as evidenced by the low DOC concentrations. Mari et al. (2007) and Weinbauer et al. (2010) also pointed out that the residence time of a water mass can also impact bioavailability of DOC to bacteria. Although it is difficult to accurately pinpoint the sources of these relatively high DOC concentrations, it is probable, given the relatively constant bacterial abundance and activity measurements at these two stations that the DOC was not of high bioavailability. This highlights the more productive environment in the Takaroa versus the Ahe atoll, probably owing to a higher water residence time than that calculated for the Ahe atoll (Andréfouët et al., 2001; Dumas et al., 2012). Lower bacterial abundances were reported in the oceanic stations compared to the atoll stations, corroborating the results from previous studies (e.g., Torréton, 1999). However, no relationship was found in this study between bacterial abundance and chlorophyll-a concentrations although bacterial production is often linked to primary production in reef systems (Rochelle-Newall et al., 2008) and many other pelagic environments (e.g., Cole et al., 1988).

Concentrations of virioplankton were similar to those occurring in near-shore oceanic coral reefs (Seymour et al., 2005; Mari et al., 2007; Dinsdale et al., 2008; Patten et al., 2011). In Ahe and Takaroa atolls, the abundances of virioplankton (min–max, 1.1–

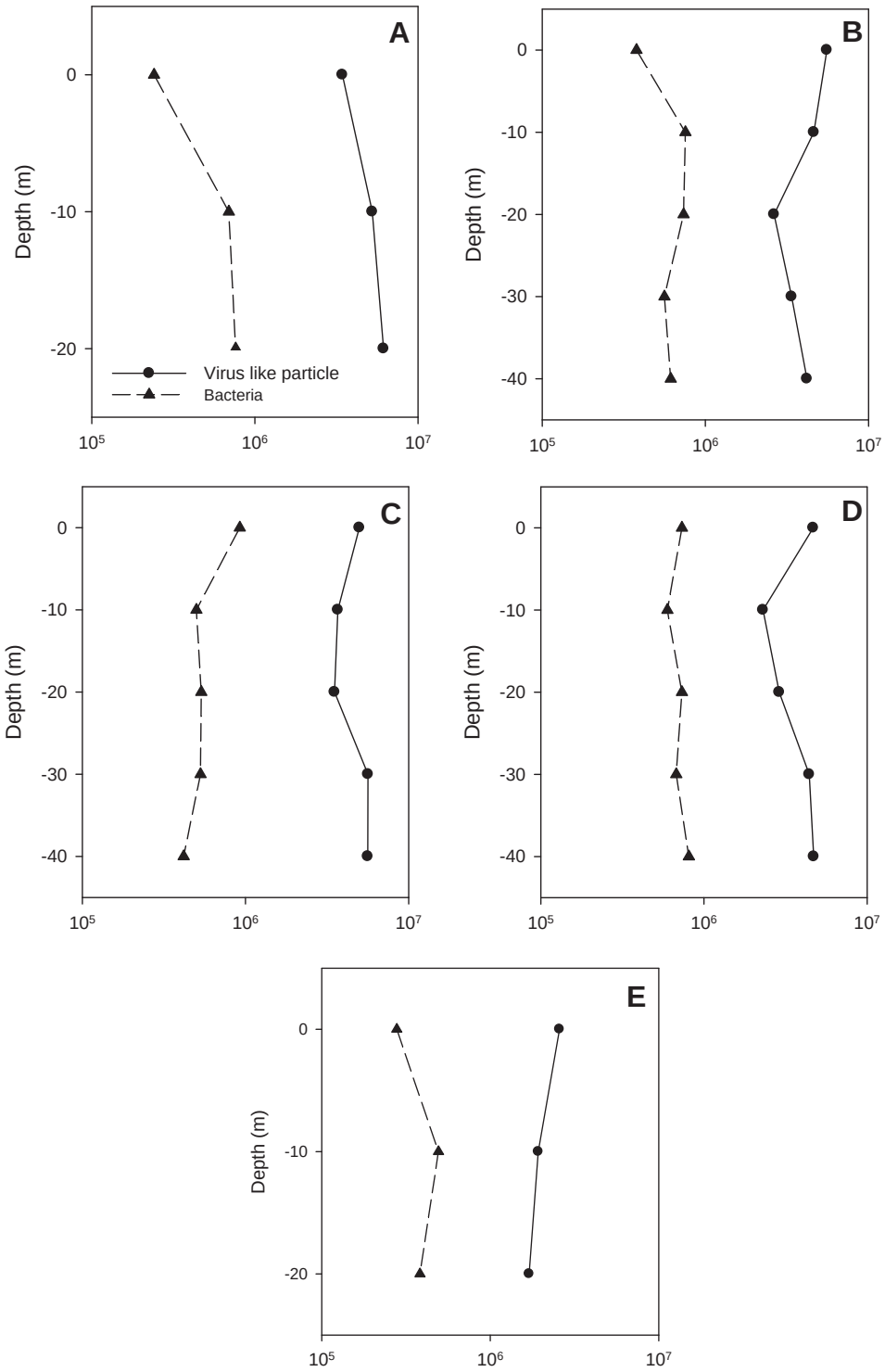

Fig. 2. Distribution of the concentrations of virus like particles (VLP ml^{-1}) and bacteria (cells ml^{-1}) in the different stations at different depth in the Ahe lagoon (A, B, C and D, respectively for A1, A3, A9 and A11) and in oceanic zone (E for OA) in August 2009.

72.0×10^7 VLPs ml^{-1}) were within the usual range (10^7–10^8 ml^{-1}) observed for temperate productive systems (Weinbauer, 2004). VLP concentrations were significantly higher ($p < 0.05$) in the lagoon than in the oceanic zones, confirming that viral abundances tend to be greater in productive, nutrient rich environments (Weinbauer et al., 1993). The results also showed that VLPs were more abundant in the Takaroa lagoon than in the Ahe lagoon, suggesting that virus abundance may be linked to the water residence time. Most (95%) virioplankton from pelagic environments in this study were smaller than 60 nm in diameter. Similar results were reported in the sea at various latitudes, including the French Atlantic coast (Auguet et al., 2006), Southern California (Cochlan et al., 1993), the Adriatic Sea (Weinbauer and Peduzzi, 1995), the Alboran Sea (Alonso et al., 2001), the Great Barrier Reef (Davy and Patten, 2007), and the Bach Dang estuary in Vietnam (Bettarel et al., 2011), indicating relative homogeneity in viral capsid size

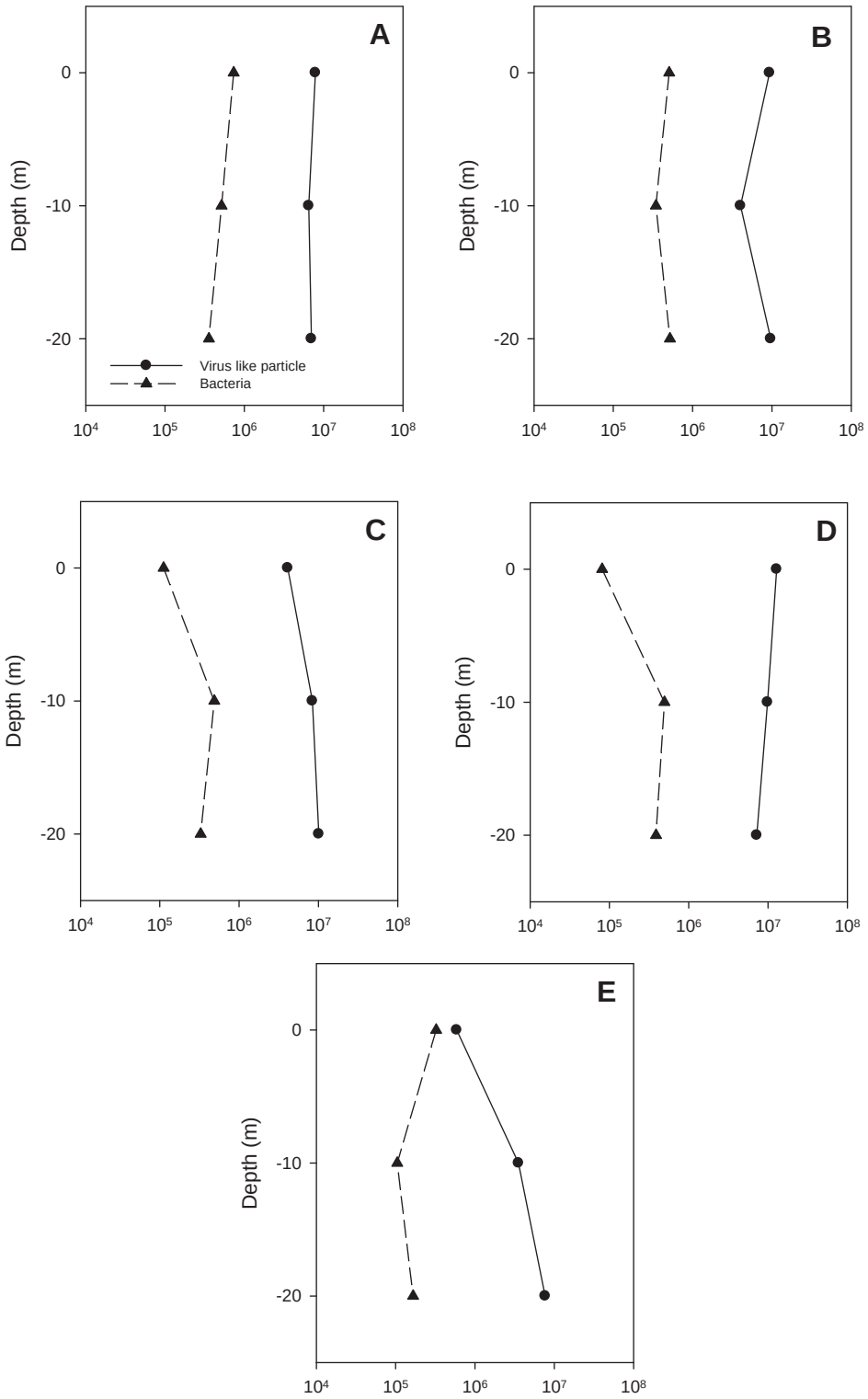

Fig. 3. Distribution of the concentrations of virus like particles (VLP ml^{-1}) and bacteria (cells ml^{-1}) in the different stations at different depth in the Takaroa lagoon (A, B, C and D, respectively for T1, T2, T3 and T4) and in oceanic zone (E for OT) in August 2009.

on a global scale. Most of the virioplankton belonged to the *Siphoviridae* characterized by a long flexible tail, confirming that 96% of all isolated phages have a tail (Ackermann, 2001).

VLP and bacterioplankton abundances did not show significant variability in most of the water columns (Figs. 2 and 3), and the slight variability in abundance with depth was generally close to the average coefficient of variation of viral and bacterial counted using epifluorescence microscopy (average CV = 20%). It was not, therefore, possible to detect any statistically significant relationship between bacterial and viral abundances in this study.

The mean virus-to-bacteria ratio (VBR) was significantly lower in Ahe than in Takaroa ($p < 0.001$) (7.6 and 17.6, respectively). This is consistent with the hypothesis that the VBR is likely to increase in environments that favor fast bacterial growth and high

Table 3
Distribution of the three caudate virus forms and of three virus size in the different stations A (Ahe lagoon) and T (Takaroa lagoon) and in the two oceanic zones in August 2009.

Station	% Myoviridae	% Siphoviridae	% Podoviridae
A1	10.0	78.0	12.0
A3	12.8	71.8	15.4
A9	14.2	66.7	19.1
A11	11.1	75.6	13.3
OA	12.7	74.5	12.8
T1	14.5	75.0	10.5
T2	11.3	75.1	13.6
T3	8.6	79.3	12.1
T4	10.2	83.6	6.2
OT	7.5	87.5	5.0
	Small (<60 nm)%	Median (60–90 nm)%	Large (>60 nm)%
A1	90.0	10.0	0.0
A3	95.1	4.9	0.0
A9	93.1	6.9	0.0
A11	87.3	10.9	1.8
OA	94.3	5.7	0.0
T1	90.4	5.8	3.8
T2	94.6	1.8	3.6
T3	92.9	7.1	0.0
T4	92.0	6.0	2.0
OT	95.0	3.3	1.7

OA and OT: oceanic stations. Number of viruses counted for this analysis varied from 95 to 112 according to their abundance.

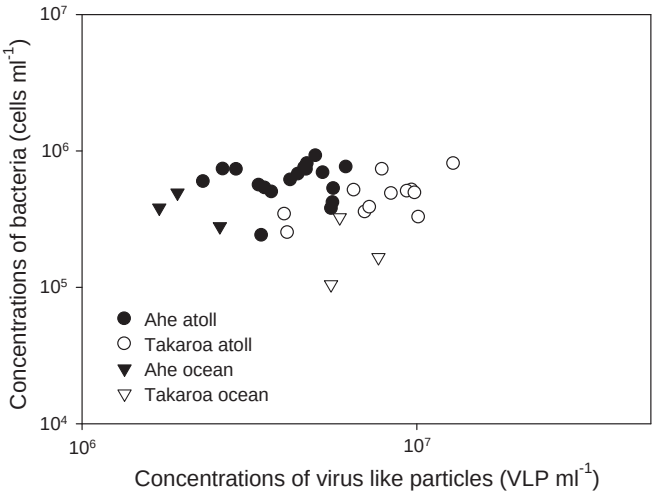

Fig. 4. Distribution of virus like particle and bacteria in lagoon and ocean of the two atolls (Ahe and Takaroa). Regression coefficient between the two variables: $r = 0.008$; $p = 0.963$; $n = 36$.

production (Wommack and Colwell, 2000; Bonilla-Findji et al., 2009). This result also confirms that the Takaroa atoll can be defined as a more productive lagoon system than the Ahe atoll. In most aquatic environments, viral abundance is closely correlated to bacterial biomass (Drake et al., 1998; Filippini and Middelboe, 2007) and activity (Heldal and Bratbak, 1991; Middelboe et al., 2003). These positive relationships suggest that viral replication relies strongly on the host abundance and metabolism (Danovaro et al., 2008). Nevertheless, bacterial abundance distribution appeared to be independent of the virus abundance in Ahe and Takaroa (Fig. 4), with no coupling between the patterns of the two variables (regression coefficient $r = 0.008$; $p = 0.963$; $n = 36$). As concluded by Dinsdale et al. (2008), these results suggest that the characteristics of these relationships are not static but may be associated with the local conditions in each atoll. The reason for this lack of coupling may also be due to the dominance of virioplankton from sources other than bacterioplankton, such as cyanobacteria (*Synechococcus* and *Prochlorococcus*), which are of the same order of magnitude as the abundance of bacterioplankton at the study sites (Thomas et al., 2010; Boury et al., 2012).

The two major viral reproductive strategies are lysogeny (bacteria containing inductible prophages) and lytic viral infection (bacteria in a lytic stage of infection). Our results indicate that virioplankton are not the main agent of bacterial mortality via the lytic cycle. Fractions of infected bacterial cells (FIC) were all extremely low (mean = 0.15%), among the lowest recorded in both marine and freshwater systems [see Table 6 in Weinbauer (2004)], regardless of the depth sampled. Nevertheless, to determine how many bacterial cells need to die to maintain the standing stock of virioplankton, it is also necessary to know how many virioplankton are released when one cell lyses. This is the burst size. An average burst size of 25 has been calculated for natural marine communities (Wommack and Colwell, 2000), and this study confirms this for the few infected cells analyzed by TEM (mean burst size 28.2 ± 21.5). This low percentage of infected cells may be attributed to the virucidal properties of solar radiation, especially UV wavelengths, which are often reported to have a significant effect on viral stocks and infectivity (Bettarel et al., 2006). High FLC was reported for some stations (close to 8% at stations A3 and T1), with the highest value at station A1 (88 ± 17%; Table 2).

Lysogeny is thought to be a strategy for virus propagation in systems with poor growth conditions for their bacterial hosts that would be unfavorable for their replication (Weinbauer et al., 2003; Fuhrman, 1999). Mitomycin C and UVC radiation are the most powerful agents inducing the lytic cycle in lysogenized bacterial communities (Ackermann and DuBow, 1987). Weinbauer and Suttle (1999) found that solar radiation caused prophase induction in 86% of the samples. This may well explain the low percentages of FLC reported in the oceanic zone in the study (2.5–8%), where there was probably continuous prophase induction due to the high solar radiation, releasing virioplankton (lytic cycle) outside the bacterial cells. Weinbauer (2004) reported that lysogeny in natural communities as determined by prophage induction due to mitomycin C ranged from not detectable to almost 100. Given the small dataset in this study, it is only possible to suggest that lysogeny is an advantage in situations where the bacterial abundance is insufficient, especially owing to the oligotrophic nutrient concentrations. This conclusion clearly merits further study in coral reef systems.

The potentially small contribution of virioplankton to the control of bacterioplankton may be associated with strong predation pressure from protists. The lack of coupling between bacterioplankton and virioplankton and the very low FIC% observed in this study suggest that the release of labile organic material from dead bacterial cells (viral shunt) did not appear to be the major factor source of nutrient regeneration. This conclusion differs from results published for temperate coastal regions demonstrating the viral shunt is an essential source of labile organic carbon in many ecosystems (Fuhrman, 1999; Wilhelm and Suttle, 1999; Suttle, 2005).

Bacterial and viral parameters were also studied in the benthic compartment at one site of Ahe. Few data are available about coral reef sediment (e.g., Paul et al., 1993; Patten et al., 2008), especially for bacterial production. Our values of benthic bacterial production (5.2×10^{11} cells l^{-1} d^{-1}) were within the range of values from marine littoral sediments (1.5 to 8.7 $\times 10^{11}$ cells l^{-1} d^{-1}; Gulf of Riga; Tuomi et al., 1999). These values were significantly lower than those reported from freshwater sediments in tropical zones (1.9×10^{12} cells l^{-1} d^{-1}; Bettarel et al., 2006). When compared to the pelagic bacterial production at the same station A11 (3.1×10^{8} cells l^{-1} d^{-1}), benthic bacterial production was higher

and seemed to be as significant as in elemental cycling by heterotrophic metabolism. As for all other studies where virus have been studied in both water column and sediment compartments (Hewson et al., 2001; Mei and Danovaro, 2004; Weinbauer, 2004), abundances in sediment exceeded those in water column by 2000. Mei and Danovaro (2004) recently calculated from the literature that a mean benthic-to-pelagic ratio of 20 for viral abundance in both marine and freshwater systems. In this study, the counts gave a ratio of 40. High abundances of virus in sediments suggest that they are important players in benthic systems but the limited observations available on the role of viruses in sediment tend to be conflicting (Filippini and Middelboe, 2007). In freshwater sediment, Filippini et al. (2006) and Bettarel et al. (2006) reported high viral abundance and an absence of infected bacterial cells. The high VBR found in Ahe atoll (mean of 51) confirms that viruses in benthic environments are an apparently dynamic and potentially ecologically relevant element, within reef ecosystems.

The characteristics of the bacterial and viral communities in the two atolls depend on the characteristics of the seawater, which are affected by regional oceanographic differences, including local circulation, effects of lagoons, run-off from the land and the community structure in the benthic environment, including the activities of the many large oyster farms. Given increasing concern about the widespread decline of the world's coral reefs (Hoegh-Guldberg, 1999; Knowlton, 2001; Gardner et al., 2003), it would be advisable to take into account the potential importance of virioplankton within these systems. Although these results should be interpreted with caution since they were obtained during only one season, the distribution patterns of virioplankton are apparently not coupled to the spatial dynamics of the bacterioplankton communities. Viral infection is, therefore, probably not the major agent responsible for bacterial mortality in these coral reef systems.

Acknowledgements

This work was supported by the European Development Fund, in collaboration with the Service de la Perliculture and the University of French Polynesia. We should like to thank P. Calquin and P. Bonin for their valuable help in collecting samples. Constructive comments and suggestions were provided by the reviewers.

References

Ackermann, H.W., 2001. Frequency of morphological phage description in the year 2000. Arch. Virol. 146, 843–857.

Ackermann, H.W., DuBow, M.S., 1987. Viruses of Prokaryotes, Natural Groups of Bacteriophages. vol. 2. CRC Press.

Alonso, M., Jimenez-Gomez, F., Rodriguez, J., Borrego, H., 2001. Distribution of virus-like particles in an oligotrophic marine environment (Alborean Sea, Western Mediterranean). Microb. Ecol. 42, 407–415.

Andréfouët, S., Charpy, L., Lo-Yat, A., Lo, C., 2012. Recent reseach for pearl oyster aquaculture management in French Polynesia. Mar. Pollut. Bull. 65, 407–418.

Andréfouët, S., Pagès, J., Tartinville, B., 2001. Water renewal time for classification of atoll lagoons in the Tuamotu Archipelago (French Polynesia). Coral Reefs 20, 399–408.

Auguet, J.C., Montanie, H., Lebaron, P., 2006. Structure of virioplankton in the Charente estuary (France): transmission electron microscopy versus pulsed field gel electrophoresis. Microb. Ecol. 5, 197–208.

Bettarel, Y., Bouvy, M., Dumont, C., Sime-Ngando, T., 2006. Virus-bacterium interactions in water and sediment of West African inland aquatic systems. Appl. Environ. Microbiol. 72, 5274–5282.

Bettarel, Y., Desnues, A., Rochelle-Newall, E., 2010. Lytic failure in cross-inoculation assays between phages and prokaryotes from three aquatic sites of contrasting salinity. FEMS Microbiol. Lett. 311, 113–118.

Bettarel, Y., Bouvier, T., Agis, M., Bouvier, C., Chu, T.V., Combe, M., Mari, X., Nghiem, M.N., Nguyen, T.T., Pham, T.T., Pringault, O., Rochelle-Newall, E., Torréton, J.-P., Tran, H.Q., 2011. distribution and life strategies in the Bach Dang estuary, Vietnam. Microb. Ecol. 62, 143154.

Bonilla-Findji, O., Herndl, G.J., Gatusso, J.P., Weinbauer, M.G., 2009. Viral and flagellate control of prokaryotic production and community structure in offshore Mediterranean waters. Appl. Environ. Microbiol. 75, 4801–4812.

Bouvy, M., Dupuy, C., Pagano, M., Barani, A., Charpy, L., 2012. Do human activities affect the picoplankton structure of the Ahe atoll lagoon (Tuamotu Archipelago, French Polynesia)? Mar. Pollut. Bull. 65, 516–524.

Charpy, L., 1996. Phytoplankton biomass and production in two Tuamotu Atoll lagoons (French Polynesia). Mar. Ecol. Prog. Ser. 145, 133–142.

Charpy, L., Blanchot, J., 1996. *Prochlorococcus* contribution to phytoplankton biomass and production of Takapoto Atoll (Tuamotu Archipelago). C.R. Acad. Sci. Paris 319, 131–137.

Cochlan, W.P., Wikner, J., Steward, G.F., Smith, D.C., Azam, F., 1993. Spatial distribution of viruses, bacteria and chlorophyll-*a* in neritic, oceanic and estuarine environments. Mar. Ecol. Prog. Ser. 92, 77–87.

Cole, J.J., Findlay, S., Pace, M.L., 1988. Bacterial production in fresh and saltwater ecosystems: a cross-system overview. Mar. Ecol. Prog. Ser. 43, 1–10.

Danovaro, R., Dell'anno, A., Trucco, A., Serresi, M., Vanucci, S., 2001. Determination of virus abundance in marine sediments. Appl. Environ. Microbiol. 67, 1384–1387.

Danovaro, R., Dell'Anno, A., Corinaldesi, C., Magagnini, M., Noble, R., Tamburini, C., Weinbauer, M., 2008. Major viral impact on the functioning of benthic deep-sea ecosystems. Nature 454, 1084–1088.

Davy, J.E., Patten, N.L., 2007. Morphological diversity of virus-like particles within the surface microlayer of scleractinian corals. Aquat. Microb. Ecol. 47, 37–44.

Del Giorgio, P.A., Davies, J., 2003. Patterns in dissolved organic matter availability and consumption across aquatic ecosystems. In: Findlay, S., Sinsabaugh, R.L. (Eds.), Aquatic Ecosystems: Interactivity of Dissolved Organic Matter. Academic Press, Amsterdam, pp. 399–424.

Dinsdale, E.A., Pantos, O., Smrigs, S., Edwards, R.A., Angly, F., et al., 2008. Microbial ecology of four coral atolls in the northern line islands. PLoS ONE 3, 1–17.

Drake, L.A., Choi, K.H., Haskell, A.G.E., Dobbs, F.C., 1998. Vertical profiles of virus-like particles and bacteria in the water column and sediments of Chesapeake Bay, USA. Aquat. Microb. Ecol. 16, 17–25.

Ducklow, H.W., 1990. The biomass, production and fate of bacteria in coral reefs. In: Dubinsky, Z. (Ed.), Coral Reefs. Elsevier, Amsterdam, pp. 265–290.

Dumas, F., Le Gendre, R., Thomas, Y., Andréfouët, S., 2012. Tidal flushing and wind driven circulation of Ahe atoll lagoon (Tuamotu Archipelago, French Polynesia) from in situ observations and numerical modelling. Mar. Pollut. Bull. 65, 425–440.

Ferrier-Pages, C., Gattuso, J.P., Cauwet, G., Jaubert, J., Allemand, D., 1998. Release of dissolved organic matter and nitrogen by the zooxanthellate coral *Galaxa fascicularis*. Mar. Ecol. Prog. Ser. 172, 263–274.

Filippini, M., Middelboe, M., 2007. Viral abundance and genome size distribution in the sediment and water column of marine and freshwater ecosystems. Microb. Ecol. 60, 397–410.

Filippini, M., Buesing, N., Bettarel, Y., Sime-Ngando, T., Gessner, M.O., 2006. Infection paradox: high abundance but low impact of freshwater benthic viruses. Appl. Environ. Microbiol. 72, 4893–4898.

Frias-Lopez, J., Zerkle, A.L., Bonheyo, G.T., Fouke, B.W., 2002. Partitioning of bacterial communities between seawater and healthy, black band diseased, and dead coral surfaces. Appl. Environ. Microbiol. 68, 2214–2228.

Fuhrman, J.A., 1999. Marine viruses and their biogeochemical and ecological effects. Nature 399, 541–548.

Gardner, T.A., Cote, I.M., Gill, J.A., Grant, A., Watkinson, A.R., 2003. Long-term region-wide declines in Caribbean corals. Science 301, 958–960.

Gast, G.J., Wiegman, S., Wieringa, E., van Duyl, F.C., Bak, R.P.M., 1998. Bacteria in coral reef water types: removal of cells, stimulation of growth and mineralization. Mar. Ecol. Prog. Ser. 167, 37–45.

Haglund, A.-L., Lantz, P., Tornblom, E., Tranvik, L., 2003. Depth distribution of active bacteria and bacterial activity in lake sediment. FEMS Microbiol. Ecol. 46, 31–38.

Heldal, M., Bratbak, G., 1991. Production and decay of viruses in aquatic environments. Mar. Ecol. Prog. Ser. 72, 205–212.

Hewson, I., O'Neil, J.M., Fuhrman, J.A., Dennison, W.C., 2001. Virus-like particle distribution and abundance in sediments and overlaying waters along eutrophication gradients in two subtropical estuaries. Limnol. Oceanogr. 46, 1734–1746.

Hoegh-Guldberg, O., 1999. Coral bleaching, climate change and the future of the worlds coral reefs. Mar. Freshw. Res. 50, 839–866.

Hoppe, H.G., Schramm, W., Bacold, P., 1988. Spatial and temporal distribution of pelagic microorganisms and their proteolytic activity over a partly destroyed coral reef. Mar. Ecol. Prog. Ser. 44, 95–102.

Kirscher, A.K.T., Velimirov, B., 1999. Benthic bacterial secondary production measured via simultaneously 3H-thymidine and 14C-leucine incorporation and its implication for the carbon cycle of a shallow macrophytic-dominated black water system. Limnol. Oceanogr. 44, 1871–1881.

Knowlton, N., 2001. The future of coral reefs. Proc. Natl. Acad. Sci. USA 98, 5419–5425.

Loret, P., Le Gall, S., Dupuy, C., Blanchot, J., Pastoureaud, A., Delesalle, B., Caisey, X., Jonquières, G., 2000. Heterotrophic protists as a trophic link between picocyanobacteria and the peral oyster Pinctada margaritifera in the Takapoto lagoon (Tuamotu Archipelago, French Polynesia). Aquat. Microb. Ecol. 22, 215–226.

Mari, X., Kerros, M.E., Weinbauer, M.G., 2007. Virus attachment to transparent exopolymeric particles along trophic gradients in the southwest lagoon in New Caledonia. Appl. Environ. Microbiol. 73, 5245–5252.

Middelboe, M., Glud, R.N., Finster, K., 2003. Distribution of viruses and bacteria in relation to diagenetic activity in an estuarine sediment. Limnol. Oceanogr. 48, 1447–1456.

Mei, M.L., Danovaro, R., 2004. Virus production and life strategies in aquatic sediments. Limnol. Oceanogr. 49, 459–470.
Moriarty, D.J.W., 1979. Biomass of suspended bacteria over coral reefs. Mar. Biol. 53, 193–200.
Moriarty, D.J.W., Pollard, P.C., Hunt, W.G., 1985. Temporal and spatial variation in bacterial production in the water column over a coral reef. Mar. Biol. 85, 285–292.
Pagès, J., Andréfouët, S., Delesalle, B., Prasil, V., 2001. Hydrology and trophic state in Takapoto Atoll lagoon: comparison with other Tuamotu lagoons. Aquat. Living Res. 14, 183–193.
Patel, A., Noble, R.T., Steele, J.A., Schwalbach, M.S., Hewson, I., Fuhrman, J.A., 2007. Virus and prokaryote enumeration from planktonic aquatic environments by epifluorescence microscopy with SYBR Green I. Nat. Protoc. 2, 269–276.
Patten, N.L., Mitchell, J.G., Middelboe, M., Eyre, B.D., Seuront, L., Harrison, P.L., Glud, R.N., 2008. Bacterial and viral dynamics during a mass coral spawning period on the Great Barrier Reef. Aquat. Microb. Ecol. 50, 209–220.
Patten, N.L., Wyatt, A.S.J., Lowe, R.J., Waite, A.M., 2011. Upstage of picophytoplankton, bacterioplankton and virioplankton by a fringing coral reef community (Ningaloo Reef, Australia). Coral Reefs 30, 555–567.
Paul, J.H., DeFlaun, M.F., Jeffrey, W.H., 1986. Elevated levels of microbial activity in the coral surface microlayer. Mar. Ecol. Prog. Ser. 33, 29–40.
Paul, J.H., Rose, J.B., Jiang, S.C., Kellogg, C.A., Dickson, L., 1993. Distribution of viral abundance in the reef environment of Key Largo, Florida. Appl. Environ. Microbiol. 59, 718–724.
Porter, K.G., Feig, Y.S., 1980. The use of DAPI for identifying and counting aquatic microflora. Limnol. Oceanogr. 25, 943–948.
Pouvreau, S., Jonquières, G., Buestel, D., 1999. Filtration by the pearl oyster *Pinctada margaritifera*, under conditions of low seston load and small particles size in a tropical lagoon habitat. Aquaculture 176, 295–314.
Proctor, L.M., Fuhrman, J.A., 1990. Viral mortality of marine bacteria and cyanobacteria. Nature 343, 60–62.
Robarts, R.D., Zohary, T., 1993. Fact or fiction–bacterial growth rates and production as determined by (methyl-3H)-thymidine? Adv. Microb. Ecol. 13, 371–425.
Rochelle-Newall, E.J., Torréton, J.-P., Mari, X., Pringault, O., 2008. Phytoplankton–bacterioplankton coupling in a subtropical South Pacfic coral reef lagoon. Aquat. Microb. Ecol. 50, 221–229.
Rohwer, F., Seguritan, V., Azam, F., Knowlton, N., 2002. Diversity and distribution of coral associated bacteria. Mar. Ecol. Prog. Ser. 243, 1–10.
Seymour, J.R., Pattern, N., Bourne, D.G., Mitchell, J.G., 2005. Spatial dynamics of virus like particles and heterotrophic bacteria within a shallow coral reef system. Mar. Ecol. Prog. Ser. 288, 1–8.
Suttle, C.A., 2005. Viruses in the sea. Nature 437, 356–361.
Thingstad, T.F., 2000. Elements of a theory for the mechanisms controlling abundance, diversity and biogeochemical role of lytic bacterial viruses in aquatic systems. Limnol. Oceanogr. 45, 1320–1328.
Thomas, Y., Garen, P., Courties, C., Charpy, L., 2010. Spatial and temporal variability of the pico-and nanophytoplankton and bacterioplankton in a deep Polynesian atoll lagoon. Aquat. Microb. Ecol. 59, 89–101.
Torréton, J.P., 1999. Biomass, production and heterotrophic activity of bacterioplankton in the Great Astrolabe Reef lagoon (Fidji). Coral Reefs 18, 43–53.
Torréton, J.P., Dufour, P., 1996. Temporal and spatial stability of bacterioplankton biomass and productivity in an atoll lagoon. Aquat. Microb. Ecol. 11, 251–261.
Tuomi, P., Lundsgaard, C., Ekebom, J., Olli, K., Künnis, K., 1999. The production and potential loss mechanisms of bacterial biomass in the southern Gulf of Riga. J. Mar. Syst. 23, 185–196.
van Duyl, F.C., Gast, G.J., 2001. Linkage of small-scale spatial variations in DOC, inorganic nutrients and bacterioplankton growth with different coral reef water types. Aquat. Microb. Ecol. 24, 17–26.
Weil, E., Smith, G., Gil-Agudelo, D.L., 2006. Status and progress in coral reef disease research. Dis. Aquat. Org. 69, 1–7.
Weinbauer, M.G., 2004. Ecology of prokaryotic viruses. FEMS Microbiol. Rev. 28, 127–181.
Weinbauer, M.G., Fuchs, D., Peduzzi, P., 1993. Distribution of viruses and dissolved DNA along a coastal trophic gradient in the northern Adriatic Sea. Appl. Environ. Microbiol. 59, 4074–4082.
Weinbauer, M.G., Höfle, M.G., 1998. Size-specific mortality of lake bacterioplankton by natural virus communities. Aquat. Microb. Ecol. 15, 103–113.
Weinbauer, M.G., Peduzzi, P., 1995. Significance of viruses versus heterotrophic nanoflagellates for controlling bacterial abundance in the northern Adriatic Sea. J. Plankton Res. 17, 1851–1856.
Weinbauer, M.G., Winter, C., Hofle, M., 2002. Reconsidering transmission electron microscopy based estimates of viral infection of bacterioplankton using conversion factors derived from natural communities. Aquat. Microb. Ecol. 27, 103–110.
Weinbauer, M.G., Nedoma, J., Christaki, U., Simek, K., 2003. Comparing the effects of resource enrichment and grazing on viral production in a meso-eutrophic reservoir. Aquat. Microbiol. Ecol. 31, 137–144.
Weinbauer, M.G., Kerros, M.-E., Motegi, C., Wilhartiz, I.C., Rassoulzadegan, F., Torréton, J.-P., Mari, X., 2010. Bacterial community composition and potential controlling mechanisms along a trophic gradient in a barrier reef system. Aquat. Microb. Ecol. 60, 15–28.
Wild, C., Huettel, M., Klueter, A., Kremb, S.G., Rasheed, M.Y.M., Jorgensen, B.B., 2004. Coral mucus functions as an energy carrier and particle trap in the reef ecosystem. Nature 428, 66–70.
Wilhelm, S.W., Suttle, C.A., 1999. Viruses and nutrient cycles in the sea. Bioscience 49, 781–788.
Wommack, K.E., Colwell, R.A., 2000. Virioplankton: viruses in aquatic ecosystems. Microbiol. Mol. Biol. Rev. 64, 69–114.
Yentsch, C.S., Menzel, D.W., 1963. A method for the determination of phytoplankton, chlorophyll and phaeophytin by fluorescence. Deep-Sea Res. 10, 221–231.

Marine Pollution Bulletin 65 (2012) 516–524

Contents lists available at SciVerse ScienceDirect

Marine Pollution Bulletin

journal homepage: www.elsevier.com/locate/marpolbul

Do human activities affect the picoplankton structure of the Ahe atoll lagoon (Tuamotu Archipelago, French Polynesia)?

Marc Bouvy [a,*], Christine Dupuy [b], Marc Pagano [c], Aude Barani [d], Loic Charpy [e]

[a] UMR 5119, ECOSYM, Ecologie des Systèmes Marins Côtiers (UM2, CNRS, IRD, Ifremer, UM1), Université Montpellier 2, Place Eugène Bataillon, Case 093, 34095 Montpellier Cedex 5, France
[b] Littoral, Environnement et SociétéS (LIENSs), Université de La Rochelle, UMR 6250 CNRS-ULR, 2 rue Olympe de Gouges, 17000 La Rochelle Cedex, France
[c] IRD – UMR MIO (Mediterannean Institut of Oceanography), Campus de Luminy Case 901, 13288 Marseille Cedex 09, France
[d] PRECYM Platform, UMS 2196, Campus de Luminy, Case 901, 13288 Marseille Cedex 09, France
[e] UMR MIO, Center of Tahiti, BP 529, 98713 Papeete, French Polynesia

ARTICLE INFO

Keywords:
Picoplankton
Enrichment experience
Human sewage
Atoll

ABSTRACT

The spatial variations of the picoplankton (photoautotrophic and heterotrophic microorganisms) in the Ahe atoll lagoon were studied in May and October 2008 to assess whether they were affected by human activities along the atoll. Spatial patterns were studied using 10 sampling stations chosen according to the location of the anthropogenic activities (pearl farming, harbor). Experiments were also carried out to determine whether bacterial growth, with or without predators, was limited by inorganic (N and P) substrates. The results showed that heterotrophic bacterioplankton abundance was superior to the photoautotrophic organisms, especially in May. Significant increases in bacterial abundance were observed in May after 24 h incubation with +P and +N (but not in October). All samples complied with the quality levels for fecal indicator bacteria (FIB) defined by the European Union and there was no evidence that human sewage had any impact on picoplankton over the whole atoll.

1. Introduction

Human activities have a major impact on marine ecosystems. The pressures exerted are diverse and result from a wide range of activities such as coastal engineering, sediment dredging, pollution, fishing, aquaculture, urban development, maritime transport, tourism, mining, oil extraction, transport and refining of oil, agricultural and industrial activities (Islam and Tanaka, 2004; Halpern et al., 2008). All these activities have an effect on the components of the marine food web, from microorganisms to top animal predators. A recent report analyzed the ecological impact of anthropogenic activities in the oceans worldwide, focusing on stressors that can be evaluated at global scale (Halpern et al., 2008). All the analyzed ocean ecosystems (coral reefs, mangroves, seagrass meadows, seamounts, rocky reefs, soft shallow areas, continental shelf areas, slope areas, pelagic waters and the deep sea) can be considered to be affected by anthropogenic activities, although to different degrees (Nogales et al., 2011).

In a context of eutrophication, the composition and structure of microbial communities are also basic indicators of ecosystem status, including phytoplankton bloom and the heterotrophic activity of aerobic and anaerobic bacteria (Paerl et al., 2002; Bouvy et al., 2010). Nutrient availability (bottom-up control), predation by protozoa (top-down control) and viral lysis are the most important factors regulating bacterial communities. Organic carbon has usually been considered to be the main factor limiting the growth of pelagic heterotrophic bacteria. However, studies on nutrient limitation of such communities have shown that mineral limitation of growth rate is widespread in various marine ecosystems (Torréton et al., 2000; Carlsson and Caron, 2001). Nutrient enrichment is a direct consequence of eutrophication, modifying the biological abundance and activity at each trophic level and, for example, increasing bacterial standing stocks and production (Ducklow and Shiah, 1993). Nutrient enrichment bioassays are the most direct method for assessing the nutrient status of phytoplankton and bacterioplankton communities and this method has been widely used (Torréton et al., 2000; Bouvy et al., 2004).

Although viral infection is now considered to be one of the major structuring processes in the dynamics of marine microbial communities (Fuhrman, 1999), grazing by heterotrophic nanoflagellates (HNF) has been identified as the main limiting factor affecting bacteria and has been shown to hinder bacterial production, thus regulating bacterial biomass in a large number of pelagic ecosystems (Solic and Krstulovic, 1994; Christaki et al., 1999; Ferrier-Pagès and Furla, 2001). Size-selective grazing coupled with resource availability has been shown to be a shaping force in both the taxonomic and phenotypic structures of bacterial communities (Jürgens

* Corresponding author. Tel.: +33 467144128.
E-mail address: marc.bouvy@ird.fr (M. Bouvy).

0025-326X/$ - see front matter © 2012 Elsevier Ltd. All rights reserved.
doi:10.1016/j.marpolbul.2012.01.008

Table 1
List of stations studied in Ahe atoll with their geographical coordinates. Maximum depth and average temperature of the water column are reported for the two surveys (May and October 2008).

Station code	Station name	Latitude south	Longitude west	Depth (m)
1	Raita pension	14°27′ 10″	146°13′18″	2.0
2	Motu Tahiri farm	14°30′39″	146°15′53″	3.7
3	Maruata farm	14°31′18″	146°18′32″	2.5
4	Aito pearl farm	14°31′28″	146°19′03″	1.8
5	Apeang farm	14°31′14″	146°19′44″	3.4
6	Harbor village	14°32′17″	146°21′24″	2.5
7	Manuia farm	14°31′17″	146°22′51″	1.7
8	Kamoka farm	14°28′53″	146°22′67″	10.0
9	Mamaha farm	14°26′29″	146°19′38″	1.8
10	Pang Fat Kyn farm	14°25′57″	146°16′23″	3.8

and Matz, 2002). However, although factors controlling bacterial communities in temperate and tropical areas have been studied, little research has been undertaken to study these microorganisms in atolls (Gonzalez et al., 1998; Ferrier-Pagès and Furla, 2001).

In addition to their role in the organic matter mineralization and in the diet for heterotrophic nanoflagellates, micro-organisms are effective descriptors for evaluating and predicting the environmental impact of human activities. Continental waters are often polluted by pathogenic microorganisms from recreational marinas, sewage disposal sites, septic tanks, rainfall runoff from urban areas and many other sources (Lipp et al., 2001; Aslan-Yilmaz et al., 2004). Fecal indicator bacteria (FIB) including thermo tolerant coliforms (TTC) and fecal streptococci (FS) are used as surrogates for human and animal pathogens for assessing water quality. In epidemiological studies, FIB are documented as being associated with an increased risk of contracting gastrointestinal and respiratory illnesses after contact with waters with high concentrations (Haile et al., 1999). Their origin has always been presumed to be anthropogenic (e.g. sewage, agricultural and urban runoff). An important criterion for assessing the potential health risk for recreational waters is the FIB density. Although FIB do not necessarily induce illness, they are often associated with pathogenic bacteria, viruses and parasites in domestic sewage. Microbial water quality varies according to the magnitude of inputs and the flow and dispersion of organisms as a result of near-shore hydrodynamics such as tides and currents (Davies-Colley et al., 1994).

French Polynesia made up of several lagoons are of great importance to the economy of the region, where farming of pearl oyster, *Pinctada margaritifera*, is the major source of export earnings, especially from Ahe atoll (Thomas et al., 2010; Andréfouët et al., 2012). The main objective of this study was to estimate the impacts of human activities along the Ahe atoll by determining fecal indicator bacteria (FIB) and by describing the abundance of heterotrophic and autotrophic picoplankton in the lagoon. For this, spatial patterns (10 sampling stations) and temporal patterns (before and after the rainy season) were studied using 10 biological indicators. Bacterial responses to nutrient enrichment based on bioassay experiments at one station were also studied for the two periods.

2. Material and methods

2.1. Study site and sample collection

This study was conducted in the Ahe atoll, 500 km northeast of Tahiti, in the north of the Tuamotu Archipelago (Fig. 1; see details in Thomas et al., 2010). Ahe lagoon is 142 km^2 in area, with a maximum depth close to 70 m, and can be defined as a semi-enclosed atoll. There is one passage to the west of the lagoon and there are several reef-flats (less than 50 cm depth) along the reef rim.

This study was conducted at the end of dry season (May 2008, temperature: 28.61 ± 0.04 °C) and at the end of the rainy season (October 2008, temperature: 27.12 ± 0.06 °C). Ten stations (S1 to S10; see Table 1) were sampled, near pearl farms mostly found along the shoreline of the atoll. Samples were taken at a depth of 0.5 m, using 2 l sterile acid-cleaned bottles.

2.2. Biological analyses

Heterotrophic bacteria and picoautotrophic cells were fixed with 0.2 μm filtered formaldehyde (final concentration 2%) and frozen in liquid nitrogen. All samples were analyzed using a MoFlo™ flow cytometer (Beckman-Coulter) equipped with a dual line, water-cooled, Coherent™ argon laser (351 and 488 nm). All data were collected in log scale, stored in list mode and analyzed with the Summit™ software package (Beckman-Coulter, Miami, FL). Standard protocols were used to enumerate phytoplankton and heterotrophic prokaryotes (Marie et al., 1999). A 1 ml formaldehyde-fixed subsample was incubated with DAPI at a final concentration of 1/10,000 for 15 min at room temperature in the dark. Fluorescent beads (2 μm Fluoresbrite™ Polysciences Inc., Warrington, PA, USA) were added to each sample to normalize and control the flow cytometer settings. For heterotrophic bacteria analysis, the side (SSC) light scatter of the photons from the 488 nm laser beam was used as trigger signal and DAPI fluorescence, excited by the UV laser, was collected in the range 405/30 nm (FL4). Combining DAPI fluorescence and light scattering unambiguously distinguishes cells from inorganic particles, detritus and free DNA (Marie et al., 1999). Picophytoplankton (*Prochlorococcus* sp. and *Synechococcus* sp. cells) and autotrophic picoeukaryotes counts were performed using the red fluorescence emission (from the 488 nm laser beam) as trigger signal. Cells were detected and enumerated according to their SSC and FSC properties, and their orange fluorescence (580/30 nm) and red fluorescence (>640 nm) from phycoerythrin and chlorophyll pigments, respectively.

The net bacterial production was estimated from the DNA synthesis rates measured by (^{3}H-methyl) thymidine (^{3}H-TdR) incorporation by microcentrifuge (Smith and Azam, 1992). A subsample was added to a sterile polystyrene snap cap tube containing a final saturating concentration of 20 nM of ^{3}H-TdR (specific activity 53 Ci mmol^{-1}, Amersham). Triplicate live samples and a control were run for each assay. The bacterial growth was measured in the dark at *in situ* temperature for a short incubation time (no longer than 1 h). Incorporation was terminated by adding TCA (5% final concentration) and samples were then stored for at least 2 h at 4 °C. After centrifugation, the precipitates were rinsed three times with 5% TCA and then resuspended in a liquid scintillation cocktail (Ultima Gold LLT, Perkin–Elmer) before the radioactivity was determined using a liquid scintillation counter (Beckman LS 6500). The results were expressed as μgC l^{-1} h^{-1} using the conversion factors determined by Gundersen et al. (2002) of 14fC per bacteria and our unpublished data of 8.6×10^{17} cells per mole of thymidine incorporated.

The chlorophyll concentrations were determined by fluorometry after filtration of samples onto Whatman GF/F fiberglass filters, directly extracted using methanol (Welschmeyer, 1994).

2.3. Fecal indicator bacteria

For FIB, a membrane filtration method was used to count thermo tolerant coliform (TTC) and fecal streptococci (FS) as colony forming units per 100 ml of the sample. TTC were counted as the number of blue colonies of 1–2 mm developed on mFC medium (Sartorius) after 24 h incubation at 44.5 °C. Small red to reddish-brown colonies of FS (~1 mm) were counted on Slanetz and Bartley medium (Sartorius) after 48 h incubation at 37 °C.

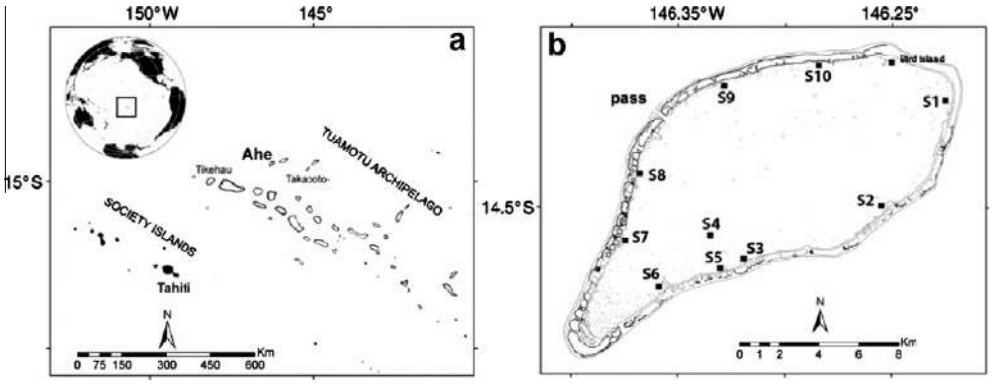

Fig. 1. Location of the Tuamotu Archipelago and of the 10 stations studied in Ahe atoll. Location of the pass (between S8 and S9) is noted.

2.4. Enrichment bioassay

Samples for the bioassays were taken from station S1 in front of the laboratory in the northeast of the atoll. Lagoon water samples were taken at 0.5 m depth. Two bioassay series were conducted to compare the responses of the bacterial community to inorganic enrichment with 100% of predators (using <50 μm-filtered water) and with 1% (using 99% of 0.22 μm-filtered water and 1% of <50 μm-filtered water) bacterial predators. Each of these was homogenized and distributed equally into two series of 4×100 ml Whirl-Pak® polyethylene sterile bags which allow the transmission of 70% UV radiation. At time zero ($t0$), inorganic nitrogen (mixture of 20 μM as NH_4Cl and 20 μM as NO_3) and inorganic phosphorus (2 μM as NaH_2PO_4) were added alone or in combination: +N, +P, +NP; nothing was added to the controls called C. All assays were performed in triplicate with a total of 24 Whirlpaks per experiment. All Whirlpaks were incubated for 24 h in a floating enclosure held at 2 m below the surface of the water. The water temperature stayed fairly constant during the experiments (28.6 ± 0.55 °C in May and 27.03 ± 0.37 °C in October). Subsamples were removed at time zero ($t0$) and after 24 h ($t24$) incubation to measure the bacterial abundance. The bacterioplankton growth rates in each triplicate were calculated as $\mu = (\ln N24 - \ln N0)/t$, where t was the incubation time and N24 and N0 were the bacterial concentration at the end and at the beginning of the incubation time. The grazing rates were calculated as the difference between apparent growth rate ($\mu + g$) and net growth rate (μ). The ingestion rate of HNF (I, bact HNF^{-1} h^{-1}) was calculated according to Davies and Sieburth (1984):

$$I = g \times N_{bact}/N_{HNF}$$

where g was the grazing rate (h^{-1}) and N_{bact} and N_{HNF} were the average concentrations of bacteria and HNF. To enumerate the nanoplanktonic cells, water samples (25 ml) were fixed and preserved with paraformaldehyde (1% final concentration). Samples were concentrated to 10 ml using a filtration tower with 0.8 μm pore size black polycarbonate filters (Nuclepore) and stained with DAPI (2.5×10^{-4} g l^{-1} final concentration). The stained nanoplanktonic cells were enumerated under UV light excitation on at least 15 randomly selected fields, at a magnification of ×1000. The method used in this study made it possible to distinguish pigmented nanoflagellates (PNF) from heterotrophic nanoflagellates (HNF) by repeatedly interchanging the filter sets (Caron, 1983): phototrophic cells (crimson under UV 365 nm excitation and red colored under green 450–490 nm excitation) and heterotrophic cells (blue under UV excitation and invisible under green excitation) were enumerated separately. Ciliates were enumerated using the Utermöhl method.

2.5. Data processing

The relationships between chlorophyll *a*, bacteria and picoautotroph abundances, fecal coliforms and streptococci were studied using multivariate analysis. All data was $x \rightarrow \log(x + 1)$ transformed and a centered Principal Component Analysis (PCA) was performed to identify the major sources of temporal and spatial variability in the microbial communities. Two variables Bravais–Pearson correlation was conducted on data log ($x + 1$). The data was processed using ADE-4 (Thioulouse et al., 1997). The differences between dates and stations for all parameters studied were tested using the non-parametric Mann–Whitney U-test. Differences were considered as significant when $p < 0.05$ (Sigma Stat version 3.5).

3. Results

The highest values for chlorophyll *a* were recorded in May 2008 (0.55 μg l^{-1} at station S7), with a mean value of 0.34 μg l^{-1}, significantly different from the mean recorded in October (0.21 μg l^{-1}, $p = 0.013$, Table 2). The total abundance of bacteria (BACT-A) was higher in May than in October ($p < 0.001$) with the highest values generally observed in the north of the atoll (Stations S9 and S10). However, the mean values for bacterial production (BACT-P) were similar in both surveys, with the highest values recorded in May at station S9 (15.22 μgC l^{-1} d^{-1}). Of the FIB, thermo-tolerant coliforms (TTC) were abundant in some stations with maximum values recorded at stations S9 and S10 in May (94 and 200 CFU 100 ml^{-1}, respectively). No significant differences were noted between the two surveys. A different pattern was observed for fecal streptococci (FS), with values significantly higher in May ($p = 0.003$), which were present in 80% of samples. The FS concentrations measured in October did not exceed 2 CFU 100 ml^{-1} in two stations. No significant correlation was observed between TTC and SF concentrations for any of the data ($r = 0.045$; $n = 20$). The average values were all below the EU guide level for marine water quality of 500 CFU 100 ml^{-1} for TTC and 100 CFU 100 ml^{-1} for FS.

Among the phytoplankton, there were two groups of cyanobacteria, *Synechococcus* (SYNE) and *Prochlorococcus* (PROC). *Synechococcus* abundances were similar in both surveys (9.6×10^4 cells ml^{-1} and 8.4×10^4 cells ml^{-1}), whereas *Prochlorococcus* concentrations were significantly lower in May (mean of 0.5×10^4 cells ml^{-1}) than in October (mean of 3.1×10^4 cells ml^{-1}; $p < 0.001$), with the highest values recorded at stations S8–S10 (Table 2). Picoeukaryotes (PICO) populations were similar for the two surveys, with no distinct distribution pattern irrespective of the season. Ratio between heterotrophic bacteria and picoautotroph abundances was significantly higher in May (mean ratio of 7.72) than in October (ratio of 1.64) ($p < 0.001$). In May, maximum values were recorded at stations S3,

Table 2
Mean and standard deviation (STD) for the parameters studied at each station during the two surveys (May and October 2008). Differences between surveys were tested using the non-parametric Mann–Whitney U-test. (ns. non significant = $p > 0.05$). Abbreviation: Chlo-a: chlorophyll-a; Bact-A: bacterial abundance; Bact-P: bacterial production; TTC: concentrations of thermotolerant coliforms; FS: concentration of faecal streptococci; SYNE: *Synechococcus* abundance; PROC: *Prochlorococcus* abundance; PICO: Pigmented picoeukaryote abundance; AUTO: Picoautotroph abundance; H/A: ratio between heterotroph (bacteria) and picoautotroph abundance. nd: non determined.

Station code	CHLOR (μg l^{-1})	BACT-A (cells ml^{-1})	BACT-P (μgC l^{-1} d^{-1})	TTC (CFU 100 ml^{-1})	SF (CFU 100 ml^{-1})	SYNE (cells ml^{-1})	PROC (cells ml^{-1})	PICOEUK (cells ml^{-1})	AUTO (cells ml^{-1})	H/A
May 2008										
S1	0.39	4.9×10^5	1.04	0	0	9.9×10^4	0.3×10^4	4.1×10^3	1.1×10^5	4.58
S2	0.23	6.3×10^5	0.58	1	5	12.0×10^4	0.6×10^4	5.0×10^3	1.3×10^5	4.67
S3	0.35	9.2×10^5	7.38	0	23	5.2×10^4	0.5×10^4	2.3×10^3	5.9×10^4	15.50
S4	0.33	6.3×10^5	1.04	0	2	10.0×10^4	0.5×10^4	3.0×10^3	1.1×10^5	5.54
S5	0.11	5.5×10^5	4.56	2	43	6.1×10^4	0.8×10^4	3.5×10^3	7.3×10^4	7.46
S6	0.39	9.0×10^5	4.42	13	9	13.0×10^4	0.3×10^4	5.5×10^3	1.4×10^5	6.46
S7	0.55	8.1×10^5	2.80	6	9	18.0×10^4	0.3×10^4	7.3×10^3	1.9×10^5	4.29
S8	0.37	5.2×10^5	0.42	7	0	7.2×10^4	0.9×10^4	4.0×10^3	8.5×10^4	6.11
S9	0.26	7.9×10^5	15.22	94	12	5.8×10^4	0.6×10^4	5.4×10^3	6.9×10^4	11.49
S10	0.37	1.1×10^6	3.50	200	8	8.6×10^4	0.5×10^4	9.8×10^3	1.0×10^5	11.13
Mean	0.34	7.4×10^5	4.10	32	11	9.6×10^4	0.5×10^4	5.0×10^3	1.1×10^5	7.72
Std	0.12	2.1×10^5	4.49	66	13	3.9×10^4	0.2×10^4	2.2×10^3	3.9×10^4	3.75
October 2008										
S1	nd	1.1×10^5	0.48	4	1	11.0×10^4	2.4×10^4	4.6×10^3	1.4×10^5	0.80
S2	0.26	2.3×10^5	12.13	0	2	6.5×10^4	4.3×10^4	2.5×10^3	1.1×10^5	2.09
S3	0.31	2.9×10^5	2.22	0	0	6.8×10^4	2.3×10^4	2.6×10^3	9.4×10^4	3.13
S4	0.24	1.8×10^5	3.46	0	0	6.2×10^4	2.5×10^4	2.4×10^3	8.9×10^4	2.03
S5	0.17	0.6×10^5	0.03	11	0	6.3×10^4	3.0×10^4	2.3×10^3	9.6×10^4	0.60
S6	0.32	1.5×10^5	2.16	0	0	18.0×10^4	2.2×10^4	8.9×10^3	2.1×10^5	0.72
S7	0.21	1.7×10^5	0.58	0	0	10.0×10^4	2.3×10^4	4.4×10^3	1.3×10^5	1.28
S8	0.15	0.8×10^5	0.05	40	0	8.3×10^4	3.1×10^4	4.3×10^3	1.2×10^5	0.66
S9	0.10	2.5×10^5	6.71	55	0	5.4×10^4	4.6×10^4	1.1×10^3	1.0×10^5	2.49
S10	0.11	2.5×10^5	4.09	15	0	5.5×10^4	3.9×10^4	9.8×10^2	9.6×10^4	2.63
Mean	0.21	1.8×10^5	3.19	13	0	8.4×10^4	3.1×10^4	3.4×10^3	1.2×10^5	1.64
Dtd	0.08	0.8×10^5	3.79	20	1	3.8×10^4	0.9×10^4	2.3×10^3	0.4×10^5	0.94
Test	0.013	<0.001	ns	ns	0.003	ns	<0.001	ns	ns	<0.001

S9 and S10 (15.5, 11.5 and 11.2, respectively) revealing a dominance of heterotrophic bacteria, whereas values decreased to 0.6 at stations S5 and S8 in October with a dominance of picoautotrophs.

During the 24 h of bioassay experiments, lower values of ciliate abundances were counted at the beginning of the experiments (236 and 130 ciliates l^{-1} in May and October, respectively). As no ciliates were found after 24 h of incubation, these potential bacterial grazers were not taken into account in these bioassays. The density of heterotrophic and pigmented nanoflagellates ranged from 1.9×10^4 cells ml^{-1} in May to 4.4×10^3 cells ml^{-1} in October. The nanoflagellate abundance did not increase significantly in the control or in the different assays ($p > 0.05$, ANOVA). The number of bacteria increased significantly in May in the samples with only 1% of the predators and the increase was more marked in presence of nutrients, whatever the nutrient added (Fig. 2). In October, the bioassay experiment did not reveal any significant increase in the number of bacteria in the samples with 1% of the predators, except when NP was added. Thus, removing 99% of bacterivorous predators caused a higher bacterial growth rate compared to the growth rate in the presence of 100% of the predators (Table 3). Higher net growth rates (μ) were observed with nutrients in May compared to the results obtained in October with similar growth rates, for all the treatments except the NP combination (Table 3). Clearly, there was a close correspondence between growth- and grazing rate values. In the presence of nutrients, grazing rates were significantly higher in May than in October (for example, 0.059 *versus* 0.010 h^{-1} with +N; 0.061 *versus* 0.052 h^{-1} with +NP). Typically, nanoflagellates (PNF and HNF) ingested between 7.23 (with +N) and 9.43 bacteria h^{-1} (with +P) in May whereas the values observed in October were lower (0.84 and 2.54 h^{-1}, respectively) (Table 3).

The two PCAs were performed on the independent datasets (10 descriptors and 10 stations). The first two eigenvalues of the PCA analysis accounted for 72.0% of the total variability in May and 69.1% in October 2008. The analysis, therefore, only considered these two first axes to highlight the relationship between descriptors along a spatial distribution of samples. In May, the variable PROC was opposed to all other variables linked to the phytoplankton (AUTO, PICO, SYNE and Chlor-A) on the first axis, as also demonstrated by the significant correlations between them (Table 4). Bacterial variables (BACT-A, BACT-P, SF and TTC) were linked to the variable H/A (heterotrophic bacteria *versus* picoautotrophs) and opposed to the variable PROC. In October, the same correlations were observed among the phytoplankton descriptors, with a clear opposition of the descriptor PROC with all the other variables. However, unlike the situation described in May, the TTC concentrations did not seem to be linked to the bacterial abundances in October. The ratio H/A was always linked to the bacterial variables and not to the autotrophic variables, as also demonstrated by the significant correlations between them (Table 4).

For both sets of measurements, the location of each station in the atoll was clearly differentiated on the first axis. In May, there were high concentrations of autotrophic cells except *Prochlorococcus* cells (PROC) at stations S6 and S9. However, the highest abundances of *Prochlorococcus* were found at stations S2–S5 (Fig. 3a). Stations S7 and S10 had high values of all the bacterial variables studied, especially the FIB concentrations. Station S7 was close to a large pearl farm, whereas station S10 was near Bird Island. In November, the distribution pattern at the stations was quite different from that observed in May. However, station S6 was always associated with high concentrations of AUTO, SYNE, PICO and Chlor-A and very low concentrations of PICO. Station S2 had the highest values of BACT-A and BACT-P but did not have high concentrations of TTC. Stations S9 and S10 near the pass had the highest values of PROC (Fig. 3b).

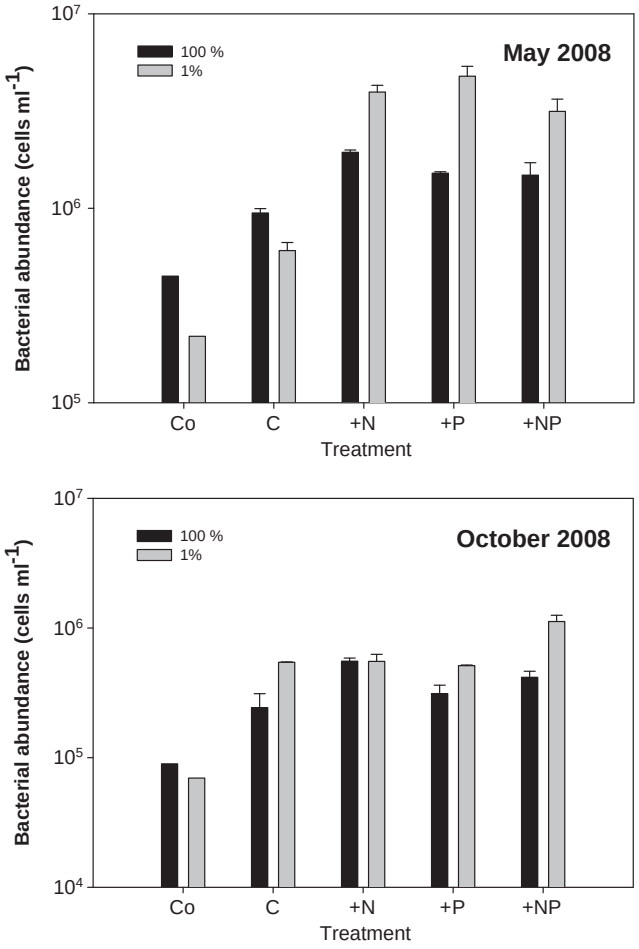

Fig. 2. Changes in bacterial abundance following different nutrient treatments (N, P and NP) between beginning of experiment (control at $t = 0$; C0) and end of incubation (24 h) conducted with (Serie 100%) and without (Serie 1%) bacterial predators. C = control at $t = 24$ h.

Table 3
Net bacterial growth rates (μ) and grazing rates of bacteria by predators (g) in May and October 2008 from dilution experiments (1% and 100%) without (control, C) and with nutrient (N, P and NP). Experiments were performed in triplicates. Ingestion rates (I) were calculated from the formula described in M&M.

May				
Dilution	100%	1%		
Variable	$\mu + g$	μ	g	I
Unit	h^{-1}	h^{-1}	h^{-1}	Bact HNF^{-1} h^{-1}
C	0.031	0.042	0.011	1.36
N	0.061	0.121	0.059	7.23
P	0.051	0.128	0.078	9.43
NP	0.050	0.111	0.061	7.44
October				
Dilution	100%	1%		
Variable	$\mu + g$	μ	g	I
Unit	(h^{-1})	(h^{-1})	(h^{-1})	Bact HNF^{-1} h^{-1}
C	0.042	0.086	0.044	3.61
N	0.076	0.086	0.010	0.84
P	0.052	0.083	0.031	2.54
NP	0.064	0.116	0.052	4.24

4. Discussion

The production of black Tahitian pearls is of key importance for the economy of the Tuamotu Archipelago (French Polynesia) but since the 2000s intensified farming has caused a reduction in quality and a collapse in prices. A multidisciplinary research program was funded by the EDF (European Development Fund) to analyze the causes of the crisis. One of the major objectives of this program was to analyze the ecological environment of the pearl-oyster, *P. margaritifera*, in Ahe atoll and its relationship with the pelagic trophic network. As explained by Thomas et al. (2010), the Ahe atoll seems to be comparable to closed atolls, mainly because of its high abundance of picophytoplankton. In fact, despite the existence of a channel and several open reef-flat spillways allowing exchanges with the surrounding ocean, the large depth of the lagoon could contribute to the reduction in water exchange. These conditions explained the increase in phytoplankton concentrations, especially of lagoonal communities like picoeukaryotes in the 11 atoll lagoons studied by Charpy and Blanchot (1998). The highest chlorophyll values were observed in the more confined, shallow area of the lagoon where pearl farming is more intensive. These high chlorophyll levels were related to high phytoplankton production linked to the recycling of nutrients by pearl oysters (Loret et al., 2000). The bacterial densities recorded during the two surveys were between 5.7×10^4 ml^{-1} (S5 in October) and 1.1×10^6 ml^{-1} (S10 in May), slightly lower than in previous studies conducted in the Ahe atoll (from April 2007 to March 2008; Thomas et al., 2010). All values were almost in the same range as values previously recorded in Takapoto (Sakka et al., 2000) and the nearby Tikehau atolls (Torréton and Dufour, 1996).

Bacterial production was close to that determined in the Tikehau and Takapoto atolls (4–5 µgC l^{-1} d^{-1}; Torréton and Dufour, 1996) and within the range of values reported in 11 other Tuamotu atolls (1.00–7.74 µgC l^{-1} d^{-1}; Torréton et al., 2002). Bacterial production (BACT-P) and abundance (BACT A) were correlated in October but not in May ($r = 0.601$; $p < 0.05$; Table 4), suggesting that bacterial communities were more controlled by resources in October (Billen et al., 1990; Bouvy et al., 1998). However, when compared to the control, no increase of bacterial numbers following the addition of nutrients was observed in the enrichment experiment performed on one single station. Others studies should be pay special attention in the future about the availability of inorganic nutrients for bacterial consumption. Top-down factors (grazing by nanoflagellates) seemed to be more responsible for the regulation of bacterial dynamics in May (see below). Picophytoplankton abundances were in the same range as values recorded by Thomas et al. (2010), except for *Prochlorococcus* concentrations. They reported mean values from $6.3 \times 10^4 \pm 4.0 \times 10^4$ cells ml^{-1} (April–May) to $13.6 \times 10^4 \pm 4.4 \times 10^4$ cells ml^{-1} (February–March) at 5 m depth, in 12 stations in the lagoon, whereas the values measured in this study were all below 46×10^3 cells ml^{-1}, possibly as the stations were very shallow, located near the coast line and *Prochlorococcus* seems more abundant in deep lagoons (Charpy and Blanchot, 1998). However, as also observed by Thomas et al. (2010), the highest values were found in October suggesting that oligotrophic situation occurs during this period in the Ahe atoll, and can be explained by a marine influence. Indeed, *Prochlorococcus* is considered to be an oceanic marker whereas picoeukaryotes are considered to be lagoon markers (Charpy, 1996). Thomas et al. (2010) reported *Synechococcus* abundances ranging from $7.7 \times 10^4 \pm 3.9 \times 10^4$ (November) to $12.2 \times 10^4 \pm 4.8 \times 10^4$ (April–May) cells ml^{-1}. These values are within the range of *Synechococcus* abundances observed during this study (Table 2). Picoeukaryote abundances found during this study were close to those measured by Thomas et al. (2010). Their abundances varied with respect to *Synechococcus* and *Prochlorococcus* concentrations in October ($r = 0.981$ and 0.609, respectively; Table 4) but not in May. These potential differences point out the variation of composition of type of resources encountered in the system, as reported in many studies (e.g. Binder et al., 1996).

In terms of water quality, one of the aims of this study was to assess the impact of human sewage by monitoring the input and

Table 4
Mann-Whitney rank correlations between the 10 biological variables studied during the two surveys (May and October 2008). Significant values are given in bold ($^{*}p < 0.05$; $^{**}p < 0.01$; $^{***}p < 0.001$). Chlo-a: chlorophyll-a; Bact-A: bacterial abundance; Bact-P: bacterial production; TTC: concentrations of thermotolerant coliforms; FS: concentration of faecal streptococci; SYNE: *Synechococcus* abundance; PROC: *Prochlorococcus* abundance; PICO: Pigmented picoeukaryote abundance; AUTO: Picoautotroph abundance; H/A: ratio between heterotroph (bacteria) and picoautotroph abundance.

	Chlo-a	Bact-A	Bact-P	TTC	SF	SYNE	PROC	PICO	AUTO	H/A
May 2008										
Chlo-a	1.000	0.328	−0.214	0.024	−0.572	**0.615***	**−0.708***	0.381	**0.602***	−0.162
Bact-A		1.000	0.379	**0.688***	0.050	0.062	−0.380	0.025	0.078	**0.606***
Bact-P			1.000	0.339	0.362	−0.448	−0.027	0.013	−0.452	**0.676***
TTC				1.000	−0.077	−0.216	0.009	0.772	−0.173	0.445
SF					1.000	−0.406	0.313	−0.246	−0.406	0.403
SYNE						1.000	**0.595***	0.410	**0.998*****	**−0.683****
PROC							1.000	−0.280	−0.561	0.076
PICO								1.000	0.454	−0.042
AUTO									1.000	**−0.686***
H/A										1.000
October 2008										
Chlo-a	1.000	0.144	0.048	**−0.766***	0.250	0.555	**−0.633***	0.569	0.453	−0.001
Bact-A		1.000	**0.601***	−0.027	0.088	0.335	0.356	−0.407	−0.291	**0.950*****
Bact-P			1.000	0.054	**0.659***	−0.337	**0.727****	−0.356	−0.196	0.532
TTC				1.000	−0.283	−0.340	**0.610***	−0.328	−0.228	0.042
SF					1.000	−0.051	0.311	−0.044	0.022	0.010
SYNE						1.000	−0.573	**0.981*****	**0.979*****	−0.578
PROC							1.000	**0.609***	−0.394	0.384
PICO								1.000	**0.951*****	**−0.629***
AUTO									1.000	−0.556
H/A										1.000

dispersion of fecal indicator bacteria (FIB). Fecal indicator bacteria (FIB) such as TTC and FS are widely accepted as being useful indicators of fecal contamination in the aquatic environment, generally associated with an increased risk of contracting gastrointestinal and respiratory illnesses (Haile et al., 1999). The analytical and statistical approaches adopted provided the first data on the trophic, health and sanitary status of the Ahe atoll. The major sewage source in the Ahe atoll was found at S9 and S10 in May, with the highest TTC and FS concentrations observed in the near shore area. In S9, the construction of a small harbor near a farm (close to twenty inhabitants) is certainly a potential source of contamination. It is also important to mention that a bird island is located near S10 (see Fig. 1); bird guano has a potential effect that was not considered in this study but that may explain some of the high FIB concentrations, as also described in some atolls located in the central Pacific by Dinsdale et al. (2008). Local currents may also explain the presence of FIB at these stations. In October, FIB concentrations were very low, especially for FS. Despite unfavorable environmental conditions encountered in the Ahe atoll (high salinity, high direct illumination), FIB concentrations remained relatively high at S9 and S10 (94 and 200 CFU 100 ml^{-1} of TTC in May). This suggests a large potential source of FIB contamination with an input from sewage discharges high enough to overcome the effects of dilution. Values of bacterial production confirm the presence of dissolved organic matter from effluent, with the highest value at S9 in May, and also at S2 in October, and suggest a temporal/spatial variability in dissolved organic matter coming from episodic human activities (pearl farming, harbor). At atoll scale, bacterioplankton abundances and productions were significantly correlated with TTC concentrations in May, and with SF in October, respectively (Table 4; Fig. 3). This may result from the direct discharge of heterotrophic bacteria and the stimulation of the autochthonous marine community by the release of sewage-derived organic substrates, as demonstrated by Cunha and Almeida (2006) in the coastal region off Aveiro (NW Portugal). The data presented here showed that the dilution and the mortality processes were not sufficient to avoid the presence of FIB in these stations. These observations corroborate previous studies in tropical zones (Senegal, West Africa) demonstrating the presence of FIB far from the sewage source (Troussellier et al., 2004; Bouvy et al., 2008). Standards and recommended guidelines based on indicators such as bacteria concentrations have been drawn up to prevent the public being exposed to pathogenic enteric microorganisms. There are no guidelines or water directives in Tuamotu Archipelago for bathing waters and so the values indicated in the EU directive were applied. The results obtained in this study show that all samples complied with the guideline value of 500 CFU 100 ml^{-1} for TTC (maximum limit of 2000 CFU 100 ml^{-1}) and 100 CFU 100 ml^{-1} for FS defined in the European Union bathing water quality directive 76/160/EEC. This study can, therefore, conclude that no evidence of human sewage was apparent at atoll scale, except for the station S9. The contamination observed at the station S10 seems to be linked to the concentration of bird guano, as reported by Choi et al. (2003). Indeed, sources of fecal bacteria other than human (i.e. birds, pets, wildlife, etc.) should not be disregarded and can introduce microbial pathogens into the marine environment (Nogales et al., 2011).

The enrichment experiments were performed in nutrient conditions comparable to those observed in 12 Tuamotu atolls (Dufour et al., 2001). In October 2010, Charpy et al. (2012) reported NH_4-N concentrations below 0.05 μmol l^{-1}, NO_3-N ranging from 0.05 to 0.10 μmol l^{-1} and concentrations of reactive orthophosphate averaging 0.26 ± 0.01 μmol l^{-1}. Thus, in this oligotrophic environment, the growth of the heterotrophic bacterial populations in the Ahe atoll can be expected to be limited by phosphorus and/or nitrogen availability, given that mineral limitation of growth rates is widespread in various marine ecosystems, including atoll systems (e.g. Torréton et al., 2000). A nutrient is considered to limit bacterial growth when the availability of this nutrient is low relative to the demand of the bacterial cells (Cotner et al., 1997). This was expressed as an increase in bacterial growth after the addition of the nutrient alone or in combination with other nutrients. In May, bacterial community dynamics were affected by a single addition of N and P or in combination N+P, especially without predators, whereas in October the responses were not significant, except with addition of NP. This contrast revealed a clear change in environmental conditions in the Ahe lagoon, explained in May by the high ratio of heterotrophic bacteria to picoautotrophs within the picoplankton compartment (mean of 7.7 *versus* 1.64 in October). In this context, carbon limitation can be

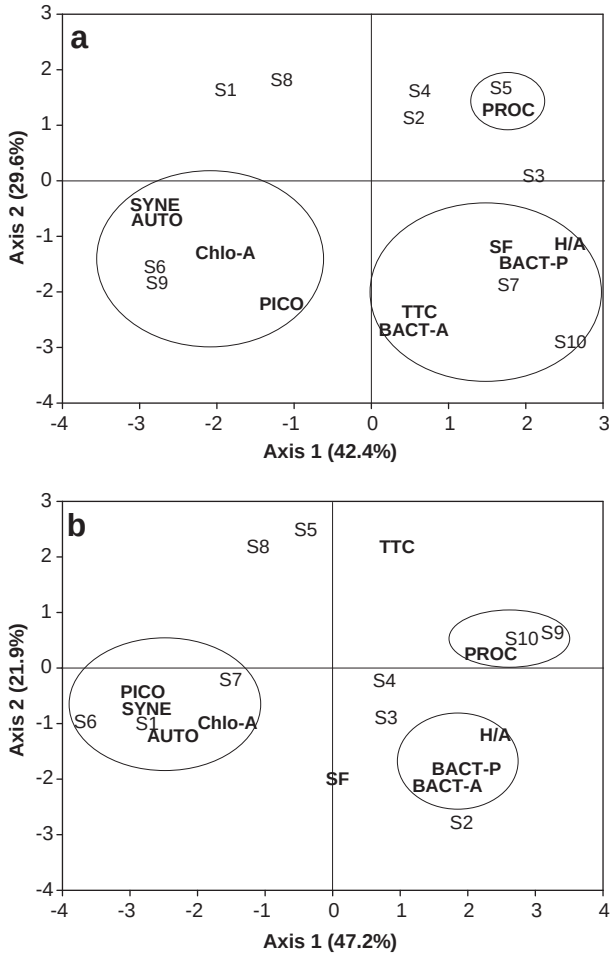

Fig. 3. Principal component analysis (PCA) on the two first axes in May (a) and October (b) 2008. Eigenvalues for each axis of the PCA are reported. Stations are identified as in Table 1. Abbreviations: Chlo-a: chlorophyll-a; Bact-A: bacterial abundance; Bact-P: bacterial production; TTC: concentrations of thermotolerant coliforms; FS: concentration of faecal streptococci; SYNE: Synechococcus abundance; PROC: Prochlorococcus abundance; PICO: Pigmented picoeukaryote abundance; AUTO: Picoautotroph abundance; H/A: ratio between heterotroph (bacteria) and picoautotroph abundance.

also advanced in May knowing that the values of the ratio between heterotrophs and autotrophs are high compared to values in October. Another hypothesis can be advanced on the major role played by the virioplanktonic community in the aquatic food web (Fuhrman, 1999; Bouvy et al., 2011). In October, viral lysis can explain the absence of increase of bacterial numbers with addition of N and P, but the absence of data did not permit to conclude on this hypothesis. However, virus and bacteria dynamics has been studied in August 2009 in Ahe atoll, and patterns observed confirm that virus communities are abundant within coral reefs but viral infection of bacterial cells seems rare (Bouvy et al., 2012).

Previous studies in atolls have always shown that bacterial communities (from 10 lagoons) responded in various ways to nutrient additions (C, N and P), mainly linked to the *in situ* concentration, the atoll morphology and benthic nitrogen fixation in the deepest open lagoons (Torréton et al., 2000). As already discussed by Thingstad et al. (1998), the hypothesis of an inorganic nutrient limitation on heterotrophic bacteria has important conceptual and functional consequences. Heterotrophic bacteria have been shown to compete successfully with phytoplankton for phosphate owing to their higher affinity for this nutrient (Kirchman, 1994). This competition suggests that nutrient limitation of primary production may have occurred in May and may have been reinforced by the bacterioplankton demand. Torréton et al. (2000) concluded that bacteria are net consumers of inorganic nitrogen and that this nitrogen is recycled by bacterioplankton grazers.

With the limited data set obtained during this study on bacterioplankton, we can only speculate that the *in situ* concentrations reflect the nutrient status of bacterioplankton in October (except with +NP), whereas phosphorus and nitrogen stimulate bacterial growth rates in May. It is not possible to state that there is an overall limitation in the Ahe atoll since the concentrations probably vary over short time-scales, responding to variations in nutrient concentrations driven by small-scale physical phenomenon such as wind (Thomas et al., 2010).

This study also investigated the growth rates of bacterial communities with and without bacterivorous predators. It is now commonly accepted that nanoflagellates are the most important grazers of bacteria in most environments (e.g. Sanders et al., 2000; Tsai et al., 2011). The ingestion rates of nanoflagellates (HNF and PNF) on natural populations of bacteria in the Ahe atoll (1.36 and 3.61 cells nanoflagellate^{-1} h^{-1} in May and October, respectively) are comparable to data in the literature (e. g. Seong et al., 2006; Tsai et al., 2011). However, our ingestion rate values are lower than those reported by Sakka et al. (2000) for the Takapoto atoll (107.6 ± 44.5 cells HNF^{-1} h^{-1}). For the treatment with NP, the mean values for grazing on bacteria were high, compared to the control, with 1.46 d^{-1} in May and 1.25 d^{-1} in October, suggesting that nitrogen and phosphorus deficiency can affect in different ways the growth and metabolism of bacteria, as suggested by Torréton et al. (2000). Sakka et al. (2000) reported an average protozoan grazing of 28% of bacterial growth. In this study, a maximum of 15.3% (May) and 63.4% (October) of the bacterial stock were ingested per day for the total nanoflagellate community (PNF and HNF) in the controls. However, in May with phosphorus addition, 66.3% of the bacterial stock was ingested per day, suggesting that, simultaneously to the increase of the bacterial growth rate due to nutrient enrichment, grazing rates also increased. In our experiment, it is obvious that grazing rates of bacteria by PNF and HNF were higher in May, concomitant with the bacterial growth rates, which provided the evidence for the close coupling of bacterial and nanoflagellate dynamics at this station. Water temperature and prey abundance are usually considered among the most important factors regulating the grazing activity of HNF (Choi, 1994). In the tropical conditions encountered in the Ahe atoll, water temperature is certainly not limiting, but the oligotrophic conditions (Charpy et al., 2012) may stimulate the ingestion of particles by PNF (pigmented nanoflagellates) (Unrein et al., 2007). Flagellates, as expected, seem to be the major protistan bacterivores in Ahe. Moreover, the alternative source of bacterial mortality, such as lysis by viruses, does not seem very important in this environment (Bouvy et al., 2012). Very few studies have been carried out on viruses in atoll lagoons (Seymour et al., 2005; Dinsdale et al., 2008; Patten et al., 2011) and nothing is known about the response of atoll lagoon bacterioplankton to the presence of viruses.

Based on sub-surface sampling, this study revealed distinctive spatial and temporal patterns in the Ahe atoll, which were characterized by microbial variables (chlorophyll-a, picoplankton structure, etc.). In marine environments, substrate availability and water temperature are considered to be important factors that regulate plankton dynamics, especially bacterioplankton (Pomeroy and Wiebe, 2000). Similar temperature data recorded in May and October cannot explain the difference between the patterns observed during the two periods. It may, therefore, be argued that the major regulator of picoplankton distribution is the substrate supply rather than the temperature. The direct influence of the ocean on the lagoon picoplankton structure was insignificant as also reported by Thomas et al. (2010). These authors explained that

wind can be the main factor driving spatial and daily variability of phytoplankton and bacterioplankton. However, station S6 (harbor village) was always associated with high concentrations of *Synechococcus* and picoeukayotes and low concentrations of *Prochlorococcus,* reflecting the possible impact of human activities with inputs from the land. The positive ratio between heterotrophic bacteria and autotrophic cells (H/A) observed during both periods reflects the high heterotrophic content in the microbial network, especially in May. According to Duarte and Agusti (1998), our result show that Ahe atoll belongs to the unproductive aquatic system, without high external inputs of inorganic nutrients issuing from human activities. Higher heterotrophic influence could be related to changes (i) in the relative contribution of the various picophytoplankton components (such as higher *Prochlorococcus* abundance) or (ii) in the nutrient concentrations (no data available to assess this hypothesis). This study, therefore, supports the idea that the planktonic communities in the Ahe atoll can act as CO_2 sources, according to Duarte and Agusti (1998). Unlike static analyses producing indices similar to those of the OECD (Organization for Economic Cooperation and Development), enrichment bioassays appear to provide a good understanding of bacterial dynamics, especially given potential nutrient input, as is the case of the Ahe atoll. Hotspots of FIB presence were found in the vicinity of some farms but the concentrations were too low to draw any conclusions on any possible impact on the microbial food web or, more generally, on the health of the oysters farmed (*P. margaritifera*). However, it will be useful if the authorities take measures to limit human sewage runoff into atoll waters as these waters are used for the pearl industry which is essential for the economy of French Polynesia.

Acknowledgements

This work was supported by the European Development Fund, in collaboration with the Service de la Perliculture and the University of French Polynesia. We should like to thank all the colleagues for their valuable help in collecting samples during the two surveys. We also thank the two anonymous reviewers for the helpful comments that have contributed to improve the manuscript.

References

Andréfouët, S., Charpy, L., Lo-Yat, A., Lo, C., 2012. Recent reseach for pearl oyster aquaculture management in French Polynesia. Mar. Pollut. Bull. 65, 407–414.

Aslan-Yilmaz, A., Okusa, E., Övez, S., 2004. Bacteriological indicators of anthropogenic impact prior to and during the recovery of water quality in an extremely polluted estuary, Golden Horn, Turkey. Mar. Pollut. Bull. 49, 951–958.

Billen, G., Servais, P., Becquevort, S., 1990. Dynamics of bacterioplankton in oligotrophic and eutrophic aquatic environments: bottom-up or top-down control? Hydrobiologia 207, 37–42.

Binder, B.J., Chisholm, S.W., Olson, R.J., Frankel, S.L., Worden, A.Z., 1996. Dynamics of pico-phytoplankton and ultra-phytoplankton, and bacteria in the central equatorial Pacific. Deep Sea Res. I (43), 907–931.

Bouvy, M., Arfi, R., Cecchi, Ph., Corbin, D., Pagano, M., Saint-Jean, L., Thomas, S., 1998. Trophic coupling between bacterial and phytoplanktonic compartments in shallow tropical reservoirs (Côte d'Ivoire, West Africa). Aquat. Microb. Ecol. 15, 25–37.

Bouvy, M., Troussellier, M., Got, P., Arfi, R., 2004. Bacterioplankton responses to bottom-up and top-down controls in a West African reservoir (Sélingué, Mali). Aquat. Microb. Ecol. 34, 301–307.

Bouvy, M., Briand, E., Lemeur, A., M'Boup, M., Got, P., Bettarel, Y., Arfi, R., 2008. Impact of sewage pollution on microbial components in a coastal tropical ecosystem. Mar. Fresh Res. 59, 614–626.

Bouvy, M., Arfi, R., Bernard, C., Carré, C., Got, P., Pagano, M., Troussellier, M., 2010. Estuarine microbial community characteristics as indicators of human-induced changes (Senegal River, West Africa). Estuarine Coastal Shelf Sci. 87, 573–582.

Bouvy, M., Bettarel, Y., Bouvier, C., Domaizon, I., Jacquet, S., Le Floc'h, E., Montanié, E., Mostajit, B., Sime-Ngando, T., Torréton, J.P., Vidussi, F., Bouvier, T., 2011. Trophic interactions between viruses, bacteria and nanoflagellates under various nutrient conditions and simulated climate change. Environ. Microbiol. 13, 1842–1857.

Bouvy, M., Combe, M., Bettarel, Y., Dupuy, C., Rochelle-Newall, E., Charpy, L., 2012. Uncoupled viral and bacterial distributions in coral reef waters of Tuamotu Archipelago (French Polynesia). Mar. Pollut. Bull. 65, 506–515.

Carlsson, P., Caron, D.A., 2001. Seasonal variation of phosphorus limitation of bacterial growth in a small lake. Limnol. Oceanogr. 46, 108–120.

Caron, D.A., 1983. Technique for enumeration of heterotrophic and phototrophic nanoplankton, using epifluorescence microscopy, and comparison with other procedures. Appl. Environ. Microbiol. 46, 491–498.

Charpy, L., 1996. Phytoplankton biomass and production in two Tuamotu atoll lagoons (French Polynesia). Mar. Ecol. Prog. Ser. 145, 133–142.

Charpy, L., Blanchot, J., 1998. Photosynthetic picoplankton in French Polynesian atoll lagoons: estimation of taxa contribution to biomass and production by flow cytometry. Mar. Ecol. Prog. Ser. 162, 57–70.

Charpy, L., Rodier, M., Fournier, J., Langlade, M.-J., Gaertner-Mazouni, N., 2012. Physical and chemical control of the phytoplankton of Ahe lagoon, French Polynesia. Mar. Pollut. Bull. 65, 471–477.

Choi, J.W., 1994. The dynamic nature of protistan ingestion response to prey abundance. J. Eukaryot. Microbiol. 41, 137–146.

Choi, S., Chu, W., Brown, J., Becker, S.J., Harwood, V.J., Jiang, S.C., 2003. Application of enterococci antibiotic resistance patterns for contamination source identification at Huntington Beach, California. Mar. Pollut. Bull. 46, 748–755.

Christaki, U., Van Wambeke, F., Dolan, J.R., 1999. Nanoflagellates (mixotrophs, heterotrophs and autotrophs) in the oligotrophic eastern Mediterranean: standing stocks, bactivory and relationships with bacterial production. Mar. Ecol. Prog. Ser. 181, 297–307.

Cotner, J.B., Ammermann, J.W., Peele, E.R., Bentzen, E., 1997. Phosphorus-limited bacterioplankton growth in the Sargasso Sea. Aquat. Microb. Ecol. 13, 141–149.

Cunha, A., Almeida, A., 2006. Influence of an estuarine plume and marine sewage outfall on the dynamics of coastal bacterioplankton communities. Aquat. Microb. Ecol. 44, 253–262.

Davies-Colley, C.M., Bell, R.G., Donnison, A.M., 1994. Sunlight inactivation of enterococci and faecal coliforms in sewage effluent diluted in seawater. Appl. Environ. Microbiol. 68, 1165–1172.

Davies, P.G., Sieburth, J.M., 1984. Estuarine and oceanic microflagellate predation of actively growing bacteria: estimation by frequency of dividing divided bacteria. Mar. Ecol. Prog. Ser. 19, 237–246.

Dinsdale, E.A., Pantos, O., Smrigs, S., Edwards, R.A., Angly, F., et al., 2008. Microbial ecology of four coral atolls in the northern line islands. PlosOne 3, 1–17.

Duarte, C.M., Agusti, S., 1998. The CO2 balance of unproductive aquatic ecosystems. Science 281, 234–236.

Ducklow, H.W., Shiah, F., 1993. Bacterial production in estuaries. In: Ford, T. (Ed.), Aquatic Microbiology: An Ecological Approach. Blackwell Scientific, Boston, MA, pp. 261–287.

Dufour, Ph., Anfréfouët, S., Charpy, L., Garcia, N., 2001. Atoll morphometry controls lagoon nutrient regime. Limnol. Oceanogr. 46, 456–461.

Ferrier-Pagès, C., Furla, P., 2001. Pico- and nanoplankton biomass and production in the two largest atoll lagoons of French Polynesia. Mar. Ecol. Prog. Ser. 211, 63–76.

Fuhrman, J.A., 1999. Marine viruses and their biogeochemical and ecological effects. Nature 399, 541–548.

Gonzalez, J.M., Torreton, J.P., Dufour, P., Charpy, L., 1998. Temporal and spatial dynamics of the pelagic microbial food web in an atoll lagoon. Aquat. Microb. Ecol. 16, 53–64.

Gundersen, K., Heldal, M., Norland, S., Purdie, D.A., Knap, A.H., 2002. Elemental C, N and P cell content of individual bacteria collected at the Bermuda Atlantic Time-series Study (BATS) site. Limnol. Oceanogr. 47, 1525–1530.

Haile, R.W., White, J.S., Gold, M., Cressey, R., Mc Gee, C., et al., 1999. The health effects of in ocean water contaminated by storm drain runoff. Epidemiology 10, 355–363.

Halpern, B.S., Walbridge, S., Selkoe, K.A., et al., 2008. A global map of human impact on marine ecosystems. Science 319, 948–952.

Islam, M.S., Tanaka, M., 2004. Impact of pollution on coastal and marine ecosystems including coastal and marine fisheries and approach for management: a review and synthesis. Mar. Pollut. Bull. 48, 624–649.

Jürgens, K., Matz, C., 2002. Predation as a shaping force for the phenotypic and genotypic composition of planktonic bacteria. Antonie van Leeuwenhoek 81, 413–434.

Kirchman, D.L., 1994. The uptake of inorganic nutrients by heterotrophic bacteria. Microb. Ecol. 28, 255–271.

Lipp, E.K., Fraarh, S.A., Rose, J.B., 2001. Assessment of impact of microbial fecal pollution and human pathogens in a coastal community. Mar. Pollut. Bull. 42, 286–293.

Loret, P., Le Gall, S., Dupuy, C., Blanchot, J., Pastoureaud, A., Delesalle, B., Caisey, X., Jonquières, G., 2000. Heterotrophic protists as a link between picocyanobacteria and the pearl oyster Pinctada margaritifera in the Takapoto lagoon (Tuamotu Archipelago, French Polynesia). Aquat. Microb. Ecol. 22, 215–226.

Marie, D., Partensky, F., Vaulot, D., Brussaart, C., 1999. Enumeration of phytoplankton, bacteria, and viruses in marine samples. In: Dressier, L.G., (Ed.), Current Protocoles of Cytometry, Suppl. 10, Unit 11, 11, pp. 1–15.

Nogales, B., Lanfranconi, M.P., Pina-Villalonga, J.M., Bosch, R., 2011. Anthropogenic perturbations in marine microbial communities. FEMS Microb. Rev. 35, 275–298.

Paerl, H.W., Dyble, J., Twomey, L., Pinckley, J.L., Nelson, J., Kerkhof, L., 2002. Characterizing man-made and natural modifications of microbial diversity and activity in coastal ecosystems. Antonie van Leeuwenhoek 81, 487–507.

Patten, N.L., Wyatt, A.S.J., Lowe, R.J., Waite, A.M., 2011. Uptake of picophytoplankton, bacterioplankton and virioplankton by a fringing coral reef community (Ningaloo reef, Australia). Coral Reefs. doi:10.1007/s00338-011-0777-8.

Pomeroy, L.R., Wiebe, W.J., 2000. Temperature and substrates as interactive limiting factors for marine heterotrophic bacteria. Aquat. Microb. Ecol. 23, 187–204.

Sakka, A., Legendre, L., Gosselin, M., Delesalle, B., 2000. Structure of the oligotrophic planktonic food web under low grazing of heterotrophic bacteria: Takapoto Atoll, French Polynesia. Mar. Ecol. Prog. Ser. 197, 1–17.

Sanders, R.W., Berninger, U.G., Lim, E.L., Kemp, P.F., Caron, D.A., 2000. Heterotrophic and mixotrophic nanoflagellates predation on picoplankton in the Sargasso Sea and Georges Bank. Mar. Ecol. Prog. Ser. 192, 103–118.

Seong, K.A., Jeong, H.J., Kim, S., Kim, G.H., Kang, J.H., 2006. Bacterivory by co-occurring red-tide algae, heterotrophic nanoflagellates, and ciliates. Mar. Ecol. Prog. Ser. 322, 85–97.

Seymour, J.R., Pattern, N., Bourne, D.G., Mitchell, J.G., 2005. Spatial dynamics of virus like particles and heterotrophic bacteria within a shallow coral reef system. Mar. Ecol. Prog. Ser. 288, 1–8.

Smith, D.C., Azam, F., 1992. A simple, economical method for measuring bacterial protein synthesis rates in seawater using ^{3}H-leucine. Mar. Microb. Food Webs 6, 107–114.

Solic, M., Krstulovic, N., 1994. Role of predation in controlling bacterial and heterotrophic nanoflagellates standing stocks in the coastal Adriatic Sea: seasonal patterns. Mar. Ecol. Prog. Ser. 114, 219–235.

Thioulouse, J., Chessel, D., Dolédec, S., Olivier, J.M., 1997. ADE 4: a multivariate analysis and graphical display software. Stat. Comput. 7, 75–83.

Thingstad, T.F., Zweifel, U.L., Rassoulzadegan, F., 1998. P limitation of heterotrophic bacteria and phytoplankton in the northwest Mediterranean. Limnol. Oceanogr. 43, 88–94.

Thomas, Y., Garen, P., Courties, C., Charpy, L., 2010. Spatial and temporal variability of the pico- and nanophytoplancton and bacterioplankton in a deep polynesian atoll lagoon. Aquat. Microb. Ecol. 59, 89–101.

Torréton, J.P., Dufour, Ph., 1996. Bacterioplankton production determined by DNA synthesis, protein synthesis, and frequency of dividing cells in Tuamotu Atoll lagoons and surrounding ocean. Microb. Ecol. 32, 185–202.

Torréton, J.P., Pagès, J., Talbo, V., 2002. Relationships between bacterioplankton and phytoplankton biomass, production and turnover rate in Tuamotu atoll lagoons Aquat. Microb. Ecol. 28, 267–277.

Torréton, J.-P., Talbot, V., Garcia, N., 2000. Nutrient stimulation of bacterioplankton growth in Tuamotu atoll lagoons. Aquat. Microb. Ecol. 21, 125–137.

Tsai, A.-Y., Gong, G.-C., Saders, R.W., Chen, W.-H., Chao, C.-F., Chiang, K.-P., 2011. Importance of bacterivory by pigmented and heterotrophic nanoflagellates during the warm season in a subtropical western Pacific coastal ecosystem. Aquat. Microb. Ecol. 63, 9–18.

Troussellier, M., Got, P., Bouvy, M., M'boup, M., Arfi, R., Lebihan, F., Monfort, P., Corbin, D., Bernard, C., 2004. Water quality and health status of the Senegal River estuary. Mar. Pollut. Bull. 48, 852–862.

Unrein, F.R., Massana, I., Alonso-Saez, L., Gasol, J.M., 2007. Significant year-round effect of small mixotrophic flagellates on bacterioplankton in an oligotrophic coastal system. Limnol. Oceanogr. 52, 456–469.

Welschmeyer, N.A., 1994. Fluorometric analysis of chlorophyll a in the presence of chlorophyll b and pheopigments. Limnol. Oceanogr. 39, 1985–1992.

Marine Pollution Bulletin 65 (2012) 525–537

Contents lists available at SciVerse ScienceDirect

Marine Pollution Bulletin

journal homepage: www.elsevier.com/locate/marpolbul

Spatio-temporal diversity of free-living and particle-attached prokaryotes in the tropical lagoon of Ahe atoll (Tuamotu Archipelago) and its surrounding oceanic waters

V. Michotey [a,b,c,d,*], S. Guasco [a,b,c,d], D. Boeuf [d], N. Morezzi [d], B. Durieux [e], L. Charpy [a,b,c,e], P. Bonin [a,b,c,d]

[a] Aix-Marseille Université, Mediterranean Institute of Oceanography (MIO), 13288 Marseille Cedex 09, France
[b] CNRS/INSU, MIO, UMR 7294, 13288 Marseille Cedex 09, France
[c] IRD, MIO, UR 235, 13288 Marseille Cedex 09, France
[d] Laboratoire de Microbiologie, de Géochimie et d'Écologie Marine, Centre d'Océanologie de Marseille, Université de la Méditerranée – Aix-Marseille Université, CNRS-UMR 6117 Campus de Luminy, Case 901, 163 Avenue de Luminy, 13288 Marseille Cedex 09, France
[e] Laboratoire d'Océanographie Physique et Biogéochimique, Centre d'Océanologie de Marseille, Université de la Méditerranée – Aix-Marseille Université, CNRS IRD-UMR 6535 Campus de Luminy, Case 901, 163 Avenue de Luminy, 13288 Marseille Cedex 09, France

ARTICLE INFO

Keywords:
Archaea
Bacteria
Biodiversity
Lagoon
Pacific Ocean

ABSTRACT

Spatio-temporal variability of prokaryotic water column communities inside and outside a Polynesian tropical lagoon subjected to pearl oysters farming was assessed in terms of abundance by quantitative PCR and diversity by DGGE. Communities and operational taxonomic units (OTUs) were analysed according to dry/rainy seasons and free-living/particle-attached state. Bacterial density was higher in the lagoon compared to ocean and a seasonal trend was observed. No influence of the localisation within lagoon or of the planktonic/attached states was noticed on bacterial abundance and diversity. The OTUs belonged to *Cyanobacteria*, to heterotrophic groups in *Proteobacteria* and *Flavobacteria*. Archaeal abundance showed seasonal tendency and particle-prevalence, but no effect of lagoon or oceanic location was observed. Lagoon and oceanic archaeal diversity were different and Euryarchaeota (MG-II, MBG, and *Halobacteria*) were detected. During the dry season, planktonic and particle-associated community differed, whereas at rainy season, both communities were similar and included members usually associated with coral.

1. Introduction

It is generally admitted that the bacterioplankton biomass is 2- or 3-fold higher than the phytoplankton biomass, increasing in proportion with oligotrophy (Karl et al., 1998). Prokaryotes are main mediators of biogeochemical cycles; they are the key-players in the mineralisation of organic matter and the only organisms able to use Dissolved Organic Matter (DOM) (Azam and Worden, 2004). The produced prokaryotic biomass is grazed by nanoplankton (nanoflagellates and ciliates), that is successively consumed by micro-zooplankton and organisms of higher Trophic levels that, in turn, produce DOM (Azam et al., 1983; Loret et al., 2000). This microbial loop allows the transfer of energy to the higher levels of the Tropic web by recycling of organic matter that would otherwise be exported from the photic layer. The activity of prokaryotes also controls the phytoplankton, by competition for nutrients such as nitrogen or phosphorus.

Atoll lagoons show distinct characteristics compared to their surrounding oceanic waters, with higher abundance of autotrophic pico and nanoplankton, as well as elevated biomass and activity (Leborgne et al., 1989; Torreton and Dufour, 1996; Charpy et al., 1997; Charpy and Blanchot, 1998; Gonzalez et al., 1998). Several Polynesian atoll lagoons are of economical importance because of their uses for pearl oysters culture (Andréfouët et al., 2012). Oysters feed on Particulate Organic Matter (POM) higher than 2 μm, however the nutritive capacity of the water column in atoll is low and the energetic content of POM is 10 times lower than in marine temperate zones (Torreton and Dufour, 1996). Although the energetic content of DOM is 25-fold more important, it is not directly accessible for oysters. Therefore, the oligotrophy of these Polynesian reef lagoons implies a bottom-up control of ecosystems productivity by prokaryotes through their capacity to use DOM and to transfer this energy to organisms that are potential preys for oysters.

The number of studies on bacterial diversity has increased in recent years, but many environments remain poorly investigated, including the water column systems of tropical coral reefs and lagoons (Dinsdale et al., 2008; Weinbauer et al., 2010). Several

* Corresponding author at: Laboratoire de Microbiologie, de Géochimie et d'Écologie Marine, Centre d'Océanologie de Marseille, Université de la Méditerranée – Aix-Marseille Université, CNRS-UMR 6117 Campus de Luminy, Case 901, 163 Avenue de Luminy, 13288 Marseille Cedex 09, France. Tel.: +33 4 91 82 93 36; fax: +33 4 91 82 91 46.
E-mail address: valerie.michotey@univ-amu.fr (V. Michotey).

0025-326X/$ - see front matter © 2012 Elsevier Ltd. All rights reserved.
doi:10.1016/j.marpolbul.2012.01.009

studies have analysed the global abundance of bacterioplankton of shallow atoll using flow cytometry and focusing mainly on *Synechococcus* and *Prochlorococcus* groups (Charpy and Blanchot, 1996, 1998, 1999; Thomas et al., 2010). Data on temporal and biogeographic diversity of heterotrophic prokaryotes including Bacteria but also Archaea are scarce in such ecosystems. Several studies have suggested that marine planktonic Archaea are metabolically active in the global ocean and that they have a potential role in oceanic carbon and nitrogen cycles (Herndl et al., 2005; Ingalls et al., 2006; Wuchter et al., 2007), however studies on spatio-temporal diversity on Archaea are still sparse and concern mainly deep or cold marine areas (Fuhrman and Davis, 1997; Lopez-Garcia et al., 2001; Murray et al., 1998; Teira et al., 2006). Archaea are known to be ubiquitously distributed throughout the world's ocean (Massana et al., 2000) and constitute a numerically dominant group of the prokaryotic community in the meso- and bathypelagic zone (Karner et al., 2001). Nevertheless, knowledge on their surface repartition needs to be improved.

In the context of optimisation of oyster cultures, a global study aimed to improve the knowledge of functioning of Ahe lagoon, a deep tropical atoll lagoon (maximal depth >70 m), of Tuamotu Archipelago (French Polynesia) and subjected to pearl production was initiated. At the time of the study, around 80 pearl farms were registered in Ahe, covering 10 km^2 of the 142 km^2 lagoon. They collectively worked on an estimated 8.1 millions of cultured pearl oysters (Andréfouët et al., 2012).

In the present study, we monitored and quantified changes in bacterial and archaeal community structure using Denaturing Gradient Gel Electrophoresis (DGGE) profiling and quantitative Polymerase Chain-Reaction (qPCR) methods in relation (i) to spatial location inside Ahe lagoon or in the nearby oceanic water, (ii) to depth, (iii) to free and particle-attached states, (iv) to seasons. We charted the spatio-temporal variability of prokaryotic community structure and employed multivariate statistical approaches to explore specific linkages between prokaryotic community structure, taxon identity and considered parameters from 4 campaigns distributed during dry and rainy seasons.

2. Materials and methods

2.1. Study site and sampling

Ahe Atoll is located in the north-western part of the French Polynesian Tuamotu Archipelago at 500 km north-east of Tahiti Island. The lagoon measures 142 km^2 and has an average depth close to 40 m. Ahe is defined as a semi-enclosed atoll and presents one active pass located in the western part of the lagoon and several reef-flat spillways (<50 cm depth) distributed along the reef rim, mainly in the southern and western parts of the lagoon. The average water residence time (ratio of lagoon volume to average water input rate) was estimated at 34 d (Pages et al., 2001) whereas the average renewal time was estimated to be around 80 d (Dumas et al., 2012). Seawater was collected during May 2008, October 2008, February 2009 and August 2009 at four stations distributed along the longest transects of Ahe lagoon (L01: 14.53°S 146.37°W; L03: 14.49°S 146.35°W, L04: 14.46°S 146.35°W, L09: 14.48°S 146.28°W, L11: 14.45°S 146.23°W). One additional station corresponding to oceanic water was located in the close vicinity of the pass (14.45°S 146.36°W) (Fig. 1). Dumas et al. (2012) using a hydrodynamic numerical 3D model found that Ahe lagoons waters were divided in three cells during regular dominant trade wind conditions: the south (L01) and the north (L11) cells have higher water residence time compared to the central one (L03, L09) which was directly impacted by the pass and its aperture to the open ocean.

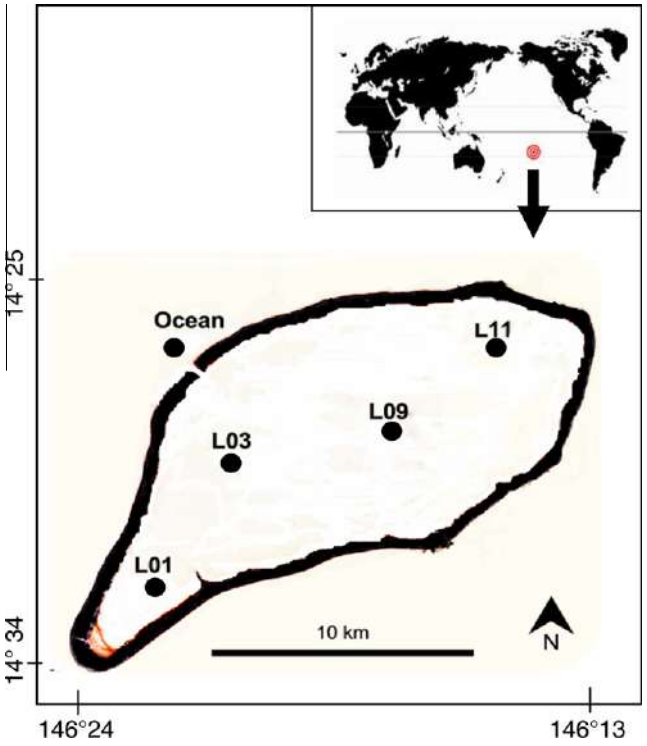

Fig. 1. Localisation of Ahe lagoon and positions of the sampling stations inside the lagoon and in the surrounding oceanic water.

Ten litres of samples were obtained from the surface with a bucket while those from 10 to 20 m depth were retrieved using a Niskin bottle. Samples of water were kept in plastic tank until processing (less than 2 h). In August 2009, two deeper sampling (30 and 40 m) were carried out.

2.2. Microscopic transparent exopolymeric particles determination

Transparent exopolymeric particles (TEP) were stained with Alcian blue (Alldredge et al., 1993) and their TEP size spectra were determined from 10 mL subsamples filtered onto 0.2-mm polycarbonate filters after transfer of the particles retained onto a microscope slide (Passow et al., 1994). TEP size spectra were determined for each slide by counting and sizing TEP at magnifications 400× with a compound light microscope. Ten images were taken per slide. The equivalent spherical diameter of each TEP (dp, mm) was calculated by measuring its cross-sectional area with an image analysis system (ImagePro Plus, MediaCybernetics).

2.3. DNA extraction

Cells from 1.5 L of sea water were recovered under gentle vacuum (~10 mm Hg) onto a 0.8 μm pore-size filter (attached community) and the cells of the filtrate containing mainly the free-living community were collected onto a 0.2 μm (free cells) pore-size polycarbonate filters respectively. Nucleic acids were extracted using MoBio Ultraclean Water DNA isolation kit (MoBio Laboratories, California) that combines bead beating and chemical reagents according to the manufacturer's protocol. Purified DNA was kept frozen at −20 °C until further use.

2.4. PCR amplification

DGGE analysis was performed using the GML5F – 907MR primer set for Bacteria (Bonin et al., 2002; Goregues et al., 2005) and

344f – 915R for Archaea (Casamayor et al., 2000) targeting the variable regions V3–V5 of SSU rRNA gene. For DGGE analysis, primers GML5F-GC or 344f-GC contained a 40-nucleotide GC-rich sequence (5′-CGCCCGCCGCGCCCCGCGCCCGTCCCGCCGCCCCCGCCCG-3′) attached to the 5′ end to improve resolution. PCR amplifications were carried out in reaction mixture containing 1.5 mM $MgCl_2$, 0.2 mM of each deoxyribonucleotide triphosphate, 50 pM of each primer, and 1 U of polymerase (Taq polymerase for bacterial amplification, Promega, USA; Hot start polymerase plus 1.5 μL of solution Q for archaeal amplification, Qiagen, Germany). Initial DNA quantity was adjusted for each sample to obtain the highest amplification yield (20–60 ng of DNA extracts for a mixture of 50 μL). The thermal cycling programs were similar to those previously described (Bonin et al., 2002; Casamayor et al., 2002). Quantification of archaeal and bacterial SSU rRNA gene copy number were determined by qPCR using either bacterial-specific (GML5F) or archaeal-specific (344f) forward primers coupled to a universal reverse primer Uni516R (Takai and Horikoshi, 2000). The LightCycler-FastStart DNA Master SYBR Green I kit (Roche diagnostic) was used for all reactions of real-time PCR with SYBR Green I detection. Concentrations of $MgCl_2$ and primers have been optimised at 2 mM of $MgCl_2$ and 0.25 pmol of each primer in a final volume of 20 μL. Before amplification, an initial denaturation step of 10 min was performed to activate the polymerase. The real time PCR cycles consisted of a denaturation step of 10-s, a hybridization step of 10-s at 55 for total bacteria and 60 °C for total Archaea, with an elongation step of 12-s. Real time data were analysed with Light Cycler software 3,5 (Roche diagnostic). Standards used for total Bacteria, and total Archaea quantification corresponded to pGEMT plasmids harbouring a Gammaproteobacterial or a MG-II Euryarchaeaotal SSU rRNA gene fragment respectively. For standard curves construction, dilution series for each standard from 9×10^6–9×10^3 to 4×10^6–4×10^3 copies for Archaea and Bacteria were used. At the end of the PCR reaction, the specificity of the amplification was checked from the first derivative of their melting curves. Prokaryotic SSU rRNA genes numbers correspond to the sum of bacterial and archaeal quantifications. All amplified products were analysed by electrophoresis on a 1% (wt./vol) agarose gel and visualised using an UV transilluminator (GelDoc 2000 Gel Documentation System, Bio-Rad). Student's *t*-test was performed on the dataset to evaluate the differences between abundance of SSU rRNA genes according to season, station, free living or particle-attached state.

2.5. Prokaryotic community structure analysis

Denaturing Gradient Gel Electrophoresis (DGGE) was performed using a D-code Universal Mutation Detection System (Bio-Rad Laboratories Inc.). Samples containing approximately equal amounts of PCR products (~300 ng of total) DNA were loaded onto 1 mm-thick, 6% (wt./vol) polyacrylamide gel with a denaturation gradient from 30% to 50% (Bacteria) or 30–60% (Archaea), where 100% of denaturation corresponds to 7 M urea and 40% formamide. Electrophoresis was run at 60 °C for 280 min at 150 V in 1× TAE buffer (40 mM Tris–HCl, 20 mM acetic acid, 1 mM EDTA). Following electrophoresis, the gel was incubated for 30 min in 1× TAE buffer containing ethidium bromide (0.5 μg mL^{-1}) and then photographed on an UV transilluminator (GelDoc 2000 Gel Documentation System, Bio-Rad). Representative bands were excised from the polyacrylamide gel. After allowing DNA to diffuse overnight at 4 °C in 100 μL of sterile water, 10 μL was used for re-amplification and the product was sequenced. Banding patterns across the gels were normalised using a previously constructed ladder composed of seven different bands that was loaded several times on each gel. Fingerprints observed on the gels were analysed using GelCompar II (Applied Maths, St-Martens-Latem, Be) software. After normalisation, automatic band detection was performed using a minimum profiling level of 5% relative to maximum. Band comparison between different profiles was settled with a 2% position tolerance and a 1% optimisation to allow for tolerance of bands shifts within and among lanes. Bands presenting similar migration under these conditions were referred to an OTU. Different bands originating from different gels and affiliated to the same OTU by this comparison were sequenced to validate gels-comparison and to phylogenetically identify OTU. For DGGE patterns, calculation of the pair-wise similarities of densitometric profiles was based on Pearson's correlation coefficient (Michener and Sokal, 1957) to construct dendrograms using the Unweighted Pair-Group Method Analysis (GelCompare II software, Applied Maths, St-Martens-Latem, Be). Tables of band presence were exported and were modified in Excel software for Canonical Correspondence Analysis (CCA). The influence of season, depth, and station on the presence of identified OTU was analysed using XLSTAT software (Addinsoft, France).

2.6. Sequencing and comparative analysis of 16S rRNA sequences

16S rRNA partial sequences obtained by the classical Sanger sequencing method were trimmed and aligned with the same region of the closest relative strains available in GenBank using the BLASTN facility (http://www2.ncbi.nlm.nih.gov/BLAST/). Sequence alignment was achieved using ClustalW improving the sensitivity of progressive multiple sequence alignment through sequence weighting, position-specific gap penalties and weight matrix choice (Thompson et al., 1994). Sequence positions and alignment uncertainties were omitted from the analysis. Phylogenetic trees were constructed using the neighbour-joining method (Saitou and Nei, 1987). A bootstrap analysis with 500 replicates was carried out to check the robustness of the tree, which was plotted using the Mega 4 program (Kumar et al., 2007). Sequences were submitted to EMBL under the accession numbers HE647133 to HE647184.

3. Results and discussion

3.1. Prokaryotic total abundance

Ahe atoll lagoon is defined as a semi-enclosed atoll (Fig. 1) and is deeper than that is usually encountered (maximum depth >70 m). It presents a relative stability of temperature, salinity and chlorophyll *a* concentration (Andréfouët et al., 2012; Dumas et al., 2012). In a previous study, over one year period, these parameters varied between 26.87 and 29.31 °C for temperature, 36.14 and 36.9 for salinity and 0.25 and 0.41 μgL^{-1} for chl *a* (Thomas et al., 2010). No vertical stratification was observed for temperature and salinity within the first 30 m (Thomas et al., 2010), although stratification was observed by Dumas et al. (2012). The dry and rainy seasons correspond to July–October and December–May, respectively. During the rainy season, winds can be intense (Dupon and Dodter, 1993).

The organic particle load under TEP (transparent exopolymeric particles) forms were measured in October in term of abundance and volume. The water of the lagoon contained more TEP (1787 ± 1020 particles mL^{-1}, corresponding to 3.9 ± 1.8 ppm) than the oceanic surrounding water (900 ±140 particles mL^{-1}, corresponding to 1.1 ± 0.4 ppm). These results are in good agreement with those reported for the lagoon of Noumea, New Caledonia (Mari et al., 2007). Analyses of prokaryotic communities of free-living and particle-attached fraction in surface (0–20 m depth) layer above the chlorophyll maximum was assessed in term of abundance and diversity. Quantitative fluorogenic PCR allowed the determination of SSU rRNA gene numbers of Bacteria and Archaea. No difference

was observed according to depth (*t*-test, $n = 80$, $p > 0.05$) in consequence average concentrations of SSU rRNA 0–20 m were reported (Table 1). Lagoon prokaryotic SSU rRNA gene (Bacteria + Archaea) concentrations were higher than that of oceanic waters and ranged between 1.82×10^5–1.18×10^7 (average 2.1×10^6) genes mL^{-1} and 1.63×10^5–1.46×10^6 (average 0.6×10^6) genes mL^{-1},

Table 1
Abundance of SSU RNA gene (average 0–20 m) determined by qPCR on particle-attached fraction (0.8 μm pore size filtration) and free fraction (subsequent 0.22 μm pore size filtration).

Station		May 2008		October 2008		February 2009		August 2009	
		Free (10^4/mL)	Attached (10^4/mL)	Free (10^4/mL)	Attached (10^4/mL)	Free (10^4/mL)	Attach (10^4/mL)	Free (10^4/mL)	Attached (10^4/mL)
L01	Bacteria	19.2 (±2.3)	31.0 (±7.5)	16.1 (±3.5)	36.7 (±30.1)	30.5 (±0.1)	121.1 (±36.4)	102.1 (±139)	68.9 (±60.1)
	Archaea	2.5 (±2.0)	0.06 (±0.02)	0.7 (±0.6)	26.2 (±20.3)	1.7 (±0.7)	11.7 (±10.7)	5.3 (±3.5)	45.6 (±31.0)
L03	Bacteria	16.3 (±9.9)	7.9 (±0.9)	107.1 (±14.3)	17.5 (±13.5)	30.2 (±10.6)	84.8 (±17.6)	15.2 (±10.4)	201.2 (±47.3)
	Archaea	0.5 (±0.1)	0.9 (±0.8)	1.0 (±0.1)	6.2 (±5.0)	0.4 (±0.1)	17.1 (±6.3)	1.5 (±1.1)	232.2 (±22.6)
L09	Bacteria	116.2 (±34.1)	32.1 (±4.8)	13.1 (±2.7)	36.6 (±30.5)	15.9 (±10.1)	76.6 (±41.6)	81.8 (±16.4)	169.1 (±59.2)
	Archaea	12.2 (±0.4)	0.04 (±0.02)	0.4 (±0.2)	26.5 (±25.5)	1.3 (±0.2)	8.1 (±1.5)	9.5 (±2.9)	143.3 (±2.2)
L11	Bacteria	56.0 (±7.3)	15.2 (±1.0)	10.1 (±4.1)	96.5 (±14.2)	22.2 (±4.6)	89.1 (±60.2)	145.1 (±47.2)	56.7 (±41.6)
	Archaea	46.8 (±26.1)	0.6 (±0.1)	1.4 (±1.8)	43.1 (±6.5)	0.9 (±0.9)	17.9 (±0.7)	107.1 (±12.2)	196.2 (±20.1)
Ocean	Bacteria	45.6 (±40.7)	3.5 (±0.9)	4.3 (±2.3)	24.2 (±0.2)	18.1 (±17.1)	40.4 (±19.3)	13.8 (±11.3)	27.5 (±26.3)
	Archaea	0.7 (±0.6)	0.02 (±0.02)	<0.01	2.1 (±2.1)	0.50 (±0.1)	0.6 (±0.5)	1.4 (±1.2)	62.9 (±17.9)

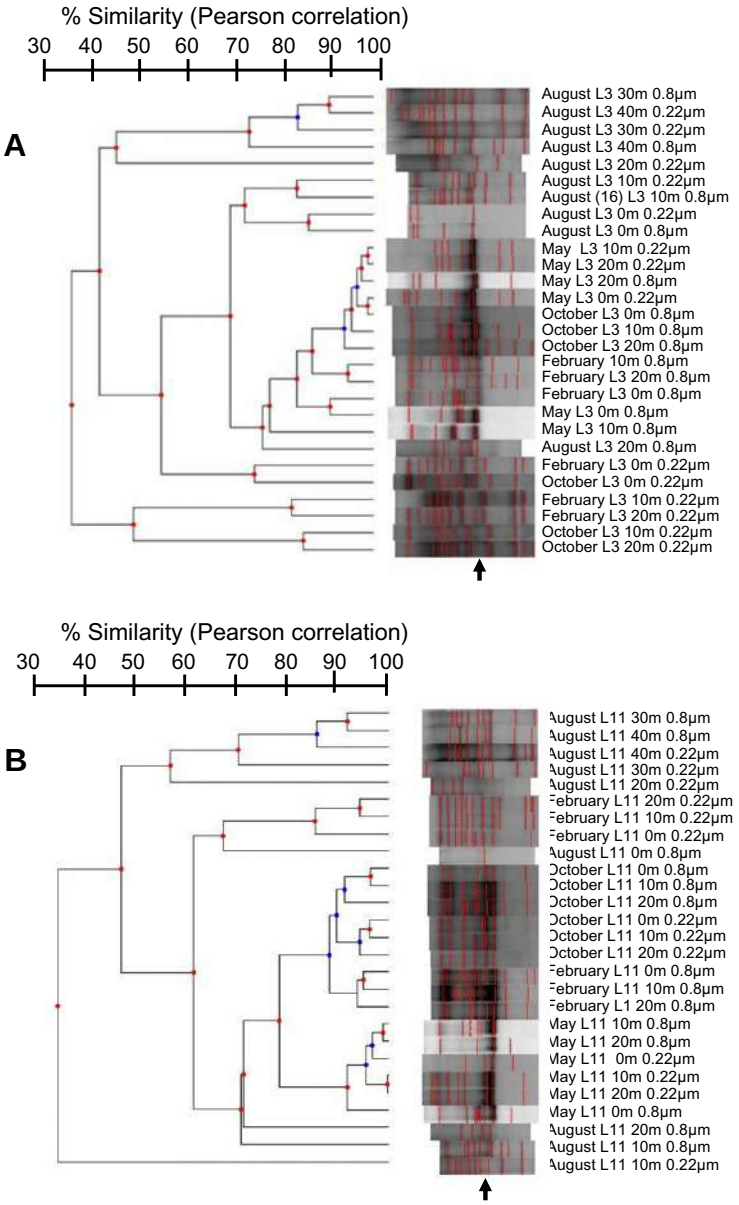

Fig. 2. Hierarchical clustering of bacterial DGGE fingerprints of stations L3 (A) and L11 (B) located inside the lagoon. Scale indicates percent similarity. Bands that have been taken into account for comparison are indicated. (0.8 μm: fraction >0.8 μm, 0.2 μm: fraction <0.8 μm). The arrows indicate the bands corresponding to *Synechococcus*.

respectively. Taking into consideration that SSU rRNA genes are in several copies per genome (average of 4.08 for Bacteria and 1.76 for Archaea; http://rrndb.cme.msu.edu), these results were slightly lower than that of cellular abundances determined at the same period by flow cytometry, except for August samples for which opposite trend was observed. For oceanic surrounding water this difference was very small (1.4 to 2-fold lower) whereas it was more pronounced for the lagoon samples (1–8-fold lower) from the same campaigns (Bouvy et al., 2012). However, cellular abundance in average are in similar range than other values obtained on the same lagoon in earlier study (in 2007, 0.3–0.99 $\times$ 10^6 cell mL^{-1} Thomas et al., 2010), for New Caledonia lagoon (0.99–1.7 $\times$ 10^6 cell mL^{-1} Weinbauer et al., 2010), or of New Caledonia oceanic area (0.6 $\times$ 10^6 cell mL^{-1}; Weinbauer et al., 2010).

3.2. Free living versus particles attached- prokaryotic abundance

The free-living and particle-attached fractions were also determined (Table 1). Percentage of particle-attached procaryotic ribosomal genes varied in a large range, between 3.5% and 98.7%, with a mean value of 63%. These values are higher than the usually reported proportion of cells attached to particles (ca. 10%) in the open ocean and in lagoons (Torreton and Dufour, 1996; Torreton, 1999; Torreton et al., 2002). However, attached prokaryotes are often more active than their free-living counterparts (Simon et al., 2002; Grossart et al., 2007). It is thus possible that this difference originated from number of ribosomal gene copies per genome that could be higher for fast-growing-particle-associated prokaryotes in comparison with slow-growing-free living one. Trends of gene abundances of the different prokaryotic communities showed that bacterial SSU rRNA numbers were significantly higher in the lagoon compared to oceanic surrounding waters (t-test, $n = 80$, $p < 0.05$) and presented a significant seasonal difference (Table 1, t-test, $n = 80$, $p < 0.05$) with a maximal value observed in August. At this time, the stations located in the middle of the lagoon (L03, L09) and directly impacted by the pass, presented the maximal number of SSU rRNA gene in the particle-attached-fraction. Those at the extremity of the lagoon-wide transect, and presenting

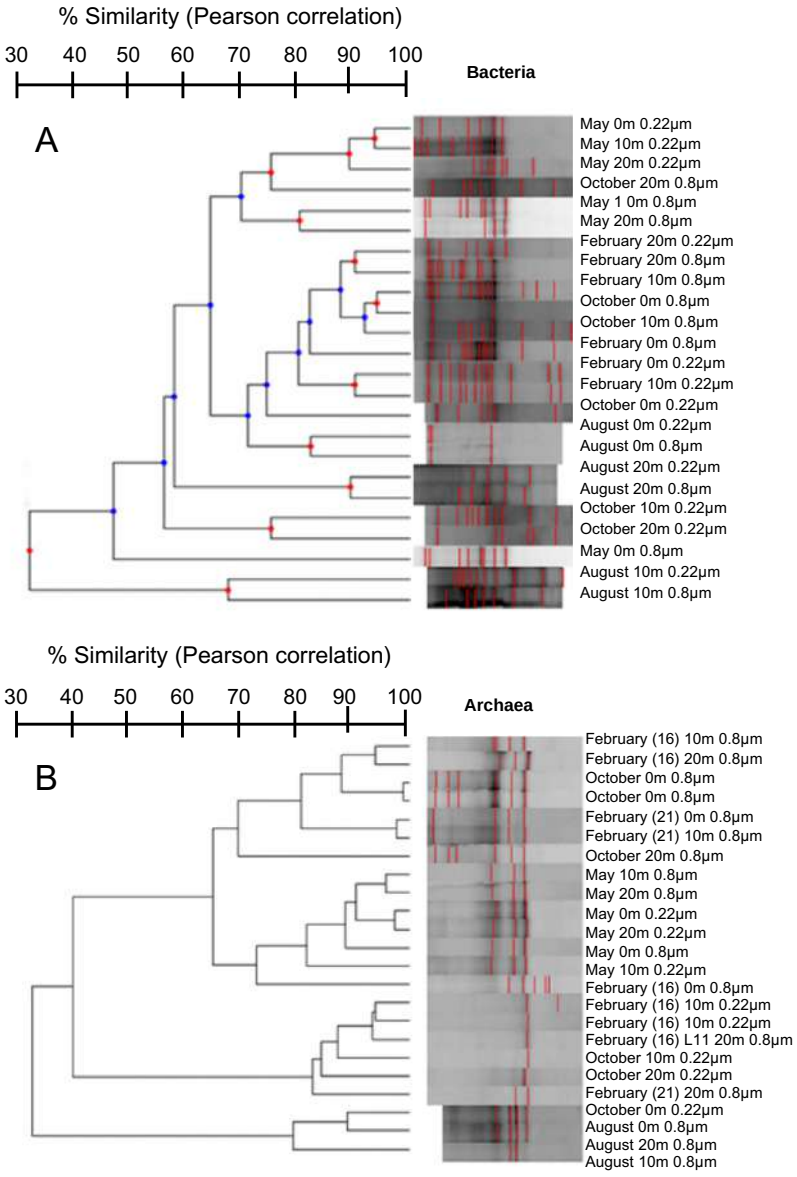

Fig. 3. Hierarchical clustering of bacterial (A) and archaeal (B) DGGE fingerprints of Ocean station. Scale indicates percent similarity. Bands that have been taken into account for comparison are indicated. (0.8 µm: fraction >0.8 µm, 0.2 µm: fraction <0.8 µm).

the higher residence time (L01, L11), showed high number of free living bacterial SSU rRNA genes. Over the year, no significant difference in bacterial SSU rRNA abundance was found according to station within the lagoon or to free-living versus particle-attached state (t-test, $n = 80$, $p > 0.05$).

In contrast to a previous study on the New Caledonia lagoon (Weinbauer et al., 2010), archaeal ribosomal genes could be amplified in Ahe lagoon. Although archaeal SSU rRNA gene abundance was lower than that of bacteria, both presented similar trends with no influence of depth and station inside Ahe lagoon (Table 1, t-test $n = 80$, $p > 0.05$). However, they differed significantly (t-test, $n = 80$, $p < 0.05$) according to the other parameters (inside/outside lagoon, Free/attached fraction, and season). In contrast to bacteria, archaeal SSU rRNA gene concentrations were similar inside and outside the lagoon, and increasing significantly (t-test $n = 80$, $p > 0.05$, $p < 0.001$) in August in comparison to other months. Archaeal SSU rRNA gene density associated to particles were also significantly higher (t-test, $n = 80$, $p > 0.05$) than that of free living cells.

3.3. Bacterial diversity

Global molecular diversity obtained from DGGE analysis, sequencing approaches and the comparative analyses of SSU rRNA gene sequences revealed the major phylogenetic types that

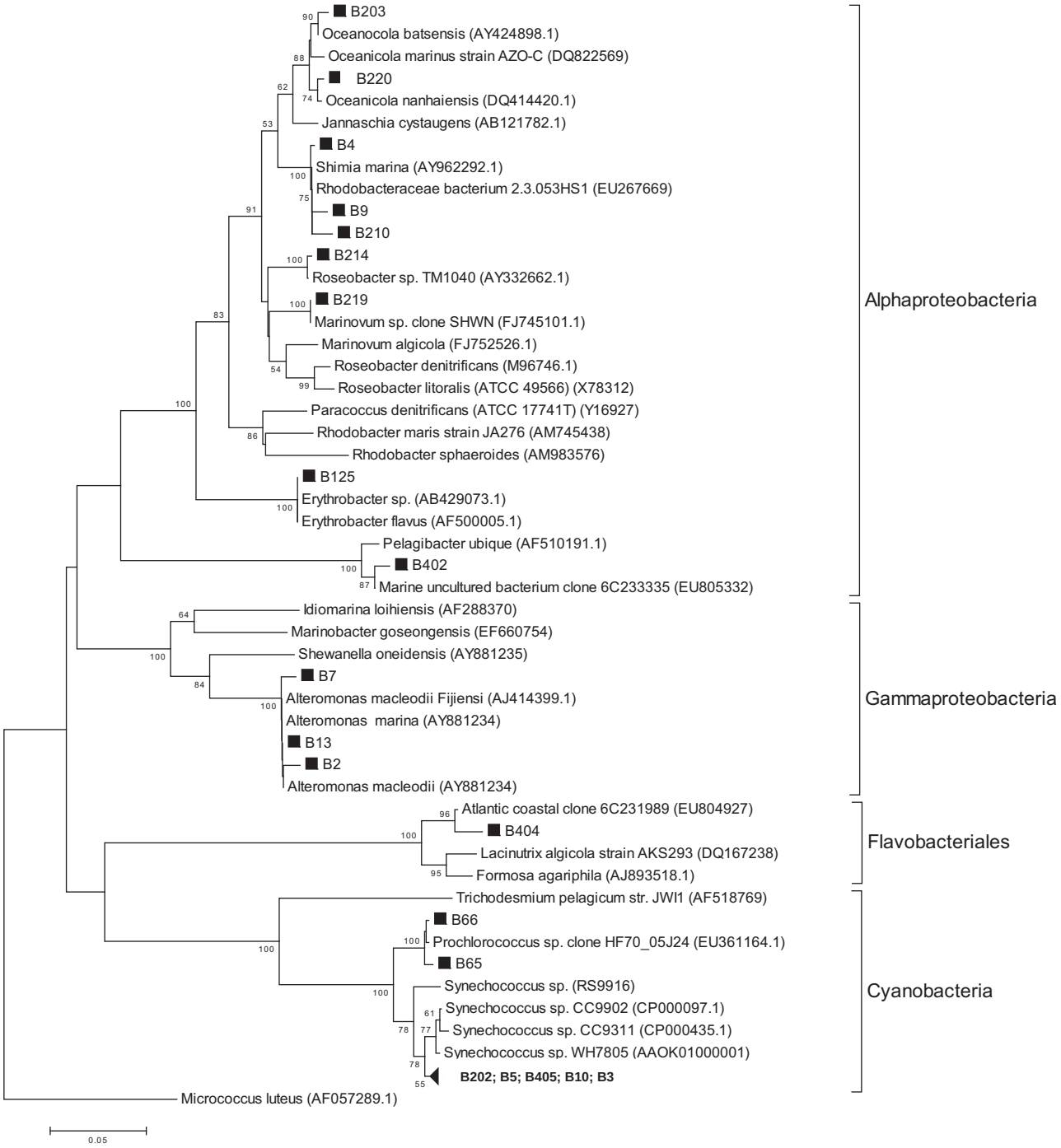

Fig. 4. Phylogenetic tree of the bacterial 16S rRNA genes of DGGE bands based on 600 nucleotides comparison. Sequences derived from this study are indicated by a square. Triangle corresponds to the compression of a sub-cluster. Bootstrap values (500 replicates) above 50% are indicated. The scale bar indicates 5% sequence divergence.

composed the lagoon and oceanic communities. All sequences retrieved in this study were affiliated within bacterial or archaeal superkingdoms, and no plastids or eukarial ribosomal gene sequences were obtained.

The structure of the free living and particle-attached bacterial communities was analysed for the four sampling periods at all depths (0, 10, 20 m and deeper at 30 m only in August) and at all stations (L01, L03, L09, L11 and Ocean), for a total of 136 samples. From analysis of the bacterial SSU rRNA gene diversity on DGGE gels, 18 different operational taxonomic units (OTUs) were identified. Within a sample, between 3 and 12 bands were observed, with the higher number of bands corresponding to the stations inside the lagoon (Fig. 2) in comparison to the oceanic station (Fig. 3A). The cluster analysis of DGGE band pattern of the lagoon station L03, in the close vicinity of the pass and subjected to oceanic influences, the station L11 located at an extremity of the transect and showing a higher water residence time and the oceanic station are presented in Figs. 2 and 3A. The community of station Ocean, L03 and L11 presented about 35% similarity within all sampling dates. No clear pattern according to seasons and no obvious distinction depending of free-living/particle-attached state could be observed. This trend could be generalised for the other stations located in the lagoon (data not shown).

The re-amplification and the sequencing of the most intense DGGE bands have shown that they belong to 3 well-defined phyla: *Cyanobacteria*, *Proteobacteria* and *Flavobacteria* (Fig. 4). The sequence of major OTU was confirmed by several sequences originating from different samples. Eight sequences retrieved from oceanic and lagoon waters and belonging to phylum *Cyanobacteria* fell in *Synechococcus* (B202; B5; B3; B405; B10; B3) and *Prochlorococcus* (B65; B66) clusters and presented 99% similarity with cultivated strains. The corresponding DGGE bands were present in almost all samples, sometimes reaching high intensity (see Fig. 2, L03, L11 stations in May 2008 samples). This finding confirms previous results obtained by flow cytometry, indicating that 83% of chl *a* extraction corresponds to picoplancton communities that were dominated in term of abundance by *Synechococcus* and *Prochlorococcus* (Thomas et al., 2010).

Despite the close phylogenetic relatedness of *Synechococcus* and *Prochlorococcus* ribosomal sequences, these two groups differ markedly in their ecologic performance, derived from different photosynthetic apparatus and nutrient physiology (Scanlan and West, 2002). *Synechococcus* is ubiquitous and is found in estuarine, coastal or offshore waters over a large range of latitudes (Olson et al., 1990b). On the other hand, *Prochloroccoccus* is confirmed to warm (45°N–40°S) and mostly nutrient-poor oceanic zone (Partensky et al., 1999; Olson et al., 1990a; Tarran et al., 2001). Among *Synechococcus*, between 10 and 16 clades have been defined based on different phylogenetic markers and physiological characteristics (Fuller et al., 2003; Rocap and Ahlgren, 2006; Muhling et al., 2006; Penno et al., 2006; Toledo et al., 1999). The phylogenetic similarities are very high between the different clades of *Synechococcus* and the size of the amplified ribosomal fragments in this study did not allow affiliating the retrieved sequences to a specific clade but to a group of clades belonging to sub-cluster 5.1 (Fuller et al., 2003). The distribution and relative abundance of member of this sub-cluster in natural environment suggest two major lifestyle strategies for marine *Synechococcus*: "open ocean/specialist" that dominate in warm-oligotrophic or temperal/polar-mesotrophic waters and "coastal/opportunist" that can be found either in coastal areas or across a broad range of ecosystems in relative low numbers, but occasionally reaching higher number in the vicinity of upwelling areas or following environmental perturbation (Dufresne et al., 2008; Scanlan et al., 2008). Sequences of majors DGGE bands belonging to *Synechococcus* and retrieved from waters of Ahe lagoon and of ocean in the close vicinity fell in "open ocean/specialist" ecotype (Fig. 4). The three OTUs (B10-3-5, B202, B405) of *Synechococcus* identified in this study was retrieved from free living as well as particle-attached fraction. However, cut-off between both fractions is low so it is not excluded that several cells may stay aggregated after division and could form small particles retained on 0.8 μm filter. The different phylotypes presented various behaviours: OTU B10-3-5 was detected at all seasons and at all stations at intermediated depths (10–20 m) whereas B202 corresponded to surface samples at rainy season and B405 to deeper samples (30 m) (Fig. 5).

Different ecotypes can also be found among *Prochlorococcus* and were defined according to their light tolerance leading to the description of Hight Light (HL) and Low Light (LH) adapted clades (Johnson et al., 2006). OTU of *Prochlorococcus* (B65–66) retrieved from Ahe lagoon waters and surrounding oceanic zone was found in particle-attached (>0.8 μm) (Fig. 5)) fraction. It fell in HL cluster and this finding is in agreement with the parameters of the sampling sites (high radiance, clear water and low depth).

Beside the cyanobacterial sequences, sequences belonging to phylum *Proteobacteria* (alpha and gamma) and *Flavobacterium* (B404) were also retrieved in this study (Fig. 4). Although ribosomal data do not provide straight forward information on metabolic traits, they allow the identification of ecophysiology of organisms. Members belonging to phylum *Proteobacteria* are important actors of the microbial community in the marine water column (Rappe et al., 2000), and present very diverse metabolisms. *Alpha-* and *Gamma-proteobacteria* identified in Ahe lagoon fell in genus *Alteromonas* (B2, B7, B13) and *Erythrobacter* (B125), in family Rhodobacteriaceae (genera *Marinovum* (B219) *Shimia* (B4, B9, B210), *Roseobacter* (B214), *Oceanicola* (B203, B11), and in SAR11

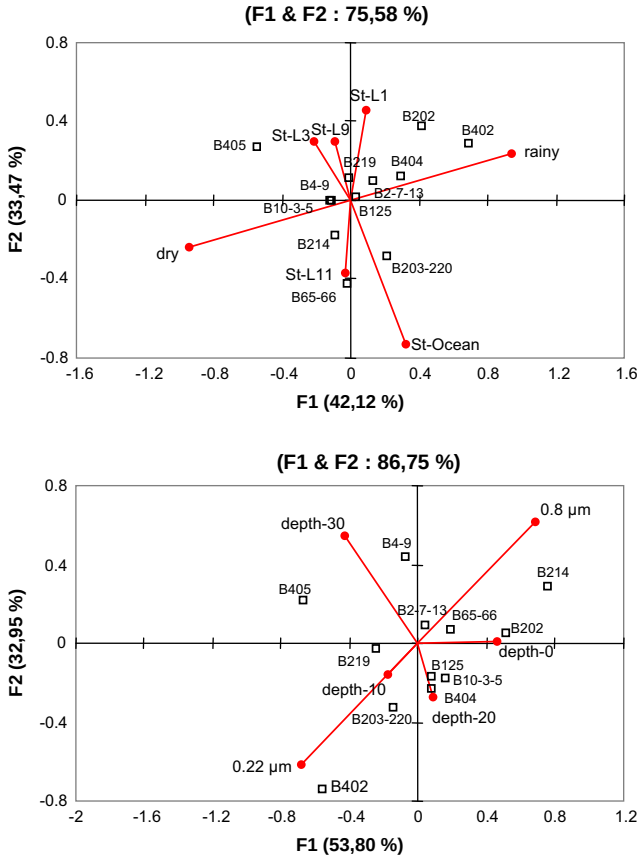

Fig. 5. Canonical Correspondence analysis (ACC) between the presence of bacterial OTU and stations, seasons, depth and free living (0.2 μm: fraction <0.8 μm) and particle-attached (0.8 μm: fraction >0.8 μm) fractions.

group (B402). Sequences belonging to similar groups have also been retrieved in the lagoon of Noumea, New Caledonia (Weinbauer et al., 2010). Many of these bacteria are described as heterotroph (Raguenes et al., 1996; Cho and Giovannoni, 2004; Martens et al., 2006). Their presence in the Ahe oligotrophic water, containing little organic matter mainly as particles, implies probably that they developed strategies to resist carbon starvation. *Marinovum* member (B219) was found in all stations, at all seasons, and in free-living and particle-attached fraction (Fig. 5). *Alteromonas* members (B2-7–13) were detected mostly at wet season from particle-attached as well as in free-living fraction (Fig. 5). The detection of Alteromonadaceae sequences is surprising, since the abundance of this group is thought to be low in oceanic water although bloom-like outbreaks have been documented (Alonso-Saez et al., 2007). The presence of *Alteromonas macleodii* is frequently detected in water column of various oceans (Muhling et al., 2008). *Alteromonadaceae* sequences have also been reported in coastal bays around Noumea. This organism was assumed to respond to disturbance such as mixing of oligotrophic offshore water with mesotrophic particle-rich bay water (Weinbauer et al., 2010). Furthermore, *Alteromonas haloplanctis* (Lebaron and Joux, 1994) has been shown to resist to carbon starvation. This property is an ecological advantage to survive in organic matter patchy environment. Other member of chemoheterotroph genus have also been detected such as OTU B4-9–210 belonging to *Shimia* that has been found preferentially in particle-attached fraction in deeper sample, as well as B203–220 belonging to *Oceanicola* which was retrieved from ocean station in free-living cell fraction (Fig. 5). Since cells of *Oceanicola* genus accumulate polyhydroxybutirate (PHB) (Cho and Giovannoni, 2004), this is another strategy to sustain carbon storage compound in an organic matter patchy environment.

The carbon-pulse conditions in Ahe tropical water could also favour mixotrophic strains belonging to *Roseobacter*, *Erythrobacter* or *Flavobacteria* genus and SAR 11 group. These groups are heterotrophs, but some strains present pigments enabling them to retrieve energy from light, sparing the few organic matter present

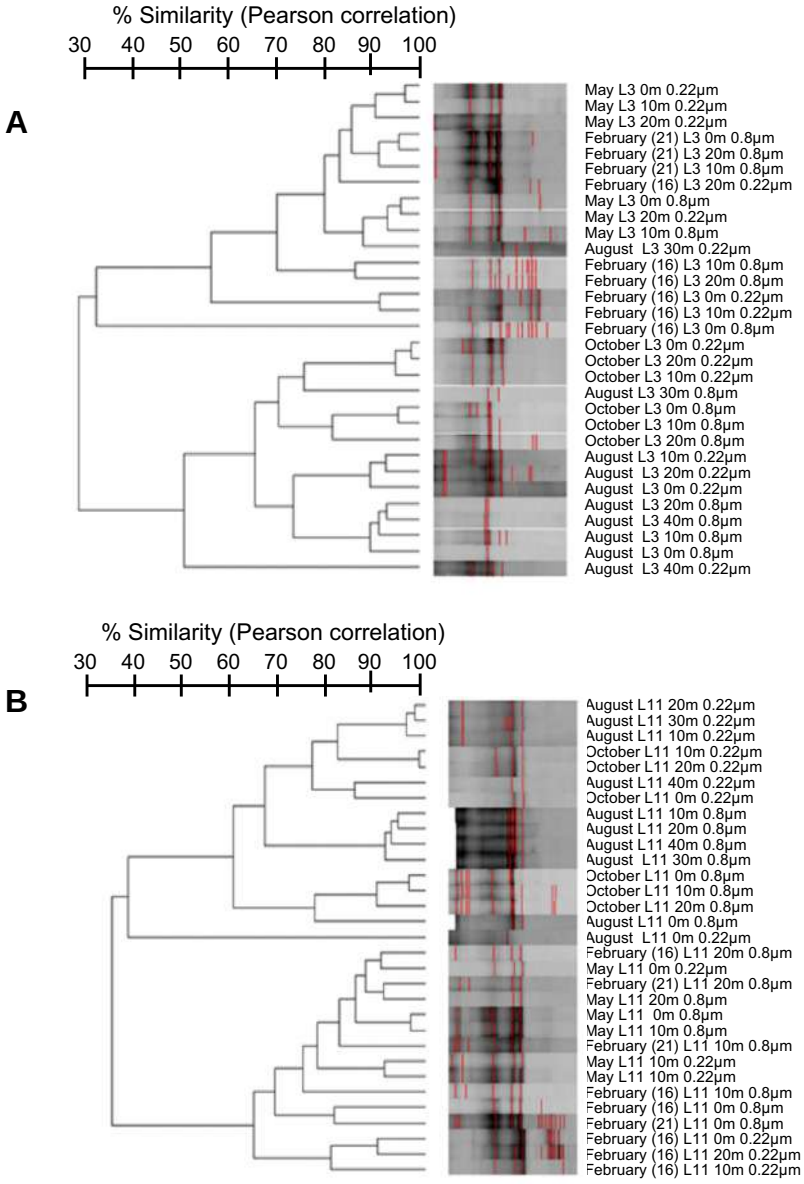

Fig. 6. Hierarchical clustering of archaeal DGGE fingerprints of stations L3 (A) and L11 (B) located inside the lagoon. Scale indicates percent similarity. Bands that have been taken into account for comparison are indicated (0.8 µm: fraction >0.8 µm, 0.2 µm: fraction <0.8 µm).

for growth or survival. These pigments are composed mainly of bacteriochlorophyll *a* for *Roseobacter* (Shiba, 1991) and *Erythrobacter* (Yurkov and Beatty, 1998) and proteorhodopsin for SAR11 members (Giovannoni et al., 2005) and *Flavobacteria* (Pinhassi et al., 2007). *Flavobacteria* (B404) and *Erythrobacter* (B215) members did not present a clear pattern of repartition in contrast to *Roseobacter* (B214) and SAR 11 members (B402). In Ahe lagoon, *Roseobacter* SSU rRNA genes (B214) have been retrieved from particle-attached surface fraction (Fig. 5) as found for other oceanic areas but localisation of this genus in planktonic fraction or associated with plankton, marine vertebrates or invertebrates have also been reported (Brinkhoff et al., 2008). *Roseobacter* is frequently encountered in oceanic area. The abundance of its SSU rRNA genes can also reach 16% of the marine surface bacterioplankton in the coastal Pacific zone (Rappe et al., 2000). SAR 11 is also a group frequently encountered in the marine environment. In this study, SAR11 (B402) OTU was detected mainly in planktonic fraction during the wet season (Fig. 5).

3.4. Archaeal diversity

The archaeal community structure was also analysed using the same DNA extract used for bacteria. For most samples, the yield of amplification was sufficient to reach the requested quantity for DGGE analysis. Within a sample, the number of DGGE bands varied between 2 and 13. Overall, 27 different OTUs were observed in this study. The cluster analysis of DGGE band pattern of the different stations inside the lagoon showed a clear separation depending of seasons i.e. May and February samples on one side and August and October samples on the other side (Fig. 6). To confirm the putative influence of seasons, a replicate of another date in February (21st) was also analysed. Although daily variation could be observed, pattern of samples from both dates in February (16th and 21st) grouped together with May samples. In consequence, for archaeal community of the lagoon, daily variations seem lower than seasonal ones. Within each cluster, the percentages of similarity were higher than 50% for most samples (Fig. 6). During the dry

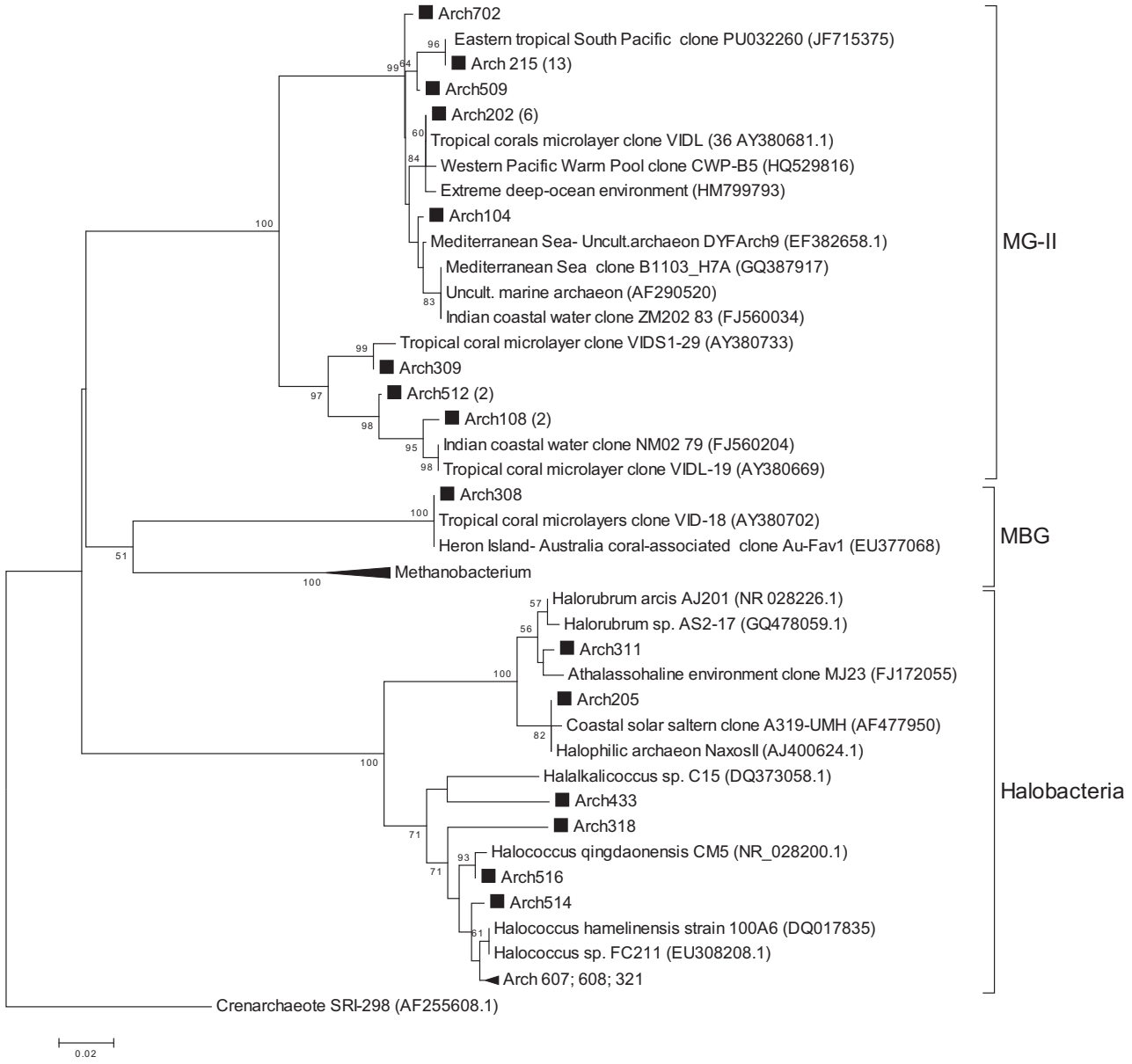

Fig. 7. Phylogenetic tree of the archaeal 16S rRNA genes of DGGE bands based on 400 nucleotides comparison. Sequences derived from this study are indicated by a square. Number of identical sequences is indicated in parenthesis. Bootstrap values (500 replicates) above 50% are noted at node. The scale bar corresponds to 2% sequence divergence.

season (October and August), communities of particles was grouped in different sub-cluster than free-living one. This distinction was not observed for the rainy season. Archaeal community in the ocean presented lower number of DGGE bands (between 6 and 1) compared to the lagoon, and no clear seasonal or free-living/particle-attached states pattern were identified (Fig. 3B).

The 14 more intense phylotypes were identified after re-amplification of DGGE band and sequencing (Fig. 7). Some intense and frequent phylotypes were confirmed by several sequences originating from different DGGE gels and samples to validate the pattern comparison. All identified OTUs were affiliated to Euryarchaeota. The sequences of OTUs were clustered in three main groups. Two of them did not possess any cultivated representative: the Marine Group II (MG-II), the Marine Benthic Group (MBG) and the class of *Halobacteria*. Members of MG-II were the most often encountered in Ahe lagoon followed by *Halobacteria* and MBG sequence (Arch 308).

MG-II or so-called "planktonic marine group euryarchaeotes" is peripherally related to Thermoplasmatales (Delong, 1992, 2003). This pelagic archaeal clade has been identified from surface waters of different marine areas and seems to be dominant here. Furthermore, MG-II members have been also found associated with tropical corals (Massana et al., 1997, 2000; Delong et al., 1999; Gallagher et al., 2004) and blooms have been observed in surface water of Monterey Bay and of the North Sea during summer (Pernthaler et al., 2002; Delong, 2003). Sequences of uncultured Archaea have been originally classified according to their geographic location. However, Teske and Sorensen (2008) analysed the phylogenetic relations between various archaeal groups and have shown that the archaeal communities group according to their local environment rather than their geographic position. Still, little is known about genetic makeup, physiology or ecology of MG-II. The closest representatives of MG-II in the Ahe sequences (Arch 702; 215; 509; 202; 104; 309:512; 108) were retrieved from Mediterranean sea, Indian Ocean, Pacific Ocean and were associated to tropical coral reefs but were outside the cluster of uncultured clones harbouring proteorhodospin gene (Frigaard et al., 2006). Except Arch 108 that was found at the oceanic station surface, the other MG-II phylotypes were characteristic of the lagoon stations (Fig. 8). Most of MG-II members were detected during rainy season sampling periods with the exception of Arch 702. The unique member of marine benthic group (Arch 308) was identical to sequence of symbiont of tropical coral and was detected mainly during the rainy season (Figs. 7 and 8). The closest relatives of several MG-II and MB sequences correspond to clones retrieved from coral microlayer. Since these OTUs were mostly detected during rainy season, their occurrence in the water column could be the result of mixing of communities associated to benthic organisms into the ambient seawater by intense winds. This mixing could result in the homogenisation of free-living and particle-associated communities as observed in Fig. 6 for May and February samples. This finding is in agreement with previous coral reef works that have shown that the release of nutrient and mucus by corals stimulate the production of Prokaryotes in nearby waters (Herndl and Velimirov, 1986; Schiller and Herndl, 1989) and fuel the food web of lagoon systems (Wild et al., 2004).

The members of class *Halobacteria* (Arch 311, 205, 433, 318, 516, 514, 607, 608, and 321) were found in lagoon samples mainly during the rainy season (Fig. 8). Cultivated strains of this class are halophilic and their presence in the marine environment could be surprising. However molecular techniques have allowed the identification of clones highly similar to *Haloarcula*, *Halorubrum* and *Haloquadratum* strains in the Gulf of Aqaba, with salinity as low as 40 (Ionescu et al., 2009). Therefore, their repartitions could be broader than previously thought. Most of the *Halobacteria* OTUs were detected in sub-surface samples, except Arch 514 that corresponds

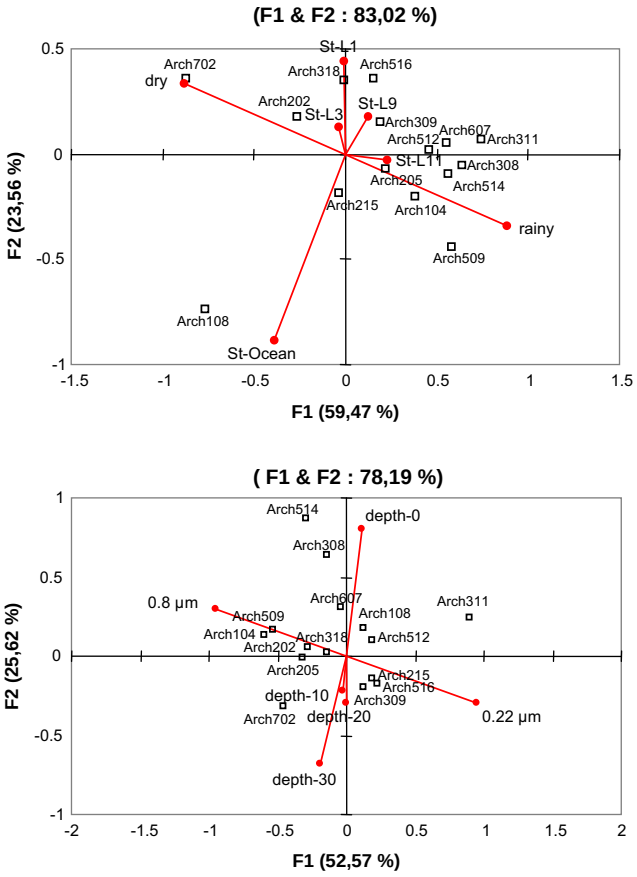

Fig. 8. Canonical correspondence analysis (ACC) between the presence of archaeal OTUs and stations, seasons, depth and free living (0.2 µm: fraction <0.8 µm) and particle-attached (0.8 µm: fraction >0.8 µm) fractions.

to surface samples. These organisms have been detected downwind area of human activity in the lagoon, and the implication of human activity on their presence cannot be excluded.

3.5. Ocean/lagoon prokaryotic relation

To understand the relation between ocean and lagoon water, the total community (free living + particle-attached) of the Ahe pass was analysed in October 2008. The period between 10–12 am, noon–1 pm and 2–4 pm corresponded to high tide (the entrance of oceanic water into the lagoon), slack water and ebb tide (the exit of the water from lagoon), respectively. The structure of bacterial surface community in the ocean and lagoon next to the pass were not different and grouped together in a cluster (Fig. 9A), however the community of the incoming water (10 am–1 pm) correspond to a different cluster and present only 30% similarity with community of ocean, of lagoon, and of outgoing water.

In contrast to bacteria, the structure of oceanic archaeal communities was different than that of the lagoon (Fig. 9B). Furthermore, the incoming archaeal community in the pass presented 92% similarity with particle-attached fraction of oceanic water. The outgoing water presented a different structure than that of the incoming one and showed 70% similarity with that of free-living and particle-attached fractions of lagoon (Fig. 9B). The DGGE finger print of incoming water presented two intense bands on the DGGE gel (OTU Arch108 and Arch 215) that were identified as members of MG-II. The sequence of most intense band (Arch108) showed 97% similarity with clones retrieved from various marine environments such as tropical coral microlayer (AY380669), deep sea hydrothermal

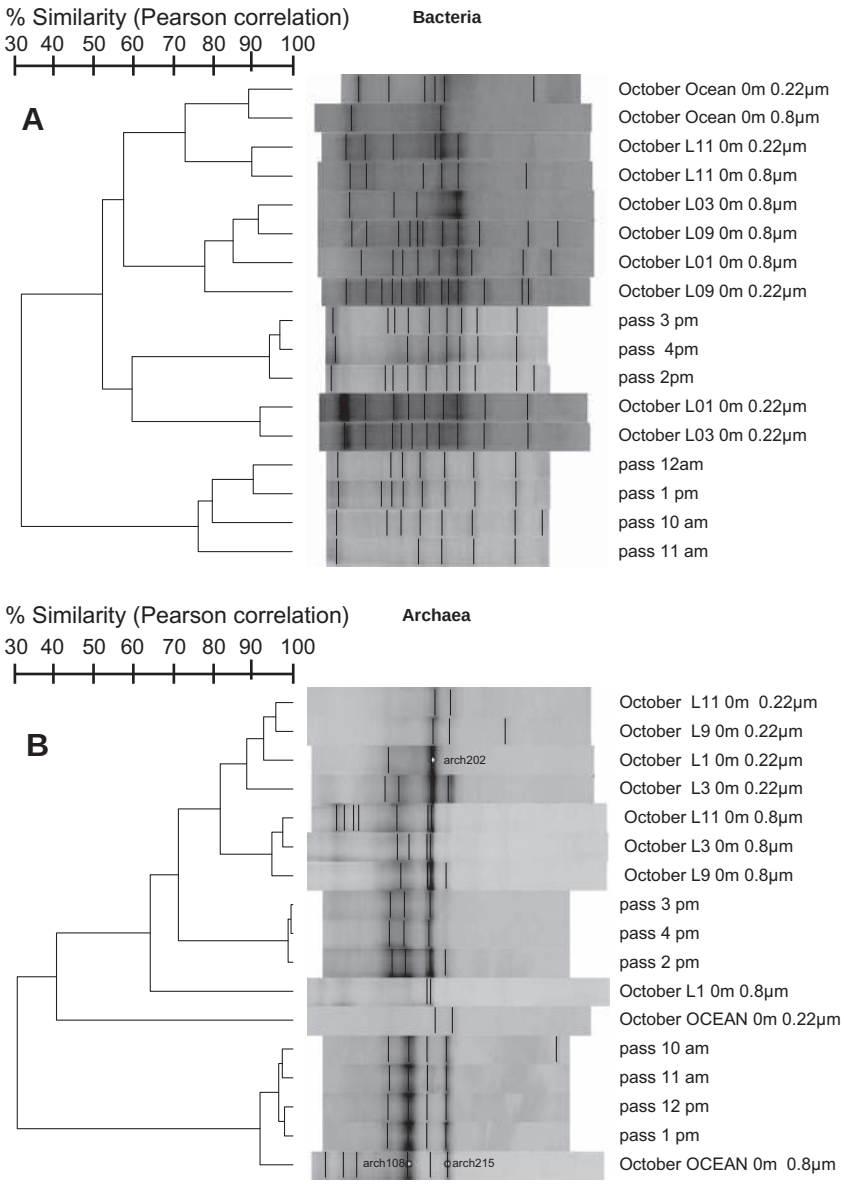

Fig. 9. Hierarchical clustering of bacterial (A) and archaeal (B) DGGE fingerprints of surface stations inside Lagoon, Ocean station, pass of the lagoon during tide. Scale indicates percent similarity. Bands that have been taken into account for comparison are indicated; (0.8 µm: fraction >0.8 µm, 0.2 µm: fraction <0.8 µm). For pass samples, the DGGE pattern correspond to the whole community (free-living + particle-attached).

deposit (AB329815), or surface water from Equatorial North Atlantic Ocean (EU237383). In October this OTU was strongly associated with oceanic particles. The second band in intensity corresponded to sequence of Arch 215 belonging to another cluster of MG-II. OTU Arch 215 appeared ubiquitous since it was detected in all stations within lagoon and in ocean, at all seasons and in free as well as in particle-attached fractions. It presented 99% similarity with sequences retrieved from various marine environments, including from the Mediterranean Sea (EF382658), Gulf of Mexico (GQ250670), central west coast of India (FJ560034), North Pacific Subtropical Gyre (DQ156474), and hydrothermal vents (AB611631). Its spatial and temporal prevalence and its free-living/particle-attached states suggest a versatile metabolism and the capacity to cope with oligotrophic environments. In the outgoing water, the intensity of Arch108 and Arch215 OTUs decreased in comparison to incoming water whereas a strong band corresponding to OTU arch202 appeared. Arch202 was ubiquitous in Ahe lagoon and the water surrounding the atoll at all seasons, but was mainly retrieved from the particle-attached fraction (Fig. 8). The closest relatives of this sequence have been found from Timor Sea marine sponges (Australia, DQ299289), from Caribbean Sea coral *Diploria labyrinthiformis* microlayer (Kellogg, 2004), in particle fraction collected at 6000 m depth in the Puerto-Rico trench at the boundary of the Caribbean Sea and the Atlantic Ocean (Eloe et al., 2010). The repartition of this cluster in Ahe lagoon and the previous reported localisation also suggests a versatile physiology and probably the requirement for organic matter. In consequence, OTU arch 202 and its close relative could be heterotrophs. Analysis of temporal succession of archaeal community in the lagoon pass during tide, confirms the cosmopolitan oceanic preference of OTU Arch108 and 215 and lagoon one for Arch202 as shown on the spatio-temporal analysis (Fig. 8). This observation underlines the influence of particles on the intensity of these OTUs, since the corresponding DGGE bands are globally more intense in this fraction.

4. Conclusion

Information obtained in Ahe atoll with molecular techniques supported previous observations obtained by flow cytometry such as (i) lower bacterial abundance in oceanic water compared to coral reefs and atoll lagoon stations (Torreton, 1999; Weinbauer et al., 2010), (ii) seasonal trend and absence of spatial variation of bacterial abundance inside Ahe lagoon and (iii) the presence of *Synechococcus* and *Prochlorococcus* in Ahe lagoon (Thomas et al., 2010). In addition, quantitative PCR allowed the distinction between bacterial and archaeal SSU rRNA gene abundance. Our survey has detected archaeal SSU rRNA genes in a Pacific lagoon which has not been reported, so far (Weinbauer et al., 2010). Archaeal density displayed a seasonal pattern and a particle-associated prevalence without effect of geographic location. The diversity of prokaryotes was analysed with DGGE fingerprint. This technique does not provide deep information of the diversity of a sample. However, it allowed the comparison of 136 samples from Ahe atoll, permitting multivariate analysis for spatio-temporal assessment of the community structure. Further, the analysis provided robust information on the occurrence of different abundant groups. In lagoon ecosystem, nutrient-depleted condition may induce carbon overflow that are exudates by phytoplankton. This leads subsequently to an increase in bacterial production and a stimulation of the microbial loop and impacts the higher trophic levels of the food web (Ferrier-Pages and Gattuso, 1998). In Ahe atoll, the microbial loop has been described as predominant (Pagano et al., 2012) and the community as heterotrophic. This finding is supported by spatio-temporal pervasiveness found in this study for heterotrophic groups such as *Marinovum*, *Flavobacteria* and *Erytrobacter*. Other groups such as *Alteromonas*, SAR11, most MGII, MGB and *Halobacteria* presented seasonal prevalence corresponding to the rainy season. Oceanic preference was identified for *Shimia* and for an OTU belonging to MG-II (Arch108). Presence of particles also seems to be an important parameter triggering archaeal community and *Roseobacter* group since many of them were encountered in particles fraction. Further, our data suggested that even in a deep lagoon such Ahe, the archaeal OTUs from the water column are tightly related to with that of coral reefs.

Acknowledgements

This study was supported by European Community via FED (Fond Européen pour le Développement) grant, and the French Polynesian "Service de la Perliculture". Special thanks to Alain Lo-Yat for the organisation of the field campaigns, Sheryl Fernandes for English checking and the two anonymous reviewers for their constructive remarks.

References

Andréfouët, S., Charpy, L., Lo-yat, A., Lo, C., 2012. Recent reseach for pearl oyster aquaculture management in French Polynesia. Marine Pollution Bulletin 65, 407–414.

Alldredge, A.L., Passow, U., Logan, B.E., 1993. The abundance and significance of a class of large, transparent organic particles in the ocean. Deep-Sea Research Part I-Oceanographic Research Papers 40, 1131–1140.

Alonso-Saez, L., Balague, V., Sa, E.L., Sanchez, O., Gonzalez, J.M., Pinhassi, J., Massana, R., Pernthaler, J., Pedros-Alio, C., Gasol, J.M., 2007. Seasonality in bacterial diversity in north-west Mediterranean coastal waters: assessment through clone libraries, fingerprinting and FISH. Fems Microbiology Ecology 60, 98–112.

Azam, F., Fenchel, T., Field, J.G., Gray, J.S., Meyerreil, L.A., Thingstad, F., 1983. The Ecological Role of Water-Column Microbes in the Sea. Marine Ecology-Progress Series 10, 257–263.

Azam, F., Worden, A.Z., 2004. Microbes, molecules, and marine ecosystems. Science 303, 1622–1624.

Bonin, P.C., Michotey, V.D., Mouzdahir, A., Rontani, J.-F., 2002. Anaerobic biodegradation of squalene: using DGGE to monitor the isolation of denitrifying Bacteria taken from enrichment cultures. FEMS Microbiology Ecology 42, 37–49.

Bouvy, M., Combe, M., Bettarel, Y., Dupuy, C., Rochelle-Newall, E., Charpy, L., 2012. Uncoupled viral and bacterial distribution in coral reef waters of Tuamotu Archipelago (French Polynesia). Marine Pollution Bulletin 65, 506–515.

Brinkhoff, T., Giebel, H.A., Simon, M., 2008. Diversity, ecology, and genomics of the Roseobacter clade: a short overview. Archives of Microbiology 189, 531–539.

Casamayor, E.O., Massana, R., Benlloch, S., Øvreås, L., Díez, B., Goddard, V.J., Gasol, J.M., Joint, I., Rodríguez-Valera, F., Pedrós-Alió, C., 2002. Changes in archaeal, bacterial and eukaryal assemblages along a salinity gradient by comparison of genetic fingerprinting methods in a multipond solar saltern. Environment Microbiology 4, 338–348.

Casamayor, E.O., Schafer, H., Baneras, L., Pedros-Alio, C., Muyzer, G., 2000. Identification of and spatio-temporal differences between microbial assemblages from two neighboring sulfurous lakes: comparison by microscopy and Denaturing Gradient Gel Electrophoresis. Applied Environment Microbiology 66, 499–508.

Charpy, L., Blanchot, J., 1996. Prochlorococcus contribution to phytoplankton biomass and production of Takapoto atoll (Tuamotu archipelago). Comptes Rendus De L Academie Des Sciences Serie Iii-Sciences De La Vie-Life Sciences 319, 131–137.

Charpy, L., Blanchot, J., 1998. Photosynthetic picoplankton in French Polynesian atoll lagoons: estimation of taxa contribution to biomass and production by flow cytometry. Marine Ecology-Progress Series 162, 57–70.

Charpy, L., Blanchot, J., 1999. Picophytoplankton biomass, community structure and productivity in the Great Astrolabe Lagoon, Fiji. Coral Reefs 18, 255–262.

Charpy, L., Dufour, P., Garcia, N., 1997. Particulate organic matter in sixteen Tuamotu atoll lagoons (French Polynesia). Marine Ecology-Progress Series 151, 55–65.

Cho, J.C., Giovannoni, S.J., 2004. Oceanicola granulosus gen. nov., sp nov and Oceanicola batsensis sp nov., poly-beta-hydroxybutyrate-producing marine bacteria in the order 'Rhodobacterales'. International Journal of Systematic and Evolutionary Microbiology 54, 1129–1136.

Delong, E.F., 1992. Archaea in Coastal Marine Environments. Proceedings of the National Academy of Sciences of the United States of America 89, 5685–5689.

Delong, E.F., 2003. Oceans of Archaea. Asm News 69, 503–511.

Delong, E.F., Taylor, L.T., Marsh, T.L., Preston, C.M., 1999. Visualization and enumeration of marine planktonic Archaea and Bacteria by using polyribonucleotide probes and fluorescent in situ hybridization. Applied and Environmental Microbiology 65, 5554–5563.

Dinsdale, E.A., Pantos, O., Smriga, S., Edwards, R.A., Angly, F., Wegley, L., Hatay, M., Hall, D., Brown, E., Haynes, M., Krause, L., Sala, E., Sandin, S.A., Thurber, R.V., Willis, B.L., Azam, F., Knowlton, N., Rohwer, F., 2008. Microbial Ecology of Four Coral Atolls in the Northern Line Islands. Plos One 3.

Dufresne, A., Ostrowski, M., Scanlan, D.J., Garczarek, L., Mazard, S., Lalenik, B., Paulen, I., Tandeau de marsac, N., Wincker, P., Dossat, C., Ferriera, S., Johnson, J., Post, A., Hess, W.R., Partensky, F., 2008. Unravelling the genomic mosaic of a ubiquitous genus of marine *cyanobacteria*. Genome biology 9, R90.

Dumas, F., Le Gendre, R., Thomas, Y., Andréfouët, S., 2012. Tidal flushing and wind driven circulation of Ahe atoll laggon (Tuamotu Archipelago, French Polynesia) from in situ observations and numerical modelling. Marine Pollution Bulletin 65, 425–440.

Dupon, J.F., Dodter, F., 1993. Les îles Tuamotu ORSTOM. Editions, 11–13.

Eloe, E., Shulse, C., Fadrosh, D., Williamson, S., Allen, E., Bartlett, D., 2010. Compositional differences in particle- associated and free-living microbial assemblages from an extreme deep-ocean environment. Environmental microbiology reports.

Ferrier-Pages, C., Gattuso, J.P., 1998. Biomass, production and grazing rates of pico- and nanoplankton in coral reef waters (Miyako Island, Japan). Microbial Ecology 35, 46–57.

Frigaard, N.U., Martinez, A., Mincer, T.J., DeLong, E.F., 2006. Proteorhodopsin lateral gene transfer between marine planktonic Bacteria and Archaea. Nature 439, 847–850.

Fuhrman, J.A., Davis, A.A., 1997. Widespread Archaea and novel bacteria from the deep sea as shown by 16S rRNA gene sequences. Marine Ecology-Progress Series 150, 275–285.

Fuller, N.J., Marie, D., Partensky, F., Vaulot, D., Post, A.F., Scanlan, D.J., 2003. Clade-specific 16S ribosomal DNA oligonucleotides reveal the predominance of a single marine Synechococcus clade throughout a stratified water column in the Red Sea. Applied and Environmental Microbiology 69, 2430–2443.

Gallagher, J.M., Carton, M.W., Eardly, D.F., Patching, J.W., 2004. Spatio-temporal variability and diversity of water column prokaryotic communities in the eastern North Atlantic. Fems Microbiology Ecology 47, 249–262.

Giovannoni, S.J., Bibbs, L., Cho, J.C., Stapels, M.D., Desiderio, R., Vergin, K.L., Rappe, M.S., Laney, S., Wilhelm, L.J., Tripp, H.J., Mathur, E.J., Barofsky, D.F., 2005. Proteorhodopsin in the ubiquitous marine bacterium SAR11. Nature 438, 82–85.

Gonzalez, J.M., Torreton, J.P., Dufour, P., Charpy, L., 1998. Temporal and spatial dynamics of the pelagic microbial food web in an atoll lagoon. Aquatic Microbial Ecology 16, 53–64.

Goregues, C.M., Michotey, V.D., Bonin, P.C., 2005. Molecular, biochemical, and physiological approaches for understanding the ecology of denitrification. Microbiology Ecology 49, 198–208.

Grossart, H.P., Tang, K.W., Kiorboe, T., Ploug, H., 2007. Comparison of cell-specific activity between free-living and attached bacteria using isolates and natural assemblages. Fems Microbiology Letters 266, 194–200.

Herndl, G.J., Reinthaler, T., Teira, E., van Aken, H., Veth, C., Pernthaler, A., Pernthaler, J., 2005. Contribution of Archaea to total prokaryotic production in the deep Atlantic Ocean. Applied and Environmental Microbiology 71, 2303–2309.

Herndl, G.J., Velimirov, B., 1986. Microheterotrophic Utilization of Mucus Released by the Mediterranean Coral Cladocora-Cespitosa. Marine Biology 90, 363–369.
Ingalls, A.E., Shah, S.R., Hansman, R.L., Aluwihare, L.I., Santos, G.M., Druffel, E.R.M., Pearson, A., 2006. Quantifying archaeal community autotrophy in the mesopelagic ocean using natural radiocarbon. Proceedings of the National Academy of Sciences of the United States of America 103, 6442–6447.
Ionescu, D., Penno, S., Haimovich, M., Rihtman, B., Goodwin, A., Schwartz, D., Hazanov, L., Chernihovsky, M., Post, A.F., Oren, A., 2009. Archaea in the Gulf of Aqaba. Fems Microbiology Ecology 69, 425–438.
Johnson, Z.I., Zinser, E.R., Coe, A., McNulty, N.P., Woodward, E.M.S., Chisholm, S.W., 2006. Niche partitioning among Prochlorococcus ecotypes along ocean-scale environmental gradients. Science 311, 1737–1740.
Karl, D.M., Hebel, D.V., Bjorkman, K., Letelier, R.M., 1998. The role of dissolved organic matter release in the productivity of the oligotrophic North Pacific Ocean. Limnology and Oceanography 43, 1270–1286.
Karner, M.B., DeLong, E.F., Karl, D.M., 2001. Archaeal dominance in the mesopelagic zone of the Pacific Ocean. Nature 409, 507–510.
Kellogg, C., 2004. Tropical Archaea: diversity associated with the surface microlayer of corals. Marine Ecology-Progress Series 273, 81–88.
Kumar, S., Tamura, K., Dudley, J., Nei, M., 2007. MEGA4: Molecular evolutionary genetics analysis (MEGA) software version 4.0. Molecular Biology and Evolution 24, 1596–1599.
Lebaron, P., Joux, F., 1994. Flow Cytometric Analysis of the Cellular DNA Content of Salmonella-Typhimurium and Alteromonas-Haloplanktis during Starvation and Recovery in Seawater. Applied and Environmental Microbiology 60, 4345–4350.
Leborgne, R., Blanchot, J., Charpy, L., 1989. Zooplankton of Tikehau Atoll (Tuamotu Archipelago) and Its Relationship to Particulate Matter. Marine Biology 102, 341–353.
Lopez-Garcia, P., Lopez-Lopez, A., Moreira, D., Rodriguez-Valera, F., 2001. Diversity of free-living prokaryotes from a deep-sea site at the Antarctic Polar Front. Fems Microbiology Ecology 36, 193–202.
Loret, P., Le Gall, S., Dupuy, C., Blanchot, J., Pastoureaud, A., Delesalle, B., Caisey, X., Jonquieres, G., 2000. Heterotrophic protists as a trophic link between picocyanobacteria and the pearl oyster Pinctada margaritifera in the Takapoto lagoon (Tuamotu Archipelago, French Polynesia). Aquatic Microbial Ecology 22, 215–226.
Mari, X., Rochelle-Newall, E., Torreton, J.P., Pringault, O., Jouon, A., Migon, C., 2007. Water residence time: A regulatory factor of the DOM to POM transfer efficiency. Limnology and Oceanography 52, 808–819.
Martens, T., Heidorn, T., Pukall, R., Simon, M., Tindall, B.J., Brinkhoff, T., 2006. Reclassification of Roseobacter gallaeciensis Ruiz-Ponte et al. 1998 as Phaeobacter gallaeciensis gen. nov., comb. nov., description of Phaeobacter inhibens sp nov., reclassification of Ruegeria algicola (Lafay et al. 1995) Uchino et al. 1999 as Marinovum algicola gen. nov., comb. nov., and emended descriptions of the genera Roseobacter, Ruegeria and Leisingera. International Journal of Systematic and Evolutionary Microbiology 56, 1293–1304.
Massana, R., DeLong, E.F., Pedros-Alio, C., 2000. A few cosmopolitan phylotypes dominate planktonic archaeal assemblages in widely different oceanic provinces. Applied and Environmental Microbiology 66, 1777–1787.
Massana, R., Murray, A.E., Preston, C.M., DeLong, E.F., 1997. Vertical distribution and phylogenetic characterization of marine planktonic Archaea in the Santa Barbara Channel. Applied and Environmental Microbiology 63, 50–56.
Michener, C.D., Sokal, R.R., 1957. A quantitative approach to a problem in classification. Evolution 11, 130–262.
Muhling, M., Fuller, N.J., Somerfield, P.J., Post, A.F., Wilson, W.H., Scanlan, D.J., Joint, I., Mann, N.H., 2006. High resolution genetic diversity studies of marine Synechococcus isolates using rpoC1-based restriction fragment length polymorphism. Aquatic Microbial Ecology 45, 263–275.
Muhling, M., Ivars-Martinez, E., D'Auria, G., Rodriguez-Valera, F., Sanchez-Porro, C., Ventosa, A., Joint, I., 2008. Biogeography of the ubiquitous marine bacterium Alteromonas macleodii determined by multilocus sequence analysis. Molecular Ecology 17, 4092–4106.
Murray, A.E., Preston, C.M., Massana, R., Taylor, L.T., Blakis, A., Wu, K., DeLong, E.F., 1998. Seasonal and spatial variability of bacterial and archaeal assemblages in the coastal waters near Anvers Island, Antarctica. Applied and Environmental Microbiology 64, 2585–2595.
Olson, R.J., Chisholm, S.W., Zettler, E.R., Altabet, M.A., Dusenberry, J.A., 1990a. Spatial and Temporal Distributions of Prochlorophyte Picoplankton in the North-Atlantic Ocean. Deep-Sea Research Part a-Oceanographic Research Papers 37, 1033–1051.
Olson, R.J., Chisholm, S.W., Zettler, E.R., Armbrust, E.V., 1990b. Pigments, Size, and Distribution of Synechococcus in the North-Atlantic and Pacific Oceans. Limnology and Oceanography 35, 45–58.
Pagano, M., Sagarra, P.B., Champalbert, G., Dupuy, C., Thomas, Y., Charpy, L., 2012. Metazooplankton communities in Ahe atoll lagoon (Tuamotu Archipelago, French Polunesia), Spatio-temporal variations and trophic relationships. Marine Pollution Bulletin 65, 538–548.
Pages, J., Andrefouet, S., Delesalle, B., Prasil, V., 2001. Hydrology and trophic state in Takapoto Atoll lagoon: comparison with other Tuamotu lagoons. Aquatic Living Resources 14, 183–193.
Partensky, F., Hess, W.R., Vaulot, D., 1999. Prochlorococcus, a marine photosynthetic prokaryote of global significance. Microbiology and Molecular Biology Reviews 63, 106.
Passow, U., Alldredge, A.L., Logan, B.E., 1994. The Role of Particulate Carbohydrate Exudates in the Flocculation of Diatom Blooms. Deep-Sea Research Part I-Oceanographic Research Papers 41, 335–357.
Penno, S., Lindell, D., Post, A.F., 2006. Diversity of Synechococcus and Prochlorococcus populations determined from DNA sequences of the N-regulatory gene ntcA. Environmental Microbiology 8, 1200–1211.
Pernthaler, A., Preston, C.M., Pernthaler, J., DeLong, E.F., Amann, R., 2002. Comparison of fluorescently labeled oligonucleotide and polynucleotide probes for the detection of pelagic marine bacteria and Archaea. Applied and Environmental Microbiology 68, 661–667.
Pinhassi, J., Gomez-Consarnau, L., Gonzalez, J.M., Coll-Llado, M., Gourdon, P., Pascher, T., Neutze, R., Pedros-Alio, C., 2007. Light stimulates growth of proteorhodopsin-containing marine *Flavobacteria*. Nature 445, 210–213.
Raguenes, G., Pignet, P., Gauthier, G., Peres, A., Christen, R., Rougeaux, H., Barbier, G., Guezennec, J., 1996. Description of a new polymer-secreting bacterium from a deep-sea hydrothermal vent, Alteromonas macleodii subsp fijiensis, and preliminary characterization of the polymer. Applied and Environmental Microbiology 62, 67–73.
Rappe, M.S., Vergin, K., Giovannoni, S.J., 2000. Phylogenetic comparisons of a coastal bacterioplankton community with its counterparts in open ocean and freshwater systems. Fems Microbiology Ecology 33, 219–232.
Rocap, G., Ahlgren, N.A., 2006. Culture isolation and culture-independent clone libraries reveal new marine Synechococcus ecotypes with distinctive light and N physiologies. Applied and Environmental Microbiology 72, 7193–7204.
Saitou, N., Nei, M., 1987. The Neighbor-joining method: A new method for reconstructing phylogenetic trees. Molecular Biology Evolution 4, 406–425.
Scanlan, D.J., West, N.J., 2002. Molecular ecology of the marine cyanobacterial genera Prochlorococcus and Synechococcus. Fems Microbiology Ecology 40, 1–12.
Scanlan, D.J., Zwirglmaier, K., Jardillier, L., Ostrowski, M., Mazard, S., Garczarek, L., Vaulot, D., Not, F., Massana, R., Ulloa, O., 2008. Global phylogeography of marine Synechococcus and Prochlorococcus reveals a distinct partitioning of lineages among oceanic biomes. Environmental Microbiology 10, 147–161.
Schiller, C., Herndl, G.J., 1989. Evidence of Enhanced Microbial Activity in the Interstitial Space of Branched Corals - Possible Implications for Coral Metabolism. Coral Reefs 7, 179–184.
Shiba, T., 1991. Roseobacter-Litoralis Gen-Nov, Sp-Nov, and Roseobacter-Denitrificans Sp-Nov, Aerobic Pink-Pigmented Bacteria Which Contain Bacteriochlorophyll-A. Systematic and Applied Microbiology 14, 140–145.
Simon, M., Grossart, H.P., Schweitzer, B., Ploug, H., 2002. Microbial ecology of organic aggregates in aquatic ecosystems. Aquatic Microbial Ecology 28, 175–211.
Takai, K., Horikoshi, K., 2000. Rapid detection and quantification of members of the archaeal community by quantitative PCR using fluorogenic probes. Applied and Environmental Microbiology 66, 5066.
Tarran, G.A., Zubkov, M.V., Sleigh, M.A., Burkill, P.H., Yallop, M., 2001. Microbial community structure and standing stocks in the NE Atlantic in June and July of 1996. Deep-Sea Research Part Ii-Topical Studies in Oceanography 48, 963–985.
Teira, E., Lebaron, P., van Aken, H., Herndl, G.J., 2006. Distribution and activity of Bacteria and Archaea in the deep water masses of the North Atlantic. Limnology and Oceanography 51, 2131–2144.
Teske, A., Sorensen, K.B., 2008. Uncultured Archaea in deep marine subsurface sediments: have we caught them all? Isme Journal 2, 3–18.
Thomas, Y., Garen, P., Courties, C., Charpy, L., 2010. Spatial and temporal variability of the pico- and nanophytoplankton and bacterioplankton in a deep Polynesian atoll lagoon. Aquatic Microbial Ecology 59, 89–101.
Thompson, J.D., Higgins, D.G., Gibson, T.J., 1994. CLUSTAL W: improving the sensitivity of progressive multiple sequence alignment through sequence weighting, position-specific gap penalties and weight matrix choice. Nucleic Acids Residues 22, 4673–4680.
Toledo, G., Palenik, B., Brahamsha, B., 1999. Swimming marine Synechococcus strains with widely different photosynthetic pigment ratios form a monophyletic group. Applied and Environmental Microbiology 65, 5247–5251.
Torreton, J.P., 1999. Biomass, production and heterotrophic activity of bacterioplankton in the Great Astrolabe Reef lagoon (Fiji). Coral Reefs 18, 43–53.
Torreton, J.P., Dufour, P., 1996. Bacterioplankton production determined by DNA synthesis, protein synthesis, and frequency of dividing cells Tuamotu atoll lagoons and surrounding ocean. Microbial Ecology 32, 185–202.
Torreton, J.P., Pages, J., Talbot, V., 2002. Relationships between bacterioplankton and phytoplankton biomass, production and turnover rate in Tuamotu atoll lagoons. Aquatic Microbial Ecology 28, 267–277.
Weinbauer, M.G., Kerros, M.E., Motegi, C., Wilhartitz, I.C., Rassoulzadegan, F., Torreton, J.P., Mari, X., 2010. Bacterial community composition and potential controlling mechanisms along a trophic gradient in a barrier reef system. Aquatic Microbial Ecology 60, 15–28.
Wild, C., Huettel, M., Klueter, A., Kremb, S.G., Rasheed, M.Y.M., Jorgensen, B.B., 2004. Coral mucus functions as an energy carrier and particle trap in the reef ecosystem. Nature 428, 66–70.
Wuchter, C., Abbas, B., Coolen, M.J.L., Herfort, L., van Bleijswijk, J., Timmers, P., Strous, M., Teira, E., Herndl, G.J., Middelburg, J.J., Schouten, S., Damste, J.S.S., 2007. Archaeal nitrification in the ocean. Proceedings of the National Academy of Sciences of the United States of America 104, 5704 (vol. 103, pp. 12317, 2006).
Yurkov, V.V., Beatty, J.T., 1998. Aerobic anoxygenic phototrophic bacteria. Microbiology and Molecular Biology Reviews 62, 695.

Marine Pollution Bulletin 65 (2012) 538–548

Contents lists available at SciVerse ScienceDirect

Marine Pollution Bulletin

journal homepage: www.elsevier.com/locate/marpolbul

Metazooplankton communities in the Ahe atoll lagoon (Tuamotu Archipelago, French Polynesia): Spatiotemporal variations and trophic relationships

Marc Pagano [a,*], Pascual-Boi Sagarra [a], Gisèle Champalbert [a], Marc Bouvy [b], Christine Dupuy [c], Yoann Thomas [d], Loïc Charpy [e]

[a] Mediterranean Institute of Oceanography (MIO), IRD, UMR 235, 13288 Marseille Cedex 09, France
[b] UMR 5119 ECOSYM, Université Montpellier II, 34095 Montpellier Cedex 5, France
[c] Laboratoire LIENSs, UMR 6250 CNRS, Université de La Rochelle, 2, rue Olympe de Gouges, 17000 La Rochelle Cedex, France
[d] Ifremer, DPFOM LPI, Presqu'île du Vivier, 29840 Argenton, France
[e] Mediterranean Institute of Oceanography (MIO), IRD, UMR 235, IRD Center of Tahiti, BP 529, 98713 Papeete, French Polynesia

ARTICLE INFO

Keywords:
Metazooplankton
Spatio-temporal patterns
Trophic relationships
Pearl oyster
Atoll lagoon
French Polynesia

ABSTRACT

Metazooplankton abundance, biomass (<80 μm, 200–500 μm and >500 μm) and community structure in the Ahe atoll were studied together with their relationships with environmental factors (temperature, salinity, wind) and trophic factors (phytoplankton, bacteria, heterotrophic nanoflagellates (HNF) and ciliates) during three periods in 2008–2009. Meroplankton, mainly bivalve and gastropod larvae, was dominant. Holoplankton was dominated by copepods, the main species being *Oithona* spp., *Paracalanus parvus*, *Clausocalanus* spp., *Corycaeus* spp., *Acartia fossae* and *Undinula vulgaris*. The results suggest a clear wind influence on the structure and horizontal distribution of the zooplankton communities. The metazooplankton appeared to be controlled mainly by food resources, suggesting a bottom-up control. The low nanophytoplankton biomass in contrast to the high abundance of picophytoplankton, HNF and nano-particle grazers (mainly *Oithona* spp., *Paracalanus* and bivalve larvae) highlighted the importance of the microbial loop in the food web.

1. Introduction

Metazooplankton plays a major role in the functioning and productivity of aquatic ecosystems through its impact on nutrient dynamics and its key position in food webs. Most mesozooplanktonic organisms exert a strong grazing impact on the phytoplankon and on the microzooplankton (Pont, 1995; Calbet, 2008). They are also a food source for organisms of the upper trophic levels such as planktivorous fish and carnivorous invertebrates (Pinel-Alloul, 1995). In coral reef and atoll lagoon environments, they are important contributors to the benthic and pelagic food webs (Bozec et al., 2004; Alldredge and King, 2009). Zooplankton organisms can also be used as biological indicators for pollution, water quality and eutrophication (Attayde and Bozelli, 1998; Webber et al., 2005). Their generation times may be short enough to respond quickly to acute stress but long enough to integrate the effects of chronic problems. These attributes can be useful to design a community ecosystem health indicator (Cairns et al., 1993). However, very few studies have dealt with zooplankton in atoll lagoons (Gerber, 1981) and only a few have concerned the Tuamotu Archipelago (Michel et al., 1971; Ricard et al., 1979; Le Borgne et al., 1989; Carleton and Doherty, 1998).

Coral reef and atoll lagoons are productive ecosystems, compared to surrounding ocean (Hatcher, 1997). They have been frequently exploited for aquaculture, as in the Tuamotu Archipelago (French Polynesia) where pearl oyster farming is a major driver of the local economy (Andrefouët et al., 2012). The planktonic pearl-oyster larvae mainly feed on nanophytoplankton with high ingestion rates (Doroudi et al., 2003). The adults, cultivated in sub-surface pelagic nets, are also important passive consumers of nanoparticles (Yukuhira et al., 1998; Fournier et al. 2012). Farmed pearl-oyster populations can be considered as components of the pelagic ecosystem in pearl farming lagoons. In these ecosystems, they share (and may compete for) food resources with several pelagic components (including zooplankton) and may serve as food for other ones. Studying the different communities of the pelagic ecosystem and evaluating their stocks and their inter-relationships are required to define the optimal conditions for the recruitment and development of oysters. This information is also necessary to determine the load capacity for cultivation (Niquil et al., 1998).

A multidisciplinary research program was funded by the European Development Fund (EDF) in 2007 to describe, among

* Corresponding author. Tel.: +33 4 91 82 91 34; fax: +33 4 91 82 65 48.
E-mail address: marc.pagano@univmed.fr (M. Pagano).

0025-326X/$ - see front matter © 2012 Elsevier Ltd. All rights reserved.
doi:10.1016/j.marpolbul.2012.01.025

other goals, the ecological environment of the pearl-oyster *Pinctada margaritifera* (Linnaeus, 1758) and its relationship with the pelagic trophic network.

Our study is part of this multidisciplinary study on the trophic environment of *P. margaritifera*. It aimed at analyzing within a farmed lagoon the spatiotemporal variations of metazooplankton standing stock and community composition according to the main environmental and trophic parameters.

2. Methods

2.1. Study site and sampling strategy

The Ahe atoll (14°29′S; 146°18′S) to the north west of the Tuamotu Archipelago in the Pacific Ocean is 23.5 km long and a maximum of 12.2 km wide (Fig. 1). The lagoon is 142 km^2 in area with maximum depth of 70 m in the central zone. The atoll rim which surrounds the lagoon is not completely closed: there is a passage (300 m long and about 20 m deep) to the northwest between the lagoon and the ocean, and several spillways mostly in the southern part of the rim. The climate is wet tropical with one rainy season from November to April with the maximum precipitation being in January and December. The annual air temperature variation is low (25–29 °C) with a regular seasonal trend. The dominant winds (NE trade-winds) are strongest in October–November.

Meteorological data (monthly averages of air temperature, rainfalls, and wind speed) were available from the meteorological station of Takaroa (Tuamotu; 14°28′S–146°2′W) for a period bracketing our surveys, in 2007–2009 (Fig. 2). The station is only 130 km from Ahe (see Fig. 1) and given the lack of any orographic effects on these low lying islands, Takaroa data were deemed representative of the conditions in Ahe atoll.

Three sampling surveys were carried out in May 2008, October 2008 and February 2009. During each period, four lagoon stations (Station 1, 23 m depth, Station 3, 50 m depth, Station 9, 50 m depth and Station 11, 45 m depth) were sampled on 2 (October 16 and 20, 2008) and 3 (May 14, 20 and 23, 2008; February 17, 20 and 24, 2009) occasions.

2.2. Environmental and trophic variables

Vertical profiles of salinity and temperature were recorded using a YSI 600 probe, from surface to bottom. Water samples were collected at two (0.5, 10 m; stations 1 and 11) and three (0.5, 10 and 20 m; stations 3 and 9) depths using a 5 L Niskin bottle. Chlorophyll *a* (Chl *a*) concentrations of particles retained on Whatman GF/F filters (0.7 μm of porosity) were measured on 400 ml water samples using a Turner Designs TD 700 fluorometer after methanol extraction (Welschmeyer, 1994). Particle fractionation using 2 μm pore size Nuclepore membranes gave an estimate of Chl *a* concentration for 0.7–2, and >2 μm size classes. The fraction of Chl *a* not retained by a 2-μm membrane was assigned to picophytoplankton biomass.

Bacteria and picoautotrophic cells were fixed with 0.2 μm filtered formaldehyde (final concentration 2%) and frozen in liquid nitrogen. Bacterial cells were enumerated by flow cytometry using the method described by Marie et al. (1999). A 1 ml formaldehyde-fixed subsample was incubated with DAPI at a final concentration of 1/10,000 for 15 min at room temperature in the dark. Each subsample was counted using a MoFlo cytometer (DAKO). Stained bacterial cells, excited at 488 nm, were enumerated according to their right-angle light scatter (RALS) and green fluorescence (FL1) measured using a 530/30 nm filter. These cell parameters were plotted onto 1024 channels and recorded on a 4-decade logarithmic scale. Fluorescent beads (0.94 μm, Polysciences Inc., Warrington, PA, USA) were added to each sample. Standardized RALS and FL1 values (RALS and FL1 for the cells divided by the RALS and FL1 for 0.94 μm beads,) were used to estimate the relative size and nucleic acid content of the bacterial cells (Troussellier et al., 1999). The list mode files were analyzed using SUMMIT software (Dako Colorado Incorporation).

Picophytoplankton (*Prochlorococcus* sp. and *Synechococcus* sp. cells) and autotrophic picoeukaryotes counts were performed using the same flow cytometer. Cells excited at 488 nm were detected and directly enumerated according to their FALS and RALS properties and their orange (585/42 nm) and red fluorescence (>650 nm) from phycoerythrin and chlorophyll pigments, respectively. Fluorescent beads (0.94 μm) were also added to each sample. The list mode files were analyzed using SUMMIT software (Dako Colorado Incorporation).

For microzooplankton enumeration (ciliates), water samples (1 L) were fixed with alkaline lugol iodine (2% final concentration). A first sedimentation was conducted for 24 h and the top 900 ml of the samples was slowly siphoned off using small-bore tubing. The remaining 100 ml was then stored at 4 °C in the dark before enumeration. After sedimentation in a Utermöhl settling chamber (Hydro-Bios combined plate chamber), cells were enumerated at a magnification of ×200 using a Zeiss axiovert inverted microscope with interference contrast.

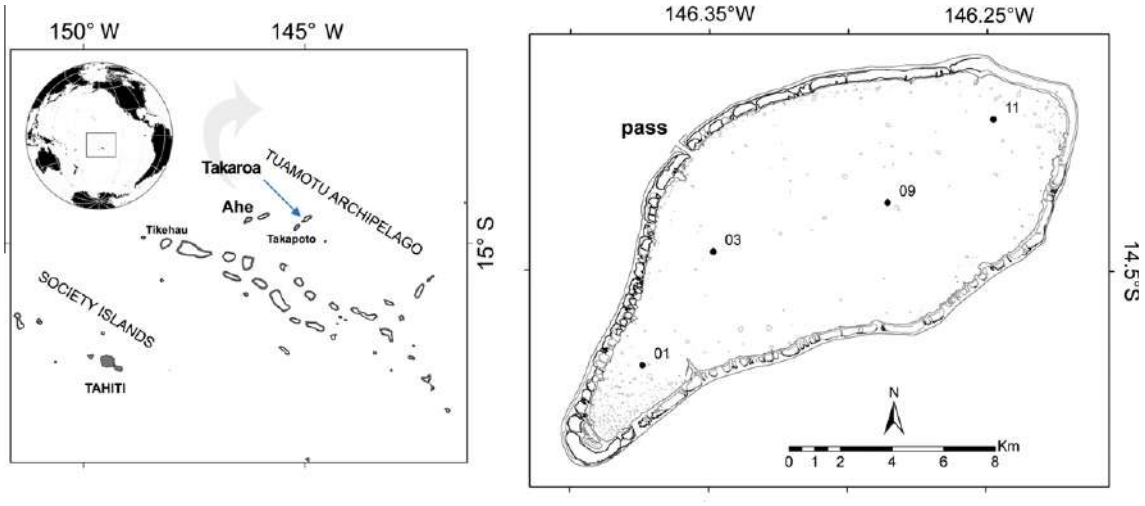

Fig. 1. Left: Location of Ahe (sampling sites) and Takaroa (meteo station) atolls. Right: Positions of the sampling stations in the Ahe lagoon.

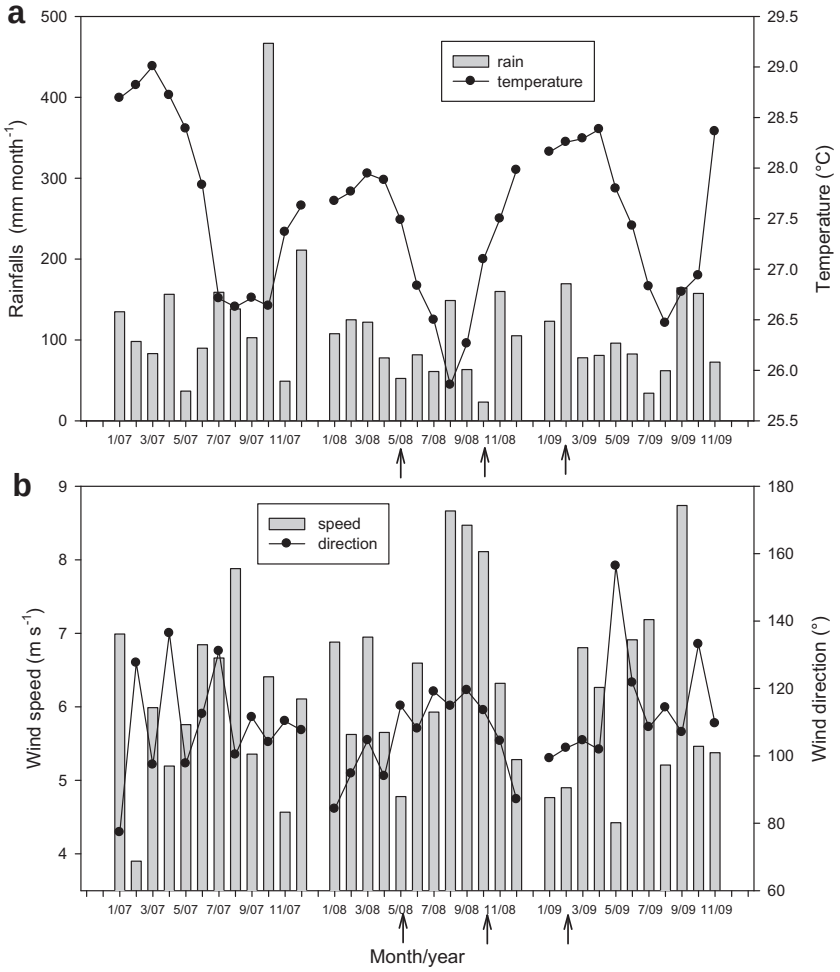

Fig. 2. Average values of (a) rainfalls and air temperature and (b) wind speed and direction recorded at Takaroa meteorological station. Sampling periods are indicated with arrows.

Nanoflagellates (in 25 ml water samples) were fixed with buffered paraformaldehyde (final concentration 1%), stained with DAPI (2.5×10^{-4} g L^{-1} final concentration) and counted on 0.8 μm black polycarbonate filters by epifluorescence microscopy (Sherr et al., 1994). Heterotrophic nanoflagellates (HNF) were distinguished from pigmented (autotrophic) nanoflagellates (PNF) by the absence of chlorophyll fluorescence.

The following factors were used to convert abundance into carbon biomass:

Bacteria: 14 fgC/cell (Gundersen et al., 2002).
Prochlorococcus: 60 fgC/cell (Charpy and Blanchot, 1998).
Synechococcus: 178 fgC/cell (Charpy and Blanchot, 1998).
Picoeukaryote: 836 fgC/cell (Verity et al., 1992).
Nanoflagellates: 3140 fgC/cell (Pelegri et al., 1999).
Ciliates: 2318 pgC/cell (Putt and Stoecker, 1989).

2.3. Zooplankton

Zooplankton was sampled by vertical hauls (bottom to surface) using a 80 μm mesh-size WP2 net equipped with a Hydrodata flowmeter. Each sample was divided into two equal sub-samples using a Motoda-type splitter. One sub-sample was used for biomass measurements and the second was fixed with formaldehyde at 4% final concentration and used for identification and enumeration of the taxa. Biomass measurements (dry weight, DW, 60 °C desiccation during 48 h; Lovegrove, 1966) were made after size-fractionation using 80 μm, 200 μm, 500 μm and 1000 μm nylon sieves. The taxa were identified and enumerated using sub samples taken by wide bore piston pipettes (0.5–5 ml). At least 100 individuals of the main taxa were counted in each sub-sample under a dissecting microscope (Olympus SZX200, magnification ×200 to ×500). The rarest taxa were estimated from the whole sample. Zooplankton taxa were identified according to Tregouboff and Rose (1957), Razouls et al. (2005–2011) and Conway et al. (2003).

The individual weight of each taxon was estimated from their size measured under a dissecting microscope (objective 50, ocular 10). The organism carbon weights were then estimated using the length-weight relationships found in the literature (Uye, 1982; Chisholm and Roff, 1990; Mauchline, 1998; Doroudi et al., 2003). The size were considered as: prosome length for copepods, from the eye base to the junction of abdomen and telson for euphausiids, from the base of the head to the base of junction of abdomen and telson for amphipods, the anterior nectophore length measurement for siphonopores, shell length for bivalve larvae and total length for other taxa.

2.4. Data analysis

Correlations between zooplankton abundance and environmental factors were computed using Statistica V6 software. The significance of each correlation was examined after Bonferroni correction for the effects of multiple comparisons.

The spatial and temporal variability of environmental variables and zooplankton communities was assessed by multivariate analysis. Two data sets were considered: the abundance of all the zooplankton taxa identified and the environmental variables. Factorial correspondence analysis (FCA) was performed on the first data set and principal component analysis (PCA) on the second. The results of the two analyses were associated by co-inertia analysis (Dolédec and Chessel, 1994). A cluster classification of observation scores from the first factorial plane was applied to partition taxa and stations (Ward's aggregation criterion). Analyses were performed using ADE4 software (Thioulouse et al., 1997).

The spatial and temporal variability of the trophic groups (biomass as $\mu g\ C\ L^{-1}$) was assessed by PCA. The groups considered were picophytoplankton (*Prochlorococcus* sp., *Synechococcus* sp., and picoeukaryotes), autotrophic nanoflagellates, bacteria, heterotrophic nanoflagellates (HNF), ciliates, predators (chaetognaths, medusae, ctenophores, *Labidocera* spp., *Candacia* spp., *Corycaeus* spp., *Oncaea* spp. and fish larvae), picoparticle feeders (salps and appendicularians), bivalve larvae and other nanoparticle feeders (other metazooplankton organisms). Picoparticle feeders, nanoparticle feeders and predators were distinguished according to Ohtsuka and Onbé (1991), Turner (1984) and Mauchline (1998).

All analyses were performed on $\log X + 1$ transformed data.

3. Results

3.1. Environmental and trophic variables

Different meteorological conditions were observed during the 3 sampling periods (Fig. 2). Rainfall were high in February 2009 (70 mm $month^{-1}$) compared to May and October 2008 (52 and 23 mm $month^{-1}$, respectively). Wind speed was lower during the May 2008 survey (0–7.7 m s^{-1} during the sampling period) than for the other surveys (6.1–11.5 m s^{-1} and 3.0–11.5 m s^{-1} in October 2008 and February 2009, respectively). Water temperature and salinity showed significant variations between sampling seasons (Fig. 3). The lowest salinity and highest temperature were recorded in February 2009, during the rainy season. In May 2008, at the beginning of the dry season, mean salinity and temperature were high while temperature was minimal in October 2008, at the end of the dry season.

Total Chl *a* was higher in May and February than in October and relative contributions of the two fractions (Chl *a* <2 μm and >2 μm) were similar between periods (Fig. 4a). The smaller fraction (Chl *a* <2 μm) was always dominant, representing 72–82% of the total. In May and October (dry season), stations 1 and 11 displayed higher

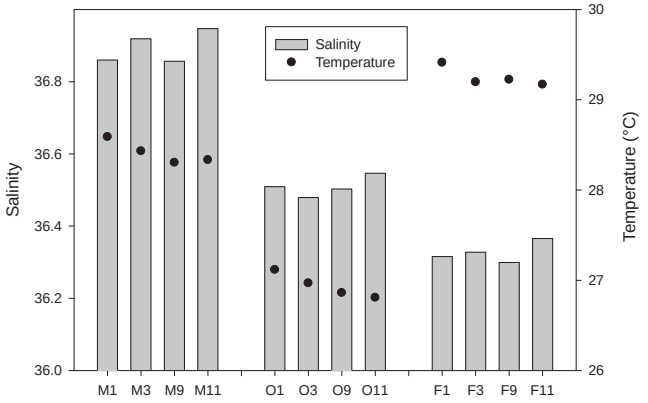

Fig. 3. Mean water column (between sampling dates) temperature and salinity at the four sampled stations (1, 3, 9, 11) during the three surveys: May 2008 (M1, M3, M9, M11), October 2008 (O1, O3, O9, O11) and February 2009 (F1, F3, F9, F11).

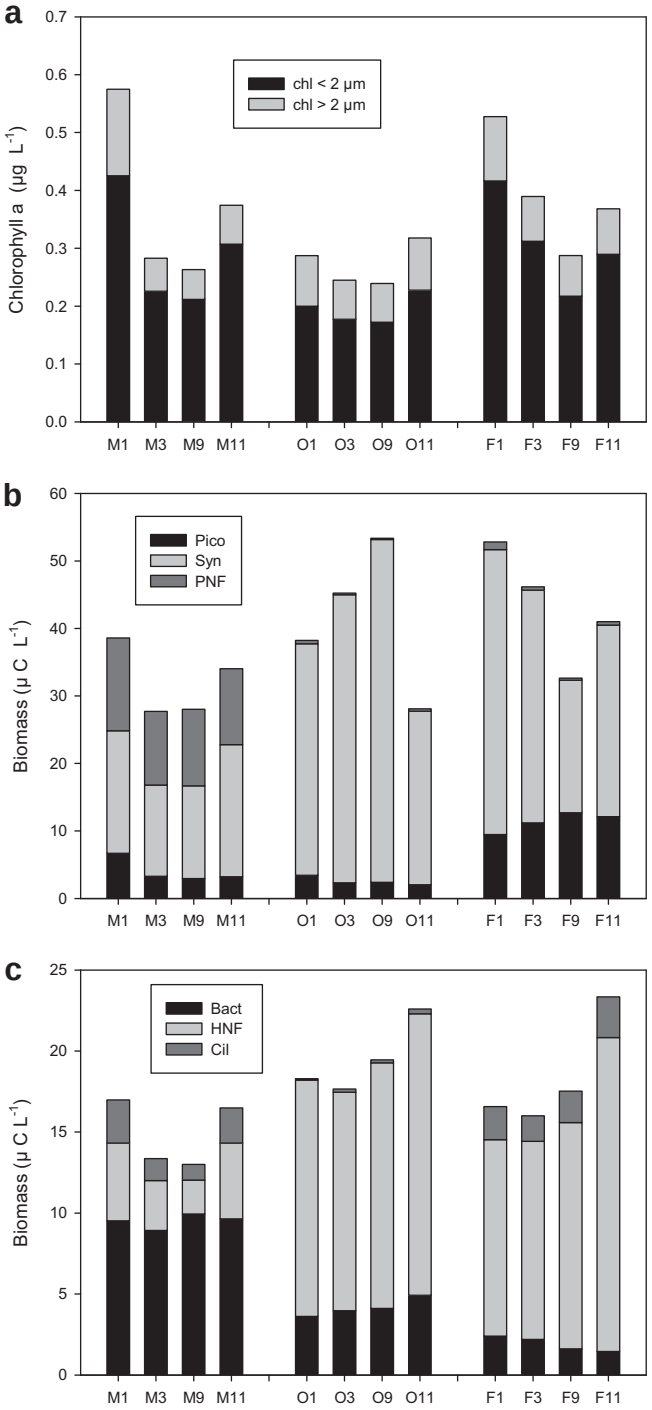

Fig. 4. Mean water column values (between sampling dates) of (a) Chlorophyll *a* (two size-fractions), (b) autotrophic microorganisms (picoeukaryotes, Pico, Synechococcus, Syn, and pigmented nano flagellates, PNF) and (c) heterotrophic migoorganisms (bacteria, Bact, heterotrophic nanoflagellates, HNF and ciliates, Cil) at the four sampled stations (1, 3, 9, 11) during the three surveys: May 2008 (M1, M3, M9, M11), October 2008 (O1, O3, O9, O11) and February 2009 (F1, F3, F9, F11).

Chl *a* concentrations than stations 9 and 3. The total autotrophic organism biomass (picoeukaryotes, *Synechococcus* and pigmented nanoflagellates, PNF) had the same spatial patterns as chlorophyll in May and February but not in October (Fig. 4b). The PNF fraction was very high in May, whereas the *Synechococcus* fraction was very high in October and February. The heterotrophic microorganism biomass was more balanced between groups (bacteria, HNF and

ciliates) in May than in October and February (predominance of HNF) (Fig. 4c).

3.2. Zooplankton

Forty two taxa were identified in the samples, 31 holoplanktonic (18 Copepods, including copepod nauplii, and 13 other organisms) and 11 meroplanktonic ones (Table 1). Copepods were the most abundant group among the holoplankton, the main taxa being *Oithona* spp., Paracalanidae (*Paracalanus parvus* and *Clausocalanus* spp.), *Corycaeus* spp. and *Acartia fossae*. The other holopankton taxa were mainly appendicularians, chaetognaths and pteropods (*Limacina* spp. and *Creseis* spp.). Meroplankton comprised mainly bivalves (including *P. margaritifera*) and gastropod larvae.

Meroplankton was more abundant than holoplankton in almost all the stations (mainly due to the number of bivalve larvae) except at stations 1 and 3 in October 2008. Zooplankton total abundance (Table 1) and biomass (Fig. 5) were strongly correlated ($r = 0.74$; $p = 0.0058$). They were both higher in February 2009 than in May and October 2008 (Fig. 5a and b). They also displayed the same spatial pattern in May 2008 with higher values at stations 1 and 11 than at stations 3 and 9, for all biomass size-fractions and taxa (Fig. 5a and b).

3.3. Relationships between zooplankton and environmental variables

3.3.1. Correlation analysis

Total zooplankton abundance was positively correlated with temperature, total and <2 μm Chl *a* and ciliates (Table 2). Total meroplankton and bivalve larvae abundances were positively correlated with total and <2 μm Chl *a*. Copepod, bivalve larvae and meroplankton abundances as well as total biomass and all size-classes showed no significant relationship with any of the environmental and trophic variables. Other holoplanktonic organisms showed significant negative correlations with salinity and bacteria.

Table 1
Mean values between sampling dates of taxa numbers, total zooplankton abundance and percentage contribution of taxa in the four sampled stations during the three surveys: May 2008 (M1, M3, M9, M11), October 2008 (O1, O3, O9, O11) and February 2009 (F1, F3, F9 and F11). The symbols of the taxa for the multivariate analyses are indicated in the second column.

		May 2008				October 2008				February 2009			
		M1	M3	M9	M11	O1	O3	O9	O11	F1	F3	F9	F11
Copepoda (%)		24.5	44.6	39.2	35.2	67.9	56.9	32.4	33.5	34.2	32.9	39.7	27.9
Nauplii	NAU	12.28	11.92	12.37	11.37	27.02	23.50	13.09	17.80	7.12	11.68	16.83	12.45
Unidentified	COPI	0.37	0.04	0.09	0.08	0.22	0.45	0.68	0.55	1.53	2.10	1.42	0.73
Paracalanus/Clausocalanus	Par	3.74	8.18	7.92	9.72	8.10	7.77	4.96	3.58	7.20	5.57	6.67	8.14
Acartia spp.	Aca	0.34	0.09	0.14	0.09	1.79	0.26			0.41	0.07	0.07	0.16
Undinula vulgaris	Und	0.14	0.21	0.24	0.08	0.14	0.25	0.10	0.04	0.05	0.07	0.20	0.32
Candacia pachydactyla	Cpa		<0.01	<0.01	0.01								
Candacia varicans	Cva		0.01										
Calanopia minor	Cmi	0.06	<0.01	0.04	0.04	0.17	0.34	0.28	0.10	1.38	1.48	1.30	1.46
Labidocera sp.	Lab		<0.01	0.01				<0.01					
Corycaeus	Cor	0.08	0.92	1.41	0.29	0.33	0.25	0.90	1.18	0.38	0.64	0.90	0.79
Oncaea	Onc			0.02				<0.01		0.07	0.12	0.03	0.01
Oithona sp.	Oit	7.51	23.17	16.76	12.98	29.06	23.78	12.23	9.90	15.99	10.87	12.18	3.57
Oithona plumifera	Opl		0.03	0.23	0.55								
Sapphirinidae	Sap		0.01									<0.01	0.01
Microsetella sp.	Mic	<0.01	<0.01	<0.01		0.02	0.10	0.21	0.05	0.01	0.12	0.06	0.12
Tisbe sp.	Tis					0.52	0.09		0.14	0.02	0.07	0.03	0.04
Harpacticoid unidentified	HAR			0.01							<0.01	0.01	0.04
Tisbe sp.	Tis					0.52	0.09		0.14	0.02	0.07	0.03	0.04
Other holoplankton (%)		1.1	4.9	5.0	1.7	7.7	8.6	5.3	4.4	12.0	21.2	9.4	10.7
Appendicularians	APP		2.02	0.92	0.73	2.86	4.07	2.24	1.77	1.69	5.08	2.73	2.80
Chaetognaths	CHA	0.84	0.68	1.28	0.72	3.28	1.59	1.19	1.30	1.02	1.74	1.35	2.55
Pteropods	PTE	0.13	0.55	0.17	0.22	1.27	2.92	1.87	1.34	9.11	14.34	5.27	5.18
Isopods	ISO	0.02			0.01							<0.01	
Ostracods	OST	0.01	0.10	0.11	0.02		0.03	0.02	0.03	0.04	<0.01	0.02	0.06
Salps	SAL	0.09	1.47	2.49	<0.01	0.01	<0.01		<0.01		<0.01		
Medusae	MED					0.03	<0.01			<0.01			
Lucifer	LEU	<0.01				<0.01		<0.01		0.03	<0.01	<0.01	0.02
Amphipoda	AMP	0.01	0.03	0.08	0.03					0.01	0.02	0.03	0.06
Ctenophora	CTE	0.01		<0.01								<0.01	
Water mites	WMI	<0.01											
Foraminifera	FOR		<0.01	<0.01									
Protozoans	PRO					0.25		0.01		0.07	0.02		0.06
Larva (meroplankton) (%)		73.0	50.5	55.7	63.0	24.9	34.6	62.2	62.2	53.9	46.0	50.9	61.4
Gastropod	LGA	16.49	7.54	7.47	16.94	11.86	9.13	8.30	11.20	19.81	12.63	10.72	11.56
Bivalve	LBI	56.01	42.85	47.78	45.87	11.47	19.26	52.57	50.41	33.71	32.92	39.64	49.45
Euphausid	LEU	0.02				0.15	0.02	<0.01		0.01	<0.01	<0.01	0.01
Decapod	LDE	0.31	0.08	0.08	0.03	0.23	0.03	0.04	0.06	0.09	0.02	0.04	0.09
Zoea	LZO	<0.01	<0.01	0.01	0.02	0.19	0.01	0.03	0.01	0.03	0.02	0.01	0.01
Fish	LFI	0.06	0.04	0.02	0.03	0.11	0.01		0.00	0.02	0.01	0.04	0.05
Polychaete	LPY	0.01	<0.01	0.07	0.01	0.09	0.08	0.05	0.06	0.11	0.07	0.03	0.09
Echinoderm	LEC	0.07	0.03	0.29	0.14	0.83	5.67	1.17	0.44	0.05	0.24	0.40	0.17
Actinotroch	LAC	<0.01									<0.01		
Cirriped	LCI									0.01	0.05		
Asteroid	LAS					0.02	0.39	0.06	0.03	0.01	0.04	0.01	0.01
Total abundance (ind. m^{-3})		23,324	5830	6501	21,222	5058	9098	18,451	17,134	27,173	17,660	13,055	17,795
Nb Taxa		28	28	29	24	26	25	24	22	29	31	30	29

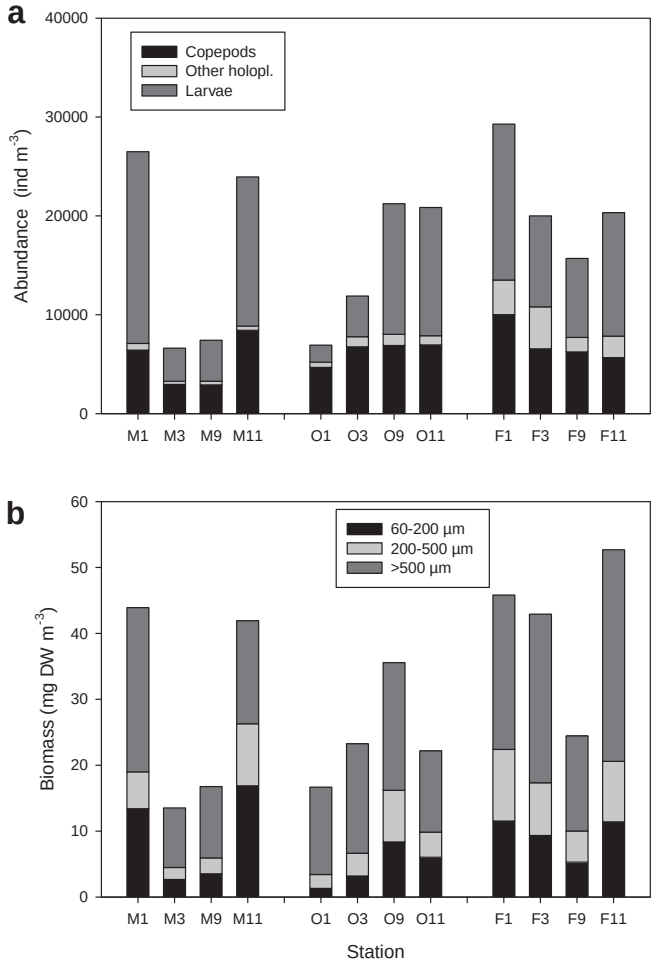

Fig. 5. Mean values (between sampling dates) of (a) abundance of the main zooplankton groups (copepods, other holoplankon and larvae) and (b) zooplankton biomass (by size-classes) as expressed in mg Dry weight (DW) per cubic meter at the four sampled stations (1, 3, 9, 11) during the three surveys: May 2008 (M1, M3, M9, M11), October 2008 (O1, O3, O9, O11) and February 2009 (F1, F3, F9, F11).

There were positive correlations between biomasses of the various functional metazooplankton groups (predators, nano and picoparticle feeders) except for bivalve larvae (Table 3). Predators were significantly and negatively correlated to the biomasses of bacteria and PNF and positively to picophytoplankton and HNF.

3.3.2. Multivariate analysis

The first factorial plane of the co-inertia analysis explained 88% of the variance, mainly on the first axis (60%). In both systems (Environment and Zooplankton), the first axis showed a seasonal distinction between the May 2008 survey (M1, M3, M9 and M11) and the two other surveys (October 2008 and February 2009) (Fig. 6). May samples were characterized by high salinity and high PNF and bacteria abundance. They were also associated with several copepod taxa: Candacia spp., *Labidocera* sp. and *Oithona plumifera* and with salps, ctenophores, isopods, foraminifers and water mites. Values recorded in October and February were correlated with HNF, *Synechococcus*, *Prochorococcus* and picoeukaryotes and with several zooplankton taxa including harpacticoid (*Microsetella* sp., *Tisbe* sp. and undetermined genera) and cyclopoid (*Oncaea* sp.) copepods, medusae, annelid and cirriped larvae. The second axis mainly opposed the February survey (on the top of the axis) to the October survey (on the bottom) and, within each survey, station 1 (top) to the other stations. The February survey and station 1 were characterized by higher temperature, chlorophyll, picoeukaryote and ciliate values and by several rare zooplankton taxa such as ctenophores, *Lucifer* spp., isopods, water mites, Cirriped and Actinotroch larvae.

In the PCA of the trophic-functional groups, the first factorial plane explained 89% of the variance, mainly on the first axis (67%). The first axis showed a clear opposition between the May 2008 survey which was characterized by high PNF and bacteria abundances and the surveys in February 2009 (mainly) and October 2008 (to a lesser extent) which were characterized by high picophytoplankton and HNF abundances and by the functional zooplankton groups (predators, pico- particle feeders, bivalves and other nano-particle feeders) (Fig. 7). It is also interesting to note the associations between HNF and picophytoplankton, between particle feeders and predators and between bivalve larvae and ciliates.

4. Discussion

4.1. Hydrobiological context

The phytoplanktonic biomass, as inferred from Chl *a*, measured in the Ahe lagoon was comparable to that in other oligotrophic ecosystems and similar to that in other lagoons of the Tuamotu Archipelago (Rancher and Rougerie, 1995). The proportion of picoplankton was close to that recorded in other atoll lagoons and in agreement with additional measurements in Ahe made in 2009 and 2010 (Charpy, 1996; Charpy et al., 2012).

High spatio-temporal variations of chlorophyll, autotrophic (picoeukaryotes, *Synechococcus* and autotrophic nanoflagellates, PNF) and heterotrophic (bacteria, HNF and ciliates) organisms were observed (see Fig. 4). A large part of this variability may be linked to water circulation within the lagoon and with the exchanges with the ocean, as discussed by Lefebvre et al. (2012) for photosynthetic parameters. Dumas et al. (2012), using one year field data and a 3D hydrodynamic model, showed how the wind influences the water circulation in Ahe atoll. They identified 3 residual circulation cells when climatological wind is activated: the south and north cells (including stations 1 and 11, respectively) with a residence time longer than in a central cell (including stations 3 and 9) more directly under the influence of the pass. In October 2008 and February 2009 during high wind speed condition from the east (7–9 m s^{-1}), the observed little difference between stations may be the consequence of water homogenization by the overturning lagoon-scale current that may affect in the same way the depth sampled here (0–10, and 0–20 m depending on stations). In May, the clear spatial differences of chlorophyll and autotrophic organisms between central (stations 3 and 9) and coastal (stations 1 and 11) stations may be partly explained by lighter winds (<2–4 m s^{-1}) stronger pass influence, and by the difference in residence time between the atoll sectors, as suggested by Lefebvre et al. (2012). The effect of wind on biological properties was already shown by Charpy and Charpy-Roubaud (1991) and Torréton et al. (2007).

The incidence of pearl farming on the variability of microorganisms can also be pointed out as suggested by Lefebvre et al. (2012). In May, the highest biomass values were observed at station 1, in the more confined, southwest shallow area of the lagoon where pearl farming is more intensive. The highest chlorophyll values reported there correspond to highest phytoplankton production values provided by both Charpy et al. (2012) and Lefebvre et al. (2012). According to Loret et al. (2000) for Takapoto Atoll, these observations could be linked to the recycling of nutrients by pearl oysters.

Table 2
Pearson's correlation coefficients between zooplankton biomass (total and by size classes) and abundance (total and for the main groups) and environmental and trophic factors. Significant values after Bonferroni correction for multiple comparison ($p < 0.005$) are in bold characters. $N = 12$. Proc. = *Prochlorococcus* sp., Syn. = *Synechococcus* sp., Pico. = picoeukaryotes, PNF = Pigmented (autotrophic) nanoflagellates, Bact. = bacteria, HNF = heterotrophic nanoflagellates, Cil. = ciliates.

	Biomass				Abundance				
	Total	>500 μm	200–500 μm	80–200 μm	Total	Copepods	Others	Mero plankton	Bivalve larvae
T	0.444 $p = 0.148$	0.412 $p = 0.183$	0.430 $p = 0.163$	0.456 $p = 0.136$	**0.757** **$p = 0.005$**	0.057 $p = 0.861$	0.423 $p = 0.171$	0.317 $p = 0.315$	0.255 $p = 0.424$
S	−0.317 $p = 0.316$	−0.492 $p = 0.105$	−0.370 $p = 0.236$	−0.023 $p = 0.942$	−0.165 $p = 0.608$	−0.442 $p = 0.150$	**−0.862** **$p = 0.000$**	−0.094 $p = 0.771$	−0.003 $p = 0.992$
Chl tot	0.660 $p = 0.019$	0.601 $p = 0.039$	0.540 $p = 0.070$	0.667 $p = 0.018$	**0.754** **$p = 0.005$**	0.469 $p = 0.124$	0.348 $p = 0.268$	0.622 $p = 0.031$	0.609 $p = 0.036$
Chl <2 μm	0.676 $p = 0.016$	0.591 $p = 0.043$	0.578 $p = 0.049$	0.705 $p = 0.010$	**0.802** **$p = 0.002$**	0.441 $p = 0.151$	0.352 $p = 0.261$	0.628 $p = 0.029$	0.602 $p = 0.038$
Chl >2 μm	0.471 $p = 0.122$	0.513 $p = 0.088$	0.299 $p = 0.345$	0.410 $p = 0.185$	0.452 $p = 0.140$	0.455 $p = 0.137$	0.247 $p = 0.439$	0.483 $p = 0.112$	0.513 $p = 0.088$
Proc	−0.049 $p = 0.880$	−0.049 $p = 0.879$	0.055 $p = 0.866$	−0.080 $p = 0.804$	−0.403 $p = 0.194$	0.212 $p = 0.507$	0.174 $p = 0.589$	0.091 $p = 0.779$	0.077 $p = 0.812$
Pico	0.555 $p = 0.061$	0.638 $p = 0.026$	0.505 $p = 0.094$	0.412 $p = 0.184$	0.704 $p = 0.011$	0.244 $p = 0.445$	0.689 $p = 0.013$	0.330 $p = 0.294$	0.271 $p = 0.395$
Syn	0.387 $p = 0.215$	0.502 $p = 0.097$	0.437 $p = 0.156$	0.086 $p = 0.791$	0.081 $p = 0.803$	0.617 $p = 0.032$	0.628 $p = 0.029$	0.125 $p = 0.699$	0.059 $p = 0.855$
PNF	−0.129 $p = 0.690$	−0.296 $p = 0.351$	−0.200 $p = 0.533$	0.152 $p = 0.637$	0.157 $p = 0.625$	−0.408 $p = 0.189$	−0.662 $p = 0.019$	0.037 $p = 0.908$	0.099 $p = 0.759$
Bact	−0.353 $p = 0.261$	−0.523 $p = 0.081$	−0.398 $p = 0.200$	−0.058 $p = 0.857$	−0.225 $p = 0.483$	−0.389 $p = 0.211$	**−0.836** **$p = 0.001$**	−0.085 $p = 0.793$	−0.003 $p = 0.992$
HNF	0.328 $p = 0.298$	0.463 $p = 0.130$	0.356 $p = 0.255$	0.052 $p = 0.871$	0.006 $p = 0.986$	0.565 $p = 0.056$	0.677 $p = 0.016$	0.160 $p = 0.619$	0.119 $p = 0.712$
Cil	0.563 $p = 0.057$	0.447 $p = 0.146$	0.505 $p = 0.094$	0.665 $p = 0.018$	**0.821** **$p = 0.001$**	0.152 $p = 0.638$	0.234 $p = 0.463$	0.536 $p = 0.073$	0.507 $p = 0.093$

Table 3
Pearson's correlation coefficients between the different trophic groups: picophytoplankton (=sum of *Prochlorococcus* sp., *Synechococcus* sp., and picoeukaryotes), pigmented (autotrophic) nanoflagellates (PNF), bacteria (Bact), heterotrophic nanoflagellates (HNF), ciliates.(Cil), predators (=sum of Chaetognaths, medusae, ctenophores, *Labidocera* spp., *Candacia* spp., *Corycaeus* spp., *Oncaea* spp. and fish larvae), picoparticle feeders (pico F = sum of salps and appendicularians), bivalves and other nanoparticle feeders (nano F = other metazooplankton organisms). Significant values after Bonferroni correction for multiple comparison ($p < 0.006$) are in bold characters. $N = 12$.

	Picophyto	PNF	Bact	HNF	Cil	Predators	Nano F	Pico F
PNF	**−0.889** **$p = 0.000$**							
Bact	**−0.754** **$p = 0.005$**	**0.848** **$p = 0.000$**						
HNF	**0.892** **$p = 0.000$**	**−0.944** **$p = 0.000$**	**−0.837** **$p = 0.001$**					
Cil	−0.329 $p = 0.296$	0.453 $p = 0.139$	−0.042 $p = 0.897$	−0.298 $p = 0.348$				
Predators	**0.771** **$p = 0.003$**	**−0.665** **$p = 0.018$**	**−0.802** **$p = 0.002$**	**0.787** **$p = 0.002$**	0.209 $p = 0.514$			
Nano F	0.644 $p = 0.024$	−0.429 $p = 0.164$	−0.668 $p = 0.017$	0.540 $p = 0.070$	0.444 $p = 0.148$	**0.871** **$p = 0.000$**		
Pico F	0.683 $p = 0.014$	−0.584 $p = 0.046$	−0.689 $p = 0.013$	0.575 $p = 0.051$	0.163 $p = 0.613$	**0.739** **$p = 0.006$**	**0.808** **$p = 0.001$**	
Bivalves	0.165 $p = 0.608$	0.099 $p = 0.759$	−0.003 $p = 0.992$	0.119 $p = 0.712$	0.507 $p = 0.093$	0.461 $p = 0.131$	0.498 $p = 0.099$	0.298 $p = 0.347$

4.2. Zooplankton community: dominance of meroplankton and bivalve larvae

The mean total zooplankton biomass and abundance in the Ahe lagoon were similar to those found in other Tuamotu atolls (Ricard et al., 1979; Le Borgne et al., 1989). Furthermore, the holoplanktonic community (dominated by the copepods *Oithona* spp., *P. parvus* and *Clausocalanus* spp., *Corycaeus* spp., *A. fossae* and *Undinula vulgaris*) was very close to those described in other atoll lagoons of the Tuamotu Archipelago in previous studies (Rose, 1953; Michel, 1969; Michel et al., 1971; Le Borgne et al., 1989; Sakka et al., 2002) and in other lagoon ecosystems in the Pacific Ocean (Le Borgne et al., 1997; Carassou et al., 2010). However, the proportion of meroplankton (35–74%) and bivalve larvae (19–56%) to total zooplankton was higher than observed in Takapoto (1% and <0.7%, respectively; Sakka et al., 2002) and in Tikeau (12–19%

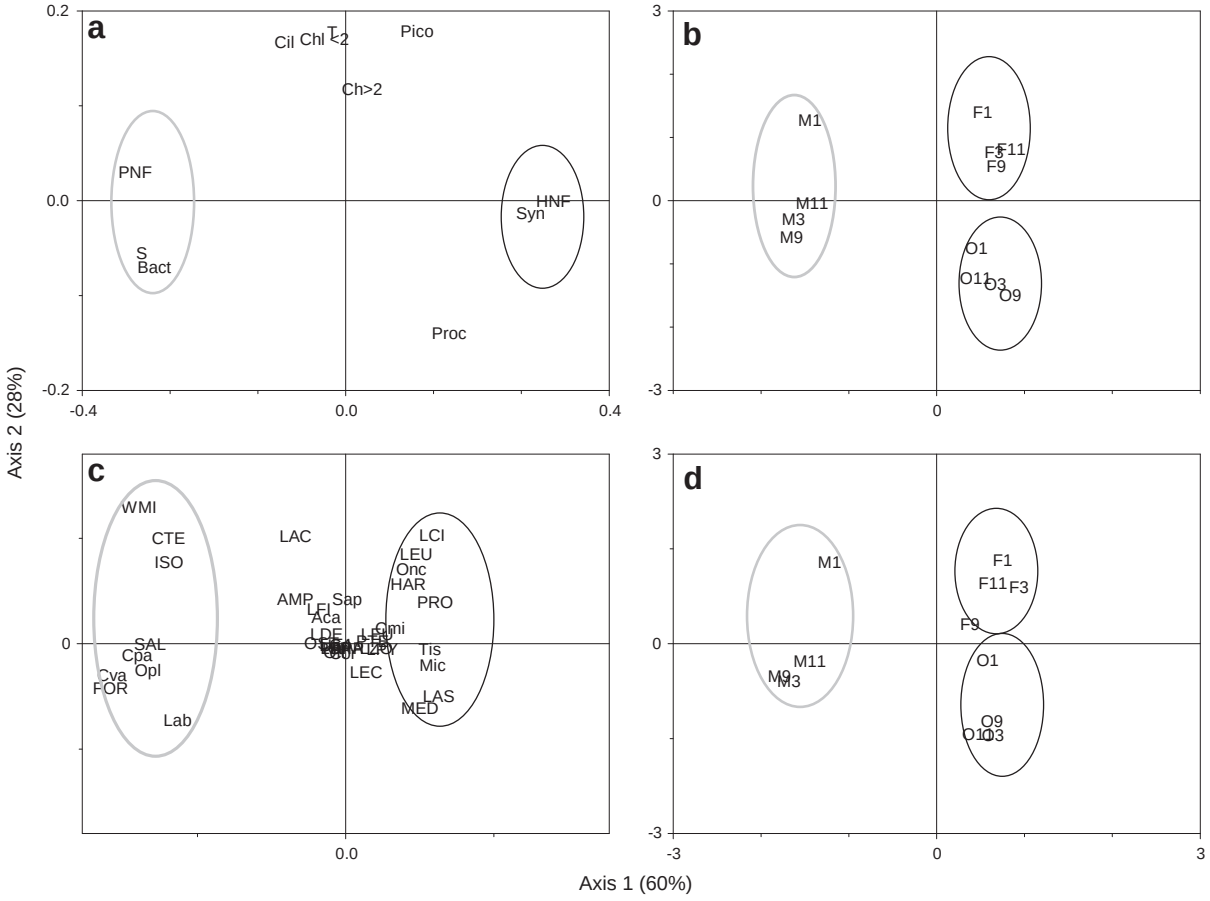

Fig. 6. Co-inertia analysis plots of (a) the environmental variables and (b) the stations in the "Environment" system and plots of (c) the taxa and (d) the stations in the "Zooplankton" system. Abbreviations as in Tables 1 and 2.

and 11–14%, respectively; Blanchot et al., 1989; see their Tables 4 and 6) or in other coral reef lagoons (e.g. 15% and 4%, respectively in New Caledonian lagoon; Carassou et al., 2010).

In Ahe lagoon, linked to pearl farming, *P. margaritifera* could constitute a large part of this important bivalve larvae stock, but Thomas et al. (2012a) estimated that the contribution of *P. margaritifera* to this stock would be low (0.5–5%) compared to wild species and in particular to *P. maculata* (65–91%). This suggests that high bivalve larvae concentration in the lagoon is not drastically modified by pearl oyster farming, despite 10% of the lagoon area dedicated to this activity. However, Thomas et al. prediction was based on experimental spat collectors immersed in the central part of the lagoon (close to stations 3 and 9) where the influence of outside oceanic water through the pass is the more important and where the pearl farming activity is the less intensive. Even with likely more than a few percent of farmed oysters, the relative abundance of bivalve larvae in the Ahe plankton is probably due to the importance of wild populations. The requirement to know the exact status of the wild population of bivalve has been pointed out by several of the study achieved in Ahe (Thomas et al., 2012a). This will be a priority in subsequent studies.

The dominance of bivalve larvae also suggests an imbalance at the bottom of the trophic pyramid, resulting in a "bottleneck" between the second (primary consumers) and third (secondary consumers) trophic levels. According to Margalef (1974), this imbalance may be related to (1) food competition between bivalve larvae and the other nanoparticle feeders and (2) dominant prey (bivalve larvae) having shells and, therefore, being difficult to consume. This second point is supported by the absence of correlation between bivalve larvae and predator, while positive correlations were found between other zooplankton prey (pico feeders and other nano feeders) and predators (see Table 3). However, further investigation on the structure and functioning of the trophic network is required to explore these hypotheses.

4.3. Spatio-temporal distribution of zooplankton

As for the aforementioned microorganisms, wind-driven water circulation may partly explain the spatiotemporal variations of zooplankton in the lagoon. It is generally accepted that, in closed or semi-closed shallow aquatic ecosystems, the wind effect on the water column mixing, combined with vertical migration (and distribution) of organisms exert a very significant influence on the zooplankton horizontal distribution (Boltovskoy et al., 1984), including in coral reef systems (Alldredge and King, 2009). Besides, in coastal marine ecosystems wind-driven circulation and the behavior of larvae of individual bivalve species have been shown to interact to produce patches of high larval abundance (Ma et al., 2006).

In this study, during the windy period (October 2008) the total abundance and biomass were lower at stations 1–3 (on the western zone) than at stations 9–11 (eastward zone). This increase was mainly due to the accumulation of bivalve larvae (Fig. 4) with copepods being relatively more abundant at stations 1–3. Such a pattern is consistent with the observations by Carleton and Doherty (1998) in another atoll of the Tuamotu Archipelago (Taiaro) where zooplankton formed distinctive, consistently different assemblages in the windward and leeward areas during the

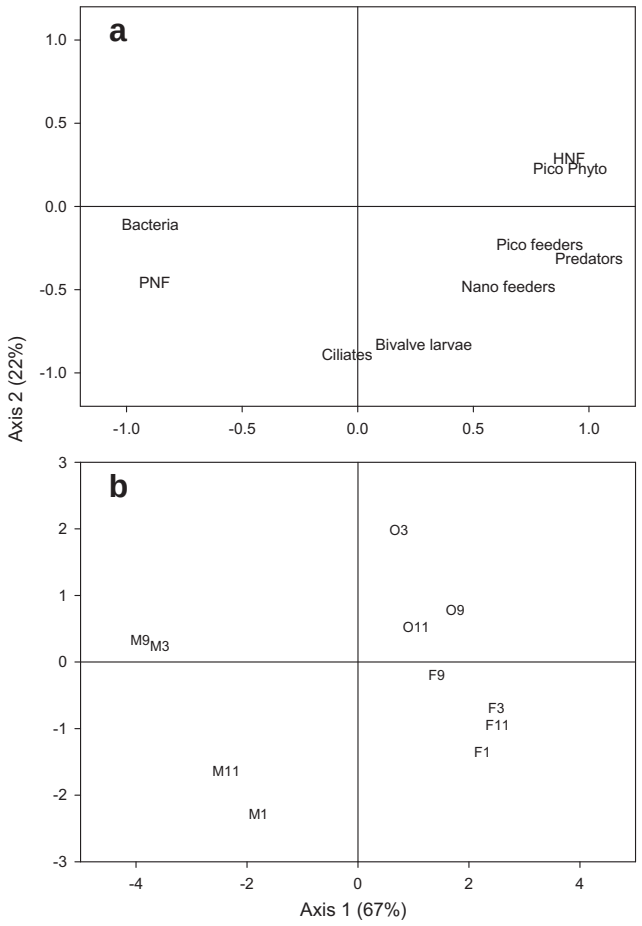

Fig. 7. Principal Component Analysis (PCA) on the trophic functional groups: plots of (a) the trophic variables and (b) the stations on the first factorial plane.

windy period. They argued that this spatial pattern probably resulted from the combination of hydrodynamic circulation within the lagoon and species specific behavior. Water circulation in closed atoll lagoons is typically dominated by wind-driven circulation with surface water moving downwind, balanced by a compensatory reverse flow near the bottom resulting in upwelling at the windward margin and downwelling at the leeward side (Michel, 1969; Atkinson et al., 1981; Dumas et al., 2012). Actively vertical migrating species should, therefore, accumulate in the downwelling zone, owing to their distribution on the surface at night, while deep-living species should prevail in the upwelling zone. According to this pattern the higher relative abundance of some copepods (*U. vulgaris*, *Paracalanus/Clausocalanus* spp., *Acartia* sp. and *Oithona* spp.) at the westward stations (stations 1–3) than at eastward stations (stations 9–11) in October 2008 (see Table 1), could be explained by their nocturnal migration to the upper water layer.

Calanoid copepods such as *Acartia*, *Paracalanus* and *Clausocalanus* (Pagano et al., 1993; Cuker and Watson, 2002; Lo et al., 2004) as well as small *Oithona* species (Tanimura et al., 2008) have been shown to exhibit typical diel vertical migrations (DVM) in contrasting habitats. We found no such evidence (nor contrary evidence) for *U. vulgaris* in the literature, but, over a 24-h sampling survey at a coastal station (5 m depth) near the field laboratory (east side of the atoll), we observed high nocturnal abundance and quasi diurnal absence of this species (unpublished data), suggesting a strong migratory behavior and possible DVM in the Ahe lagoon. On the other hand, high abundance of bivalve larvae at the eastward stations (stations 9–11) could be partly explained by their permanent concentration in the deep layers (20–30 m) as observed by Thomas et al., (2012a). These authors observed in 2007–2008 a similar large-scale distribution pattern with high concentration of bivalve larvae in the eastern part by windy conditions. They suggested that the deep vertical distribution of the larvae could explain their horizontal distribution, the larvae being passively transported by the overturning upwind deep current leading to high larval concentration along the eastern reef rim. The high transport potential for larvae observed by Thomas et al. (2012a) and the modeling study performed by Thomas et al. (2012b) has confirmed the existence of this circulation.

During the light wind period (May 2008) the central area (stations 3 and 9) was characterized by lower zooplankton biomass and abundance and lower percentages of meroplankton and bivalve larvae than at the coastal stations (stations 1 and 11). These differences can be explained by the tide-driven flush going through the pass, creating a jet-like circulation in the central area, according to the 3D hydrodynamical model by Dumas et al. (2012). The resulting higher oceanic influence in the central part of the lagoon probably explains the higher relative abundance of typical oceanic zooplankton populations such as salps and appendicularians at station 3 and 9 compared to stations 1 and 11 (see Table 1). Hamner et al. (2007) also observed tidal export–import phenomena leading to changes of zooplankton community in a coral reef system (Palau). On the other hand, higher percentage of bivalve larvae at station 1 and 11 compared to stations 3 and 9 could reflect a stronger influence of pearl oyster farming at a period where low wind-driven overturning circulation limits larval dispersion over the lagoon.

4.4. Relationships between zooplankton and environmental and trophic variables

Our study revealed clear differences in zooplankton community between the different sampling periods, probably explained by either abiotic or biotic variables (see Co-inertia analysis, Fig. 6). During the dry season survey (May 2008) characterized by high salinity (>36.8) and autotrophic-dominant trophic status (higher abundance of PNF and bacteria), the zooplankton community was mainly characterized by *Candacia* spp., *Labidocera* sp., *Oithona plumifera* and salps. During the other periods (October 2008 and February 2009), characterized by lower salinity (<36.6) and heterotrophic-dominant trophic status (higher abundance of HNF), the community was mainly characterized by harpacticoid (*Microsetella* sp., *Tisbe* sp. and undetermined genera) and cyclopid (*Oncaea* sp.) copepods, medusae, Annelid and Cirriped larvae. Salinity and trophic status, therefore, appeared to be important causes explaining the time-variations of the zooplankton community.

Total zooplankton abundance was positively correlated with temperature, mainly due to the highest abundance recorded in February during the warmest period. Zooplankton composition was also dependent on temperature as shown by the multivariate analysis with the colder (October 2008) and the warmer (February 2009) surveys opposed on the second axis. The February 2009 survey was characterized by several rare zooplankton taxa such as Ctenophores, *Lucifer*, isopods, water mites and Cirriped and Actinotroch larvae. Alvarez-Cadena et al. (2009) also showed clear distinction between the dry season (November–May), and the wet season (June–October) for the composition and abundance of zooplankton in a coral reef lagoon, in relation with variations of similar abiotic factors (temperature and salinity).

The clearly higher zooplankton abundance and biomass at the coastal stations (1 and 11) than at the central ones (3 and 9) during the light wind period (May), (see Fig. 5 and discussion above), can be related to concurrent higher phytoplankton and microheterotrophic biomass (see Fig. 4). Furthermore, we also ob-

served a significant correlation between Chl *a* and zooplankton abundance ($r = 0.75$, $p = 0.005$). These results suggest a bottom-up control of zooplankton in the lagoon. This type of control is relatively common in oligotrophic ecosystems, such as atoll lagoons, where the primary production is limited by low nutrient levels and where phytoplankton biomass availability is a limiting factor for the production of the upper trophic levels (Calbet et al., 1996). In the Ahe lagoon, the bulk of phytoplankton consists of picophytoplankton which cannot be directly consumed by most zooplankton taxa including the most abundant ones, such as bivalve larvae (Doroudi et al., 2003). To fulfill their energy needs, these organisms had to consume nano- or micro-particles such as organic detritus, transparent exopolymeres (TEP) which were abundant during this study (Durieux, pers. com.) and heterotrophic organisms produced trough the microbial loop.

The importance of detritus as food for lagoon zooplankton was shown by Gerber and Marshall (1974) in Eniwetok Lagoon (Marshall Islands), and by Le Borgne et al. (1989) in Tikehau Atoll lagoon. The use of TEP as a food source for zooplankton was suggested by Ling and Alldredge (2003), although other works have shown an inhibiting effect (Dutz et al., 2005). The importance of the microbial loop for the production of the upper trophic levels in atoll lagoons has been shown in previous studies. Sakka et al. (2002) showed that protozoa played a key role in the Takapoto atoll by exerting strong grazing pressure on picoplankton and were themselves a major food source for metazoan zooplankton. In the same lagoon, Loret et al. (2000) showed that hetero/mixotrophic protists processed the picoplanktonic resource rapidly and efficiently for filter-feeders, particularly pearl oysters. In the Ahe lagoon, the importance of the microbial loop is supported by the study of Michotey et al. (2012) showing spatiotemporal pervasiveness for heterotrophic groups such as *Marinovum*, *Flavobacteria* and *Erytrobacter*. The trophic link between metazooplankton and the microbial loop is suggested by our positive correlations between ciliates and total zooplankton ($r = 0.82$, $p = 0.01$) and by–the PCA for the functional groups (Fig. 7) which showed clear links between HNF and nano particle feeders, as well as between ciliates and bivalve larvae. It is also supported by the Co-inertia analysis (Fig. 6) which showed a clear opposition between the May 2008 survey, where the herbivory components of the food chain prevailed with the large numbers of PNF and the presence of salps, and the surveys in October 2008 and February 2009 where the predominance of the heterotrophic microbial components (higher abundance of HNF) was associated with a zooplankton community characterized by harpacticoid (*Microsetella* sp., *Tisbe* sp. and undetermined genera) and cyclopid (*Oncaea* sp.) copepods and by medusa, Annelid and Cirriped larvae. The association of salps with PNF and bacteria may be linked to their ability to graze not only on 2–200 μm phytoplankton but also on 0.5–2 μm free-living bacteria and picophytoplankton, owing to their mucus net filtering structures (Riisgard and Larsen, 2010). On the other hand, the association of harpacticoids and cyclopids with the heterotrophic network may be linked to their ability to utilize a variety of food materials including detritus, organic flocs, fecal pellets and protists (Lewis et al., 1998; Metz, 1998).

5. Conclusion

Our results showed the predominance of meroplankton and bivalve larvae in Ahe as compared to other coral reef and atoll lagoons. while the dominance of bivalve larvae suggests potentially major community change arising from aquaculture activities (pearl oyster farming), it is probably mainly due to the importance of wild populations. Our study also suggests that tide-flushing and wind driven circulation of the lagoon, as evidenced in the study by Dumas et al. (2012), plays an important role in shaping the time and space distribution of the zooplankton. Salinity, temperature and trophic status (autotrophic *vs* heterotrophic) seem to be the main forcing variables for the abundance and composition of the metazooplankton community. The preponderance of picophytoplankton within the phytoplankton community and the abundance of nanoparticle feeders are indirect evidence of the importance of the microbial loop in Ahe lagoon.

Acknowledgements

This study was funded by the 9th European Development Fund (EDF) (grant POF/001/002 N°1 to Serge Andréfouët and Loic Charpy, IRD). The authors express their gratitude to the EDF and Service de la Perliculture staff, especially Alain Lo-Yat, for their efficient help during sample collection on Ahe atoll. They also thank two anonymous reviewers for helpful criticisms and comments on the first version of the manuscript.

References

Alldredge, A.L., King, J.M., 2009. Near-surface enrichment of zooplankton over a shallow back reef: implications for coral reef food webs. Coral Reefs 28, 895–908.

Alvarez-Cadena, J.N., Ordonez-Lopez, U., Almaral-Mendivil, A.R., Uicab-Sabido, A., 2009. Composition and abundance of zooplankton groups from a coral reef lagoon in Puerto Morelos, Quintana Roo, Mexico, during an annual cycle. Revista de Biologia Tropical 57, 647–658.

Andréfouët, S., Charpy, L., Lo-Yat, A., Lo, C., 2012. Recent reseach for pearl oyster aquaculture management in French Polynesia. Marine Pollution Bulletin 65, 407–414.

Atkinson, M., Smith, S.V., Stroup, E.D., 1981. Circulation in Enewetak Atoll lagoon. Limnology and Oceanography 26, 1074–1083.

Attayde, J.L., Bozelli, R.L., 1998. Assessing the indicator properties of zooplankton assemblages to disturbance gradients by canonical correspondence analysis. Canadian Journal of Fisheries and Aquatic Sciences 55, 1789–1797.

Blanchot, J., Charpy, L., Borgne, R., 1989. Size composition of particulate organic matter in the lagoon of Tikehau Atoll (Tuamotu Archipelago). Marine Biology 102, 329–339.

Boltovskoy, D., Pedroso, F.L., Battistoni, P.A., 1984. The effects of wind and diel vertical migrations on the distribution of freshwater zooplankton. Studies on Neotropical Fauna and Environment 19, 137–154.

Bozec, Y.M., Gascuel, D., Kulbicki, M., 2004. Trophic model of lagoonal communities in a large open atoll (Uvea, Loyalty islands, New Caledonia). Aquatic Living Resources 17 (2), 151–162.

Cairns, J., McCormick, P.V., Niederlehner, B.R., 1993. A proposed framework for developing indicators of ecosystem health. Hydrobiologia 263, 1–44.

Calbet, A., 2008. The trophic roles of microzooplankton in marine systems. ICES Journal of Marine Science 65, 325–331.

Calbet, A., Alcaraz, M., Saiz, E., Estrada, M., Trepat, I., 1996. Planktonic herbivorous food webs in the catalan Sea (NW Mediterranean): temporal variability and comparison of indices of phyto-zooplankton coupling based on state variables and rate processes. Journal of Plankton Research 18, 2329–2347.

Carassou, L., Le Borgne, R., Rolland, E., Ponton, D., 2010. Spatial and temporal distribution of zooplankton related to the environmental conditions in the coral reef lagoon of New Caledonia, Southwest Pacific. Marine Pollution Bulletin 61, 367–374.

Carleton, J.H., Doherty, P.J., 1998. Tropical zooplankton in the highly-enclosed lagoon of Taiaro Atoll (Tuamotu Archipelago, French Polynesia). Coral Reefs 17, 29–35.

Charpy, L., 1996. Phytoplankton biomass and production in two Tuamotu atoll lagoons (French Polynesia). Marine Ecology Progress Series 145, 133–142.

Charpy, L., Blanchot, J., 1998. Photosynthetic picoplankton in French Polynesian atoll lagoons: estimation of taxa contribution to biomass and production by flow cytometry. Marine Ecology Progress Series 162, 57–70.

Charpy, L., Charpy-Roubaud, C., 1991. Particulate organic matter fluxes in a Tuamotu atoll lagoon. Marine Ecology Progress Series 71, 53–63.

Charpy, L., Rodier, M., Fournier, J., Langlade, M.J., Gaertner-Mazouni, N., 2012. Physical and chemical control of the phytoplankton of Ahe lagoon, French Polynesia. Marine Pollution Bulletin 65, 471–477.

Chisholm, L.A., Roff, J.C., 1990. Size-weight relationships and biomass of tropical off Kingston, Jamaica. Marine Biology 106, 71–77.

Conway, D.V.P., White, R.G., Hugues-Dit-Ciles, J., Gallienne, C.P., Robins, D.B., 2003. Guide to the coastal and surface zooplankton of the South-Western Indian Ocean. DEFRA Darwin Initiative Zooplankton Programme, Version 1, Marine Biological Association of the United Kingdom Occasional Publications, Plymouth.

Cuker, B.E., Watson, N.A., 2002. Diel vertical migration of zooplankton in contrasting habitats of the Chesapeake Bay. Estuaries 25, 296–307.

Dolédec, S., Chessel, D., 1994. Co-inertia analysis: an alternative method for studying species-environment relationships. Freshwater Biology 31, 277–294.
Doroudi, M.S., Southgate, P.C., Lucas, J.S., 2003. Variation in clearance and ingestion rates by larvae of the black-lip pearl oyster (*Pinctada margaritifera*, L.) feeding on various microalgae. Aquaculture Nutrition 9, 11–16.
Dumas, F., Le Gendre, R., Thomas, Y., Andréfouët, S., 2012. Tidal flushing and wind driven circulation of Ahe atoll lagoon (Tuamotu Archipelago, French Polynesia) from in situ observations and numerical modelling". Marine Pollution Bulletin 65, 425–440.
Dutz, J., Breteler, W., Kramer, G., 2005. Inhibition of copepod feeding by exudates and transparent exopolymer particles (TEP) derived from a *Phaeocystis globosa* dominated phytoplankton community. Harmful Algae 4 (5), 929–940.
Fournier, J., Dupuy, C., Bouvy, M., Courrodon-Real, M., Charpy, L., Pouvreau, S., Le Moullac, G., Le Pennec, M., Cochard, J.-C., 2012. Pearl oysters *Pinctada margaritifera* grazing on natural plankton in Ahe atoll lagoon (Tuamotu archipelago, French Polynesia). Marine Pollution Bulletin 65, 490–499.
Gerber, R.P., 1981. Species composition and abundance of lagoon zooplankton at Eniwetak atoll, Marshall Isalnds. Atoll research Bulletin 247, 1–22.
Gerber, R.P., Marshall, N., 1974. Ingestion of detritus by the lagoon pelagic community at Eniwetok Atoll. Limnology and Oceanography 19, 815–824.
Gundersen, K., Heldal, M., Norland, S., Purdie, D.A., Knap, A.H., 2002. Elemental C, N and P cell content of individual bacteria collected at the Bermuda Atlantic Time-series Study (BATS) site. Limnology and Oceanography 47, 1525–1530.
Hamner, W.M., Colin, P.L., Hamner, P.P., 2007. Export-import dynamics of zooplankton on a coral reef in Palau. Marine Ecology Progress Series 334, 83–92.
Hatcher, B.G., 1997. Organic production and decomposition. In: Birkeland, C. (Ed.), Life and Death of Coral Reefs. Chapman and Hall, New York, pp. 230–248.
Le Borgne, R., Blanchot, J., Charpy, L., 1989. Zooplankton of Tikehau atoll (Tuamotu archipelago) an its relationship to particulate matter. Marine Biology 102, 341–353.
Le Borgne, R., Rodier, M., LeBouteiller, A., Kulbicki, M., 1997. Plankton biomass and production in an open atoll lagoon: Uvea, New Caledonia. Journal of Experimental Marine Biology and Ecology 212, 187–210.
Lefebvre, S., Claquin, P., Orvain, F., Véron, B., Charpy, L., 2012. Spatial and temporal dynamics of size-structured photosynthetic parameters (PAM) and primary production (13C) of pico- and nano-phytoplankton in an atoll lagoon. Marine Pollution Bulletin 65, 478–489.
Lewis, A.G., Chatters, L., Raudsepp, M., 1998. Feeding structures and their functions in adult and preadult *Tigriopus californicus* (Copepoda: Harpacticoida). Journal of the Marine Biological Association of the United Kingdom 78, 451–466.
Ling, S.C., Alldredge, A.L., 2003. Does the marine copepod Calanus pacificus consume transparent exopolymer particles (TEP)? Journal of Plankton Research 25 (5), 507–515.
Lo, W.T., Shih, C.T., Hwang, J.S., 2004. Diel vertical migration of the planktonic copepods at an upwelling station north of Taiwan, western North Pacific. Journal of Plankton Research 26, 88–96.
Loret, P., Le Gall, S., Dupuy, C., Blanchot, J., Pastoureaud, A., Delesalle, B., Caisey, X., Jonquières, G., 2000. Heterotrophic protist as a trophic link between picocyanobacteria and the pearl oyster Pinctada margaritifera in the Takapoto lagoon Tuamotu Archipelago, French Polynesia). Aquatic Microbial Ecology 22, 215–226.
Lovegrove, T., 1966. The determination of the dry weight of plankton and the effect of various factors on the values obtained. In: Barnes, H. (Ed.), Some Contemporary Studies in Marine Science. Allens and Unwin Ltd., London, pp. 407–420.
Ma, H.G., Grassle, J.P., Chant, R.J., 2006. Vertical distribution of bivalve larvae along a cross-shelf transect during summer upwelling and downwelling. Marine Biology 149, 1123–1138.
Margalef, R., 1974. Ecologia. Omega (Ed.), Barcelona.
Marie, D., Partensky, F., Vaulot, D., Brussaart, C., 1999. Enumeration of phytoplankton, bacteria, and viruses in marine samples. In: Dressier, L.G. (Ed.), Current Protocoles of Cytometry. Suppl. 10, Unit 11,11, pp. 1–15.
Mauchline, J., 1998. The biology of Calanoid copepods. In: Blaxter, J.H.S., Southward, A.J., Tyler, P.A. (Eds.), Advances in Marine Biology. Academic Press, London, p. 710.
Metz, C., 1998. Feeding of *Oncaea curvata* (Poecilostomatoida, Copepoda). Marine Ecology Progress Series 169, 229–235.
Michel, A., 1969. Plancton du lagon et des abords extérieurs de l'atoll de Mururoa. Cahiers du Pacifique 13, 81–131.
Michel, A., Colin, C., Desrosières, R., Oudot, C., 1971. Observations sur l'hydrologie et le plancton des abords et de la zone de passes de l'atoll de Rangiroa (Archipel des Tuamotu, Océan Pacifique Central). Cahiers ORSTOM, Série Océanographie 9, 375–402.
Michotey, V., Guasco, S., Boeuf, D., Morezzi, N., Durieux, B., Charpy, L., 2012. Spatio-temporal diversity of free-living and particle-attached prokaryotes in the tropical lagoon of Ahe atoll (Tumotu Archipelago) and its surrounding oceanic waters. Marine Pollution Bulletin 65, 525–537.
Niquil, N., Jackson, G.A., Legendre, L., Delesalle, B., 1998. Inverse model analysis of the planktonic food web of Takapoto Atoll (French Polynesia). Marine Ecology-Progress Series 165, 17–29.
Ohtsuka, S., Onbé, T., 1991. Relationships between mouthpart structures and *in situ* feeding habits of species of the family Pontellidae (Copepoda: Calanoida). Marine Biology 111, 213–225.
Pagano, M., Gaudy, R., Thibault, D., Lochet, F., 1993. Vertical migrations and feeding rhythms of mesozooplanktonic organisms in the Rhone River plume area (North-West Mediterranean Sea). Estuarine Coastal and Shelf Science 37, 251–269.
Pelegri, S.P., Dolan, J.R., Rassoulzadegan, F.U., 1999. Use of high temperature catalytic oxidation (HTCO) to measure carbon content of microorganisms. Aquatic Microbial Ecology 16, 273–280.
Pinel-Alloul, B., 1995. Les invertébrés prédateurs du zooplancton. In: Pourriot, R., Meybeck, M. (Eds.), Limnologie Générale. Masson. Collection d'Ecologie, Paris, pp. 541–564.
Pont, D., 1995. Le zooplancton herbivore dans les chaînes alimentaires pélagiques. In: Pourriot, R., Meybeck, M. (Eds.), Limnologie Générale. Masson. Collection d'Ecologie, Paris, pp. 515–540.
Putt, M., Stoecker, D.K., 1989. An experimentally determined carbon: volume ratio for marine oligotrichous ciliates from estuarine and coastal waters. Limnology and Oceanography 34, 1097–1104.
Rancher, J., Rougerie, F., 1995. L'environnement océanique de l'archipel des Tuamotu (Polynésie française). Oceanology Acta 18, 43–60.
Razouls, C., de Bovée, F., Kouwenberg, J., Desreumaux, N., 2005-2011. Diversité et répartition géographique chez les Copépodes planctoniques marins. <http://www.copepodes.obs-banyuls.fr>. <http://www.copepodes.obs-banyuls.fr>.
Ricard, M., Gueredrat, J.A., Magnier, Y., Renon, J.P., Rochette, J.P., Rougerie, F., Sournia, A., Wauthy, B., 1979. Le plancton du lagon de Takapoto. Journal de la Société des Océanistes 35, 47–67.
Riisgard, H.U., Larsen, P.S., 2010. Particle capture mechanisms in suspension-feeding invertebrates. Marine Ecology-Progress Series 418, 255–293.
Rose, M., 1953. Quelques renseignements sur le plancton des Tuamotu. Bulletin du Muséum d'Histoire Naturelle 2eme Ser. 20, pp. 455–462 (456–462).
Sakka, A., Legendre, L., Gosselin, M., Niquil, N., Delesalle, B., 2002. Carbon budget of the planktonic food web in an atoll lagoon (Takapoto, French Polynesia). Journal of Plankton Research 24, 301–320.
Sherr, E.B., Caron, D.A., Sherr, B.F., 1994. Staining of heterotrophic protists for visualisation via epifluorescence microscopy. In: Kemp, P.F., Sherr, B.F., Sherr, E.B., Coll, J.J. (Eds.), Handbook of Methods in Aquatic Microbial Ecology. Lewis Publishers, Boca Raton, pp. 213–227.
Tanimura, A., Hattori, H., Miyamoto, Y., Hoshiai, T., Fukuchi, M., 2008. Diel changes in vertical distribution of *Oithona similis* (Cyclopoida) and *Oncaea curvata* (Poecilostomatoida) under sea ice in mid-summer near Syowa Station, Antarctica. Polar Biology 31 (5), 561–567.
Thioulouse, J., Chessel, D., Dolédec, S., Olivier, J.-M., 1997. ADE-4, a multivariate analysis and graphical display software. Statistics and Computing 7, 75–80.
Thomas, Y., Garen, P., Bennett, A., Le Pennec, M., Clavier, J., 2012a. Multi-scale distribution and dynamics of bivalve larvae in a deep atoll lagoon (Ahe, French Polynesia). Marine Pollution Bulletin 65, 453–462.
Thomas, Y., Le Gendre, R., Garen, P., Dumas, F., Andréfouët, S., 2012b. Bivalve larvae transport and connectivity within the Ahe atoll lagoon (Tuamotu Archipelago), with application to pearl oyster aquaculture management. Marine Pollution Bulletin 65, 441–452.
Torréton, J.-P., Rochelle-Newall, E., Jouon, A., Faure, V., Jacquet, S., Douillet, P., 2007. Correspondence between the distribution of hydrodynamic time parameters and the distribution of biological and chemical variables in a semi-enclosed coral reef lagoon. Estuarine Coastal and Shelf Science 74, 766–776.
Tregouboff, G., Rose, M., 1957. Manuel de planctonologie méditerranéenne. Paris.
Troussellier, M., Courties, C., Lebaron, P., Servais, P., 1999. Flow cytometric discrimination of bacterial populations in seawater based on SYTO 13 staining of nucleic acids. Microbial Ecology 29, 319–330.
Turner, J.T., 1984. The feeding ecology of some zooplankters that are important prey items of larval fish, NOAA Techn. Rept. NMFS, p. 28.
Uye, S.I., 1982. Length-weight relationships of important zooplankton froml the Inland Sea of Japan. Journal of the Oceanographical Society of Japan 38, 149–158.
Verity, P., Robertson, C., Tronzo, C., Andrews, M., Nelson, J., Sieracki, M., 1992. Relationship between cell volume and the carbon and nitrogen content of marine photosynthetic nanoplankton. Limnology and Oceanography 37, 1434–1446.
Webber, M., Edwards Myers, E., Campbell, C., Webber, D., 2005. Phytoplankton and zooplankton as indicators of water quality in Discovery Bay, Jamaica. Hydrobiologia 545, 177–193.
Welschmeyer, N.A., 1994. Fluorometric analysis of clorophyll a in the presence of chlorophyll b and phaeopigments. Limnology and Oceanography 39, 1985–1992.
Yukuhira, H., Klumpp, D.W., Lucas, J.S., 1998. Effects of body size on suspension feeding and energy budgets of the pearl oyster *Pinctada margaritifera* and *P. maxima*. Marine Ecology Progress Series, pp. 119–130.